AD-A064 436 DOUGLAS AIRCRAFT CO LONG BEACH CALIF F/G 11/9
TESTING FOR MECHANICAL PROPERTIES OF MONOLITHIC AND LAMINATED P--ETC(U)
OCT 78 F E GREENE, L P KOEGEBOEHN F33615-75-C-3105
UNCLASSIFIED MDC-J6950 AFFDL-TR-77-96-PT-1 NL

1 OF 5
AD
A064436

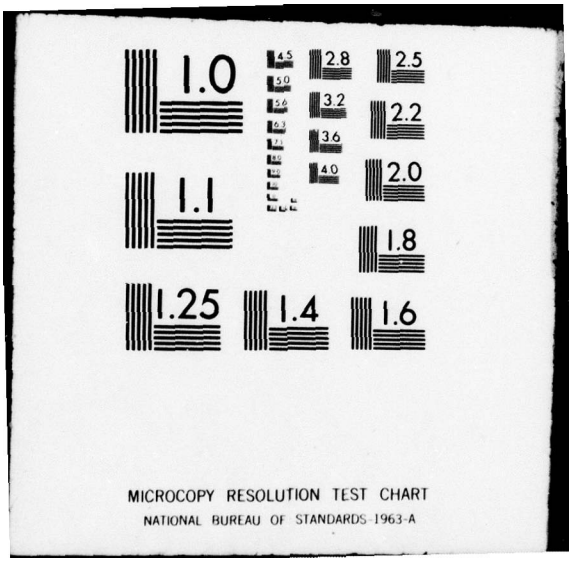
1.0
1.1
1.25
1.4
1.6
1.8
2.0
2.2
2.5
2.8
3.2
3.6
4.0
4.5
5.0
MICROCOPY RESOLUTION TEST CHART
NATIONAL BUREAU OF STANDARDS-1963-A

AFFDL-TR-77-96
PART 1

LEVEL II 2

AD A064436

TESTING FOR MECHANICAL PROPERTIES OF MONOLITHIC AND LAMINATED POLYCARBONATE MATERIALS, PART 1 TEST RESULTS AND ANALYSIS

F.E. Greene
Douglas Aircraft Company
McDonnell Douglas Corporation
3855 Lakewood Boulevard
Long Beach, California 90846

DDC FILE COPY

DDC
RECEIVED
FEB 13 1979
C

OCTOBER 1978

TECHNICAL REPORT AFFDL-TR-77-96

Final Report For Period Janury 1976-October 1978

Approved for public release; distribution unlimited

AIR FORCE FLIGHT DYNAMICS LABORATORY
AIR FORCE WRIGHT AERONAUTICAL LABORATORIES
AIR FORCE SYSTEMS COMMAND
WRIGHT-PATTERSON AIR FORCE BASE, OHIO 45433

79 02 08 007

NOTICE

When Government drawings, specifications, or other data are used for any purpose other than in connection with a definitely related Government procurement operation, the United States Government thereby incurs no responsibility, nor any obligation whatsoever; and the fact that the Government may have formulated, furnished, or in any way supplied the said drawings, specifications, or other data, is not to be regarded by implication or otherwise as in any manner licensing the holder or any other person or corporation, or conveying any rights or permission to manufacture, use, or sell any patented invention that may in any way be related thereto.

This report has been reviewed by the Information Office (OI) and is releasable to the National Technical Information Service (NTIS). At NTIS, it will be available to the general public, including foreign nations.

This technical report has been reviewed and is approved for publication.

Larry G. Moosman

LT. LARRY G. MOOSMAN
Project Manager
Improved Windshield Protection ADPO
Vehicle Equipment Division

Robert E. Wittman

ROBERT E. WITTMAN
Program Manager
Improved Windshield Protection ADPO
Vehicle Equipment Division

FOR THE COMMANDER:

Ambrose B. Nutt

AMBROSE B. NUTT
Director
Vehicle Equipment Division

Copies of this report should not be returned unless return is required by security considerations, contractual obligations, or notice on a specific document.

AIR FORCE/56780/2 February 1979 — 150

(19) TR-77-96-PT-1

SECURITY CLASSIFICATION OF THIS PAGE (When Data Entered)

REPORT DOCUMENTATION PAGE

READ INSTRUCTIONS BEFORE COMPLETING FORM

(18) 1. REPORT NUMBER: AFFDL-TR-77-96, Part 1

2. GOVT ACCESSION NO.

3. RECIPIENT'S CATALOG NUMBER

(9) 5. TYPE OF REPORT & PERIOD COVERED: Final Report, January 1976 - October 1978

(6) 4. TITLE (and Subtitle): Testing for Mechanical Properties of Monolithic and Laminated Polycarbonate Materials, Part 1, Test Results and Analysis

(14) 6. PERFORMING ORG. REPORT NUMBER: MDC-J6950

7. AUTHOR(s): F. E. Greene

(15) 8. CONTRACT OR GRANT NUMBER(s): F33615-75-C-3105

9. PERFORMING ORGANIZATION NAME AND ADDRESS: Douglas Aircraft Company, McDonnell Douglas Corporation, Long Beach, California 90846 — 116 400

10. PROGRAM ELEMENT, PROJECT, TASK AREA & WORK UNIT NUMBERS: Project: 2202, Task: 02, Work Unit: 01 — 632 11F

11. CONTROLLING OFFICE NAME AND ADDRESS: Air Force Flight Dynamics Laboratories, Air Force Wright Aeronautical Laboratories, Air Force Systems Command - Wright-Patterson AFB

(11) 12. REPORT DATE: October 1978

13. NUMBER OF PAGES: 443

14. MONITORING AGENCY NAME & ADDRESS (if different from Controlling Office)

(16) 2202, 1926

(17) 02

15. SECURITY CLASS. (of this report): Unclassified

15a. DECLASSIFICATION/DOWNGRADING SCHEDULE

16. DISTRIBUTION STATEMENT (of this Report)

Approved for public release; distribution unlimited.

(12) 448 p.

17. DISTRIBUTION STATEMENT (of the abstract entered in Block 20, if different from Report)

(10) F.E. Greene, L.P. Koegeboehn, J.H. Lawrence, R.H. Magnusson, J.W. Kazmaier

18. SUPPLEMENTARY NOTES

19. KEY WORDS (Continue on reverse side if necessary and identify by block number)

Mechanical properties
True stress-strain tensile curves
Materials property program
Ramberg-Osgood equation inputs
Aerodynamic heating and service aging effects
Polycarbonate and laminating materials testing
Design allowable stress-strain curves.

20. ABSTRACT (Continue on reverse side if necessary and identify by block number)

This report documents the studies, testing, analyses, and development of mechanical properties of high temperature polymers for use in the design of laminated windshields and canopies for supersonic aircraft.

Testing and data reduction were directed toward establishment of design allowables for polymers similar to MIL-HDBK-5B values for metals. Tests were conducted and design mechanical properties determined for static and

→ over

DD FORM 1 JAN 73 1473 EDITION OF 1 NOV 65 IS OBSOLETE

SECURITY CLASSIFICATION OF THIS PAGE (When Data Entered)

116 400 79 02 08 007

19. KEY WORDS

20. ABSTRACT

bird impact loading conditions at the operating temperature extremes of a supersonic aircraft. To provide these design mechanical properties, the following items were developed and are documented in this report.

- Testing methods at strain rates from 0.5 to 12,000 inch/inch/minute and at test temperatures from -30°F to +190°F.
- Design allowable tensile, compressive, and shear stress-strain curves.
- True tensile stress-strain curves for polycarbonate materials.
- Computerized normality test method for checking distribution of test data points using Kolmogorov-Smirnov limits.
- A computer program used for analysis of test data and development of design allowable stress-strain curves and other mechanical properties data.

Studies based on analyses of test data documented in this report are as follows:

- Aerodynamic heating and service aging effects on mechanical properties of processed polycarbonate materials.
- Strain rate and temperature effects on various high temperature polymer materials.
- Thickness effects on yield properties of processed polycarbonate materials at static and impact loading conditions.
- Comparisons of high temperature polymer materials for use in the design of laminated transparencies for supersonic aircraft.

FOREWORD

This report is one of a series of reports that describes work performed by Douglas Aircraft Company, McDonnell Douglas Corporation, 3855 Lakewood Blvd., Long Beach, California 90846, under the Windshield Technology Demonstrator Program. This work was sponsored by the U.S. Air Force Flight Dynamics Laboratory, Wright-Patterson Air Force Base, under Contract F33615-75-C-3105, Project 2202/1926.

Lieutenant L. G. Moosman (AFFDL/FEW) was the Air Force Project Manager who monitored the program.

Mr. J. H. Lawrence, Jr., was the Program Director for the Douglas Aircraft Company. Mr. F. E. Greene, Structural Engineering, was the responsible engineer and author of this report.

The principal investigators and contributing authors were:

L. P. Koegeboehn - Environmental Engineering
J. H. Lawrence - Structures - Design
R. H. Magnusson - Structures - Design
J. W. Kozmata - Material and Process Engineering

The author wishes to thank R. J. Reid, R. Lingle, K. L. DeVries, and A. H. Jones of Terra Tek, Inc., Salt Lake City, Utah for their timely efforts in performing high strain rate testing under contract to Douglas.

This report was first submitted to the Air Force in February, 1978, and the time period covered by this report was from October 1976 through January 1978.

ACCESSION for
NTIS White Section
DDC Buff Section
UNANNOUNCED
JUSTIFICATION
BY
DISTRIBUTION/AVAILABILITY CODES
Dist. SPECIAL
A

TABLE OF CONTENTS

SECTION		PAGE
I	INTRODUCTION	1
II	INDUSTRIAL SURVEY AND REVIEW OF MATERIAL DATA	9
	MATERIAL PROPERTIES DATA REVIEW	9
	MATERIALS RESEARCH	14
III	MATHEMATICAL ANALYSIS	17
	STATISTICAL AND MATHEMATICAL SOLUTION FOR DEFINING DESIGN ALLOWABLES	18
IV	AERODYNAMIC HEATING AND SERVICE AGING EFFECTS ON MECHANICAL PROPERTIES OF POLYCARBONATE	49
	TEST SPECIMEN DESCRIPTION	49
	TEST EQUIPMENT AND SETUP DESCRIPTION	53
	TEST PROCEDURES	53
	TEST REQUIREMENTS	55
	TEST RESULTS AND ANALYSIS	57
V	LOW STRAIN RATE TENSILE MECHANICAL PROPERTIES TESTING OF PROCESSED POLYCARBONATE MATERIALS	69
	TEST SPECIMEN DESCRIPTION	69
	TEST SETUP AND EQUIPMENT DESCRIPTION	73
	TEST PROCEDURE	73
	TEST REQUIREMENTS	76
	TEST RESULTS AND ANALYSIS	77
VI	LOW STRAIN RATE COMPRESSIVE MECHANICAL PROPERTIES TESTING OF PROCESSED POLYCARBONATE MATERIALS	181
	TEST SPECIMEN DESCRIPTION	181
	TEST SETUP AND EQUIPMENT DESCRIPTION	183
	TEST PROCEDURE	183
	TEST REQUIREMENTS	185
	TEST RESULTS AND ANALYSIS	185
VII	LOW STRAIN RATE SHEAR MECHANICAL PROPERTIES TESTING OF LAMINATED INTERLAYER MATERIALS	213
	TEST SPECIMEN DESCRIPTION	213

REPRODUCIBILITY OF THE ORIGINAL PAGE IS POOR

SECTION PAGE

TEST SETUP AND EQUIPMENT DESCRIPTION. 218
TEST PROCEDURES 218
TEST REQUIREMENTS 223
TEST RESULTS AND ANALYSIS 224

VIII HIGH STRAIN RATE TENSILE MECHANICAL PROPERTIES TESTING OF MONOLITHIC POLYCARBONATE MATERIALS. 275
TEST SPECIMEN DESCRIPTION 275
TEST SETUP AND EQUIPMENT DESCRIPTION. 278
TEST PROCEDURE. 283
TEST REQUIREMENTS 283
TEST RESULTS AND ANALYSIS 285

IX HIGH STRAIN RATE COMPRESSIVE MECHANICAL PROPERTIES OF MONOLITHIC POLYCARBONATE MATERIAL 351
TEST SPECIMEN DESCRIPTION 351
TEST SETUP AND EQUIPMENT DESCRIPTION. 353
TEST PROCEDURE. 359
TEST REQUIREMENTS 359
TEST RESULTS AND ANALYSIS 360

X HIGH STRAIN RATE SHEAR MECHANICAL PROPERTIES TESTING OF LAMINATED INTERLAYER MATERIALS. 373
TEST SPECIMEN DESCRIPTION 373
TEST SETUP AND EQUIPMENT DESCRIPTION. 375
TEST PROCEDURE. 381
TEST RESULTS AND ANALYSIS 382

XI CONCLUSIONS AND RECOMMENDATIONS. 427
CORE PLY MATERIALS - PROCESSED POLYCARBONATE. 427
INTERLAYER MATERIALS. 429
MATERIAL DESIGN ALLOWABLES. 431
TEST OBSERVATIONS 432

APPENDICES PAGE

A TENSILE STRESS-STRAIN CURVE DATA 95

B COMPRESSION STRESS-STRAIN CURVE DATA 193

C SHEAR STRESS-STRAIN CURVE DATA 239

D TENSILE STRESS-STRAIN CURVE DATA 297

E COMPRESSION STRESS-STRAIN DATA 365

F SHEAR STRESS-STRAIN CURVE DATA 395

REFERENCES 442

LIST OF ILLUSTRATIONS

NUMBER		PAGE
1	Block Diagram - Design Curve Development.	19
2	True Tensile Stress-Strain Curve Development.	23
3	Design Tensile Stress-Strain Curve Development.	26
4	Design Shear and Compression Stress-Strain Curve Development	27
5	Graphical Presentation of Normality Check	29
6	Normal Population Distribution Factor K vs N	30
7	Ramberg-Osgood Curve Development	32
8	Material Properties Computer Programs Diagram	33
9	Tensile Specimen (Z7942633-503)	51
10	Tensile Specimen (Z7942633-541, -571, -605)	52
11	Impact Test Specimen (Z7942633-1)	52
12	Tensile Test Specimen Indexing and Alignment Fixture . . .	54
13	Tensile Stress-Strain Test Setup	54
14	Impact Resistance Test Setup (Izod Type)	56
15	Tensile Average Curves - Thermal Conditioning Effects . . .	59
16	Tensile Average Curves - Thermal Conditioning Effects . . .	60
17	Tensile Average Curves - Service Aging Effects	61
18	Tensile Average Curves - Service Aging Effects	63
19	Before and After Storage for Four Years at 293-393K in a Dark Dry Location (Adapted from Reference 6).	64
20	Average Mechanical Properties Versus Thermal Conditioning for SL3000 Polycarbonate Material	65
21	Average Mechanical Properties Versus Thermal Conditioning for "TUFFAK" Polycarbonate Material	66
22	Tensile Specimen (Z7942633-503)	71
23	Tensile Specimen (Z7942633-541, -507, -571, -605)	71
24	Tensile Specimen (Z7942633-509)	72
25	Tensile Specimen (Z7942633-517, -543)	72
26	Tensile Test Setup	74
27	Tensile Test Setup	75
28	Tensile Test Specimen Indexing and Alignment Fixture . . .	76

PRECEDING PAGE NOT FILMED BLANK

LIST OF ILLUSTRATIONS (Continued)

NUMBER		PAGE
29	Tensile Average Curves - Material Comparisons	82
30	Tensile Average Curve - Processing Effects	84
31	Tensile Average Curve - Processing Effects	85
32	Tensile Average Curves - Forming Effects.	86
33	Tensile Average Curves - Strain Rate Effects	87
34	Tensile Average Curves - Strain Rate Effects	88
35	Tensile Average Curves - Temperature Effects	90
36	Tensile Average Curves - Temperature Effects	91
37	Tensile Average Curves - Thickness Effects.	92
38	Compression Test Specimen (Z7942633-511, -545)	182
39	Compression Test Specimen (Z7942633-513, -515, -527, -547)	182
40	Compression Test Setup	184
41	Compression Average Curves - Processing Effects	190
42	Shear Test Specimen (Z7942633-529)	215
43	Shear Test Specimen (Z7942633-531, -533, -623, -627).	215
44	Shear Test Specimen (Z7942633-535, -539)	216
45	Torsional Shear Test Specimen (Z7942633-537)	217
46	Compressive Shear Test Setup	219
47	Shear Test Fixture	220
48	Torsional Shear Test Setup	221
49	Shear Average Curves - Temperature Effects	229
50	Shear Average Curves - Temperature Effects	230
51	Shear Average Curves - Temperature Effects	232
52	Shear Average Curves - Temperature Effects	233
53	Shear Average Curves - Material Comparisons	234
54	Shear Average Curves - Material Comparisons	235
55	Shear Average Curves - Material Comparisons	236
56	Shear Average Curves - Test Methods Comparisons	238
57	Tensile Specimen (Z7942633-523)	276
58	Tensile Specimen (Z7942633-569)	276

LIST OF ILLUSTRATIONS (Continued)

NUMBER		PAGE
59	Tensile Specimen (Z7942633-601)	277
60	Tensile Specimen (Z7942633-611)	277
61	Medium Strain Rate Test Facility	279
62	Schematic of Medium Strain Rate Machine	280
63	High Strain Rate Gas Actuator	282
64	Tensile Test Configuration	284
65	Tensile Average Curves - Processing Effects	289
66	Tensile Average Curves - Temperature Effects	290
67	Tensile Average Curves - Thickness Effects	291
68	Tensile Average Curves - Forming Effects.	293
69	Tensile Average Curves - Material Comparisons	294
70	Compression Specimen (Z7942633-525)	352
71	Medium Strain Rate Test Facility	354
72	Schematic of Medium Strain Rate Machine	355
73	High Strain Rate Gas Actuator	356
74	Compression Test Configuration	358
75	Compression Average Curves - Temperature Effects	363
76	Shear Test Specimen (Z7942633-519, -625)	374
77	Shear Test Specimen (Z7942633-521)	374
78	Shear Test Specimen (Z7942633-603)	374
79	Medium Strain Rate Test Facility	376
80	Schematic of Medium Strain Rate Machine	377
81	High Strain Rate Gas Actuator	378
82	Tensile Test Configuration	380
83	Shear Average Curves - Temperature Effects	386
84	Shear Average Curves - Temperature Effects	387
85	Shear Average Curves - Temperature Effects	388
86	Shear Average Curves - Temperature Effects	389
87	Shear Average Curves - Temperature Effects	390
88	Shear Average Curves - Material Comparisons	391

LIST OF ILLUSTRATIONS (Continued)

NUMBER		PAGE
89	Shear Average Curves - Material Comparisons	392
90	Tensile Strain Rate and Temperature Effects	393
91	Tensile Strain Rate and Temperature Effects	427
92	Shear Strain Rate and Temperature Effects	431
93	Yield Strength as a Function of Temperature. From Reference 16.	435
94	Stress-Strain Curve in Cold Drawing. Inset is the Appearance of the Test-Piece Itself. (a) Undrawn (b) Drawn Regions Respectively. From Reference 11	437
95	Effect of Loaindg Rate on Fracture Surface of Glassy Polymers. From Reference 20.	438
96	Sample That Did Not Draw (x 40)	440
97	Sample That Necked and was Drawn Over Large Part of Gauge Length.	441

LIST OF TABLES

TABLE		PAGE
1	RAW MATERIAL SUPPLIERS AND LAMINATORS	10
2	TYPICAL PROPERTIES OF TRANSPARENT HIGH TEMPERATURE STRUCTURAL MATERIALS	12
3	TYPICAL PROPERTIES OF TRANSPARENT HIGH TEMPERATURE INTERLAYER MATERIALS	13
4	0.975 FRACTILES OF THE F DISTRIBUTION ASSOCIATED WITH n_1 AND n_2 DEGREES OF FREEDOM $F_{0.975}(n_1, n_2)$	46
5	0.95 AND 0.975 FRACTILES OF THE t DISTRIBUTION ASSOCIATED WITH df DEGREES OF FREEDOM	47
6	TEST SPECIMEN THERMAL CONDITIONING	51
7	TENSILE AND IMPACT TEST DATA (SL3000) TASK 1, TEST SERIES 1	59
8	TENSILE TEST DATA (TUFFAK) TASK 1, SERIES 2	60
9	TENSILE TEST DATA TASK 1, TEST SERIES 3	61
10	TENSILE TEST DATA, TASK 2	63
11	TENSILE STRENGTH DATA TASK I	78
12	TENSILE STRENGTH DATA TASK II	80
13	TENSILE STRENGTH DATA TASK III	81
14	PROPOSED TENSILE DESIGN ALLOWABLES	94
15	COMPRESSION STRENGTH DATA TASK I	187
16	COMPRESSION STRENGTH DATA TASK II	188
17	PROPOSED COMPRESSION DESIGN ALLOWABLES	191
18	SHEAR STRENGTH DATA, TASK I	225
19	SHEAR STRENGTH DATA TASK II	226
20	SHEAR STRENGTH DATA, TASK III	228
21	TENSILE STRENGTH DATA	286
22	TENSILE STRENGTH DATA	287
23	PROPOSED TENSILE DESIGN ALLOWABLES	296
24	COMPRESSION STRENGTH DATA	361
25	SHEAR STRENGTH DATA	383

SECTION I
INTRODUCTION

Bird impact hazards to high speed, high performance, low flying aircraft have become one of the major flight safety problems of the jet age. This safety problem accompanied with the need for design engineers to design lightweight transparencies poses many problems in the selection of materials for windshields and canopies.

This report describes studies that were conducted and the material testing accomplished to establish mechanical properties of transparency materials that could withstand the harsh environment to which a windshield or canopy is exposed on a high speed, low flying supersonic aircraft. It was estimated that aerodynamic heating could cause the transparency surface temperature to reach 300°F, and these high temperatures could occur at low altitude where the potential for a birdstrike is greatest. Based on these requirements, materials testing was accomplished on monolithic and laminated transparency materials that had been processed by qualified vendors. Seven series of tests were performed on these selected high temperature polymer materials.

Based on prior transparency design reports and an assessment of bird impact testing results, it became apparent that a knowledge of the load carrying ability was necessary for transparency materials subjected to varying strain-rate loading conditions under wide temperature extremes. The low strain-rate (0.01 in./in./min. to 20 in./in./min.) mechanical properties of transparency materials are required to design for cabin pressure, thermodynamic, aerodynamic and structural carry-through loading. The high strain-rate (100 in./in./min. to 12,000 in./in./min.) mechanical properties of the transparency materials are required to design for bird strike loading. In the case of low strain-rate loading, the inherent load-carrying ability of a transparency must be such that the limit load can be sustained without excessive deformation or permanent set, requiring a knowledge of the elastic properties of the materials.

The load-carrying ability of a transparency under high strain-rate conditions requires a knowledge of the materials in the plastic range, where excessive deformation can be a design asset due to absorption of the bird impact shock load. To provide these mechanical properties the complete stress-strain histories of candidate materials are required. To be of maximum usage, the required material properties should consider the effects of:

1. Rate of strain at appropriate testing temperatures.
2. Processing thermal history, manufacturing methods and procedures.
3. In-service aerodynamic heating and service aging.

INDUSTRY SURVEY

An intensive library and industry survey was undertaken to identify transparency materials, vendor capabilities, and tabulate known mechanical properties of available transparency materials. The results of this effort is documented in Section II.

STATISTICAL ANALYSES

The accuracies of the industry established mechanical properties of transparency materials, at best, are approximations.

The paragraphs that follow provide an overview of the statistical approach, presented in Section III that should be utilized to establish more reliable values needed in the design of windshields or canopies.

Historically, the way of describing a material property has been one number which characterizes the "average" property quantitatively. Such a description of material property tells nothing about the variability of the particular materials. Unfortunately, many transparent material properties are listed in this fashion in Vendor's and Processor's literature in textbooks, and even in the latest edition of MIL-HDBK-17A, Part II. On page 1-2 of this handbook it states:

"The data on the mechanical, thermal, optical and other properties of transparent plastics and glass have been selected from a number of specifications and reports. Sufficient test data were not available on all materials for establishing design allowables. Therefore, some material property data are only representative values and should be considered as such. Because most configurations are complex, the designer should prepare test specimens of the final design configuration and conduct confirmation tests of all critical design factors". (underlining by author)

It should be mentioned that in MIL-HDBK-17A, Part II, no indication is given for any material as to whether "sufficient test data" were available for it, or whether or not its "material property data are only representative values". As any transparency designer is aware, these "ball park" values are the only information easily available.

An example of an excellent source for metallic properties is Military Handbook-5B. This military design handbook is the standard source book in the aircraft industry for the design strength properties of various metals and elements. The strength information is based on statistical data and is listed for materials of various forms (sheets, bars, casting, etc.) and of various heat treatments. The design allowable value for the material strength properties are given such that a certain high percentage of all like material is expected to exceed these values. The statistical techniques employed are a means of maintaining a high level of assurance in the reported values.

Section 9 of MIL-HDBK-5B fully describes the statistical techniques required to present acceptable design allowable material property values. Douglas adopted the methods outlined in MIL-HDBK-5B in the preparation of statistical-accurate design allowables for the transparent material tested, which is documented in Section III of this report.

SPECIMEN TESTING, RESULTS AND ANALYSIS

The most viable transparent material, capable of meeting bird impact requirements at minimum weight, was found to be polycarbonate. Polycarbonate has potential applications as a monolithic, as well as, in combination with other materials in a laminated form. As a laminate, the latest generation of interlayer materials must be used to sustain the high temperatures expected on high speed aircraft.

The testing descriptions, results and analyses for seven series of tests are contained in Sections IV through X with brief descriptions noted in the paragraphs that follow. In an endeavor to provide meaningful and consistent data, where possible, ASTM test methods or ASTM methods that are in the development stages were utilized in defining the configuration of specimens, the test methods and the data documentation format. Average and design allowable stress-strain curves were developed from tests noted in Sections V through X and are shown as appendices to the respective sections. These curves were the basis for the tabulated data shown within each section.

Section IV presents a series of tests covering aerodynamic heating and service aging effects on mechanical properties of monolithic polycarbonate. Previously it has been demonstrated that exposure of bisphenol, a thin film polycarbonate material, to temperatures above 80°C (176°F) became increasingly less ductile. This was evidenced by accumulative decreases in impact strength, fracture energy, extension to break, and increases in tensile yield strength. Other evidence indicated a degrading of these mechanical properties due to weathering and storage. To determine if mechanical property changes occur in sheet polycarbonate due to aerodynamic heating, a series of tensile and impact tests were conducted at room temperature on two types of monolithic polycarbonate specimens that had been exposed to thermal conditioning representative of the exposure a supersonic aircraft would encounter during its lifetime. To determine if mechanical property changes occur in sheet polycarbonate due to service aging, a series of tensile tests were conducted at room temperature on fusion bonded monolithic polycarbonate specimens removed from a four year old service-aged canopy and newly made transparencies.

Section V presents the low strain rate tensile mechanical properties testing of processed polycarbonate materials. This test series was conducted to establish complete tensile stress-strain curves and mechanical properties for monolithic polycarbonate materials at various temperature conditions and at low strain rates. Test specimens were made from instrumented beams and bird impact test windshield/canopies, or from material (both sheet and specimen configurations) furnished by transparency fabricators. The primary use for these tests was to provide average (actual) and design allowables for development, and future design use in computer programs. Additional uses were to provide for evaluation of materials and processors, trade-off design studies, windshield static load design analysis, and to provide test criteria for future transparency design specification control documents. Maximum and minimum test temperatures were established for tests based on the flight profile of a supersonic aircraft.

Section VI presents the low strain rate compressive mechanical properties testing of processed polycarbonate materials. This test series was conducted to establish compressive mechanical properties of monolithic polycarbonate materials as processed by specific transparency fabricators. The primary use for these tests was to provide average (actual) and design allowables of processed polycarbonate materials for development, and future design use in computer programs. Additional use was to provide for static load design analysis and for evaluation of vendors processes. Test specimens were made from instrumented beams and bird impacted test windshields, or furnished by specific transparency fabricators.

Section VII presents the low strain rate shear mechanical properties testing of laminated interlayer materials. This series of tests was conducted to establish complete shear mechanical properties of interlayer materials as processed by specific transparency fabricators. The primary use for these tests was to provide average (actual) mechanical properties and design allowables for processed interlayer materials for development, and future design use in computer programs. Additional uses were:

evaluation of materials and processors, trade-off design studies, windshield static load analysis, and test criteria for the windshield/canopy design specification control documents. Test specimens were made from instrumented beams and bird impacted test windshields, or from material (both laminated sheet and specimen configurations) furnished by specific transparency fabricators. Two types of shear tests were conducted: (1) a generally used compression double shear test, and (2) a unique torsional shear test. Results of these two types of testing were compared to arrive at the most accurate means of testing. Maximum and minimum test temperatures were established for tests based on the flight profile of a supersonic aircraft.

Section VIII presents the high strain rate tensile mechanical properties testing of processed polycarbonate materials. This series of tests was conducted to provide average (actual) mechanical properties and design allowables for monolithic polycarbonate materials processed by specific transparency fabricators. The primary use for these mechanical properties was for development and future design use in computer analysis of a bird strike. These data are also useful in evaluating materials processed by transparency fabricators. Tests were conducted at the maximum and minimum temperature conditions established by the flight profile of a supersonic aircraft. Maximum strain rates due to a bird strike were determined from bird impact tests of actual full size transparencies. Tests were accomplished at Terra Tek, Inc., Salt Lake City, Utah under contract to Douglas for high strain rate testing. Test specimens were designed to specifications furnished by Terra Tek, Inc., and manufactured by specific fabricators receiving the same processing as a laminated aircraft transparency.

Section IX presents the high strain rate compressive mechanical properties of processed polycarbonate material. This series of tests was conducted to provide average (actual) mechanical properties and design allowables for monolithic polycarbonate materials as processed by specific transparency fabricators. The primary use for these mechanical properties was for development and future design use in computer analysis

of bird strike. Additional uses were to provide for evaluation of materials and processors. Tests were conducted at the maximum and minimum temperature conditions established by the flight profile of a supersonic aircraft. Maximum strain rates due to a bird strike were determined from bird impact tests of actual full size transparencies. Compression testing was accomplished at Terra Tek, Inc., Salt Lake City, Utah, under contract to Douglas for high strain rate testing. Test specimens were designed to specifications furnished by Terra Tek, Inc., and manufactured by specific fabricators receiving the same processing as a laminated aircraft transparency.

Section X presents the high strain rate shear mechanical properties testing of laminated interlayer materials. This series of tests was conducted to provide average (actual) shear mechanical properties and design allowables for laminated interlayer materials as processed by specific transparency fabricators. The primary use for these mechanical properties was for development and future design use in computer analysis of a bird strike. This data is also useful in evaluating materials processed by transparency fabricators. Tests were conducted at maximum and minimum temperature conditions established by the flight profile of a supersonic aircraft. The strain rates utilized were based on maximum strain rates determined from bird impact tests of actual full size windshields. Tests were conducted at Terra Tek, Inc., Salt Lake City, Utah, under contract to Douglas for high strain rate testing. Test specimens were designed to specifications furnished by Terra Tek, Inc., and manufactured by specific fabricators receiving the same processing as a laminated transparency.

Section XI presents conclusions and recommendations based on data analysis and observations of Sections IV through X as well as data previously generated by others.

SECTION II
INDUSTRIAL SURVEY AND REVIEW OF MATERIAL DATA

The selection of materials and processors were based on design requirements for a windshield on a supersonic bomber (reference 1), and a formed canopy on a supersonic fighter (reference 2). General design concepts were developed using high temperature materials that were currently in military flight status, and newly developed materials. Design concepts using structural core plies of multilayered laminated glass, multilayered laminated polycarbonate and monolithic polycarbonate construction were investigated. Several types of laminating interlayer materials were selected, both currently used and newly developed materials. An industry survey was undertaken to identify qualified laminators and materials to provide these requirements. The results of this survey, completed in December 1976, are documented in Table 1.

MATERIAL PROPERTIES DATA REVIEW

An exhaustive search was made to gather mechanical properties data for the Windshield Technology Demonstrator Program. Literature searches were initiated at NASA Scientific and Technical Division, at the Defense Documentation Center, at private and public libraries, at the Air Force Flight Dynamics Laboratories, and from material suppliers.

Current industry tests and publications were found to offer incomplete and/or inadequate information concerning high-performance material properties of many promising aircraft transparency materials. Such properties are essential to effect a proper balance of structural efficiency, safety, minimum weight designs, provide a solid basis for design trade-off studies, and material/fabrication specification tests.

PRECEDING PAGE NOT FILMED
BLANK

TABLE 1.

RAW MATERIAL SUPPLIERS AND LAMINATORS

MATERIAL	VENDOR DESIGNATION	MIL SPEC	INDEX OF REFRACTION	HAZE	MAX. MAT'L TEMPERATURE RANGE	THICKNESS AVAIL-ABILITY	RAW MATERIAL SUPPLIERS	LAMINATORS	LIGHT TRANS-MISSION
As-Cast Acrylic	PLEXIGLAS II SWEDLOW TYPE 320	MIL-P-5425	1.49	1%	-65 to 190°F	0.060-0.188	Rohm & Haas Swedlow	PPG Sierracin Swedlow Goodyear	92%
As-Cast modified and partially cross-linked acrylic	PLEXIGLASS 55 SWEDLOW TYPE 350	MIL-P-8184	1.50	1%	-65 to 190°F	0.080-0.188	Rohm & Haas Swedlow	PPG Sierracin Swedlow Goodyear	91%
Stretched Acrylic	STRETCH PLEXIGLASS 55 STRETCH SWEDLOW TYPE 350S	MIL-P-25690	1.499	1%	-65 to 180°F	0.060 - 0.970	Sierracin Goodyear Swedlow	Sierracin Goodyear Swedlow PPG	91%
Poly-carbonate	SL3000	MIL-P-83310	1.586 (avg)	>1%	-65 to 320°F	0.125-0.500	General Electric	Texstar Sierracin Swedlow Goodyear PPG	90%
	TUFFAK						Rohm & Haas		
Cast-In-Place (CIP) Silicone	S-100		1.44	1%	-70 to 350°F		Sierracin	Sierracin	91%
	SS-5272Y		1.409	1%	-70 to 350°F		Swedlow	Swedlow	91%
	FAX-28			0.13%	-65 to 250°F		Goodyear	Goodyear	90.1%
Polyurethane	PPG112		1.4967	0.5%		0.030 per ply	PPG	PPG	85%
	F5X-3A		1.536	1.2%			Goodyear	Goodyear	87.8%
	S-120		1.490	0.3%	-65 to 240°F		Sierracin	Sierracin	86.0%
Copolymer	S-130		1.52				Sierracin	Sierracin	89 - 91%

Prior industry work in the determination of mechanical properties was concerned with materials testing at low strain rate and moderate temperatures. Properties so obtained were found to be typical elastic mechanical properties without reference to strength variation. Such material properties were considered inaccurate and incomplete for design and specification tests of this program. Existing American Society of Testing Materials (ASTM) and Federal Standard Methods of Testing procedures, if followed, would have provided much of this needed data (see * data below). Existing test data reports were found to provide inadequate or none of the following required test data:

1. *Complete identification of material tested
2. *Conditioning procedures used
3. *Atmospheric conditions in test room
4. *Number of specimens tested (5 minimum)
5. *Speed of testing
6. *Stress value at yield or break, average value and standard deviation.
7. *Modulus of elasticity, average value and standard deviation
8. True ultimate tensile stress at break, average value and standard deviation
9. Secant modulus, average value and standard deviation
10. True ultimate strain value to break point, average value and standard deviation.

By use of this reported test data the designer can reconstruct the complete stress-strain history (elastic and plastic properties) of the test material, and can calculate a design allowable or minimum anticipated value by statistical methods where required for a specific processed material.

Tables 2 and 3 show the typical, single value, physical and mechanical properties as published on specific materials of interest for this program. Stress-strain data curves are not included, as published data were either not available, inadequate, or incomplete.

TABLE 2. TYPICAL PROPERTIES OF TRANSPARENT HIGH TEMPERATURE STRUCTURAL MATERIALS

PHYSICAL OR MECHANICAL PROPERTY	STANDARD TEST METHOD USED	SYMBOL AND/OR UNITS	BASIC MATERIAL DESCRIPTION/MATERIAL PROPERTIES SOURCE MIL-HDBK-17A, PART II AND NOTED						
			POLYCARBONATE MIL-P-83310	AS-CAST ACRYLIC MIL-P-5425	AS-CAST ACRYLIC MIL-P-8184	STRETCH ACRYLIC MIL-P-25690	SODA LIME GLASS MIL-G-25667	SODA LIME GLASS MODIFIED MIL-G-25667	CHEM STR GLASS MIL-G-25667-V
Tensile Strength	FTMS 406-1011 ASTM:D-638	PSI x 10^3	9.8-10.5 at 0.2 IN./MIN	10.0 at 0.2 IN./IN./MIN	10.5-11.0 at 0.2 IN./MIN	11.5-11.9 at 0.2 IN./MIN			
Compressive Strength	FTMS 406-1021 ASTM:D-695	PSI x 10^3	12.6	18.0	19.0	17.0			
Tensile Modulus	FTMS 406-1011 ASTM:D747	E PSI x 10^5	3.0-3.6	4.5-4.6	4.5	4.5-4.9			
Compressive Modulus	FTMS 406-1021 ASTM:D695	G PSI x 10^5		4.5	4.5	5.0			
Coefficient of Thermal Expansion	FTMS 406-2031 ASTM:D696	IN./IN./°F x 10^{-5}	3.47	4.1	4.1		0.46 WADC-T12-53-99	0.46 WADC-T12-53-99	0.49 SIERRACIN
Coefficient of Thermal Conductivity	ASTM:C177	BTU-IN./HR/FT^2/°F	1.5 SIERRACIN	1.3 SWEDLOW	1.2-1.55	1.15	6.5	6.5	7.1 SIERRACIN
Specific Heat	ASTM:C351-54	CPI/BTU/LB/°F	0.28	0.35	0.35	0.35	0.19	0.19	0.20
Density	ASTM:C177	LB/IN.^{3}	0.043	0.043	0.043	0.043	0.091	0.091	0.091
Bearing Strength	LP406b-1051	PSI x 10^3	7.0 E/D = 1.5			15.2			
Poisson's Ratio	–	–	0.36 AFFDL-TR-25-2	0.35	0.35	0.35	0.22	0.22	0.22
Shear Modulus of Elasticity	ASTM:D732	G/PSI	130° AFFDL-TR-25-2						
Abraded Modulus of Rupture		/PSI					21,990	21,990	40,430

NOTES: 1.) Tests conducted at standard room temperatures.
2.) Crosshead speed noted (if available).
3.) See standard test method for definition of symbols.

TABLE 3. TYPICAL PROPERTIES OF TRANSPARENT HIGH TEMPERATURE INTERLAYER MATERIALS

PHYSICAL OR MECHANICAL PROPERTY	TEST METHOD USED	SYMBOL AND/OR UNITS	BASIC MATERIAL SUPPLIER AND MATERIAL PROPERTIES SOURCE						
			SIERRACIN			SWEDLOW, INC.	GOODYEAR AEROSPACE CORP.		PPG INDUSTRIES
			S-100 (CIP) SILICONE	S-120 URETHANE	S-130 COPOLYMER	SS5272Y (CIP) SILICONE	F-4X-28 (CIP) SILICONE	F5X-3A URETHANE	PPG 112 URETHANE
Tensile Strength	ASTM:D-412	PSI	460	2700	3200 - 3400	830 - 950		6000	6700 at 20 IN./MIN
Shear Strength	ASTM:D732 *FED MMA-132	PSI	230	1100	-	190	300	3200	3800 AFFDL-TR-74-75
Tensile Modulus of Elasticity	ASTM:D747	E PSI	-	-	-	-	-	-	1000
Coefficient of Thermal Expansion	ASTM:D696	IN./IN./°F	15×10^{-5}	11×10^{-5}	9.9×10^{-5}	21.2×10^{-5}	20×10^{-5}	-	-
Coefficient of Thermal Conductivity	ASTM:C177	BTU-IN./HR/FT^2/°F	1.147	-	1.30	0.76	1.28	-	2.00
Specific Heat	ASTM:C351-54	CPI/BTU/LB/°F	0.36	-	0.00	0.35	0.37		0.44 at 117°C
Density	ASTM:C177	LB/IN.^{3}	0.037	0.037	0.038	0.037	0.04	0.04	0.04
Poisson's Ratio	-	-	0.33	-	0.42	-	-	-	0.43 AFFDL-TR-75-2
Shear Modulus	ASTM:D732	G/PSI	65	-	-	-	-	180	400* AFFDL-TR-75-2

NOTES: 1.) Tests conducted at standard room temperatures unless otherwise noted.
2.) Crosshead speed noted (if available).

Most tensile stress-strain curves were found to show only the portion of the stress-strain relation through yield stress, and/or did not take into account the reduced area of the test section in the plastic portion of the curve, giving an erroneous value for rupture stress and rupture strain.

MATERIALS RESEARCH

Plycarbonate Plastic Material

The 1/4- and 1/2-inch thick "Tuffak" polycarbonate sheets manufactured by Rohm & Haas Co., were furnished to DAC to be evaluated and compared with SL3000 polycarbonate manufactured by General Electric Co. The basic polycarbonate resin used in extruding these polycarbonate sheets was manufactured by Mobay Chemical Co. These polycarbonate sheets have a UV absorber added to give it superior outdoor weathering characteristics. Rohm & Haas used Mobay's low molecular weight resin, designated as M-40, to achieve better optical properties, specifically light transmission and low haze content. High haze content is usually contributed to small amounts of contaminants and trace reaction chemicals.

"Merlon" is the trade name for Mobay's polycarbonate resin. This thermoplastic resin is a linear aromatic polyester of carbonic acid. Its structure is:

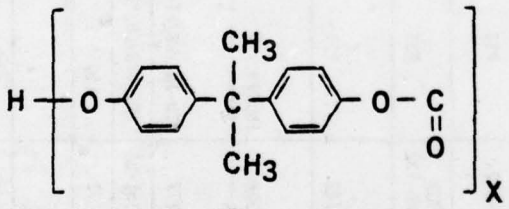

X may represent 100 to 800 units or more

The molecular wieght of a single unit is 254. Polymers may have a molecular weight of 25,000 to more than 200,000. In commercial practice, however, the molecular weight range is 25,000 to 70,000.

Basically, there is no significant difference between G.E. "Lexan" and Mobay's "Merlon" polycarbonate resin. The only difference in the chemical process used to manufacture this linear aromatic polyester of carbonic acid is the trace reaction chemical impurities and contaminations. Either of these constituents can influence physical, chemical, or optical properties of polycarbonate resin. Inorganic as well as organic contaminants can seriously reduce the physical or mechanical properties of the resin. This condition can be improved or further degraded by improper extrusion of the polycarbonate sheet.

Viscosity index and compression moldings are used by Rohm & Haas as a Quality Control Inspection for Mobay's incoming polycarbonate resin. The viscosity index is used to check overall molding and extruding properties. The compression molding is chiefly used to evaluate the haze and light transmission properties of the resin and to quantitatively determine the amount of contamination in the resin.

The extreme high and low molecular weight are generally not used to produce quality polycarbonate sheet for aircraft glazing. The lower and light molecular fractions are generally used for adjusting injection molding properties and characteristics, such as flow, viscosity, melt index, and other chemical properties. Intrinsic viscosity is used by industry as an analytical quality control tool for determining the molecular weight spectrum of organic polymers. Molecular weight plotted against intrinsic viscosity can be readily established (reference 3). Mechanical properties can be correlated to specific molecular weights or ranges (reference 4). The molecular weights range and/or intrinsic viscosity limits can be easily established for controlling material physical properties. G.E. representatives stated that mechanical property variance from batch-to-batch of resin should be small due to the viscosity control of SL3000 sheet material.

SECTION III
MATHEMATICAL ANALYSIS

The basic effort of this report was to establish design allowables for laminated transparency plastic materials. These design allowables of specific plastic structural ply and interlayer materials were to be developed on a basis similar to the requirements of MIL-HDBK-5B. To meet the requirements for the statistical minimum (design allowable) stress-strain curves, points from developed test stress-strain curves were statistically analyzed for normal (Gaussian) distribution and points on the design curve calculated by methods outlined in MIL-HDBK-5B. These procedures allowed the development of design allowable stress-strain curves by taking into account the sample size, and the desired confidence level. After generating the design curve, specific design allowables were determined for use in the Ramberg-Osgood curve formula (Reference 5), which provided for the complete design stress-strain curve input into a computer program for bird strike analysis.

Design mechanical properties allowables presented in this report are based on small samples and a limited number of heat lots of a material. These heat lots are based on specific proprietary manufacturing methods and interlayer formulations which may change. Therefore, the definition of the statistical propulation must be sufficiently restrictive to ensure that the design allowables are realistic and useful. This is accomplished by establishing the range of products for which the given mechanical property allowable can be characterized by a single statistical population. The statistical population of a processed material can be compared with the published design allowable of the test material by application of appropriate statistical tests of significance. In this section, two tests (the F and t tests) are described for use in determining whether a sample belongs to the same population as the published design allowable of the test material.

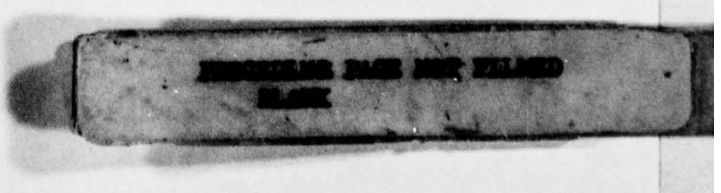

STATISTICAL AND MATHEMATICAL SOLUTION FOR DEFINING DESIGN ALLOWABLES

The steps taken in the development of mechanical property design allowables is presented in diagram form in Figure 1. The following paragraphs in this section define these steps in detail.

Definitions

The following definitions define the terms used in this section and following sections of this report.

1. Load Rate (crosshead rate) - The change in load carried by the specimen per unit time in units of inches per minute or inches per second.

2. Strain Rate - The rate of loading the test specimen per inch of gage length, in units of inches per inch per minute or inches per inch per second.

3. Gage Length (l_o) - The original length of that portion of the specimen over which strain or change in length is determined.

4. Yield Strength - The stress at which deformations cease to be elastic and become permanent, due to the onset of plastic flow. The maximum load point for polycarbonate.

5. Shear Strain (radians) - Shear strain is defined by the equation

$$V = \tan^{-1} \frac{h}{t}$$

where h is the amount of shear deformation of an interlayer
t is the interlayer thickness
V is the shear strain.

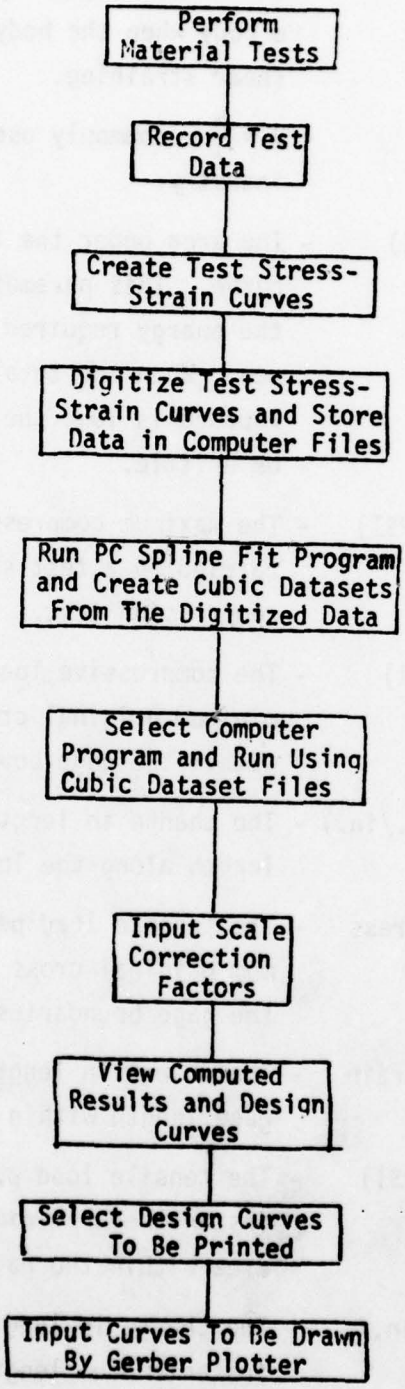

Figure 1. Block Diagram - Design Curve Development.

		Shear strain is the angular change between two originally orthogonal lines in a body when the body is subjected to shear straining.
6.	Shear Strain (in./in.)	- $V = \frac{h}{t}$ commonly used by the transparency industry.
7.	Relative Toughness (PSI)	- The area under the tensile stress-strain curve. This parameter is a measure of the energy required to break the specimen. When the total work to affect rupture is low, the material is said to be brittle.
8.	Compressive Strength (PSI)	- The maximum compressive stress (nominal) carried by a test specimen during a compression test.
9.	Compressive Stress (PSI)	- The compressive load per unit area of minimum original cross section area within the gage boundaries.
10.	Compressive Strain (in./in.)	- The change in length per unit of original length along the longitudinal axis.
11.	Engineering Tensile Stress (PSI)	- The tensile load per unit area of minimum original cross section area within the gage boundaries.
12.	Engineering Tensile Strain (in./in.)	- The change in length per unit of original gage length within the gage boundaries.
13.	True Tensile Stress (PSI)	- The tensile load per unit of the instantaneous minimum cross section area within the gage boundaries.
14.	True Tensile Strain (in./in.)	- The change in length per unit of instantaneous length within the gage boundaries.

15. Significance Level - Risk of concluding that two samples were drawn from different populations when, in fact, they were drawn from the same population. A significance level of $\alpha = 0.05$ is employed throughout these Guidelines.*

16. Confidence Interval Estimate- Range of values, computed from the sample, that is expected to include the population variance or mean.

17. Degrees of Freedom - Number of independent comparisons afforded by a sample.

18. Design Allowable - The calculated minimum mechanical property for a specific heat lot or several heat lots of material. The statistical confidence associated with these design allowables is 95 percent.*

19. Heat - All material of the same composition or product type. (A heat may be divided into several lots by subsequent processing.)

20. Lot - All material from a heat or the same product type having the same subsequent processing (thermal and mechanical).

True Tensile Stress-Strain Curve Development

The engineering stress-strain curve does not give a true indication of the deformation characteristics of a material because it is based entirely on the original dimensions of the specimen. These dimensions change continuously during the test. This dimensional change is quite noticeable when the specimen undergoes appreciable change in cross-sectional

*This is appropriate, since a confidence level $1 - \alpha = 0.95$ is used in establishing A, B and C values.

area. This commonly occurs in the highly elongated regions of plastic materials. Thus, measures of stress and strain which are based on the instantaneous dimensions are needed. Since dimensional changes are small in elastic deformation, it is not necessary to make this distinction in this region. The derivation of true stress and true strain and its application to material properties follows.

Test curve data are received as a plot of load (pounds) versus strain (inches). Test specimen measurement data furnished with each curve includes gage length (ℓ_g), initial cross sectional area (A_o), cross sectional area measured after rupture (A_p), and elongation of specimen to rupture (ℓ_r). The tensile load-strain curve is converted to a tensile stress-strain curve by establishing stress (σ) and strain (ε) scales, plotting the rupture point, and drawing a line tangent to the elastic portion of the curve to the rupture point as illustrated in Figure 2. The vertical stress scale is established by dividing the load increment (ΔP) by A_o. The horizontal strain scale is established by dividing strain ($\Delta\ell$) by ℓ_g. The tensile curve rupture point true stress ($\bar{\sigma}_r$) and true strain ($\bar{\varepsilon}_r$) coordinates were determined as follows:

$$\sigma = \frac{P}{A_o}$$

where P is the tensile load on the test specimen, and A_o is the initial cross sectional area of the test specimen.

The true stress, by definition, is

$$\sigma = \frac{P}{A} \qquad (2)$$

where A is the instantaneous sectional area of the test specimen under the load P. A is approximately equal to A_p when the plastic strains are

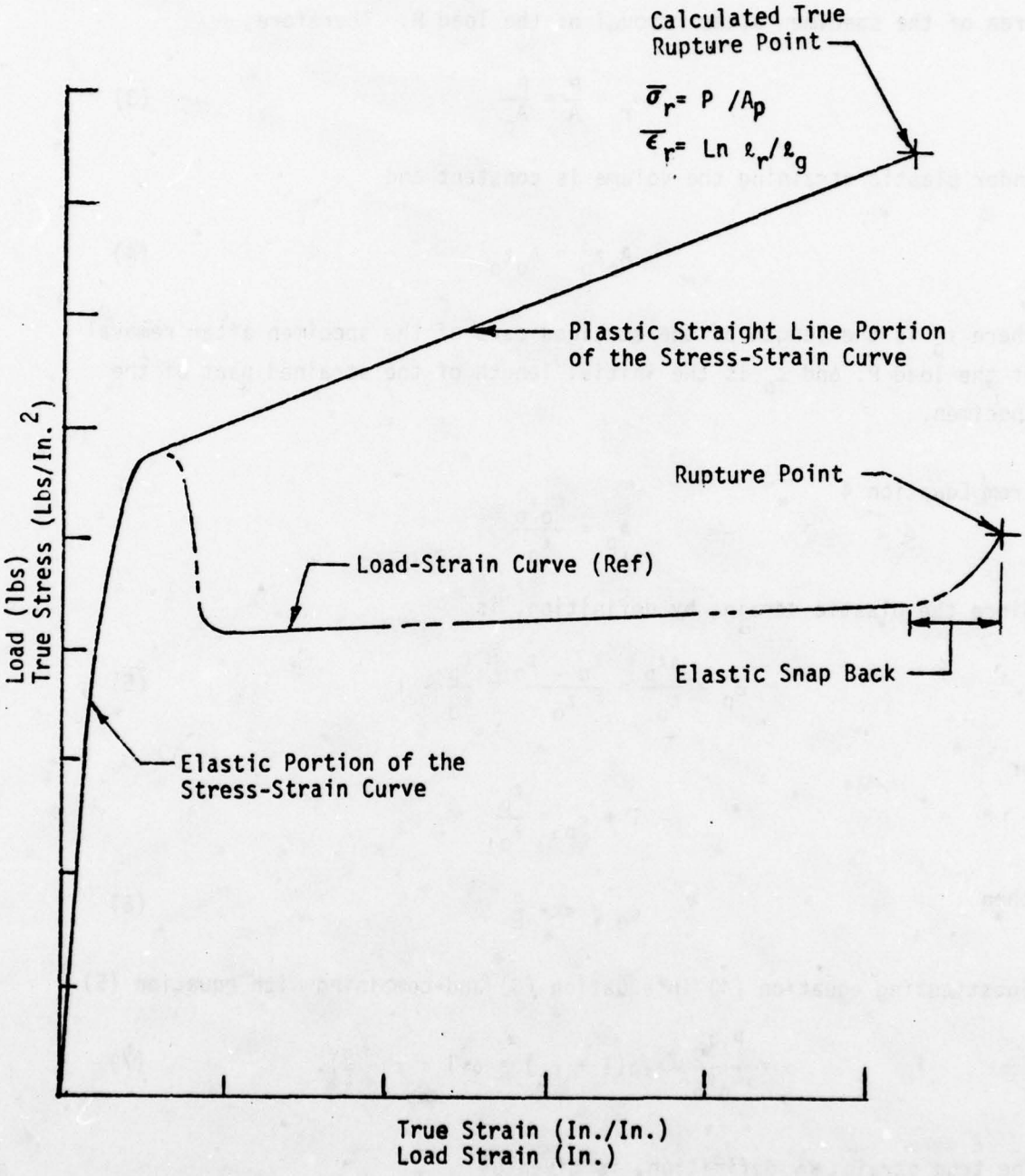

Figure 2. True Tensile Stress-Strain Curve Development

large compared with the elastic strains. A_p is the minimum cross sectional area of the specimen after removal of the load P. Therefore,

$$\sigma_r = \frac{P}{A} = \frac{P}{A_p} \tag{3}$$

under plastic straining the volume is constant and

$$A_p \ell_p = A_o \ell_o \tag{4}$$

where ℓ_p is the length of the strained part of the specimen after removal of the load P, and ℓ_o is the initial length of the strained part of the specimen.

From Equation 4

$$A_p = \frac{A_o \ell_o}{\ell_p} .$$

Since the plastic strain, by definition, is

$$\varepsilon_p = \frac{\Delta \ell_p}{\ell_o} = \frac{\ell_p - \ell_o}{\ell_o} = \frac{\ell_p}{\ell_o} - 1 \tag{5}$$

or

$$1 + \varepsilon_p = \frac{\ell_p}{\ell_o}$$

then

$$\varepsilon_p = \varepsilon - \frac{\sigma}{E} \tag{6}$$

Substituting equation (4) in equation (3) and combining with equation (5)

$$\sigma = \frac{P \ell_p}{A_o \ell_o} = \sigma(1 + \varepsilon_p) = \sigma(1 + \varepsilon - \frac{\sigma}{E}). \tag{7}$$

The true strain, by definition, is given by

$$\varepsilon = \int_{\ell_o}^{\ell_p} d\varepsilon_T = \int_{\ell_o}^{\ell_p} \frac{d\ell}{\ell} = \text{Ln} \frac{\ell_p}{\ell_o} \tag{3}$$

thus considering equation (4)

$$\varepsilon = \text{Ln} \frac{A_o}{A_p} .$$

The plastic range of the true stress-strain curve was drawn as a straight line because means were not available to accurately determine test specimen cross sectional area reduction versus load during plastic elongation. The straight line assumption for the plastic portion of the curve is considered conservative as the final area, A_p, was calculated after the observed elastic snap-back. An approximation of the cross sectional area increase based on the observed gap after snap-back gave a ten percent higher value for stress at ruptures.

Design Allowable Stress- Strain Curve Development

To meet the requirement for design allowable stress-strain curves, the developed stress-strain curves for a series of repeated tests were statistically analyzed using methods outlined below for normal (or gaussian) distribution. The statistical methods used in MIL-HDBK-5B are normally used in determining specific design strength values such as tensile ultimate strength, tensile yield strengths, compressive yield strength, etc. In a similar manner these methods were adapted to determine specific stress or strain values on the design allowable curve for a number (n) of stress or strain values (X_i) on the tensile stress-strain curve as illustrated in Figure 3, and compression, shear stress-strain curve as illustrated in Figure 4.

From the analysis of the sample size (N), the mean stress ($\overline{X}$),

$$\overline{X} = \Sigma X_i / N , \qquad (9)$$

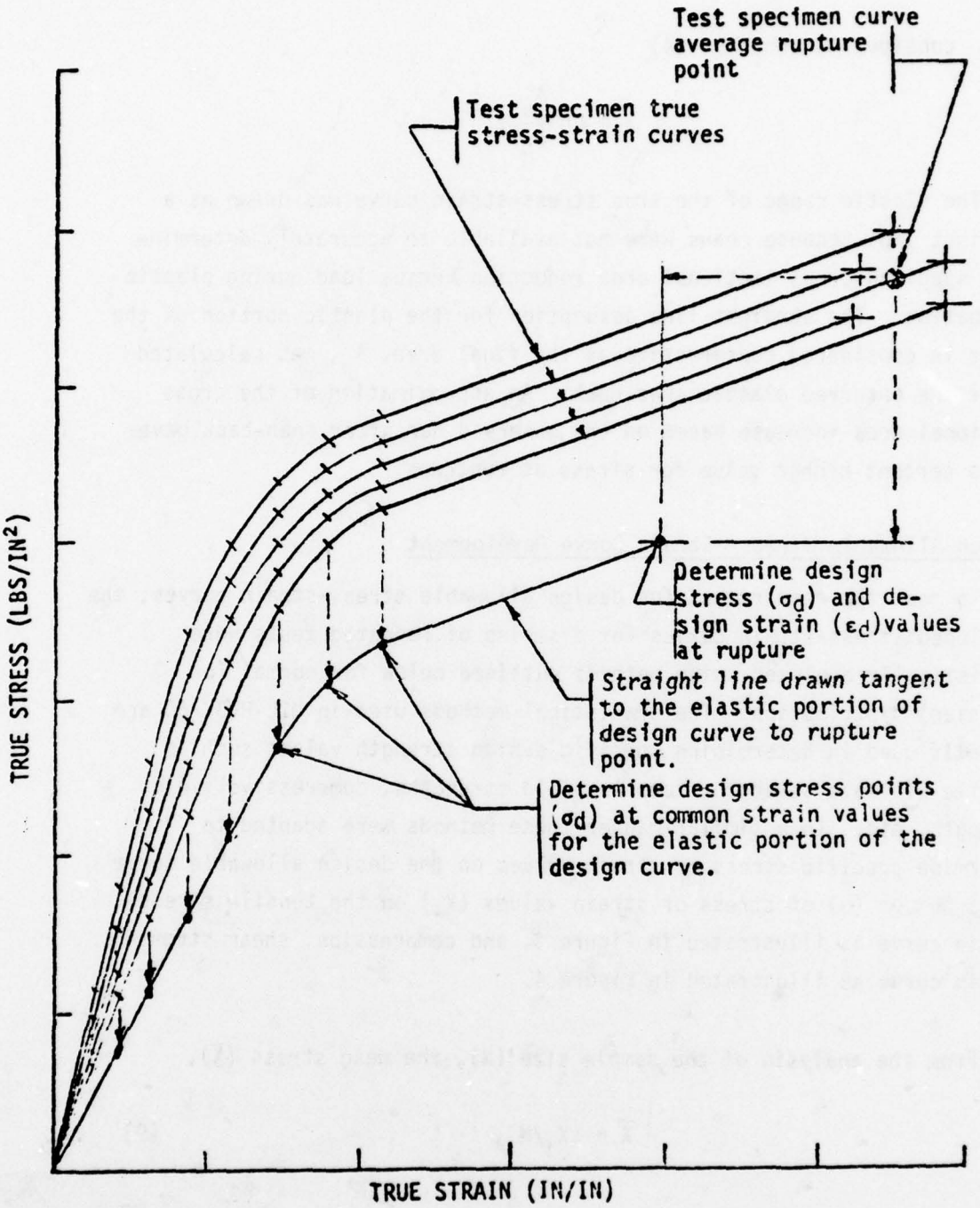

Figure 3. Design Tensile Stress-Strain Curve Development

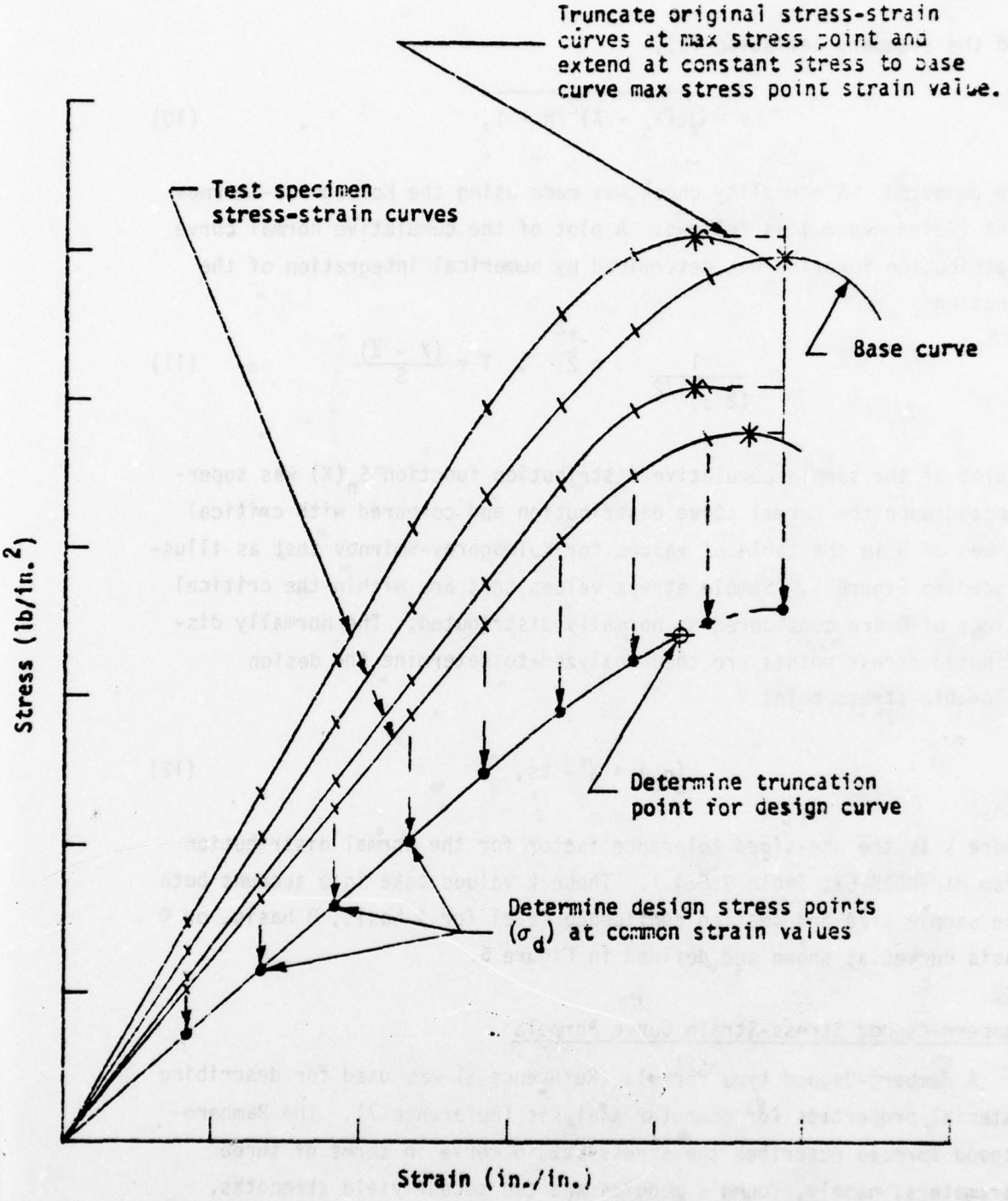

Figure 4. Design Shear and Compression Stress-Strain Curve Development.

and the standard deviation (s),

$$s = \sqrt{\Sigma(X_i - X)^2/N - 1}, \tag{10}$$

are computed. A normality check was made using the Kolmogorov-Smirnov test (Reference 6) as follows: A plot of the cumulative normal curve distribution function was determined by numerical integration of the function

$$\frac{1}{(2\pi)^{1/2}} \cdot e^{\frac{-T^2}{2}} \quad ; \quad T = \frac{(X - \bar{X})}{S} \tag{11}$$

A plot of the sample cumulative distribution function $S_n(X)$ was superimposed upon the normal curve distribution and compared with critical values of D in the table of values for Kolmogorov-Smirnov test as illustrated in Figure 5. Sample stress values that are within the critical values of D are considered as normally distributed. The normally distributed stress points are then analyzed to determine the design allowable stress point

$$(\sigma_d) = \bar{X} - ks, \tag{12}$$

where k is the one-sided tolerance factor for the normal distribution from MIL-HDBK-5B, Table 9.6.4.1. These k values take into account both the sample size and desired confidence level for A basis, B basis, or C basis curves as shown and defined in Figure 6.

Ramberg-Osgood Stress-Strain Curve Formula

A Ramberg-Osgood type formula (Reference 5) was used for describing material properties for computer analysis (Reference 7). The Ramberg-Osgood formula describes the stress-strain curve in terms of three parameters; namely, Young's modulus and two secant yield strengths.

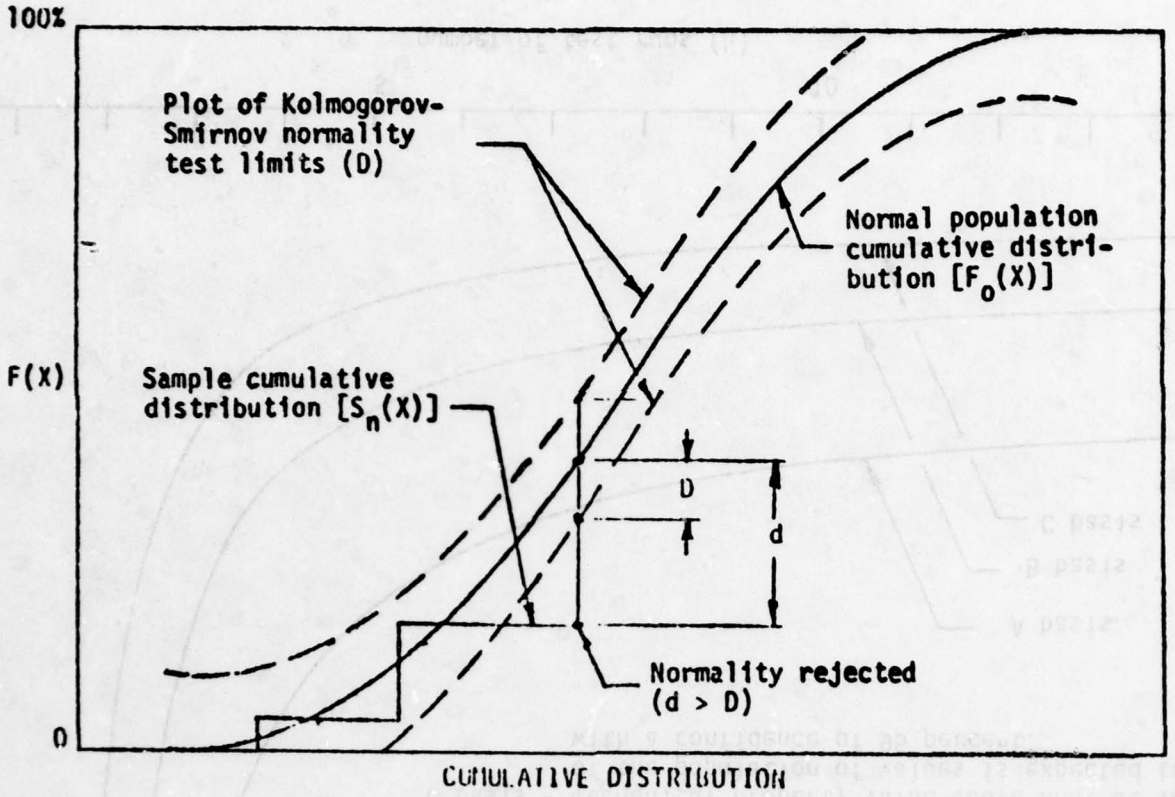

Figure 5. Graphical Presentation of Normality Check.

A basis - mechanical property value above which at least 99 percent of the population of values is expected to fall, with a confidence of 95 percent.

B basis - mechanical property value above which at least 90 percent of the population of values is expected to fall, with a confidence of 95 percent.

C basis - mechanical property value above what at least 75% of the population of values is expected to fall, with a confidence of 95 percent.

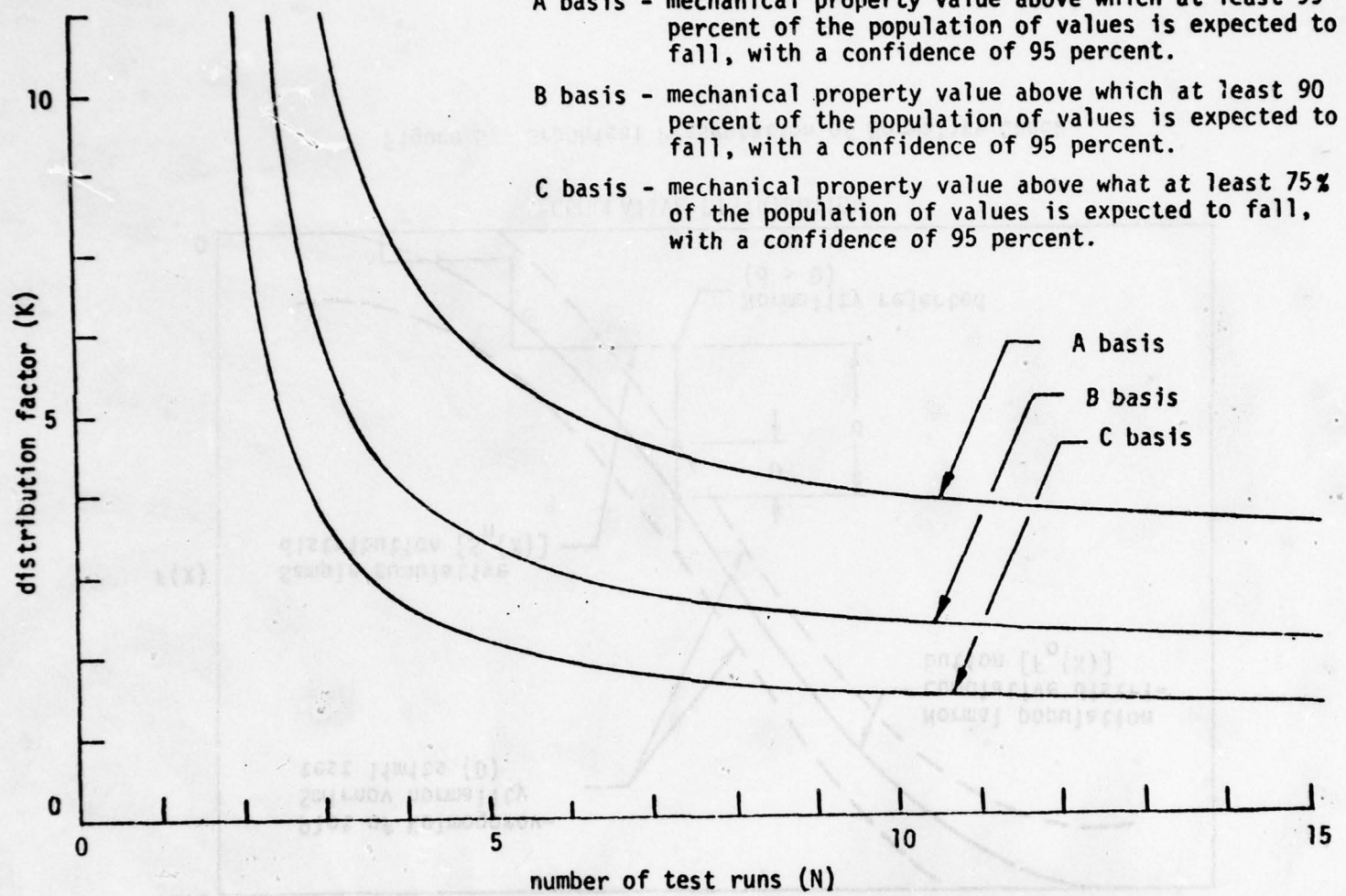

Figure 6. Normal Population Distribution Factor K vs N.

Dimensionless charts are derived from this formula for determining the stress-strain curve for which these three parameters are known. The Ramberg-Osgood formula

$$\frac{\varepsilon}{\varepsilon_o} = \frac{\sigma}{\sigma_o} + K' \left(\frac{\sigma}{\sigma_o}\right)^n$$

describes the dimensionless diagram as shown in Figure 7 where k' and n are material properties. The secant modulus (E_o) that best describes the design curve for polycarbonate was found to be the tangent of the stress-strain point at the intersection of the elastic and plastic portions of the stress-strain curve which is reported for each design curve. The term K' is determined from the ratio

$$K' = \frac{1}{R} - 1; \; R = \frac{E_o}{E}$$

The n term is determined by solving the Ramberg-Osgood formula, knowing K' and the quantities ε_o, σ_o, ε_r, σ_r, as shown from the design stress-strain curve in Figure 7.

Material Properties Computer Program Development

The design allowable stress-strain curves were constructed by computer programs developed specifically for this project in conjunction with existing Douglas programs. The steps taken in the computer programs are diagramed in Figure 8, and defined in the following paragraphs.

The true tensile stress-strain test curves were converted to a format that was usable in a computer program. The method selected uses parametric cubic (PC) geometry, which is a mathematical technique for describing bounded 3-dimensional curves and surfaces in a form that satisfies the need for speed, accuracy, and manipulative flexibility. This particular case was limited to 2-dimensional curves (Reference 8). Proprietary Douglas subroutines were used to accomplish these parametric cubic operations.

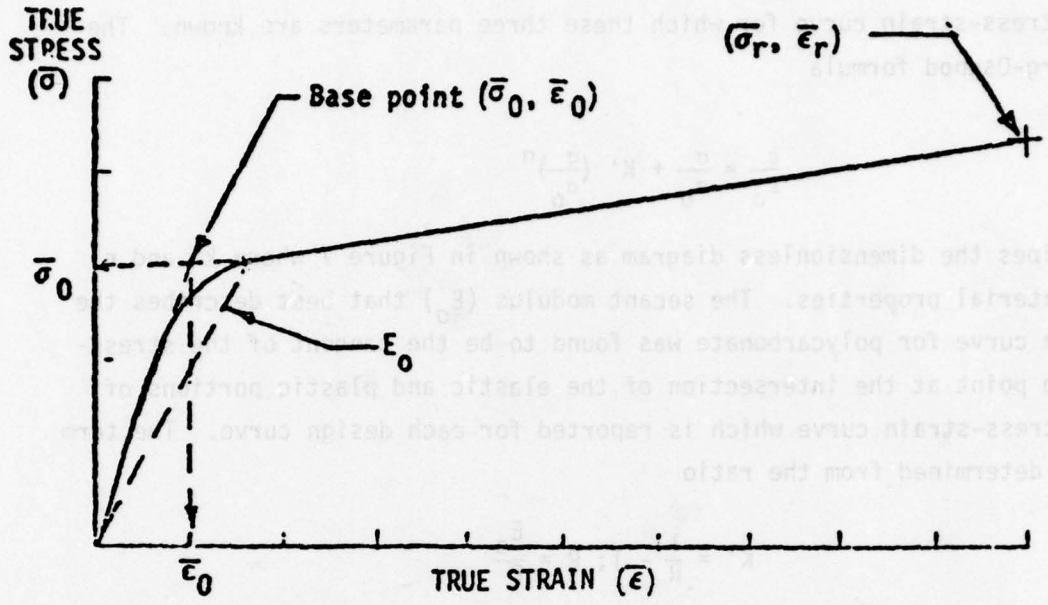

DESIGN STRESS-STRAIN CURVE

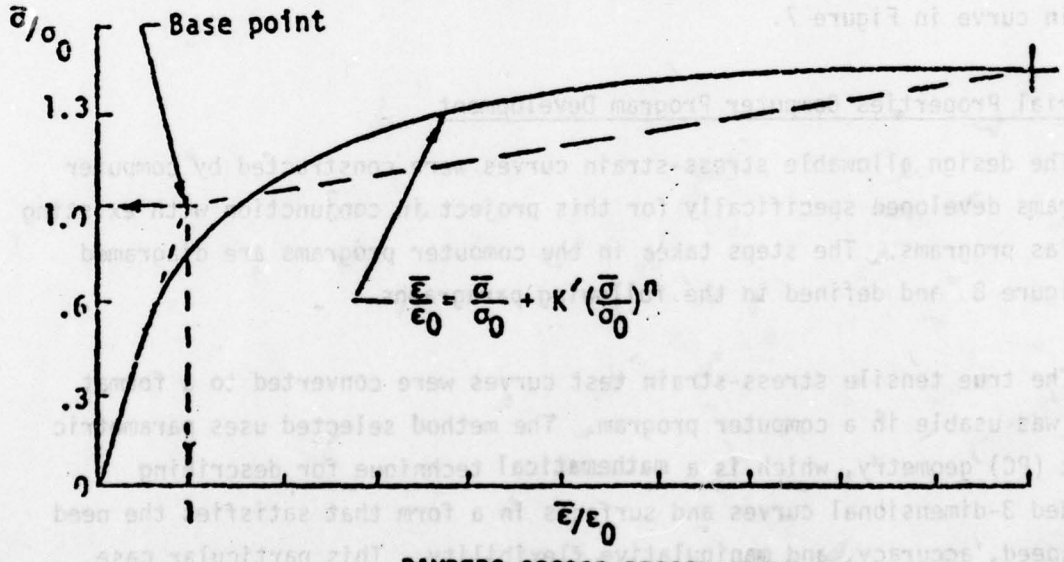

RAMBERG-OSGOOD DESIGN CURVE

Figure 7. Ramberg-Osgood Curve Development.

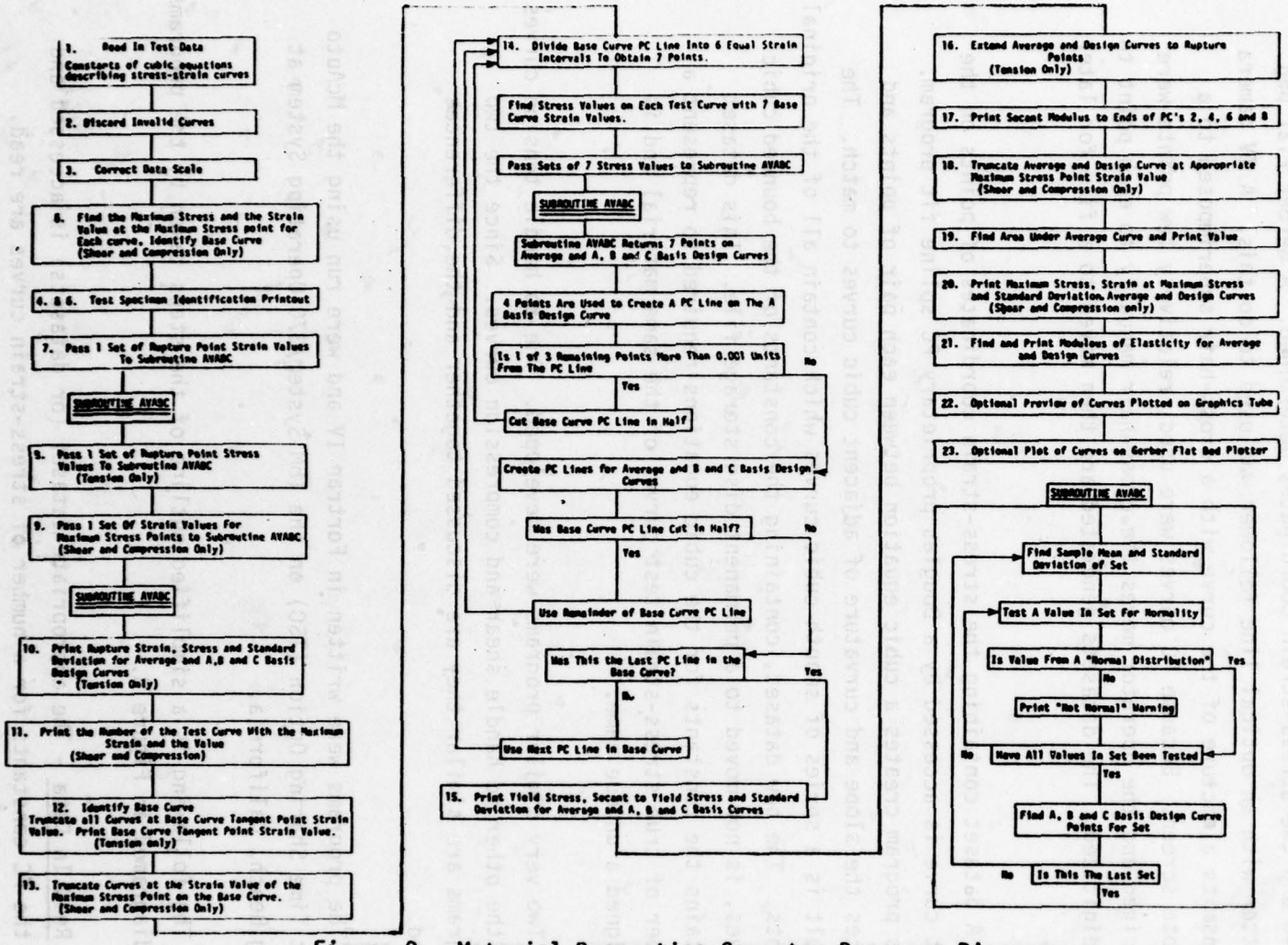

Figure 8. Material Properties Computer Programs Diagram.

THIS PAGE IS BEST QUALITY PRACTICABLE
FROM COPY FURNISHED TO DDC

The true stress-strain test curves must first be "digitized", that is, a sufficient number of points to ensure accuracy must be selected on each curve and the stress-strain coordinates determined. A Gerber Flat Bed Plotter with an optical line follower was used to do this. A TV camera transmits a picture of the curve with a cross-hair superimposed to a remote screen. Because PC curves were used, relatively few points were required and the operator moves the cross-hair manually to each point to be digitized. The datasets generated are then moved to a file for later use.

A dataset containing the stress-strain coordinates of points on the test curve is accessed by a Douglas proprietary PC spline fit program. This program creates a cubic equation between each pair of points and forces the slope and curvature of adjacent cubic curves to match. The result is a series of smooth cubic curves which contain all of the original points. The new dataset, containing the constants of the bounded cubic curves, is now moved to a permanent disc storage file. This dataset contains the constants for the cubic equations required to represent a number of true stress-strain test curves of the same material and is assigned a unique name.

Two very similar programs were developed. One to handle tension curves and the other to handle shear and compression curves. Since the two programs are similar they are discussed together and the differences noted.

The programs were written in Fortran IV and were run using the McAuto West Time Sharing Option (TSO) on the IBM System/370 Operating System at Long Beach, California.

The following is a simplified outline of the steps taken by the programs, as diagramed in Figure 8.

1. Read In Data - The appropriate dataset (or datasets) is accessed and the PC constants for a number of stress-strain curves are read.

2. Discard Curves - At this point it is possible to discard one or more of the stress-strain curves. This would be done if for some reason, it was determined that a particular curve did not belong in this family of curves. A mechanical flaw in a test specimen would be a typical cause for discarding a curve.

3. Correct Data Scale - The stress and strain scales of the digitized curves are sometimes factored to facilitate the PC spline fit. If this was done, corrective scale factors would be entered at this point.

4. Test Specimen Printout (Tension Only) - The identification of each stress-strain curve and the end point (rupture point) stress and strain values are printed.

5. Find Maximum Stress and Strain at Maximum Stress for Each Test Curve - (Shear and Compression Only) - Find the maximum stress point on each PC (parametric cubic curve) in a test curve. Select the maximum stress point from this group of points and find the strain value at that point. Repeat this step for each test curve. The test curve with the maximum stress point will be the base curve for other calculations.

6. Test Specimen Printout (Shear and Compression Only) - The identification of each stress-strain curve, the maximum stress value and the strain value at the maximum stress point are printed.

7. Find the Strain Values and the Standard Deviation for the Average Curve and the A Basis, B Basis, and C Basis Design Curve Rupture Points. (Tension Only) - Pass the rupture point (end point) strain values for each test curve to subroutine AVABC (call AVABC).

Subroutine AVABC:

A. Find the sample mean (average value) and standard deviation of a set of values per MIL-HDBK-5B, Section 9.2.2.3.

B. Test each value for normality using "The Kolmogorov-Smirnov Test for Normality with Mean and Variance Unknown". (Reference 6). This is accomplished by first calculating the difference between the sample cumulative distribution function and the cumulative normal distribution function. This difference is compared with a critical value taken from a table of critical values for sample sizes up to 40 and has a level of significance of 0.05 (confidence level of 95 percent) (Reference 6). The point is from a normal distribution if the difference is less than or equal to the critical value. If the difference is greater than the critical value a "not normal" warning printout is made. The strain and stress values of the point, the critical value, and the calculated difference are printed. The program continues regardless of normality.

C. Find the A basis, B basis, and C basis design curve points for the set of values by multiplying the sample standard deviation by a one-sided tolerance factor and subtracting from the sample mean as indicated in MIL-HDBK-5B, Section 9.2.7.2. The one-sided tolerance limit factor corresponds to a proportion at least 0.99 of a normal distribution and a confidence coefficient of 0.95 for an A basis curve point. (0.90 for B basis curve and 0.75 for a C basis curve with a confidence coefficient of 0.95). These factors were taken from MIL-HDBK-5B, Table 9.6.4.1, Section 9.6.4.

D. Return to main program at point of call to subroutine AVABC.

8. Find the Stress Values and the Standard Deviation for the Average Curve and the A Basis, B Basis, and C Basis Design Curve Rupture Points (Tension Only) - Pass the rupture point (end point) stress values for each test curve to subroutine AVABC (call AVABC). See Subroutine AVABC in Step 7.

9. Find the Strain Values and the Standard Deviation for the Average Curve and the A Basis, B Basis, and C Basis Design Curve Maximum Stress Points (Shear and Compression Only) - Pass the maximum stress point strain values for each test curve to subroutine AVABC (call AVABC). See Subroutine AVABC in Step 7.

10. Rupture Printout (Tension Only) - Rupture strain and stress and standard deviation values are printed for the average curve and the A basis, B basis, and C basis design curves.

11. Maximum Strain on the Test Curves (Shear and Compression only) - The number of the test curve with the maximum strain and the maximum strain value are printed out.

12. Truncate Test Curves (Tension Only) - Each test curve has a straight line, tangent to the test curve, to the rupture point. The test curve that has the tangent point with the maximum strain is identified as the base curve. All of the test curves are then truncated at the strain value of the tangent point on the base curve or extended at the slope of the tangent line to the strain value at the base curve tangent point. The number of the base curve and strain value at which the test curves are truncated are printed.

13. Truncate Test Curves (Shear and Compression Only) - If the strain value at the maximum stress point on a test curve is less than the strain value at the maximum stress point on the base curve, the test curve is truncated at the maximum stress

point and then extended at a constant stress value to the strain value of the base curve maximum stress point. If the strain value of the test curve maximum stress point is equal to the strain value of the base curve maximum stress point, the test curve is truncated at the strain value of the base curve maximum stress point.

14. Calculate Stress and Strain Values for Points on the Average Curve and A Basis, B Basis, and C Basis Design Curves - The number of PC (parametric cubic) lines in the average and design curves will be equal to or greater than the number of PC lines in the truncated base test curve. The following procedure is executed for each PC line in the base curve:

    A. Divide the base curve PC line into equal strain intervals to obtain seven strain values including the beginning and end points.

    B. Find the stress values at the points on each test curve with seven strain values from the base curve.

    C. Pass the sets of seven stress values for each test curve to subroutine AVABC. (call AVABC). See subroutine AVABC in Step 7.

    D. Subroutine AVABC will return seven stress and strain values for points on the average and A basis, B basis, and C basis design curves. Four of these points on the A basis curve (points one, three, five and seven) are used to calculate the coefficients of a PC line which will pass through the points exactly. The remaining three points (points two, four, and five) are checked to see if they are within 0.001 units of the PC line. If one of the points is more than 0.001 unit from the A basis curve PC line, the base test curve PC line is cut in half and Steps A, B, and C are repeated for the first half.

E. Calculate the coefficients for PC lines for the average and B basis and C basis design curves over the same strain interval as the A basis curve.

F. If the base test curve PC line was cut in half, repeat Steps A, B, C, D, and E for the remaining half.

15. Yield Stress, Secant Value and Standard Deviation Printout (Tension Only) - The yield stress is assumed to be at the strain value used to truncate the test curves in Step 12. The yield stress is divided by the strain at that point to give the secant value. Yield stress, secant to yield stress and standard deviation values are printed for the average and the A basis, B basis, and C basis design curves.

16. Extend the Average and Design Curves to the Rupture Points (Tension Only) - The average curve and the A basis, B basis, and C basis design curves from Step 14 are cut off at the strain value of the base test curve tangent point. The coefficients of the PC lines which will join the curves with their respective rupture points are now calculated. The rupture points were calculated in Steps 7 and 8. The average and design curves are now complete.

17. Secant Modulus of Elasticity - As an aid in establishing the modulus of elasticity it is assumed that the curve is straight line from the origin to the end point of the second PC. The modulus is obtained by dividing the end point stress by the end point strain. The end point strain (in./in.) and secant modulus ($lb/in.^2$) are printed for tension and compression design curves. The printout for shear design curves is shear strain (Radians) and shear secant modulus ($lb/in.^2$). This is repeated to the end points of the fourth, sixth and eighth PC's.

18. Truncate the Average and Design Curves at the Maximum Stress Point Strain Value (Shear and Compression Only) - The average curve and the A basis, B basis, and C basis design curves from Step 14 are limited by the strain value of the base curve maximum stress point. If this limit strain value is greater than the maximum stress point strain value calculated in Step 9, the curve is truncated at its maximum stress point strain value. The average and design curves are now complete.

19. Area Under the Average Curve is Calculated and Printed (Tension Only) - The area under each PC (parametric cubic line) in the average curve is found by a simple integration of the cubic functions. The sum of these areas is the area under the average curve.

20. Maximum Stress on Design Curves (Shear and Compression Only) The maximum stress, strain value at the maximum stress point and standard deviation are printed for the average curve and the A basis, B basis, and C basis design curves.

21. Modulus of Elasticity - The modulus of elasticity and the standard deviation are calculated at a strain value corresponding to the second digitized point on the base curve and are then printed out for the average curve and the A basis, B basis, and C basis design curves.

22. Preview Plots - The test curves, the average curve, and the A basis, B basis, and C basis design curves can be displayed on a Tektronics 4014 or Computek 400 graphic tube. Whether or not all of the design curves are usable can be determined at this point. The curves can be hard copied on a unit attached to the graphics tube but the resulting copies are not as accurate or as clear as Gerber plots.

23. Gerber Hardcopy - Any or all of the curves that can be previewed can be plotted on the Gerber Flat Bed Plotter. The output is presently on 8-1/2 x 11 herculine but could be changed easily. The program asks for the X scale (strain) and Y scale (stress) factors in units per inch of graph axis. The X axis (5 inches), the Y axis (7 inches), and the numerical values at one-inch intervals on each axis are added to the curve plots automatically.

Statistical Tests of Significance

The statistical population of a processed material can be compared with the given design allowable material by application of appropriate statistical tests of significance. In this section, two tests (the "F" and "t" tests) are described for use in determining whether a sample belongs to the same population as the published design allowable for a test material. The "F" test is used first to determine whether two sample variances differ significantly, after which the "t" test is used to evaluate whether the two sample means differ significantly. The variance(s) is the square of the standard deviation. The tests given are exact when:

1. The observations within each sample are taken randomly from a single population (heat lot).

2. The characteristic measured is normally distributed within the population.

3. Test specimens are the same configuration and thickness.

4. Test conditions are identical for the two compared samples.

The following computation methods and tables have been adopted from Military Handbook-5C, dated 15 September 1976, Section 9.6.2, Table 9.6.4.4 and Table 9.6.4.5.

The "F" Test

The "F" Test is used to determine whether the strength of two products differ with regard to variability.

Consider two products, A and B. These might represent two different processes or formulations. The statistics for the samples drawn from these products are:

	Product A	Product B
Sample Size (n)	n_A	n_B
Sample Standard Deviation (S)	s_A	s_B
Sample Mean ($\overline{X}$)	$\overline{X}_A$	$\overline{X}_B$

F is the ratio of the two sample variances (S^2), thus,

$$F = s_A^2/s_B^2$$

If the true variances of Products A and B are identical at a significance level of $\alpha = 0.05$, F should lie within the interval defined by

$$F_{0.975} \text{ (for } n_A - 1 \text{ and } n_B - 1 \text{ degrees of freedom).}$$

and

$$1/F_{0.975} \text{ (for } n_B - 1 \text{ and } n_A - 1 \text{ degrees of freedom).}^{**}$$

If F does not lie within this interval, it can be concluded that the two products differ with regard to their variability. Values of $F_{0.975}$ are presented in Table 4, Page 46.

**Since a two-sided interval is being defined for the population variance, the fractile of the F distribution corresponding to $1 - \alpha/2$ should be used, i.e., $F_{0.975}$.

Example of Test Computation - The following sample statistics are reported:

	Product A	Product B
Sample Size	20	30
Sample Standard Deviation (PSI)	4.0	5.0
Sample Mean, PSI	100.0	102.0

Perform an F test as follows:

$$F = s_A^2/s_B^2 = 4^2/5^2 = 0.64$$

$df = n_A - 1 = 19$

$= n_B - 1 = 29$

$F_{0.975}(19,29) = 2.23$

$1/F_{0.975}(29,19) = 1/2.40 = 0.42$

} From Table 4

Since 0.64 lies within the interval 0.42 to 2.23 one can conclude that there is no reason to believe that Products A and B differ with regard to their variability.

The "t" Test

The "t" test is used to determine whether two products differ with regard to their average strength. If they do, one may conclude that the two products do not belong to the same population.

In making the "t" test, it is assumed that the variances of the two products are nearly equal, as first determined from the F test. If the "F" test shows that the variances are significantly different, there is no need to conduct the "t" test.

Consider the same products, A and B. The statistics for the samples drawn from these products are:

	Product A	Product B
Sample Size (n)	n_A	n_B
Sample Standard Deviation (S)	s_A	s_B
Sample Mean ($\bar{X}$)	$\bar{X}_A$	$\bar{X}_B$

$D_{\bar{X}}$ is the absolute difference between the two sample means.

$$D_{\bar{X}} = \left| \bar{X}_A - \bar{X}_B \right|$$

If the true means of products A and B are identical, $D_{\bar{X}}$ should not exceed u, which is determined as indicated by the following equation for a significance level of $\alpha = 0.05$.

$$n = t_{0.975} s_p \sqrt{\frac{n_A + n_B}{n_A n_B}}$$

where

$t_{0.975}$ has $n_A + n_B - 2$ degrees of freedom*

and

$$s_p = \sqrt{\frac{(n_A-1)s_A^2 + (n_B-1)s_B^2}{n_A + n_B - 2}}$$

Values of $t_{0.975}$ are found in Table 5.

Example of t Test Computation - The following sample statistics are the same as those in the previous example.

	Product A	Product B
Sample Size	20	30
Sample Standard Deviation psi	4.0	5.0
Sample Mean, psi	100.0	102.0

*Since a two-sided interval is being defined for the population mean, the fractile of the t distribution corresponding to $1 - \alpha/2$ should be used, i.e., $t_{0.975}$.

$$s_p = \sqrt{\frac{(n_A - 1)s_A^2 + (n_B - 1)s_B^2}{n_A + n_B - 2}}$$

$$= \sqrt{\frac{(19)(4)^2 + (29)(5)^2}{48}} = 4.63 \text{ psi}$$

$$\sqrt{\frac{n_A + n_B}{n_A n_B}} = \sqrt{\frac{20 + 30}{(20)(30)}} = 0.2887$$

$$u = t_{0.975} s_p \sqrt{\frac{n_A + n_B}{n_A n_B}}$$

$$= (2.011)(4.63)(0.2887) = 2.7 \text{ psi}$$

$$D_{\bar{X}} = \left| \bar{X}_A - \bar{X}_B \right| = 2.0 \text{ psi}$$

Since $D_{\bar{X}}$ (2.0) is not greater than u (2.7), it may be concluded that there is no reason to believe that Products A and B differ with regard to their average strength.

On the basis of both tests in this example, the conclusion would be that the two products were drawn from the same population, and the given design allowable is valid. If the tests confirm the sample product is not from the same population, the given design allowable is not valid, and should be recomputed for this new material.

TABLE 4. 0.975 FRACTILES OF THE F DISTRIBUTION ASSOCIATED WITH n_1 AND n_2 DEGREES OF FREEDOM $F_{0.975}(n_1, n_2)$

n_1 = degrees of freedom for numerator

n_2 = degrees of freedom for denominator

n_2 \ n_1	1	2	3	4	5	6	7	8	9	10	12	15	20	24	30	40	60	120	∞
1	647.8	799.5	864.2	899.6	921.8	937.1	948.2	956.7	963.3	968.6	976.7	984.9	993.1	997.2	1001	1006	1010	1014	1018
2	38.51	39.00	39.17	39.25	39.30	39.33	39.36	39.37	39.39	39.40	39.41	39.43	39.45	39.46	39.46	39.47	39.48	39.49	39.50
3	17.44	16.04	15.44	15.10	14.88	14.73	14.62	14.54	14.47	14.42	14.34	14.25	14.17	14.12	14.08	14.04	13.99	13.95	13.90
4	12.22	10.65	9.98	9.60	9.36	9.20	9.07	8.98	8.90	8.84	8.75	8.66	8.56	8.51	8.46	8.41	8.36	8.31	8.26
5	10.01	8.43	7.76	7.39	7.15	6.98	6.85	6.76	6.68	6.62	6.52	6.43	6.33	6.28	6.23	6.18	6.12	6.07	6.02
6	8.81	7.26	6.60	6.23	5.99	5.82	5.70	5.60	5.52	5.46	5.37	5.27	5.17	5.12	5.07	5.01	4.96	4.90	4.85
7	8.07	6.54	5.89	5.52	5.29	5.12	4.99	4.90	4.82	4.76	4.67	4.57	4.47	4.42	4.36	4.31	4.25	4.20	4.14
8	7.57	6.06	5.42	5.05	4.82	4.65	4.53	4.43	4.36	4.30	4.20	4.10	4.00	3.95	3.89	3.84	3.78	3.73	3.67
9	7.21	5.71	5.08	4.72	4.48	4.32	4.20	4.10	4.03	3.96	3.87	3.77	3.67	3.61	3.56	3.51	3.45	3.39	3.33
10	6.94	5.46	4.83	4.47	4.24	4.07	3.95	3.85	3.78	3.72	3.62	3.52	3.42	3.37	3.31	3.26	3.20	3.14	3.08
11	6.72	5.26	4.63	4.28	4.04	3.88	3.76	3.66	3.59	3.53	3.43	3.33	3.23	17	3.12	3.06	3.00	2.94	2.88
12	6.55	5.10	4.47	4.12	3.89	3.73	3.61	3.51	3.44	3.37	3.28	3.18	3.07	3.02	2.96	2.91	2.85	2.79	2.72
13	6.41	4.97	4.35	4.00	3.77	3.60	3.48	3.39	3.31	3.25	3.15	3.05	2.95	2.89	2.84	2.78	2.72	2.66	2.60
14	6.30	4.86	4.24	3.89	3.66	3.50	3.38	3.29	3.21	3.15	3.05	2.95	2.84	2.79	2.13	2.67	2.61	2.55	2.49
15	6.20	4.77	4.15	3.80	3.58	3.41	3.29	3.20	3.12	3.06	2.96	2.86	2.76	2.70	2.64	2.59	2.52	2.46	2.40
16	6.12	4.69	4.08	3.73	3.50	3.34	3.22	3.12	3.05	2.99	2.89	2.79	2.68	2.63	2.57	2.51	2.45	2.38	2.32
17	6.04	4.62	4.01	3.66	3.44	3.28	3.16	3.06	2.98	2.92	2.82	2.72	2.62	2.56	2.50	2.44	2.38	2.32	2.25
18	5.98	4.56	3.95	3.61	3.38	3.22	3.10	3.01	2.93	2.87	2.77	2.67	2.56	2.50	2.44	2.38	2.32	2.26	2.19
19	5.92	4.51	3.90	3.56	3.33	3.17	3.05	2.96	2.88	2.82	2.72	2.62	2.51	2.45	2.39	2.33	2.27	2.20	2.13
20	5.87	4.46	3.86	3.51	3.29	3.13	3.01	2.91	2.84	2.77	2.68	2.57	2.46	2.41	2.35	2.29	2.22	2.16	2.09
21	5.83	4.42	3.82	3.48	3.25	3.09	2.97	2.87	2.80	2.73	2.64	2.53	2.42	2.37	2.31	2.25	2.18	2.11	2.04
22	5.79	4.38	3.78	3.44	3.22	3.05	2.93	2.84	2.76	2.70	2.60	2.50	2.39	2.33	2.27	2.21	2.14	2.08	2.00
23	5.75	4.35	3.75	3.41	3.18	3.02	2.90	2.81	2.73	2.67	2.57	2.47	2.36	2.30	2.24	2.18	2.11	2.04	2.97
24	5.72	4.32	3.72	3.38	3.15	2.99	2.87	2.78	2.70	2.64	2.54	2.44	2.33	2.27	2.21	2.15	2.08	2.01	1.94
25	5.69	4.29	3.69	3.35	3.13	2.97	2.85	2.75	2.68	2.61	2.51	2.41	2.30	2.24	2.18	2.12	2.05	2.98	1.91
26	5.66	4.27	3.67	3.33	3.10	2.94	2.82	2.73	2.65	2.59	2.49	2.39	2.28	2.22	2.16	2.09	2.03	1.95	1.88
27	5.63	4.24	3.65	3.31	3.08	2.92	2.80	2.71	2.63	2.57	2.47	2.36	2.25	2.19	2.13	2.07	2.00	1.93	1.85
28	5.61	4.22	3.63	3.29	3.06	2.90	2.78	2.69	2.61	2.55	2.45	2.34	2.23	2.17	2.11	2.05	1.98	1.91	1.83
29	5.59	4.20	3.61	3.27	3.04	2.88	2.76	2.67	2.59	2.53	2.43	2.32	2.21	2.15	2.09	2.03	1.96	1.89	1.81
30	5.57	4.18	3.59	3.25	3.03	2.87	2.75	2.65	2.57	2.51	2.41	2.31	2.20	2.14	2.07	2.01	1.94	1.87	1.79
40	5.42	4.05	3.46	3.13	2.90	2.74	2.62	2.53	2.45	2.39	2.29	2.18	2.07	2.01	1.94	1.88	1.80	1.72	1.64
60	5.29	3.93	3.34	3.01	2.79	2.63	2.51	2.41	2.33	2.27	2.17	2.06	1.94	2.88	1.82	1.74	1.67	1.58	1.48
120	5.15	3.80	3.23	2.89	2.67	2.52	2.39	2.30	2.22	2.16	2.05	1.94	1.82	1.76	69	1.61	1.53	1.43	1.31
∞	5.02	3.69	3.12	2.79	2.57	2.41	2.29	2.19	2.11	2.05	1.94	1.83	1.71	1.64	1.57	1.48	1.29	1.27	1.00

TABLE 5. 0.95 AND 0.975 FRACTILES OF THE t DISTRIBUTION ASSOCIATED WITH df DEGREES OF FREEDOM

df	$t_{.95}$	$t_{.975}$	df	$t_{.95}$	$t_{.975}$
1	6.314	12.706	21	1.721	2.080
2	2.920	4.303	22	1.717	2.074
3	2.353	3.182	23	1.714	2.069
4	2.132	2.776	24	1.711	2.064
5	2.015	2.571	25	1.708	2.060
6	1.943	2.447	26	1.706	2.056
7	1.895	2.365	27	1.703	2.052
8	1.860	2.306	28	1.701	2.048
9	1.833	2.262	29	1.699	2.045
10	1.812	2.228	30	1.697	2.042
11	1.796	2.201	40	1.684	2.021
12	1.782	2.179	50	1.676	2.009
13	1.771	2.160	60	1.671	2.000
14	1.761	2.145	80	1.664	1.990
15	1.753	2.131	100	1.660	1.984
16	1.746	2.120	120	1.658	1.980
17	1.740	2.110	200	1.653	1.972
18	1.734	2.101	500	1.648	1.965
19	1.729	2.093	∞	1.645	1.960
20	1.725	2.086			

SECTION IV
AERODYNAMIC HEATING AND SERVICE AGING EFFECTS ON MECHANICAL PROPERTIES OF POLYCARBONATE

Previously it had been demonstrated that exposure of bisphenol A thin film polycarbonate material to temperatures above 80°C (176°F) caused the material to become increasingly less ductile (Reference 9). This was evidenced by accumulative decreases in impact strength, fracture energy, extension to break, and increases in tensile yield strength. Other evidence indicated a degrading of these mechanical properties due to weathering and storage (Reference 10 and 11). To determine if mechanical property changes occur in sheet polycarbonate due to aerodynamic heating, a series of tensile and impact tests were conducted at room temperature on two types of monolithic polycarbonate specimens that had been exposed to thermal conditioning. The thermal conditioning was representative of the thermal exposure a supersonic aircraft would encounter during its lifetime. To determine if mechanical property changes occur in sheet polycarbonate due to service aging, a series of tensile tests were conducted at room temperature on fusion bonded monolithic polycarbonate specimens removed from a four-year-old service-aged canopy and newly made transparencies.

TEST SPECIMEN DESCRIPTION

The test specimens used in this test series were made from 0.250 inch thick polycarbonate sheet representative of the core plies in the B-1 alternate design laminated windshield, and from 0.50 to 0.87 inch thick fusion bonded polycarbonate sheet representative of the F-16 alternate design canopy. Two types of polycarbonate sheet were tested, SL3000 (General Electric) and "Tuffak" (Rohm and Haas). Specimens of a particular test series were orientated in the same length-width relation with respect to the basic stock. All test specimens were examined under polarized light to expose stress risers from machining operations which could have affected test results. Specimens displaying stress risers were refinished (sanded and polished) to remove such discrepancies. Machine cutting speed and feed rates were controlled to prevent heating parts above 150°F during machining to eliminate adverse thermal conditioning effects.

The Z5942633-503 tensile specimens shown in Figure 9, 60 each required, were constructed in accordance with ASTM D638-72, Type 1, except the overall length was extended to accommodate the Douglas indexing and alignment fixture. Specimens were made from "as extruded" SL3000 and Tuffak monolithic polycarbonate materials, and were thermally conditioned, as shown in Table 6, prior to testing.

The Z7942633-541 tensile specimens, 15 each required, and -571 tensile specimens, 10 each required, shown in Figure 10, were constructed in accordance with ASTM D638-72, Type III, except the overall lengths were extended, and holes were provided in each end of the test specimen to provide for the Douglas holding fixture. Specimens were made from fusion bonded SL3000 polycarbonate material removed from test canopies or furnished by transparency fabricators. Five -541 tensile specimens were made from a service aged F-15 canopy (see Part 2, Appendix G for service aging history).

The Z7942633-605 tensile specimens, 15 each, (Figure 10), were constructed in accordance with ASTM D638-72, Type III, except the overall length was extended and holes were provided in each end of the test specimen for the Douglas holding fixture. Specimens were made from an F-16 transparency of stretched, fusion bonded SL3000 polycarbonate material. Five of these specimens were thermally conditioned at 185°F for 36 hours to simulate the lifetime aerodynamic heating effects of a supersonic aircraft.

The Z7942633-1 impact test specimens were constructed in accordance with Figure 11. Specimens were made from SL3000 monolithic polycarbonate materials and thermally conditioned in accordance with Table 6 prior to testing.

Thermal Conditioning of Specimens

To provide thermal conditioning, test specimens were heated in a series of Blue "M", circulating air ovens equipped with temperature control overrides and temperature/time recording apparatus. Each oven was equipped

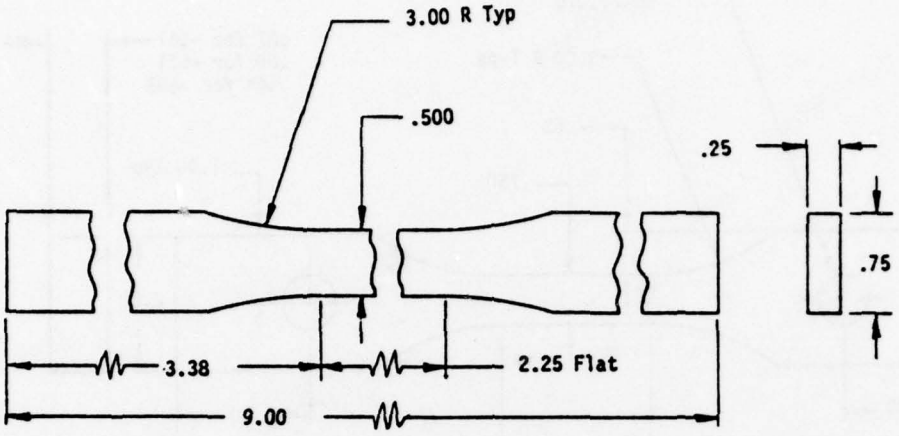

Figure 9. Tensile Specimen (Z7942633-503).

TABLE 6. TEST SPECIMEN THERMAL CONDITIONING

TEST BATCH* NUMBER		THERMAL CONDITIONING		APPROXIMATE NUMBER OF FLIGHT EXPOSURES
		TEMPERATURE (°F)	TIME (HR:MIN)	
B-1	T-1	0	0	0
B-2	T-2	180	2:00	35
B-3	T-3	180	12:00	312
B-4	T-4	180	30:00	350
B-5	T-5	185	16:30	75
B-6	T-6	180 185	30:00 16:30	425

*Each B test batch consists of five Z7942633-503 test specimens, and three Z7942633-1 test specimens. Each T test batch consists of five Z7942633-503 test specimens.

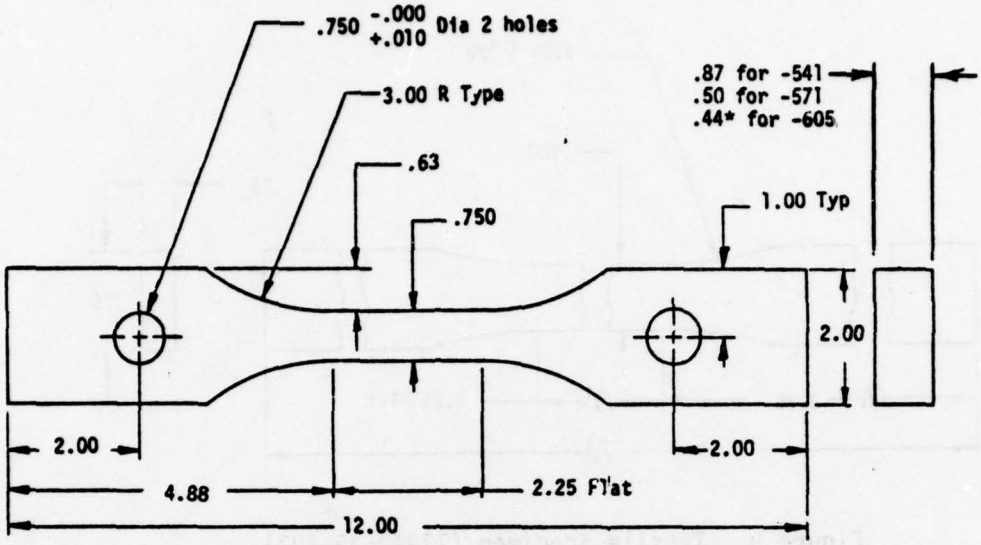

*Specimen thickness reduces approximately 10% by forming.

Figure 10. Tensile Specimen (Z7942633-541, -571, -605).

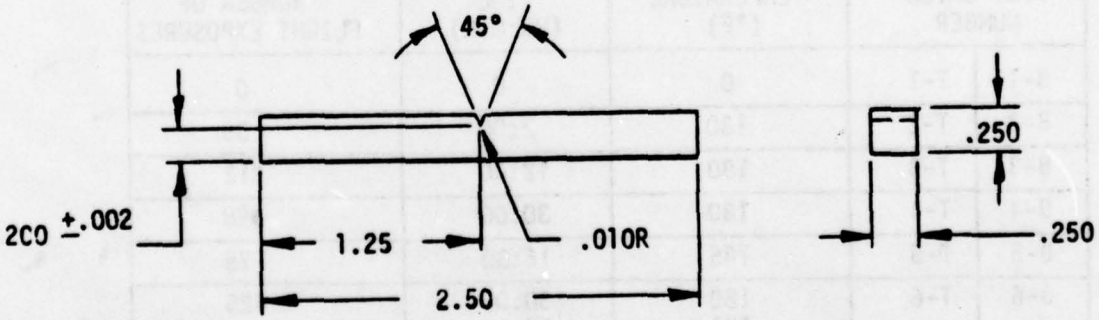

Figure 11. Impact Test Specimen (Z7942633-1).

with iron constantan thermocouples for monitoring the internal circulating air and specimen temperatures to provide automatic temperature control of ovens within ±5°F. Calibration and certification of these ovens was performed within a six-month period prior to use.

TEST EQUIPMENT AND SETUP DESCRIPTION

Tensile Tests

A tensile test specimen indexing and alignment fixture, Figure 12, was used for positive clamping and proper alignment of the test specimen. Tests were conducted on a 30,000-pound capacity Riehle universal test machine. To provide accurate means of determining strain measurements during elastic deformation, a Riehle dual range extensometer, Model DN-D10-20, was used to measure and record elongation. The tensile test setup is shown in Figure 13.

Impact Tests

Tests were conducted using a Tinius Olsen Impact Testing Machine, in which the test specimen was held as a vertical cantilever beam, as shown in Figure 14. The impact test specimen was located and clamped to maintain a constant distance from the pendulum pivot to the centerline of each specimen notch.

TEST PROCEDURES

Tensile Test Procedure

Tensile tests were conducted in accordance with standard method of test, ASTM D638-72. The test specimen gage length cross section dimensions were measured and recorded for each specimen prior to testing. The 0.250 thick specimens were mounted into the indexing and alignment fixture for attachment of clevis ends, as shown in Figure 12. The test specimen was placed in the testing machine and a dual range extensometer installed on the test specimen, as shown in Figure 13. The slack was removed from the system and a measurement made between the clevis ends of the specimen

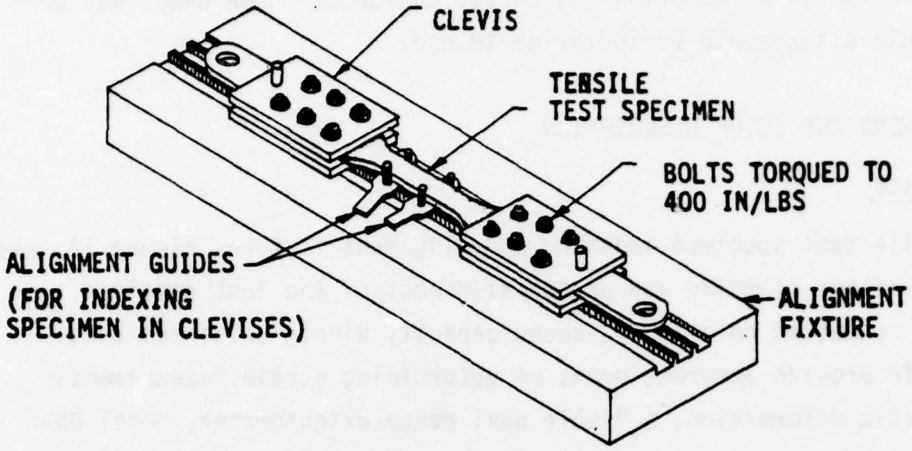

Figure 12. Tensile Test Specimen Indexing and Alignment Fixture.

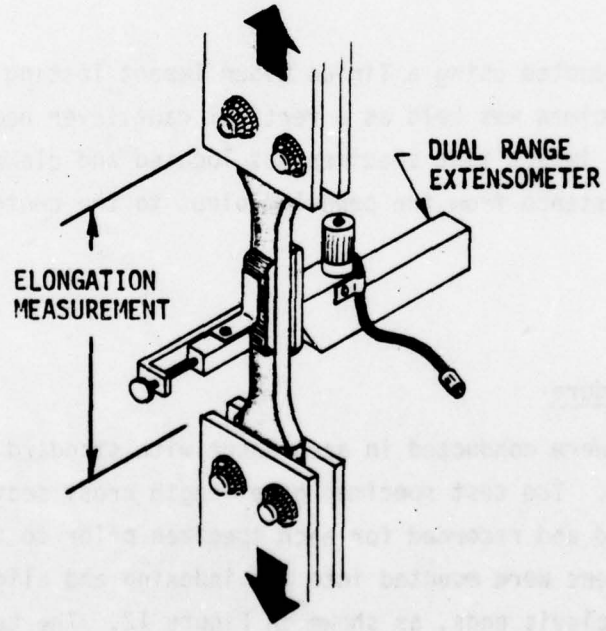

Figure 13. Tensile Stress-Strain Test Setup.

clamps, as shown in Figure 13. The room temperature was recorded and the machine speed set at 0.05-inch per minute. During the test run the maximum load was determined and recorded. The extensometer was removed during plastic deformation of the specimen to prevent instrument damage. The test specimen was then taken to rupture and a measurement made between the clevis ends of the specimen clamps to determine the elongation to failure. A load deflection curve was automatically drawn during test to the point where the extensometer was removed. Five specimens were tested for each test batch of material.

Impact Test Procedures

Impact tests were conducted in accordance with standard method of test ASTM D256-72a, Method C. Tests were conducted on a cantilever beam, izod type impact machine. The test specimen dimensions were measured and verified to be within tolerance and the notch width dimension was recorded for each specimen. A sample test specimen was placed into the test machine, as shown in Figure 14. A pendulum weight was selected that imparted enough energy to break the specimen without exceeding the excess energy scale limit. After breaking each specimen, the total impact energy and excess energy reading were recorded within $\pm$0.025-inch pounds. Specimens in the same test batch were run consecutively with the same pendulum weight and test conditions. A minimum of three specimens were tested for each test batch.

TEST REQUIREMENTS

Douglas provided facilities and services required for testing. The mechanical testing machines used were verified for accuracy per ASTM E4-72 procedure within $\pm$0.5 percent traceable to National Bureau of Standards (NBS). Instrumentation equipment was verified for a class accuracy of B1 per ASTM E83-67 procedures.

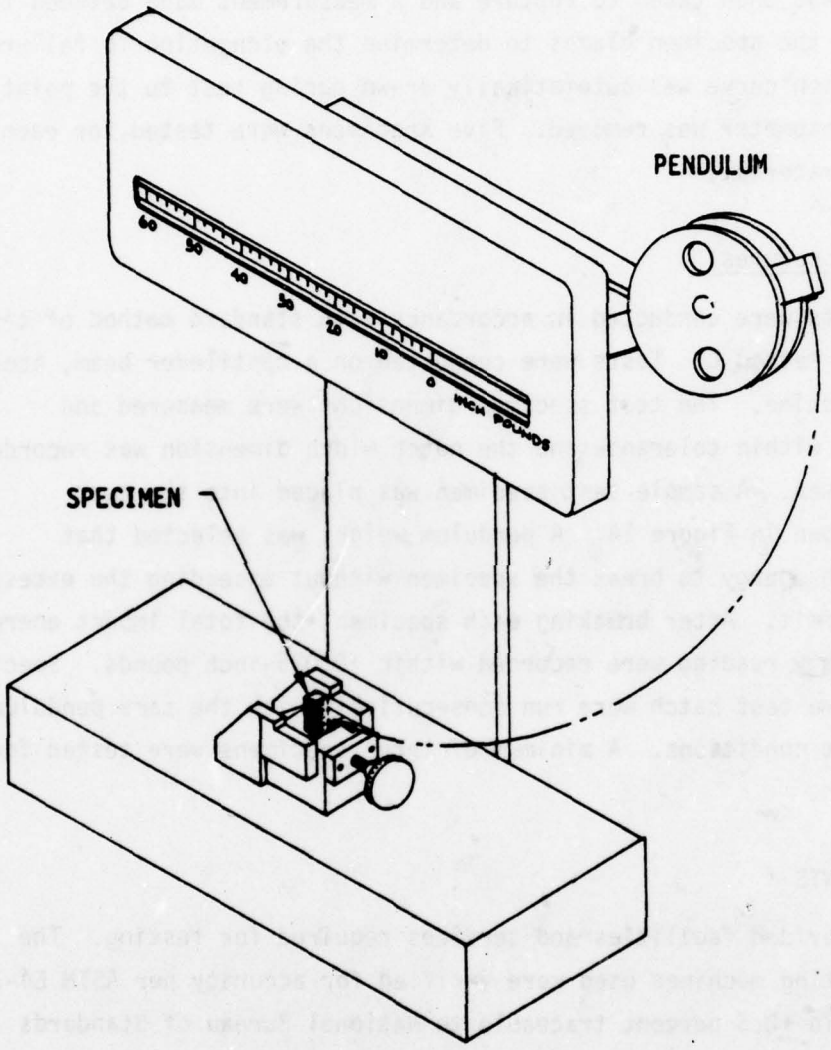

Figure 14. Impact Resistance Test Setup (Izod Type).

Tensile Tests

Tensile tests were conducted per standard method of testing, ASTM D638-72. The speed of testing was 0.05-inch per minute ±20 percent. The gage length cross section dimensions of each test specimen were measured within ±0.001-inch and recorded before and after each test. Tests were conducted at room temperature conditions. A load-deflection curve was recorded for each specimen tested through the peak load portion of the curve. A minimum of 5 test specimens for each test condition were provided. Elongation to failure was determined for each test specimen by making gage length measurements before and after each test. The peak load and rupture load was recorded for each test.

Impact Tests

Impact tests were conducted per standard method of testing, ASTM D256-72a. Tests were conducted at room temperature conditions. Tests were conducted on a standard cantilever beam (izod-type) impact machine. A minimum of three test specimens for each test condition were provided. The energy required to break the specimen within ±0.25 inch pounds was reported for each specimen.

TEST RESULTS AND ANALYSIS

Two general tasks were documented in this section of the report: Task 1, Aerodynamic Heating Effects on Polycarbonate Material Properties and Task 2, Service Aging Effects on Polycarbonate Material Properties.

Tensile test data curves, specimen photographs, test measurement data, and material properties computer runs are presented in Appendix G (Part 2) of this report.

Test data presented are the mathematical average (actual) mechanical property of a specific heat lot of material for a specified test condition.

Test Data

Task 1, Test Series 1, consisted of six test batches identified by batch numbers B-1 through B-6. Each test batch was comprised of five P/N Z7942633-503 tensile test specimens and three P/N Z7942633-501 impact test specimens made of SL3000 polycarbonate material. The average strength data for this test series is given in Table 7. The average stress-strain curves for this test series are superimposed in Figure 15.

Task 1, Test Series 2, consisted of six test batches identified by batch numbers T-1 through T-6. Each test batch is comprised of five P/N Z7942633-503 tensile test specimens made of "Tuffak" polycarbonate material. The average strength data for this test series is given in Table 8. The average stress-strain curve histories for this test series are superimposed in Figure 16.

Task 1, Test Series 3, consisted of five test batches of fusion bonded SL3000 polycarbonate material. A test batch consisted of five each P/N Z7942633-605 tensile specimens made from fusion bonded polycarbonate material removed from a Texstar test canopy and thermally conditioned at 185°F for 36 hours to simulate the life span aerodynamic heating effects of a canopy installed on a supersonic aircraft. These tests were compared with tests of five each P/N Z7942633-605, P/N Z7942633-541, and P/N Z7942633-571 specimens made of fusion bonded polycarbonate material processed by Texstar and other transparency fabricators. The average strength data for this test series is given in Table 9. The average stress-strain curve histories for this test series are superimposed in Figure 17.

Task 2 testing consisted of a series of tensile tests on fusion bonded SL3000 polycarbonate material. Five P/N Z7942633-541 tensile specimens were made of fusion bonded SL3000 polycarbonate material removed from a service aged canopy made by Sierracin/Sylmar Corp. These tests were compared with tests of five each P/N 77942633-541 and P/N Z7942633-605 tensile specimens made of fusion bonded SL3000 polycarbonate material

TABLE 7. TENSILE AND IMPACT TEST DATA (SL3000)
TASK 1, TEST SERIES 1

TENSILE TESTS					IMPACT TESTS
TEST BATCH NUMBER	AVG. YIELD STRENGTH (PSI)	AVG. % ELONGATION TO YIELD	AVG. % ELONGATION TO BREAK	AVG. MODULUS ($PSI \times 10^{-5}$)	AVERAGE IMPACT ENERGY TO BREAK (FT-LB/IN. OF NOTCH)
B-1	9287	2.53	124	3.21	9.77
B-2	9355	2.59	136	3.12	3.86
B-3	9511	2.55	82	3.28	4.60
B-4	9508	2.53	104	3.19	2.56
B-5	9446	2.45	48	3.22	2.75
B-6	9561	2.43	89	3.36	2.71

NOTES:
1. A test batch consists of five (5) tensile specimens minimum and three (3) impact specimens.
2. Test batch B-1 tests reflect the basic (as extruded) mechanical properties of all materials used in this test series.

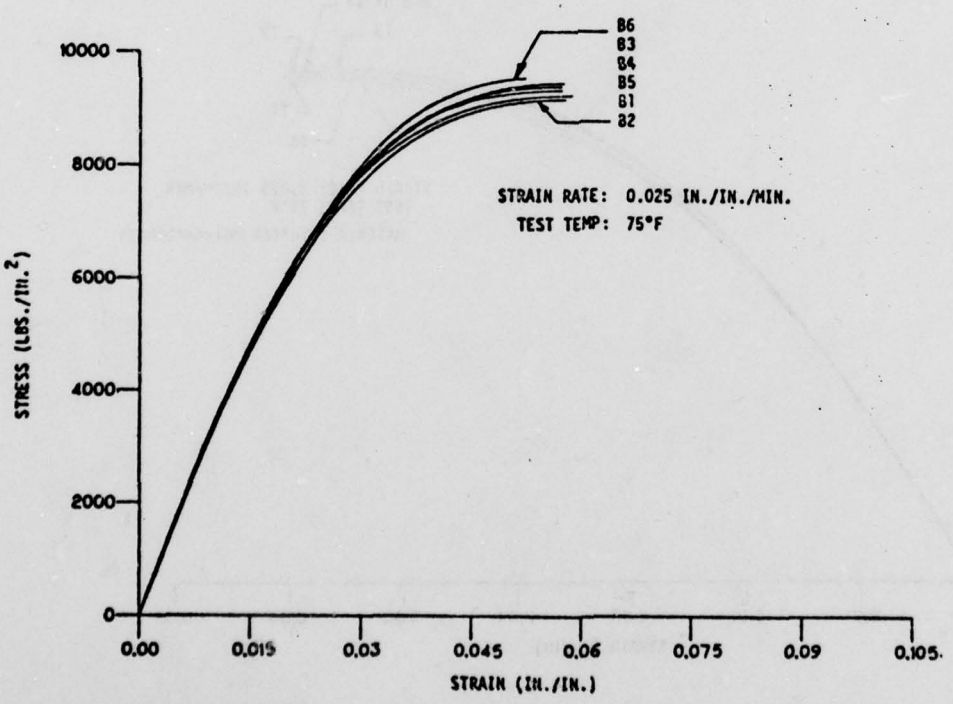

FIGURE 15. TENSILE AVERAGE CURVE - THERMAL CONDITIONING EFFECTS

TABLE 8. TENSILE TEST DATA (TUFFAK)

TASK 1, SERIES 2

SPECIMEN TEST BATCH NUMBER	YIELD STRESS (PSI)	PERCENT ELONGATION TO YIELD	PERCENT ELONGATION TO BREAK	ELASTIC MODULUS (PSIx10-5)	THERMAL CONDITIONING	
					TEMPERATURE (°F)	TIME (HR: MIN)
T-1	8858	2.79	140	3.08	---	---
T-2	8926	2.75	137	3.16	180	2:00
T-3	9037	2.73	124	3.12	180	12:00
T-4	8918	2.71	125	3.06	180	30:00
T-5	8819	2.47	113	3.08	185	16:30
T-6	8950	2.48	118	3.13	180 185	30:00 16:30

NOTES:

1. Test Batch T-1 reflects the basic (as extruded) material properties of all materials used in this test series.
2. A test batch consists of five (5) tensile specimen minimum.

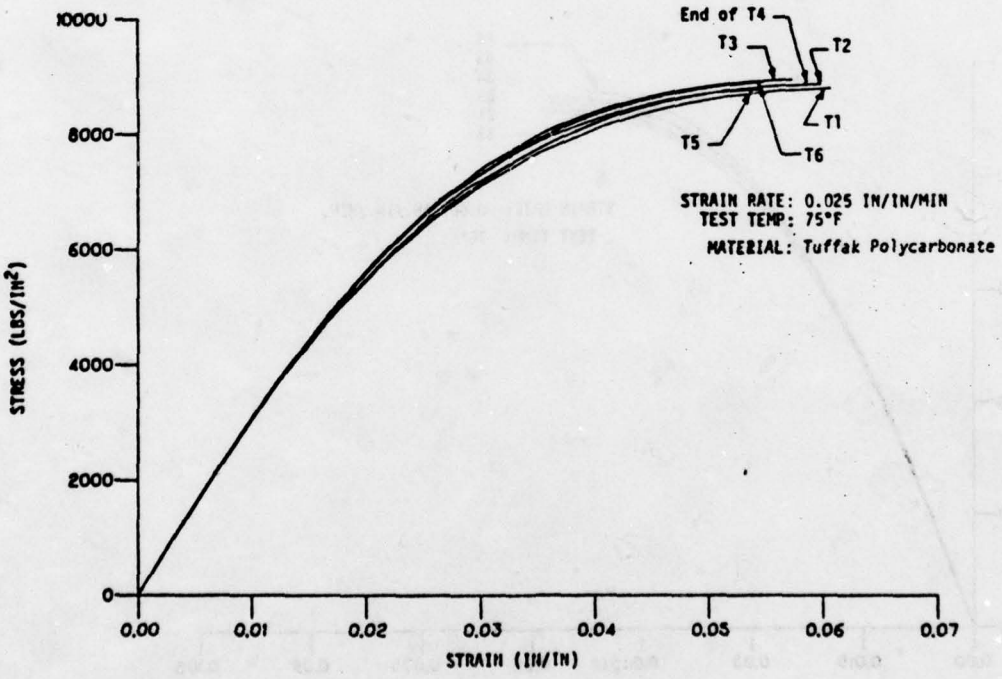

Figure 16. Tensile Average Curves - Thermal Conditioning Effects.

TABLE 9. TENSILE TEST DATA
TASK 1, TEST SERIES 3

SPECIMEN PROCESSOR AND NUMBER*	YIELD STRESS (PSI)	ULTIMATE STRESS (PSI)	ULTIMATE TRUE STRAIN (IN./IN.)	ELASTIC MODULUS (PSI x 10^5)	SECANT MODULUS (PSI x 10^5)	PERCENT ELONGATION TO YIELD	PERCENT ELONGATION TO FAILURE	FRACTURE ENERGY (PSI)
A4 TC	10,293	11,556	0.423	3.30	1.74	2.79	53	4403
A4	9,981	12,411	0.561	3.17	1.50	2.84	75	6020
D3	9,780	11,950	0.474	3.64	1.60	2.54	61	4910
B4	9,509	12,497	0.568	3.21	1.50	2.72	76	5986
C2	9,729	12,525	0.530	3.29	1.61	2.53	70	5635

* A 4 TC
- TC — Thermal Conditioned
- 4 — Part Number
- A — Processor: A, B, C, D

PROCESSOR A: Texstar Plastics Co.
B: Sierracin/Sylmar Co.
C: Swedlow, Inc.
D: PPG Industries, Inc.

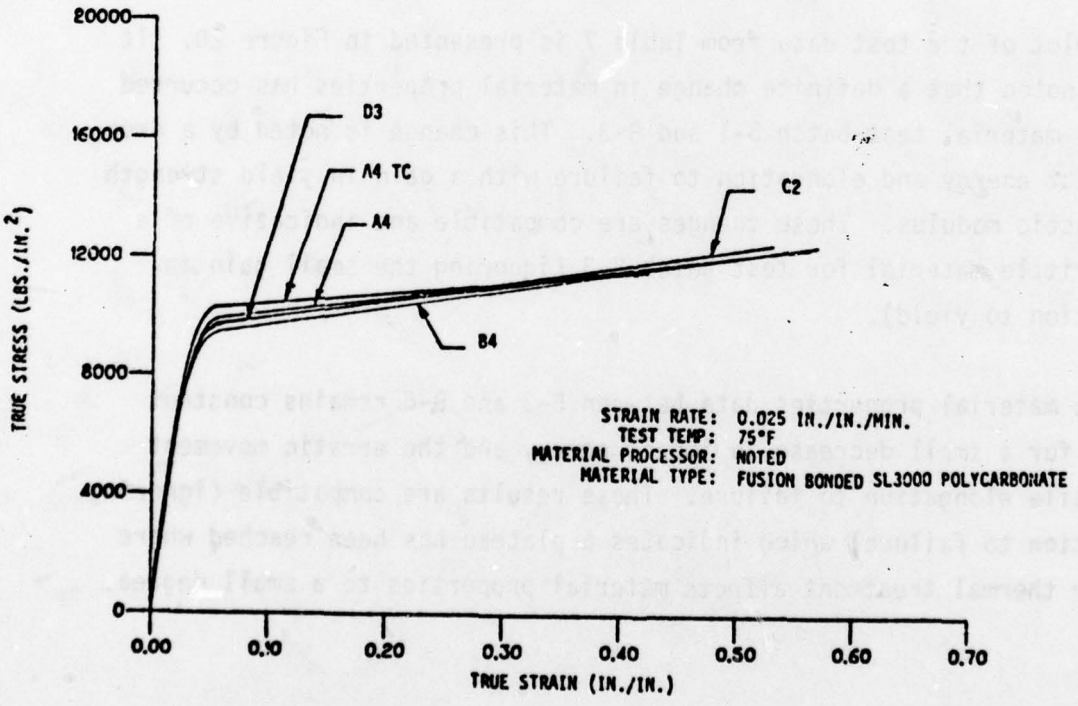

Figure 17. Tensile Average Curves - Service Aging Effects.

processed by Sierracin/Sylmar Corp., and other transparency fabricators. The average strength data for this task is given in Table 10. The average stress-strain curve histories for this test series are presented in Figure 18. Additional evidence of aging effects on polycarbonate are given by the average stress-strain curve histories presented in Figure 19 as adapted from Reference 6.

Analysis

In this analysis, all data are based on averages, therefore, any spread between stress-strain curves and other comparable data are considered within the average limits presented for each test batch. Although some data may be superfluous, it was considered better to collect and record all data that was available should any unusual trend occur.

Task 1, Test Series 1

A plot of the test data from Table 7 is presented in Figure 20. It can be noted that a definite change in material properties has occurred between material test batch B-1 and B-3. This change is noted by a drop in impact energy and elongation to failure with a gain in yield strength and elastic modulus. These changes are compatible and indicative of a more brittle material for test batch B-3 (ignoring the small gain in elongation to yield).

The material properties data between B-3 and B-6 remains constant except for a small decrease in impact energy and the erratic movement of tensile elongation to failure. These results are compatible (ignoring elongation to failure) which indicates a plateau has been reached where further thermal treatment affects material properties to a small degree.

TABLE 10. TENSILE TEST DATA

TASK 2

SPECIMEN PROCESSOR AND NUMBER*	YIELD STRESS (PSI)	ULTIMATE STRESS (PSI)	ULTIMATE TRUE STRAIN (IN./IN.)	ELASTIC MODULUS (PSI x 10^{-5})	SECANT MODULUS (PSI x 10^{-5})	PERCENT ELONGATION TO YIELD	PERCENT ELONGATION TO FAILURE	FRACTURE ENERGY (PSI)
B2 SA	10,092	12,268	0.432	3.42	1.66	2.51	54	4579
B2	10,105	13,283	0.596	3.65	1.77	2.54	81	6707
A3	9,362	12,360	0.539	3.09	1.53	2.68	71	5590
C2	9,729	12,525	0.530	3.29	1.61	2.53	70	5635
D3	9,780	11,950	0.474	3.64	1.60	2.54	61	4910

* A 4 SA
- SA — Service Aged
- 4 — Part Number
- A — Processor: A, B, C, D

PROCESSOR A: Texstar Plastics Co.
B: Sierracin/Sylmar Co.
C: Swedlow, Inc.
D: PPG Industries, Inc.

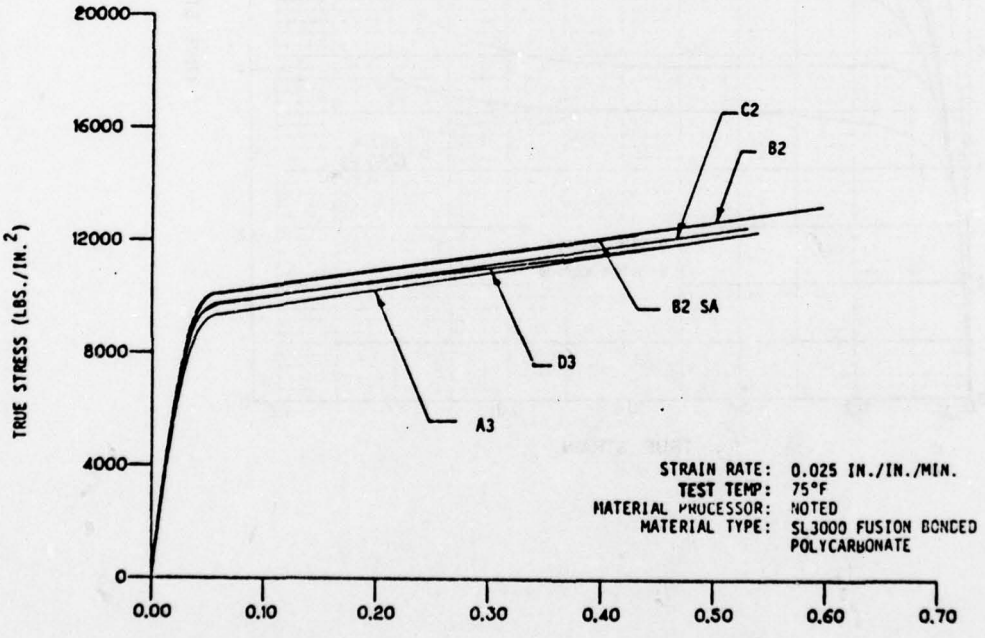

Figure 18. Tensile Average Curves - Service Aging Effects.

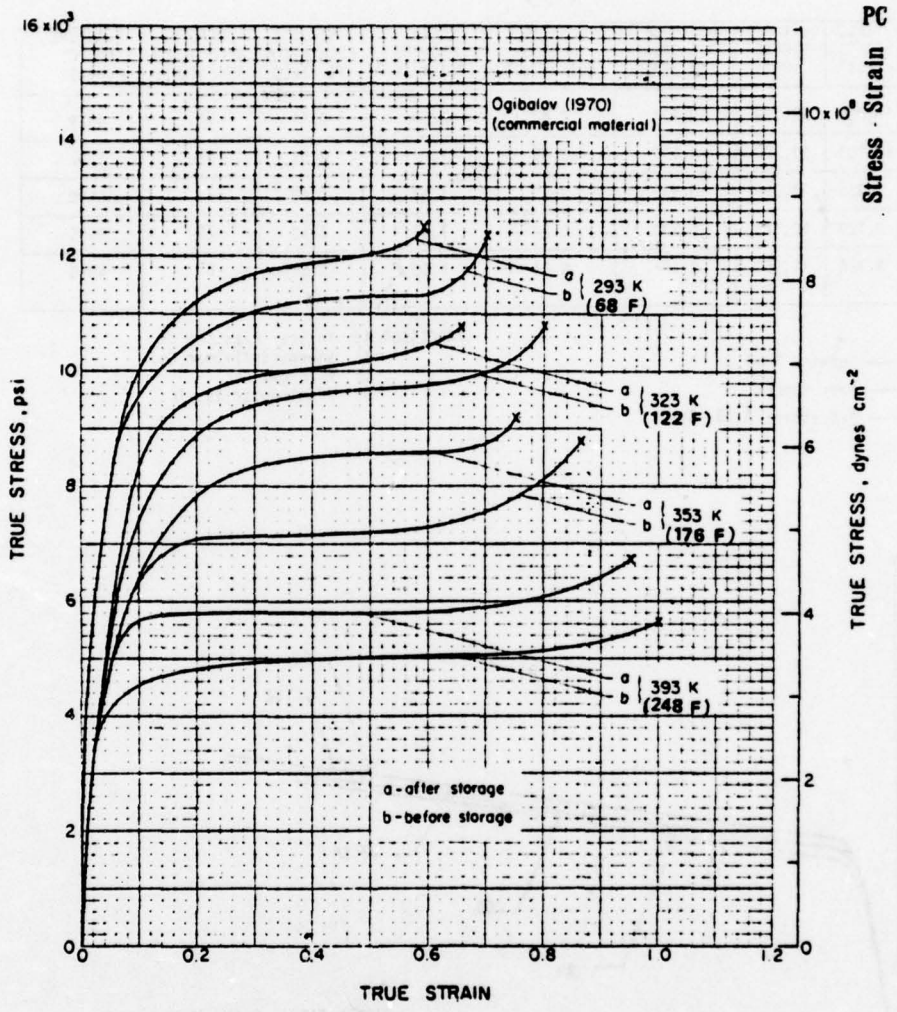

Figure 19. Before and After Storage for Four Years at 293-393K in a Dark Dry Location. (Adapted from Reference 6).

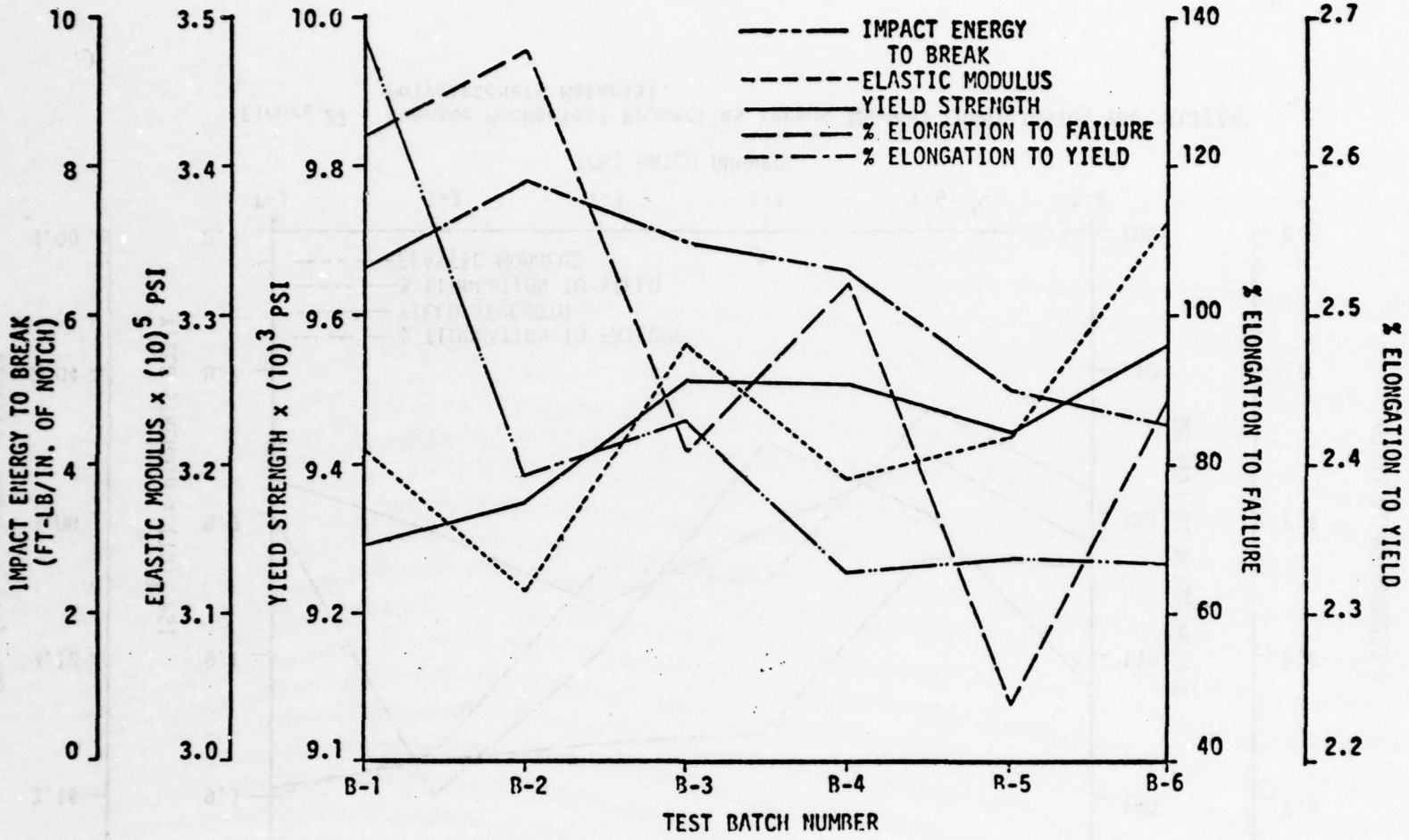

Figure 20. Average Mechanical Properties Versus Thermal Conditioning for SL3000 Polycarbonate Material.

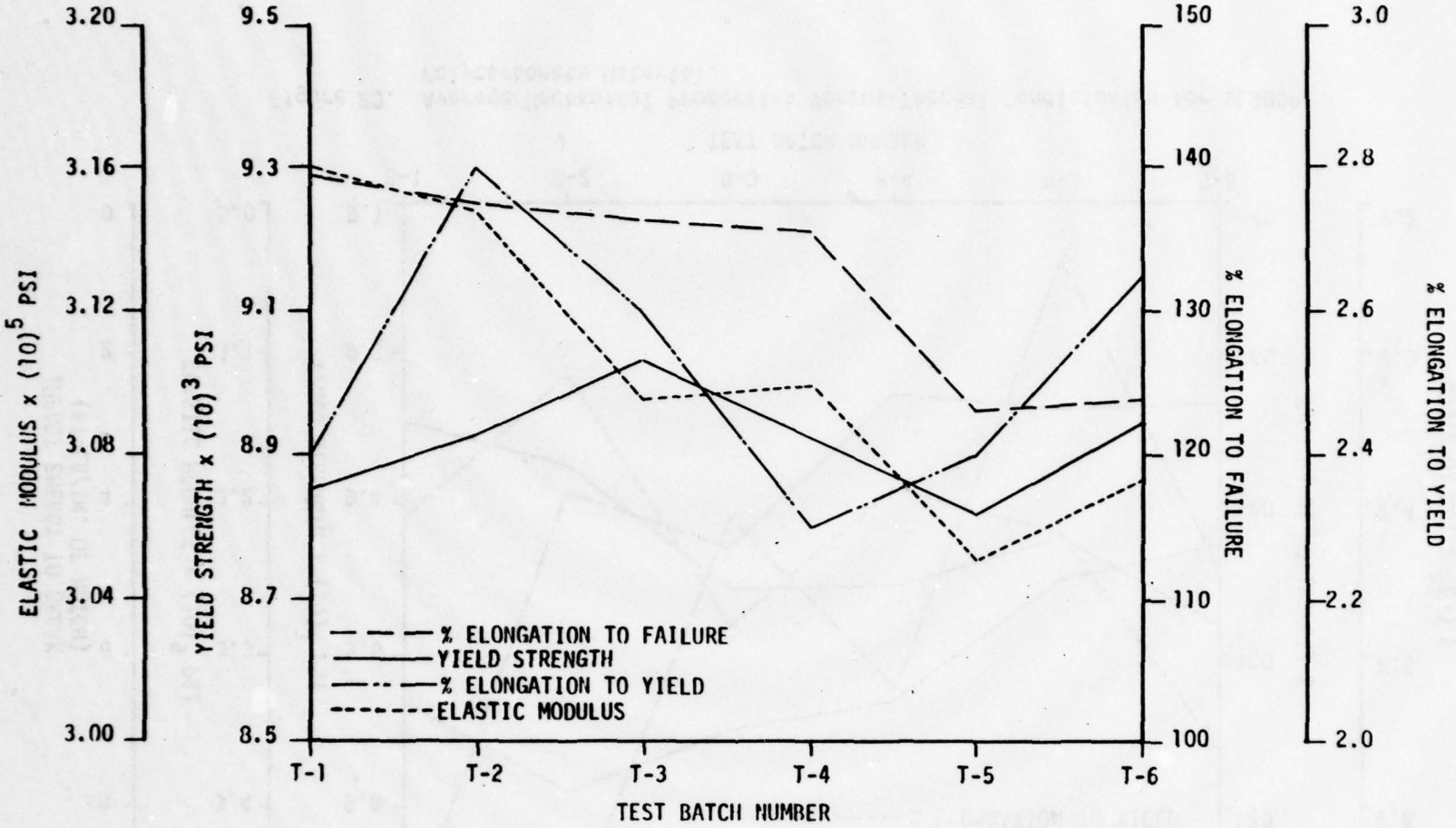

Figure 21. Average Mechanical Properties Versus Thermal Conditioning for "TUFFAK" Polycarbonate Material.

Task 1, Test Series 2

A plot of the test data from Table 8 is presented in Figure 21. It can be noted that a gradual change in material properties has occurred between T-1 and T-6. This change is noted by an increase in tensile yield, and tensile modulus, with a decrease in tensile elongation to both yield and failure. These results are compatible and are indicative of a more brittle material for test batch B-6.

Task 1, Test Series 3

Comparison of test results in Table 9 and Figure 17 for A4, D3, B4, and C2 test specimens with A4 TC thermal conditioned test specimen reveals that material embrittlement has taken place due to thermal conditioning. This change is noted by an increase in yield strength, a decrease in percent elongation to failure, and a decrease in fracture energy.

Task 2

Comparison of test results in Table 10, Figure 18 and Figure 19, reveal that material embrittlement has taken place due to service aging. This change is noted by an increase in yield strength, a decrease in percent elongation to yield and failure, and a decrease in fracture energy.

Conclusions

Conclusions based on data contained in this section and other applicable data are contained in Section XI of this report.

SECTION V
LOW STRAIN RATE TENSILE MECHANICAL PROPERTIES TESTING OF PROCESSED POLYCARBONATE MATERIALS

This test series was conducted to establish tensile mechanical properties of processed polycarbonate materials at various temperature conditions and at low strain rates. Test specimens were made from instrumented beams (Reference 12), bird impact test windshield/canopies (Reference 13), and material (both sheet and specimen configurations) furnished by transparency fabricators. The primary use for these tests was to provide average (actual) and design allowables for development and future design use in computer programs (Reference 7). Additional uses were to provide information for the evaluation of materials and processors, trade-off design studies, windshield static load design analysis, and to provide test criteria for future transparency design specification control documents. Tests were conducted per ASTM standard methods. Maximum and minimum test temperatures were established based on the flight profile of a supersonic aircraft.

TEST SPECIMEN DESCRIPTION

The test specimens for this series of tests were made from SL3000 (General Electric Co.) and Tuffak (Rohm and Haas Co.) polycarbonate sheet processed by several transparency fabricators. All test specimens were examined under polarized light to expose stress risers that resulted from machining operations and could have affected test results. Specimens displaying stress risers were refinished (sanded and polished) to remove such discrepancies. Machine cutting speed and feed rates were controlled to prevent heating parts above 150°F which could result in adverse thermal conditioning effects. Specimens of a particular test series were orientated in the same length-width relation with respect to the basic stock.

The Z5942633-503 tensile specimens (Figure 22) were constructed in accordance with ASTM D638-72, Type 1, except the overall length was

PRECEDING PAGE NOT FILMED BLANK

extended to accommodate the Douglas indexing and alignment fixture. Specimens were made from SL3000 and "Tuffak" monolithic polycarbonate materials. The test specimens received transparency fabricators processes that normally occur during the manufacture of a laminated transparency. The transparency fabricators were PPG Industries (PPG), Texstar Plastics Co. (TEX), Sierracin Corp. (SK), and Swedlow Co. (SWU).

The Z5942633-507, -541, -571, and -605 test specimens (Figure 23) were constructed in accordance with ASTM D638-72, Type III, except the overall length was extended, and holes were provided in each end of the test specimen to accommodate the Douglas holding fixture. Specimens were made from SL3000 and "Tuffak" fusion bonded polycarbonate material. The Z5942633-507 test specimen material was furnished by Sierracin Corp., and received the same processing as the Z5942626-1 and -501 transparent beam. The Z5942633-541 test specimen material was furnished by Sierracin Corp., and Swedlow Co.; Z5942633-571 test specimen material was furnished by PPG Industries; and Z5942633-605 test specimen material was furnished by Sierracin, Swedlow, and Texstar. These specimens received the same processing that a laminated transparency for a supersonic aircraft would receive.

The Z5942633-509 test specimens (Figure 24) were constructed in accordance with ASTM D638-72, Type V, except the overall length was extended to accommodate the Douglas indexing and alignment fixture. The test specimens were made of SL3000 monolithic polycarbonate material and received the same processing as the Z5942626-501 transparent beam manufactured by Sierracin Corp.

The Z5942633-517 and -543 test specimens (Figure 25) were constructed in accordance with ASTM D638-72, Type I. The test specimens were made of SL3000 monolithic polycarbonate material. The Z5942633-517 test specimen material was furnished by Sierracin Corp., and received the same processing as the Z5942626-503 and -505 transparent test beam. The Z5942633-543 test specimen material was furnished by Sierracin Corp. and Swedlow Co., and received the same processing as the laminated transparency for the B-1 supersonic aircraft transparency.

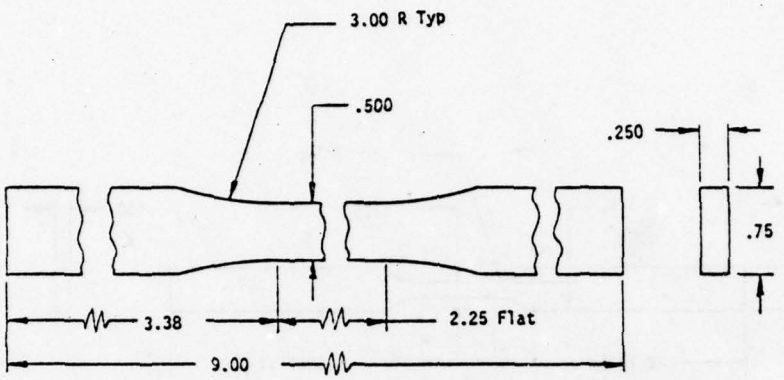

Figure 22. Tensile Specimen (Z7942633-503).

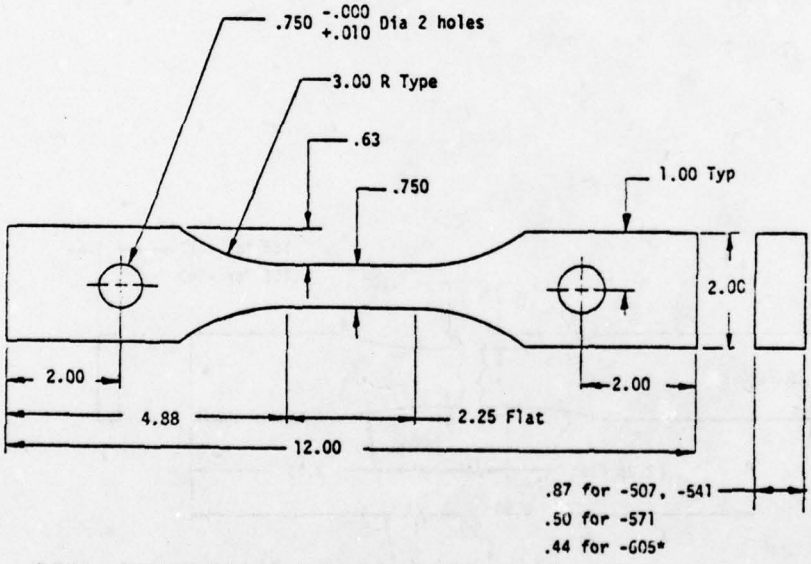

* Note: Specimen thickness to be reduced .06 by stretch forming prior to machining.

Figure 23. Tensile Specimen (Z7942633-541, -507, -571, -605).

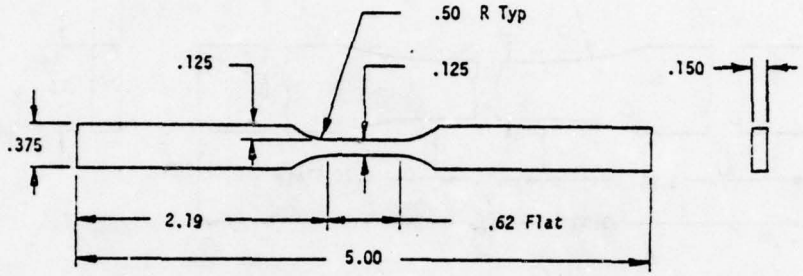

Figure 24. Tensile Specimen (Z7942633-509).

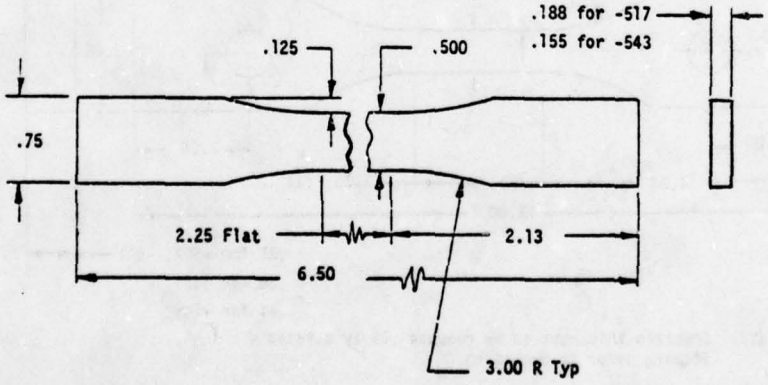

Figure 25. Tensile Specimen (Z7942633-517, -543).

TEST SETUP AND EQUIPMENT DESCRIPTION

Portions of the following tensile test setup and equipment description is the same as outlined in Section IV, and is repeated here for the convenience of the reader.

The test setup for the Z7942633-503, -509, -517 and -543 test specimens is shown in Figure 26. In this test setup the Douglas indexing and alignment fixture is used to provide for positive clamping and alignment of the test specimen. The test setup for the Z7942633-507, -541, -571 and -605 tensile specimens is shown in Figure 27. In both test setups a Riehle dual range extensometer was used to measure and record specimen elongation. Two types of test machines were used for testing, a 30,000-pound capacity Riehle mechanical test machine, and a 10,000-pound capacity Instron mechanical test machine.

TEST PROCEDURE

Tensile tests were conducted in accordance with standard method of test, ASTM D638-72. The test specimen gage length cross section dimensions were measured and recorded for each specimen prior to testing. The Z7942633-503, -509, -517, and -543 specimens were mounted into the indexing and alignment fixture for attachment of clevis ends, as shown in Figure 28. The test specimen was then placed in the test machine and a extensometer installed as shown in Figure 26. Each Z7942633-507, -541, -571, and -605 test specimen was placed in the testing machine and an extensometer installed on the test specimen, as shown in Figure 27. The slack was removed from the system and a measurement made between the ends of the specimen clamps as shown in Figures 26 and 27. The room temperature was recorded and the machine set at the desired testing speed. During the test run the maximum load was determined and recorded. The extensometer was removed from the specimen during plastic deformation of the specimen to prevent instrument damage. The test specimen was then loaded to rupture and the rupture load recorded. A measurement was again made between the ends of the specimen clamps to determine the total elongation to failure. A load deflection curve was

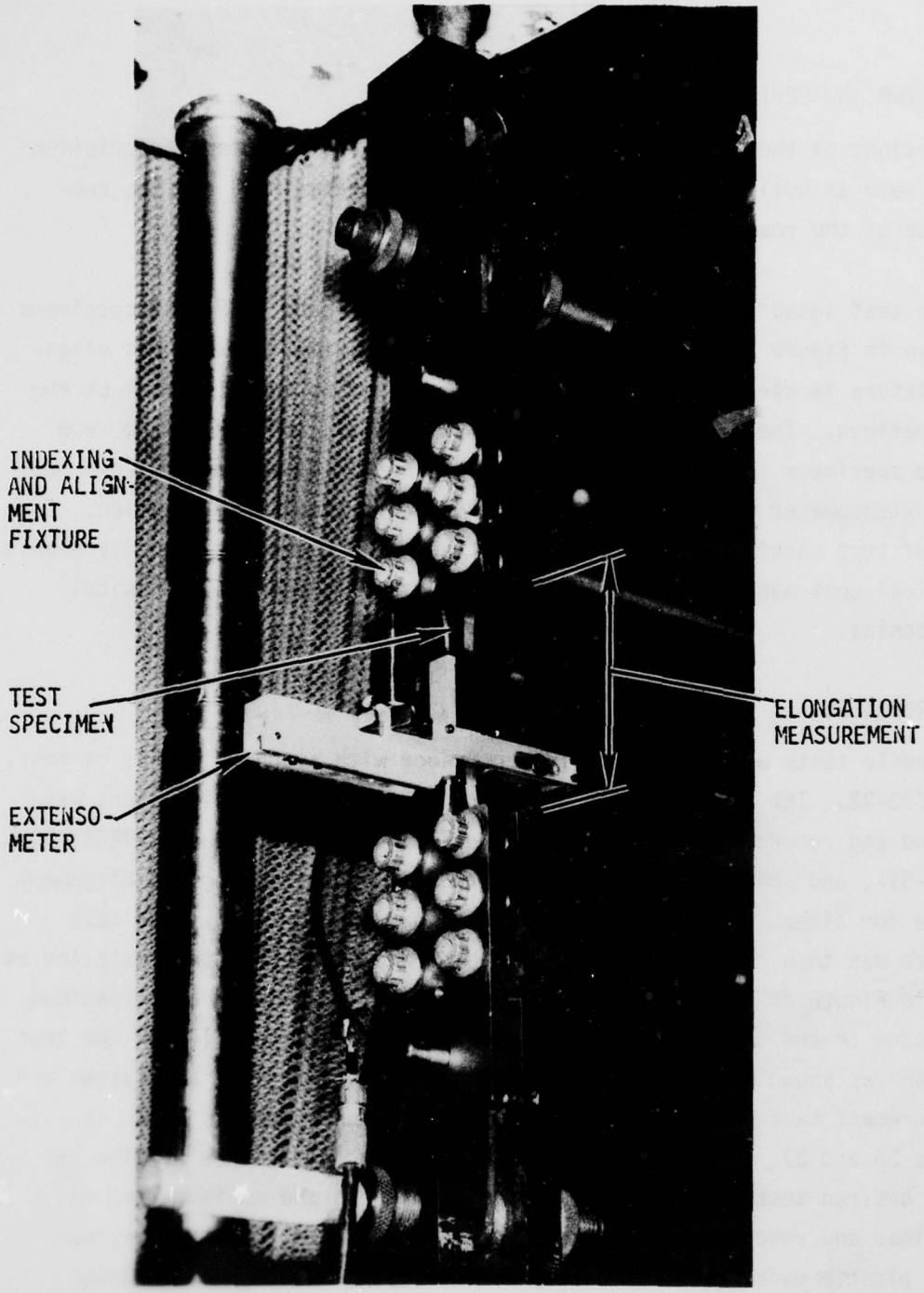

Figure 26. Tensile Test Setup

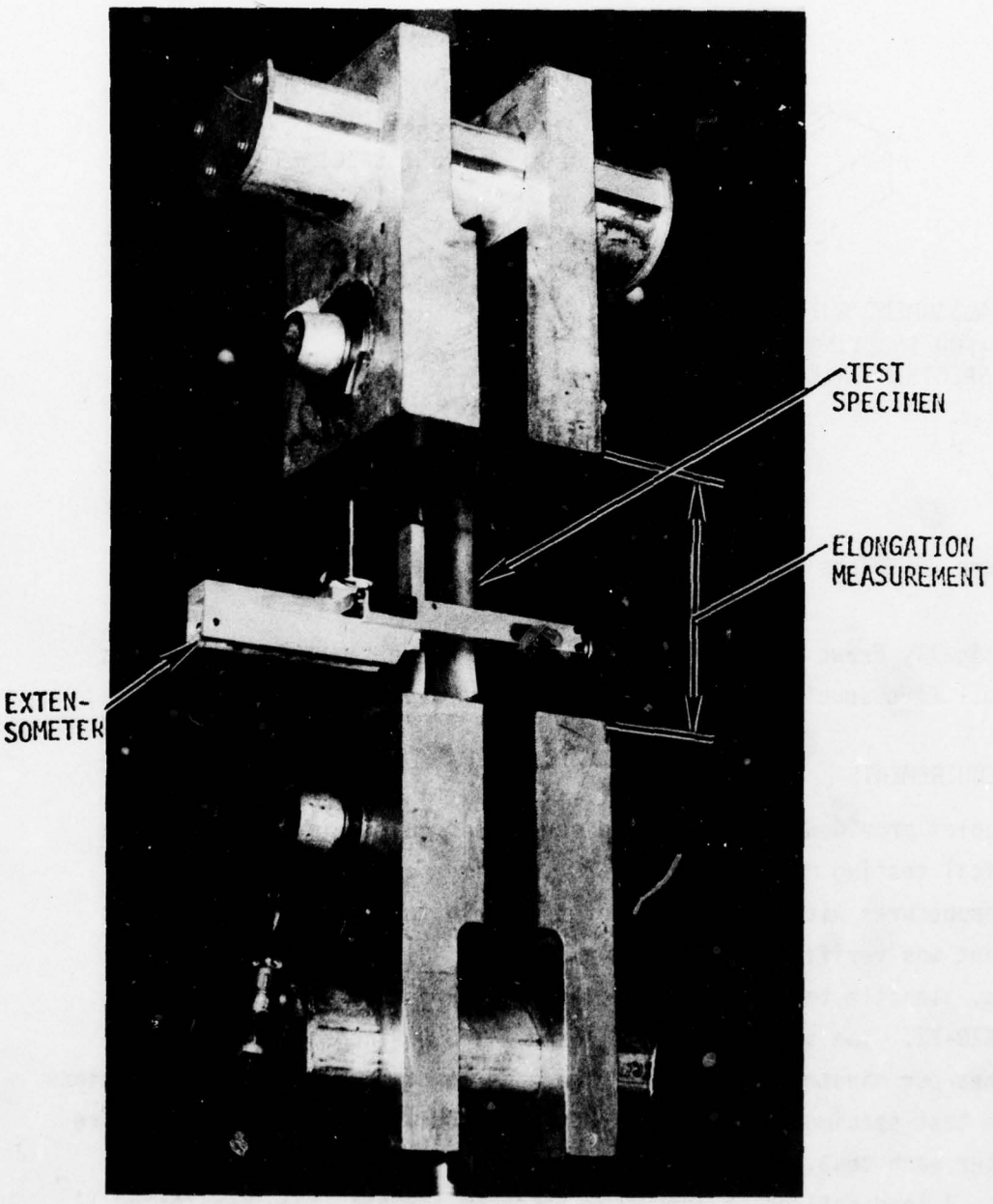

Figure 27. Tensile Test Setup

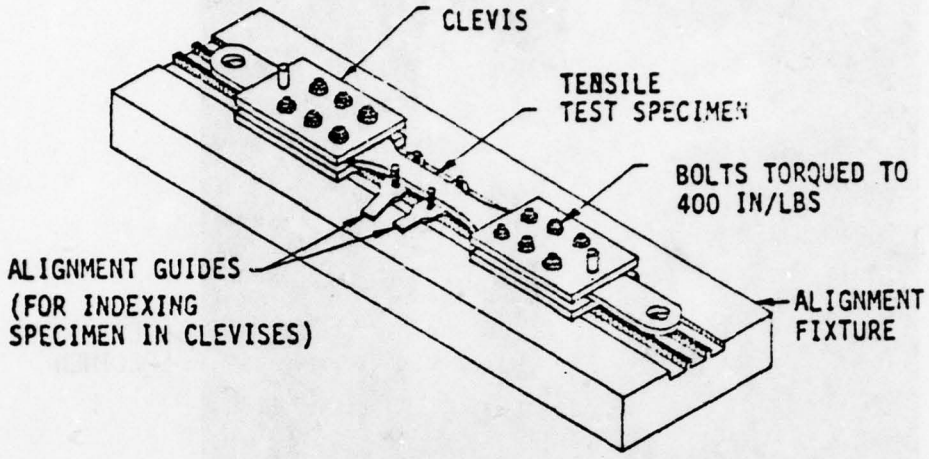

Figure 28. Tensile Test Specimen Indexing and Alignment Fixture.

automatically drawn during test to the point where the extensometer was removed. Five specimens were tested for each test batch of material.

TEST REQUIREMENTS

Douglas provided facilities and services required for testing. The mechanical testing machines used were verified for accuracies per ASTM E4-72 procedures within ±0.5 percent traceable to NBS. Instrumentation equipment was verified for a class accuracy of B1 per ASTM E83-67 procedures. Tensile tests were conducted per standard method of testing, ASTM D638-72. The speed of testing used was 0.05-inch per minute, and 10-inches per minute ±20 percent. The gage length cross section dimensions of each test specimen was measured within ±0.001-inch and recorded before and after each test. Test temperatures (±5°F) were -30°F, +75°F and +195°F. A load-deflection curve was recorded for each specimen tested through the peak load portion of the curve. A minimum of 5 test specimens for each test condition was provided. Elongation to failure was determined for each test specimen by making grip length measurements before and after each test. The peak load and rupture load was recorded for each test.

TEST RESULTS AND ANALYSIS

Three tasks were accomplished and documented in this section of the report. Task I provides average (actual) mechanical properties data for monolithic and fusion bonded polycarbonate materials removed from windshields and canopies in support of a bird strike analysis computer program (Reference 7), and for materials removed from test beams in support of the analysis of laminated beams representative of aircraft transparencies (Reference 12). Task II provided average (actual) and design allowables for monolithic polycarbonate materials as processed by PPG Industries (PPG), Texstar Plastics (TEX), Sierracin Corp. (SK), and Swedlow Co. (SWU). Task III provides average (actual) and design allowables for fusion bonded polycarbonate materials as processed by Texstar Plastics, Sierracin Corp., Swedlow Co., and PPG Industries.

The mechanical properties data presented were based on five or more test specimens made from the same batch of material and tested at identical conditions where possible. Test specimens that broke at some fortuitous flaw, did not break between predetermined gage marks, or failed in the fusion bonded area were not used in calculation of mechanical properties data. The design allowables presented were computed on a "B" basis by methods outlined in Chapter III. Where "B" basis data could not be computed, the "C" basis data were computed and presented. Where the design allowable could not be computed, due to insufficient test data, no design allowable is presented.

Test Data

Task I average (actual) tensile strength data is given in Table 11. The average true stress-strain curves from which the tabulated data were calculated are presented in Appendix A, Figures A.1 through A.13.

TABLE 11. TENSILE STRENGTH DATA TASK I

TEST SPECIMEN IDENT	TEST SPECIMEN NO.*	THICKNESS (IN.)	TEST TEMP (°F)	STRAIN RATE (IN/IN MIN)	AVERAGE STRENGTH DATA: YIELD (PSI)	STD DEV (PSI)	SEC YLD MOD (PSI 10^{-5})	ULTIMATE: TRUE STRESS (PSI)	STD DEV (PSI)	TRUE STRAIN (IN/IN)	STD DEV (IN/IN)	ELAST MOD (PSI 10^{-5})	STD DEV (PSI x 10^{-5})	MATERIAL IDENTIFICATION - BEAM NUMBER OR TRANSPARENCY IDENTIFICATION
PPG517	5	0.19	76	0.025	9198	76	1.59	17238	538	0.601	0.018	3.74	0.098	Z5942626-503 TEST BEAM
PPG517	5	0.19	77	0.025	9095	86	1.56	16901	1139	0.580	0.022	3.48	0.137	Z5942626-505
PPG517D	5	0.19	74	0.025	9232	45	1.65	15701	2005	0.553	0.055	3.63	0.080	Z5942626-505
SK507	4	0.87	76	0.025	9467	377	1.52	12584	505	0.561	0.023	3.32	0.453	Z5942626-1,-501
SK509	5	0.15	78	0.025	9175	334	1.43	13781	1590	0.566	0.049	3.27	0.331	Z5942626-501 TEST BEAM
SWU541/8	3	0.87	75	0.025	9729	215	1.61	12525	159	0.530	0.011	3.64	0.311	SWEDLOW B-1 WINDSHIELD
SWU543/8	6	0.16	76	0.025	9528	95	1.77	13319	914	0.515	0.024	3.76	0.307	SWEDLOW B-1 WINDSHIELD
TEX605/29	7	0.47	72	0.025	10019	91	1.45	12482	437	0.559	0.030	3.39	0.166	TEXSTAR F-16 TEST CANOPY
TEX605/30	5	0.46	78	0.025	10088	73	1.59	12057	728	0.517	0.057	3.45	0.082	
TEX605/48	6	0.47	72	0.025	10067	111	1.71	12177	646	0.539	0.044	3.68	0.370	
TEX605/1	5	0.57	75	0.025	9639	125	1.51	12959	383	0.706	0.027	3.14	0.196	
TEX605/27	6	0.48	76	0.025	9981	35	1.50	12411	283	0.561	0.024	3.17	0.217	
TEX605/5	5	0.57	75	0.025	9743	25	1.52	13271	504	0.738	0.032	3.03	0.077	
TEX605C43	4	0.45	71	0.025	9796	216	1.30	11918	654	0.514	0.077	2.74	0.522	TEXSTAR F-16 TEST CANOPY

*Number of specimens included in the generation of data presented.

Task II average (actual) and specific design allowables are given in Table 12. The average and design true stress-strain curves from which the tabulated values were derived are presented in Appendix A, Figures A.14 through A.44.

Task III average (actual) and specific design allowables for mechanical properties are presented in Table 13. The average and design true stress-strain curves from which the tabulated values were derived are presented in Appendix A, Figures A.45 through A.76.

Experimental test data and true stress-strain curves for test specimens are contained in Part 2, Appendix H.

Analysis

In this analysis, comparisons are made between two types of polycarbonate as processed by four aircraft transparency fabricators. The effects of processing, forming, strain rate, and test temperature are demonstrated for these processed materials. Proposed design allowables are generated from test data used in calculation of specific design strength values presented in Tables 12 and 13.

Material Comparisons

The average tensile stress-strain curves from test data of two types of processed polycarbonate material are presented in Figure 29. Tabulated strength data derived from these curves are contained in Table 13. It can be noted that material "B" at -30°F appears more brittle than material "A" based on values of true strain at rupture. The reverse appears to be true based on this criteria at +195°F. Since these differences appear only at extreme temperature conditions, and rupture strength is within anticipated scatter of a single heat lot of material, it is concluded that these processed materials are equivalent in tensile strength properties.

TABLE 12. TENSILE STRENGTH DATA TASK II

TEST SPECIMEN		THICKNESS	TEST TEMP (°F)	STRAIN RATE (IN/IN/MIN)	AVERAGE STRENGTH DATA									DESIGN ALLOWABLE					
								ULTIMATE		ULTIMATE							ULTIMATE		
IDENT.	NO.*				YIELD (PSI)	STD DEV (PSI)	SEC YLD MOD (PSI 10^{-5})	TRUE STRESS (PSI)	STD DEV (PSI)	TRUE STRAIN (IN/IN)	STD DEV IN/IN)	ELAST MOD (PSI 10^{-5})	STD DEV (PSI x 10^{-5})	DES BAS	YIELD (PSI)	SEC YLD MOD (PSI	TRUE STRESS (PSI)	TRUE STRAIN (IN/IN)	ELAST MOD (PSI x 10^{-5})
PPG503	4	.25	75	0.025	9707	62	1.74	14141	1739	0.510	0.017	3.61	0.052	C	9545	1.71	9589	0.466	3.55
PPG503	5	.25	76	4.44	10213	57	1.87	15903	1443	0.625	0.042	2.62	0.172	B	10017	1.84	10985	0.481	3.17
PPG503	5	.25	-30	4.44	12240	1031	1.00	15422	2097	0.481	0.121	1.39	0.218	C	10024	0.82	10912	0.221	0.95
PPG503	5	.25	195	4.44	7658	118	1.06	11036	1314	0.680	0.040	1.26	0.051	C	7405	1.03	8210	0.594	1.09
PPG517	5	.188	76	0.025	10315	654	0.64	16603	1638	0.597	0.065	3.03	1.039	C	8907	0.55	13082	0.456	0.87
SK503	5	.25	75	0.025	9816	72	1.80	12618	171	0.570	0.010	3.38	0.056	B	9569	1.76	12035	0.536	3.28
SK503	5	.25	75	4.44	10725	45	1.55	13704	667	0.564	0.042	2.03	0.423	B	10570	1.53	11432	0.422	0.82
SK503	5	.25	76	0.025	9178	155	1.68	16972	1570	0.588	0.048	2.99	0.550	B	8649	1.58	11623	0.424	2.05
SK503	5	.25	-30	4.44	11780	322	3.00	14840	269	0.517	0.035	3.54	0.695	B	10680	2.72	13923	0.398	1.17
SK503	5	.25	195	4.44	8159	82	1.74	11163	938	0.702	0.025	2.28	0.080	B	7880	1.68	7967	0.615	2.08
SWU503	4	.250	75	0.025	9637	73	1.78	11744	379	0.457	0.019	3.94	0.200	B	9445	1.74	10751	0.407	3.05
SWU503	5	.25	76	5.00	10296	261	1.88	13374	732	0.580	0.047	2.77	0.261	B	9408	1.71	10880	0.421	1.93
SWU503	3	.25	-30	4.44	12076	1582	1.11	15202	1953	0.507	0.038	1.61	0.231						
SWU503	5	.25	195	4.44	7792	150	1.19	10637	762	0.689	0.019	1.36	0.093	B	7281	1.11	8042	0.623	1.08
TEX503X	4	.25	75	0.025	9797	65	1.84	12205	971	0.481	0.036	3.55	0.148	C	9625	1.81	9664	0.386	2.87

*Number of specimens included in the generation of data presented.

TABLE 13. TENSILE STRENGTH DATA TASK III

TEST SPECIMEN		THICKNESS	TEST TEMP (°F)	STRAIN RATE (IN/IN/MIN)	AVERAGE STRENGTH DATA									DESIGN ALLOWABLE					
								ULTIMATE									ULTIMATE		
IDENT.	NO*				YIELD (PSI)	STD DEV (PSI)	SEC YLD MOD (PSI 10^{-5})	TRUE STRESS (PSI)	STD DEV (PSI)	TRUE STRAIN (IN/IN)	STD DEV (IN/IN)	ELAST MOD (PSI x 10^{-5})	STD DEV (PSI x 10^{-5})	DES BAS	YIELD (PSI)	SEC YLD MOD (PSI	TRUE STRESS (PSI)	TRUE STRAIN (IN/IN)	ELAST MOD (PSI 10^{-5})
PPG571	5	.50	74	0.025	9780	245	1.60	11950	527	0.474	0.038	3.64	0.129	B	8944	1.46	10153	0.344	3.24
PPG571	5	.50	75	0.025	10027	105	1.61	10914	1284	0.419	0.132	3.47	0.038						
SK541	4	.94	75	0.022	10106	133	1.77	13283	379	0.596	0.016	3.65	0.103	B	9550	1.67	11706	0.530	3.23
SK605	5	.50	72	0.025	9509	127	1.50	12497	165	0.568	0.011	3.13	0.179	B	9076	1.43	11936	0.531	2.55
SK605	2	.50	-30	4.44	13148	530	1.56	16773	75	0.388	0.096	2.65	0.213						
SK605	3	.50	195	4.44	7961	173	1.47	10170	1286	0.651	0.090	2.12	0.377						
SWU605	5	.50	75	4.44	10221	74	1.60	13901	610	0.580	0.023	2.88	0.429	B	9970	1.56	11822	0.501	1.44
SWU605	5	.50	-30	4.44	12484	735	1.50	15894	803	0.485	0.021	2.91	0.268	B	9978	1.20	13159	0.412	2.67
SWU605	6	.50	195	4.44	7128	190	1.56	10771	1662	0.645	0.111	2.15	0.066	C	6769	1.48	7622	0.434	2.14
SWU605RH	5	.50	75	4.44	10401	638	1.57	13702	395	0.564	0.034	2.65	0.357	B	8227	1.24	12354	0.446	1.56
SWU605RH	5	.50	-30	4.44	13224	1093	1.34	16210	1011	0.447	0.075	2.90	0.406	C	10874	1.10	14036	0.285	2.15
SWU605RH	6	.50	195	4.44	7137	146	1.56	11972	1094	0.700	0.022	2.39	0.255	B	6700	1.46	8682	0.632	1.89
TEX571	4	.50	72	0.025	9362	139	1.53	12360	790	0.539	0.016	3.09	0.056						
TEX571RH	6	.50	72	0.025	9030	96	1.52	13203	1416	0.548	0.069	2.99	0.038	B	8741	1.47	8945	0.341	2.96
TEX605	5	.50	75	4.44	10317	87	1.67	13915	698	0.556	0.018	2.77	0.330	B	10020	1.62	11538	0.495	1.95
TEX605	5	.50	-30	4.44	13605	1598	1.49	17369	2464	0.448	0.033	3.01	0.518	C	8186	0.89	12071	0.377	1.48
TEX605	6	.50	195	4.44	7448	283	1.60	10554	1708	0.658	0.073	2.45	0.234	C	6913	1.48	7317	0.519	2.38
TEX605X	6	.50	72	4.44	11043	94	0.68	14277	672	0.545	0.042	1.02	0.115	B	10762	0.66	12257	0.420	0.79

* Number of specimens included in the generation of data presented.

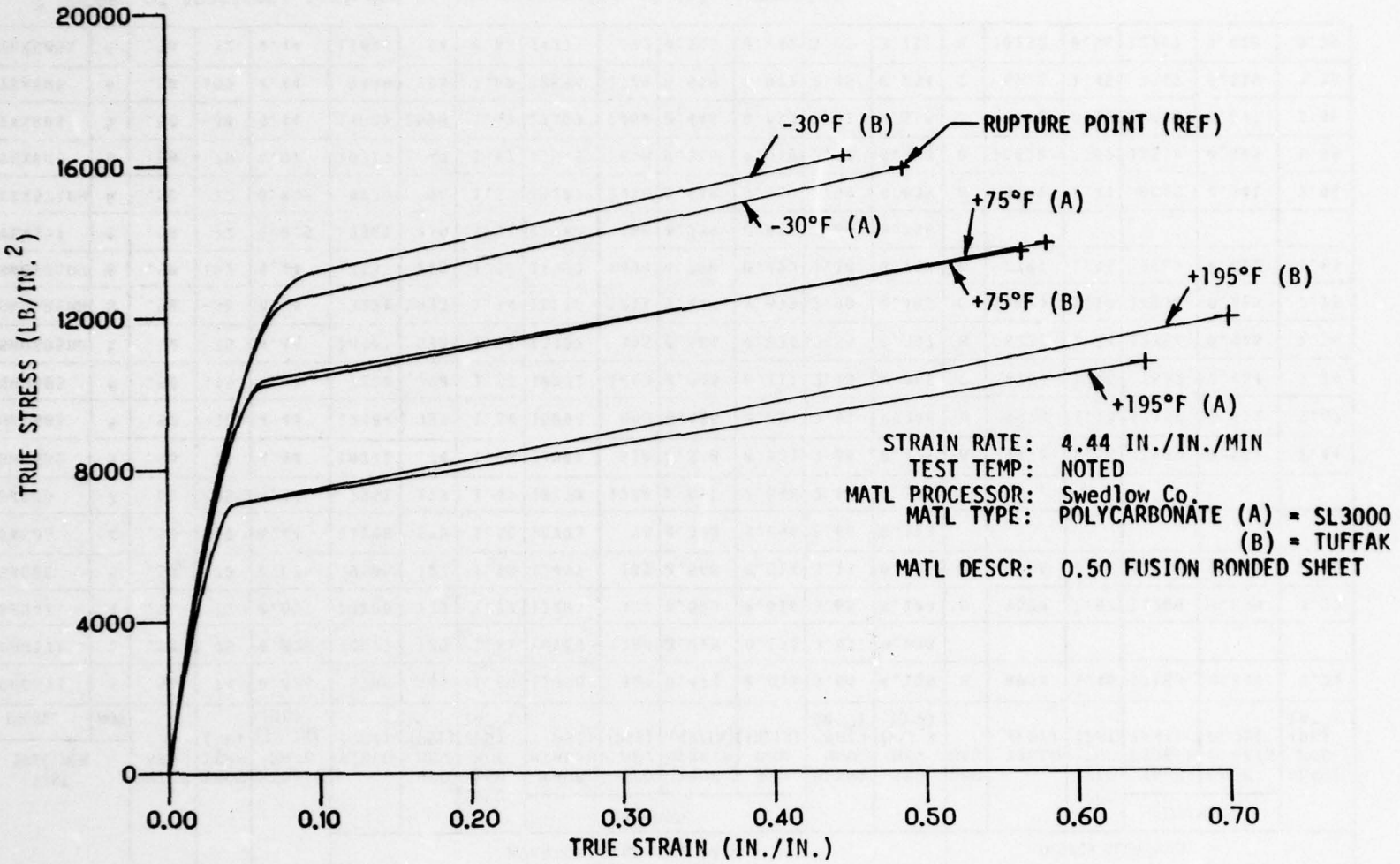

Figure 29. Tensile Average Curves - Material Comparisons.

Processing Effects

A plot of the average tensile stress-strain curves comparing processed monolithic and fusion bonded SL3000 polycarbonate sheet material from four transparency fabricators are presented in Figures 30 and 31. Average curves are the same as contained in Appendix A for strength data in Tables 12 and 13. It can be noted that a definite difference exists in the plastic range of the stress-strain curves due to the different processing methods of the four transparency fabricators represented. Note that material processing affects plastic properties, and to some extent elastic properties of polycarbonate materials. This results in changes in elastic modulus, yield strength, secant modulus, rupture stress, and rupture strain mechanical properties. The stress-strain curve with the least strain at rupture (the shortest curve) indicates the least ductile processed material, and the curve with the greatest strain at rupture (the longest curve) indicates the most ductile processed material.

Forming Effects

A plot of average tensile stress-strain curves comparing processed fusion bonded SL3000 polycarbonate sheet material removed from several formed test canopies are presented in Figure 32. Average curves are the same as contained in Appendix A for strength data in Table 11. It is noted that forming affects elastic and plastic tensile properties of polycarbonate materials. Forming appears to decrease elastic modulus, yield strength, secant modulus, rupture stress, and rupture strain values at the 10 percent level. Little change is noted up to the 8 percent reduction in thickness.

Strain Rate Effects

A plot of average tensile stress-strain curves comparing processed monolithic and fusion bonded SL3000 polycarbonate materials at two strain rates is presented in Figures 33 and 34. The stress-strain curves presented are a general industry average of like materials as processed by several transparency fabricators and is the same test data used to

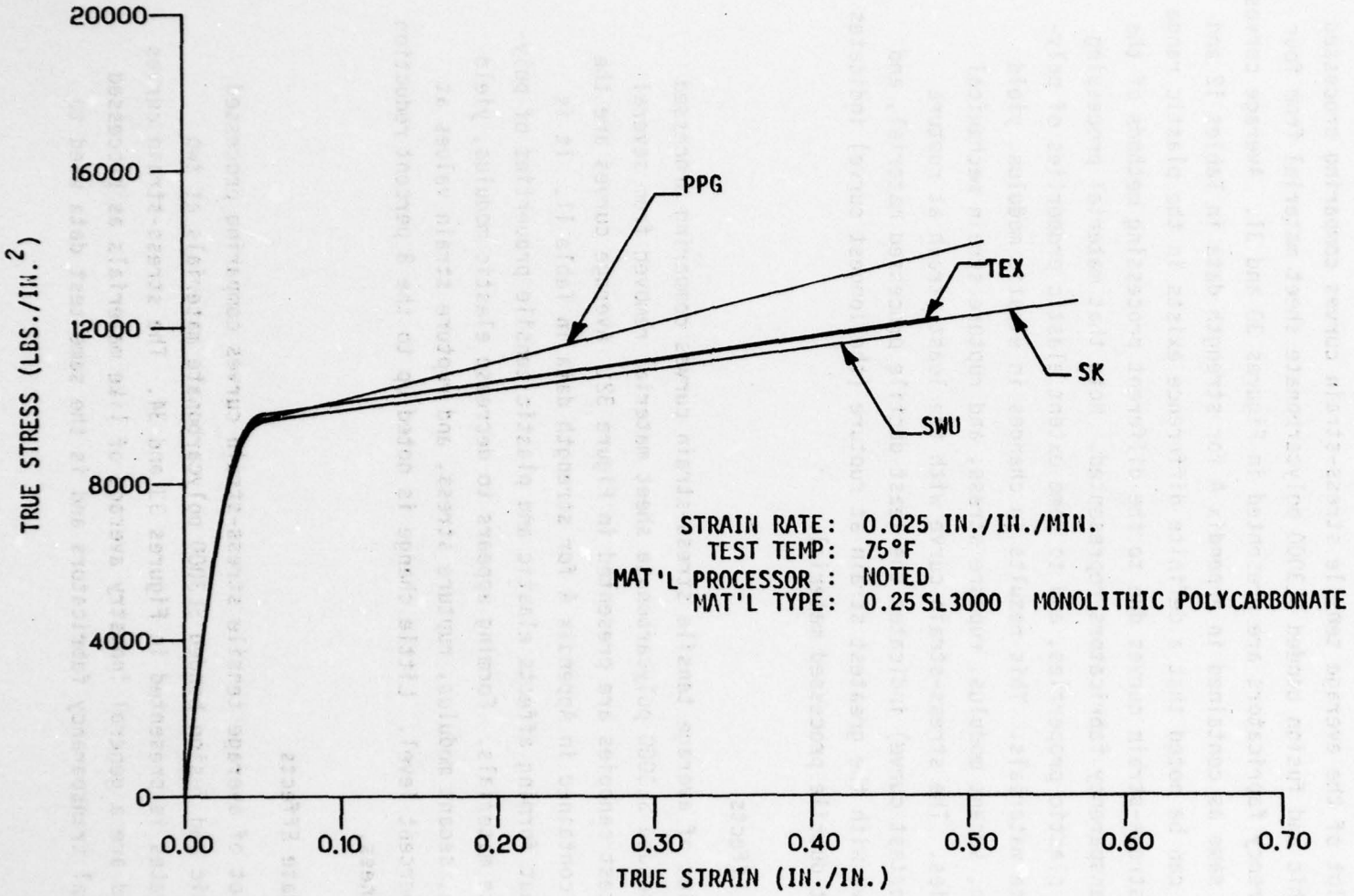

Figure 30. Tensile Average Curve - Processing Effects.

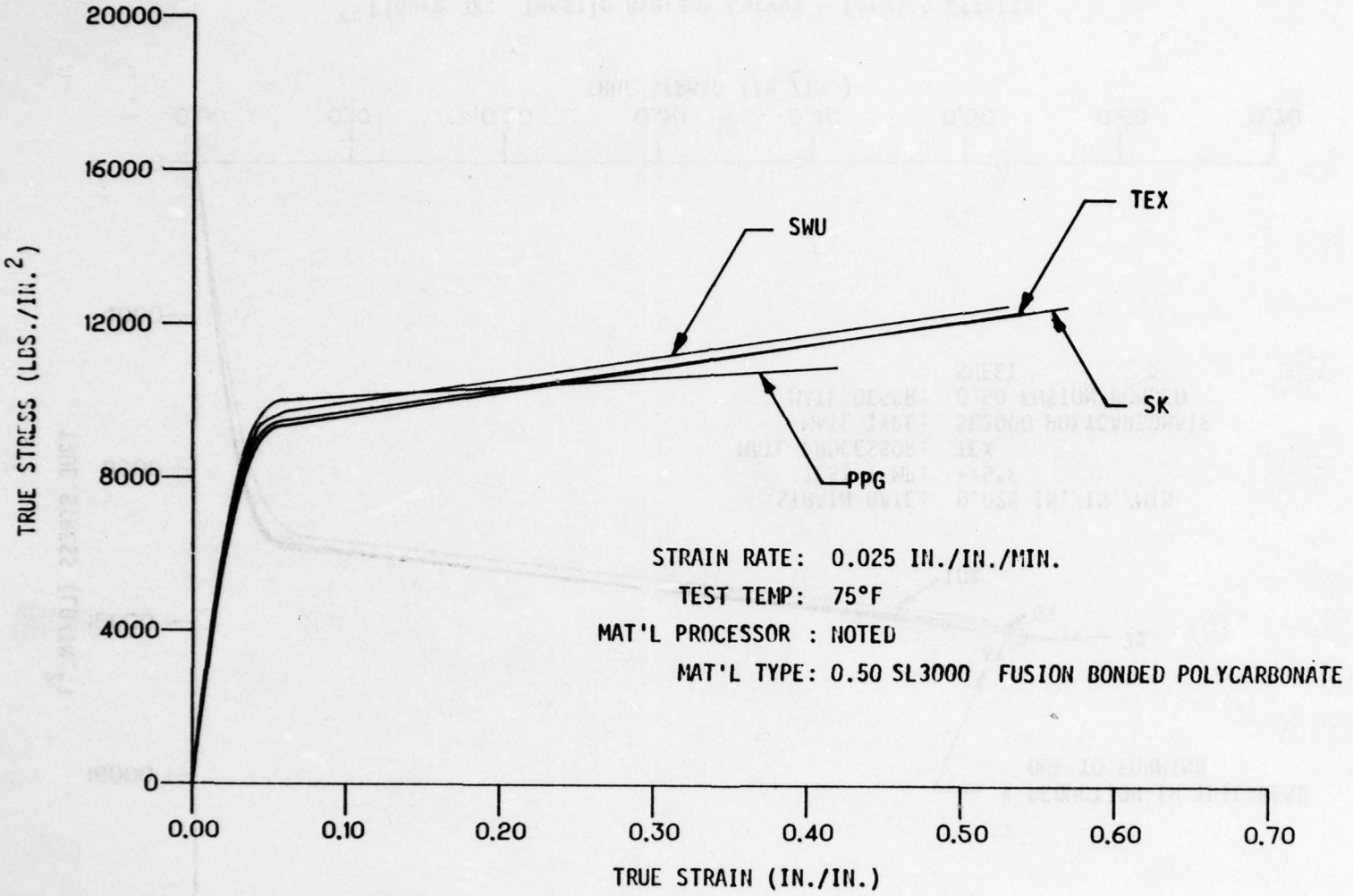

Figure 31. Tensile Average Curve - Processing Effects.

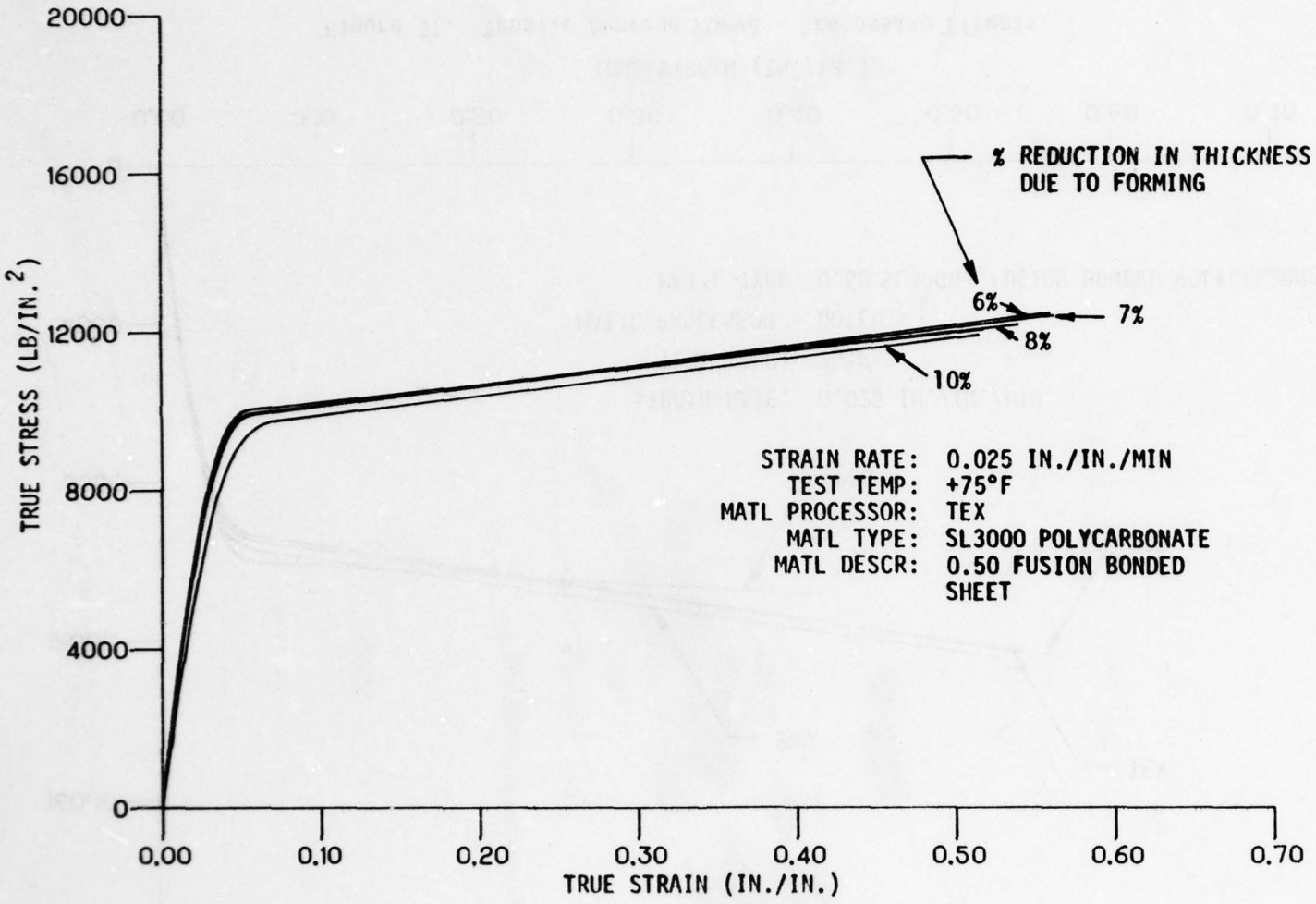

Figure 32. Tensile Average Curves - Forming Effects.

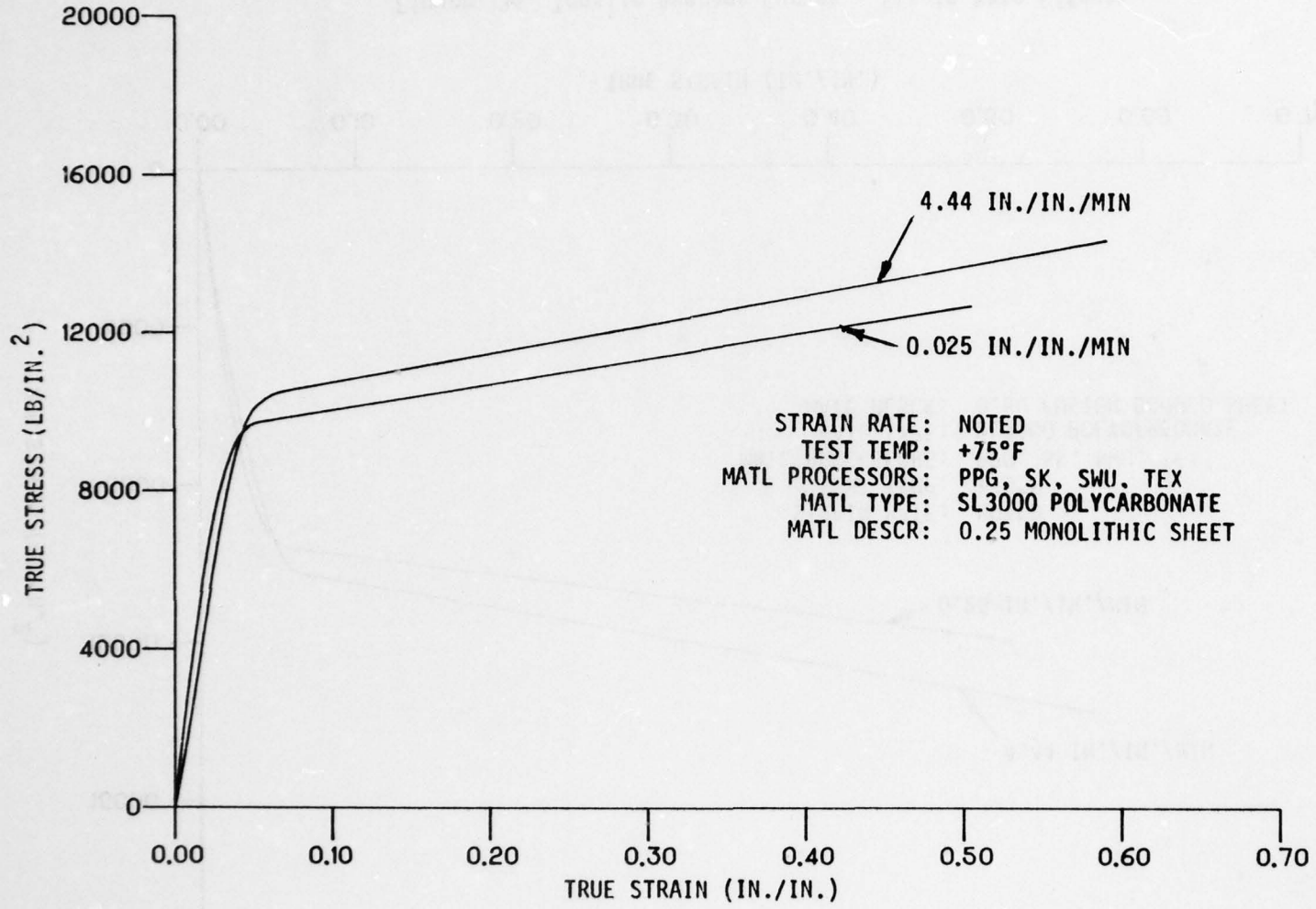

Figure 33. Tensile Average Curves - Strain Rate Effects.

AD-A064 436 DOUGLAS AIRCRAFT CO LONG BEACH CALIF F/G 11/9
TESTING FOR MECHANICAL PROPERTIES OF MONOLITHIC AND LAMINATED P--ETC(U)
OCT 78 F E GREENE, L P KOEGEBOEHN F33615-75-C-3105
UNCLASSIFIED MDC-J6950 AFFDL-TR-77-96-PT-1 NL

2 OF 5
AD
AD A064436

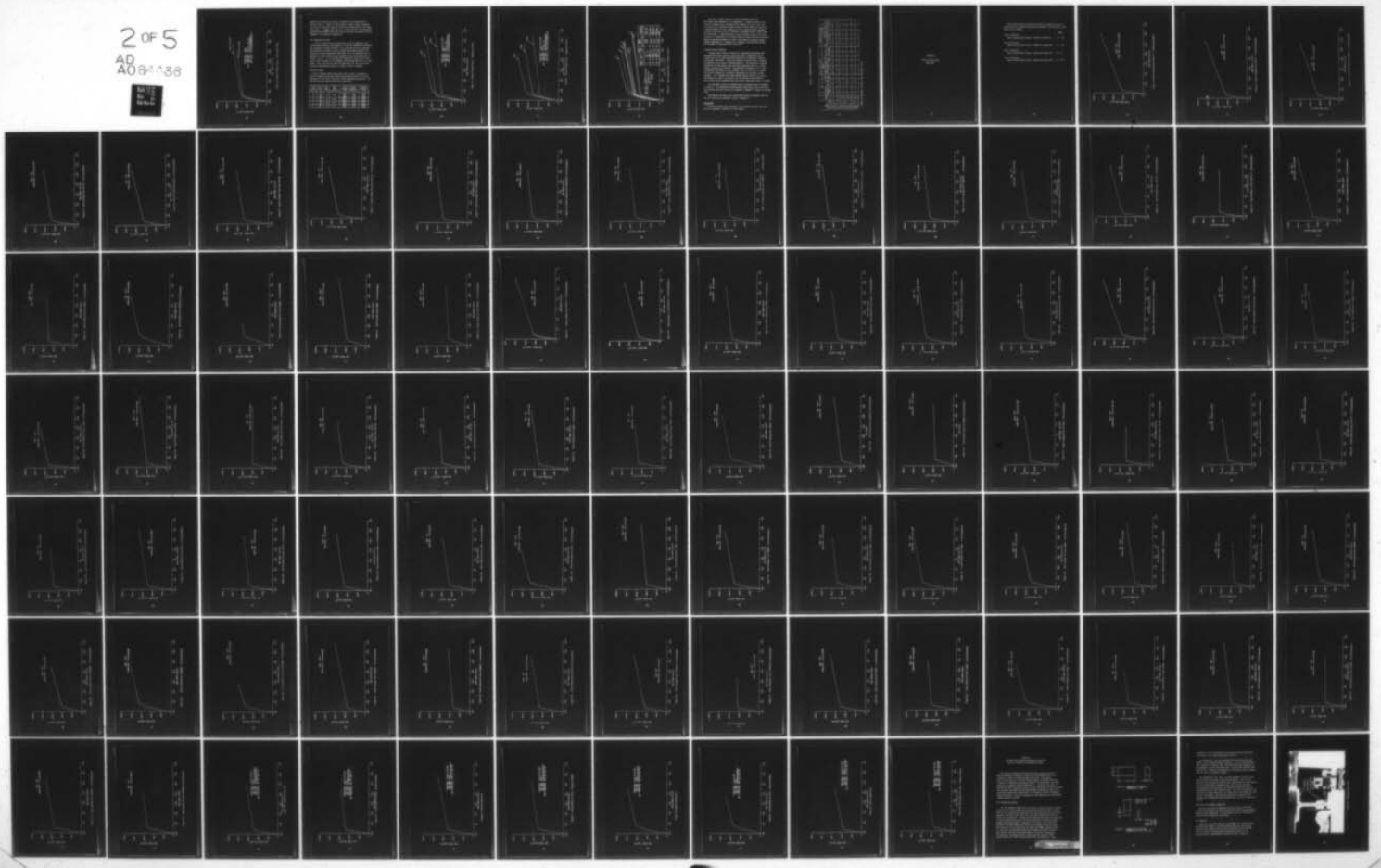

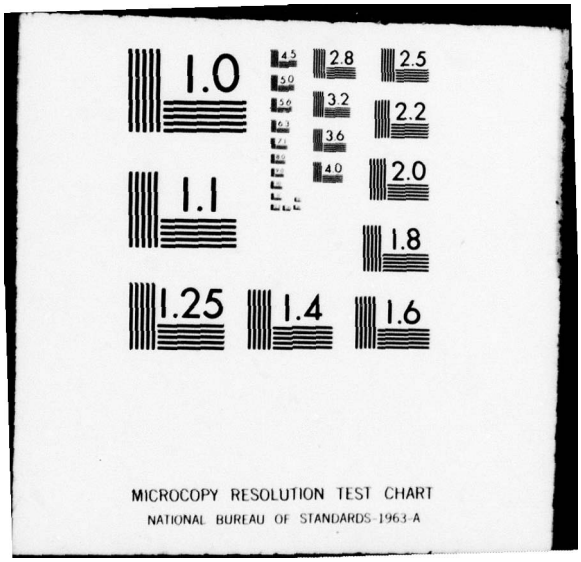
1.0
1.1
1.25
1.4
1.6
1.8
2.0
2.2
2.5
2.8
3.2
3.6
4.0
4.5
5.0
MICROCOPY RESOLUTION TEST CHART
NATIONAL BUREAU OF STANDARDS-1963-A

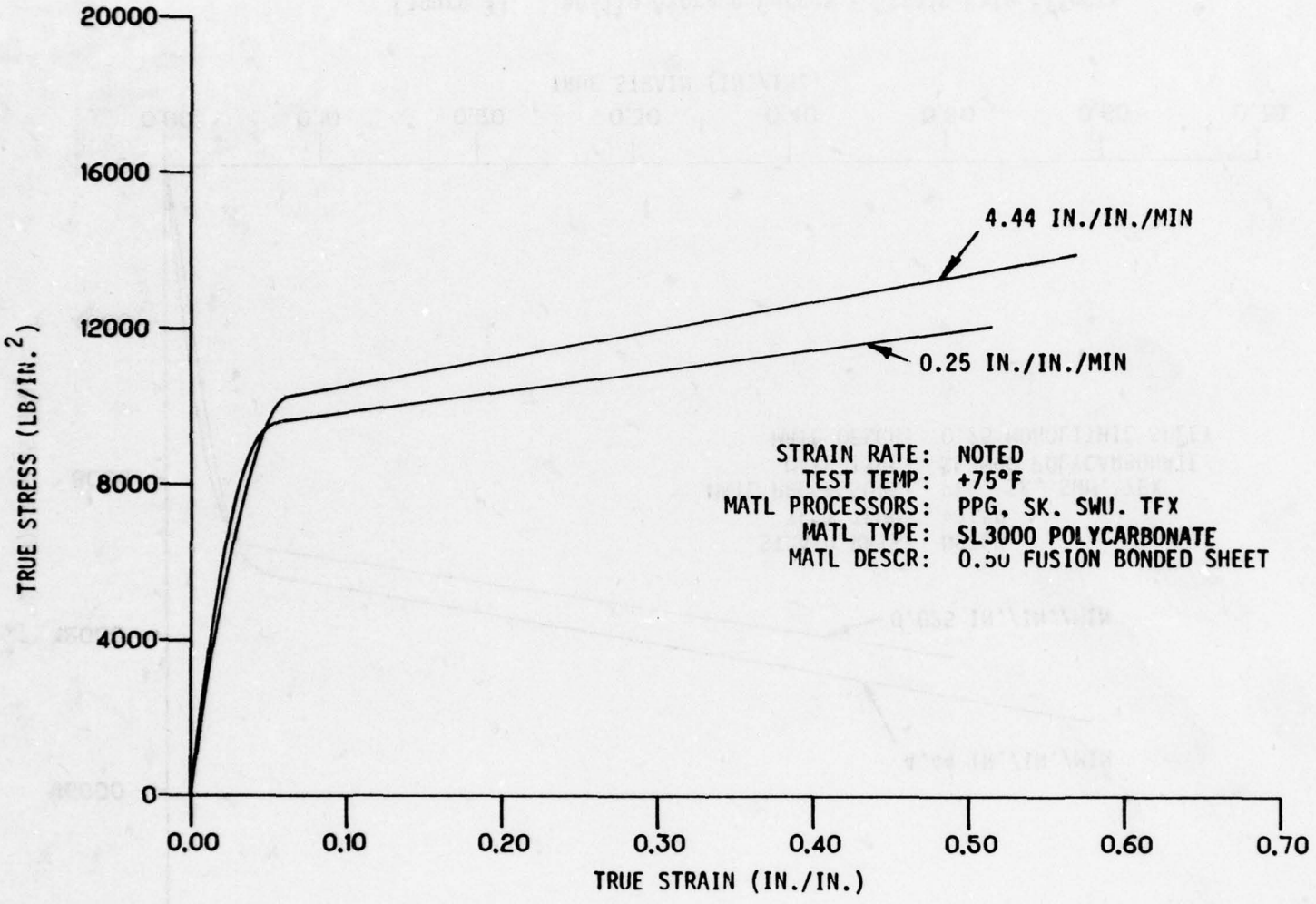

Figure 34. Tensile Average Curves - Strain Rate Effects.

generate the stress-strain curves in Appendix A and strength data in Tables 12 and 13. Figures 33 and 34 reveal a higher relative toughness for both 0.25 monolithic sheet and 0.50 fusion bonded sheet at the higher strain rate. It appears that the 4.44 in./in./min strain rate more nearly approaches the assumed ideal strain rate to generate the greatest relative toughness of the material (Reference 9).

Test Temperature Effects

A plot of average tensile stress-strain curves for monolithic and fusion bonded processed polycarbonate at three test temperature conditions are presented in Figures 35 and 36. The stress-strain curves presented were generated from tensile tests of SL3000 polycarbonate materials as processed by three transparency fabricators and is the same data used to generate the stress-strain curves in Appendix A and the strength data in Tables 11 and 12. It can be noted that temperature affects elastic and plastic tensile properties of processed polycarbonate materials to a large extent. Also note that the lower the temperature the less ductile the processed polycarbonate material is, based on strain to rupture.

Thickness Effects

A plot of average tensile **true** stress-strain curves is presented in Figure 37 comparing processed SL3000 polycarbonate materials of various thicknesses at two strain rates and at three temperature conditions. The affected strength properties data are listed below.

Curve Ident (Fig 34)	Thickness (in)	Test Temp (°F)	Strain Rate (in/In/Min)	Yield Strength (PSI)	Elastic Modulus (PSIX10-5)	Relative Toughness (PSI)
A	.16	75	0.025	9325	3.41	6302
B	.25			9747	3.50	5409
C	.50			9665	3.44	5335
D	.25	75	4.44	10510	2.20	6944
E	.50			10276	2.90	6517
F	.25	-30	4.44	13105	2.93	6193
G	.50			12910	2.72	6129
H	.25	195	4.44	7733	1.75	5920
J	.50			7457	2.12	5652

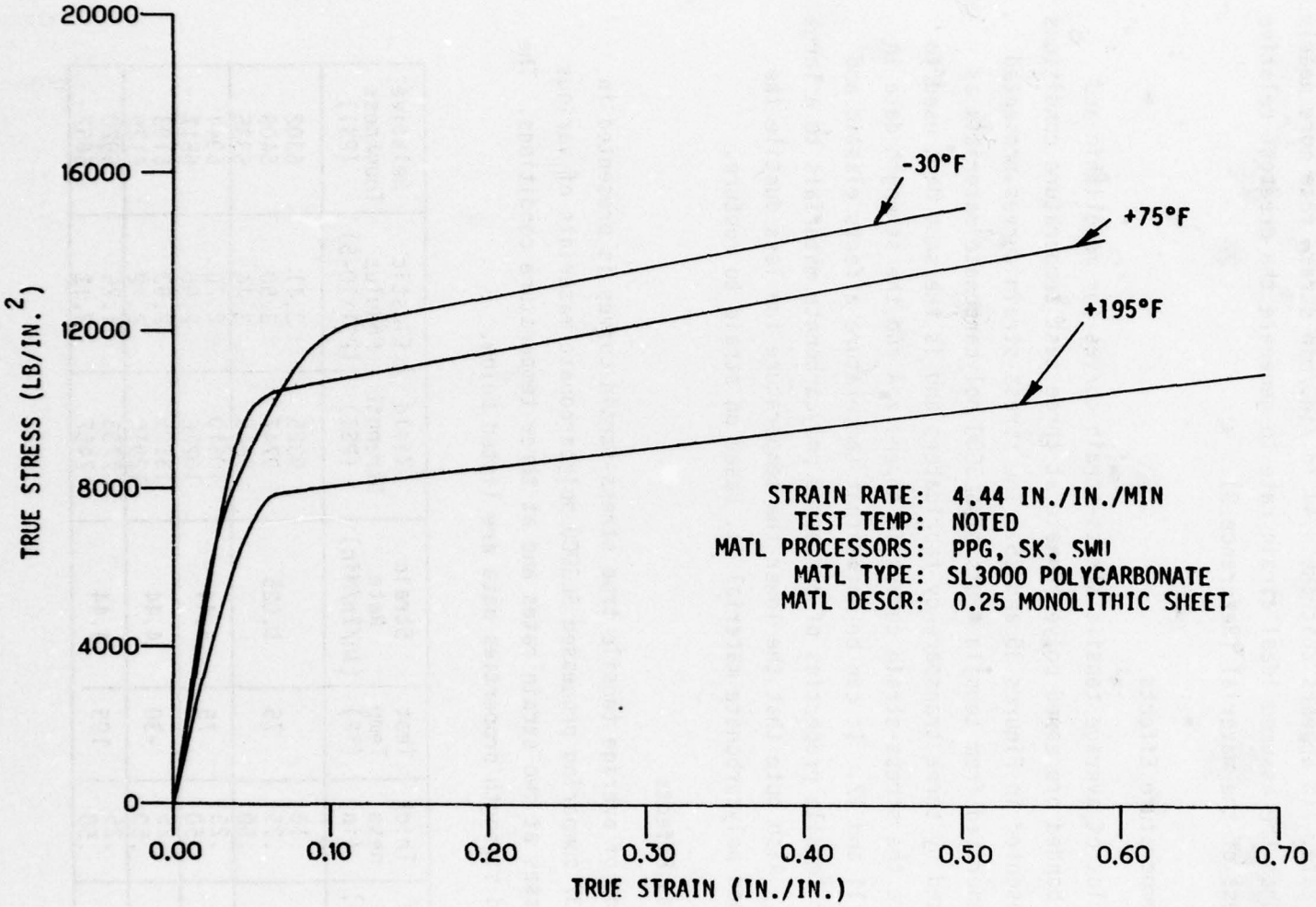

Figure 35. Tensile Average Curves - Temperature Effects.

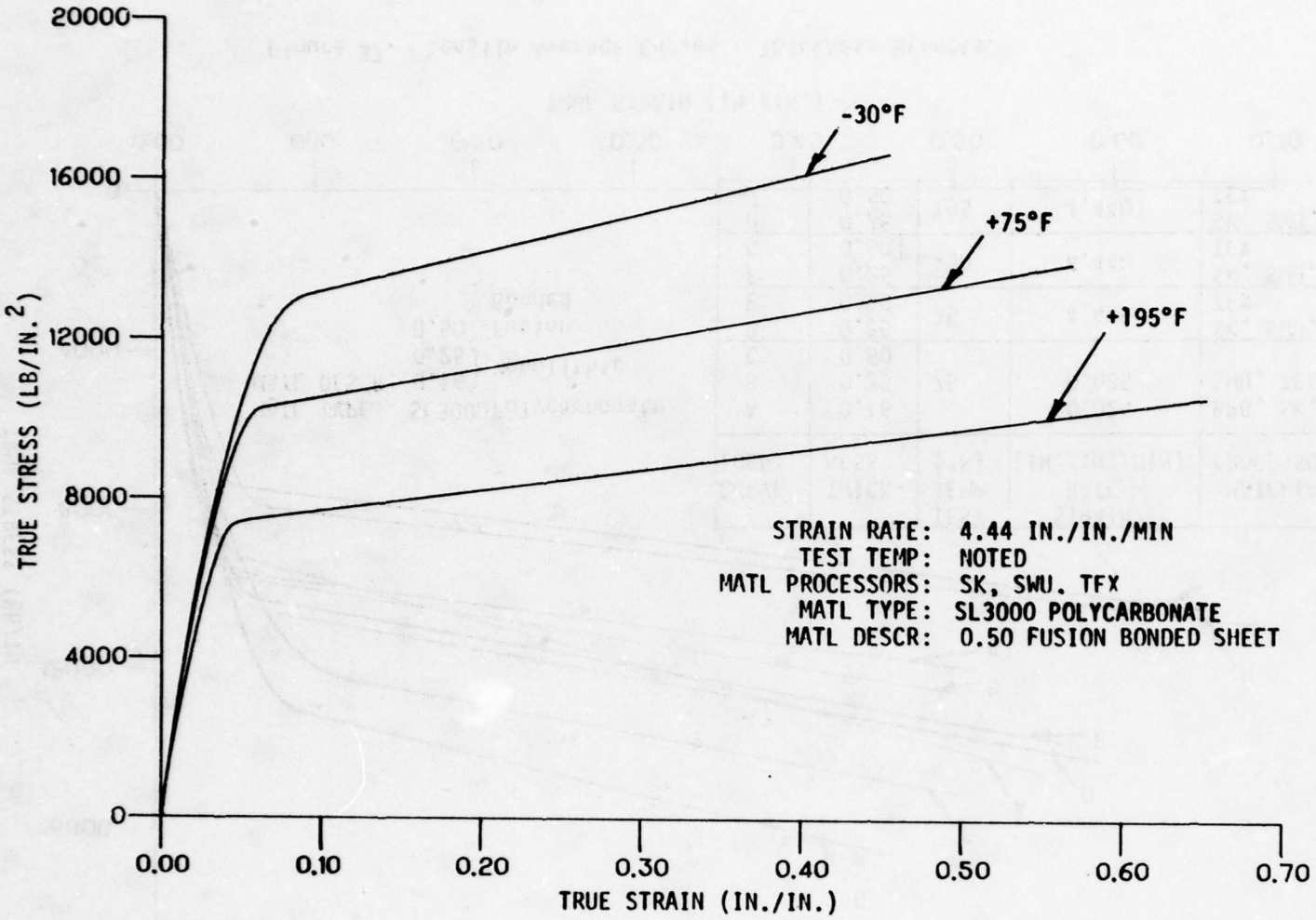

Figure 36. Tensile Average Curves - Temperature Effects.

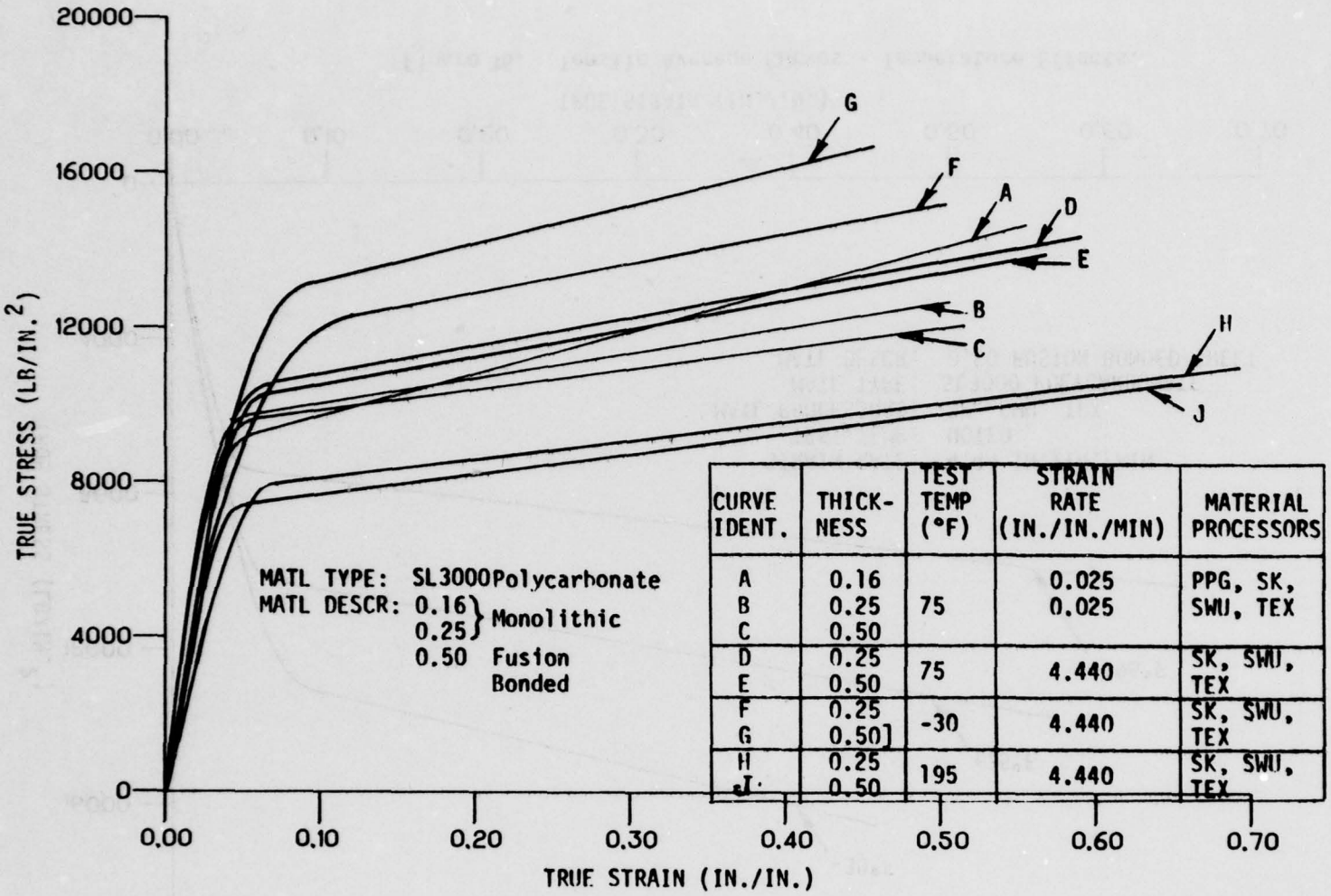

CURVE IDENT.	THICK-NESS	TEST TEMP (°F)	STRAIN RATE (IN./IN./MIN)	MATERIAL PROCESSORS
A	0.16	75	0.025	PPG, SK, SWU, TEX
B	0.25		0.025	
C	0.50			
D	0.25	75	4.440	SK, SWU, TEX
E	0.50			
F	0.25	-30	4.440	SK, SWU, TEX
G	0.50			
H	0.25	195	4.440	SK, SWU, TEX
I	0.50			

Figure 37. Tensile Average Curves - Thickness Effects.

Note that a slight increase in relative toughness exists for the thinner test specimens at all temperatures. A marked increase in the relative toughness with a decreased yield strength for curve A over that of curves B and C indicates thickness effect at these noted test conditions. A marked decrease in elastic modulus with an increased relative toughness of curve H over that of curve J indicates a thickness effect at these noted test conditions. A marked decrease in yield strength of curve G over that of curve F is indicative of a thickness effect at these noted test conditions. Based on conclusions reached for strain rate effects on previous investigations (Reference 14) it appears that thickness is not the only variable, but thickness in combination with strain rate.

Proposed Design Allowables

Proposed tensile design allowables for processed polycarbonate were developed from tensile test data previously used in determining design strength data for SL 3000 polycarbonate material as processed by specific transparency fabricators. These were combined to provide design allowables representing a wide range of processed material. The fabrication processes represented include drying, press polishing, mechanical polishing, fusion bonding, forming, and laminating. Representative specimens from all known transparency fabricators are not included, but it is felt that all normal fabrication processes of a laminated transparency are included in these averages. It is intended that these proposed design allowables be used by the designer for static load analysis and for material test minimums in design specification documents where the specific fabrication source is unknown.

The developed averages and proposed design allowables data are presented in Table 14. The average and proposed design stress-strain curves from which the tabulated data were derived are presented in Appendix A, Figures A76 through A 83.

Experimental test data, test stress-strain curves and computer data runs for this analysis are contained in Part 2, Appendix H.

Conclusions

Conclusions based on data presented in this section and other applicable data are contained in Section XI of this report.

TABLE 14. PROPOSED TENSILE DESIGN ALLOWABLES

TEST SPECIMEN IDENT	NO.*	THICKNESS	TEST TEMP (°F)	STRAIN RATE (IN./IN. MIN)	AVERAGE STRENGTH DATA: YIELD (PSI)	STD DEV (PSI)	SEC YLD MOD (PSI 10^{-5})	ULTIMATE: TRUE STRESS (PSI)	STD DEV (PSI)	TRUE STRAIN (IN./IN.)	STD DEV (IN/IN)	ELAST MOD (PSI 10^{-5})	STD DEV (PSI x 10^{-5})	PROPOSED DESIGN ALLOWABLE: DES BAS	YIELD (PSI)	SEC YLD MOD (PSI 10^{-5})	ULTIMATE: TRUE STRESS (PSI)	ULTIMATE: TRUE STRAIN (IN/IN)	ELAST MOD (PSI 10^{-5})
PPG503 SK503 SWU503 TEX503	17	.25	75	0.025	9750	98	1.75	12673	1260	0.508	0.049	3.50	0.110	C	9632	1.72	11136	0.450	3.39
PPG503 SK503 SWU605 TEX605	20	.25 .25 .50 .50	75	4.44	10419	202	1.51	14159	1219	0.581	0.041	2.47	0.510	C	10196	1.47	12815	0.540	1.93
PPG503 SK503 SWU503 SK605 SWU605 TEX605	25	.25 .25 .25 .50 .50 .50	-30	4.44	12910	1284	1.06	15869	1708	0.468	0.084	2.72	1.270	C	11506	0.94	14002	0.380	1.36
PPG503 SK503 SWU503 SK605 TEX605	24	.25 .25 .25 .50 .50	195	4.44	7733	374	1.07	10755	1273	0.671	0.067	1.81	0.460	C	7337	1.02	9407	0.600	1.42

* Number of specimens included in the generation of data.

APPENDIX A

TENSILE STRESS-STRAIN CURVE DATA

The following tensile stress-strain curves are presented for use in conjunction with tabulated strength data presented in the following listed tables of this section.

PAGES

Table 11 (Page 78)

Tensile stress-strain curves - Figures A1 through A14 . . . 97 - 110

Table 12 (Page 80)

Tensile stress-strain curves - Figures A15 through A43 . .110 - 139

Table 13 (Page 81)

Tensile stress-strain curves - Figures A44 through A75 . .140 - 171

Table 14 (Page 94)

Tensile stress-strain curves - Figures A76 through A83 . .172 - 179

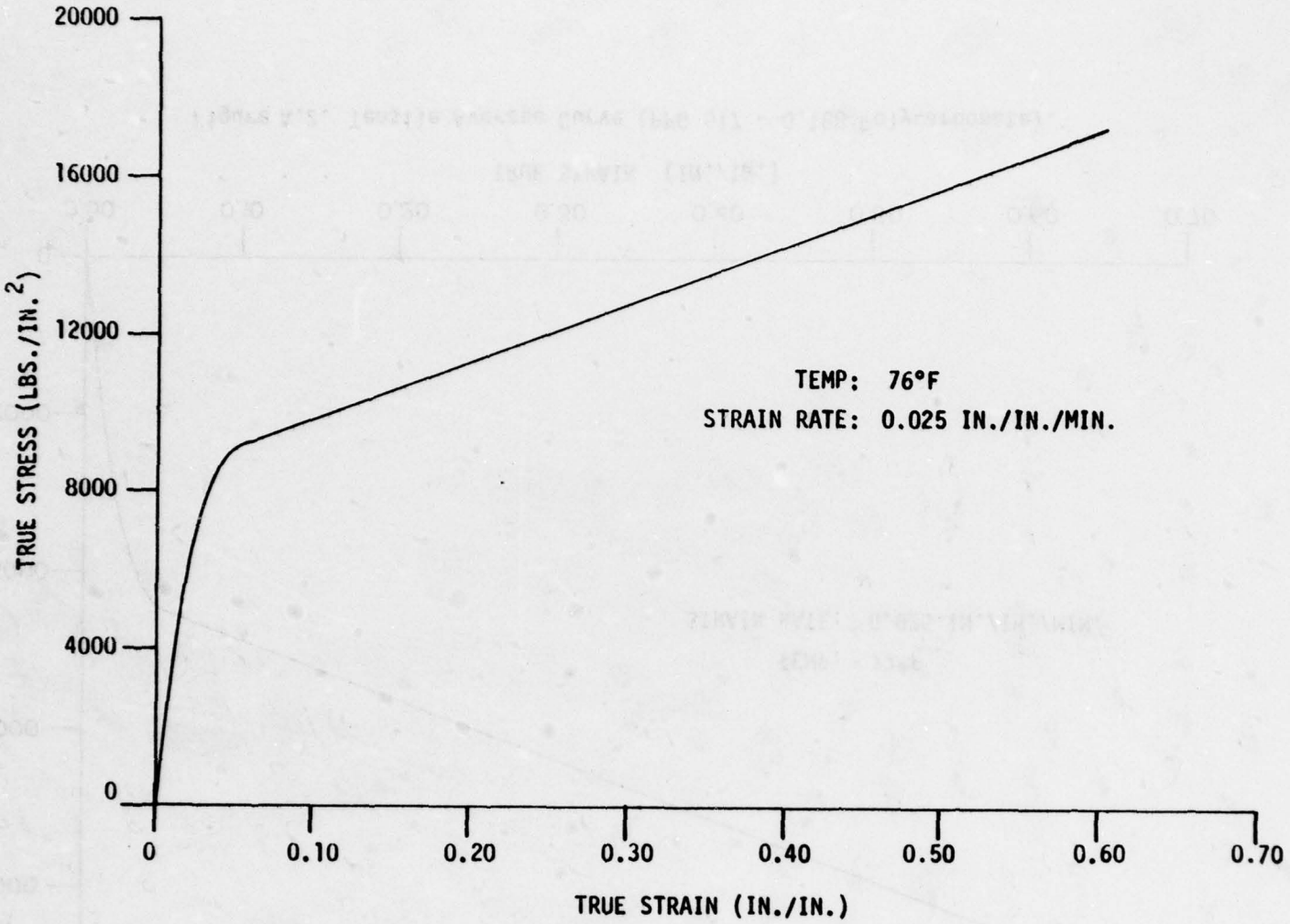

Figure A.1.Tensile Average Curve (PPG 517 - 0.188 Polycarbonate).

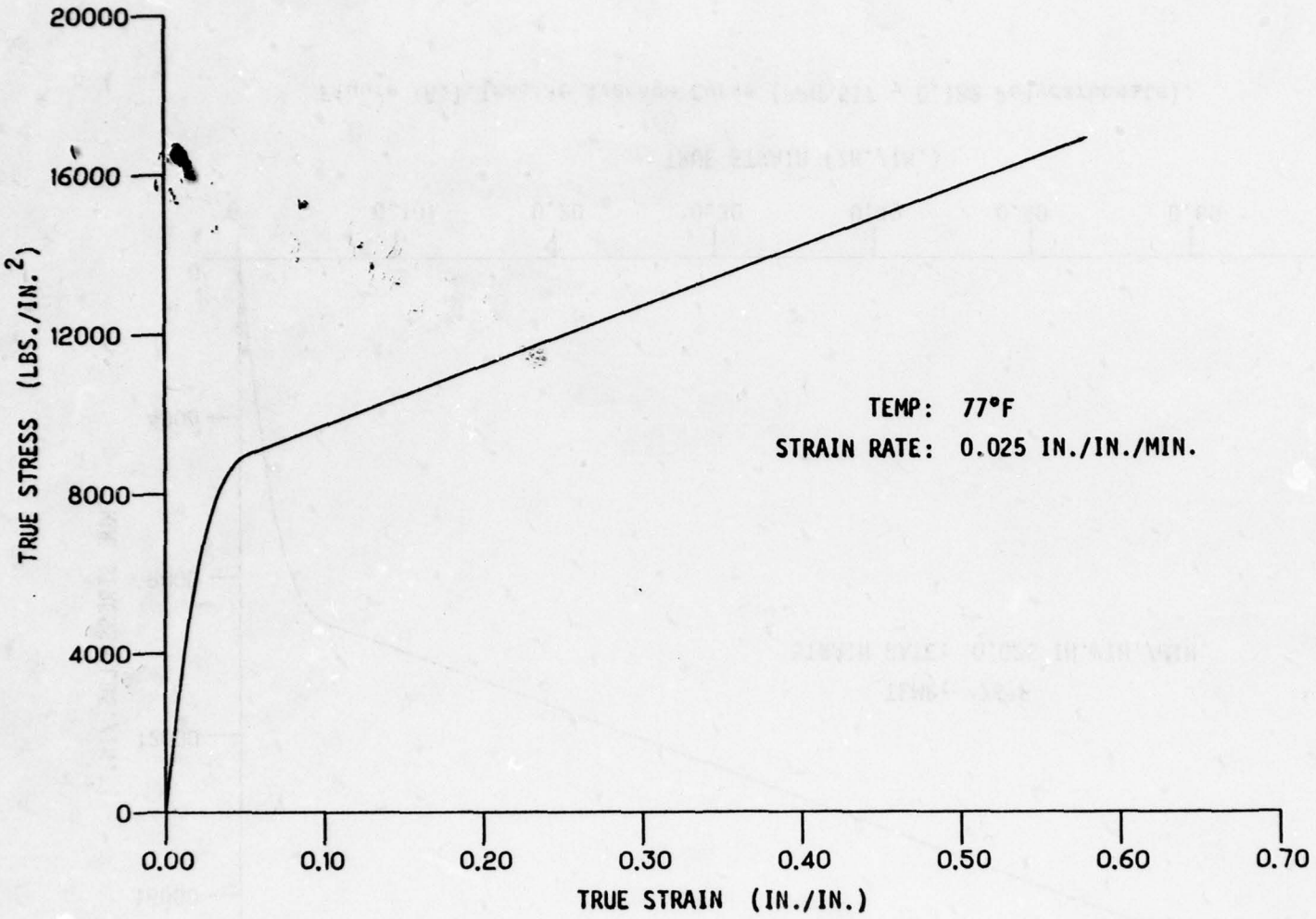

Figure A.2. Tensile Average Curve (PPG 517 - 0.188 Polycarbonate).

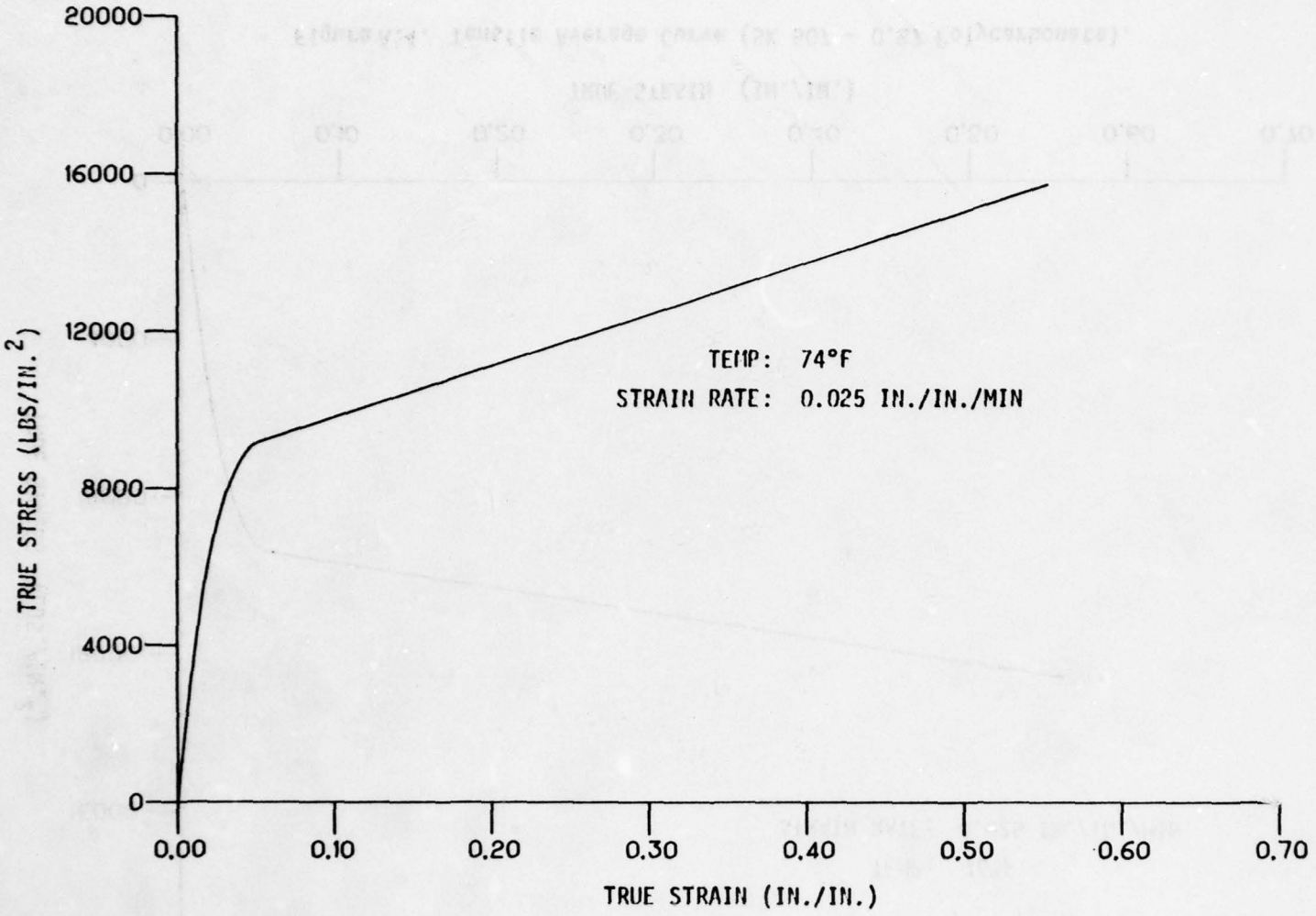

Figure A.3. Tensile Average Curve (PPG517D - 0.19 Polycarbonate).

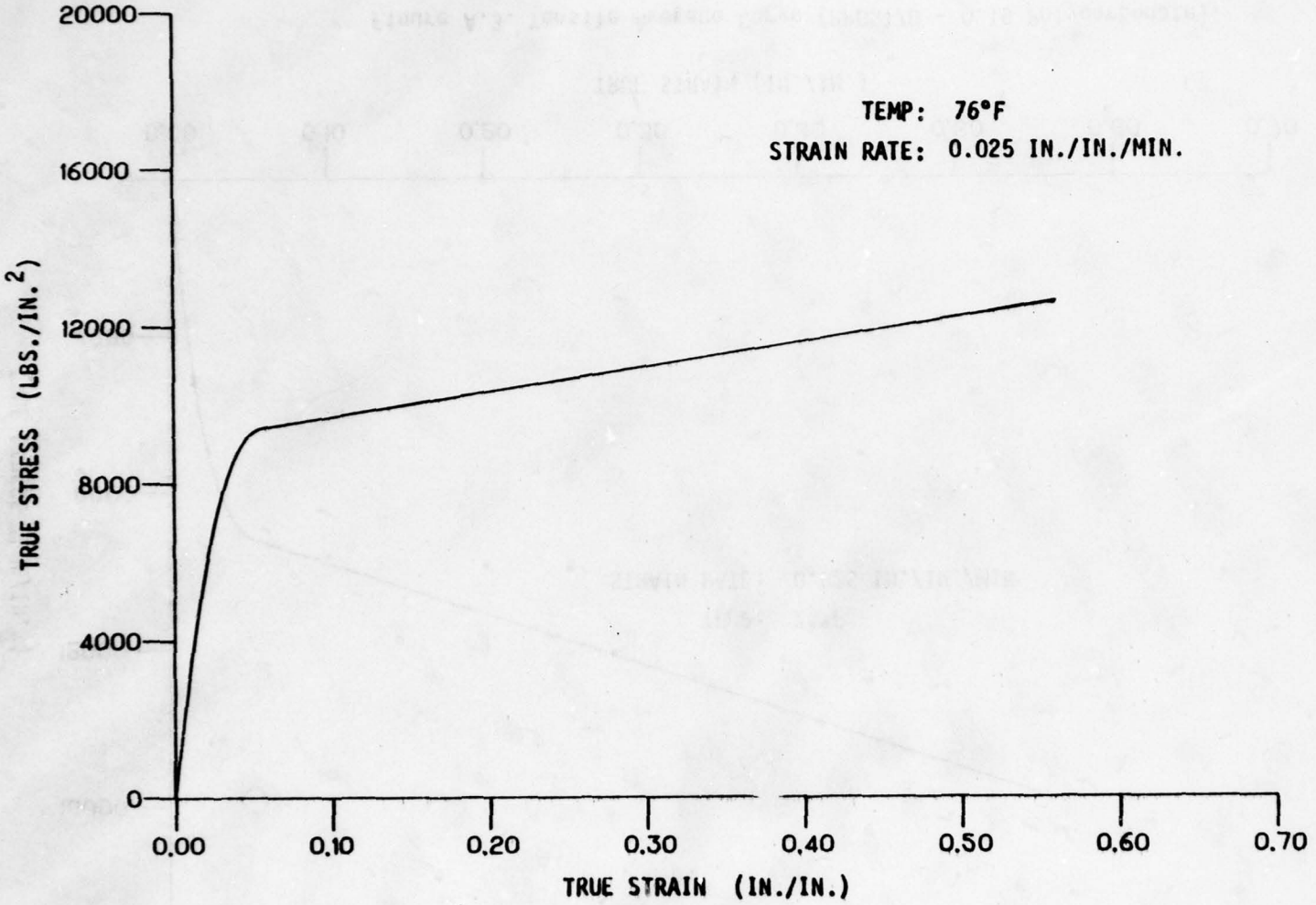

Figure A.4. Tensile Average Curve (SK 507 - 0.87 Polycarbonate).

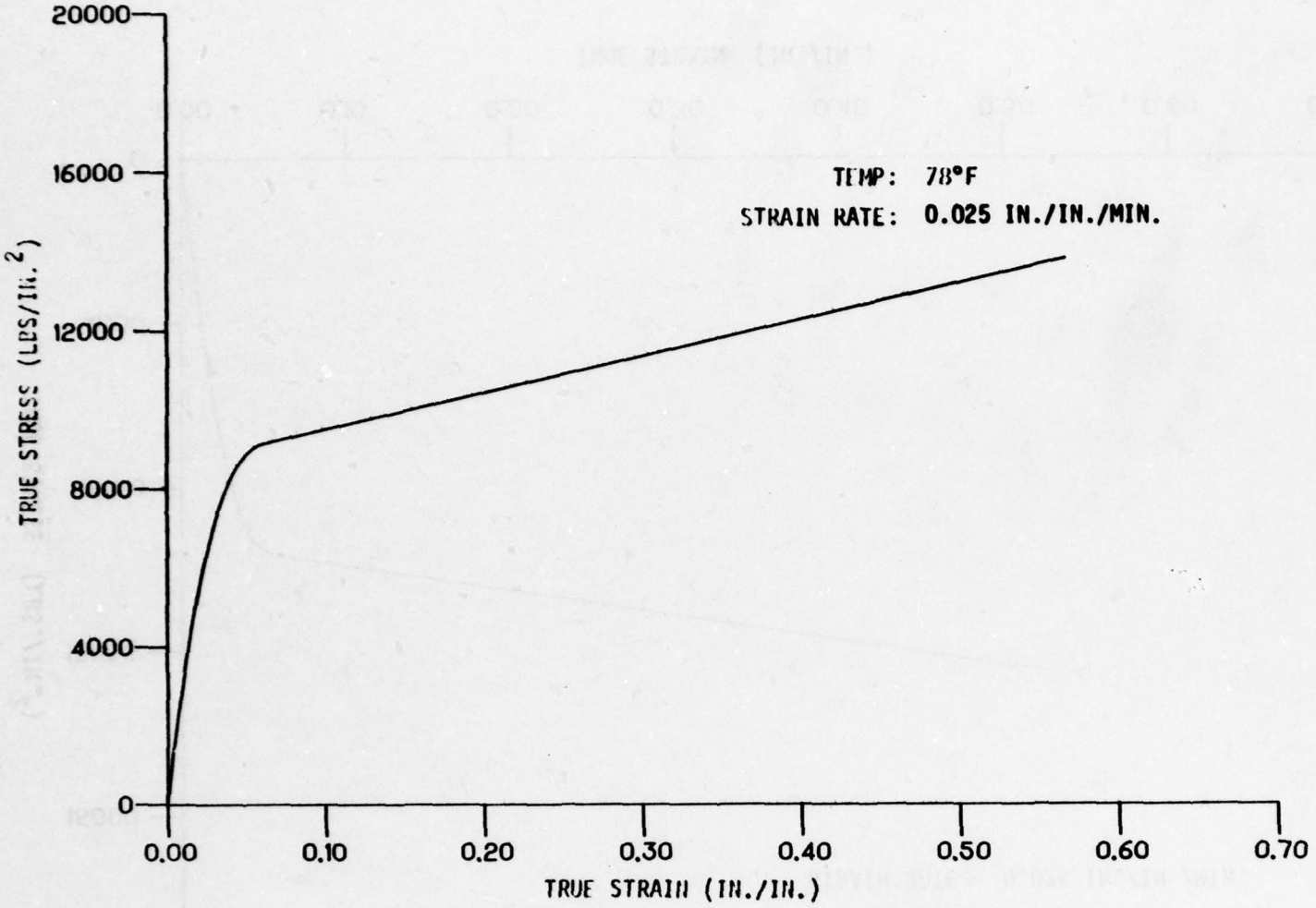

Figure A.5. Tensile Average Curve (SK509 - 0.150 Polycarbonate).

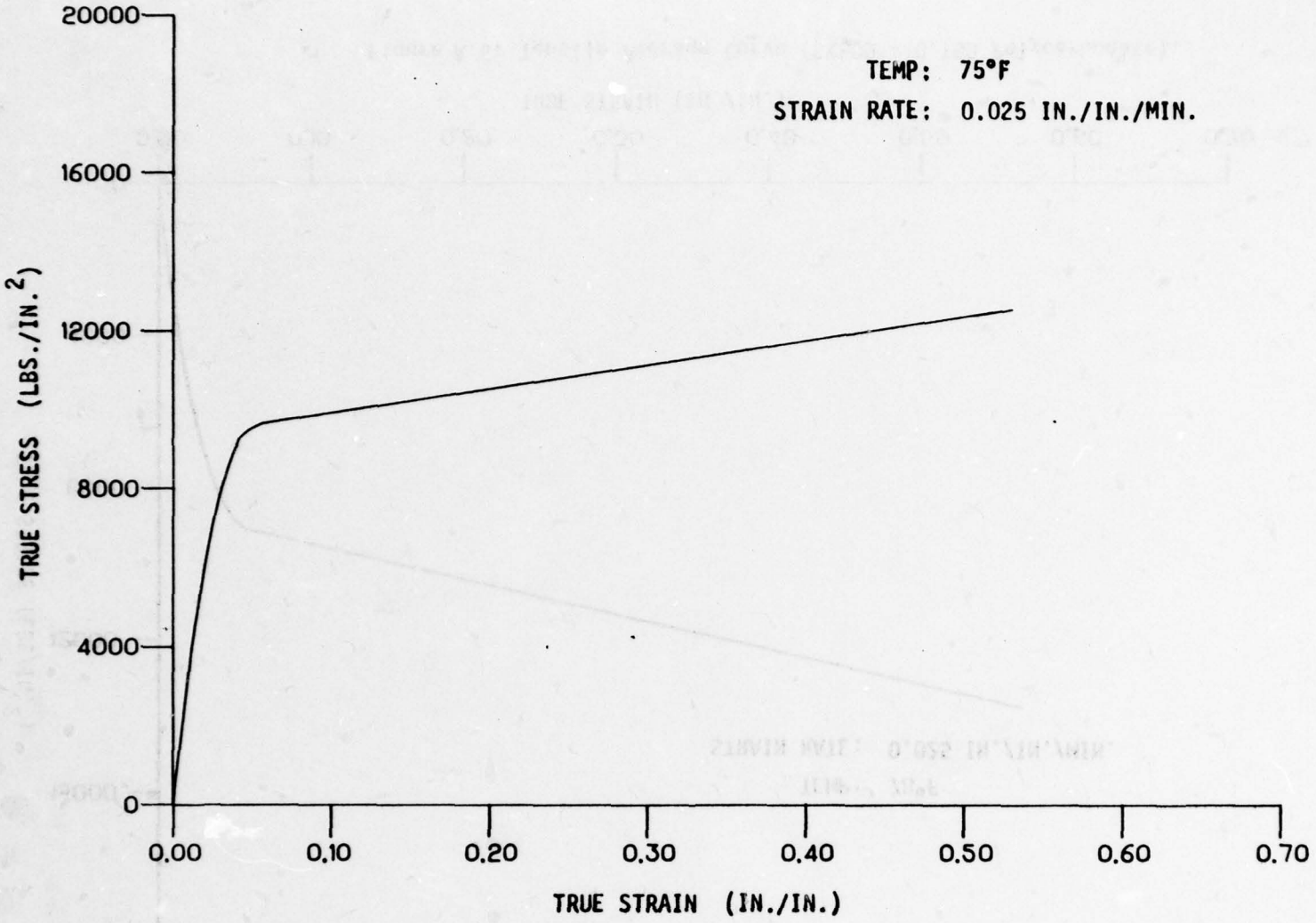

Figure A.6. Tensile Average Curve (SWU 541(108) - 0.87 Polycarbonate).

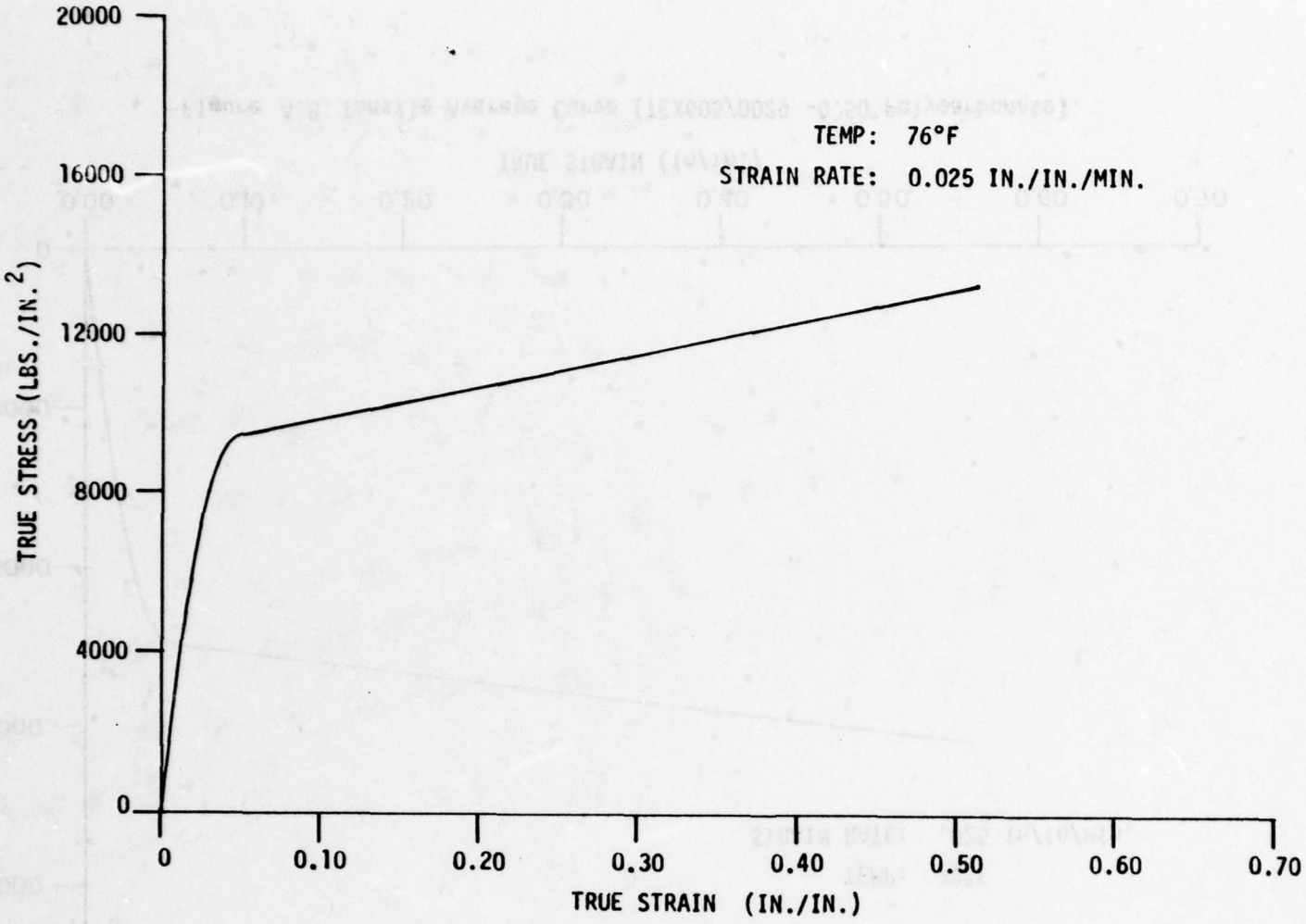

Figure A.7. Tensile Average Curve (SWU 543 108 - 0.155 Polycarbonate).

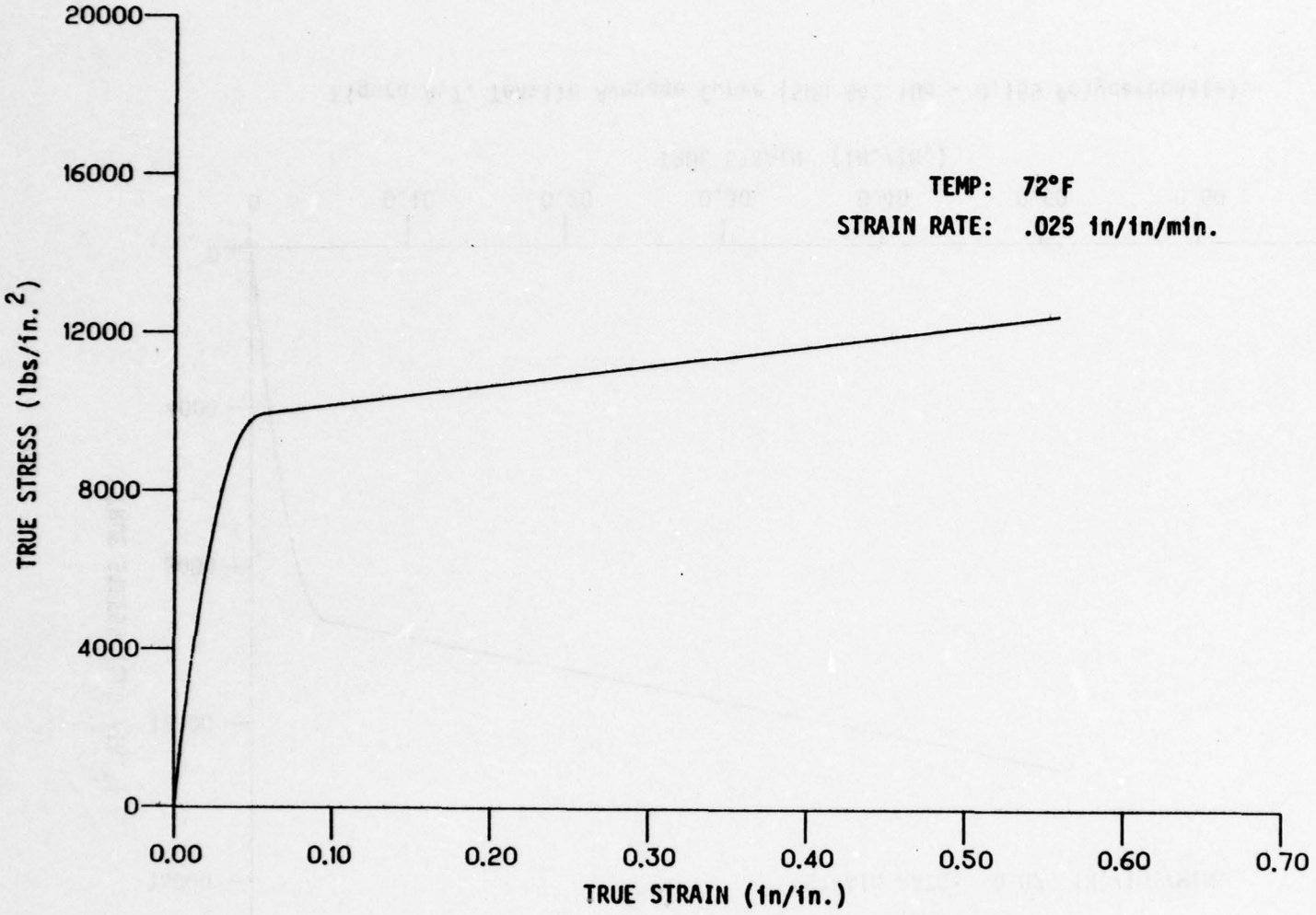

Figure A.8. Tensile Average Curve (TEX605/0029 -0.50 Polycarbonate).

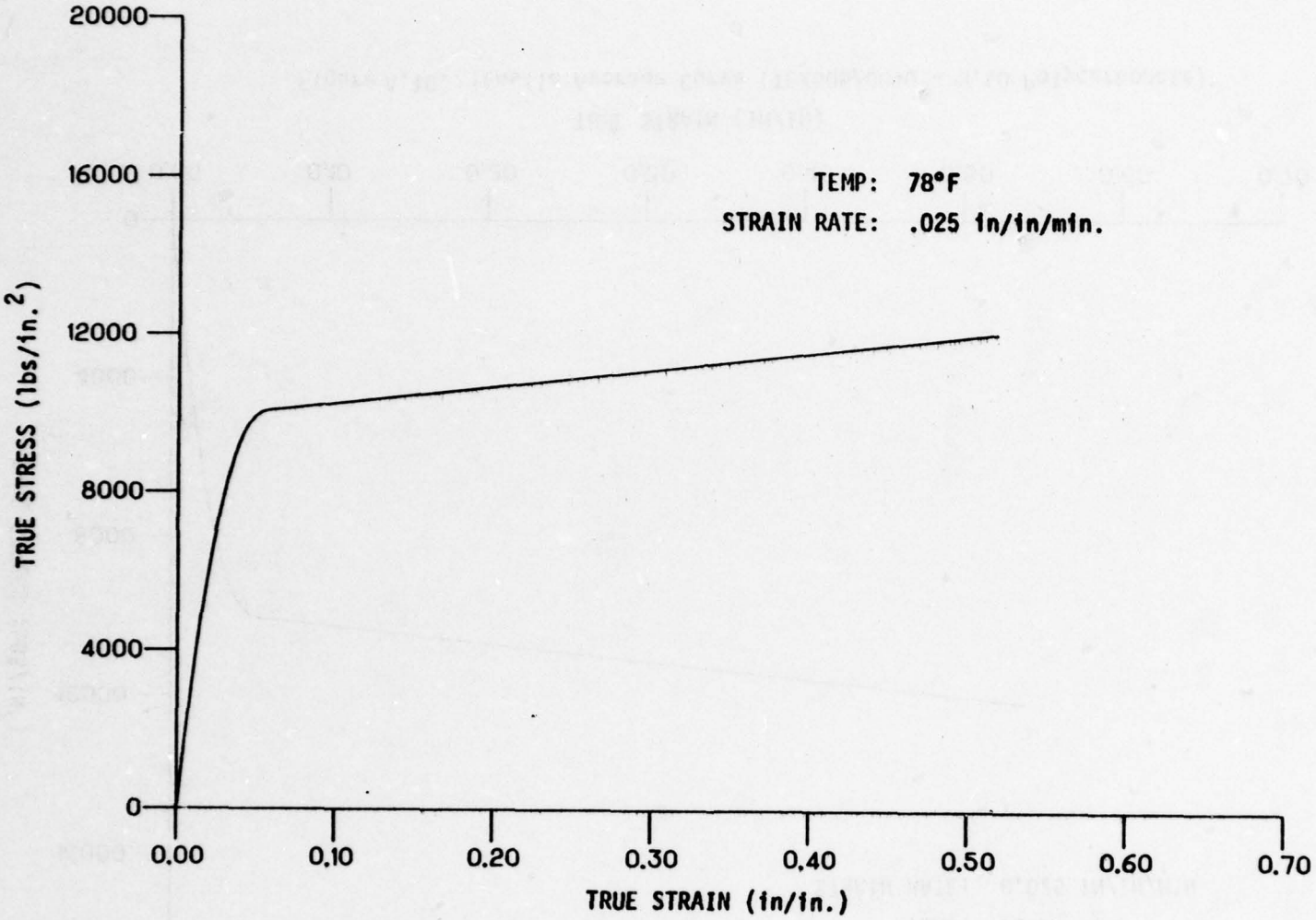

Figure A.9. Tensile Average Curve (TEX605/0030 -0.50 Polycarbonate).

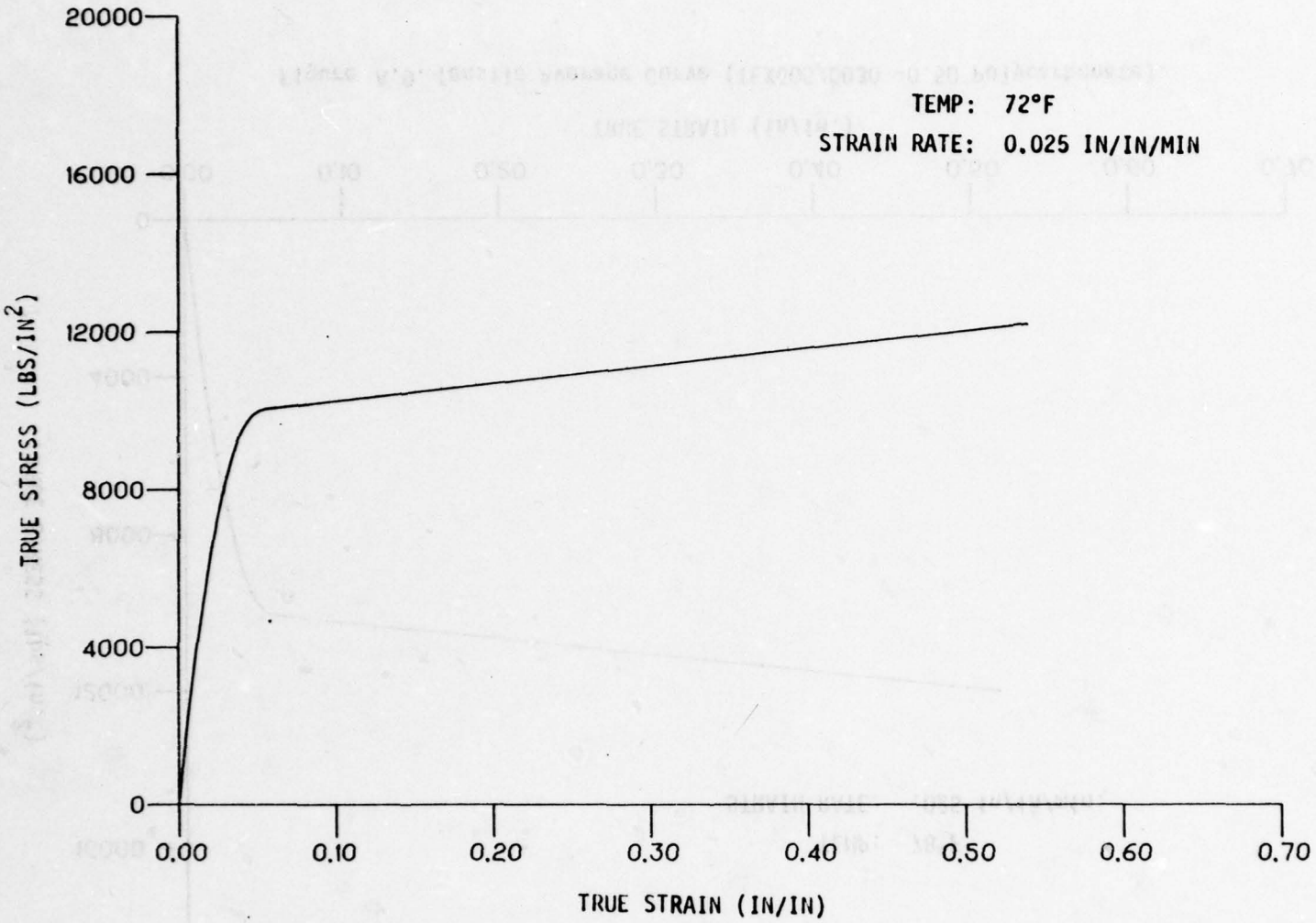

Figure A.10. Tensile Average Curve (TEX605/0040 - 0.50 Polycarbonate)

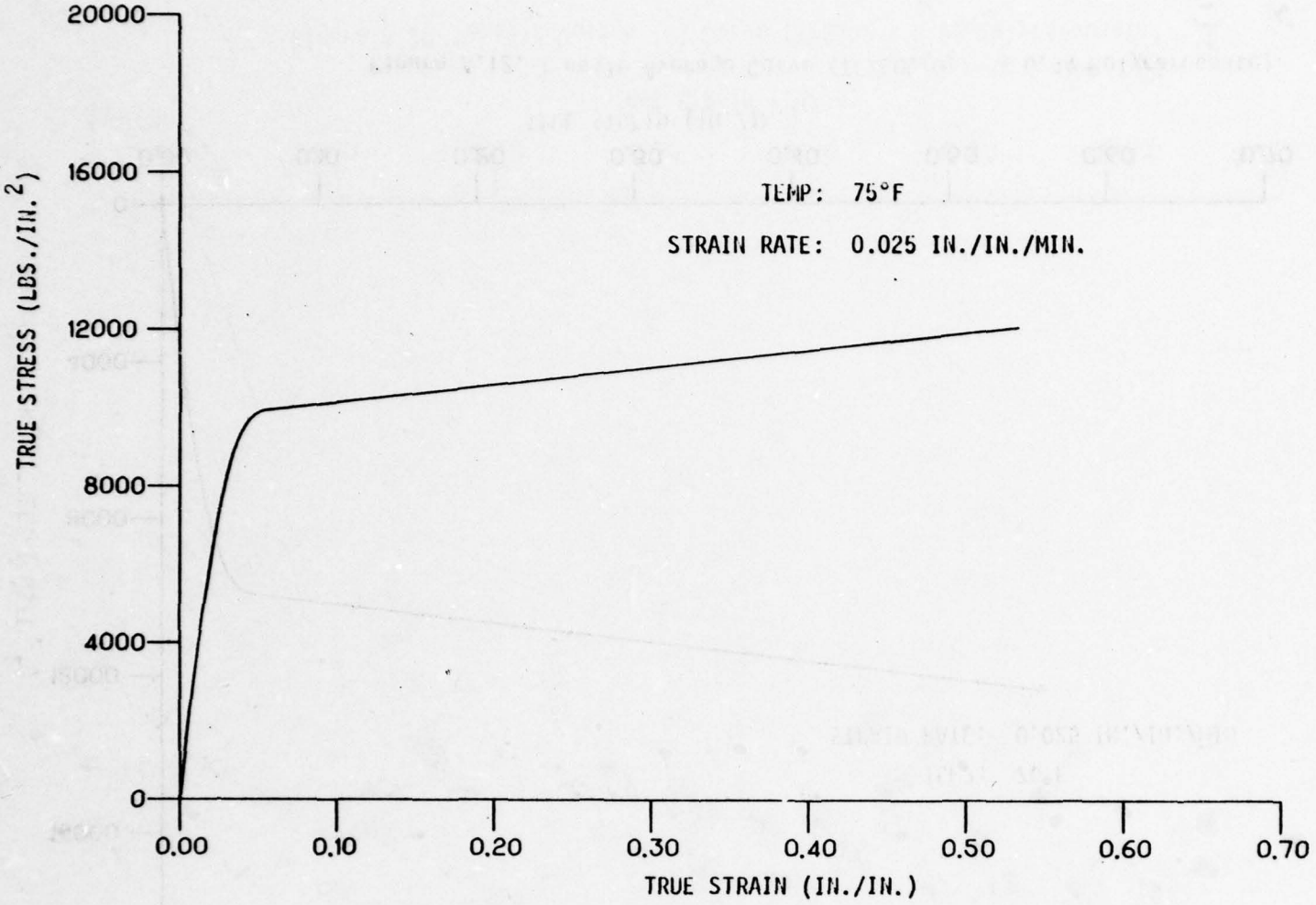

Figure A.11.Tensile Average Curve (TEX605/01 - 0.44 Polycarbonate)

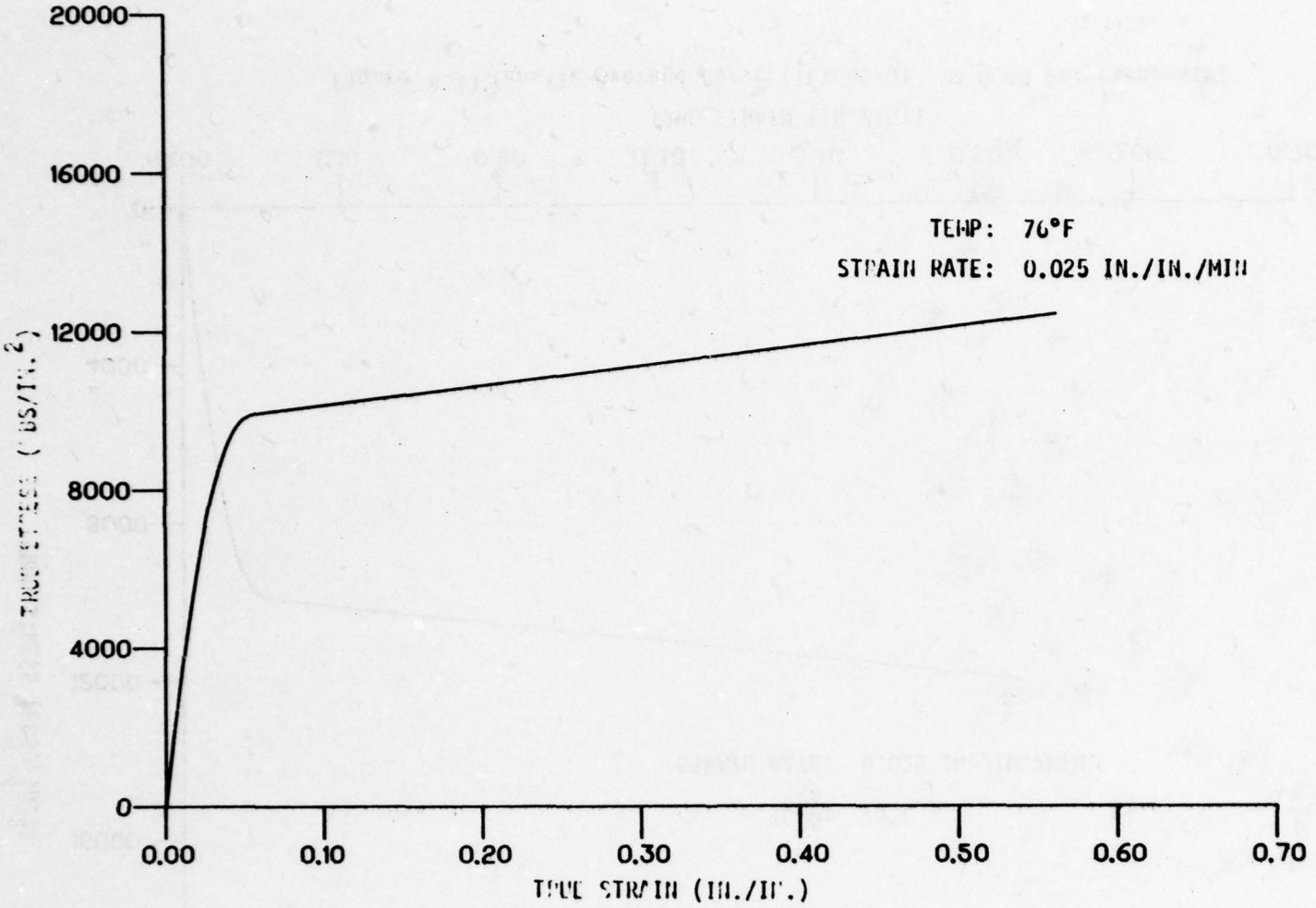

Figure A.12. Tensile Average Curve (TEX605/027 - 0.44 Polycarbonate).

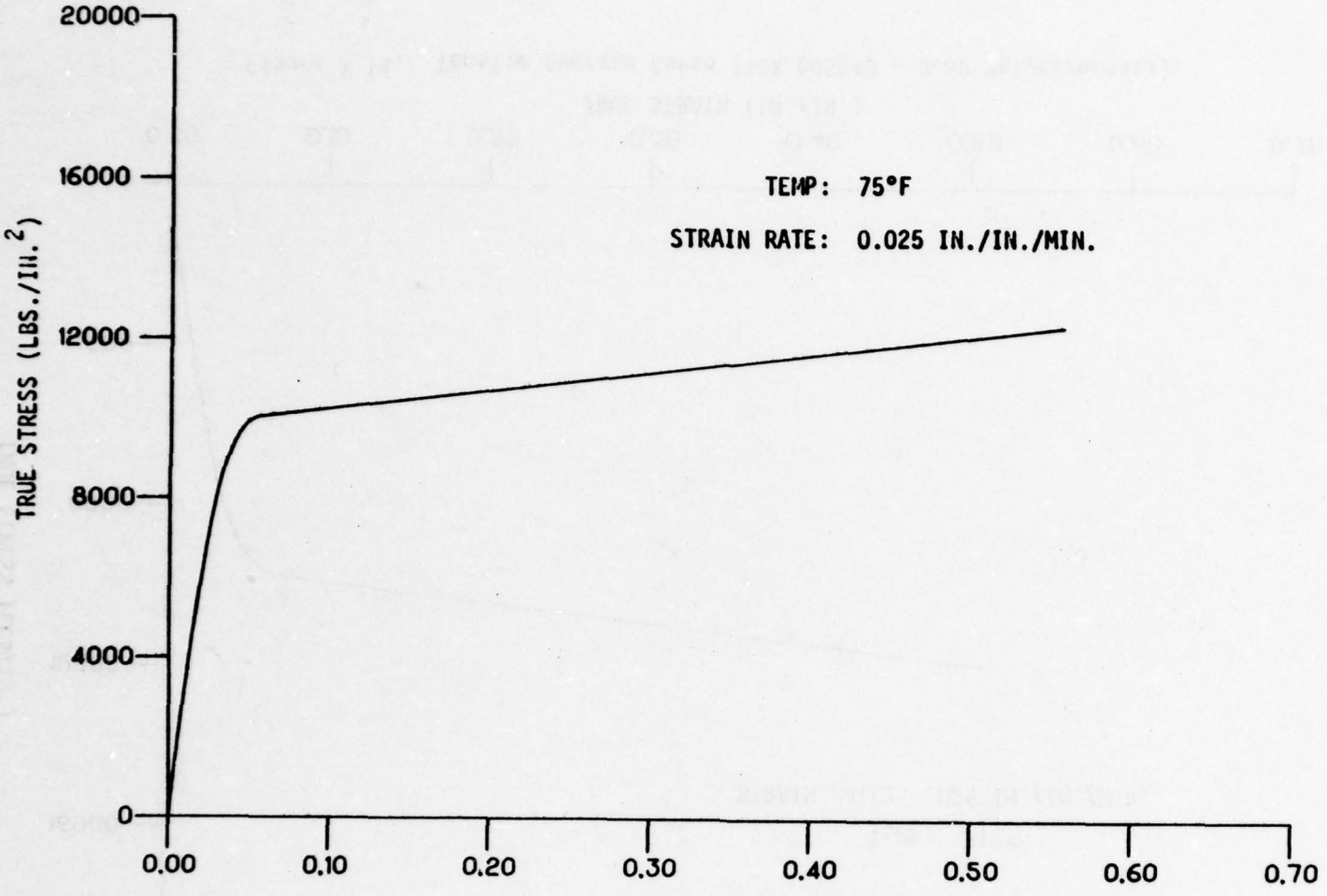

Figure A.13. Tensile Average Curve (TEX605/05 - 0.44 Polycarbonate)

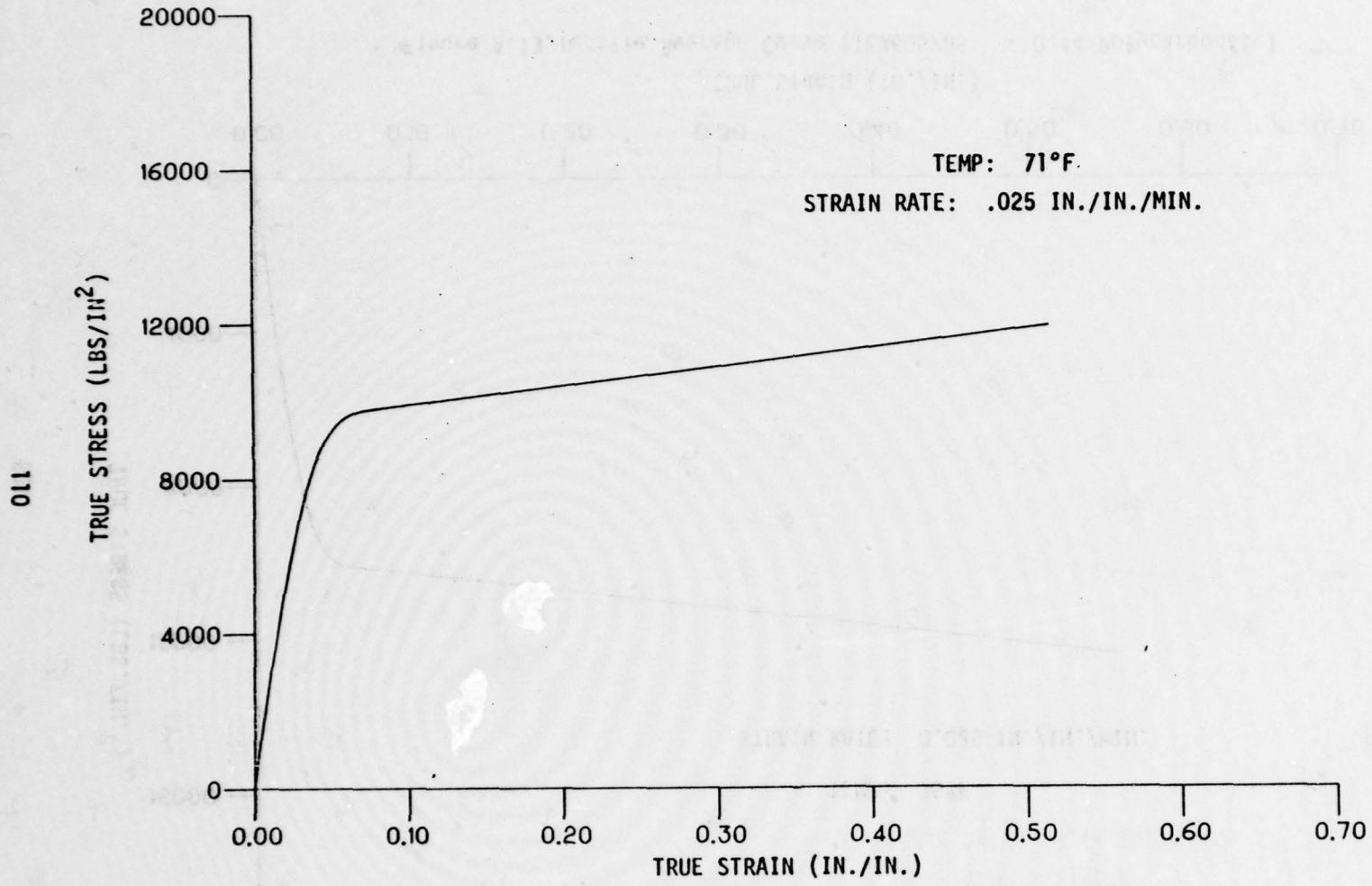

Figure A.14. Tensile Average Curve (TEX 605C43 - 0.50 Polycarbonate).

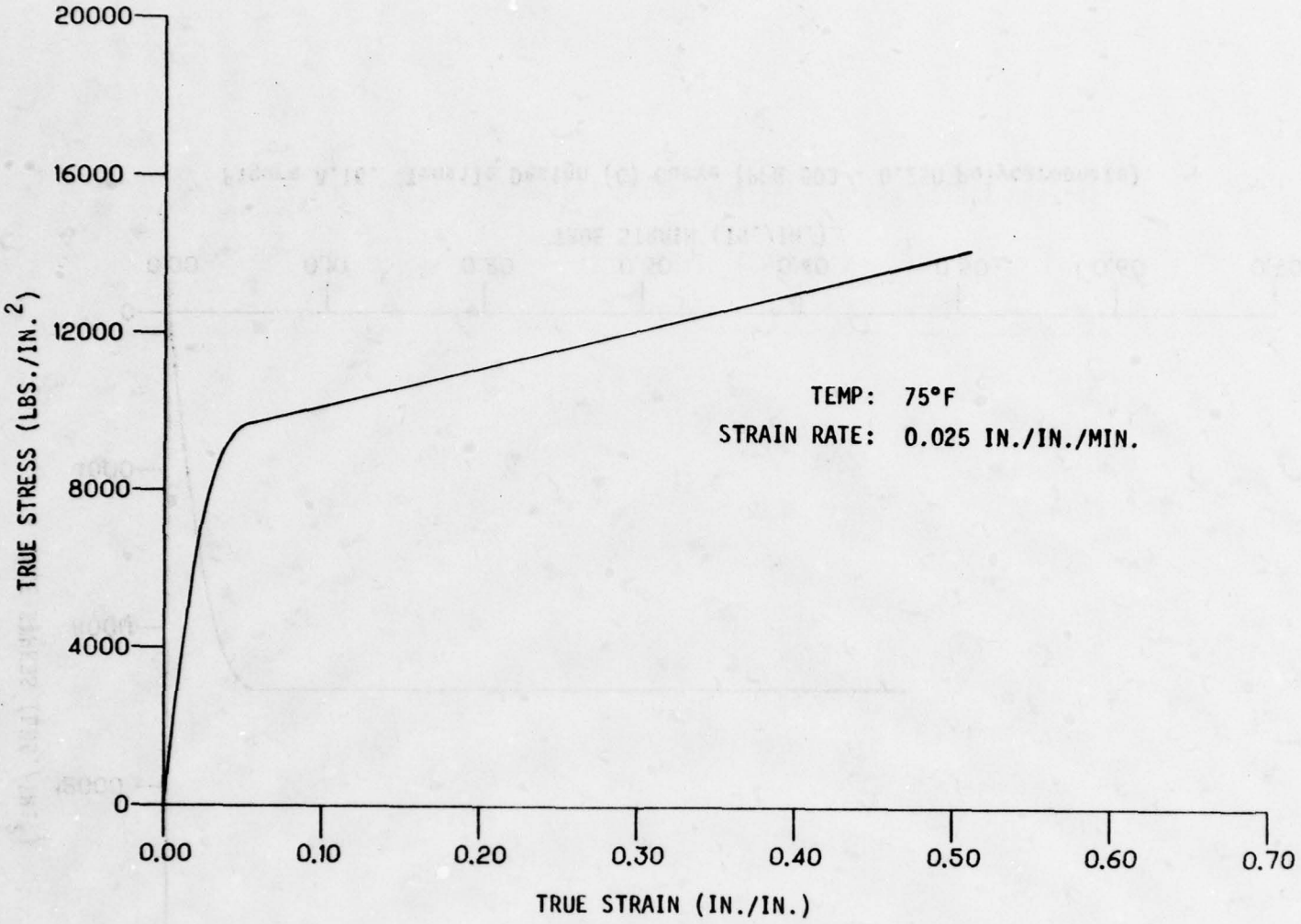

Figure A.15. Tensile Average Curve (PPG 503 - 0.250 Polycarbonate).

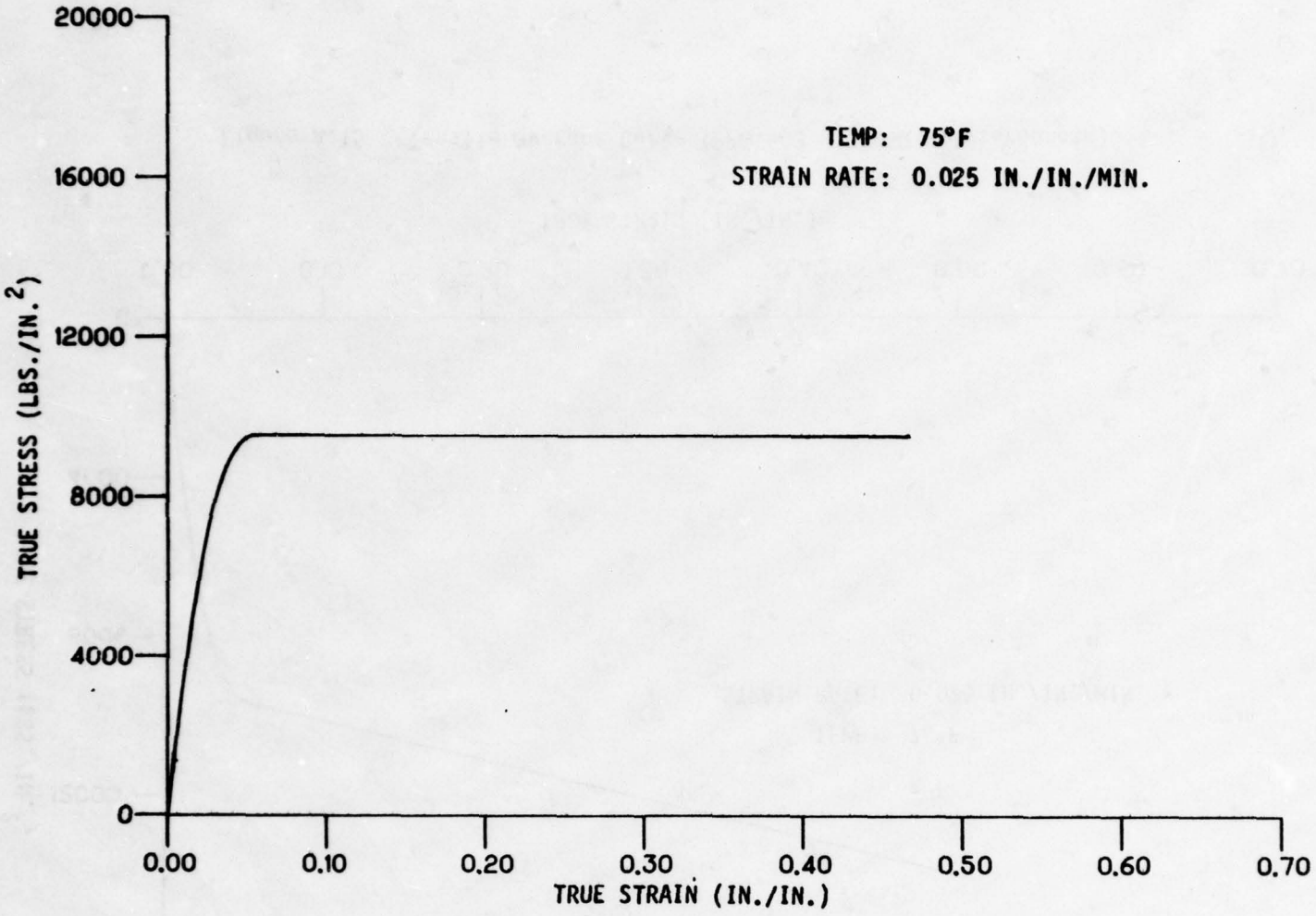

Figure A.16. Tensile Design (C) Curve (PPG 503 - 0.250 Polycarbonate).

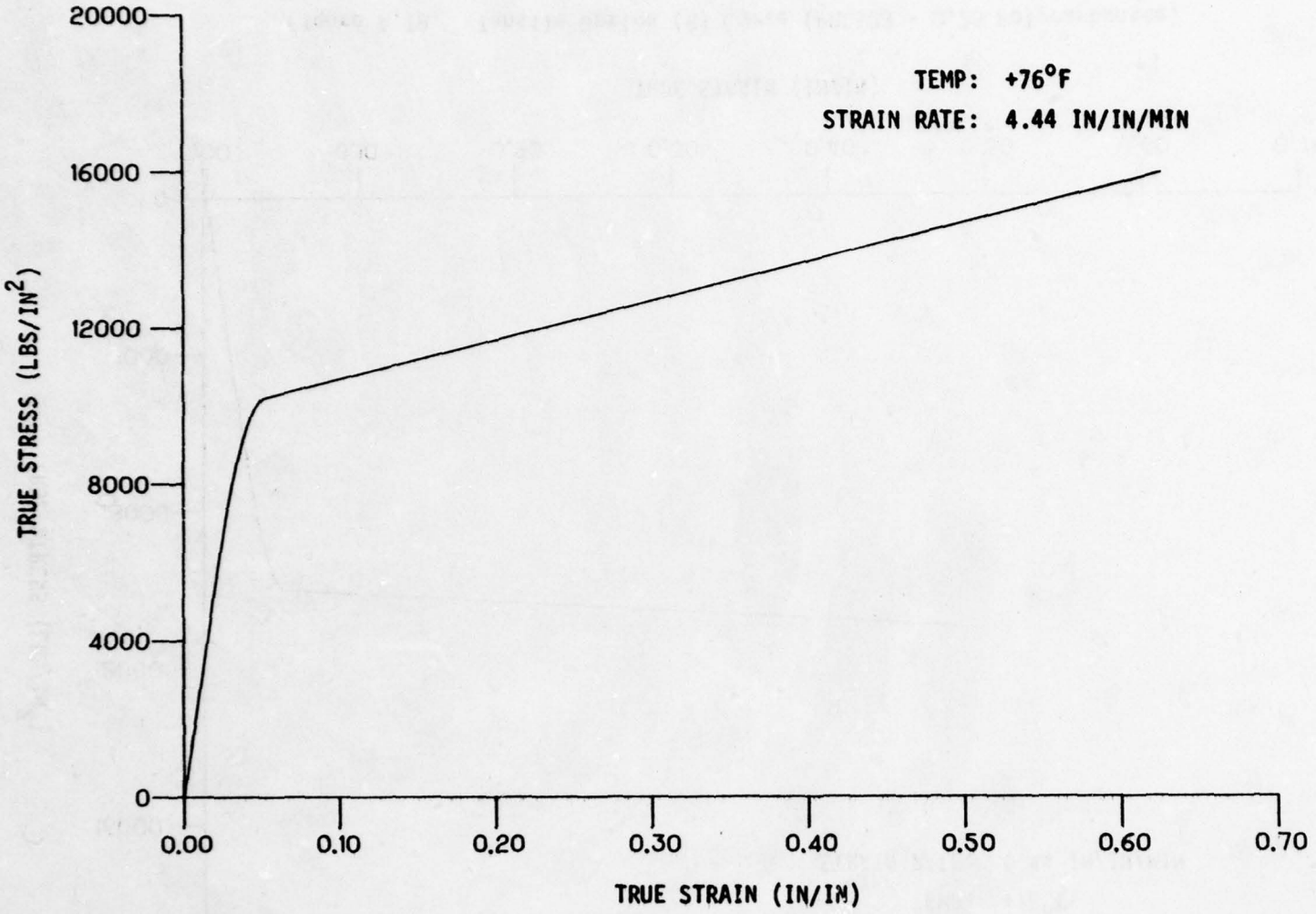

Figure A.17. Tensile Average Curve (PPG503 - 0.25 Polycarbonate)

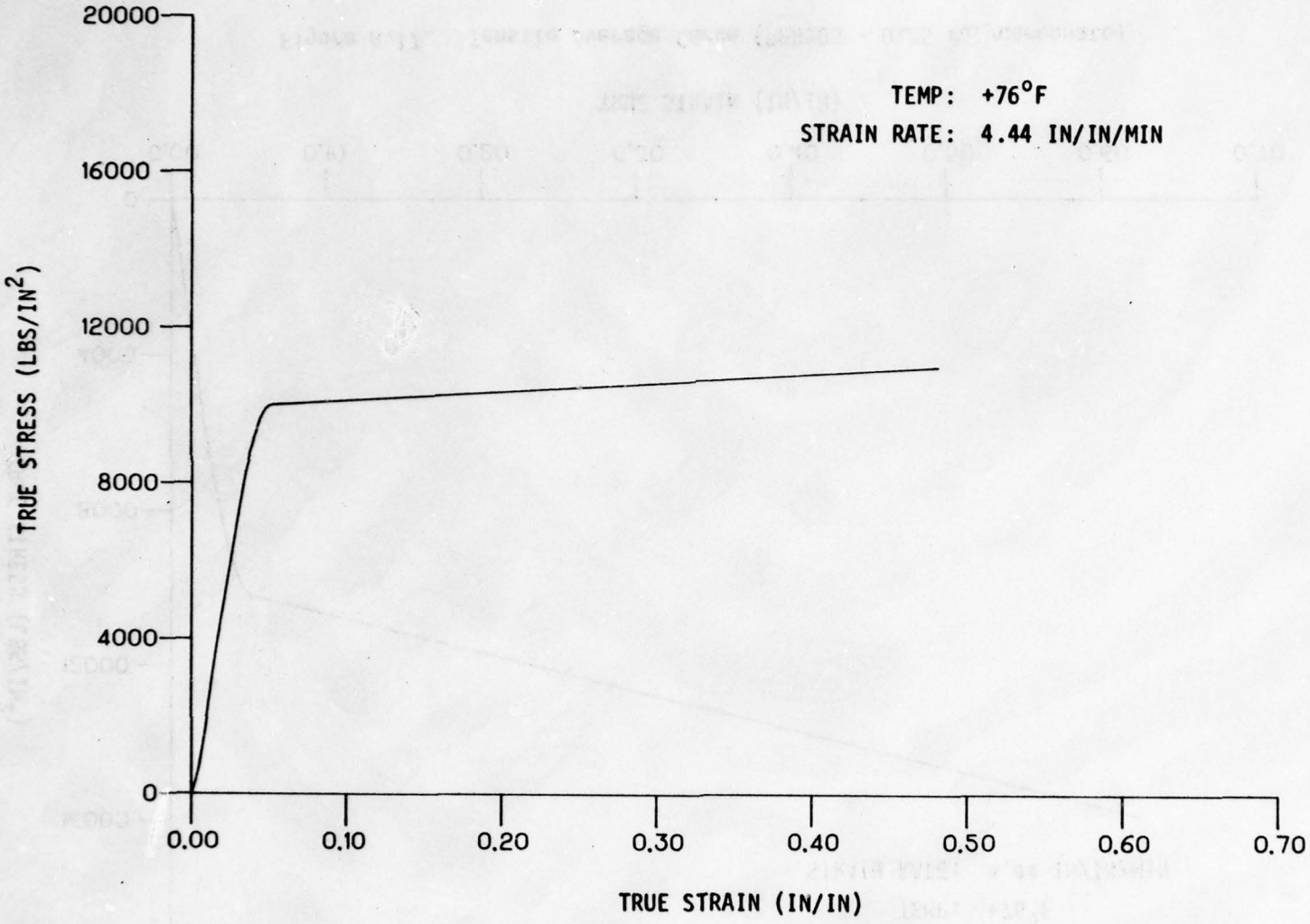

Figure A.18. Tensile Design (B) Curve (PPG503 - 0.25 Polycarbonate)

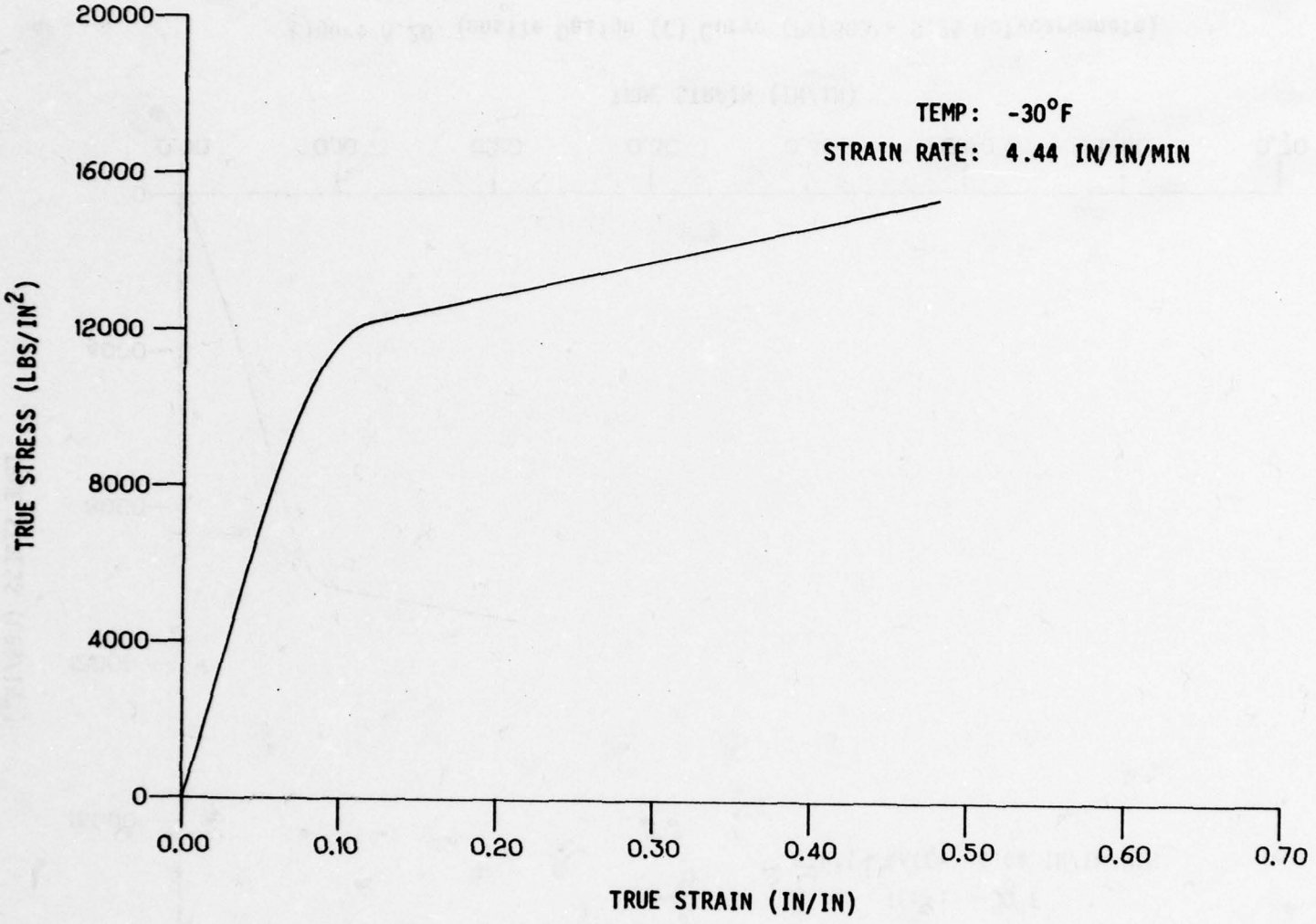

Figure A.19. Tensile Average Curve (PPG503-0.25 Polycarbonate)

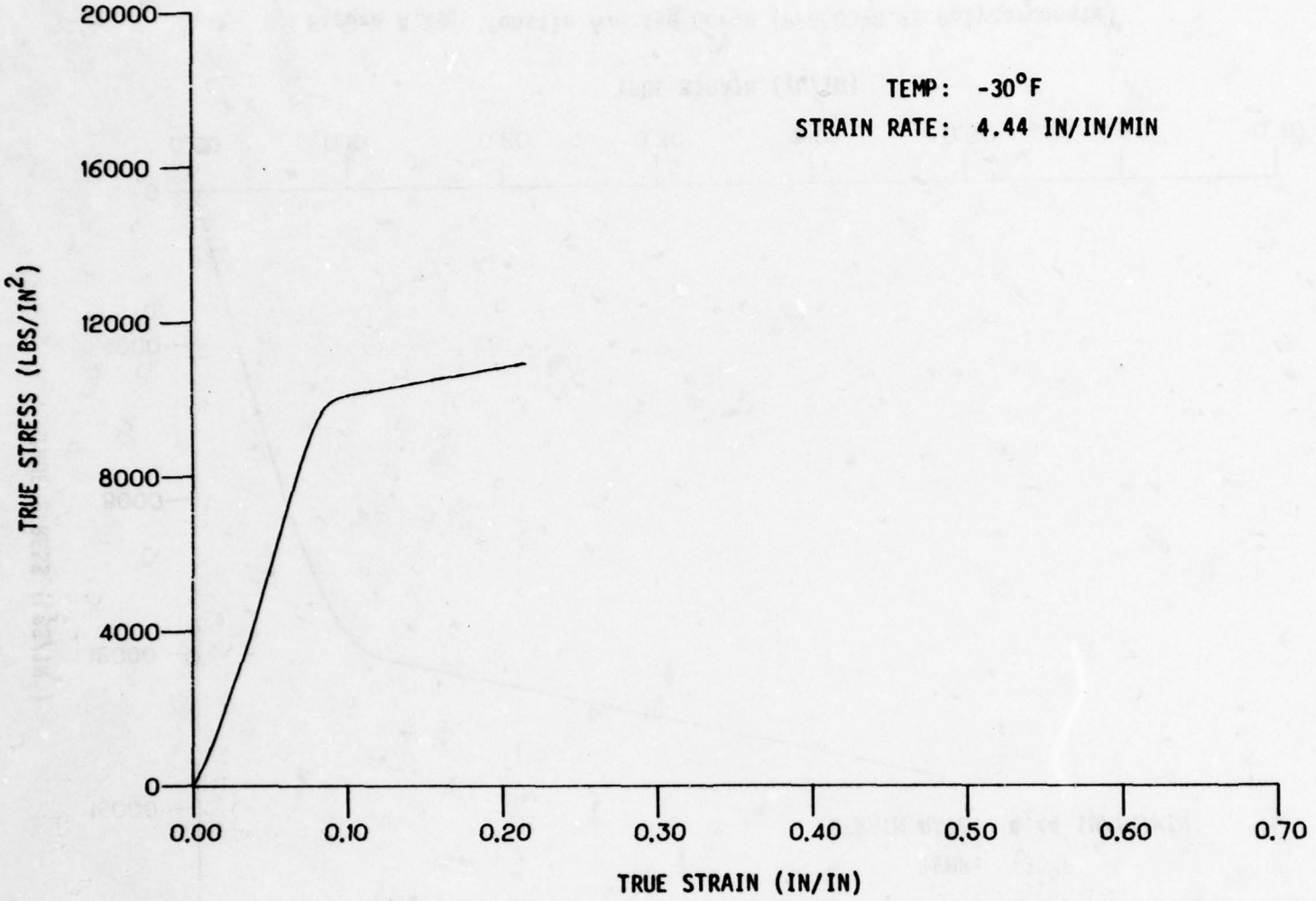

Figure A.20. Tensile Design (C) Curve (PPG503 - 0.25 Polycarbonate)

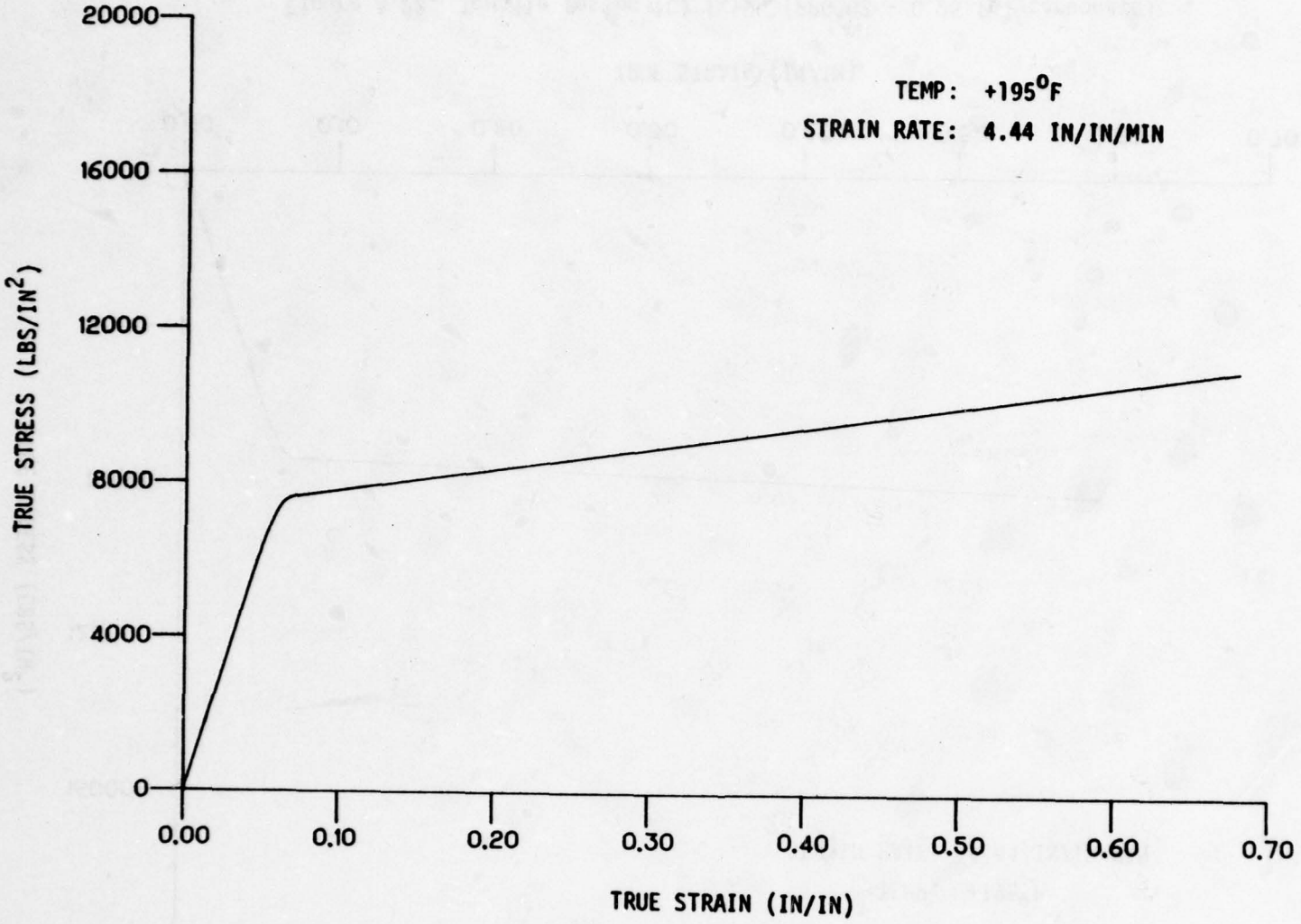

Figure A.21. Tensile Average Curve (PPG503 - 0.25 Polycarbonate)

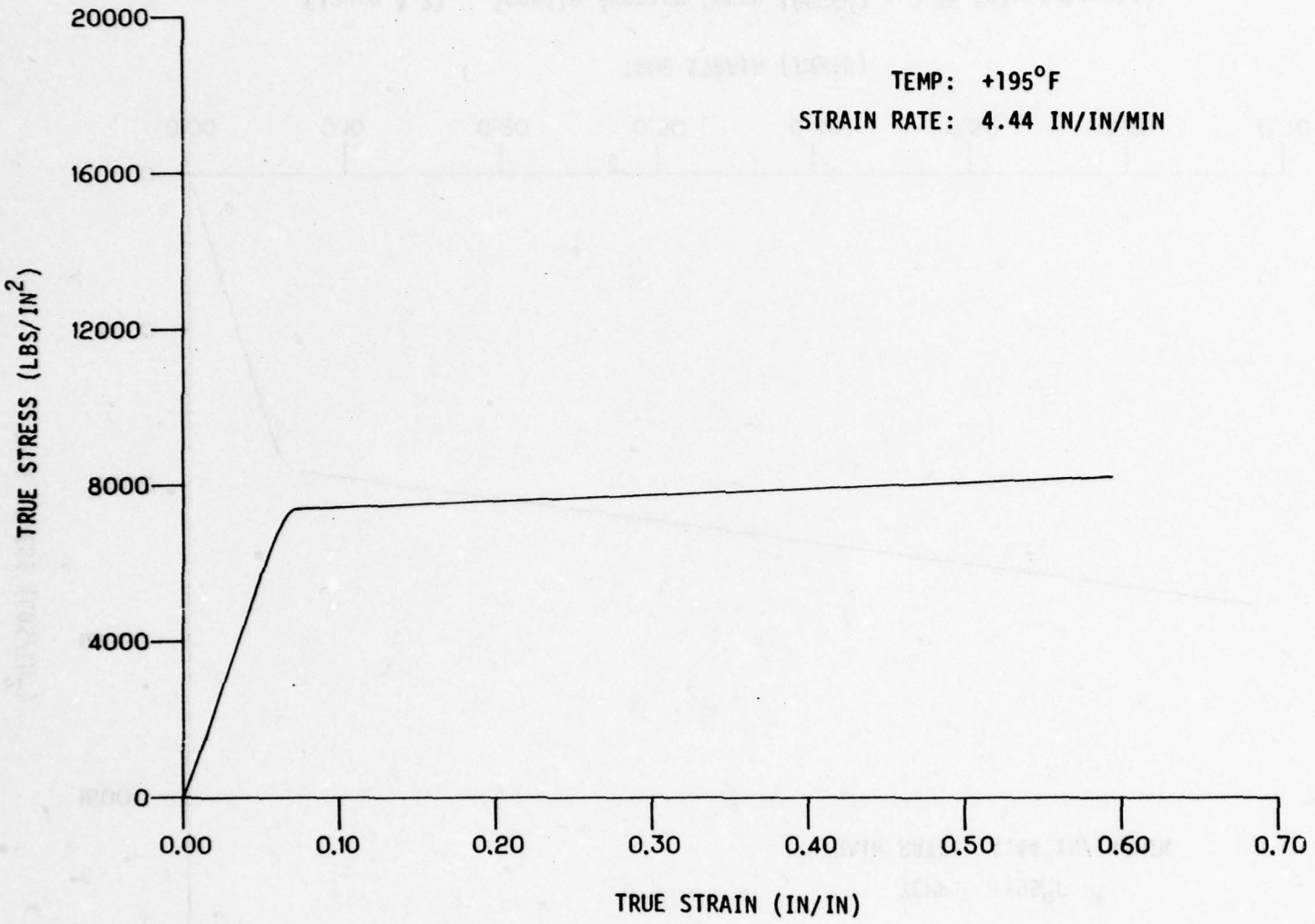

Figure A.22. Tensile Design (C) Curve (PPG503 - 0.25 Polycarbonate)

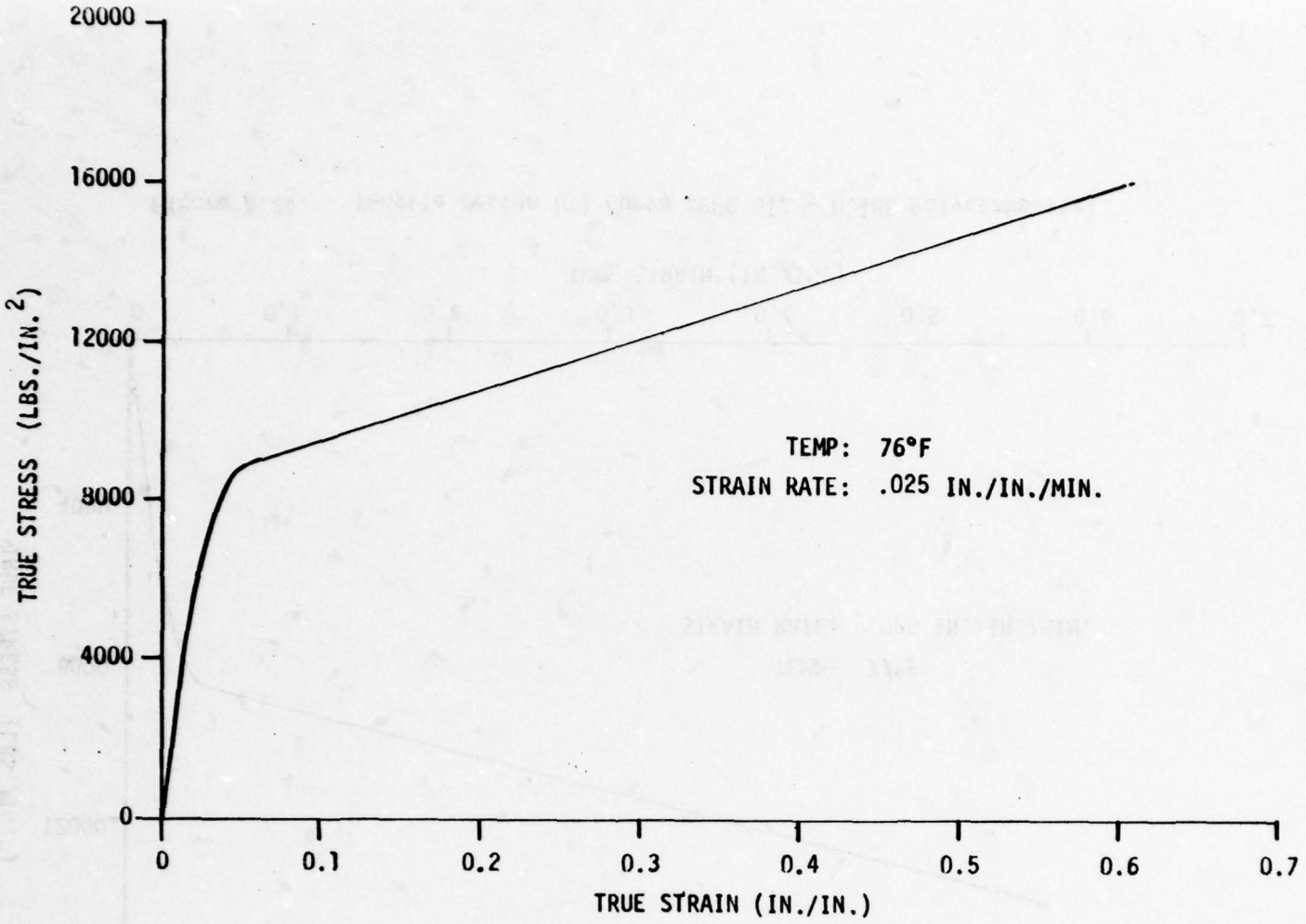

Figure A.23. Tensile Average Curve (PPG 517 - 0.188 Polycarbonate).

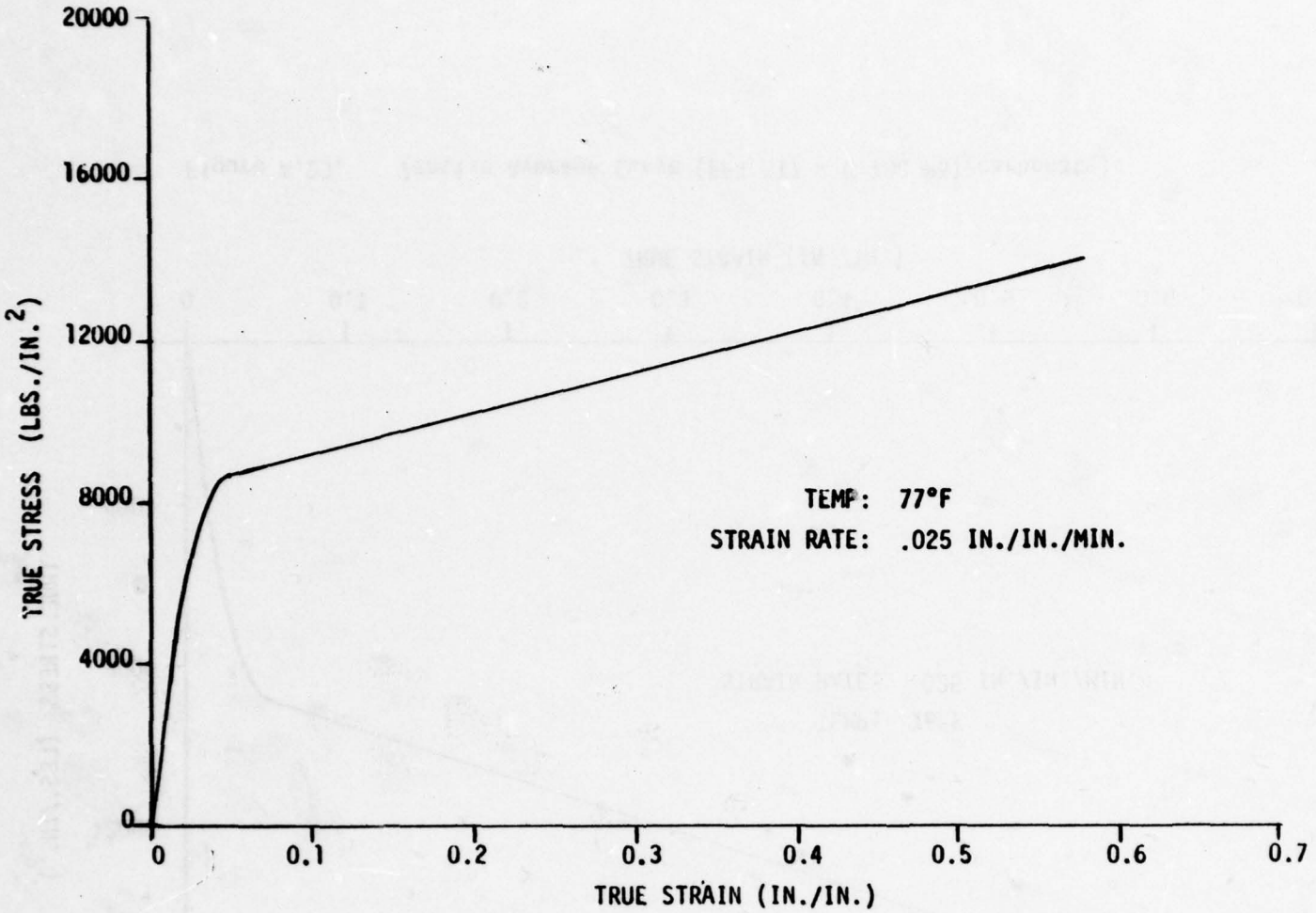

Figure A.24. Tensile Design (C) Curve (PPG 517 - 0.188 Polycarbonate).

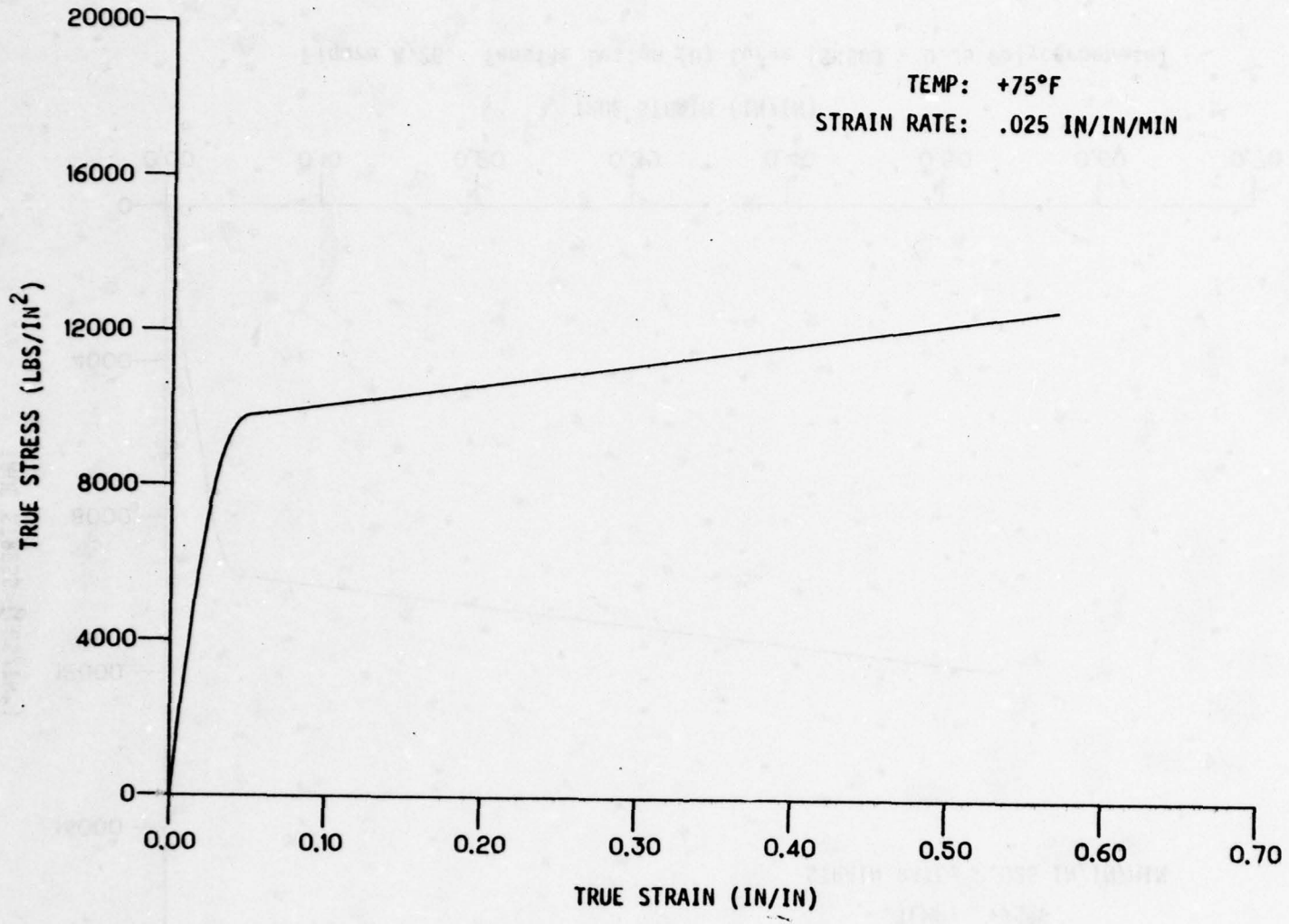

Figure A.25. Tensile Average Curve (SK503 - 0.25 Polycarbonate)

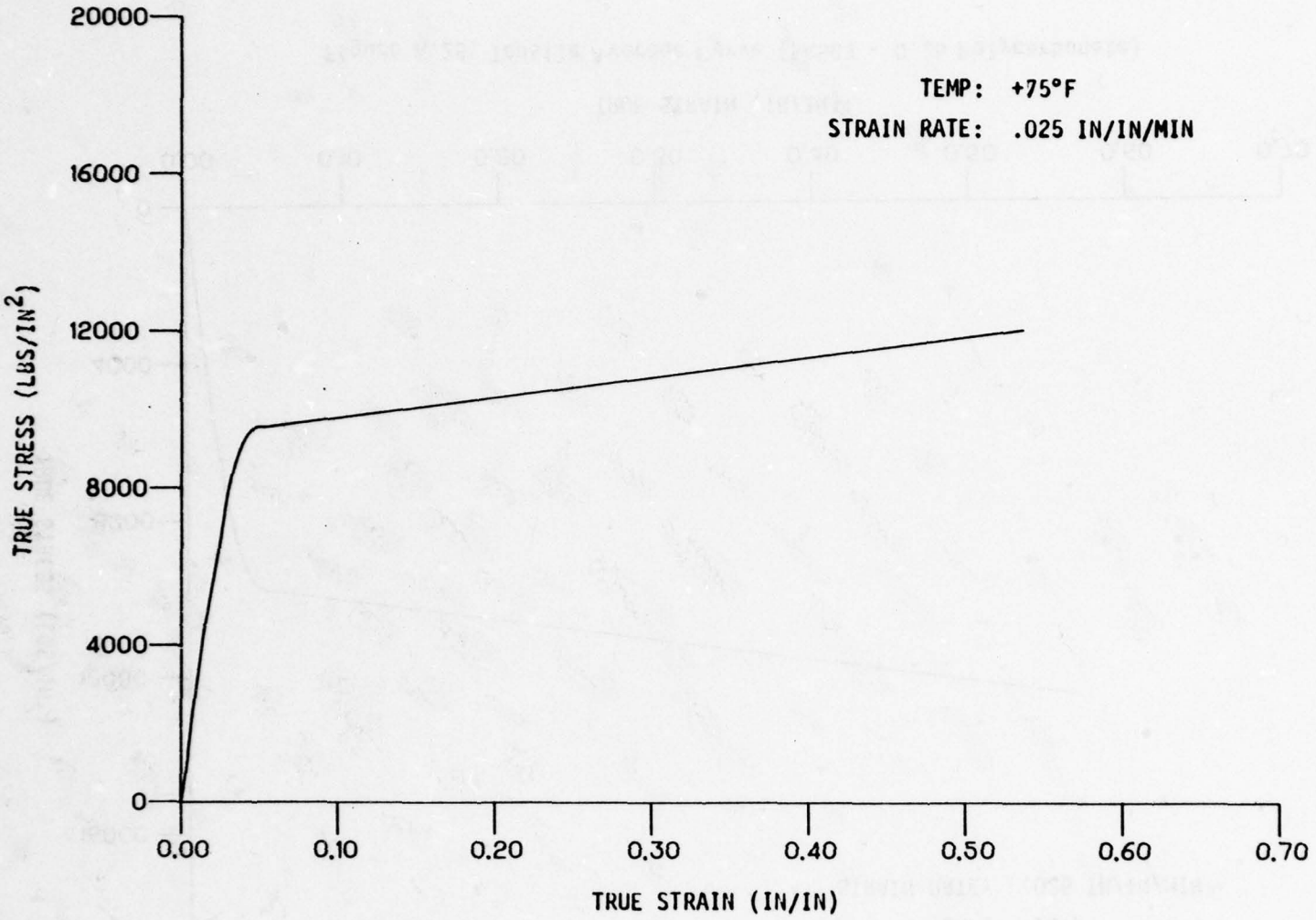

Figure A.26. Tensile Design (B) Curve (SK503 - 0.25 Polycarbonate)

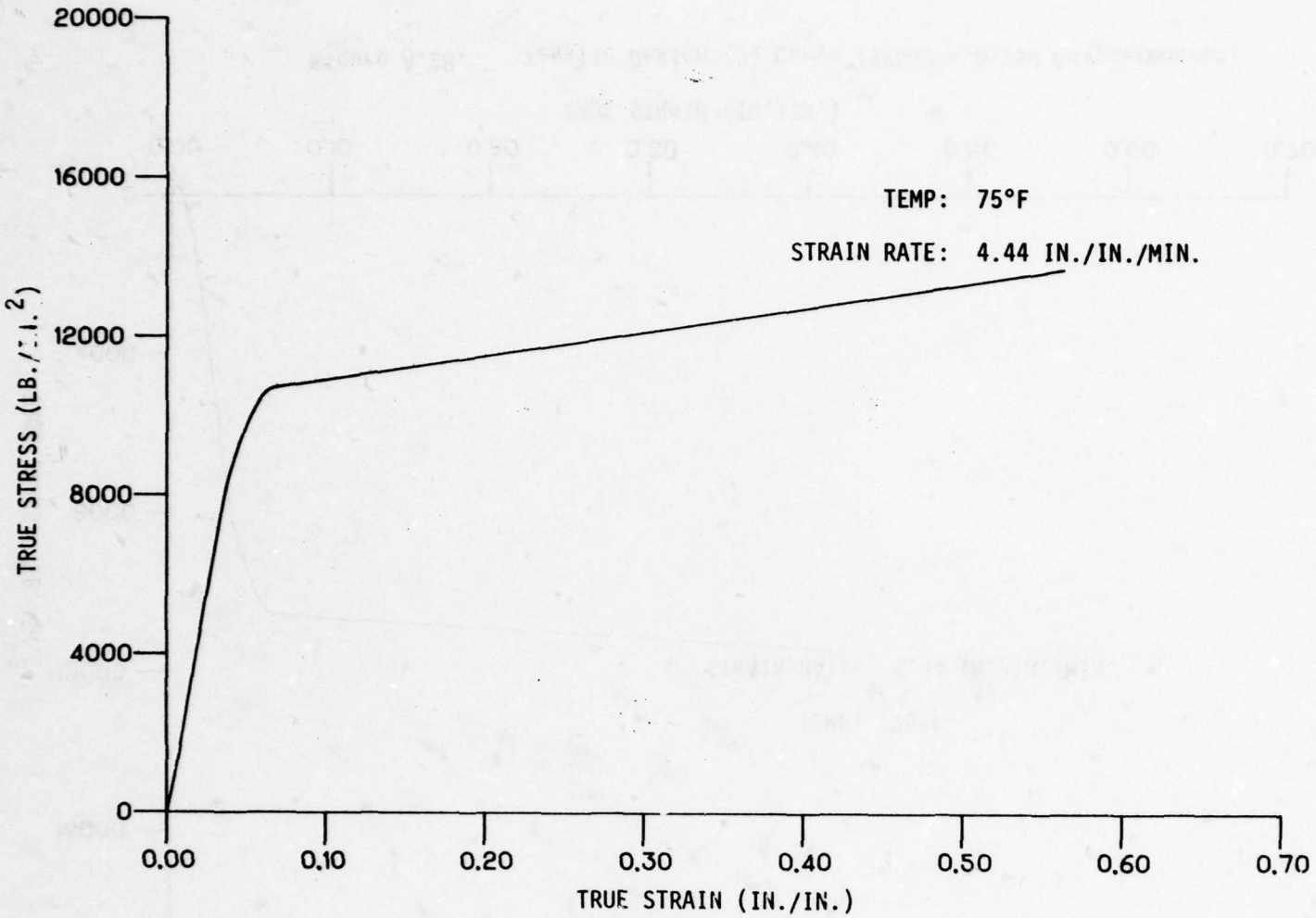

Figure A.27. Tensile Average Curve (SK503 - 0.250 Polycarbonate).

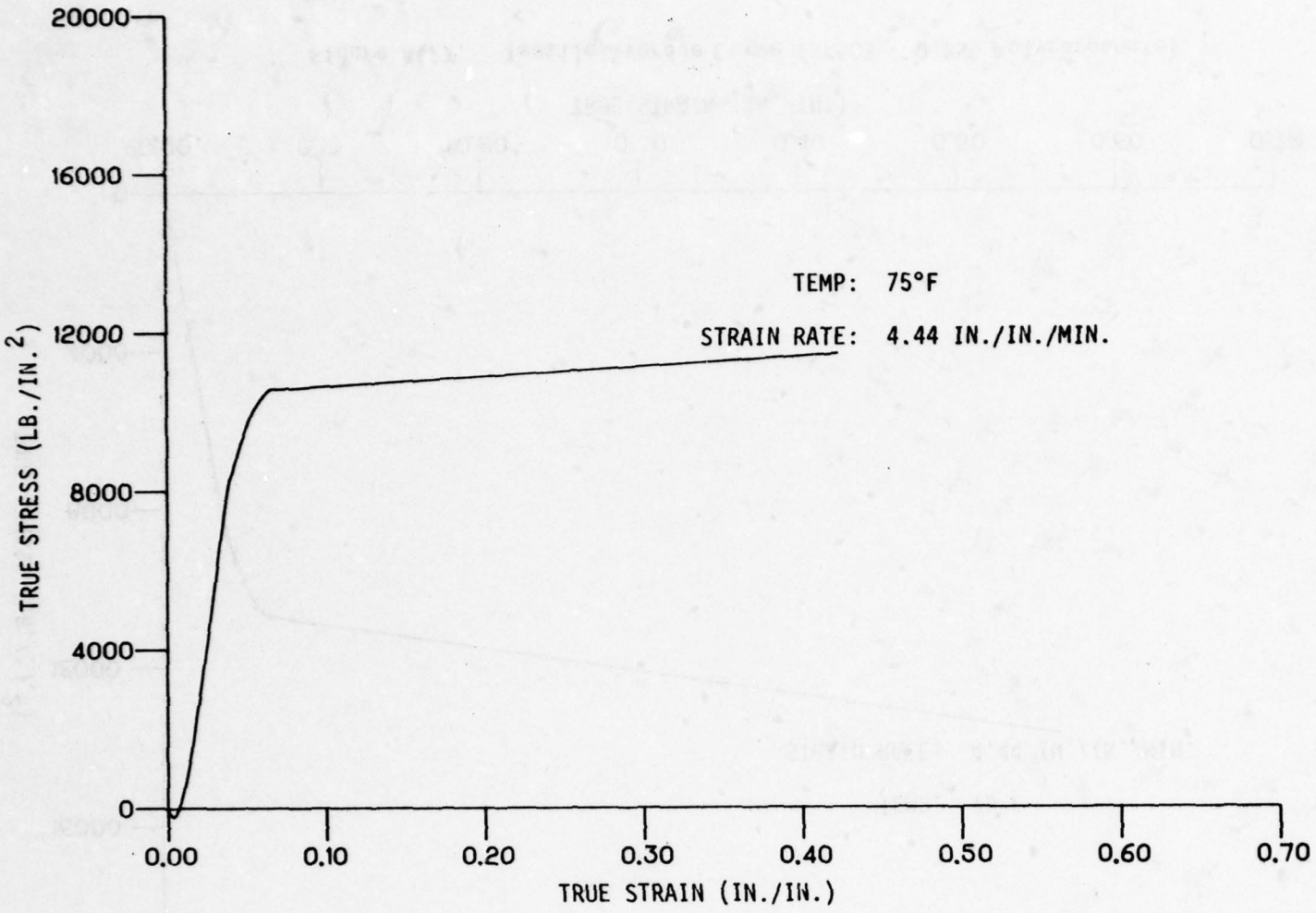

Figure A.28. Tensile Design (B) Curve (SK503 - 0.250 Polycarbonate)

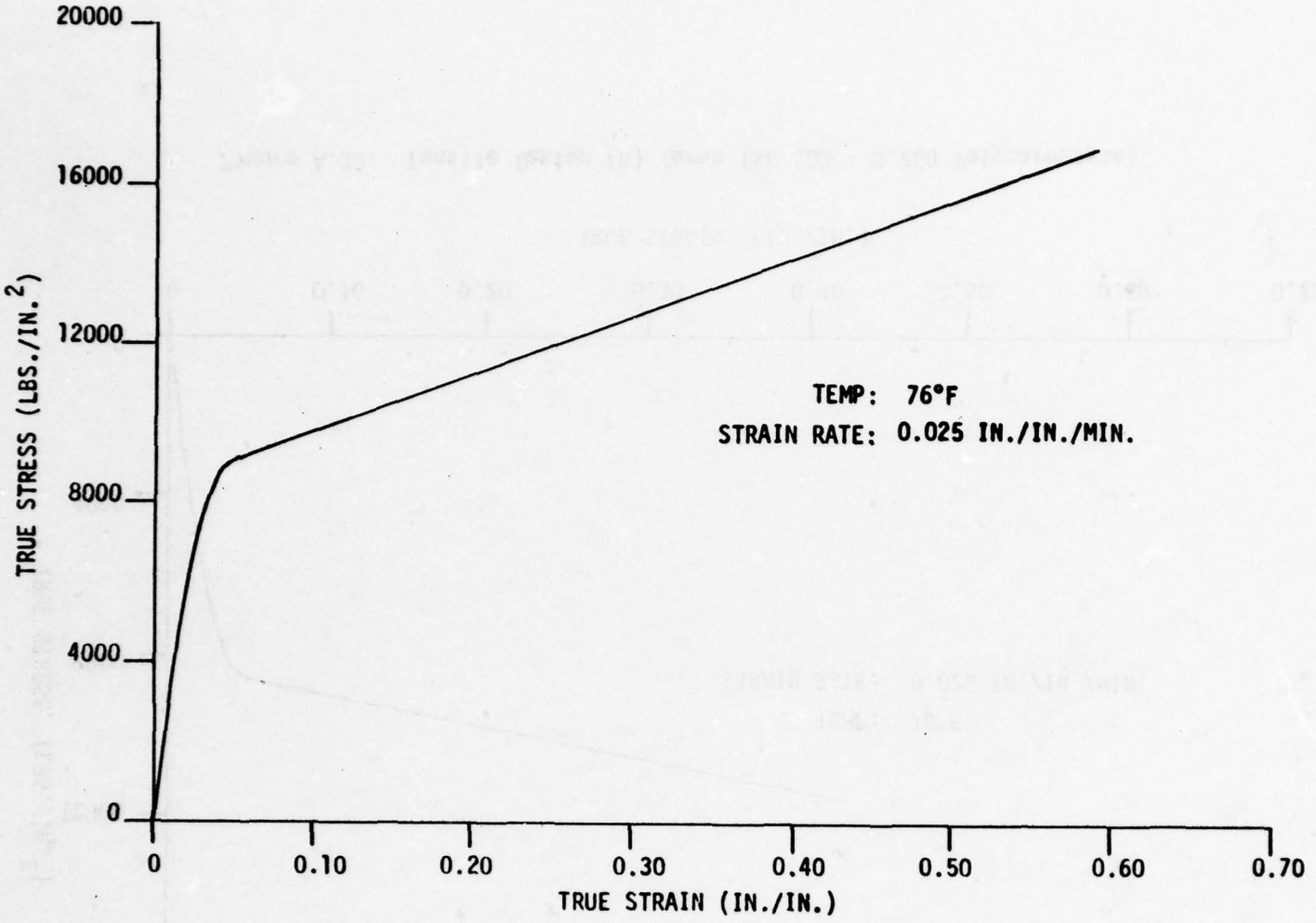

Figure A.29. Tensile Average Curve (SK 503 - 0.250 Polycarbonate).

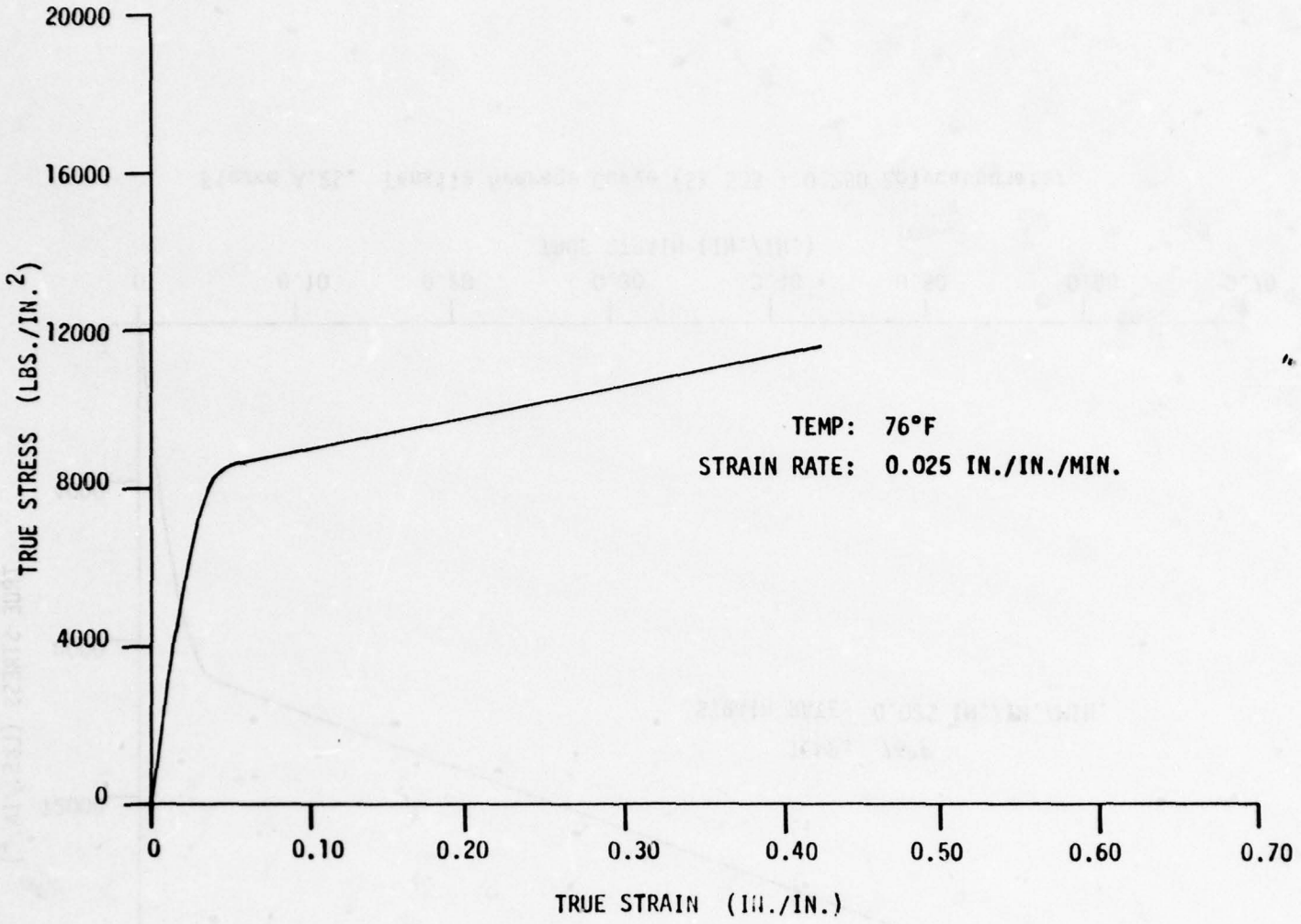

Figure A.30. Tensile Design (B) Curve (SK 503 - 0.250 Polycarbonate).

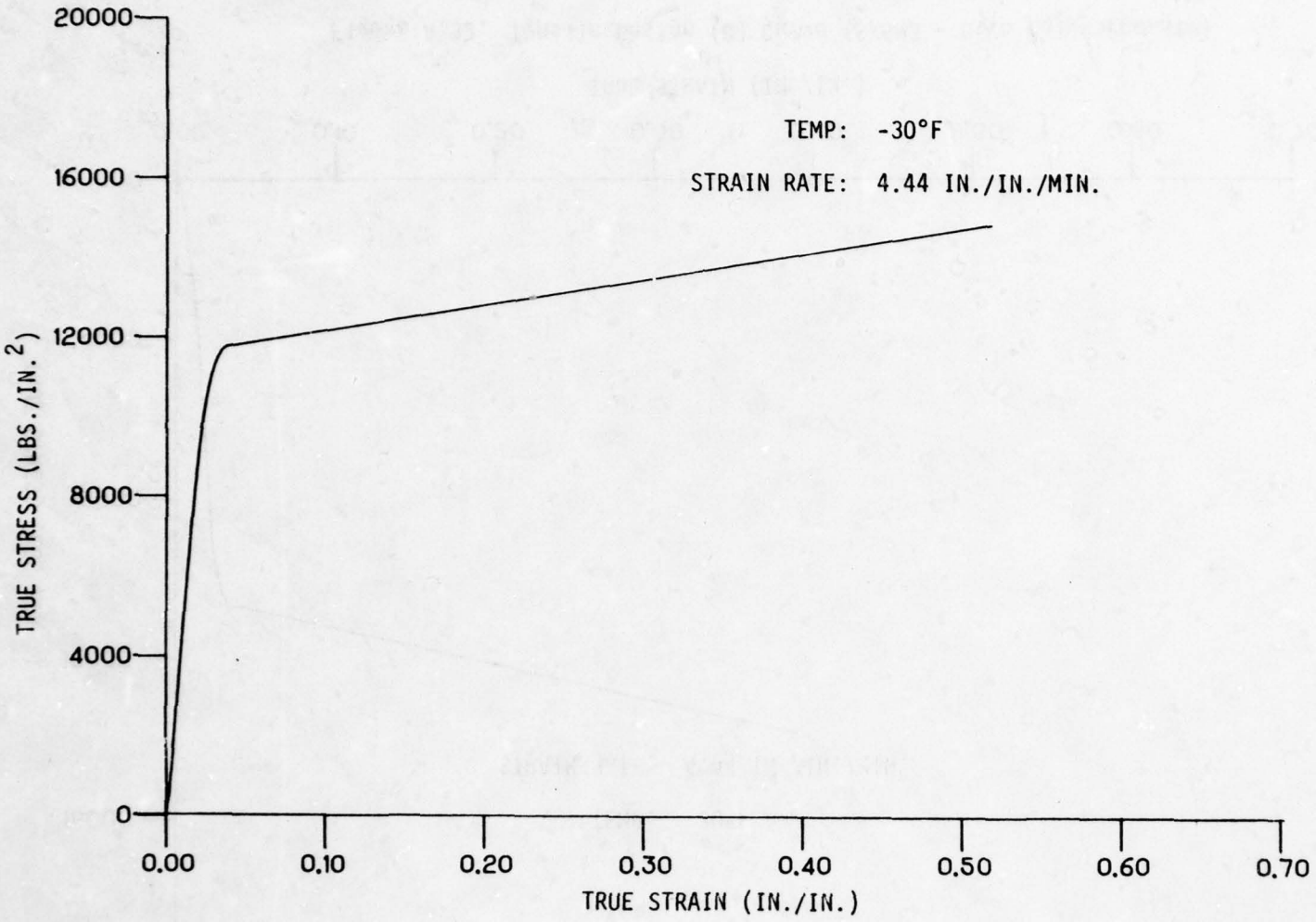

Figure A.31. Tensile Average Curve (SK503 - 0.25 Polycarbonate)

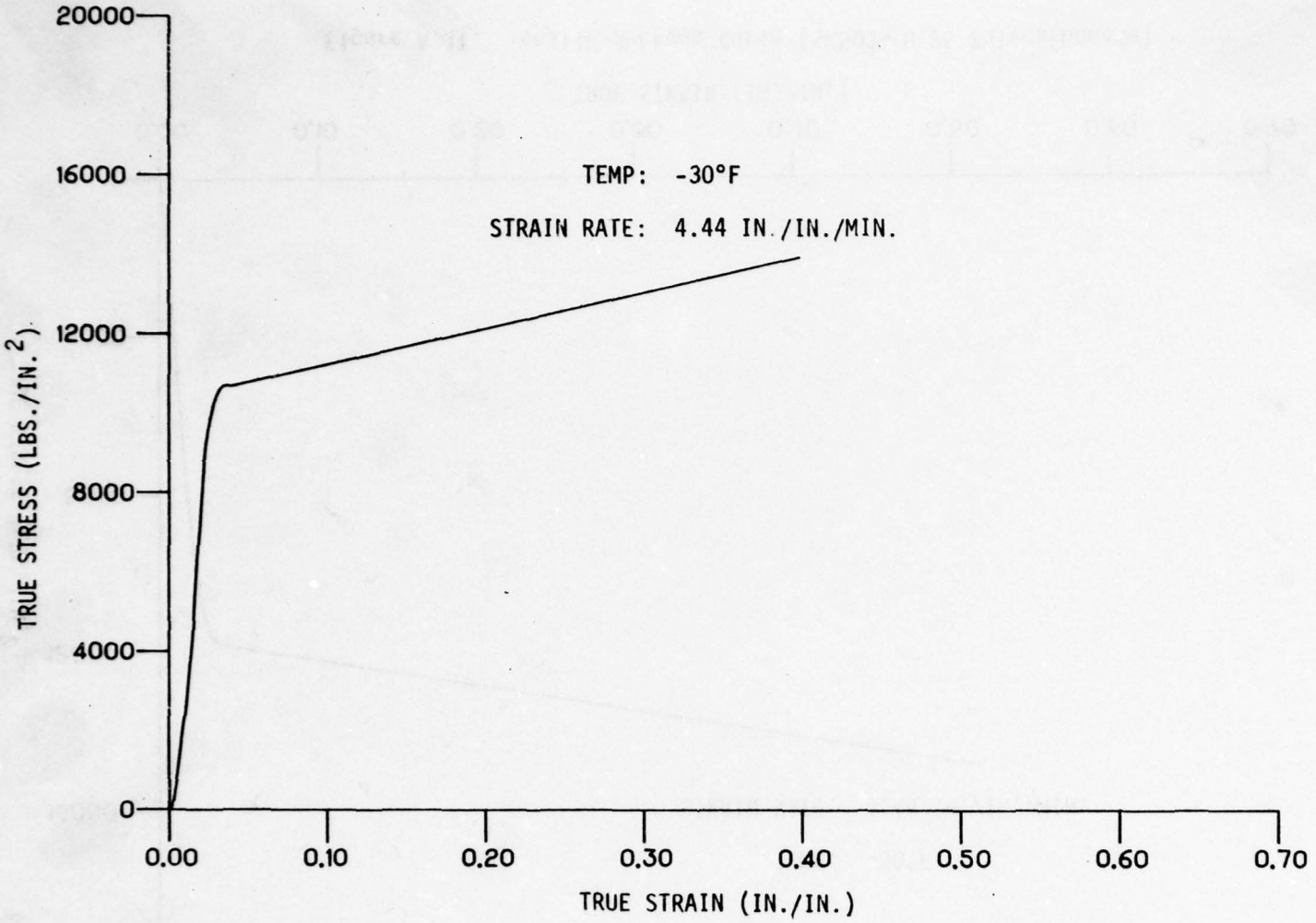

Figure A.32. Tensile Design (B) Curve (SK503 - 0.25 Polycarbonate)

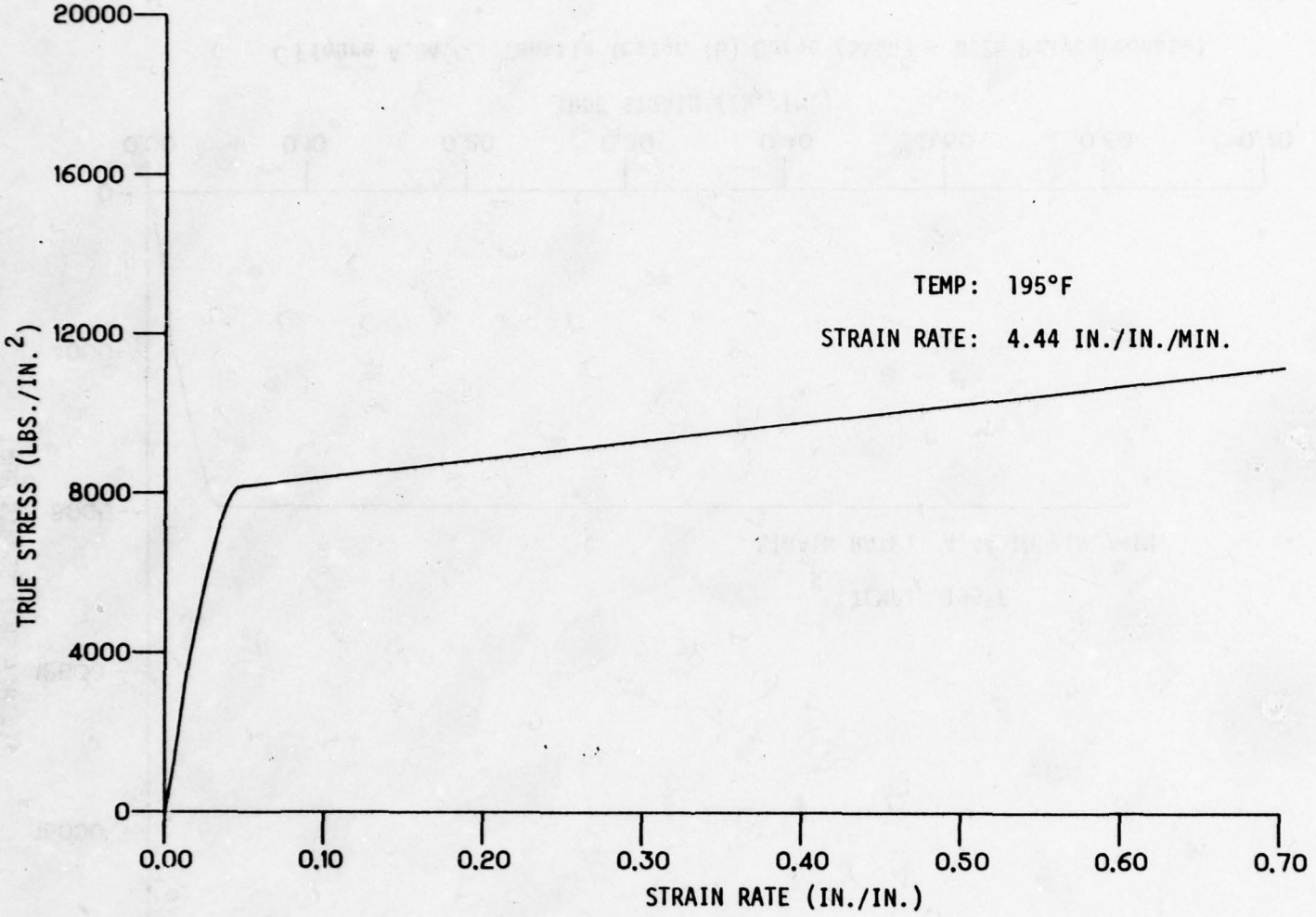

Figure A.33. Tensile Average Curve (SK503 - 0.25 Polycarbonate).

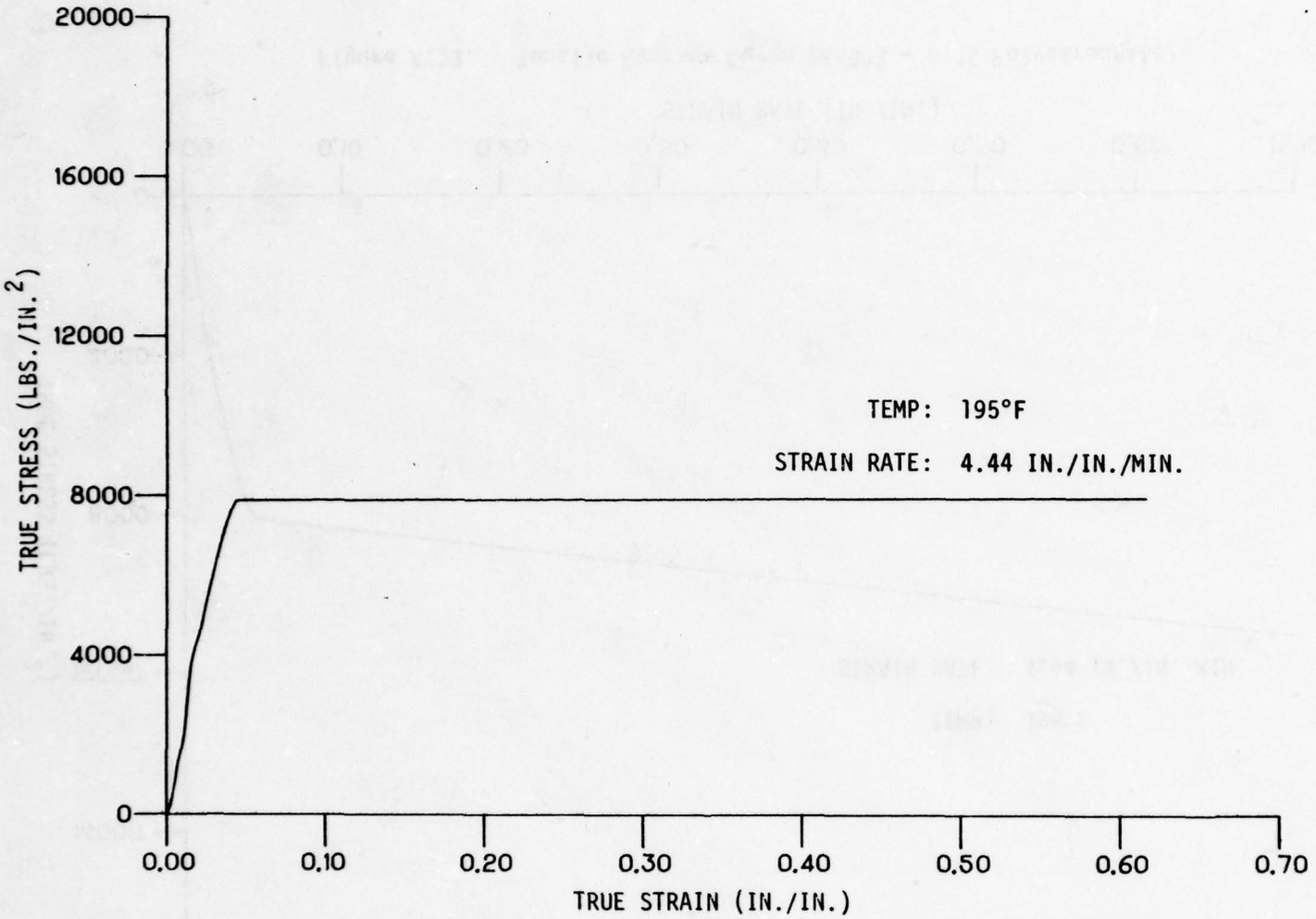

Figure A.34. Tensile Design (B) Curve (SK503 - 0.25 Polycarbonate)

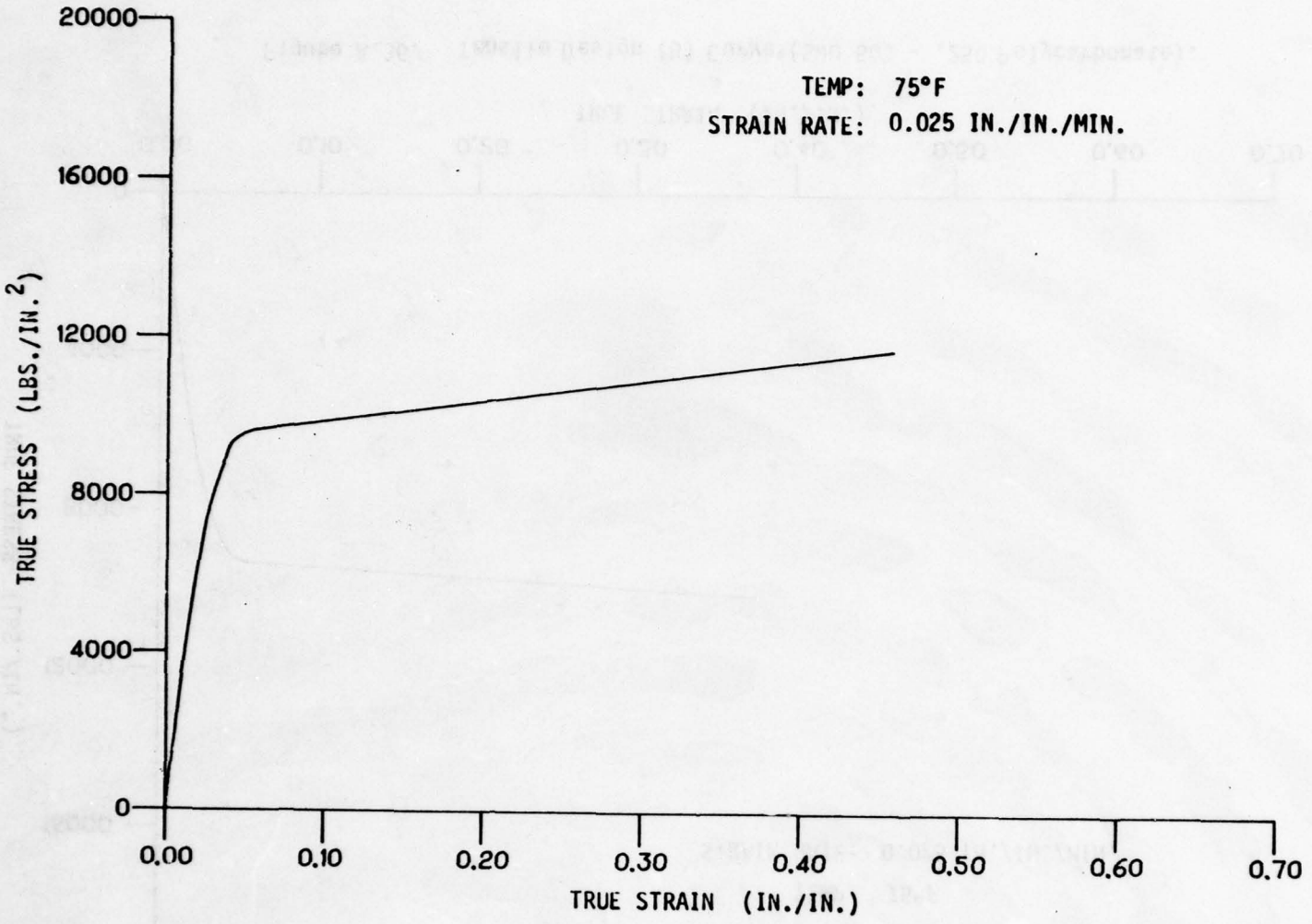

Figure A.35. Tensile Average Curve (SWU 503 - .250 Polycarbonate).

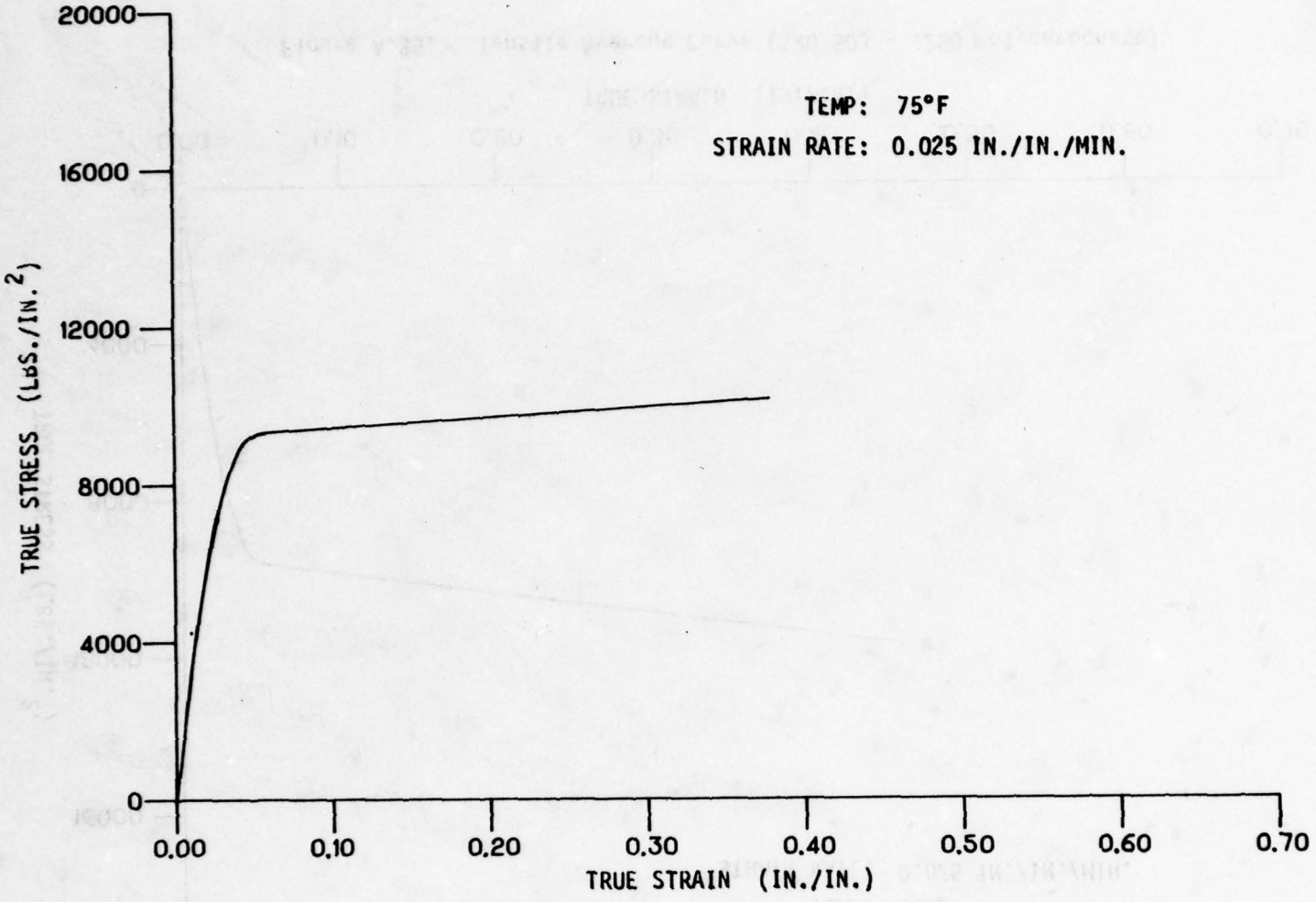

Figure A.36. Tensile Design (B) Curve (SWU 503 - .250 Polycarbonate).

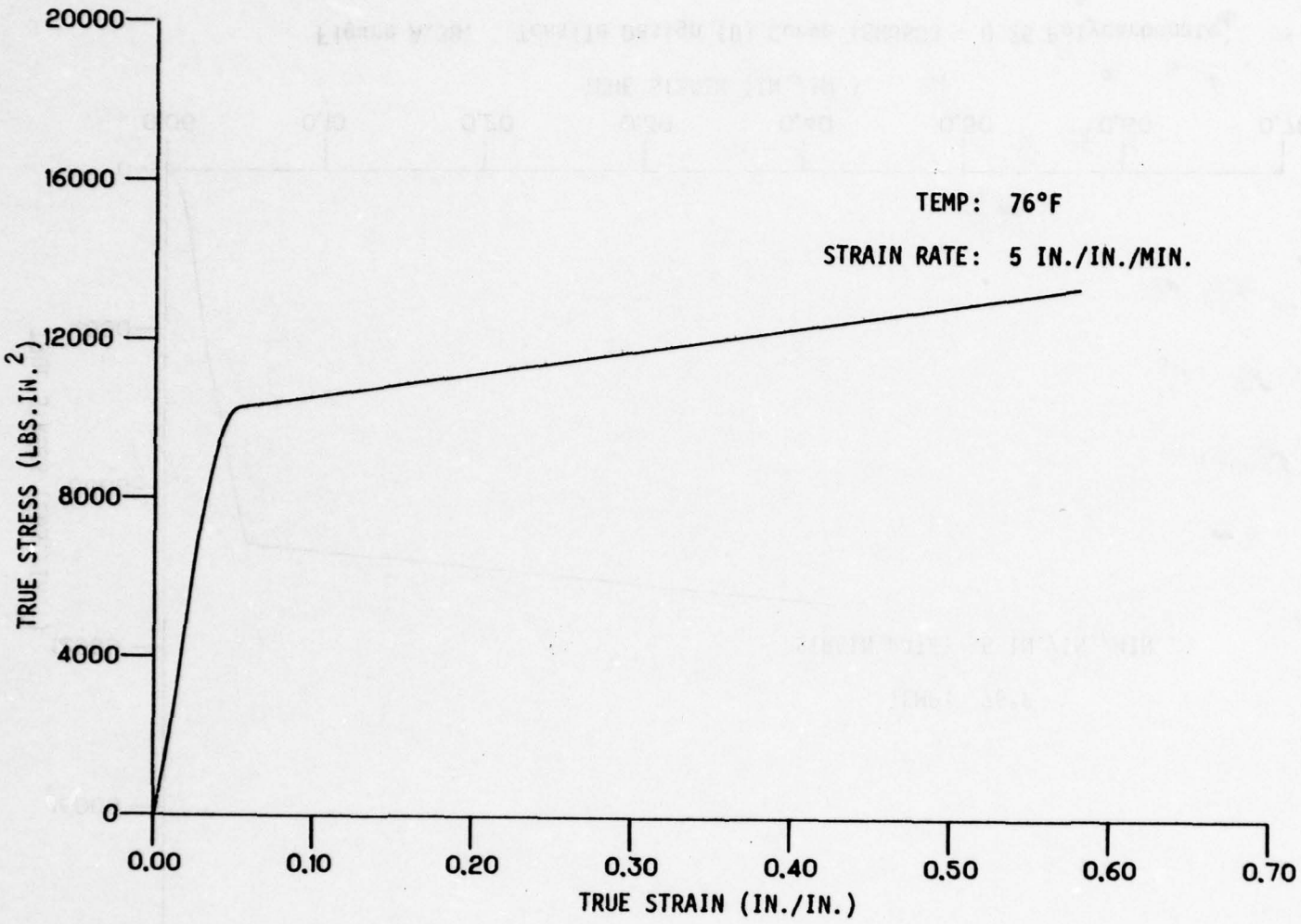

Figure A.37. Tensile Average Curve (SWU503 - 0.25 Polycarbonate)

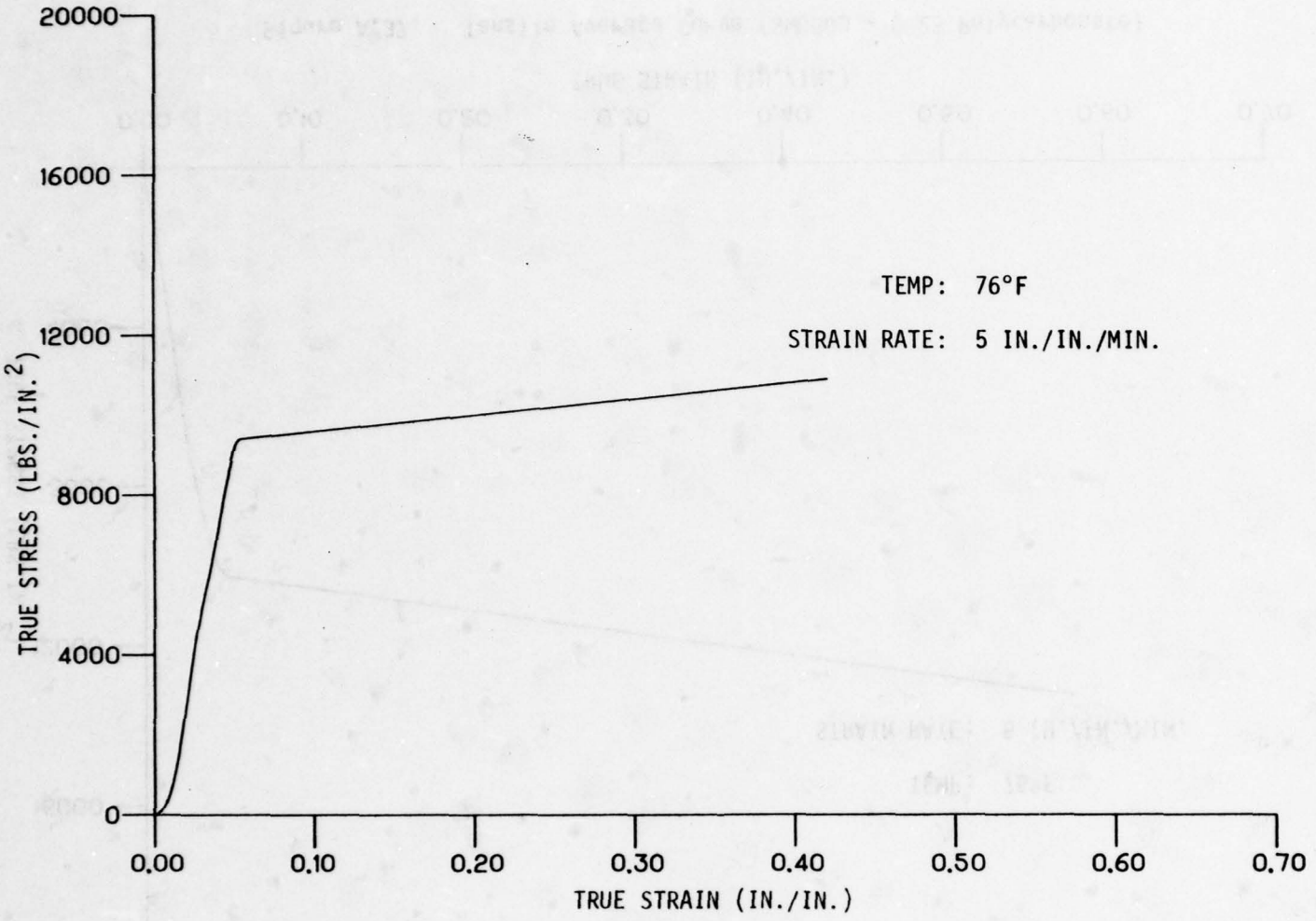

Figure A.38. Tensile Design (B) Curve (SWU503 - 0.25 Polycarbonate)

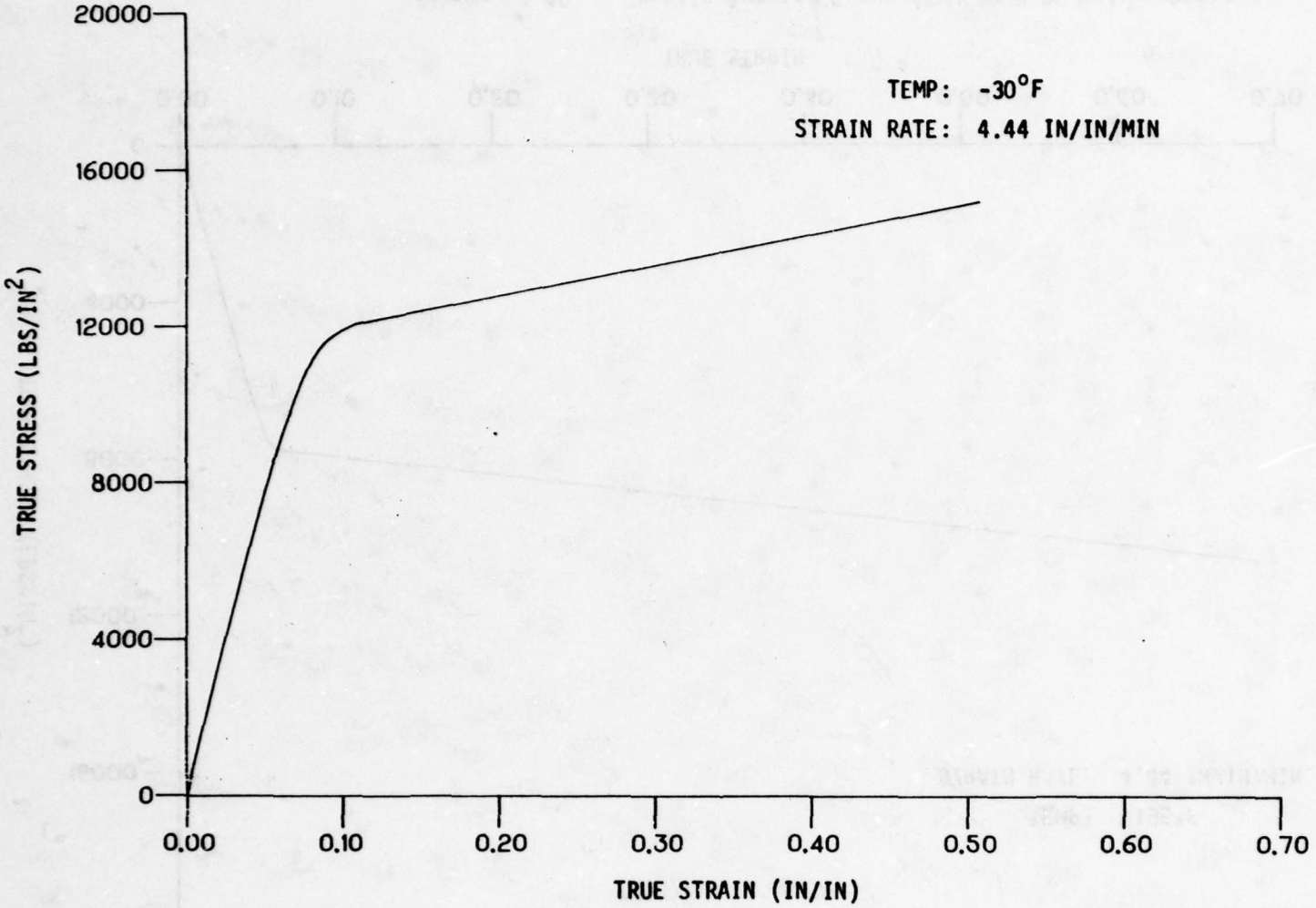

Figure A.39. Tensile Average Curve (SWU503 - 0.250 Polycarbonate)

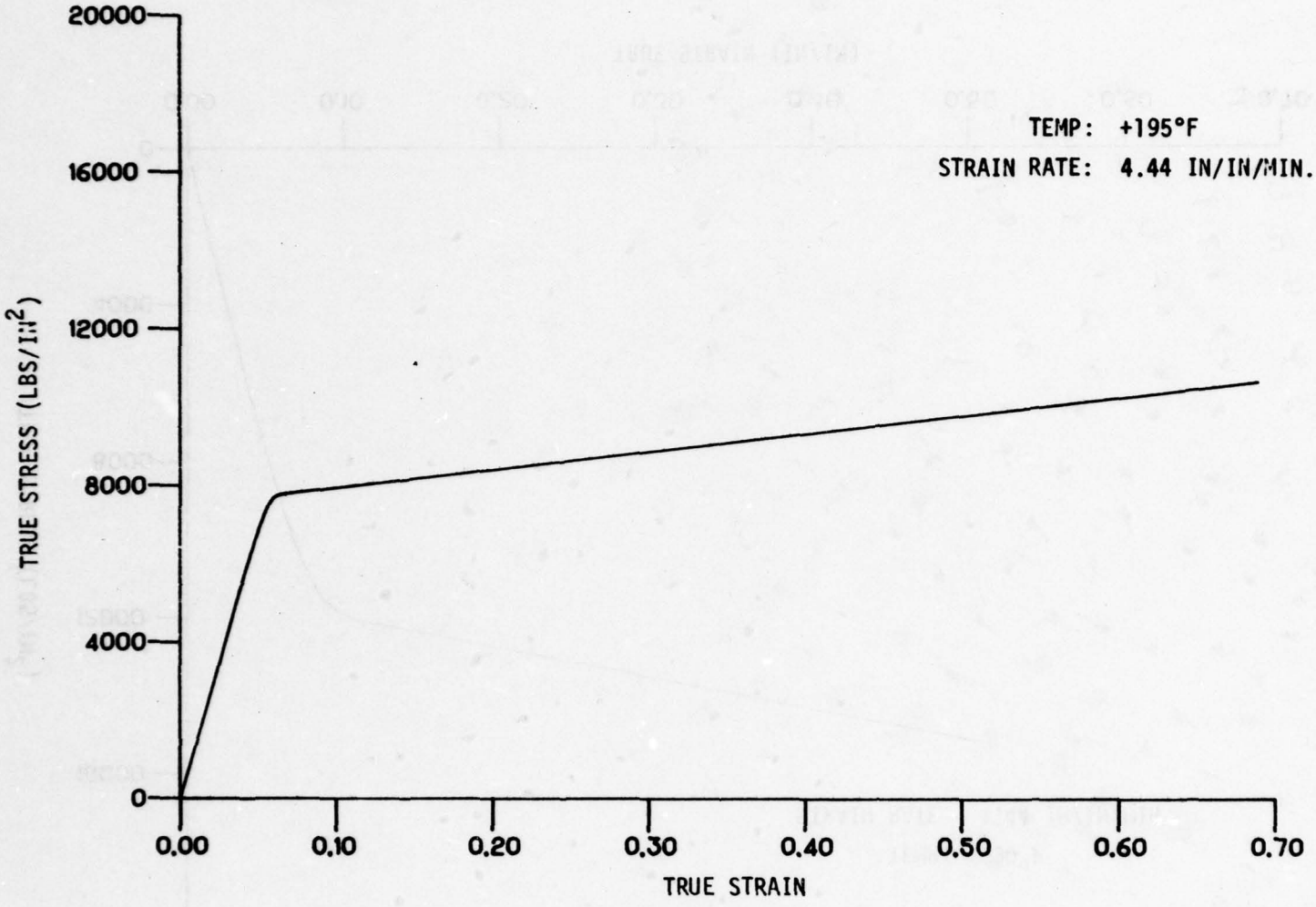

Figure A.40. Tensile Average Curve (SWU503-0.25 Polycarbonate).

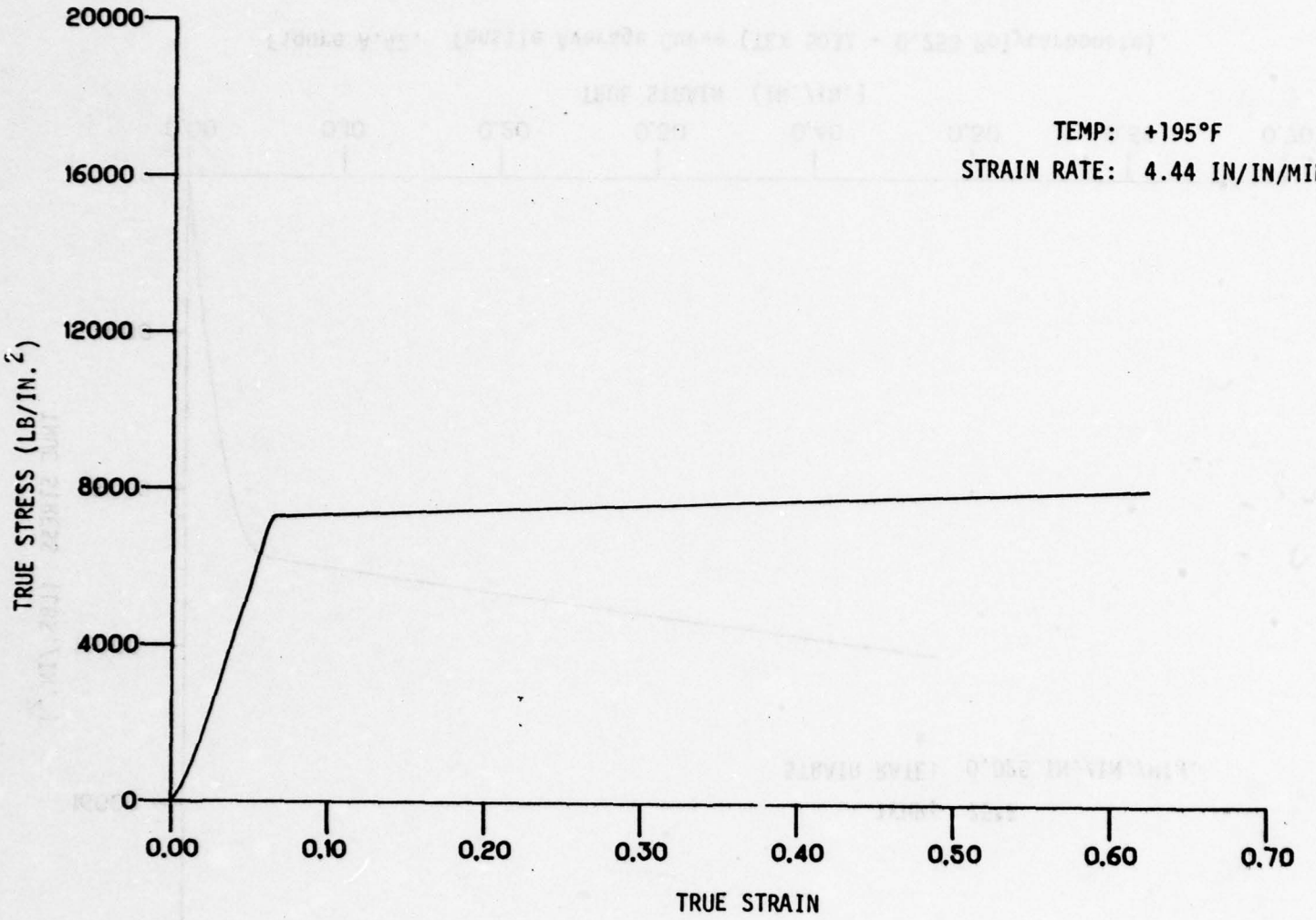

Figure A.41. Tensile Design (B) Curve (SWU503-0.25 Polycarbonate).

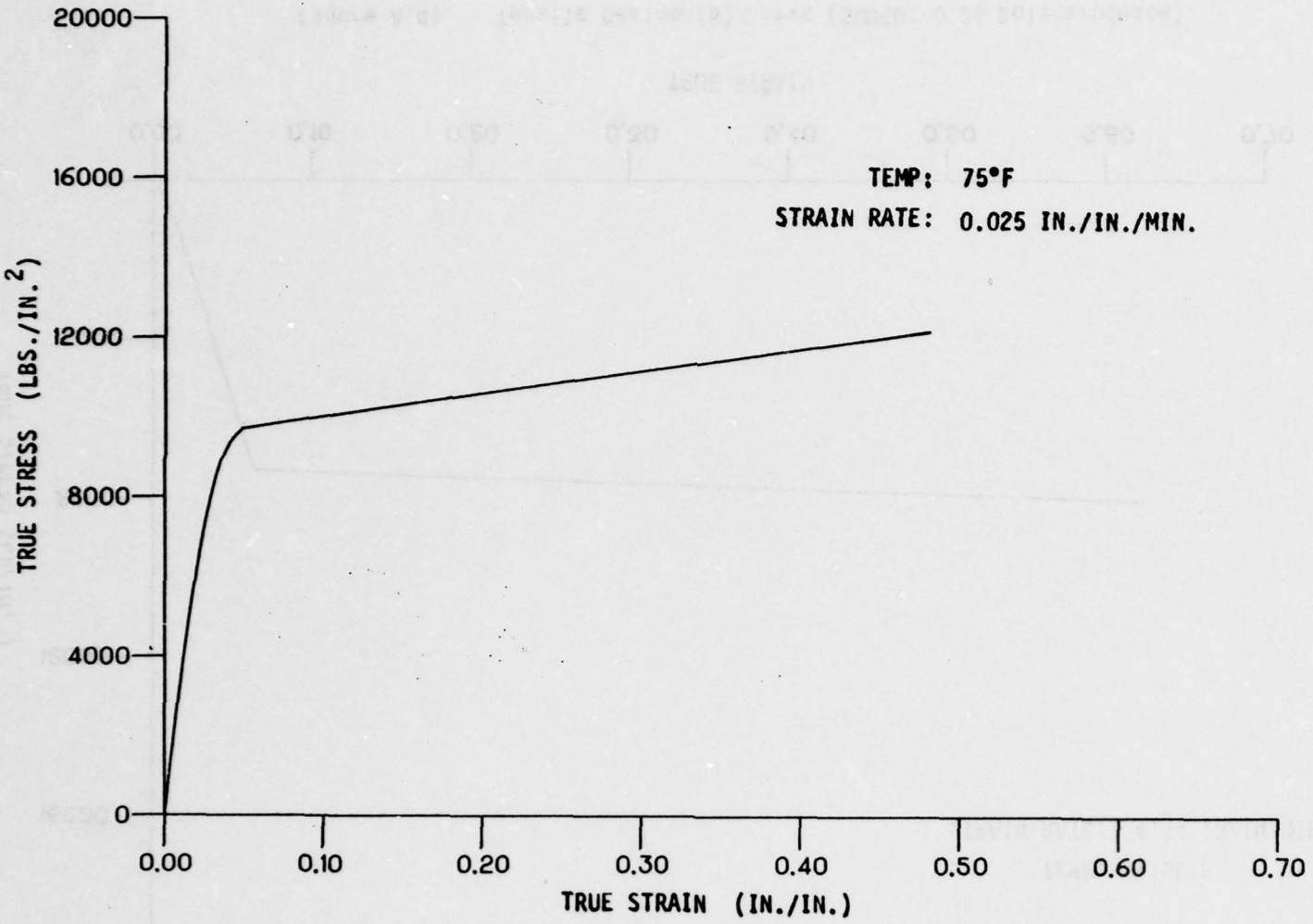

Figure A.42. Tensile Average Curve (TEX 503X - 0.250 Polycarbonate).

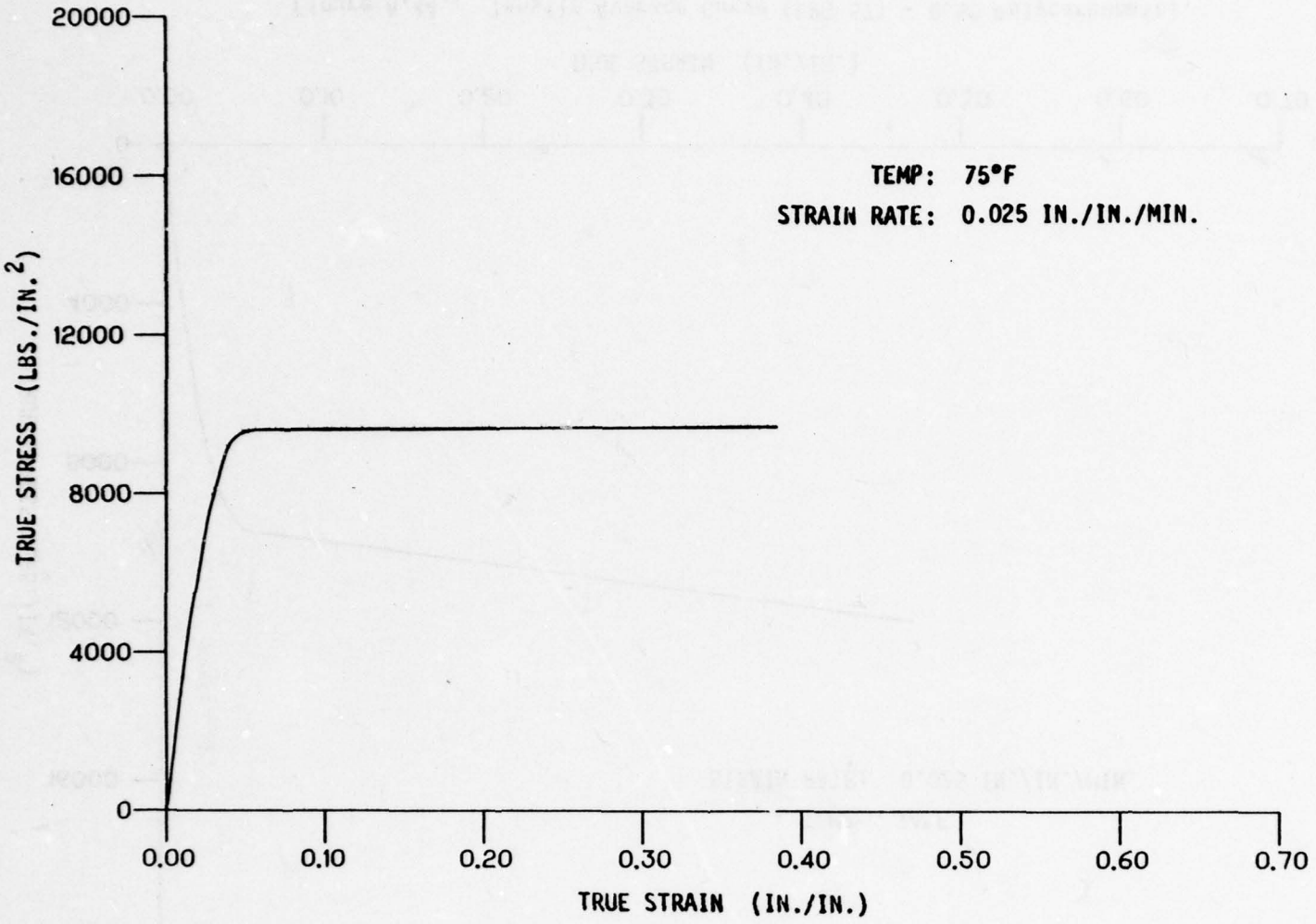

Figure A.43. Tensile Design (C) Curve (TEX 503X - 0.250 Polycarbonate).

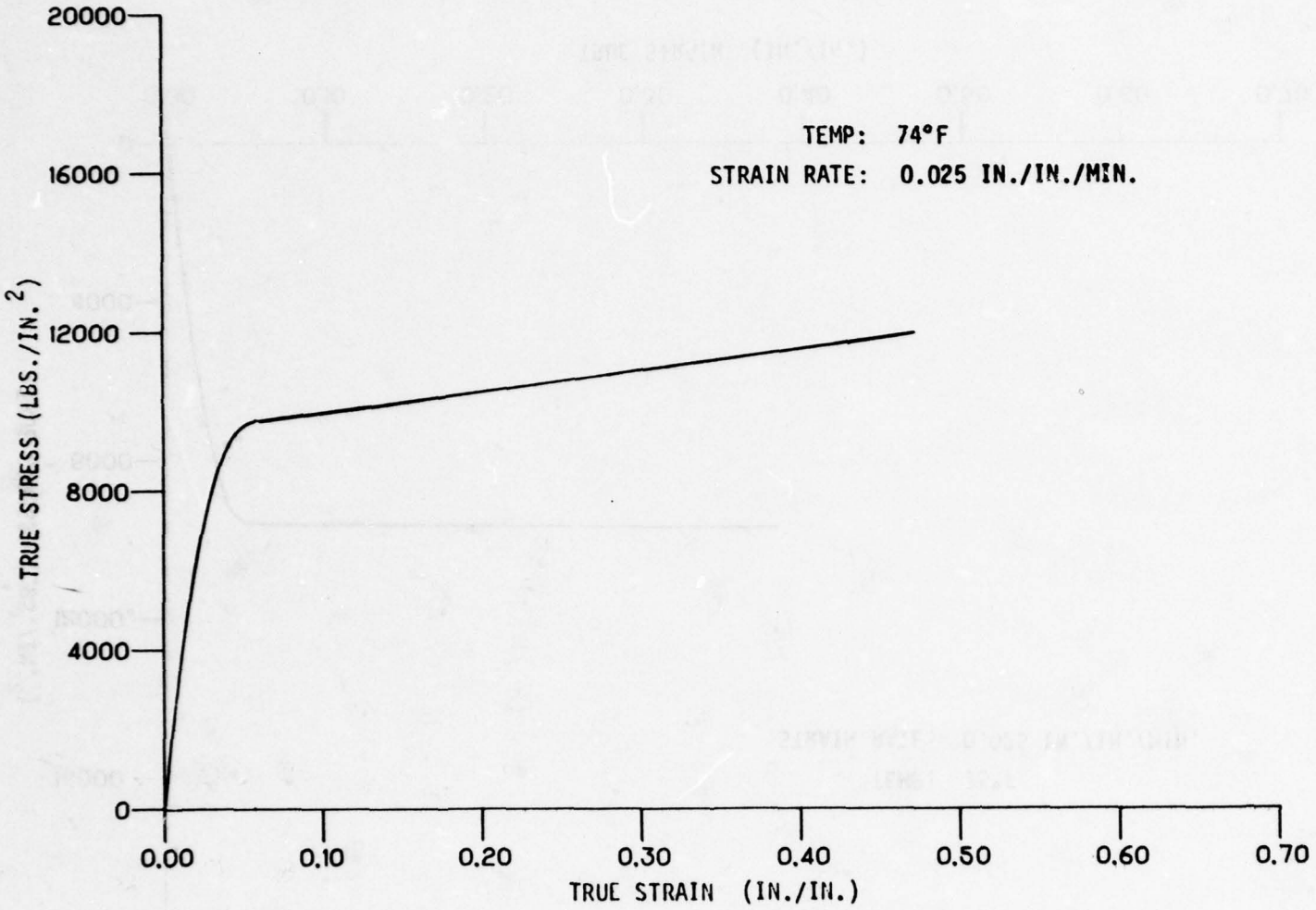

Figure A.44.. Tensile Average Curve (PPG 571 - 0.50 Polycarbonate).

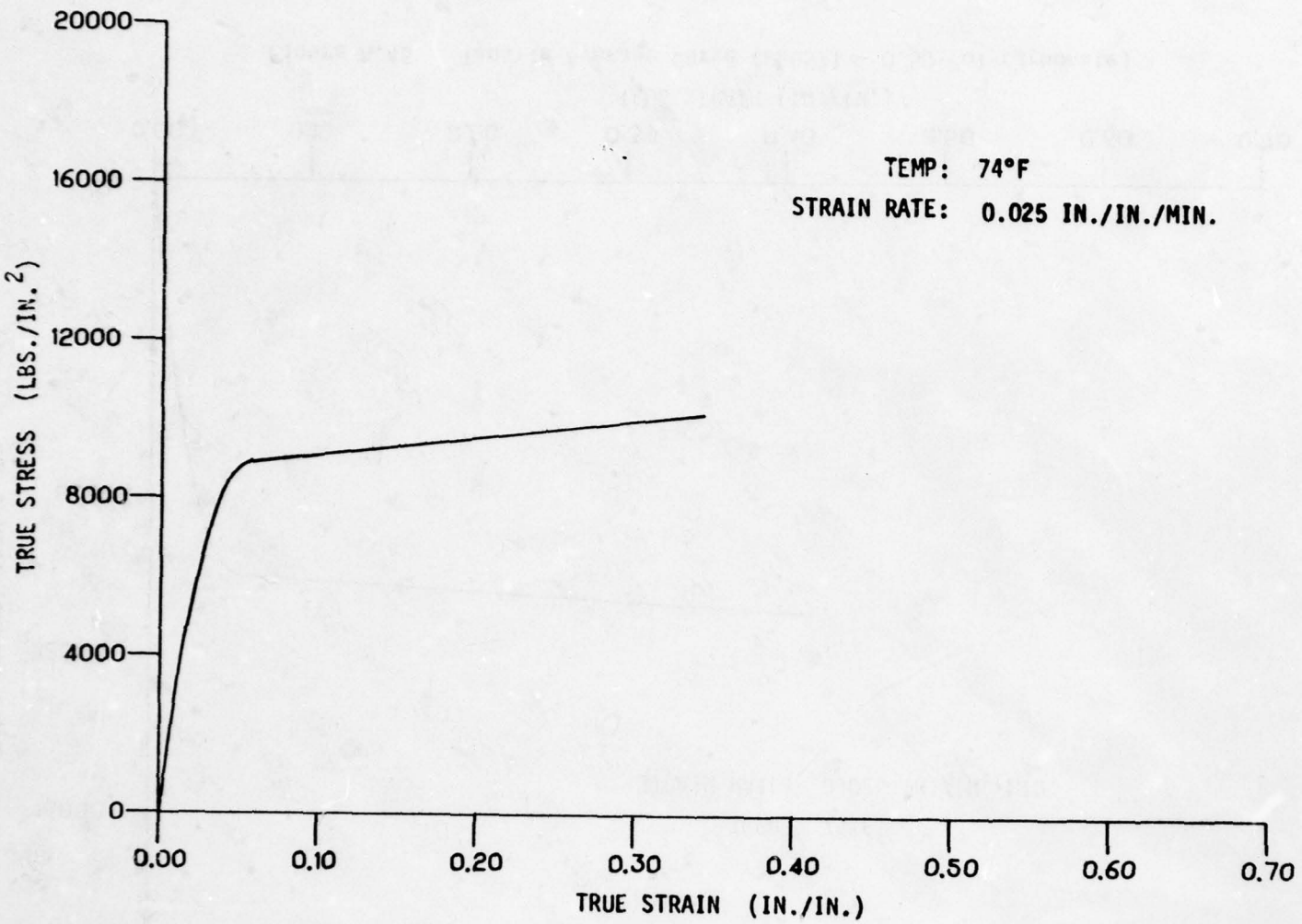

Figure A.45. Tensile Design (B) Curve (PPG 571 - 0.50 Polycarbonate).

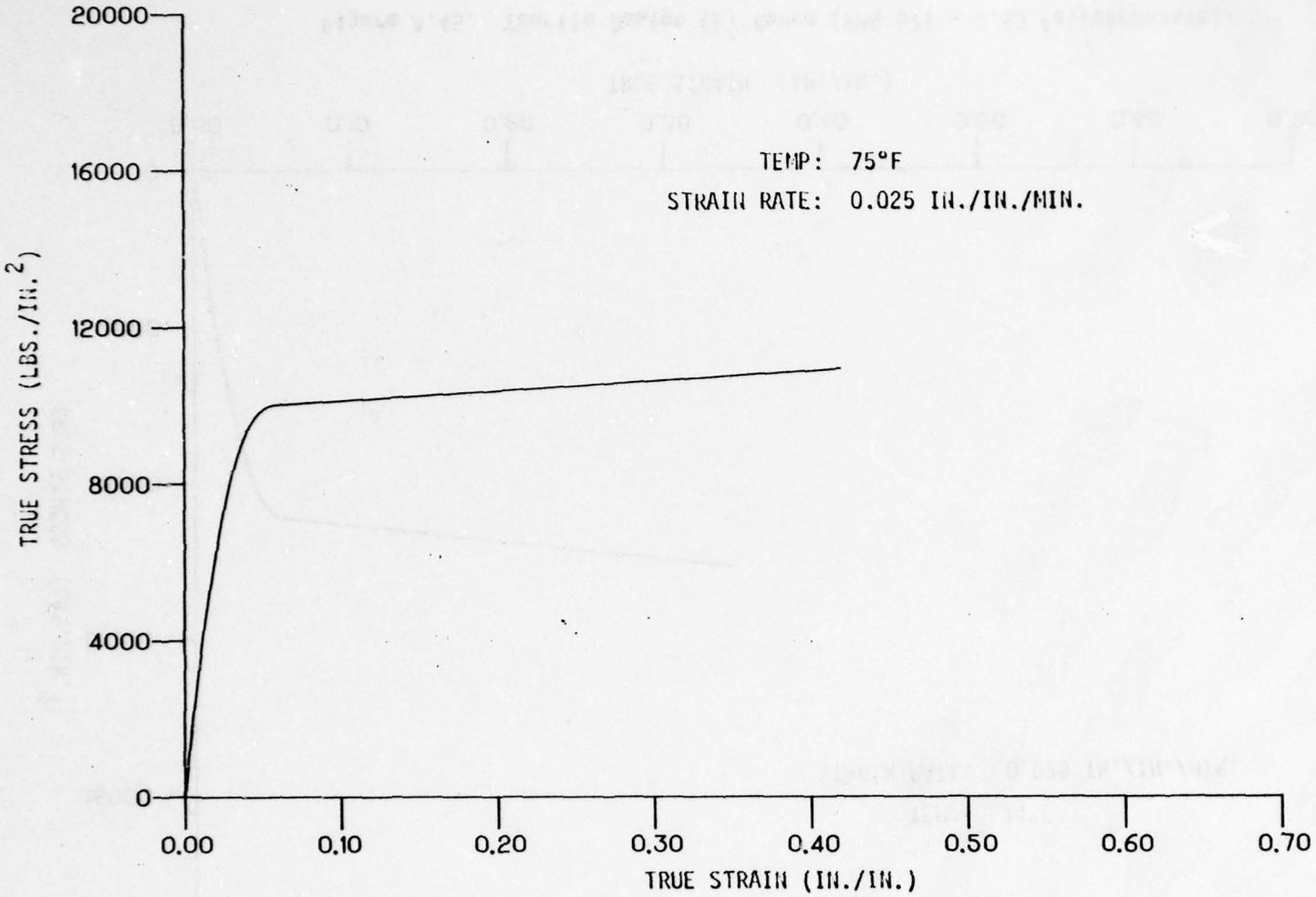

Figure A.46. Tensile Average Curve (PPG571 - 0.50 Polycarbonate)

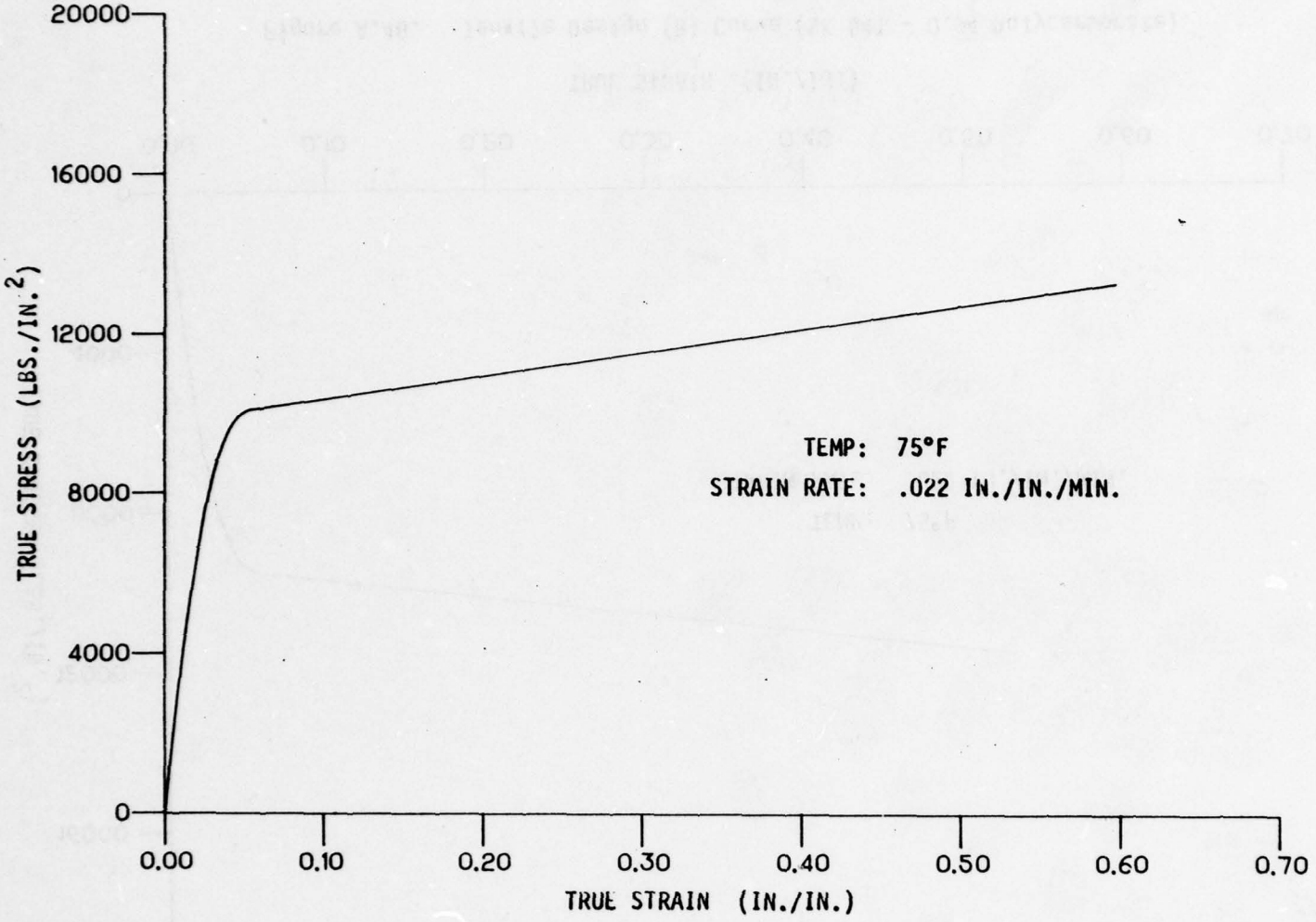

Figure A.47. Tensile Average Curve (SK 541 - 0.94 Polycarbonate).

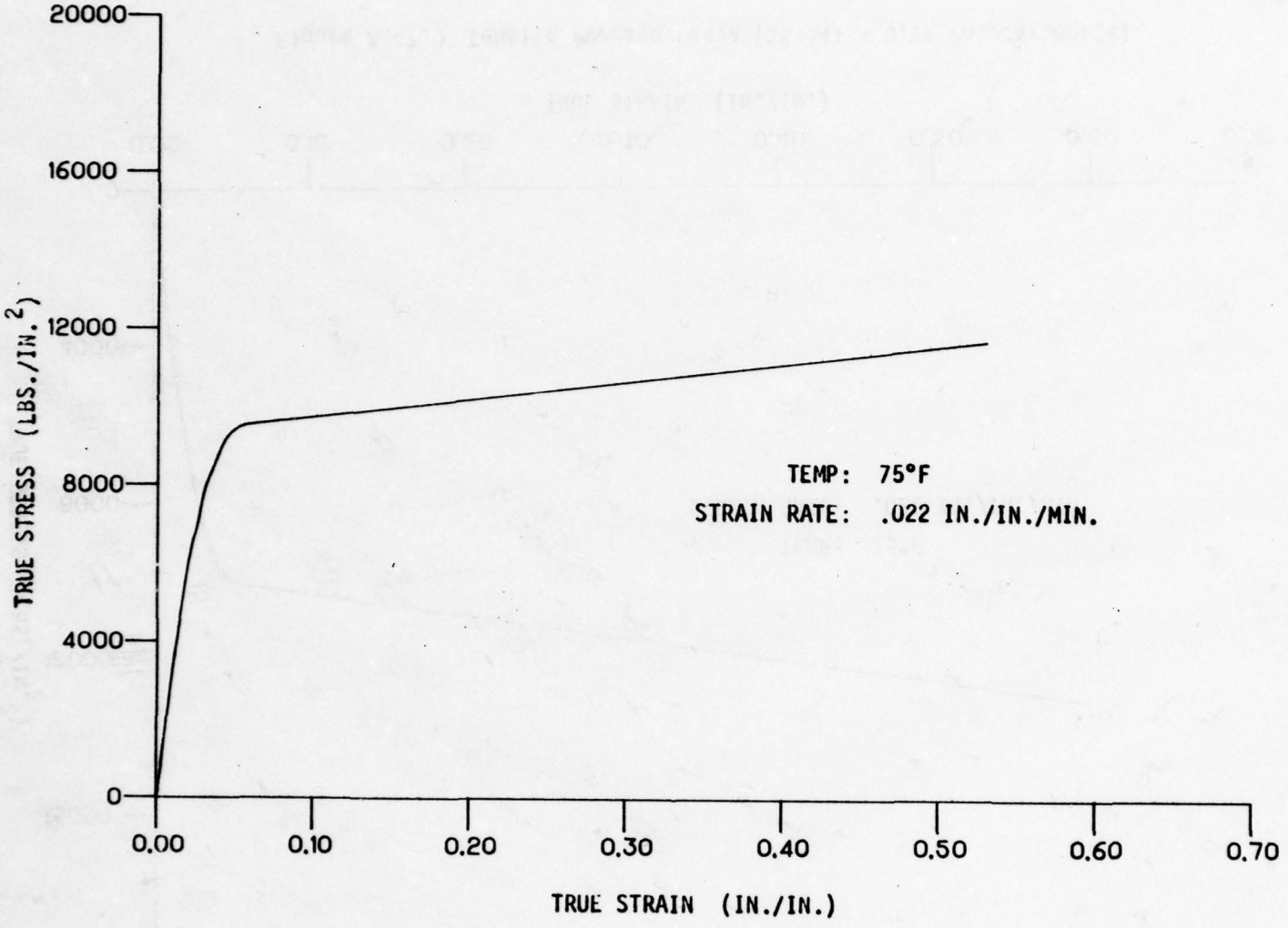

Figure A.48. Tensile Design (B) Curve (SK 541 - 0.94 Polycarbonate).

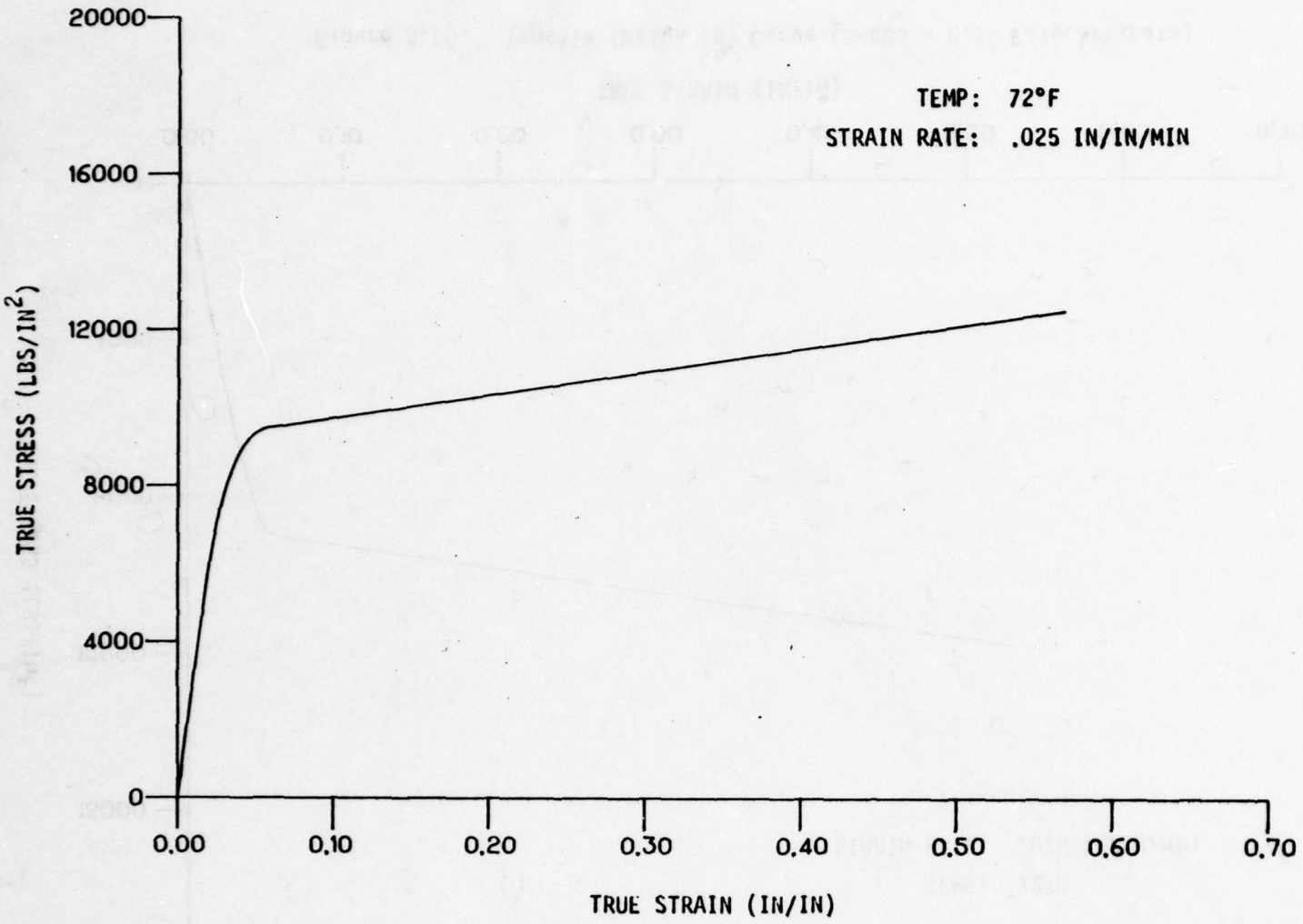

Figure A.49. Tensile Average Curve (SK605 - 0.50 Polycarbonate)

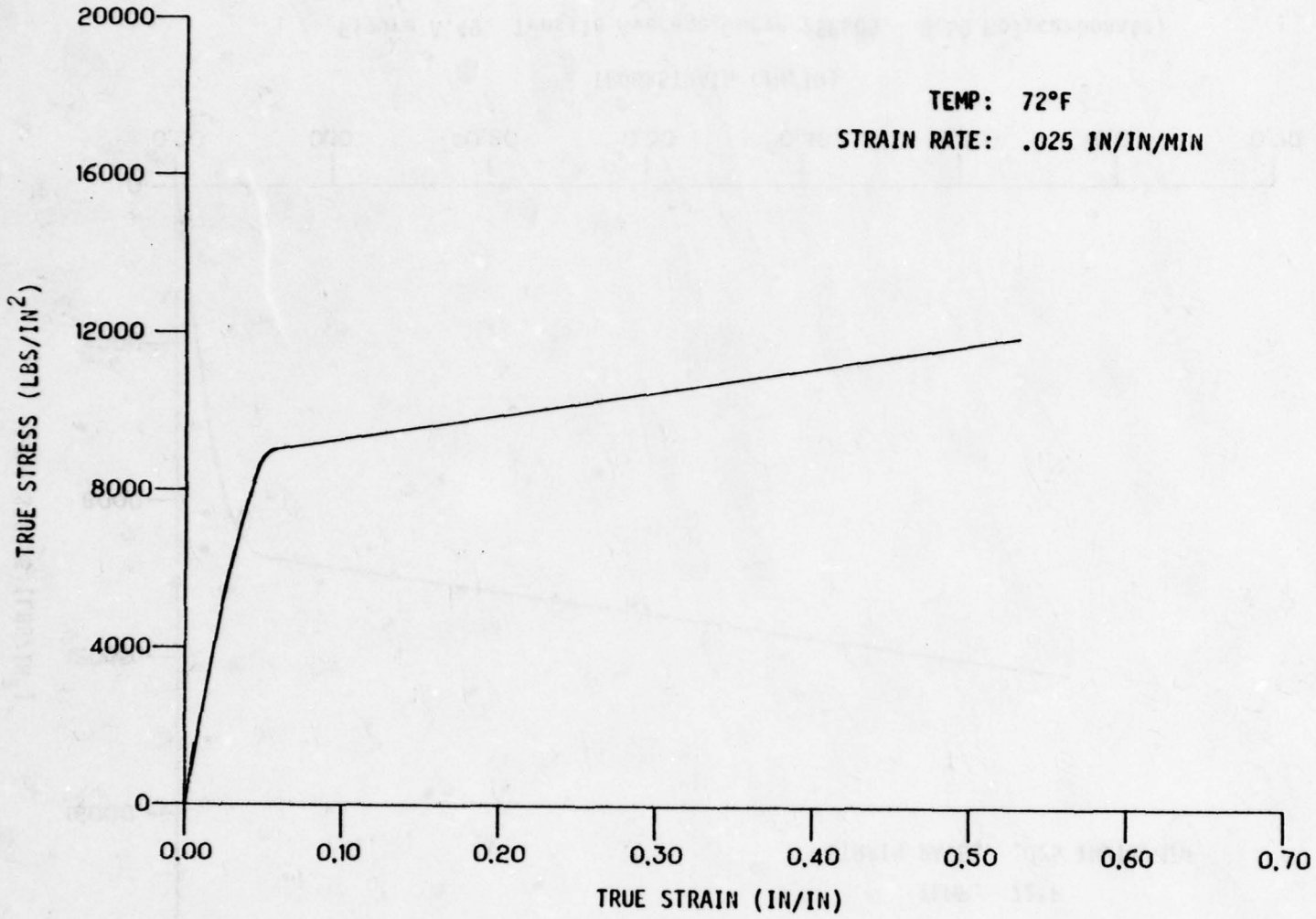

Figure A.50. Tensile Design (B) Curve (SK605 - 0.50 Polycarbonate)

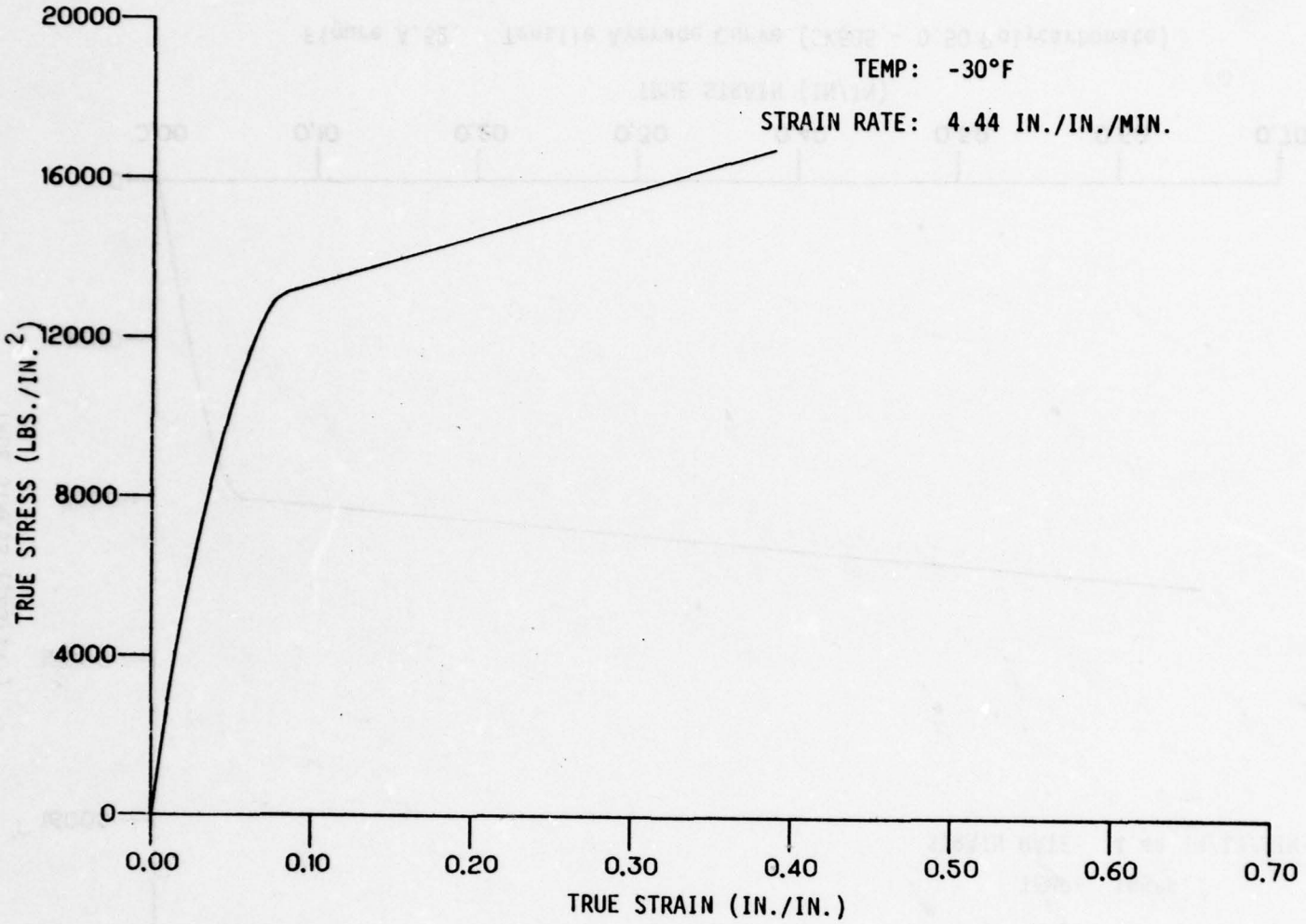

Figure A.51. Tensile Average Curve (SK605 - 0.50 Polycarbonate)

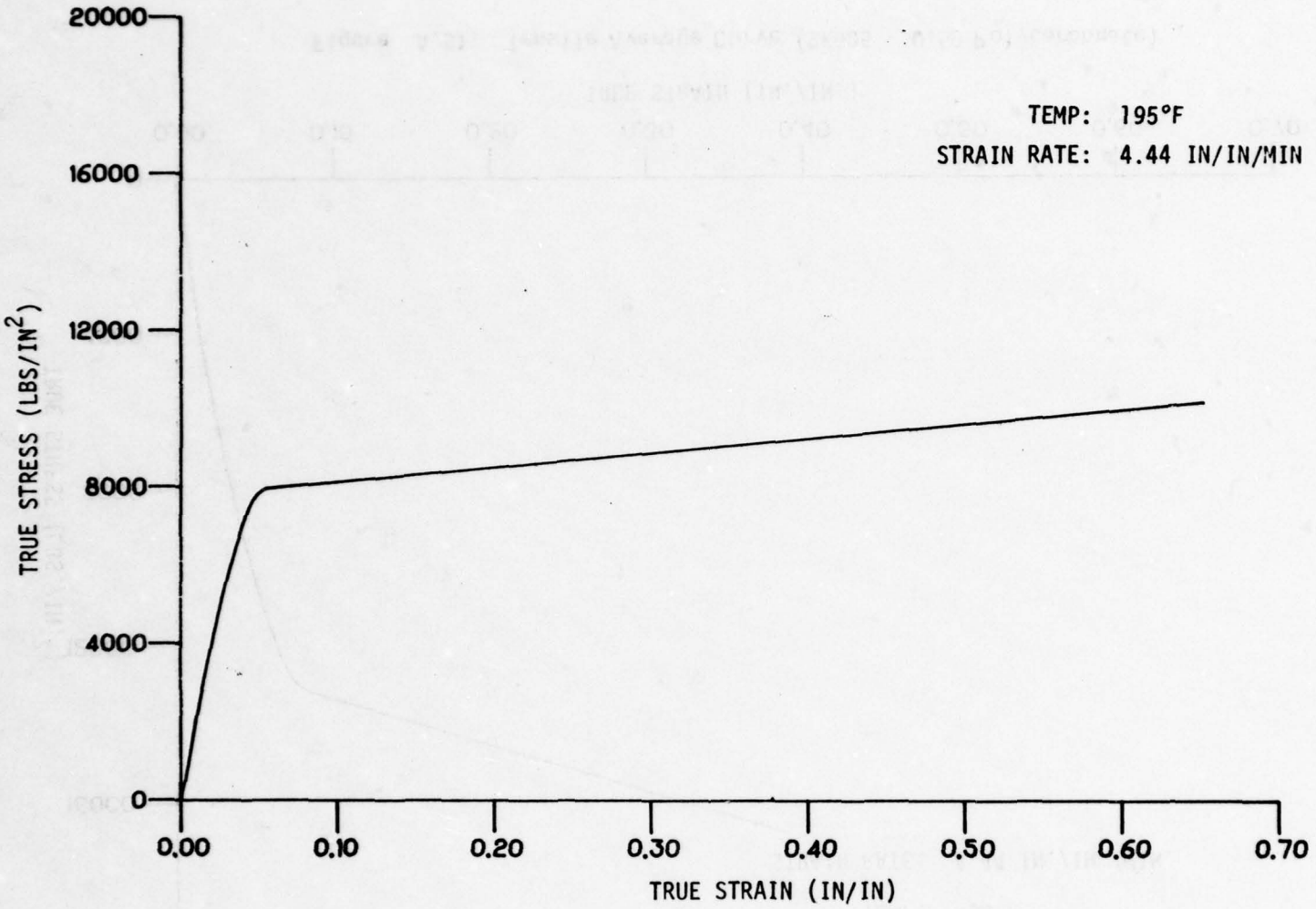

Figure A.52. Tensile Average Curve (SK605 - 0.50 Polycarbonate)

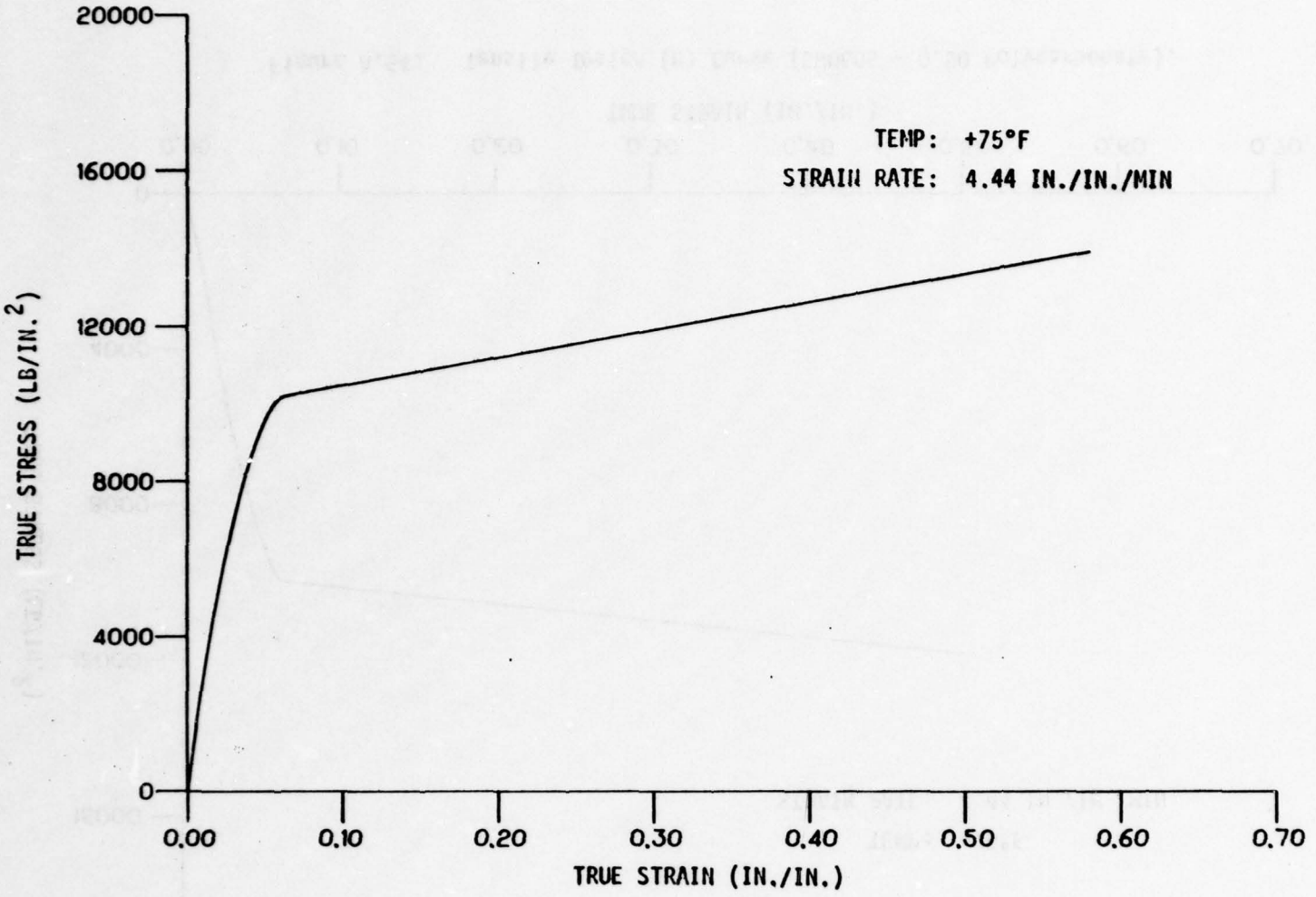

Figure A.53. Tensile Average Curve (SWU605 - 0.50 Polycarbonate).

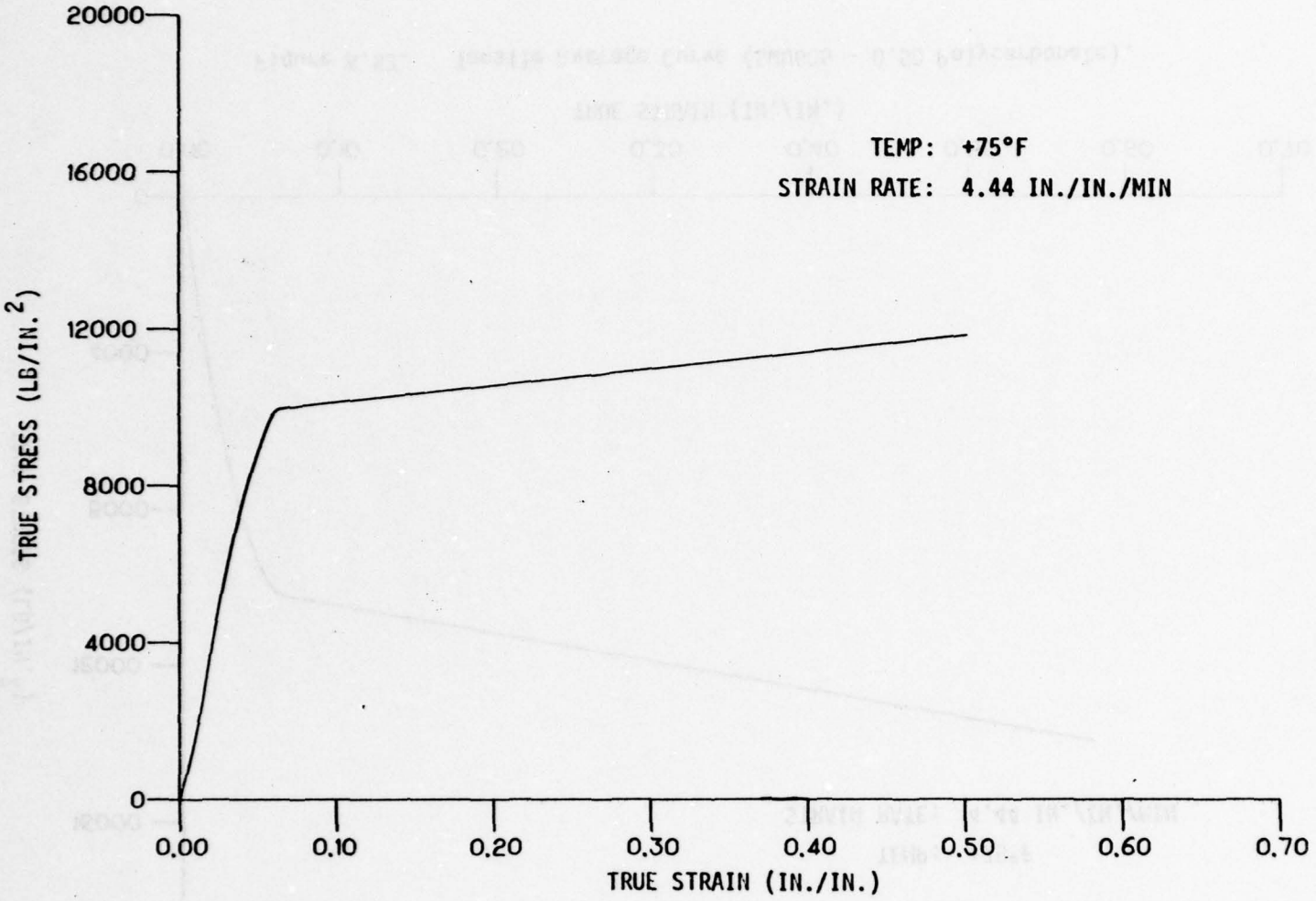

Figure A.54. Tensile Design (B) Curve (SWU605 - 0.50 Polycarbonate).

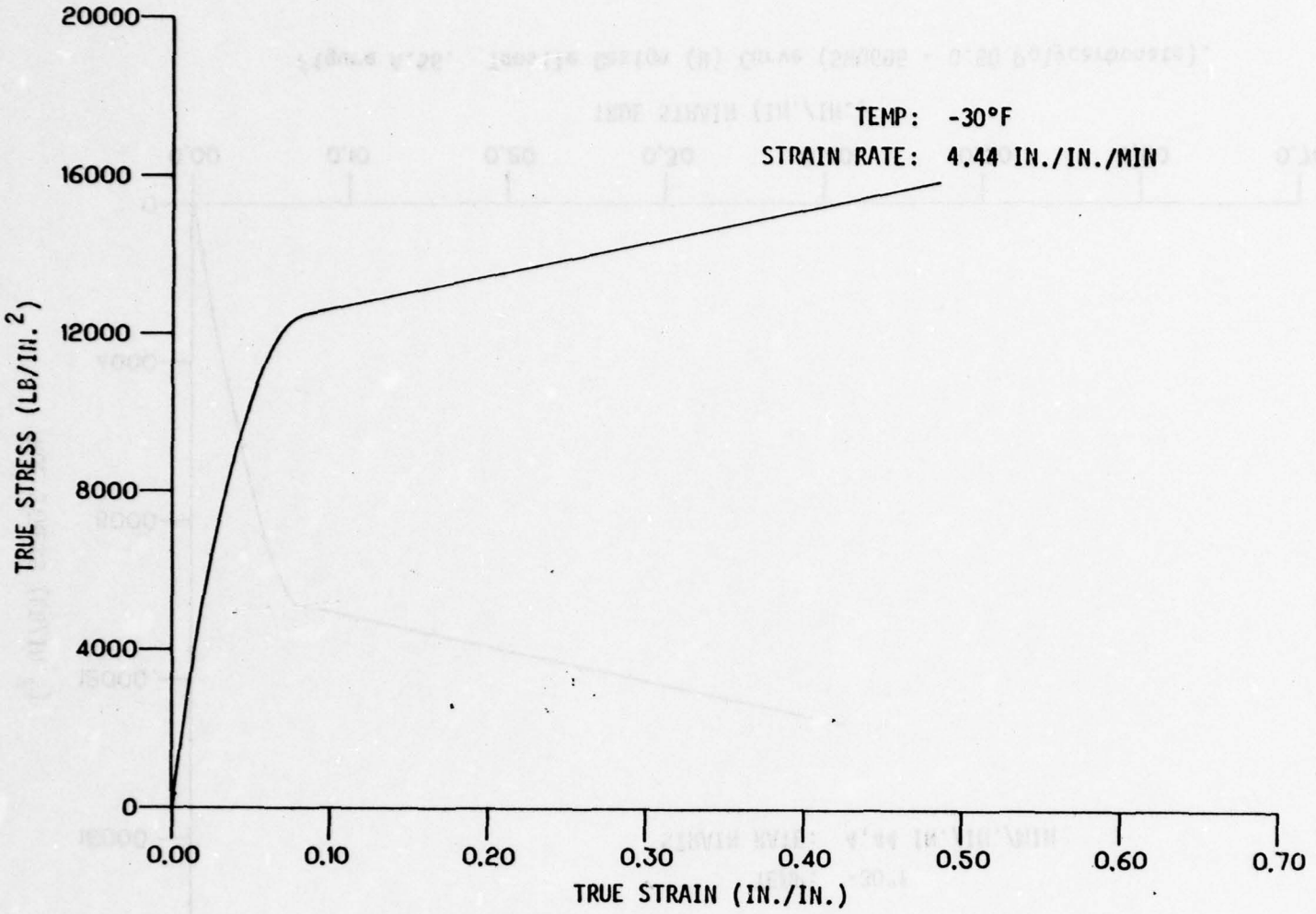

Figure A.55 Tensile Average Curve (SWU605 - 0.50 Polycarbonate).

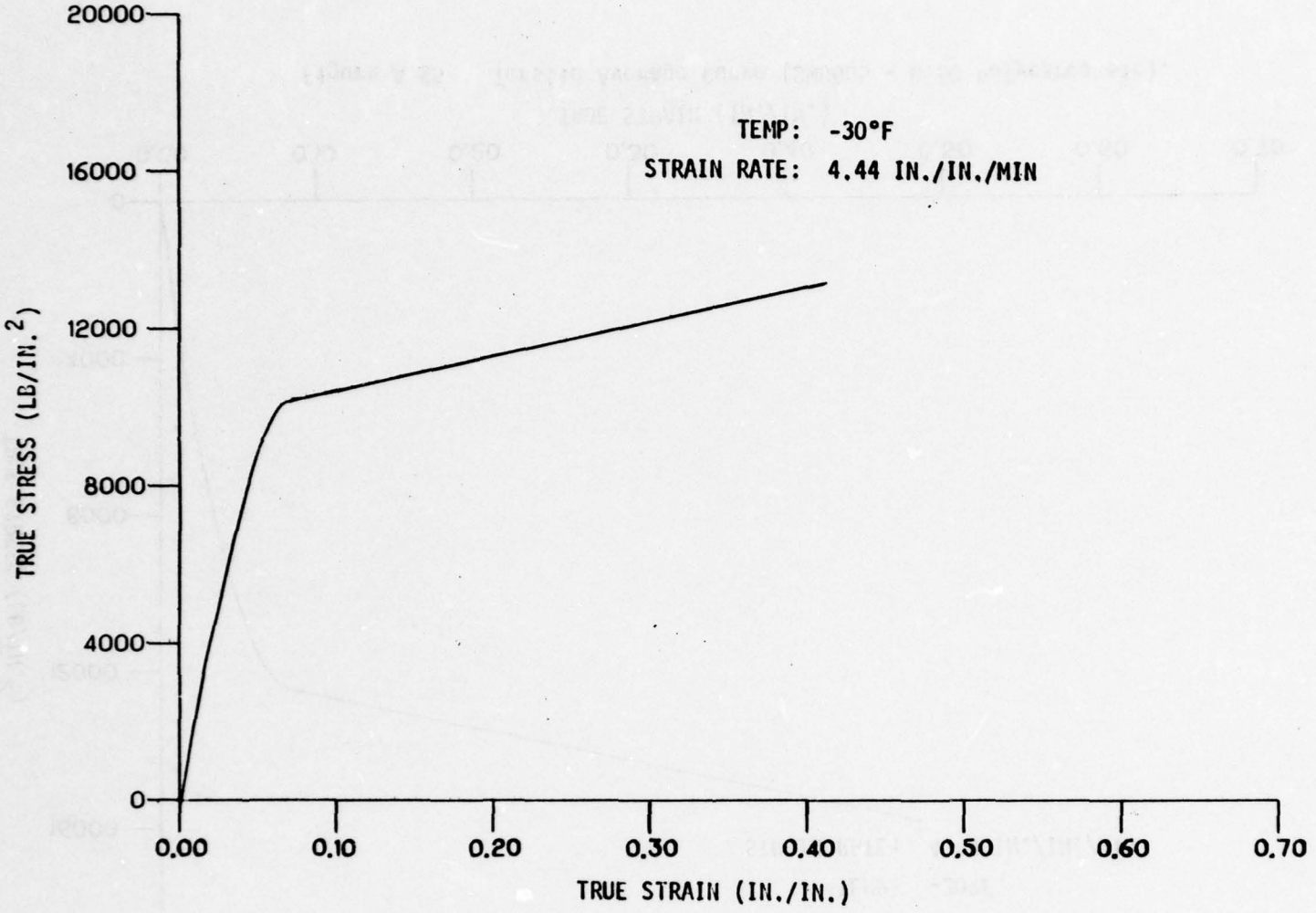

Figure A.56. Tensile Design (B) Curve (SWU605 - 0.50 Polycarbonate).

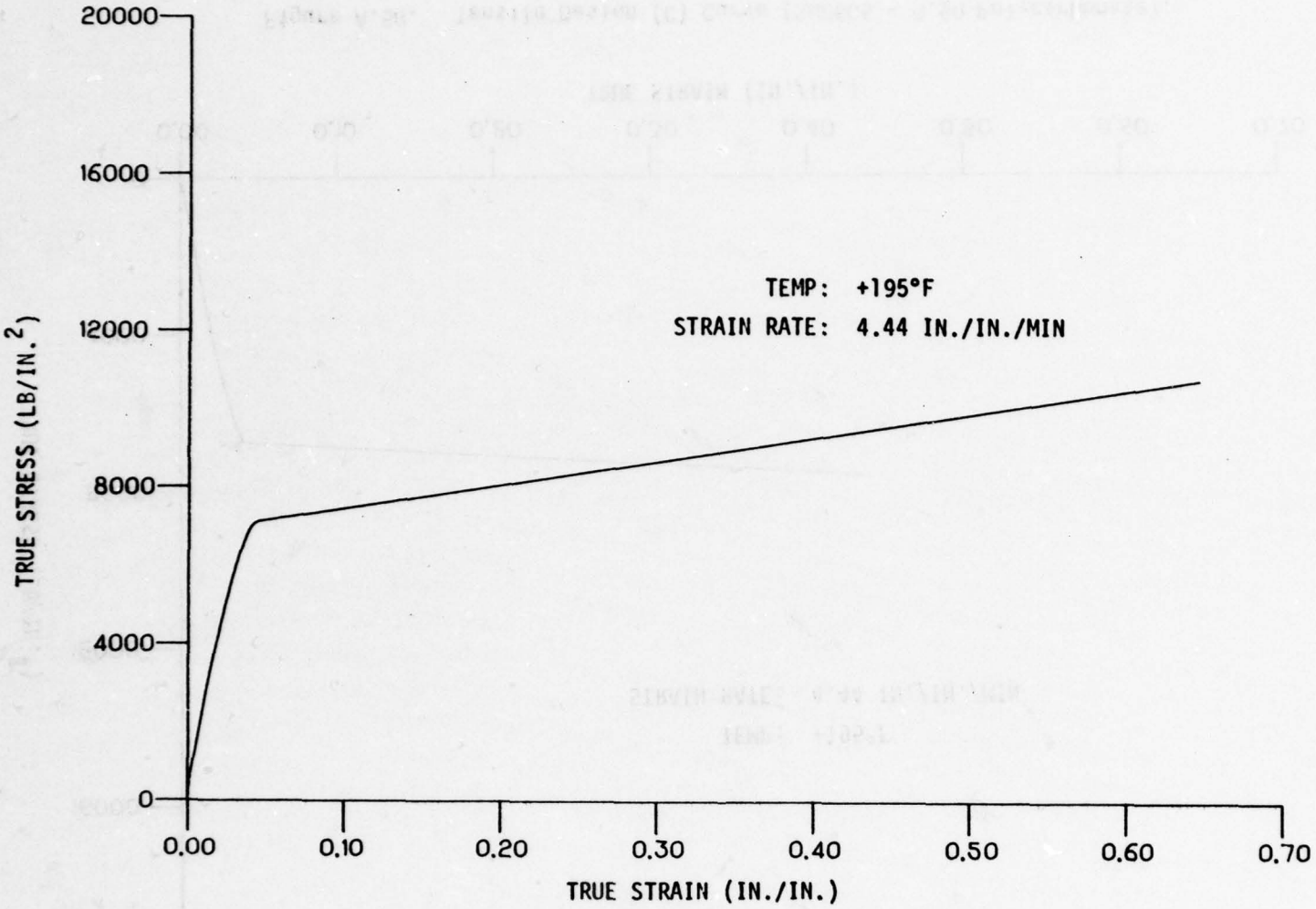

Figure A.57. Tensile Average Curve (SWU605 - 0.50 Polycarbonate).

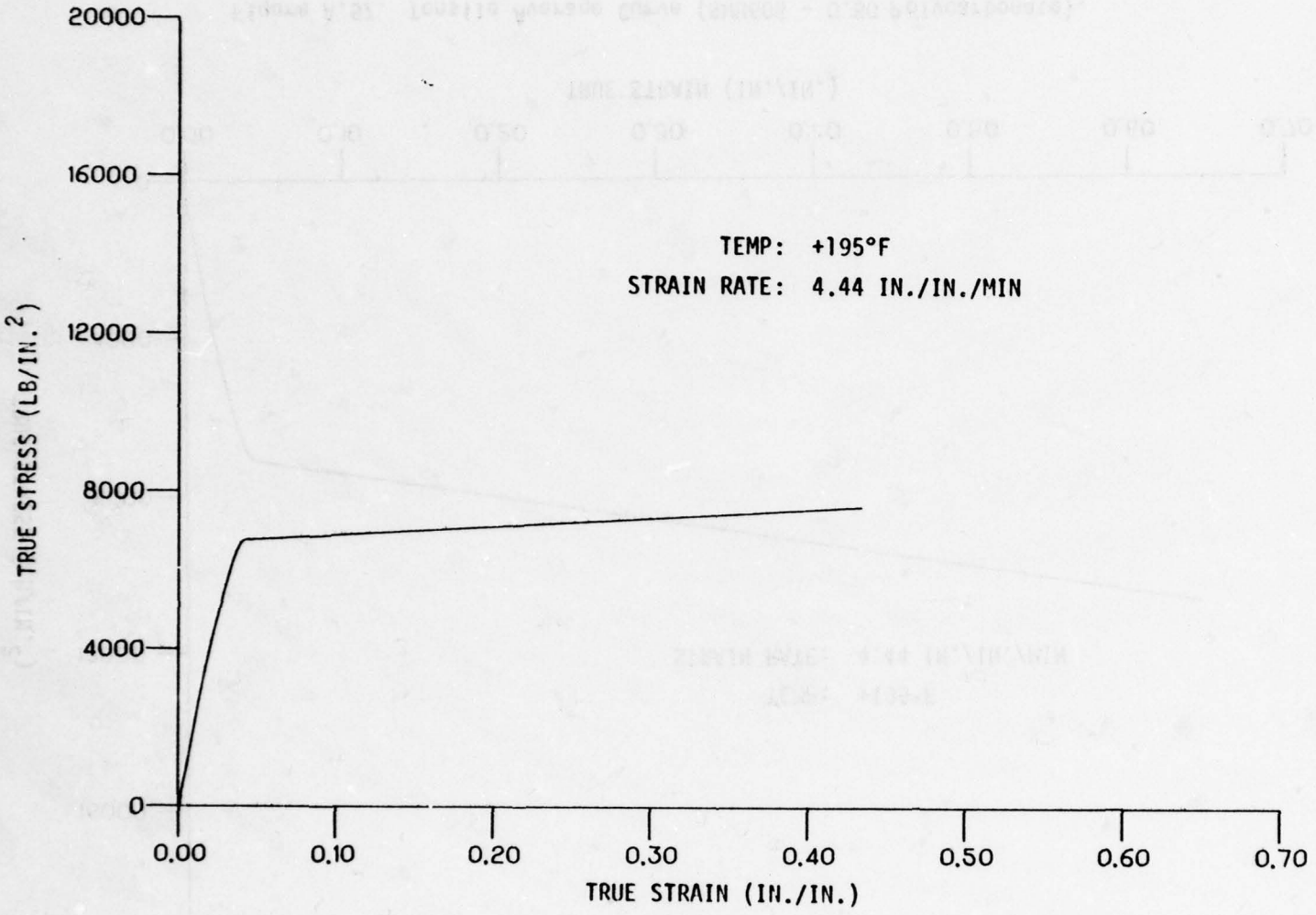

Figure A.58. Tensile Design (C) Curve (SWU605 - 0.50 Polycarbonate).

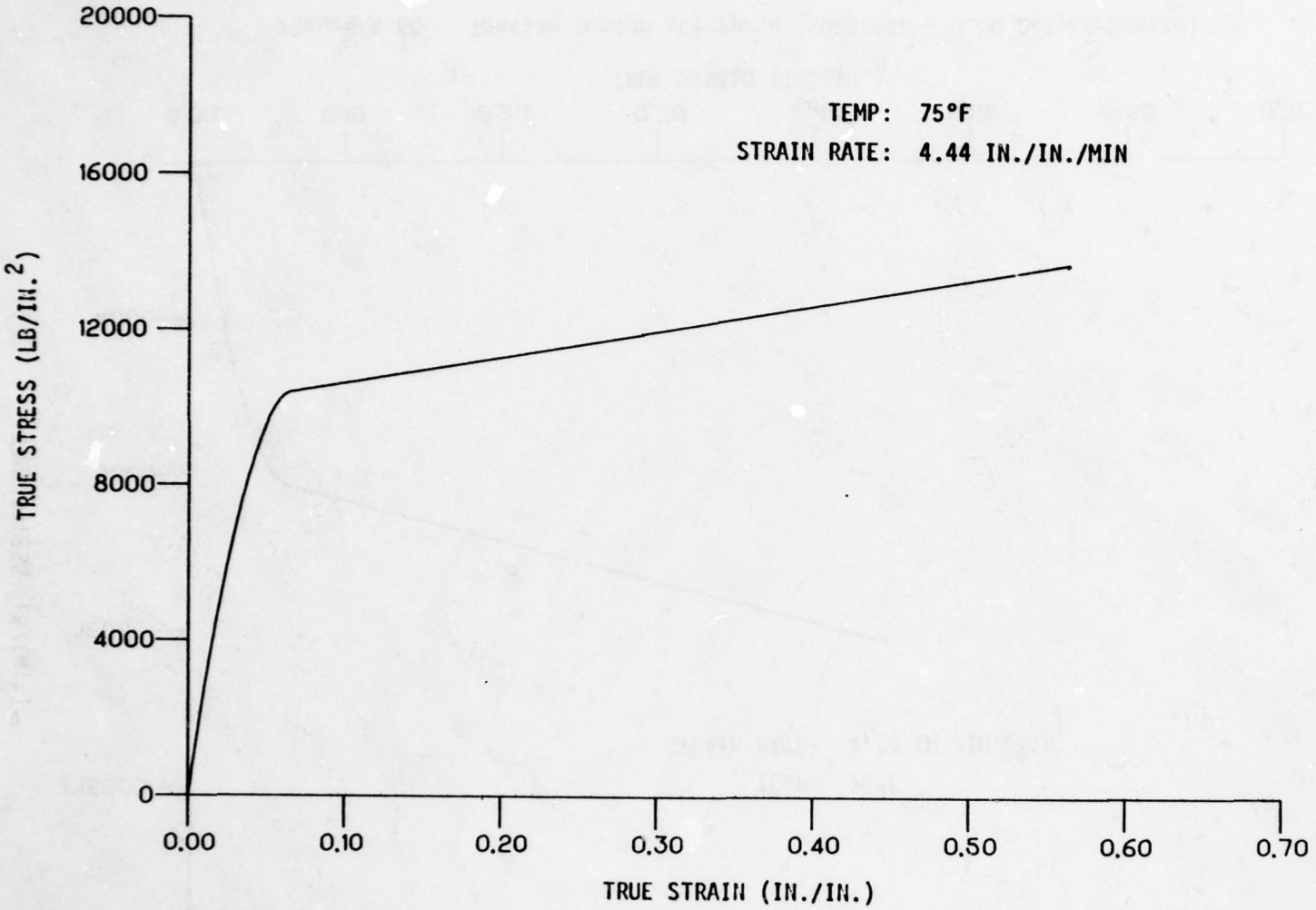

Figure A.59. Tensile Average Curve (SWU605RH - 0.50 Polycarbonate).

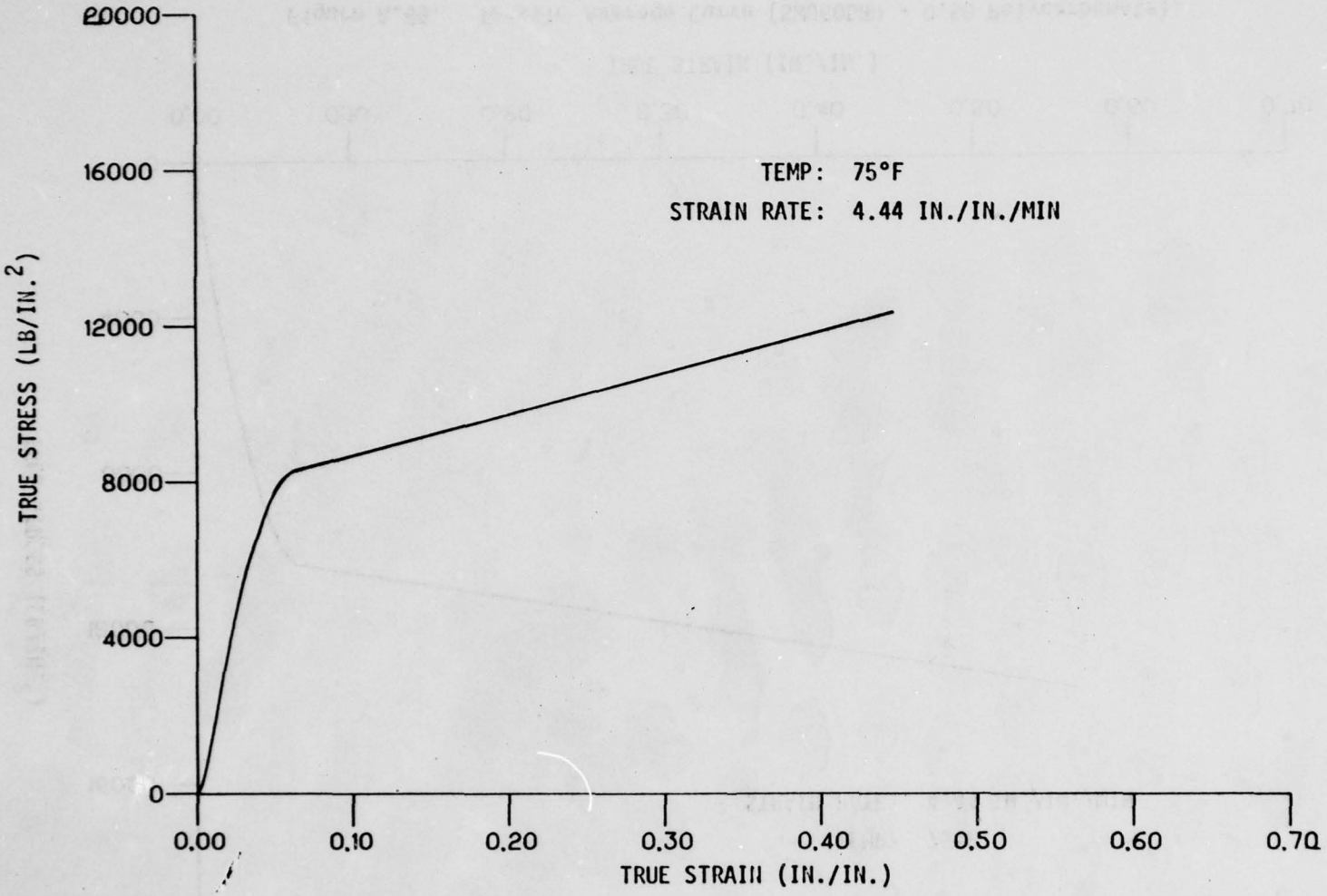

Figure A.60. Tensile Design (B) Curve (SWU605RH - 0.50 Polycarbonate).

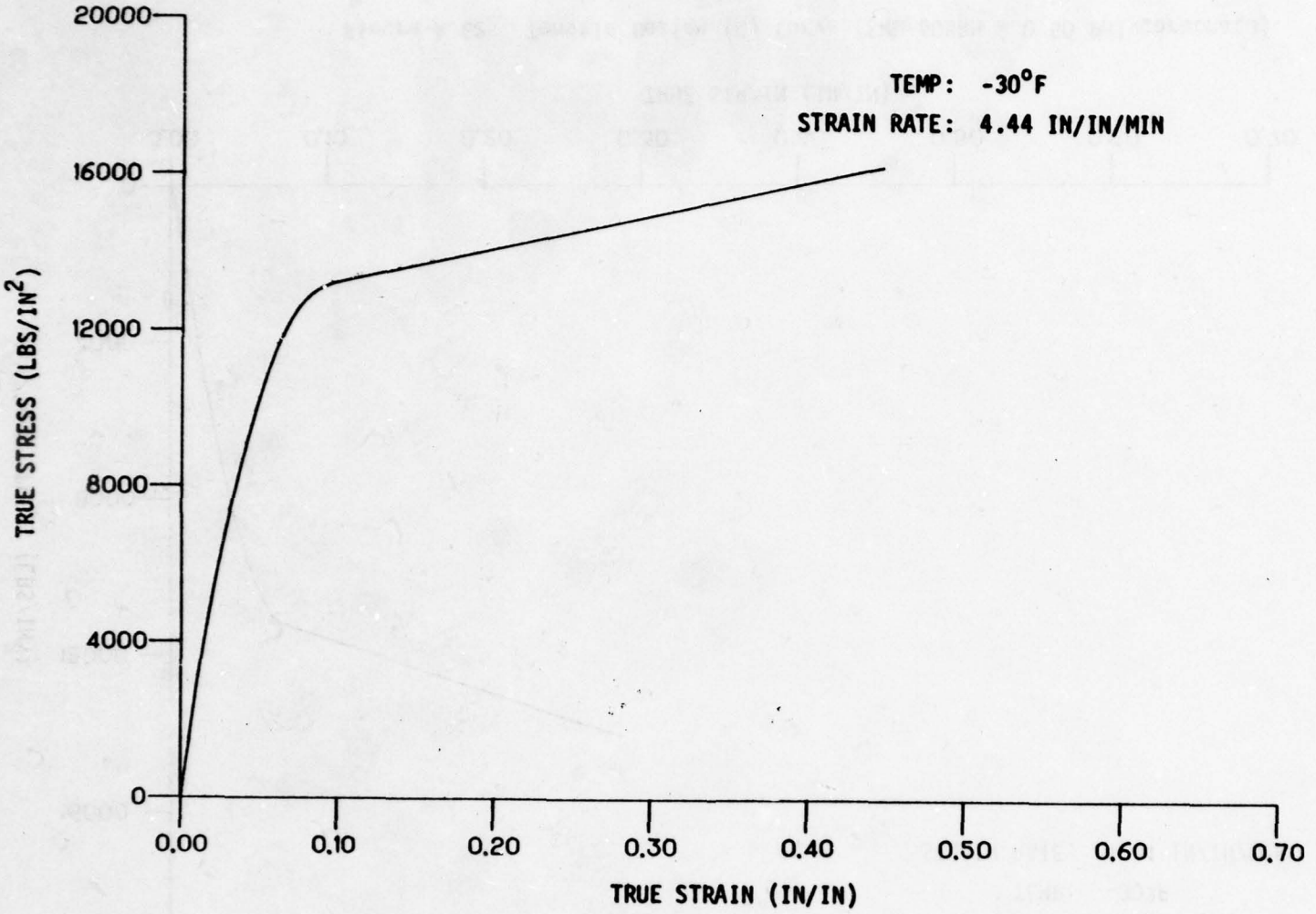

Figure A.61. Tensile Average Curve (SWU605RH - 0.50 Polycarbonate)

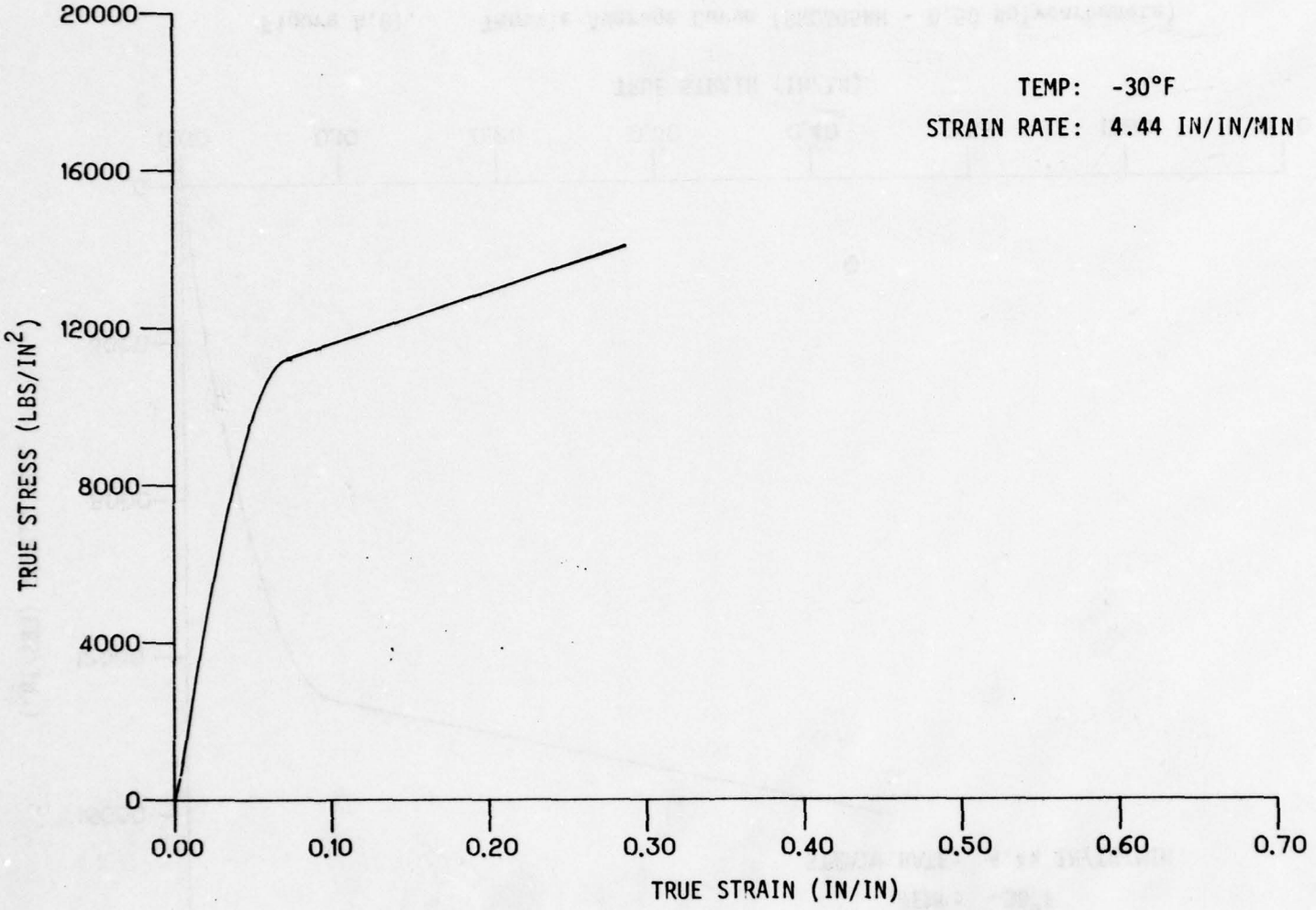

Figure A.62 Tensile Design (C) Curve (SWU 605RH - 0.50 Polycarbonate).

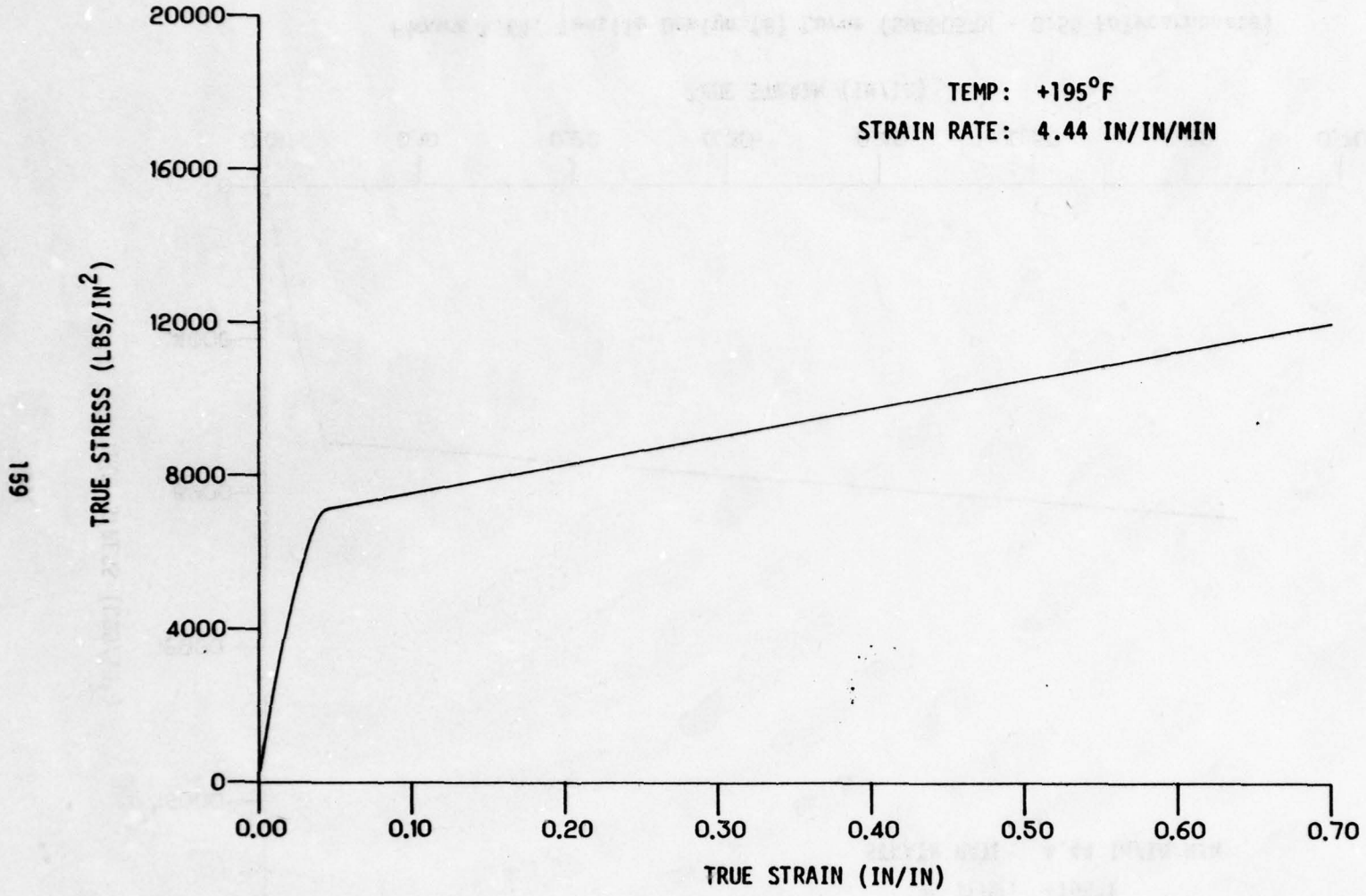

Figure A.63. Tensile Average Curve (SWU605RH - 0.50 Polycarbonate)

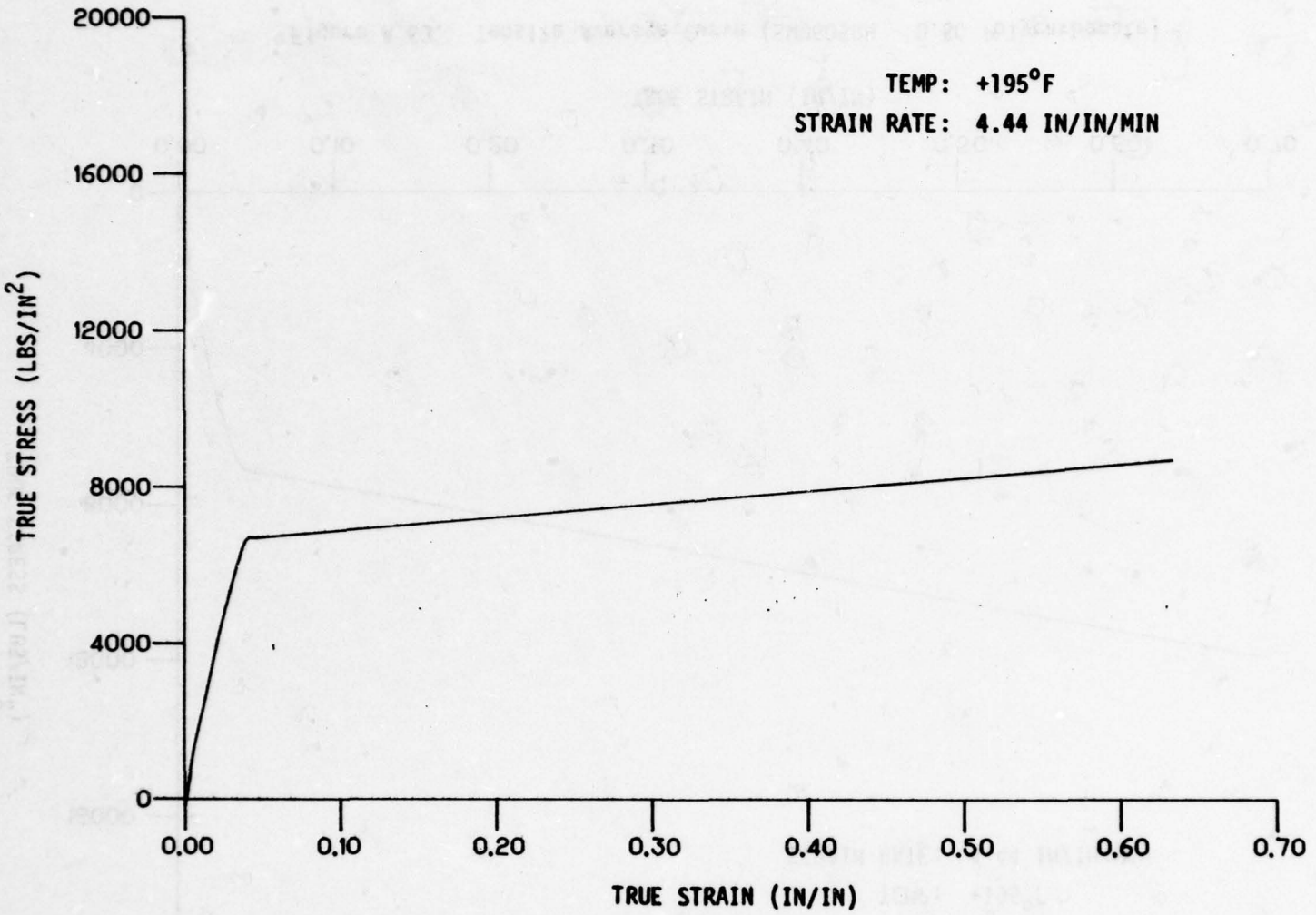

Figure A.64. Tensile Design (B) Curve (SWU605RH - 0.50 Polycarbonate)

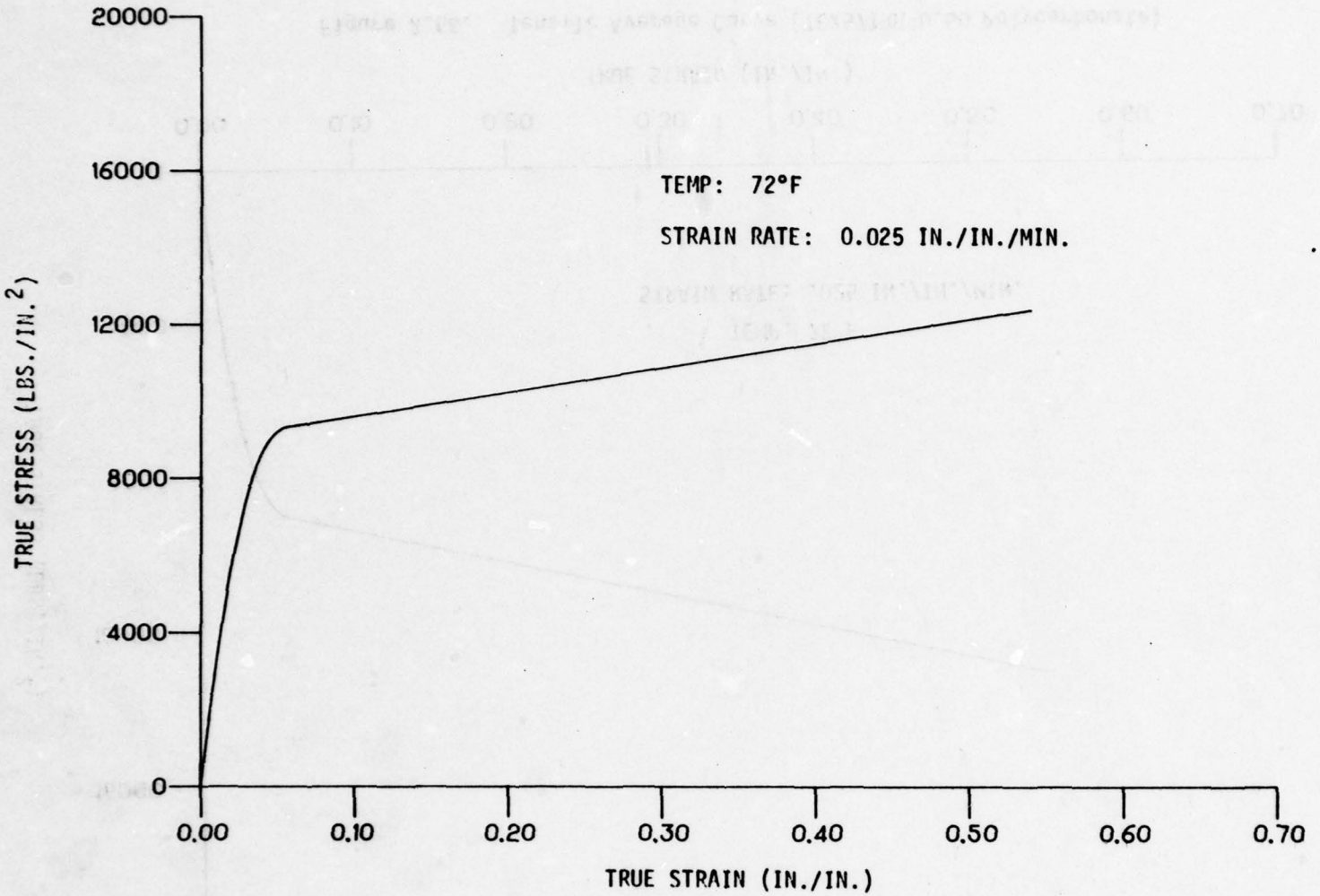

Figure A.65. Tensile Average Curve (TEX571-0.50 Polycarbonate).

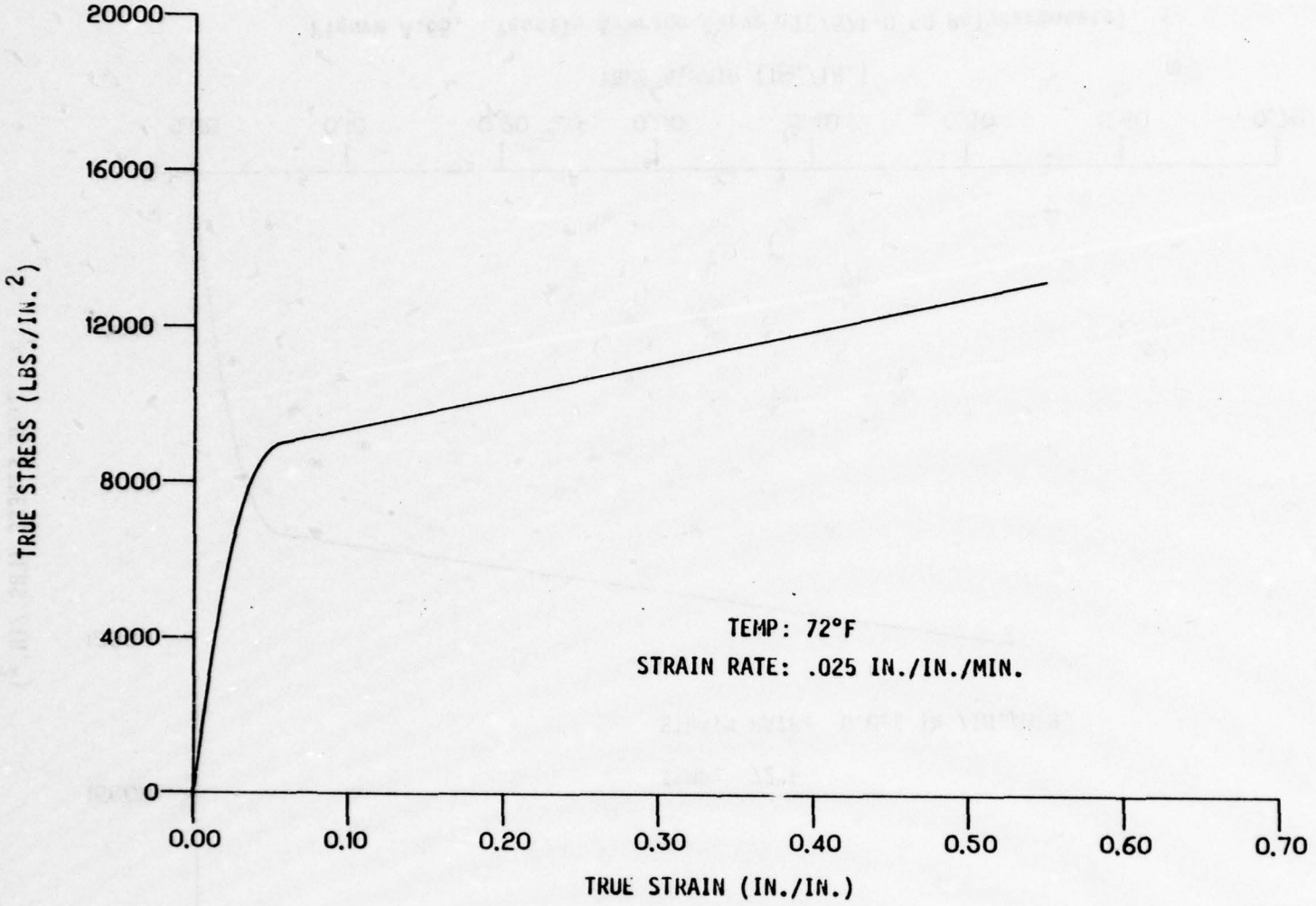

Figure A.66. Tensile Average Curve (TEX571RH-0.50 Polycarbonate)

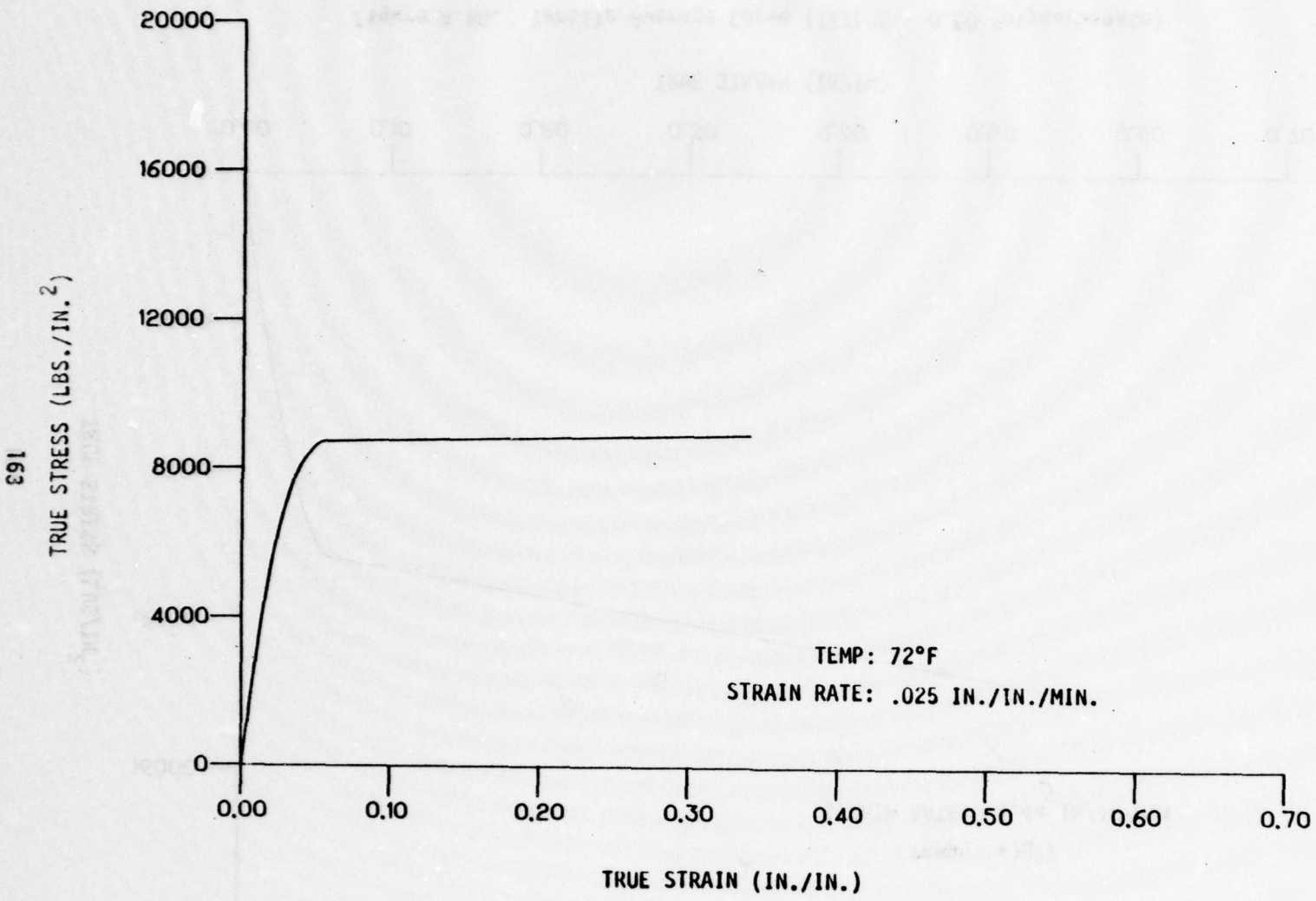

Figure A.67. Tensile Design (B) Curve (TEX571RH-0.50 Polycarbonate)

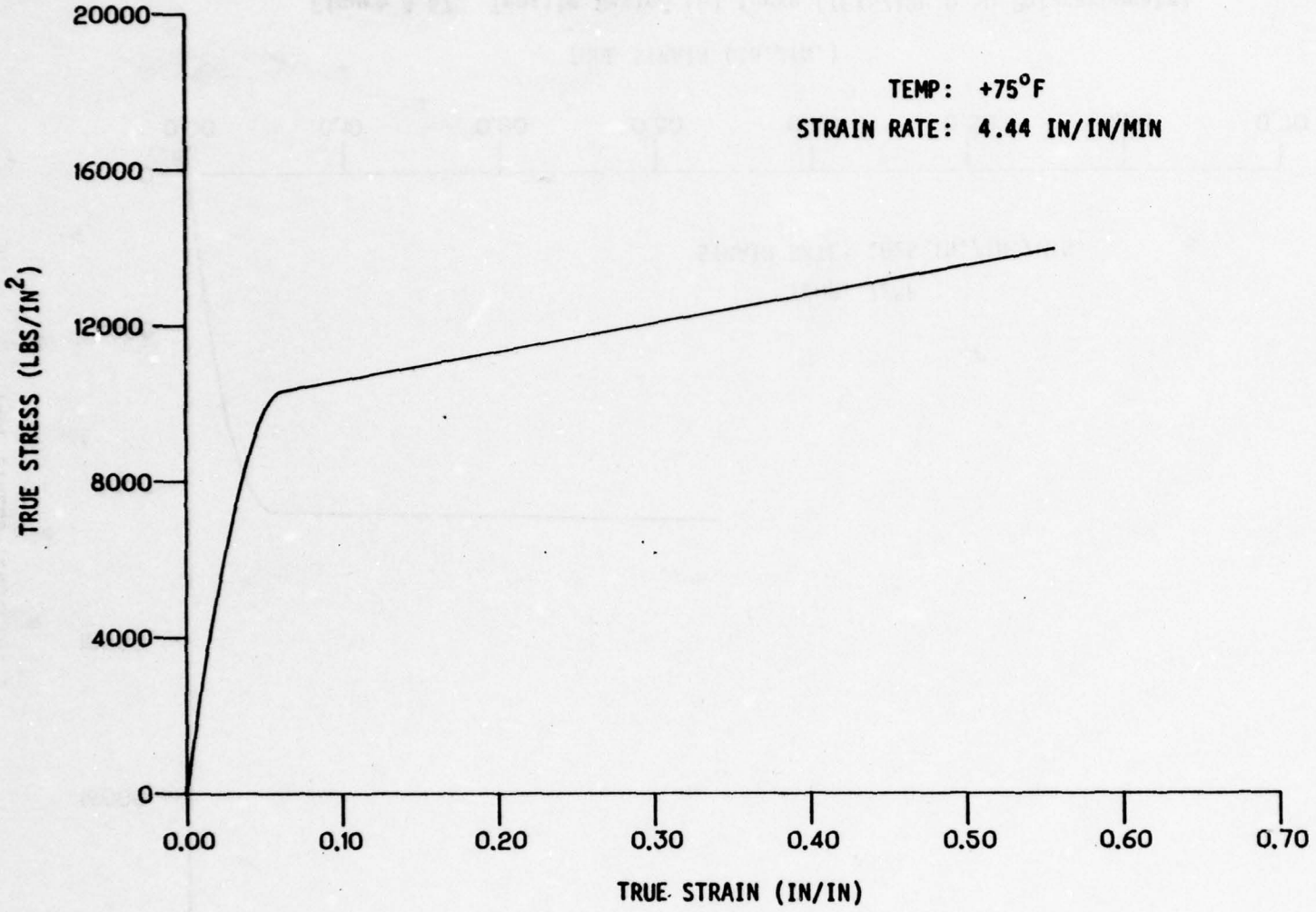

Figure A.68. Tensile Average Curve (TEX605 - 0.50 Polycarbonate)

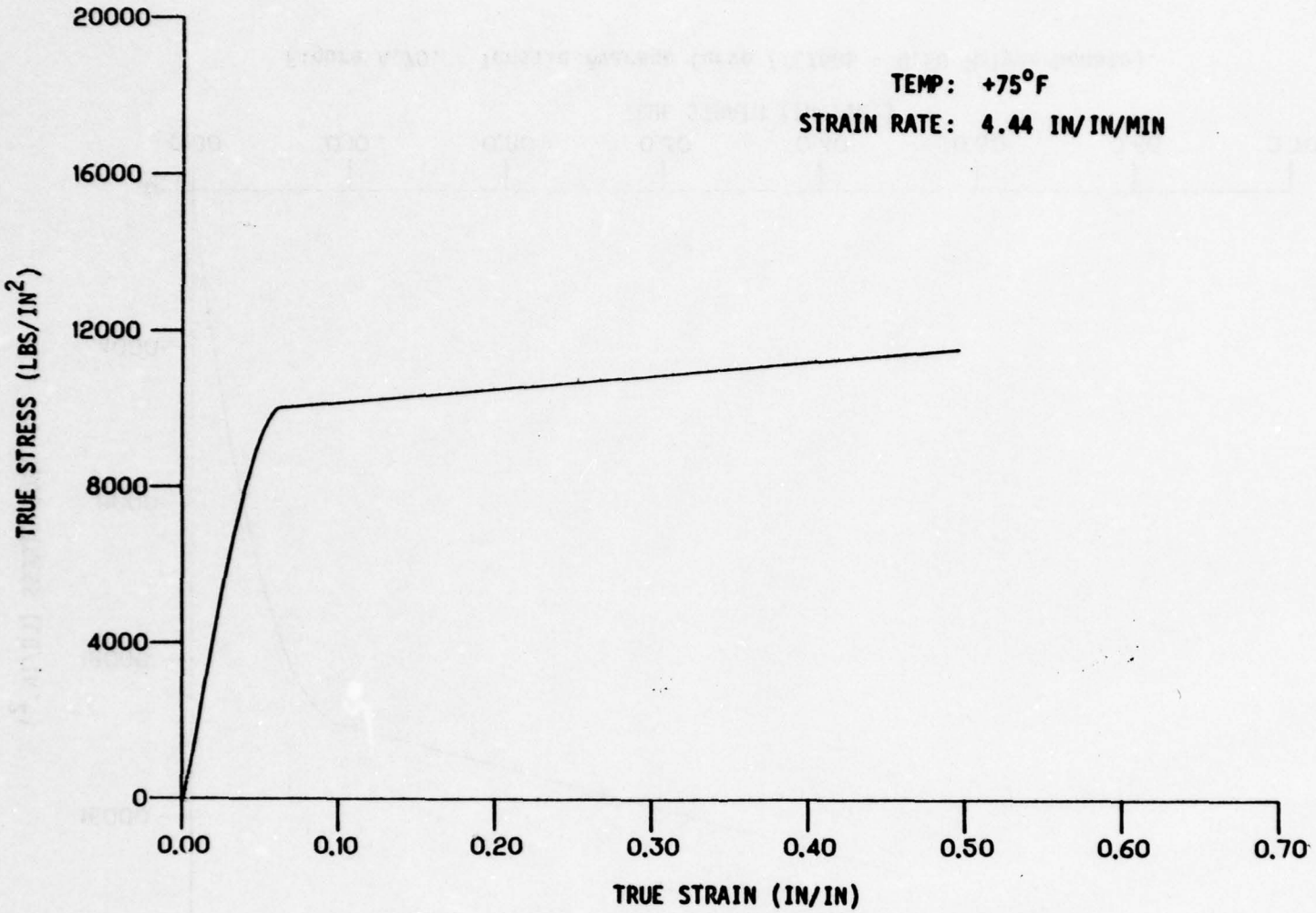

Figure A.69. Tensile Design (B) Curve (TEX605 - 0.50 Polycarbonate)

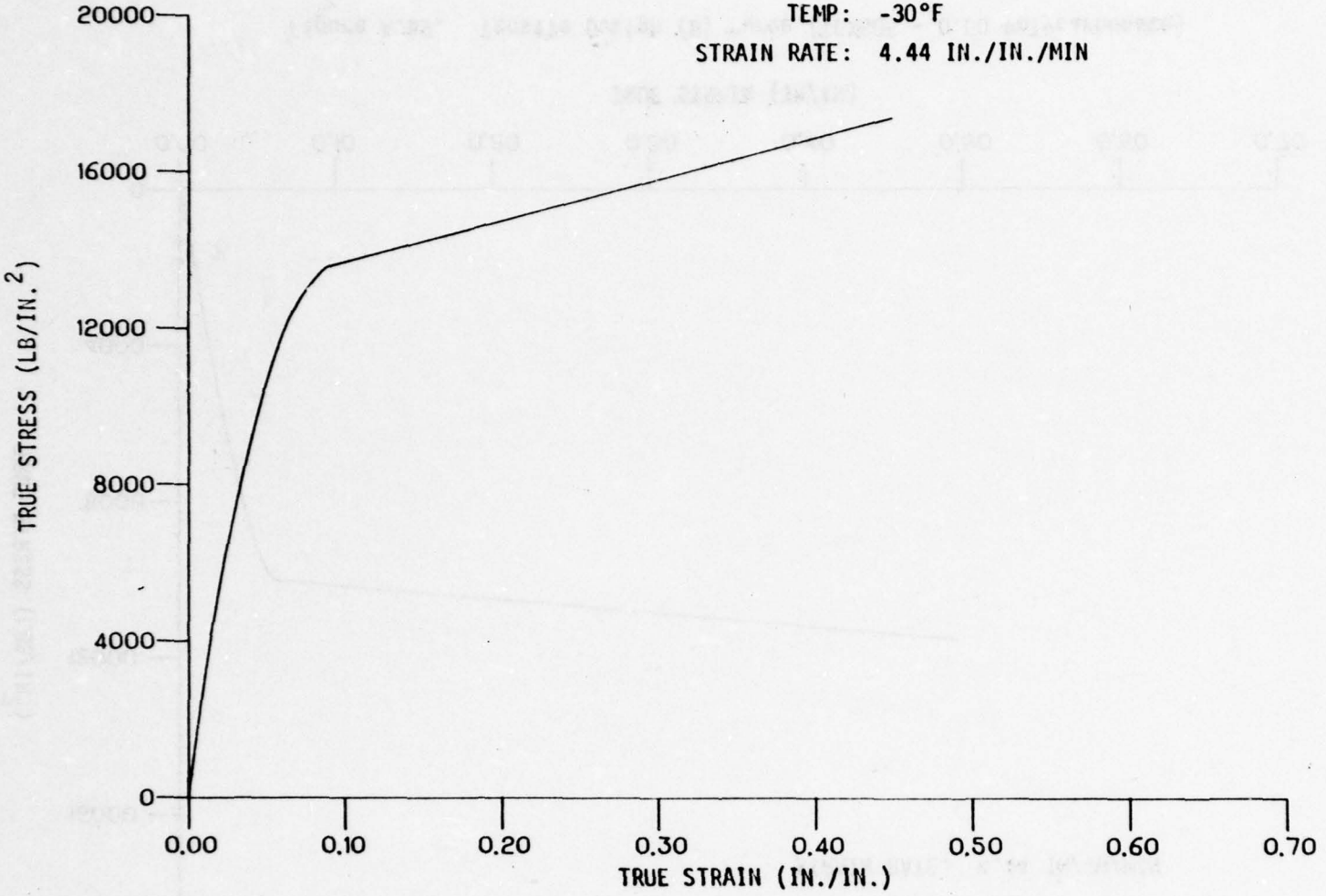

Figure A.70. Tensile Average Curve (TEX605 - 0.50 Polycarbonate).

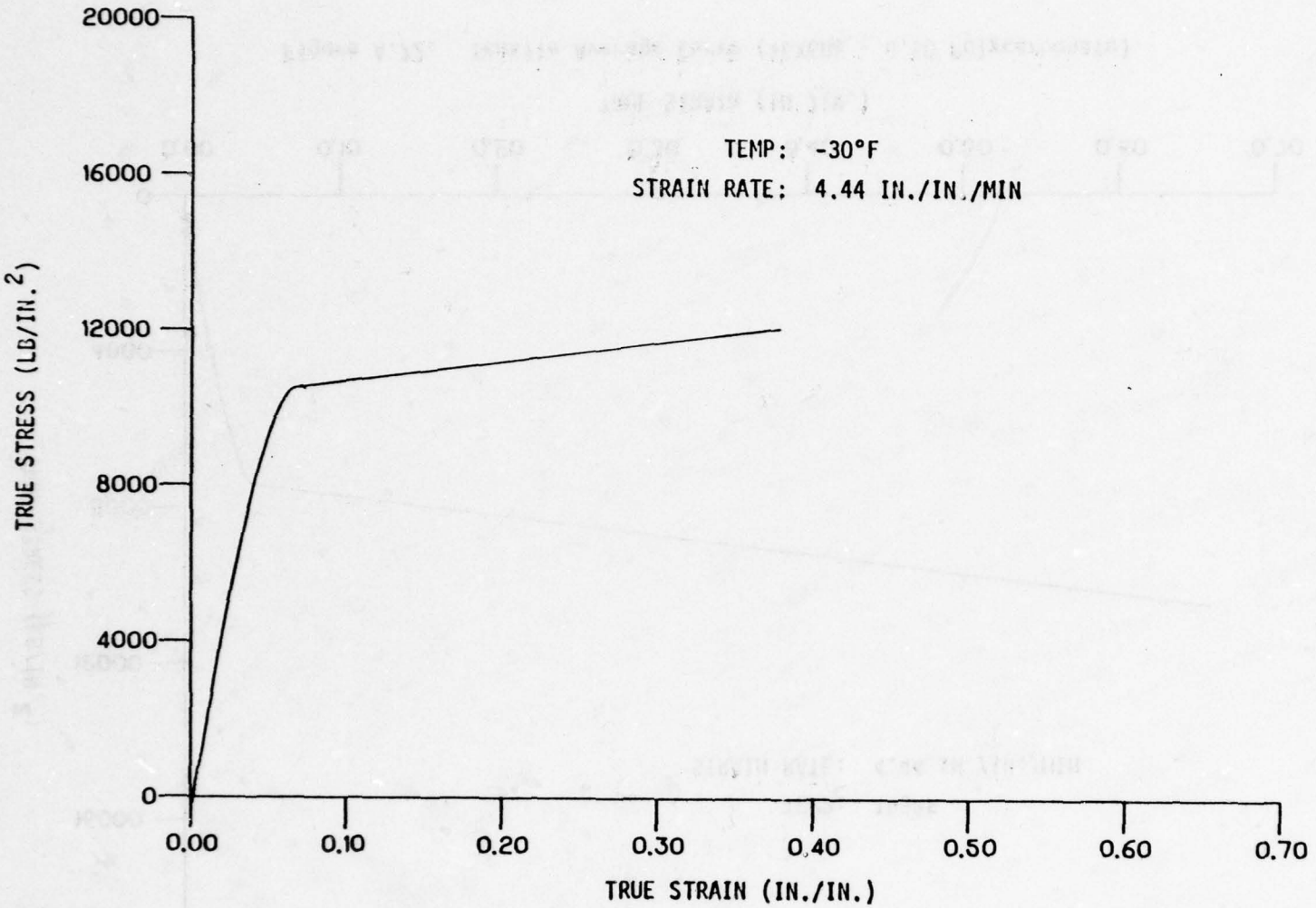

Figure A.71. Tensile Design (C) Curve (TEX605 - 0.50 Polycarbonate).

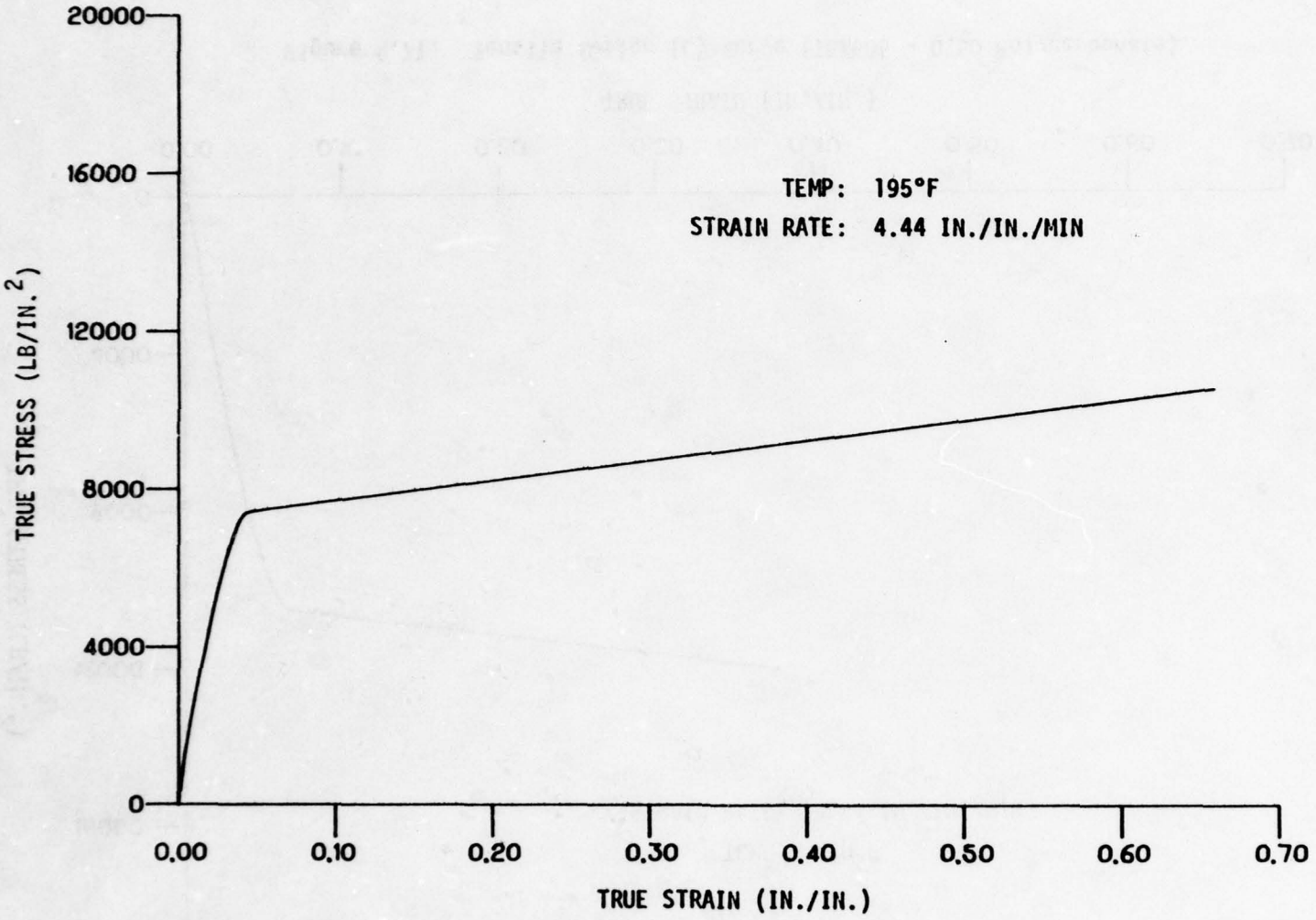

Figure A.72. Tensile Average Curve (TEX605 - 0.50 Polycarbonate).

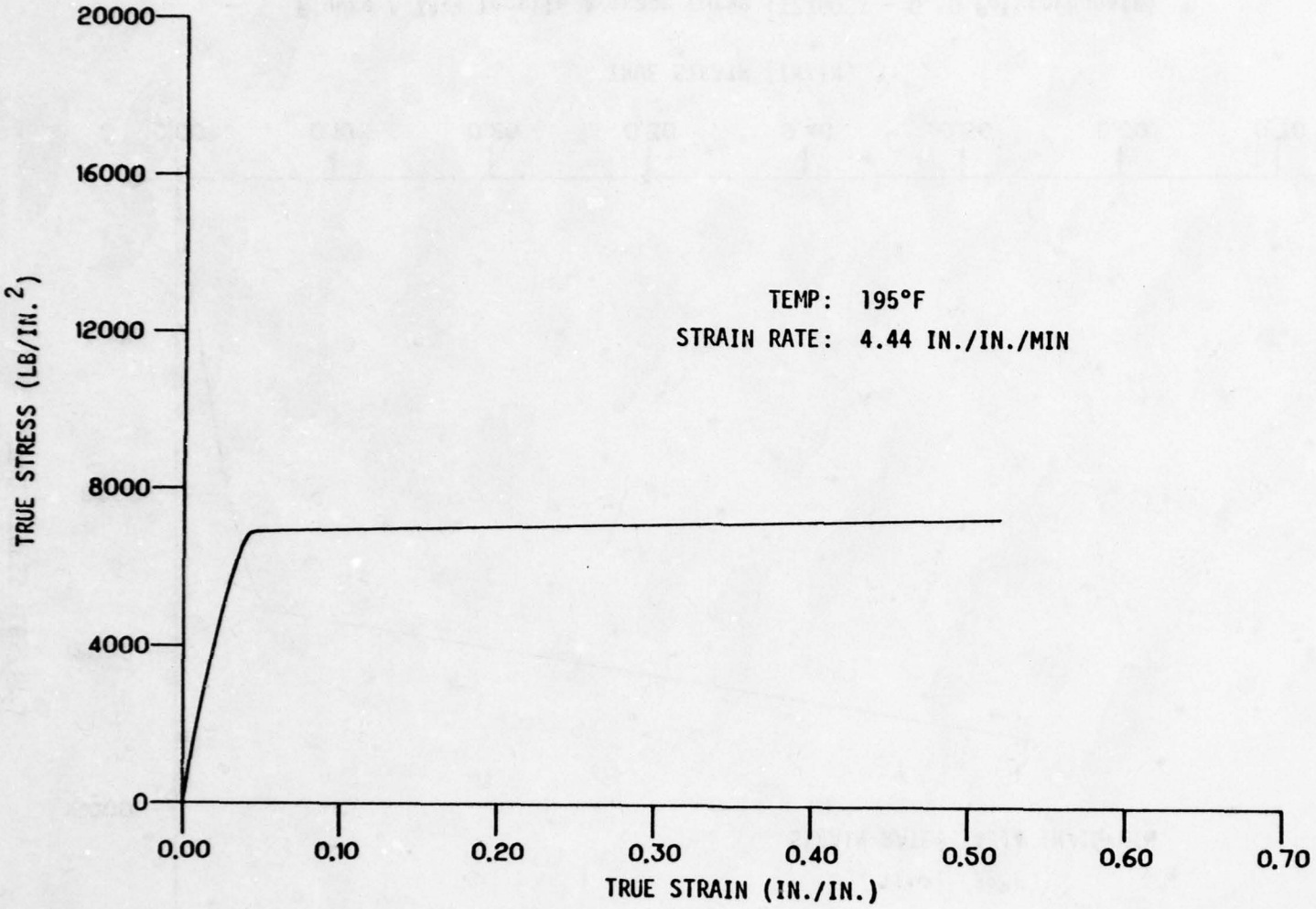

Figure A.73. Tensile Design (C) Curve (TEX605 - 0.50 Polycarbonate).

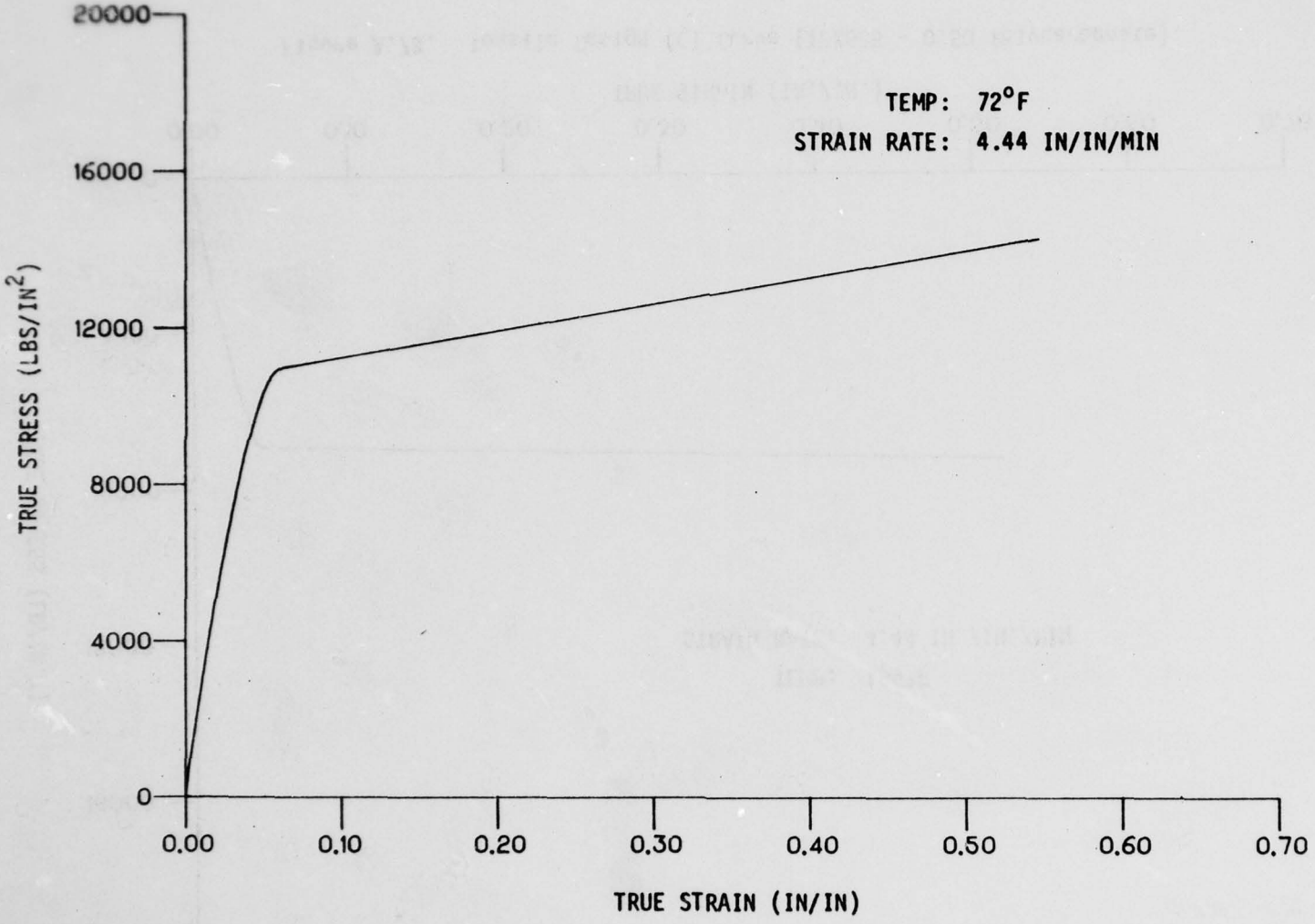

Figure A.74. Tensile Average Curve (TEX605X - 0.50 Polycarbonate)

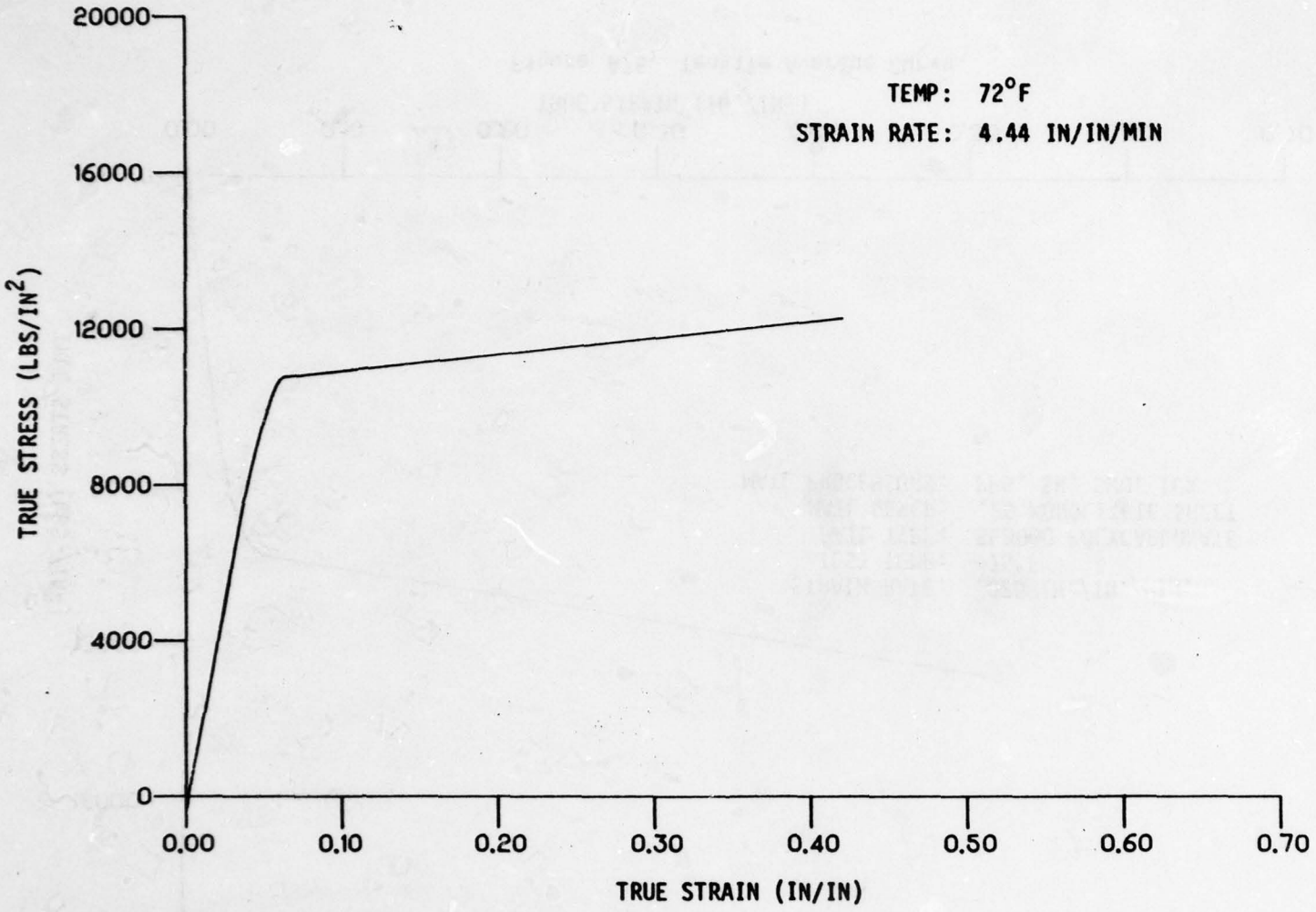

Figure A.75. Tensile Design (B) Curve (TEX605X-0.50 Polycarbonate)

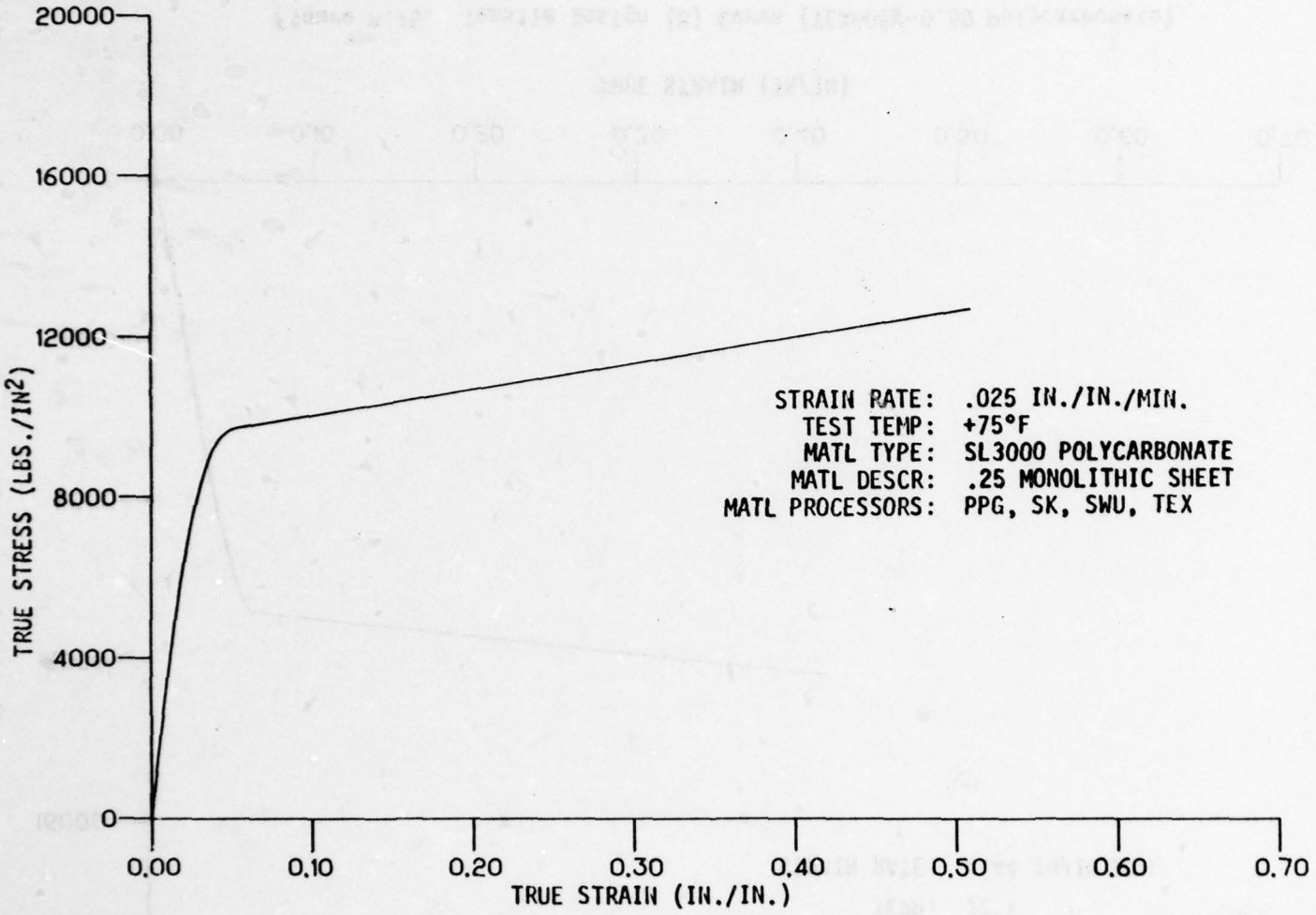

Figure A76. Tensile Average Curve.

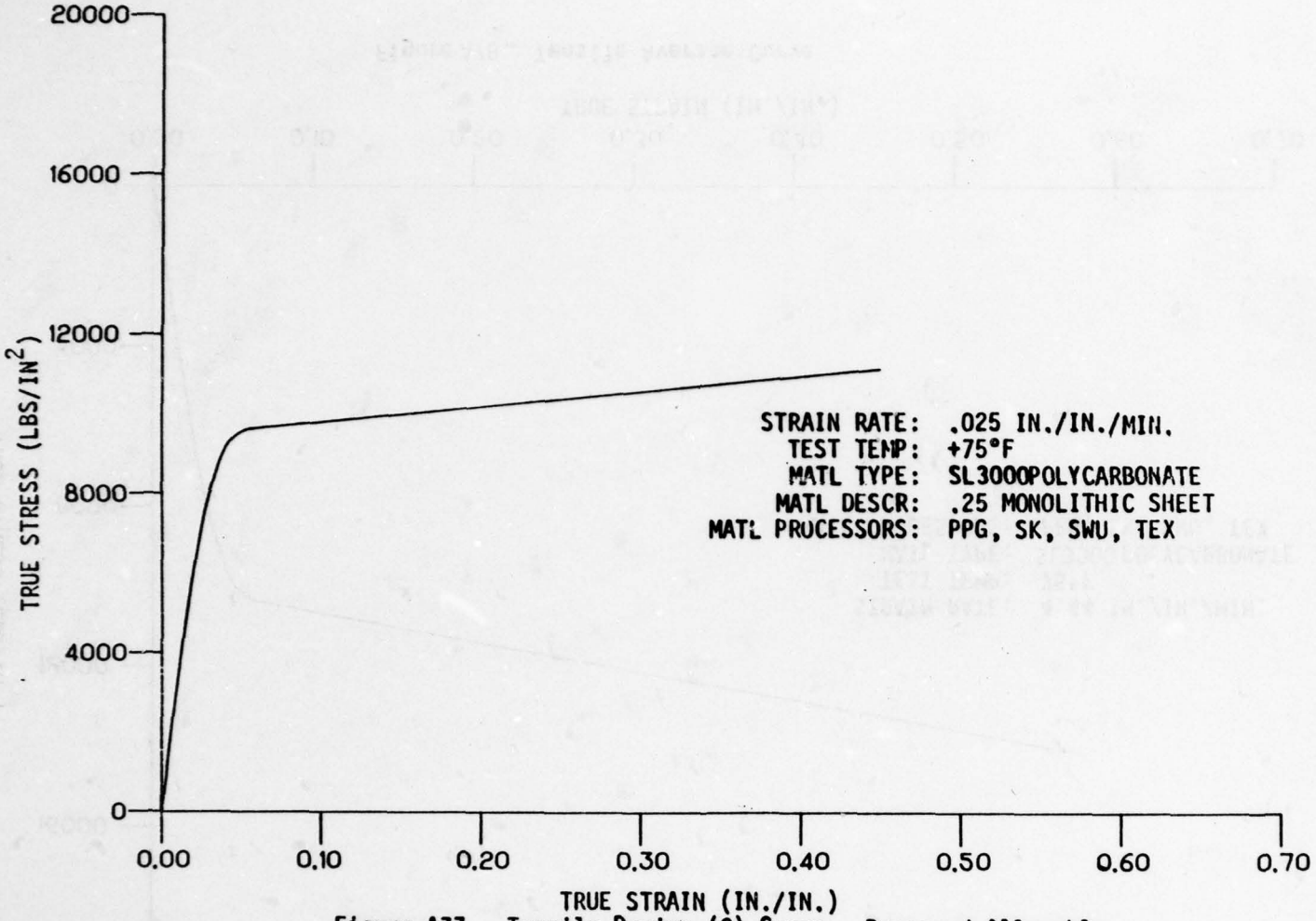

Figure A77. Tensile Design (C) Curve - Proposed Allowable

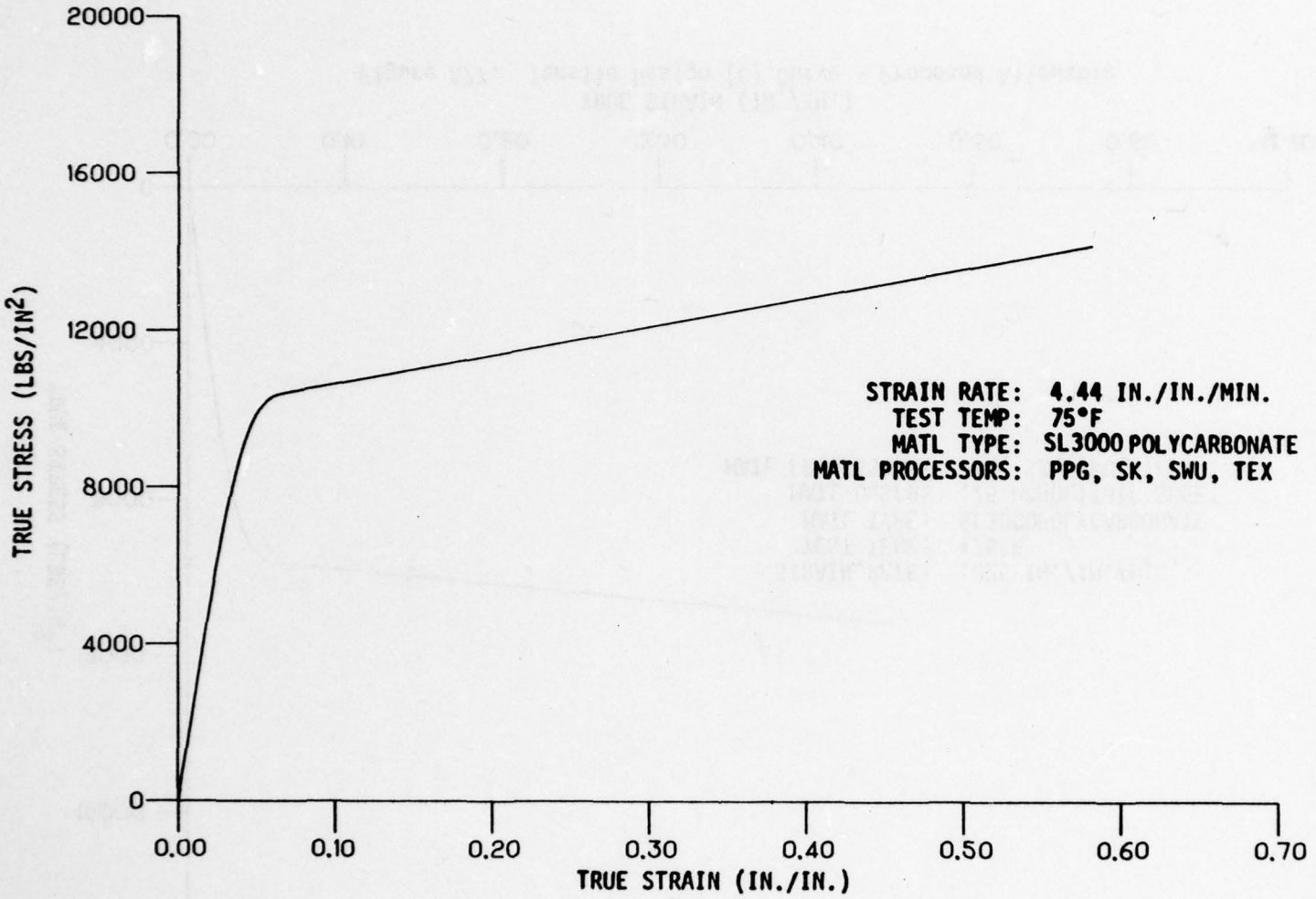

Figure A78. Tensile Average Curve

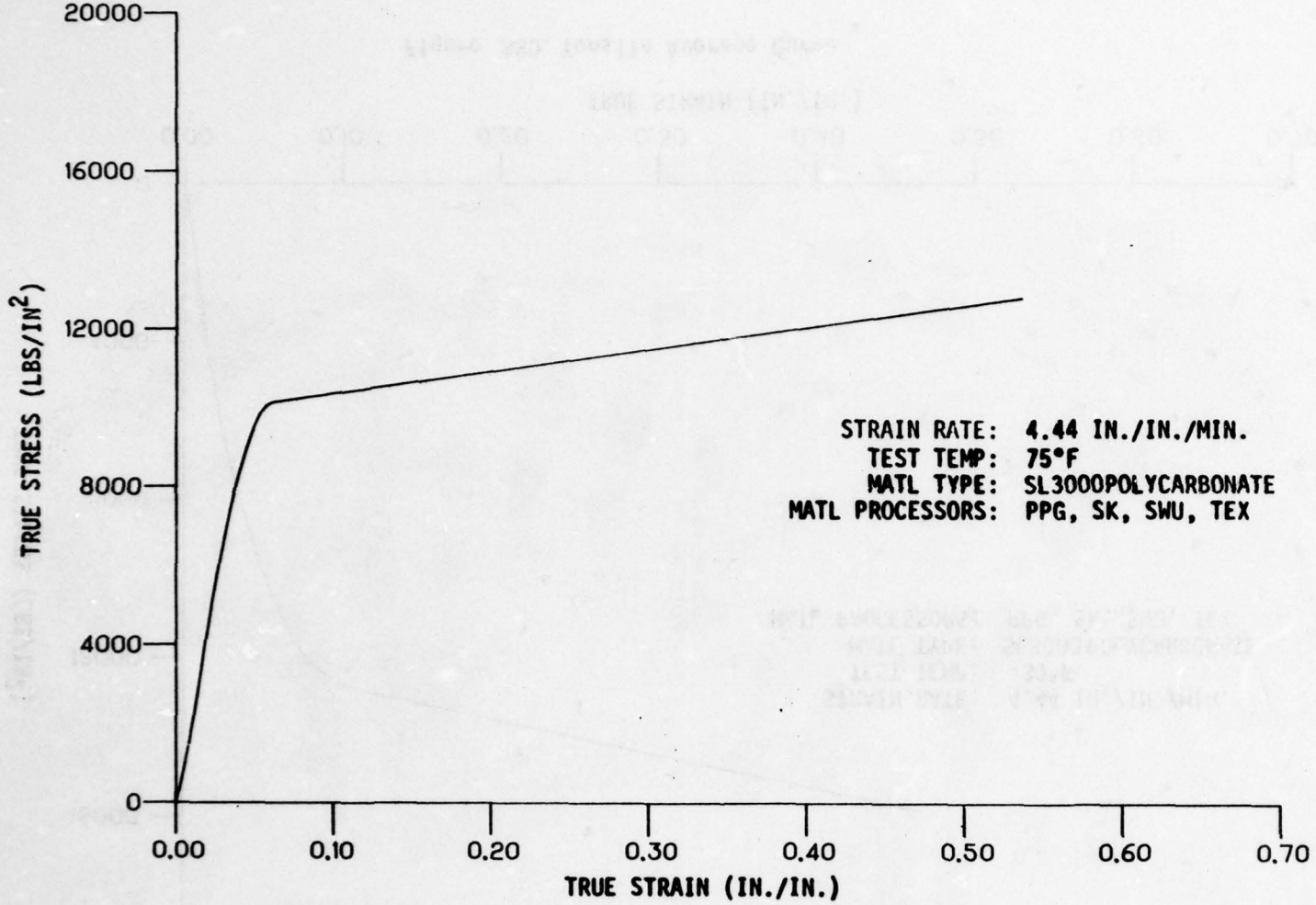

Figure A79. Tensile Design (C) Curve - Proposed Allowable

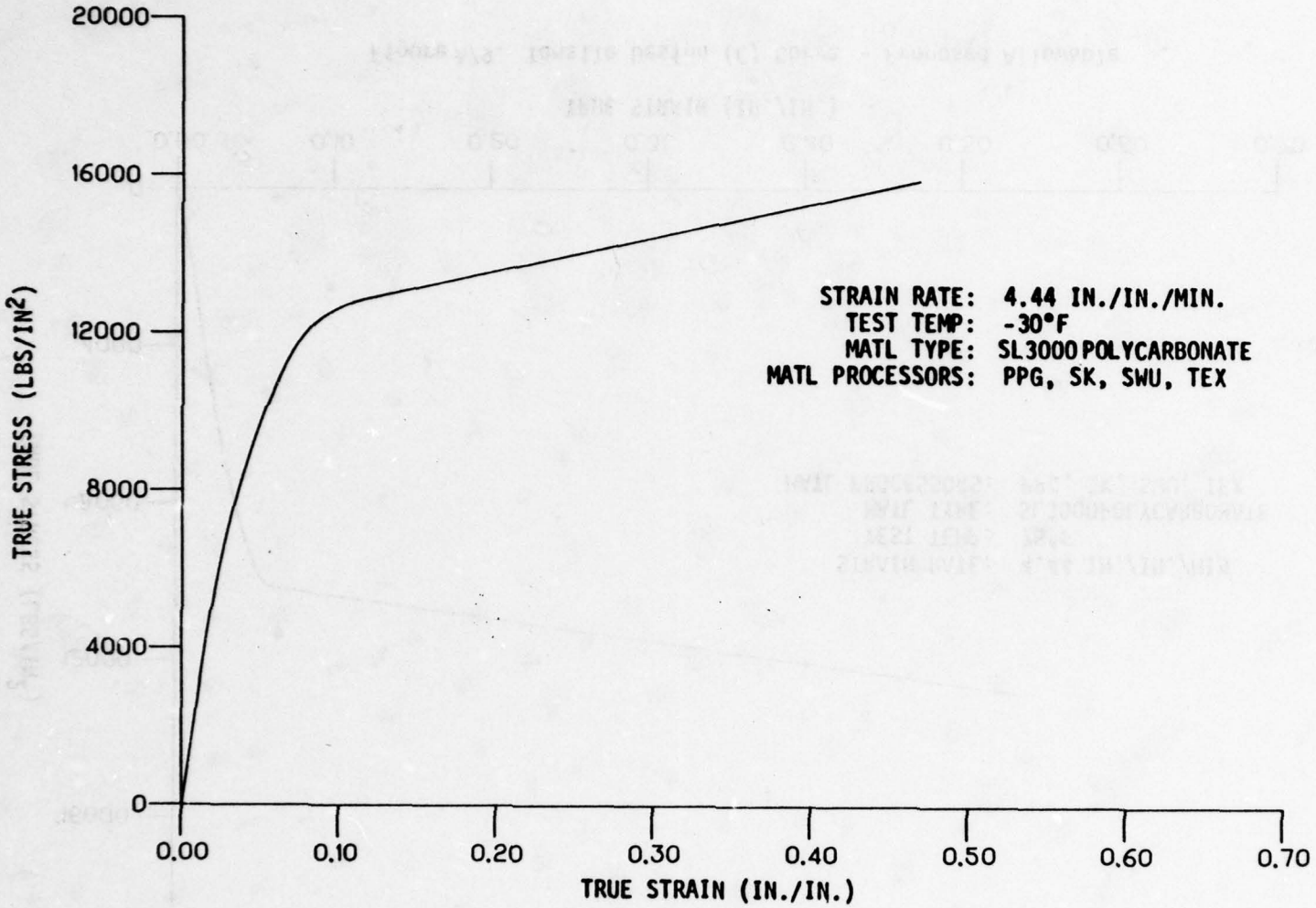

Figure A80. Tensile Average Curve

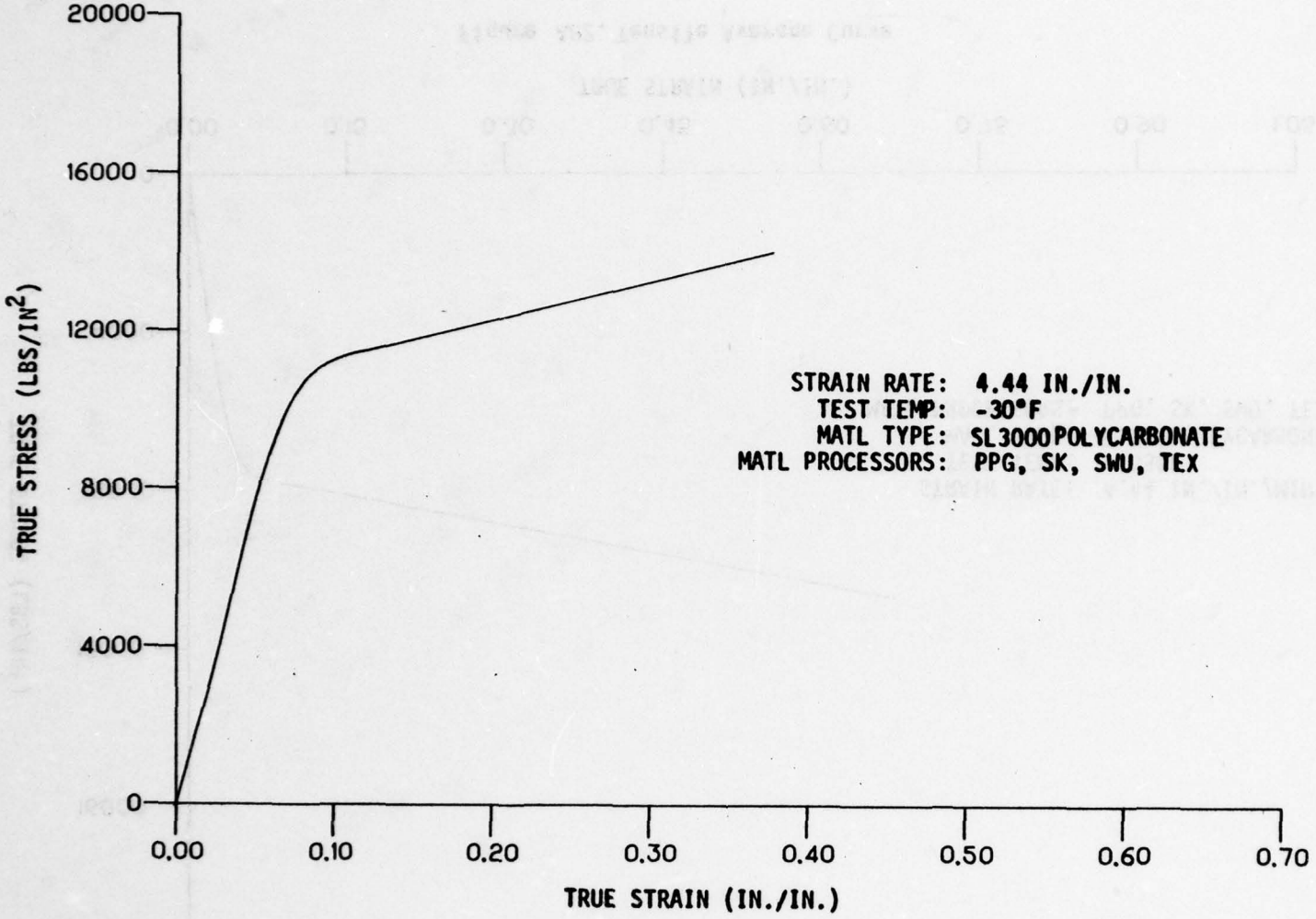

Figure A81. Tensile Design (C) Curve - Proposed Allowable

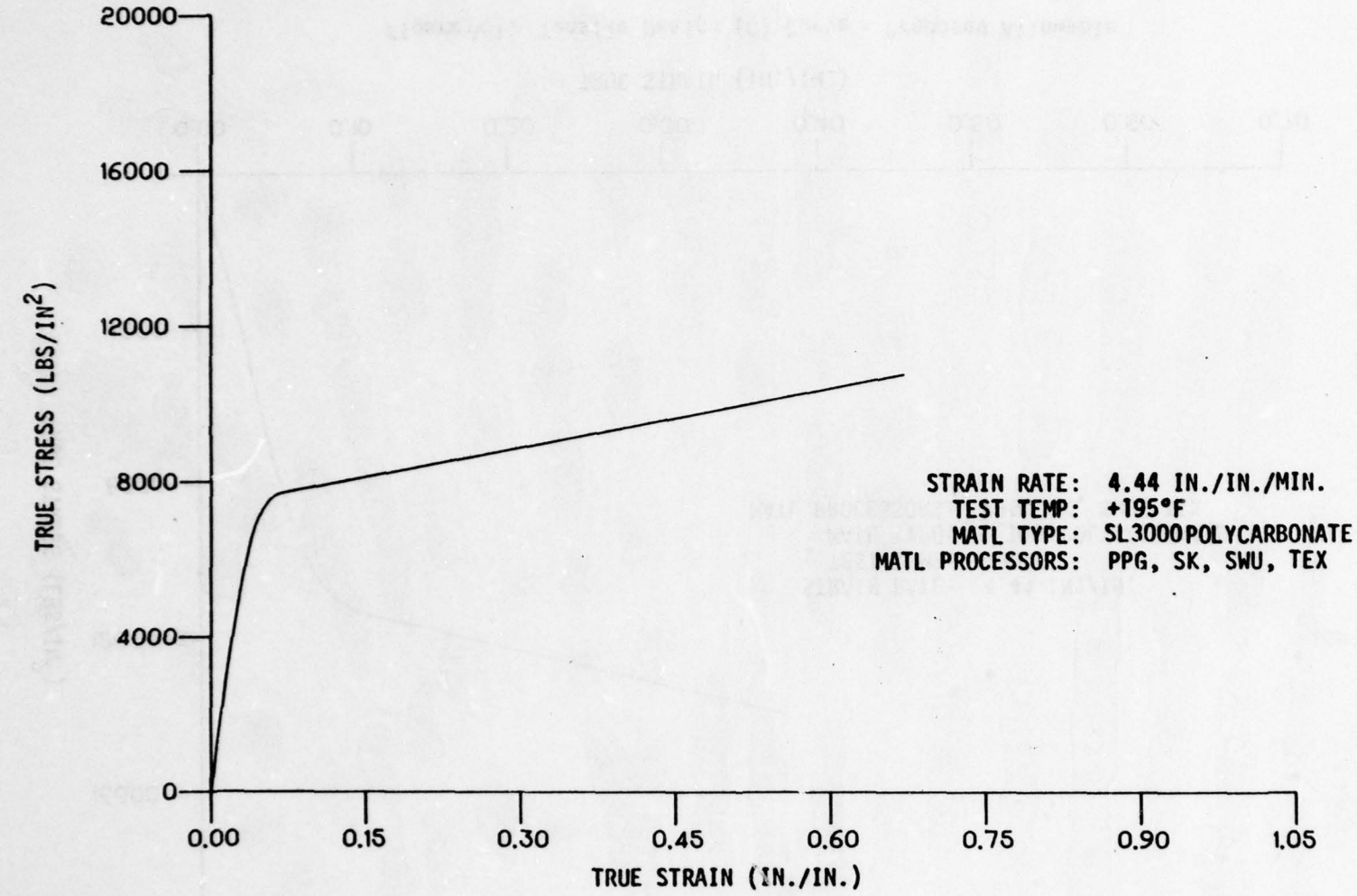

Figure A82. Tensile Average Curve

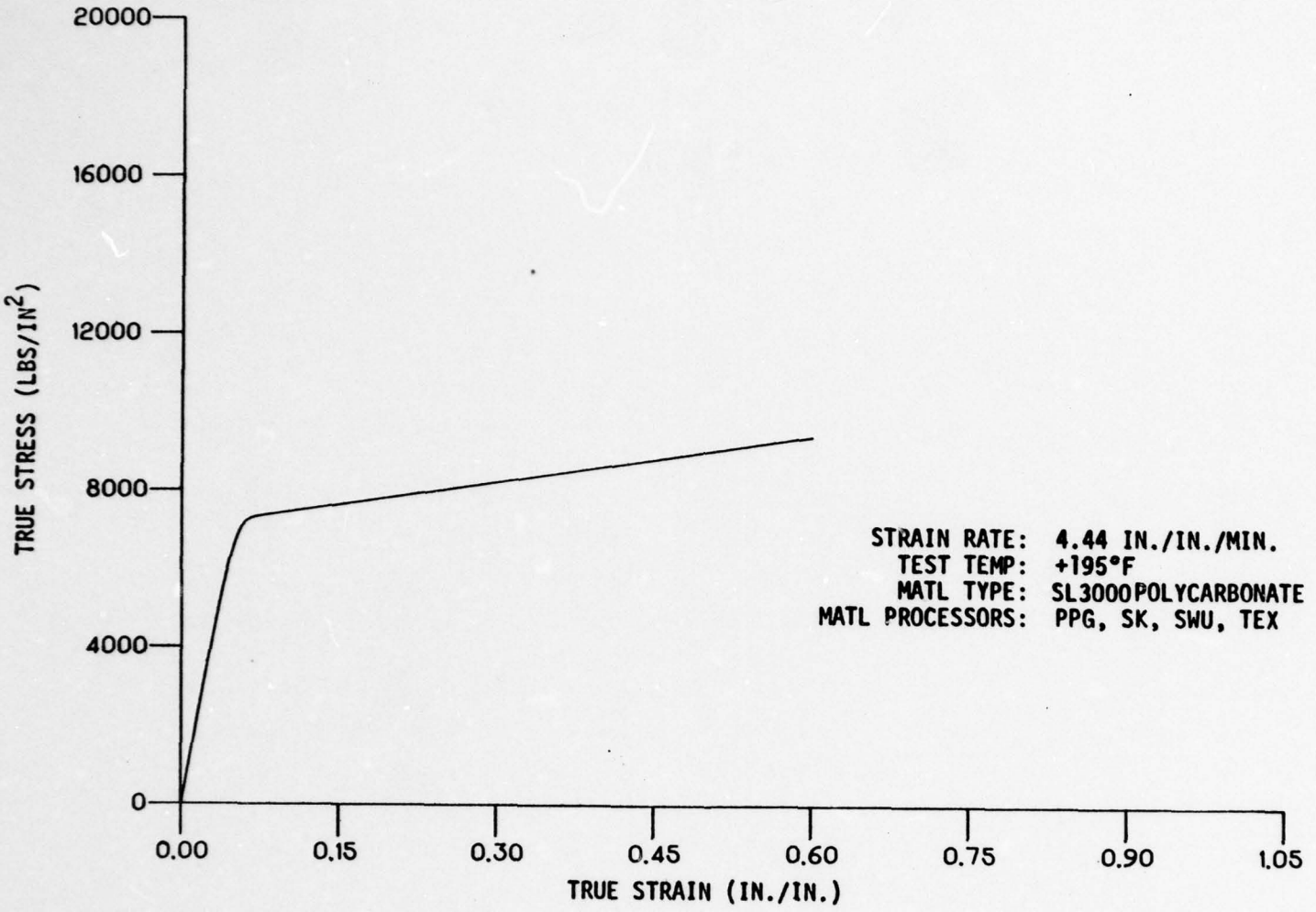

Figure A83. Tensile Design (C) Curve - Proposed Allowable

SECTION VI

LOW STRAIN RATE COMPRESSIVE MECHANICAL PROPERTIES TESTING OF PROCESSED POLYCARBONATE MATERIALS

This series of tests was conducted to provide low strain rate compressive mechanical properties of monolithic polycarbonate materials as processed by specific windshield/canopy fabricators. The primary use for these tests was to provide average (actual) and design compression allowables of processed polycarbonate materials for development, and future design use in computer programs (Reference 7). Additional uses were to provide for static load design analysis and for evaluation of vendors processes. Test Specimens were made from instrumented beams (Reference 12), and bird impacted test windshields (Reference 13), or furnished by specific windshield/canopy fabricators. Tests were conducted at room temperature per ASTM D695-69 standard method of testing.

TEST SPECIMEN DESCRIPTION

The test specimens required for this series of tests are shown in Figures 38 and 39. All test specimens were examined under polarized light to expose stress risers from machining operations which could have affected test results. Specimens displaying stress risers were refinished (sanded and polished) to remove such discrepancies. Machine cutting speed and feed rates were controlled to prevent heating parts above 150°F during machining to eliminate adverse thermal conditioning effects. Specimens of a particular test series were oriented in the same length-width relation with respect to the basic stock. Test specimens for this test series were made from SL3000 (General Electric Co.) monolithic polycarbonate material and received fabricators processes that normally occur during the manufacture of an aircraft transparency. The fabricator's processed materials tested were PPG Industries (PPG), Texstar Plastics Co. (TEX), Sierracin Corp. (SK), and Swedlow Inc. (SWU).

PRECEDING PAGE NOT FILMED
BLANK

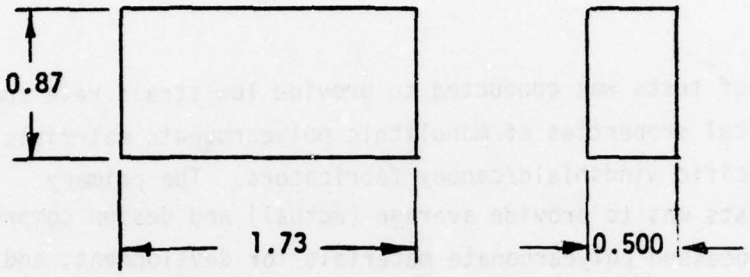

Figure 38. Compression Test Specimen
(Z7942633-511, -545).

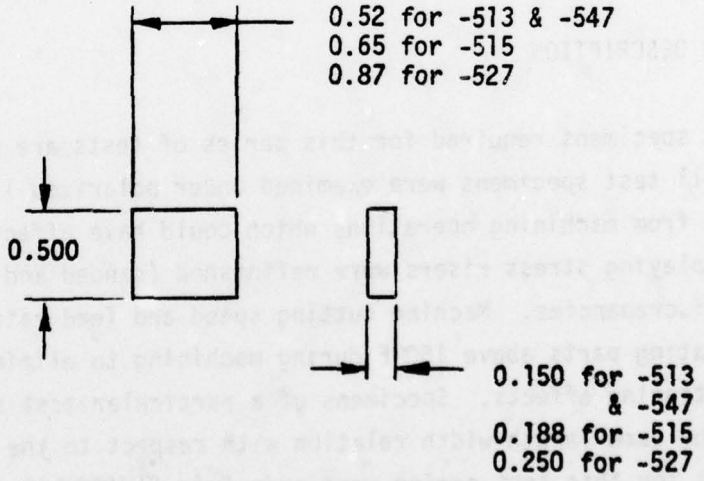

Figure 39. Compression Test Specimen
(Z7942633-513, -515, -527, -547).

A minimum of five (5) specimens of the following configurations were constructed by each noted transparency fabricator.

The Z5942633-511, -545 test specimens (Figure 38) were made from SL3000 fusion bonded polycarbonate material. The -511 test specimens were furnished by Sierracin Corp., and received the same processing as the Z5942626-1 and -501 transparent beam. The -545 test specimens were removed from a laminated bird impacted test transparency made by Swedlow Corp. for the B-1 supersonic aircraft.

The Z5942633-513, -515, -527, -547 test specimens (Figure 39) were made from monolithic SL3000 polycarbonate material. The -513 test specimens were furnished by Sierracin Corp. and received the same processing as the Z5942626-501 transparent beam. The -515 test specimens were furnished by PPG Industries, and received the same processing as the Z5942626-503 and -505 transparent beam. The -527 test specimens were furnished by Texstar Plastics Co., and received the same processing as an aircraft transparency. The -547 test specimens were removed from a laminated test transparency made by Swedlow Corp. for the B-1 supersonic aircraft.

TEST SETUP AND EQUIPMENT DESCRIPTION

The test setup used for compression testing is shown in Figure 40. A Baldwin deflectometer was used to measure and record crosshead movement during specimen compression. The test machine used was a 60,000-pound capacity Baldwin mechanical test machine.

TEST PROCEDURE

Compression tests were conducted in accordance with standard method of testing ASTM D695-69. The test specimen length and cross section dimensions were measured within $\pm$0.001 and recorded for each specimen prior to testing. The test specimen was then positioned in the test machine and a deflectometer installed as shown in Figure 40.

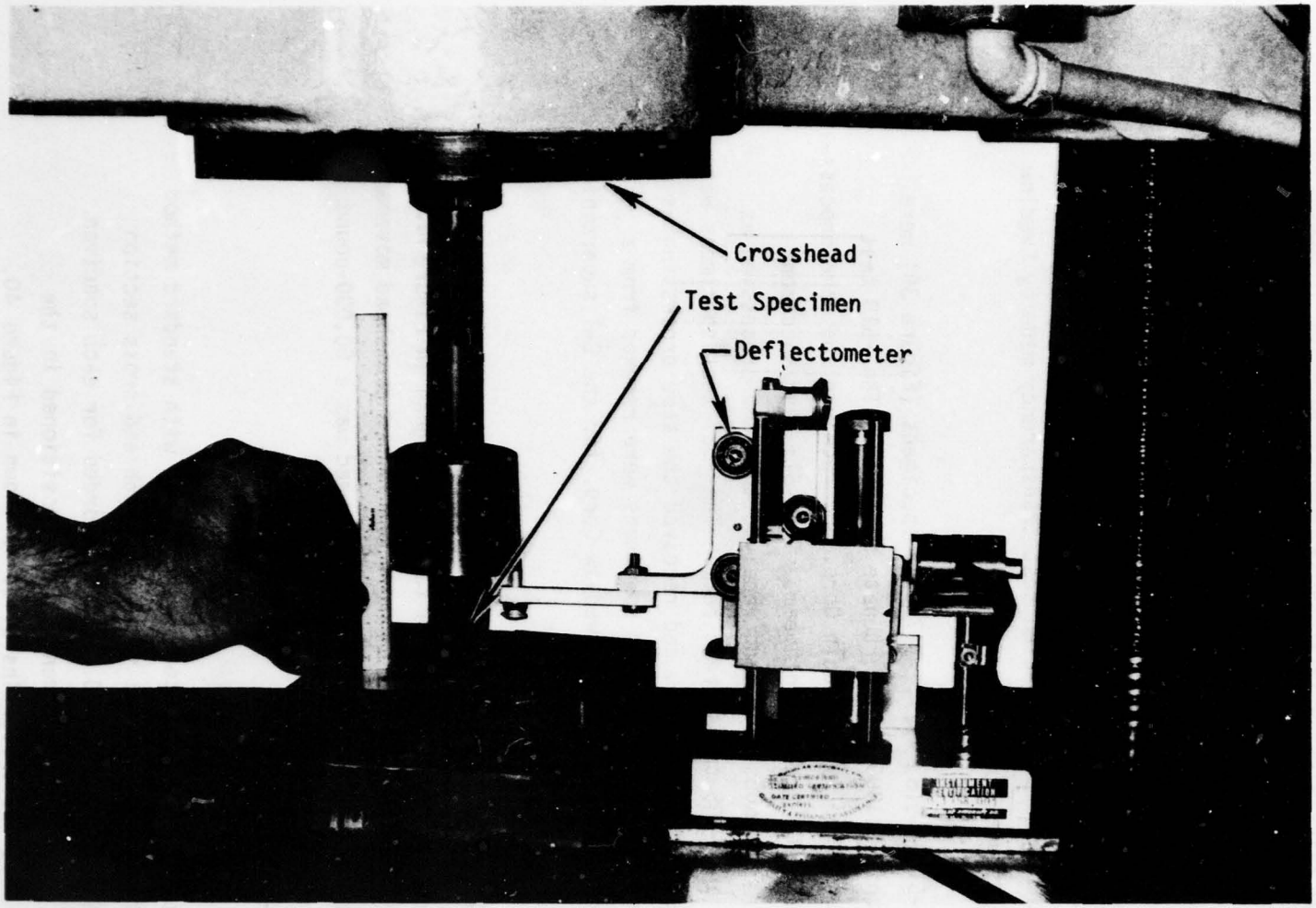

Figure 40. Compression Test Setup.

AD-A064 436 DOUGLAS AIRCRAFT CO LONG BEACH CALIF F/G 11/9
TESTING FOR MECHANICAL PROPERTIES OF MONOLITHIC AND LAMINATED P--ETC(U)
OCT 78 F E GREENE, L P KOEGEBOEHN F33615-75-C-3105
UNCLASSIFIED MDC-J6950 AFFDL-TR-77-96-PT-1 NL

3 OF 5
AD
A064436

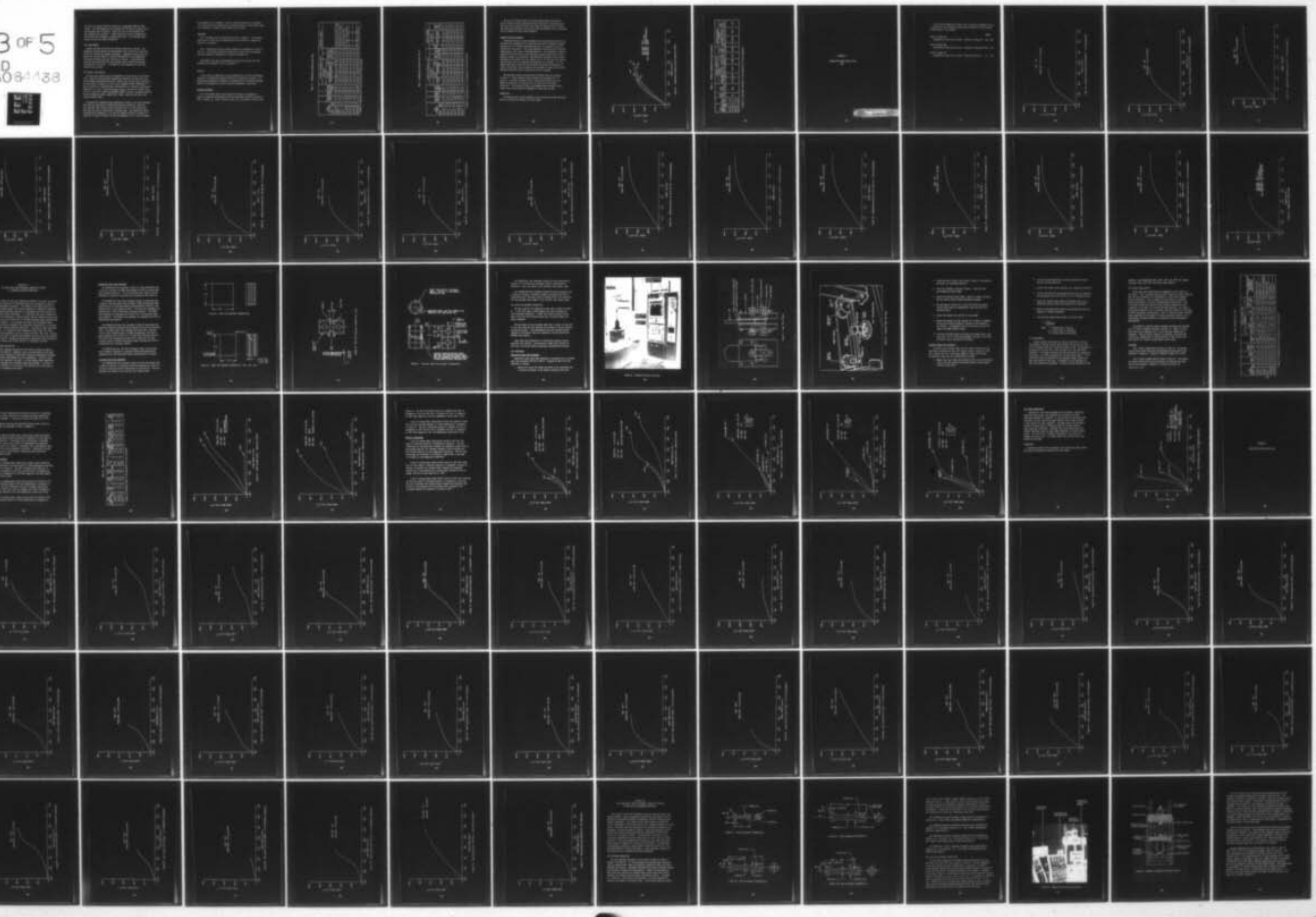

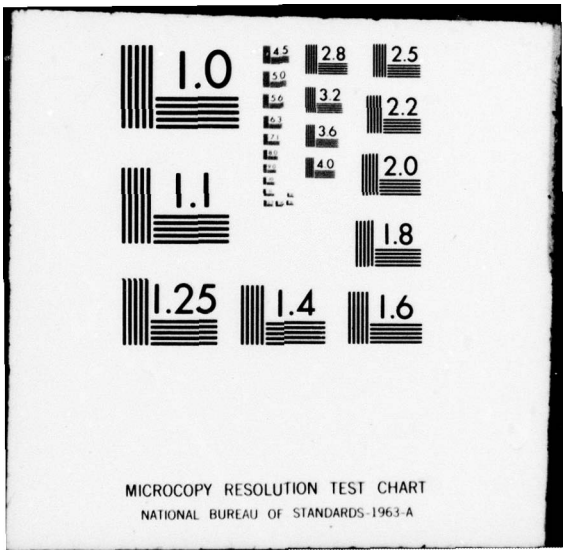
1.0
1.1
1.25
1.4
1.6
1.8
2.0
2.2
2.5
2.8
3.2
3.6
4.0
4.5
5.0
5.6
6.3
7.1
8.0
9.0
10.0
11.2
12.5
14.0
16.0
18.0
20.0
22.4
25.0
28.0
32.0
36.0
40.0
MICROCOPY RESOLUTION TEST CHART
NATIONAL BUREAU OF STANDARDS-1963-A

The slack was removed from the system and a measurement made for gage length. The room temperature was recorded and the machine rate was set at the designed speed of testing. During the test run the maximum load was determined and recorded. A load deflection curve was automatically drawn during test through the maximum load point. Five specimens were tested for each test batch of material.

TEST REQUIREMENTS

Douglas provided facilities and services required for testing. The mechanical testing machine and deflectometer were verified for accuracies within $\pm$0.5 percent per Douglas procedures. Compression testing was conducted per standard method of testing ASTM D695-69 at room temperature. The speed of testing used was 0.05-inch per minute. A load-deflection curve was machine plotted for each specimen tested through the maximum load portion of the curve. A minimum of 5 test specimens for each test condition was provided.

TEST RESULTS AND ANALYSIS

Two tasks were accomplished and documented in this section of the report. Task I provides average (actual) compressive properties of monolithic and fusion bonded polycarbonate materials removed from aircraft test windshields and test beams in support of a bird strike computer program (Reference 7) and the analysis of laminated beams representative of aircraft transparencies (Reference 12). Task II provides average (actual) and specific design allowables for monolithic SL3000 polycarbonate material based on processed material from PPG Industries (PPG), Swedlow Corp. (SWU), Sierracin Corp (SK), and Texstar Plastics (TEX).

The compressive properties data presented are based on five test specimens made from the same batch of material and tested at identical conditions. Test specimens that failed at some fortuitous flaw or in the fusion bond area were not used in calculation of strength data. The compression design allowables were computed on a "B" basis by methods outlined in Chapter III. Where the "B" basis allowable could not be computed, the "C" basis allowable

was computed and is presented. Where no design allowables are presented, the data could not be computed due to large deviations in test results that gave negative or illogical stress and/or strain values.

Test Data

Task I average (actual) properties are given in Table 15. The average stress-strain curves for the tabulated data are presented in Appendix B, Figures B.1 through B.7.

Task II average and specific design compression allowables are given in Table 16. The average and design stress-strain curves for the tabulated data are presented in Appendix B, Figures B.8 through B.16.

Experimental test data and engineering stress-strain curves for test specimens are contained in Part 2, Appendix J.

ANALYSIS

In this analysis comparisons are made between four aircraft transparency processors to demonstrate processing effects on mechanical strength. Proposed design compression allowables are presented for SL 3000 polycarbonate material as processed by the four aircraft transparency fabricators.

Processing Effects

A plot of average compression stress-strain curves is presented in Figure 41 comparing the processed SL3000 polycarbonate from PPG Industries (PPG), Swedlow, Inc. (SWU), Sierracin Corp. (SK), and Texstar Plastics (TEX).

TABLE 15. COMPRESSION STRENGTH DATA TASK I

TEST SPECIMEN IDENT	NO*	THICKNESS (IN.)	TEST TEMP (°F)	STRN RATE (IN./IN/MIN)	AVERAGE STRENGTH DATA: ULTIMATE STRESS (PSI)	STD DEV (PSI)	STRAIN (IN/IN)	STD DEV (IN/IN)	SHEAR MOD (PSI 10^{-5})	STD DEV (PSI x 10^{-5})	MATERIAL SOURCE
PPG515/26	3	.19	75	0.077	10640	1066	0.071	0.005	2.86	0.397	Z5942626-503,-505 BEAM
SK511	5	.50	78	0.03	11841	494	0.070	0.001	2.77	0.111	Z5942626-1,-501 BEAM
SK513	5	.15	78	0.10	12052	158	0.083	0.004	2.23	0.106	Z5942626-501 BEAM
SWU545/7	6	.500	78	0.03	12005	184	0.067	0.001	2.98	0.248	B-1 TEST WINDSHIELD
SWU545/7	6	.500	78	0.03	11942	180	0.067	0.002	2.62	0.197	
SWU547/7	6	.150	78	0.10	12463	109	0.059	0.003	3.35	0.613	
SWU547/8	7	.15	75	0.096	11486	94	0.062	0.001	3.56	0.314	B-1 TEST WINDSHIELD

* Number of specimens used in the generation of data presented.

TABLE 16. COMPRESSION STRENGTH DATA TASK II

TEST SPECIMEN IDENT	NO.*	THICKNESS (IN.)	TEST TEMP (°F)	STRN RATE (IN/IN MIN)	AVERAGE STRENGTH DATA: ULTIMATE STRESS (PSI)	STD DEV	STRAIN (IN/IN)	STD DEV (IN/IN)	SHEAR MOD (PSI x 10^{-5})	STD DEV (PSI x 10-5)	DESIGN ALLOWABLE: DES BAS	ULTIMATE STRESS (PSI)	ULTIMATE STRAIN (IN/IN)	SHEAR MOD (PSI x 10^{-5})
PPG515	6	.19	75	0.10	11259	232	0.077	0.003	2.40	0.088	B	10352	0.067	2.17
SK511	5	.50	78	0.03	11841	494	0.070	0.001	2.77	0.111	B	10193	0.065	2.61
SK513	5	.15	78	0.10	12052	158	0.083	0.004	2.23	0.106	B	11162	0.070	1.88
SWU515	5	.188	78	0.076	11868	186	0.067	0.004	3.01	0.216	B	11115	0.053	2.17
SWU545/7	6	.500	78	0.03	12005	184	0.067	0.001	2.98	0.248	B	11443	0.065	2.23
TEX527	5	.25	75	0.057	11186	296	0.061	0.002	3.27	0.383	B	10149	0.054	1.94

* Number of specimens used in the generation of data presented.

It can be seen from Figure 41 that processing affects the material elastic modulus, maximum compressive stress, and strain to maximum stress. The stress-strain curve with the least strain to maximum stress indicates the least ductile material and the curve with the greatest strain to maximum stress indicates the most ductile material.

Proposed Design Allowables

Proposed compression design allowables for processed polycarbonate were developed from compression test data previously used in determining design strength data for SL3000 polycarbonate material as processed by specific transparency fabricators. These were combined to provide design allowables representing a wide range of processed material. The fabrication processes represented include drying, press polishing, mechanical polishing, fusion bonding, forming, and laminating. Representative specimens from all known transparency fabricators are not included, but it is felt that most fabrication processes used for laminated transparencies are included. It is intended that these proposed design allowables be used by the designer for static load analysis and for material test minimums in design specification documents where the specific fabrication source is unknown.

The developed average proposed design allowable data are presented in Table 17. These proposed design allowable are presented on a "C" basis as it includes specimens from all the participating vendors and would be unrealistic if presented on a "B" basis due to the large deviations. The developed average and proposed design allowable stress-strain curves are presented in Appendix B, Figures B17 and B18.

CONCLUSIONS

Conclusions based on data contained in this section and other applicable data are contained in Section XI of this report.

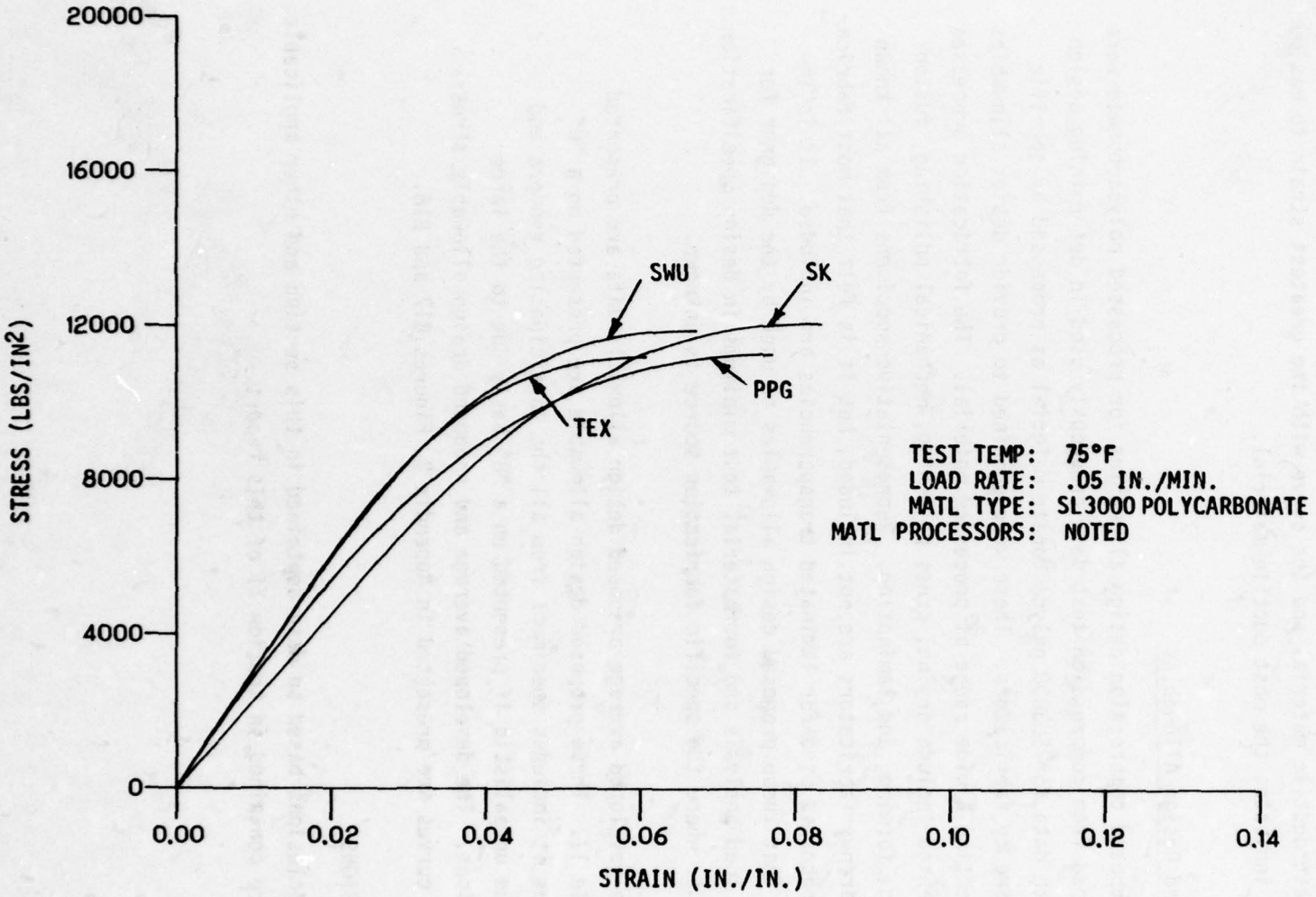

Figure 41. Compression Average Curves-Processing Effects

TABLE 17. PROPOSED COMPRESSION DESIGN ALLOWABLES

TEST SPECIMEN IDENT.	NO. *	THICK-NESS	TEST TEMP (°F)	LOAD RATE (IN./MIN)	AVERAGE STRENGTH DATA						DESIGN ALLOWABLE			
					MAXIMUM				MOD (PSI x 10^{-5})	STD DEV (PSI 10^{-5})	DES BAS	MAXIMUM		MOD (PSI x 10^{-5})
					STRESS (PSI)	STD DEV (PSI)	STRAIN (IN./IN.)	STD DEV (IN/IN)				STRESS (PSI)	STRAIN (IN./IN.)	
PPG515		0.19												
SK513	21	0.15	76	0.05	11,535	439	0.072	0.009	2.87	0.046	C	10,829	0.061	2.38
SWU515		0.19												
TEX527		0.25												

* Number of specimens included in the generation of data presented.

APPENDIX B

COMPRESSION STRESS-STRAIN CURVE DATA

The following compression stress-strain curves are presented for use in conjunction with tabulated strength data presented in the following listed tables of this section.

PAGES

Table 15 (Page 187)

Compression stress-strain curves - Figures B1 through B7 . 195 - 201

Table 16 (Page 188)

Compression stress-strain curves - Figures B 8 through B16.202 - 210

Table 17 (Page 191)

Compression stress-strain curves - Figures B17 and B18. . .211 - 212

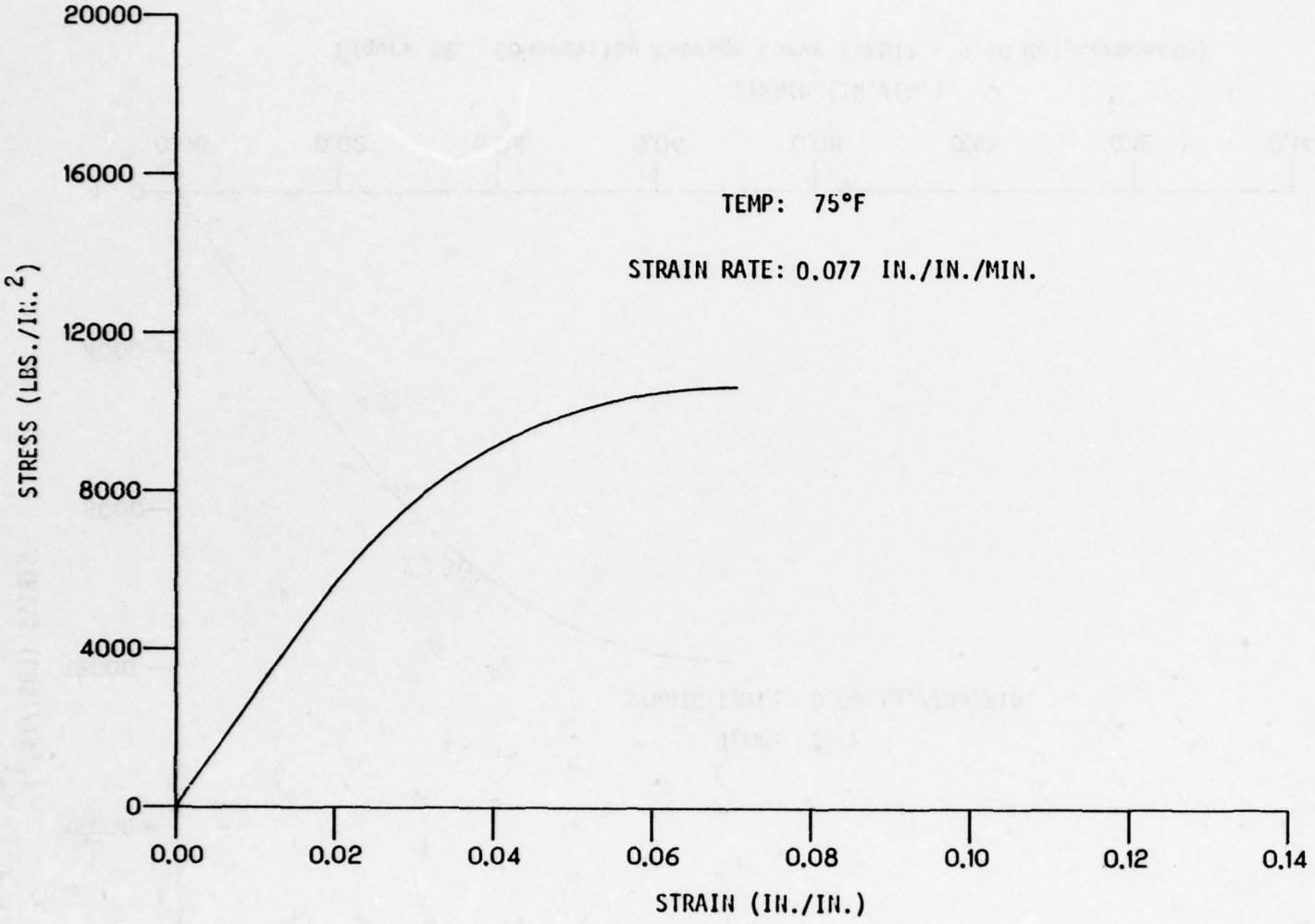

Figure B1. Compression Average Curve (PPG515/26 - 0.19 Polycarbonate)

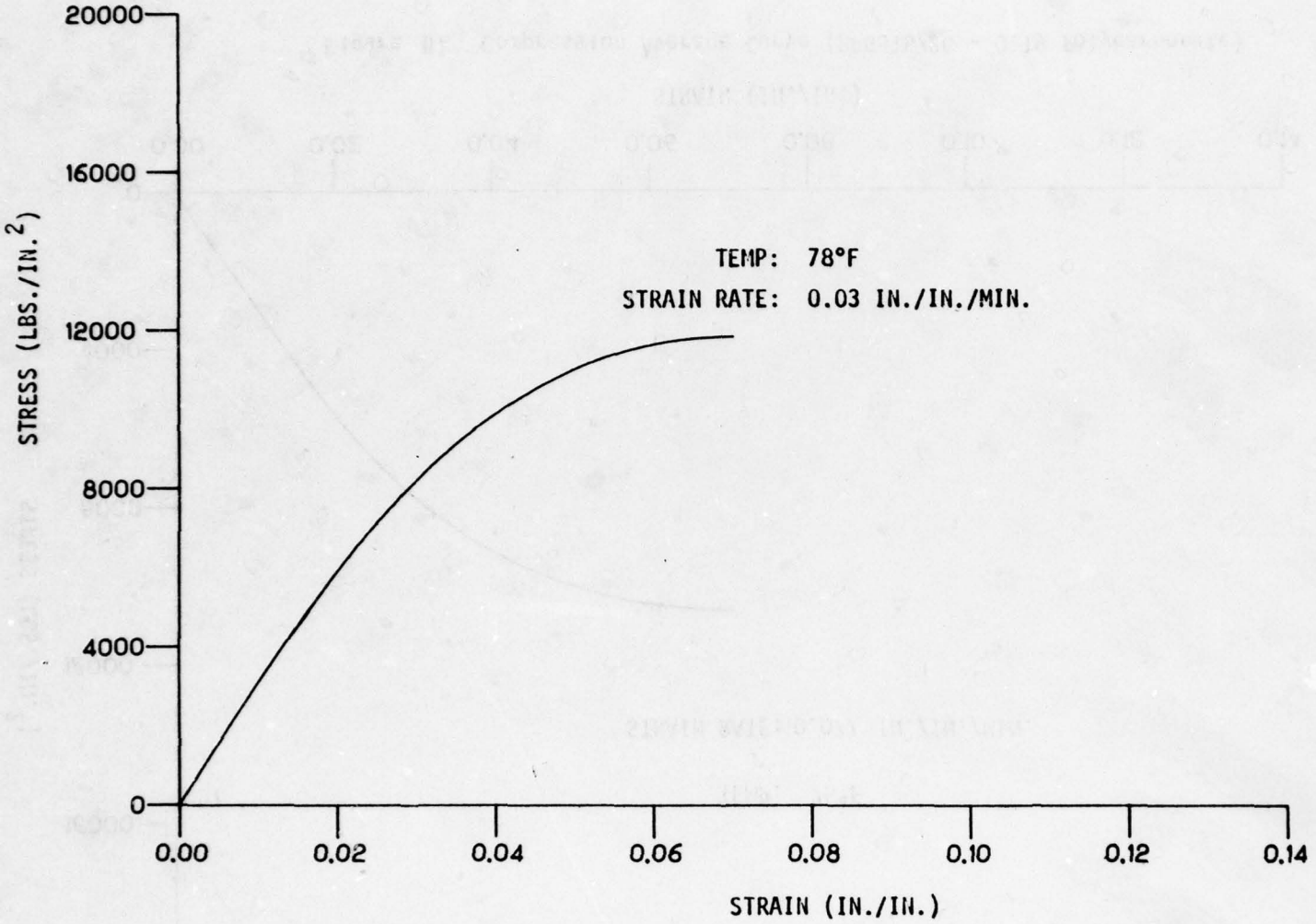

Figure B2. Compression Average Curve (SK511 - 0.50 Polycarbonate)

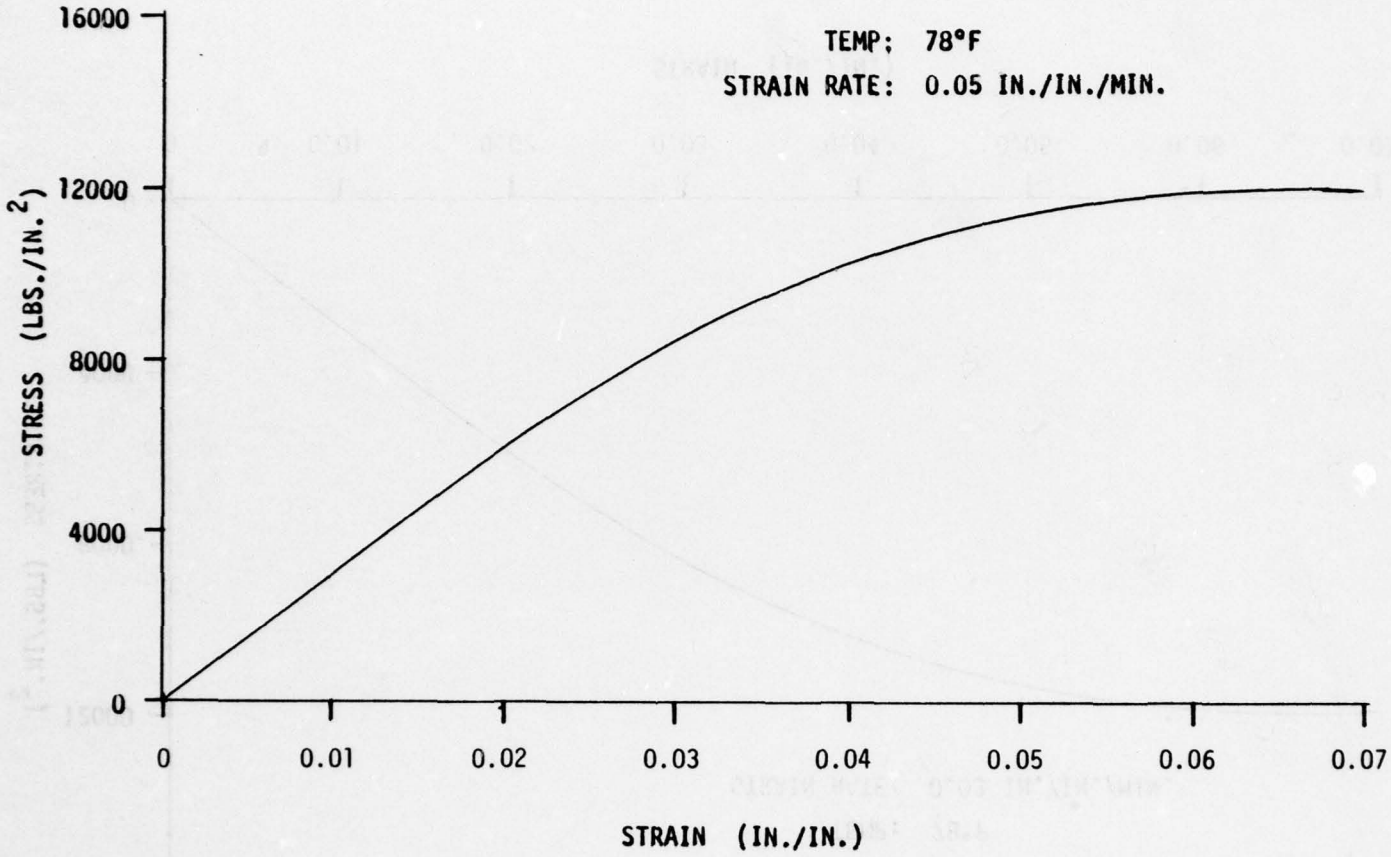

Figure B3. Compression Average Curve (SK 513 - 0.150 Polycarbonate).

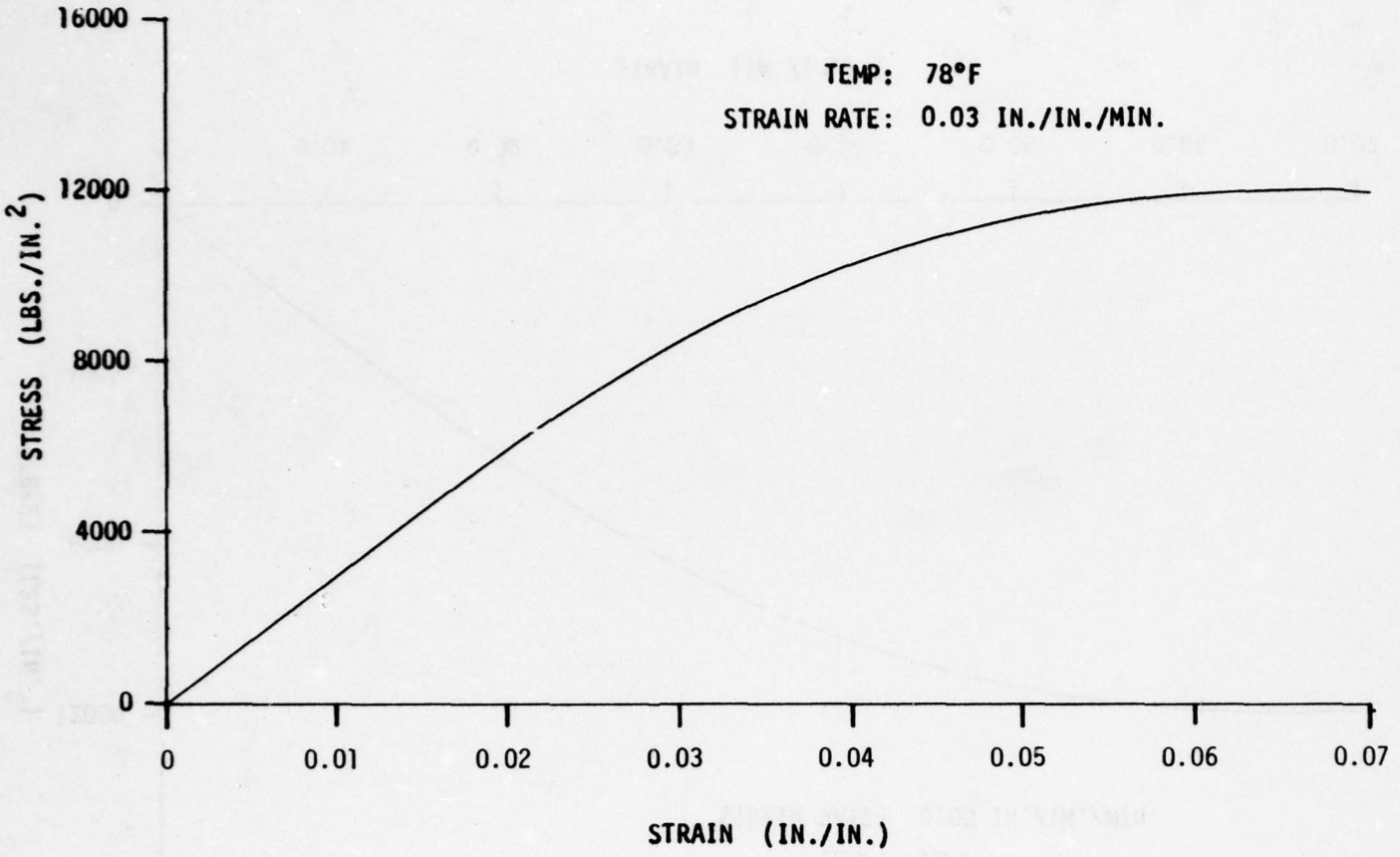

Figure B4 . Compression Average Curve (SWU 545/107 - 0.500 Polycarbonate B-1 W/S).

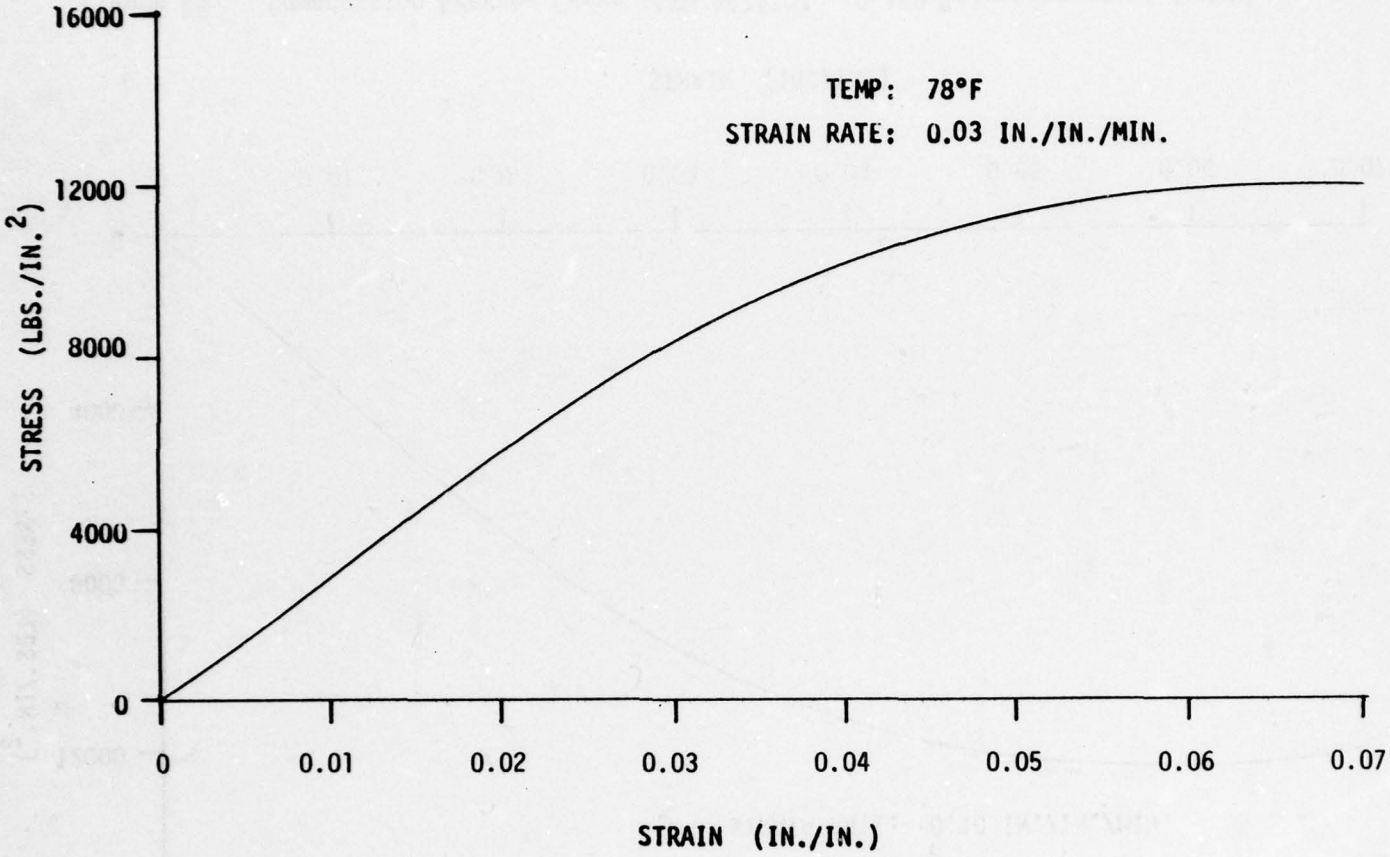

Figure B5 . Compression Average Curve (SWU 545-108 - 0.500 Polycarbonate).

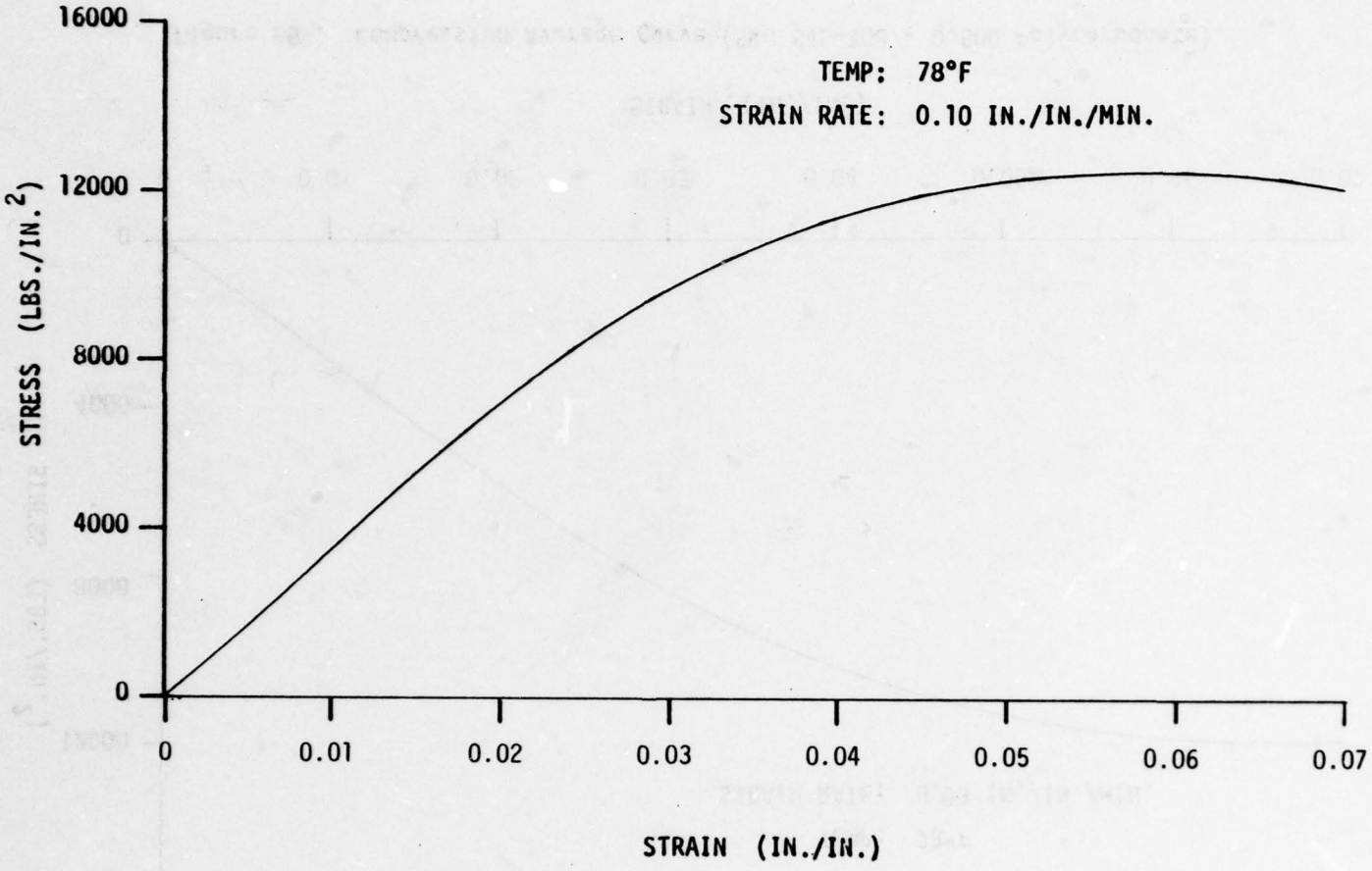

Figure B6 . Compression Average Curve (SWU 547/107 - 0.150 Polycarbonate B-1 W/S).

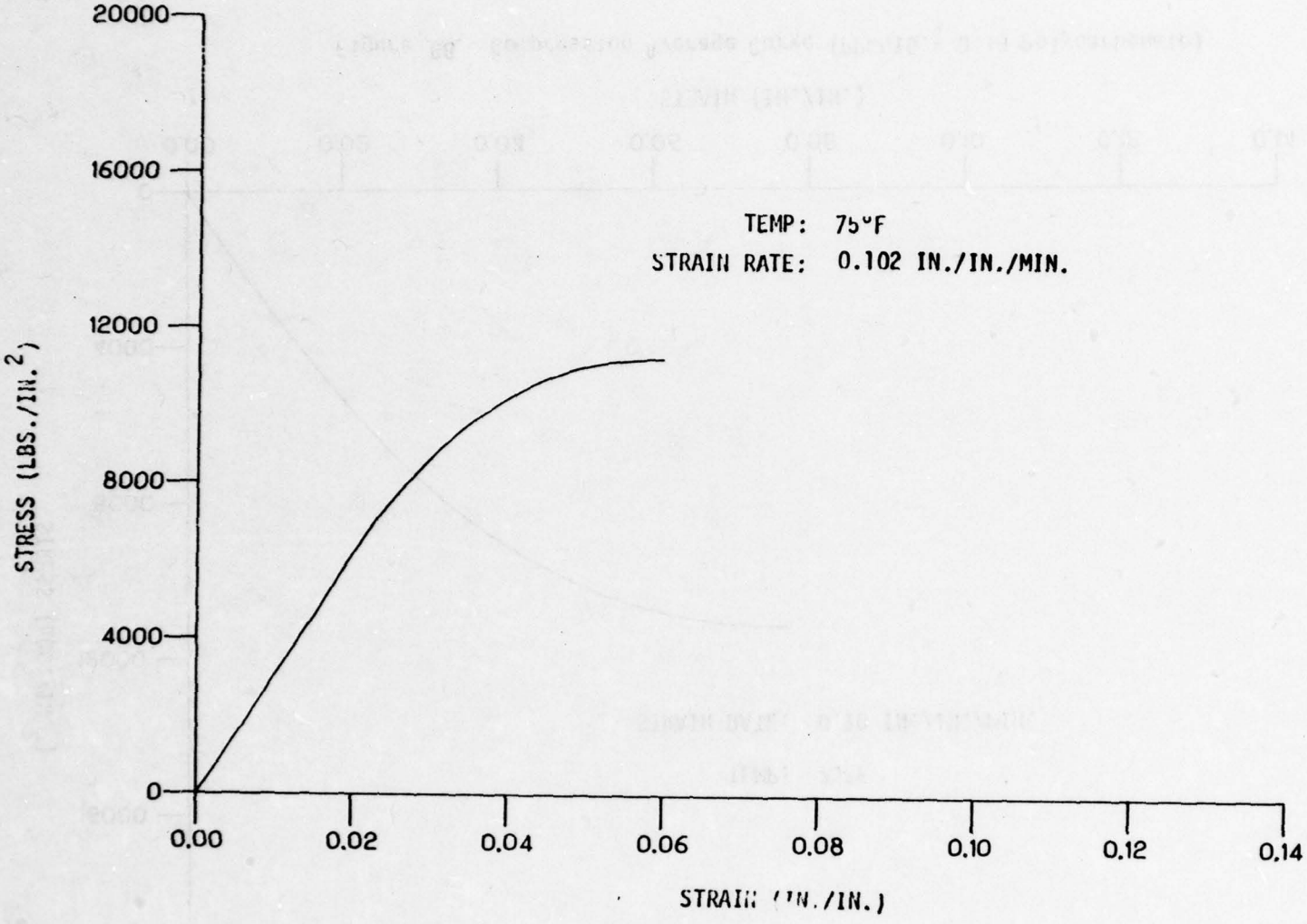

Figure B7. Compression Average Curve (SWU 547/108 - 0.15 Polycarbonate).

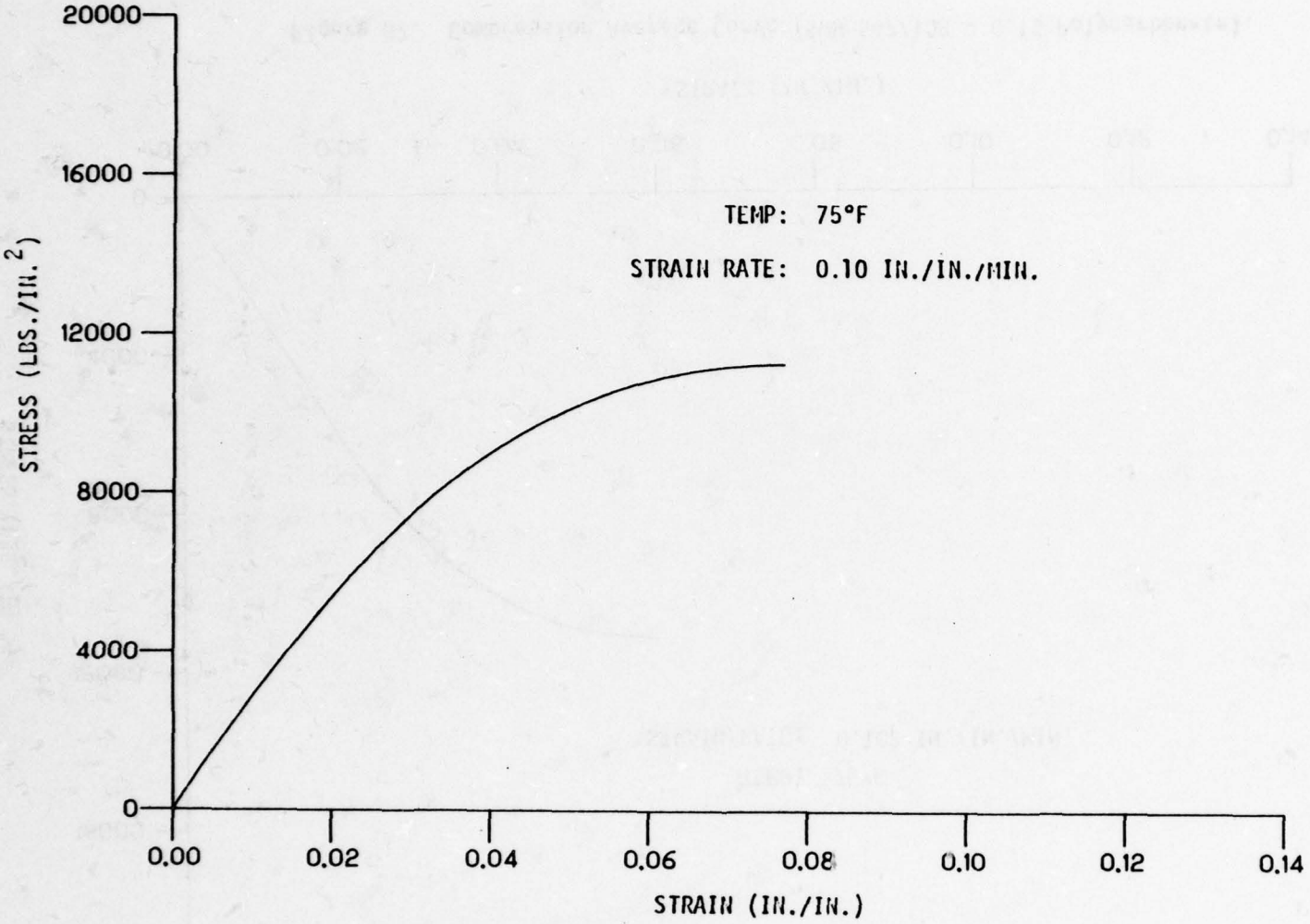

Figure B8. Compression Average Curve (PPG515 - 0.19 Polycarbonate)

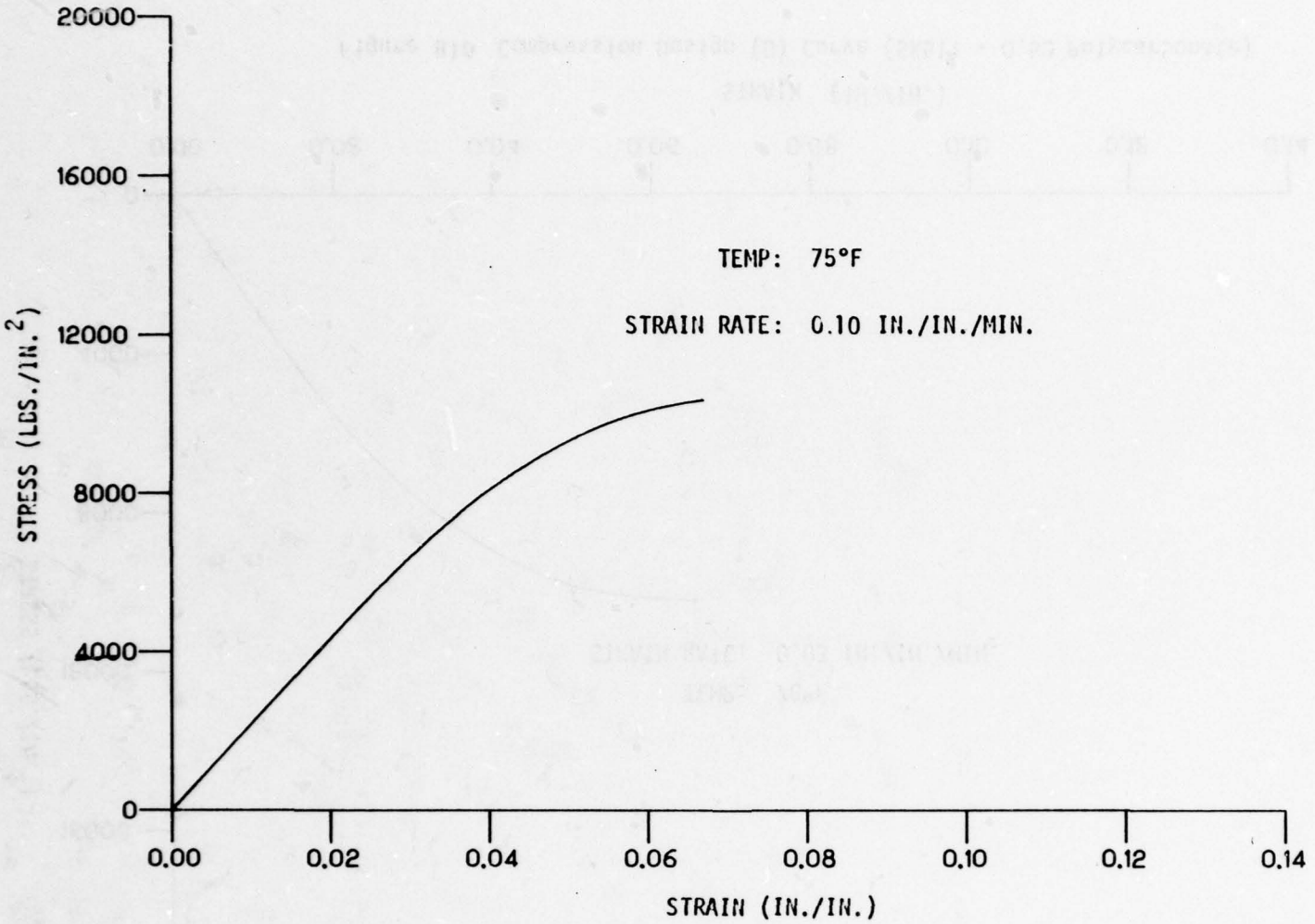

Figure B9. Compression Design (B) Curve (PPG515 - 0.19 Polycarbonate).

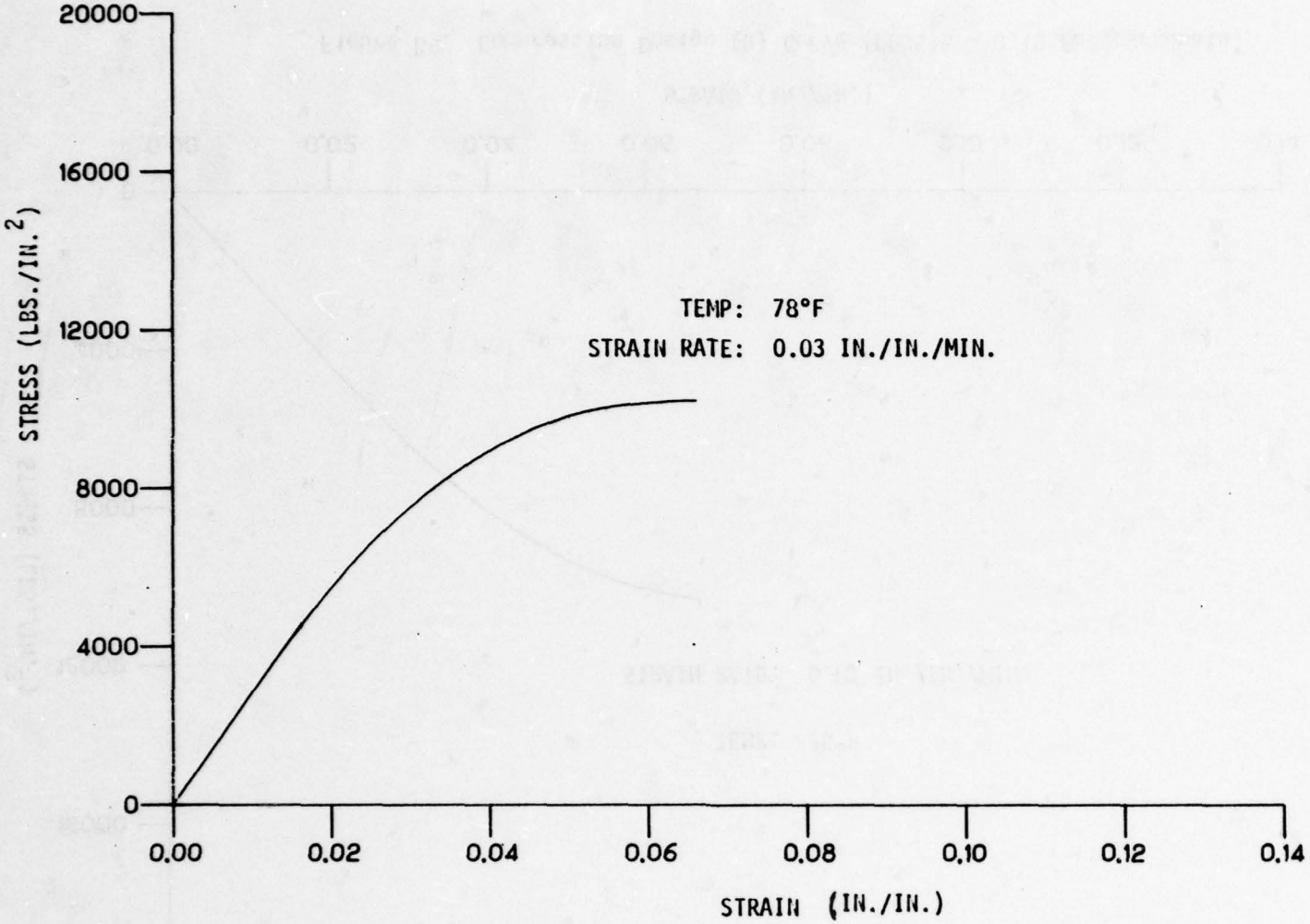

Figure B10 Compression Design (B) Curve (SK511 - 0.50 Polycarbonate)

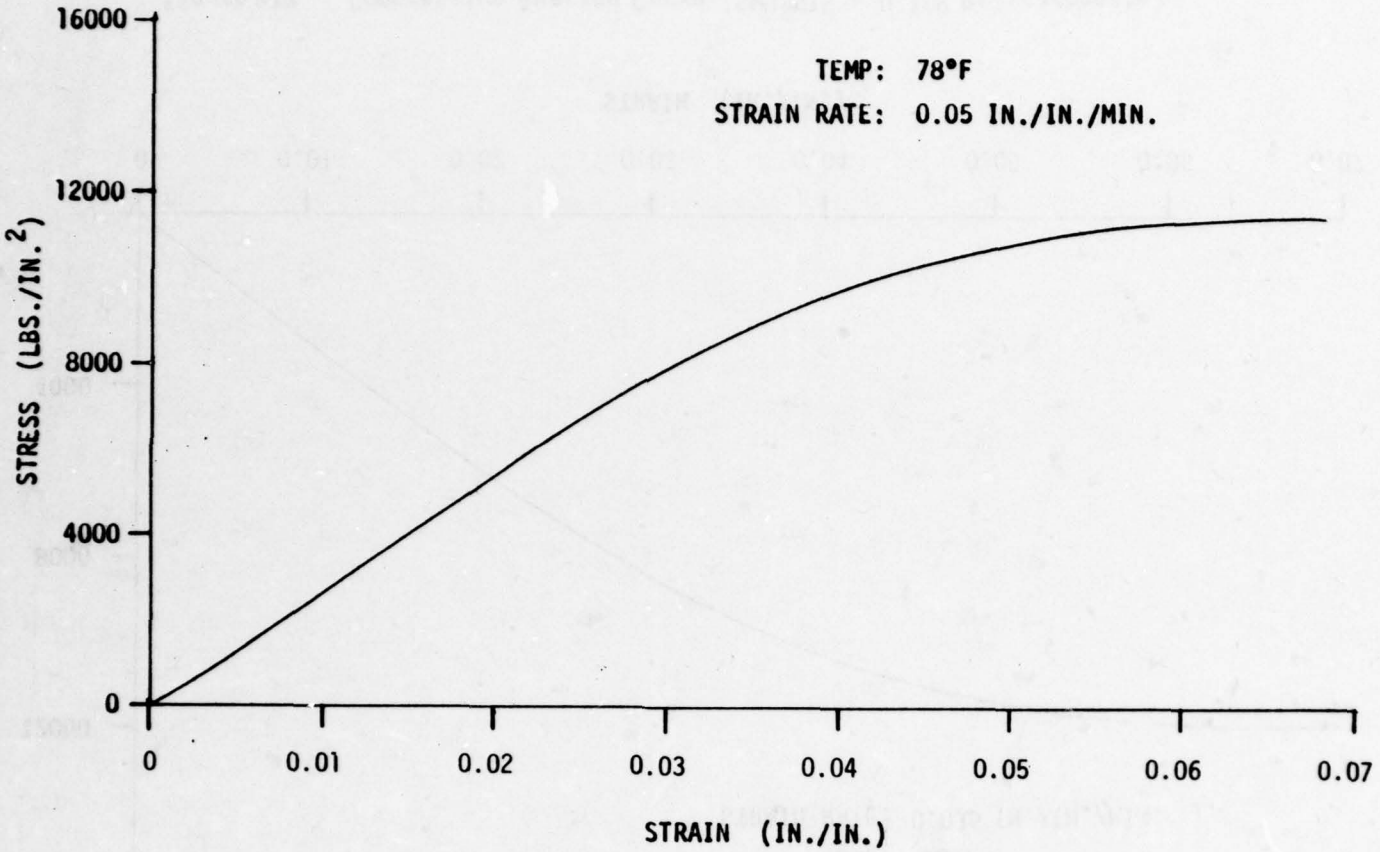

Figure B11. Compression Design (B) Curve (SK 513 - 0.150 Polycarbonate).

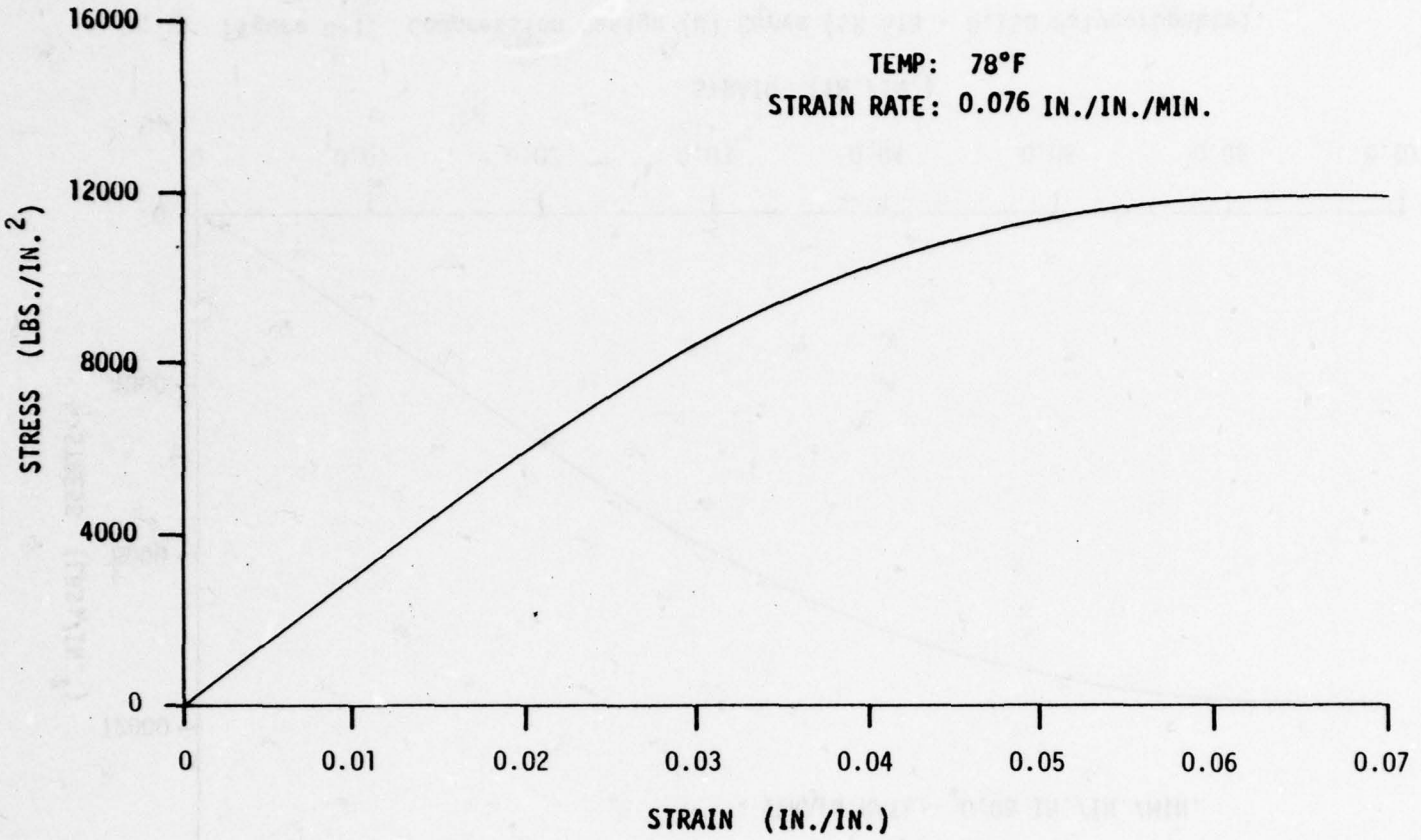

Figure B12. Compression Average Curve (SWU 515 - 0.188 Polycarbonate).

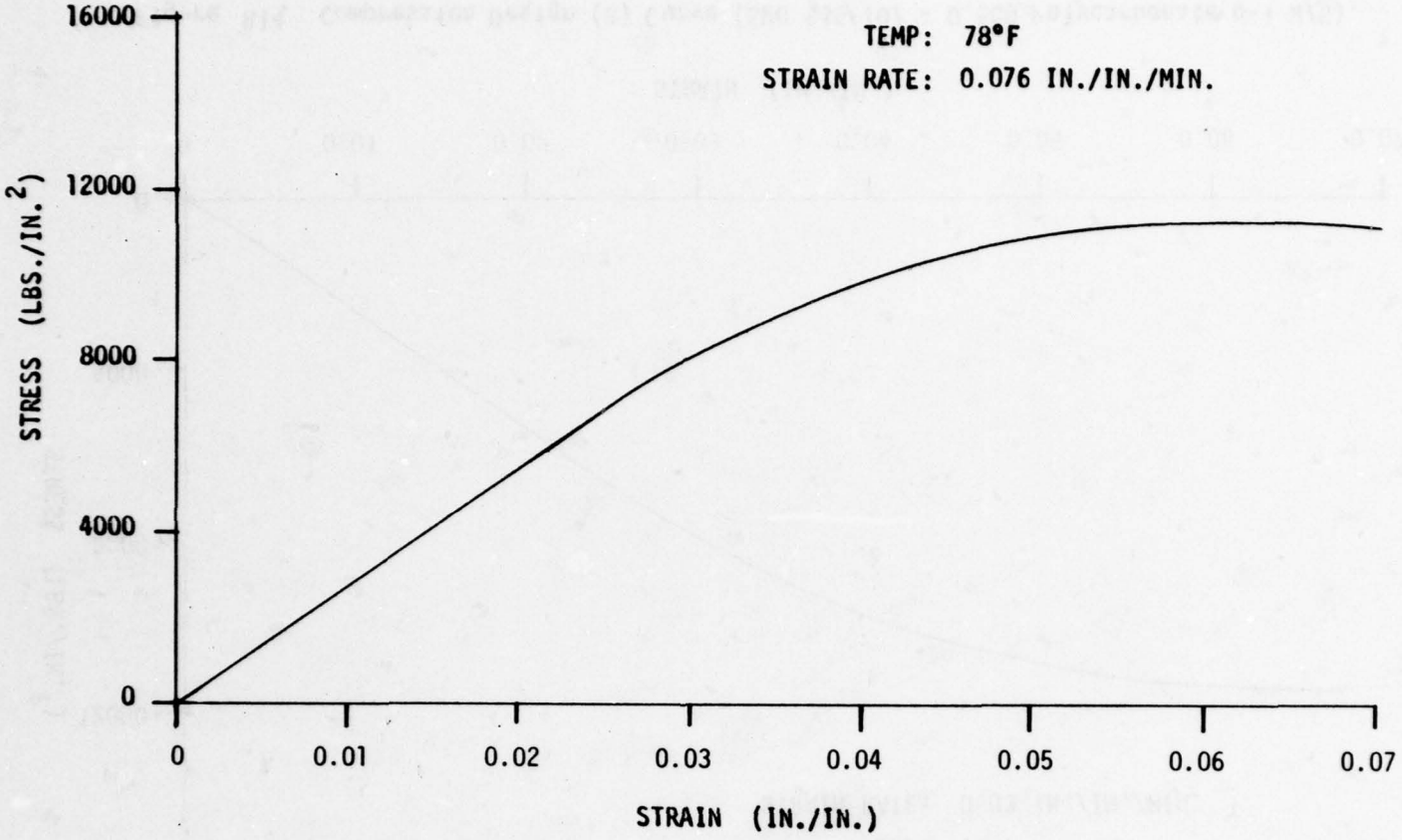

Figure B13 Compression Design (b) Curve (SWU 515 - 0.188 Polycarbonate).

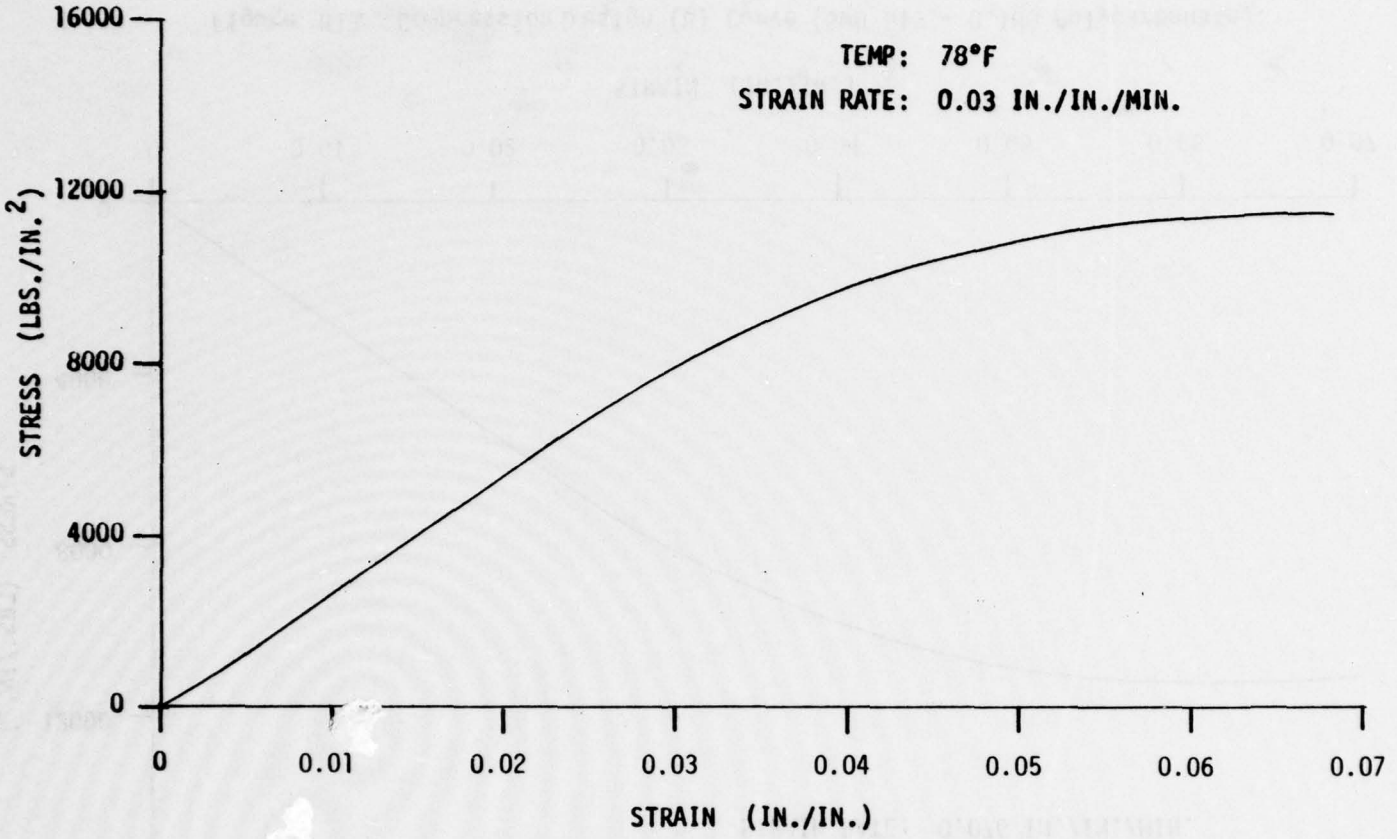

Figure B14 Compression Design (B) Curve (SWU 545/107 - 0.500 Polycarbonate B-1 W/S).

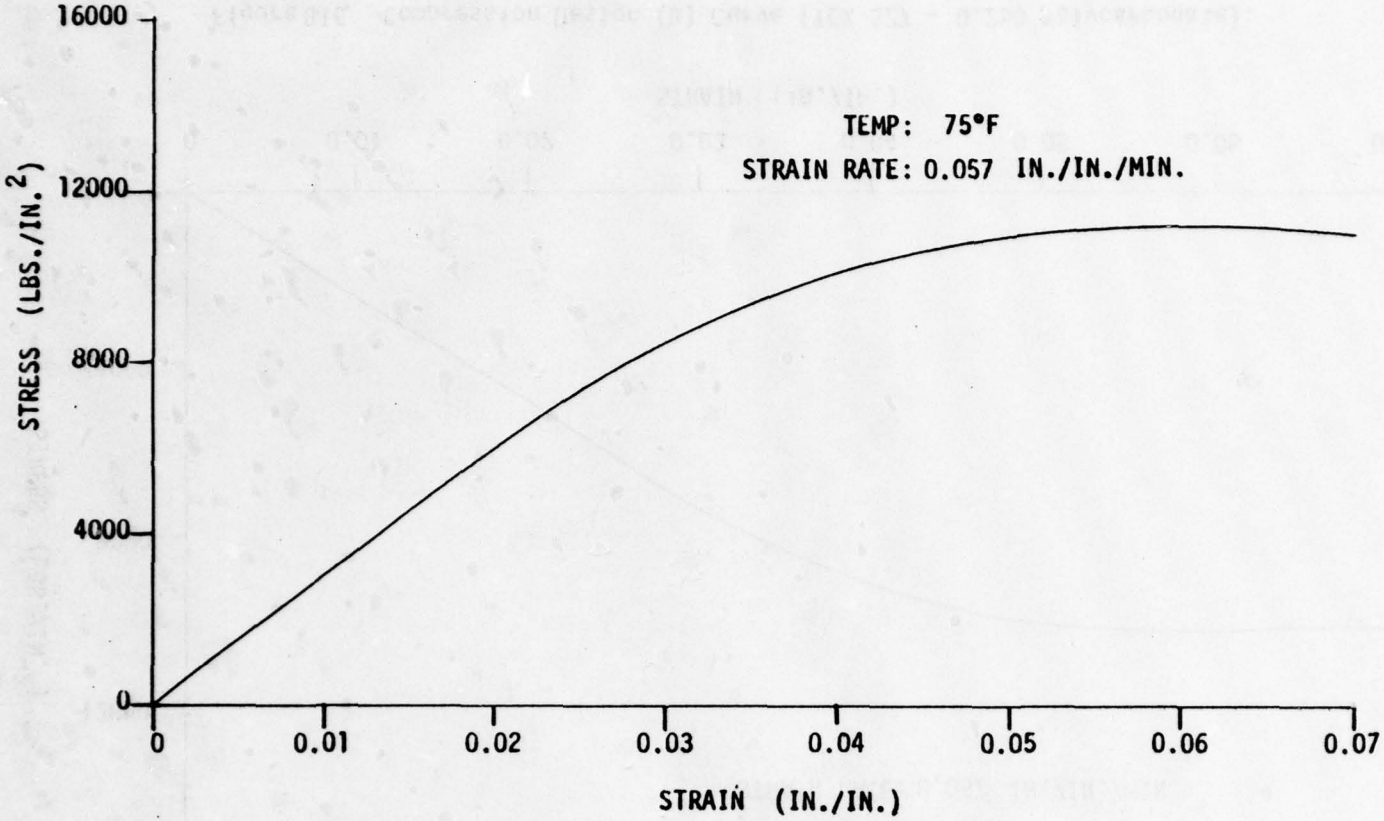

Figure B15. Compression Average Curve (TEX 527 - 0.250 Polycarbonate).

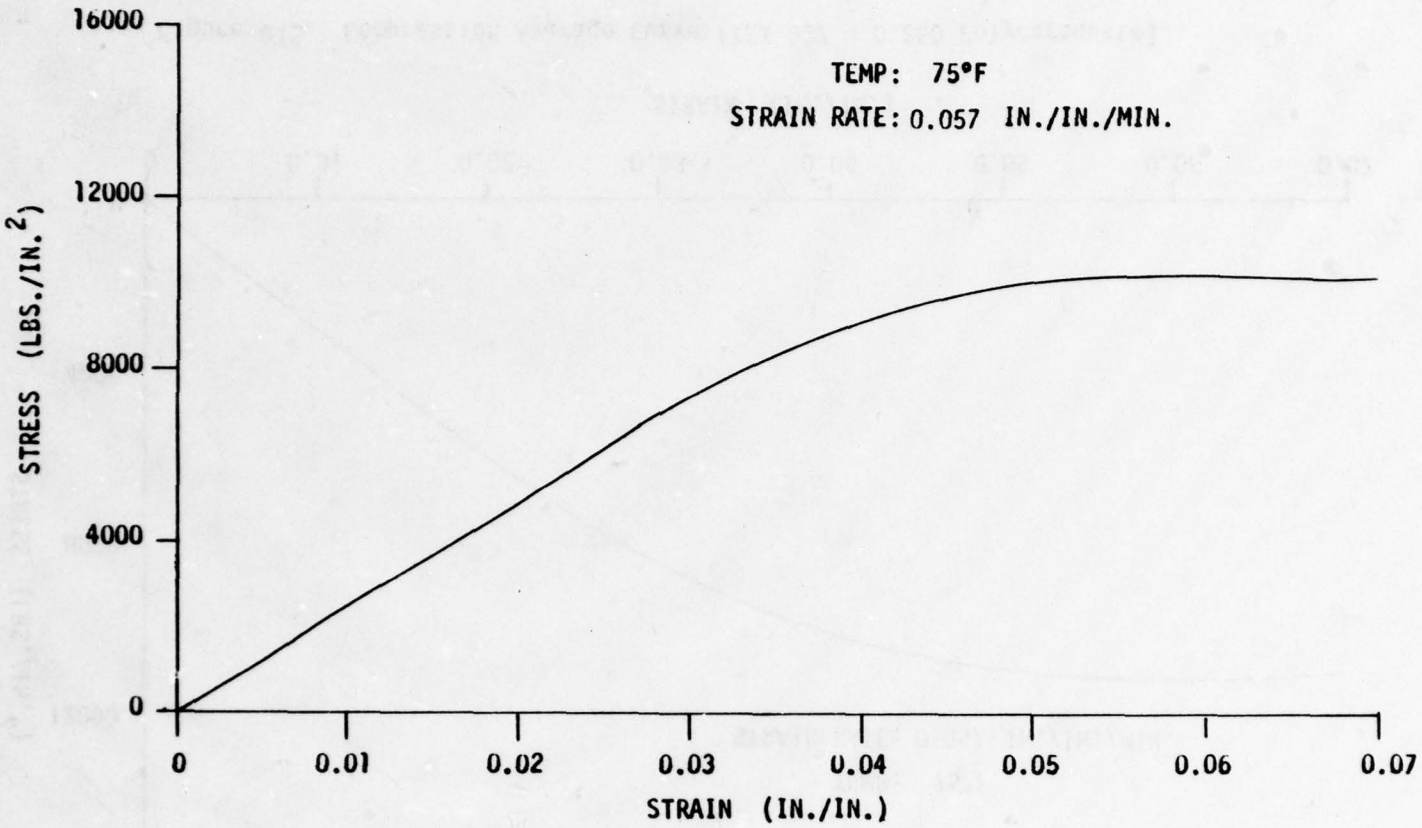

Figure B16. Compression Design (B) Curve (TEX 527 - 0.250 Polycarbonate).

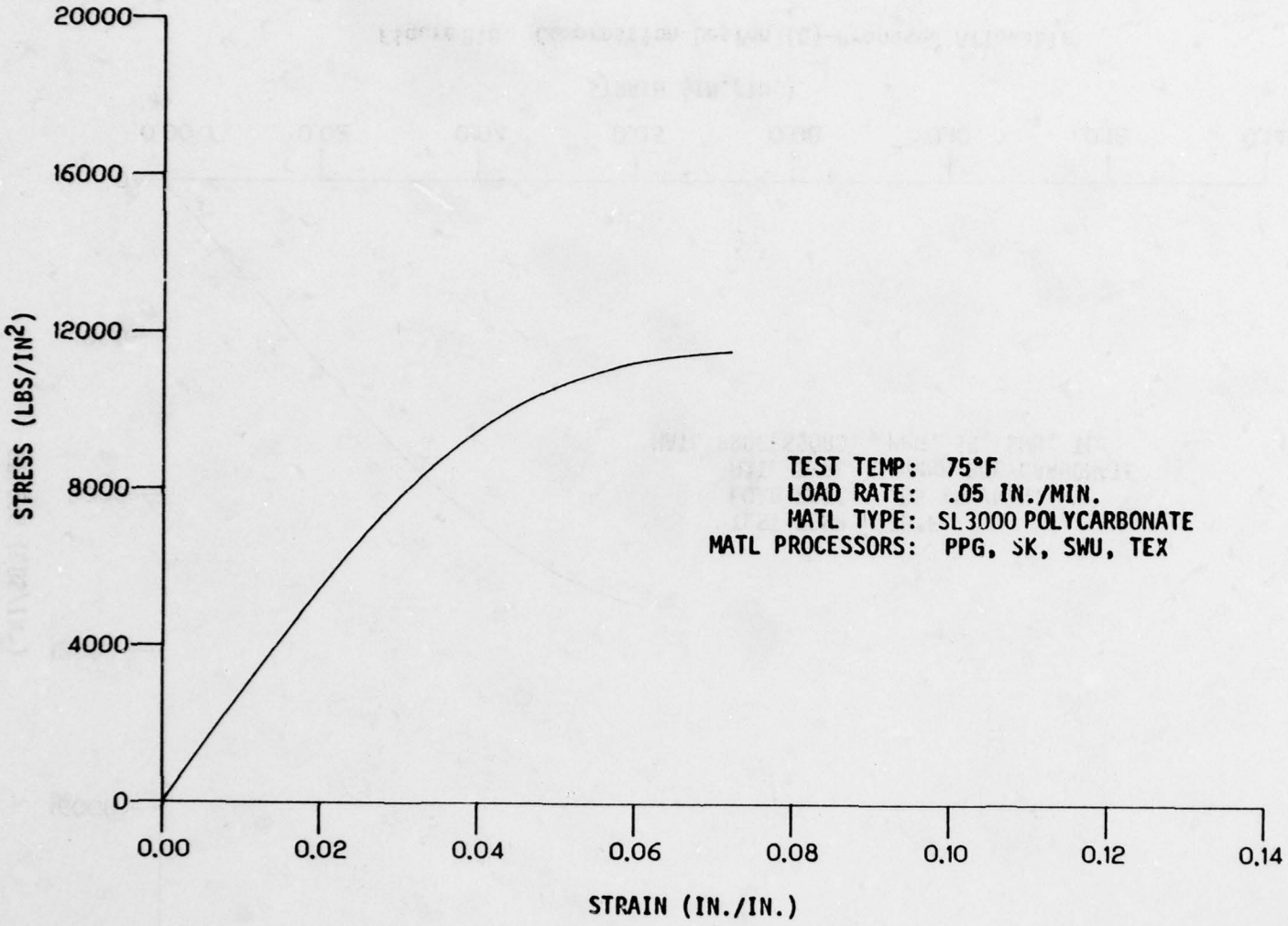

Figure B17. Compression Average Curve

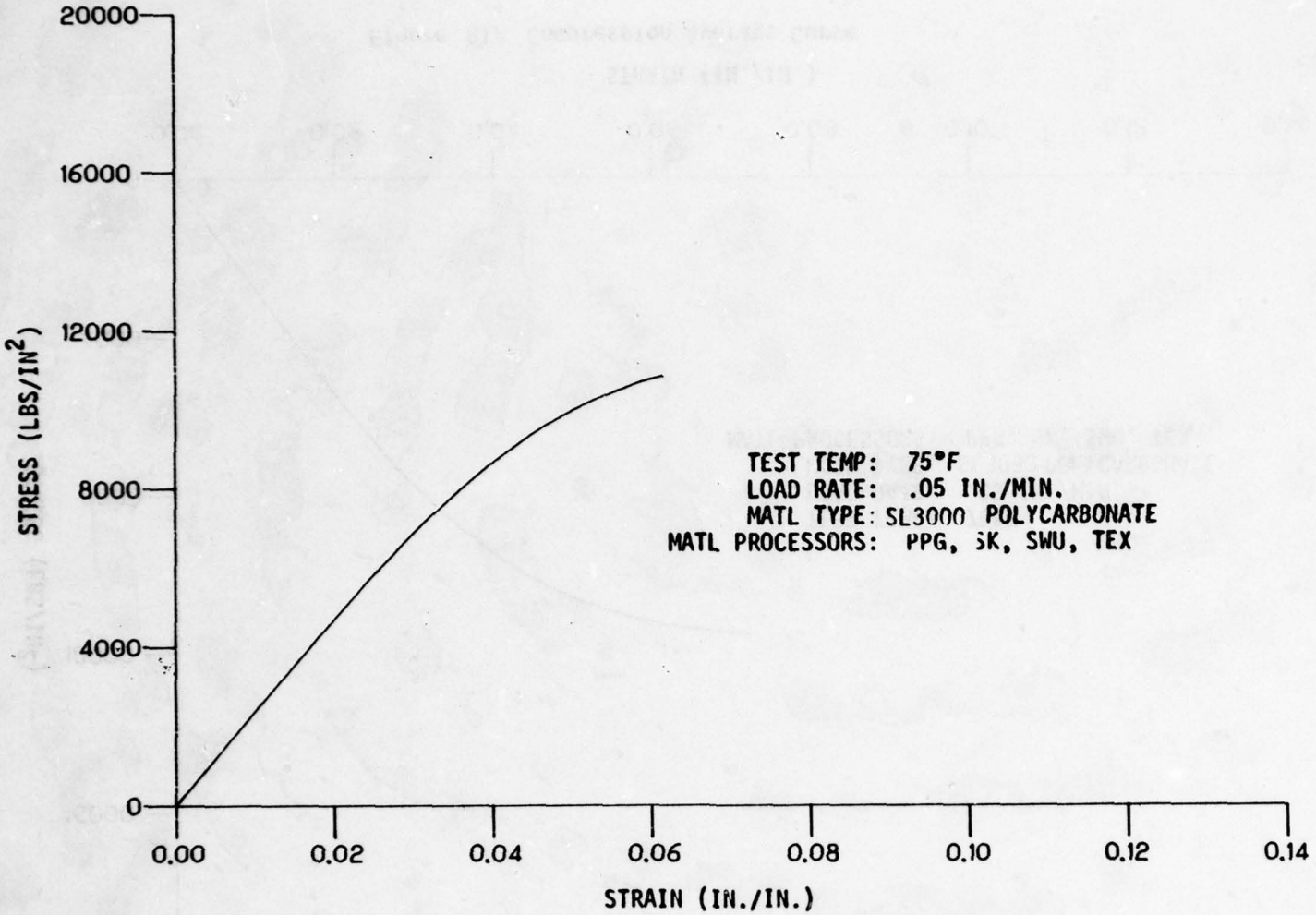

Figure B18. Compression Design (C)-Proposed Allowable

SECTION VII
LOW STRAIN RATE SHEAR MECHANICAL PROPERTIES TESTING OF LAMINATED INTERLAYER MATERIALS

This series of tests was conducted to establish low strain rate shear mechanical properties of interlayer materials as processed by specific windshield/canopy fabricators. The primary use for these tests was to provide average (actual) and design allowables for mechanical properties of processed interlayer materials for development and future design use in computer analysis (Reference 7). Additional uses were: evaluation of materials and processors, trade-off design studies, windshield static load analysis, and test criteria for the windshield/canopy design specification control documents. Test specimens were made from instrumented beams (Reference 12), bird impacted test windshields (Reference 13), or furnished by specific windshield/canopy fabricators. Two types of shear tests were conducted: (1) a generally used compression double shear test (ASTM standard being prepared), and (2) a unique torsional shear test. Results of these two types of testing were compared to arrive at the most accurate means of testing. Maximum and minimum test temperatures were established for tests based on the flight profile of a supersonic aircraft.

TEST SPECIMEN DESCRIPTION

The test specimens required for this series of tests are shown in Figures 42 through 45. Materials used in the fabrication of the shear specimens were subjected to the normal forming and fabrication processes of a laminated polycarbonate aircraft transparency. Two basic types of shear test specimens are shown, a five-ply double shear compression type test specimen and a torsional shear test specimen. A minimum of five (5) specimens of the following configurations were constructed by each noted transparency fabricator.

Compression Shear Test Specimens

The Z7942633-529 test specimens (Figure 42) were constructed from a seven ply laminate of SL3000 polycarbonate and PPG-112 polyurethene base interlayer materials. The test specimens were removed from the Z5942626-505 laminated transparent beam furnished by PPG Industries.

The Z5942633-531 shear test specimens (Figure 43) were made from a three-ply laminate constructed processed SL3000 polycarbonate sheet laminated with an interlayer material manufactured by Sierracin (SK), Swedlow (SWU), or PPG Industries (PPG). The SK531 test specimens are laminated with S-100 silicone base interlayer material. The SWU531 test specimens are laminated with SS-5272Y (HT) silicone base interlayer material. The PPG-531 test specimens are laminated with PPG-112 polyurethene base material.

The Z5942633-533 shear test specimens (Figure 43) were made from laminated windshields manufactured by Swedlow (SWU) and PPG Industries (PPG). The SWU533 shear test specimens were made from a three-ply B-1 bird test windshield made of SL3000 polycarbonate, and acrylic sheet laminated with SS-5272Y (HT) silicone base interlayer material. The PPG-533 test specimens were made from an eight-ply bird test windshield made of SL3000 polycarbonate sheet laminated with PPG-112 polyurethane base interlayer material.

The Z5942633-623 and -627 test specimens (Figure 43) were made from a three-ply laminate of processed SL3000 polycarbonate sheet laminated with S-130 interlayer material manufactured by Sierracin.

Torsional Shear Test Specimens

The Z7942633-535 test specimens (Figure 44) were constructed from a three-ply laminate of processed SL3000 polycarbonate and S-100 silicone base interlayer material manufactured by Sierracin Co. The test specimens were bonded to the torsional test adapter tubes.

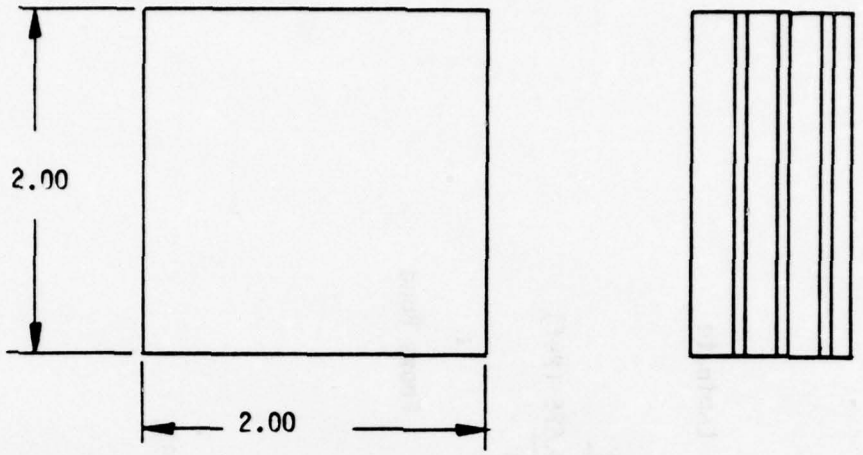

Figure 42. Shear Test Specimen (Z7942633-529).

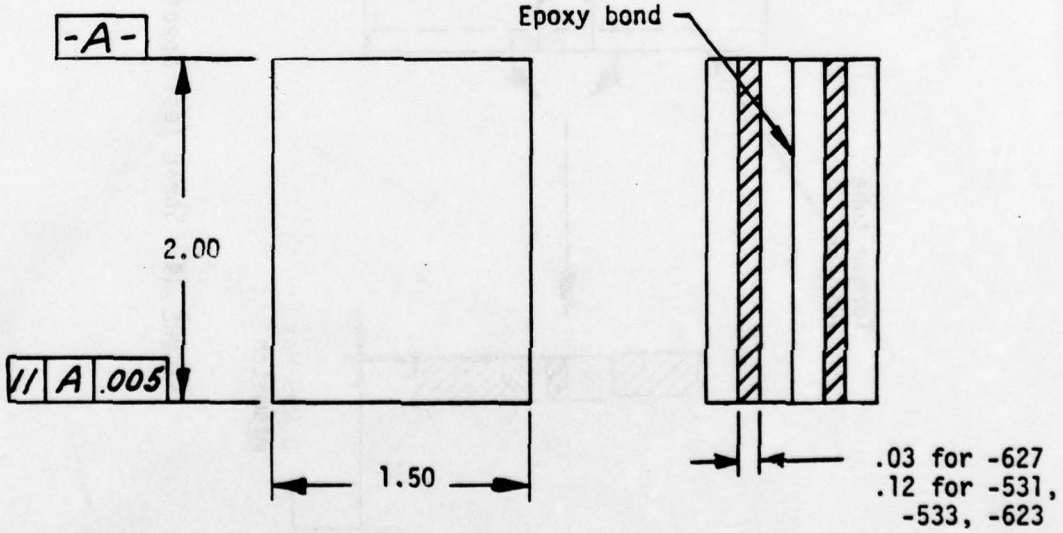

Figure 43. Shear Test Specimen (Z7942633-531, -533, -623, -627).

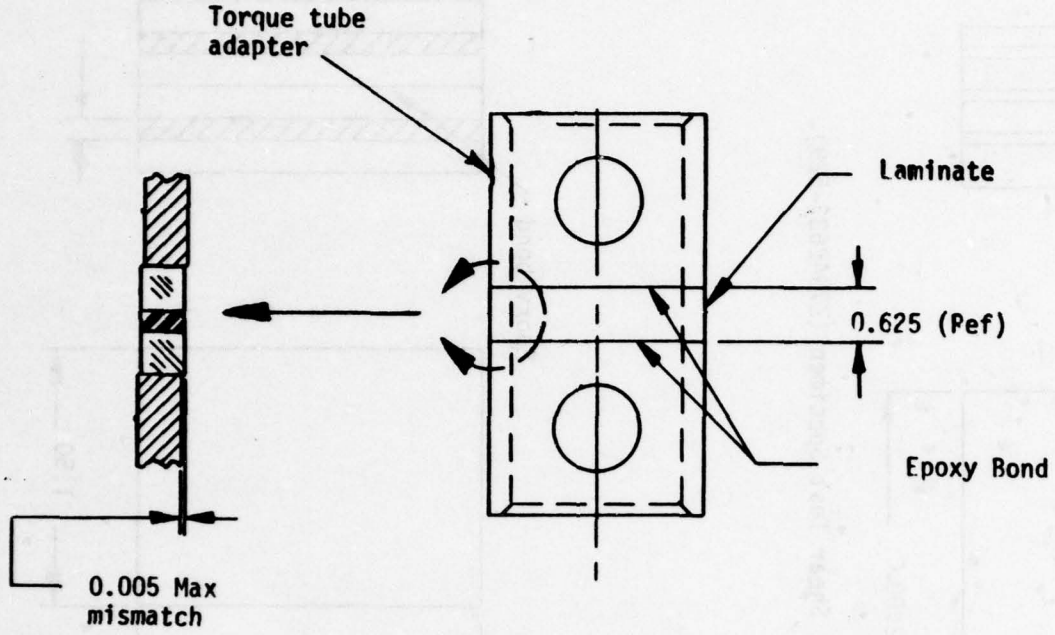

FIGURE 44. Shear Test Specimen (Z7942633-535, -539).

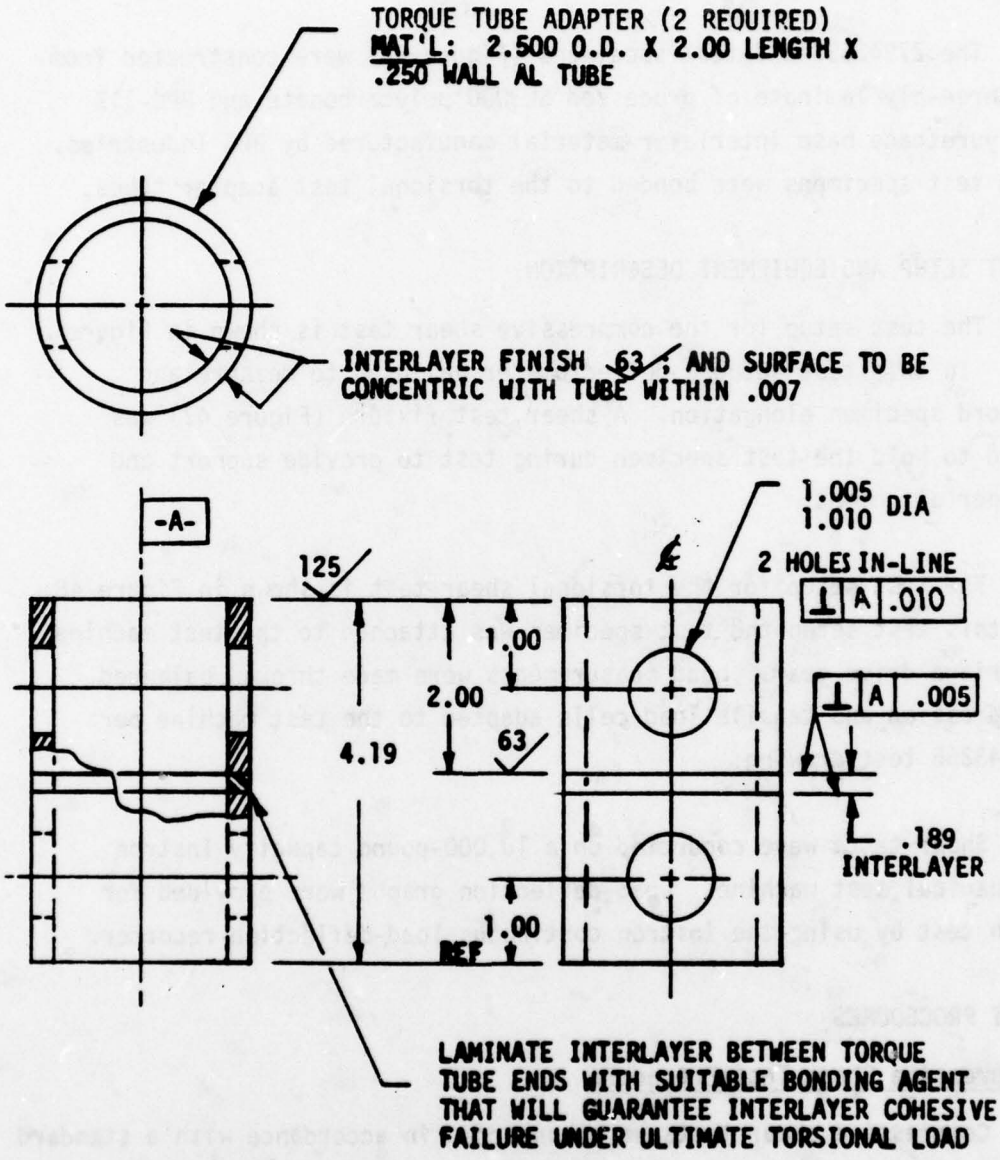

FIGURE 45. Torsional Shear Test Specimen (Z7942633-537).

The Z7942633-537 test specimens (Figure 45) were constructed of SS-5272Y (HT) silicone base interlayer material manufactured by Swedlow Co., which was bonded to the torsional test adapter tubes.

The Z7942633-539 test specimens (Figure 44) were constructed from a three-ply laminate of processed SL3000 polycarbonate and PPG-112 polyurethane base interlayer material manufactured by PPG Industries. The test specimens were bonded to the torsional test adapter tubes.

TEST SETUP AND EQUIPMENT DESCRIPTION

The test setup for the compressive shear test is shown in Figure 46. In this test setup a deflectometer was used to measure and record specimen elongation. A shear test fixture (Figure 47) was used to hold the test specimen during test to provide support and proper alignment.

The test setup for the torsional shear test is shown in Figure 48. In this test setup the test specimen was attached to the test machine carriage drive gear. Load measurements were made through balanced compression and tensile load cells adapted to the test machine per Z5943265 test drawing.

Shear tests were conducted on a 10,000-pound capacity Instron mechanical test machine. Load-deflection graphs were provided for each test by using the Instron continuous load-deflection recorder.

TEST PROCEDURES

Compressive Shear Test Procedure

Compressive shear tests were conducted in accordance with a standard shear test procedure ASTM STD-F-705-76. Proposed by ASTM F7.08 Sub-committee as follows:

1. Measure and record the length and width of the interlayer with a suitable micrometer to the nearest 0.025-mm (0.001-inch).

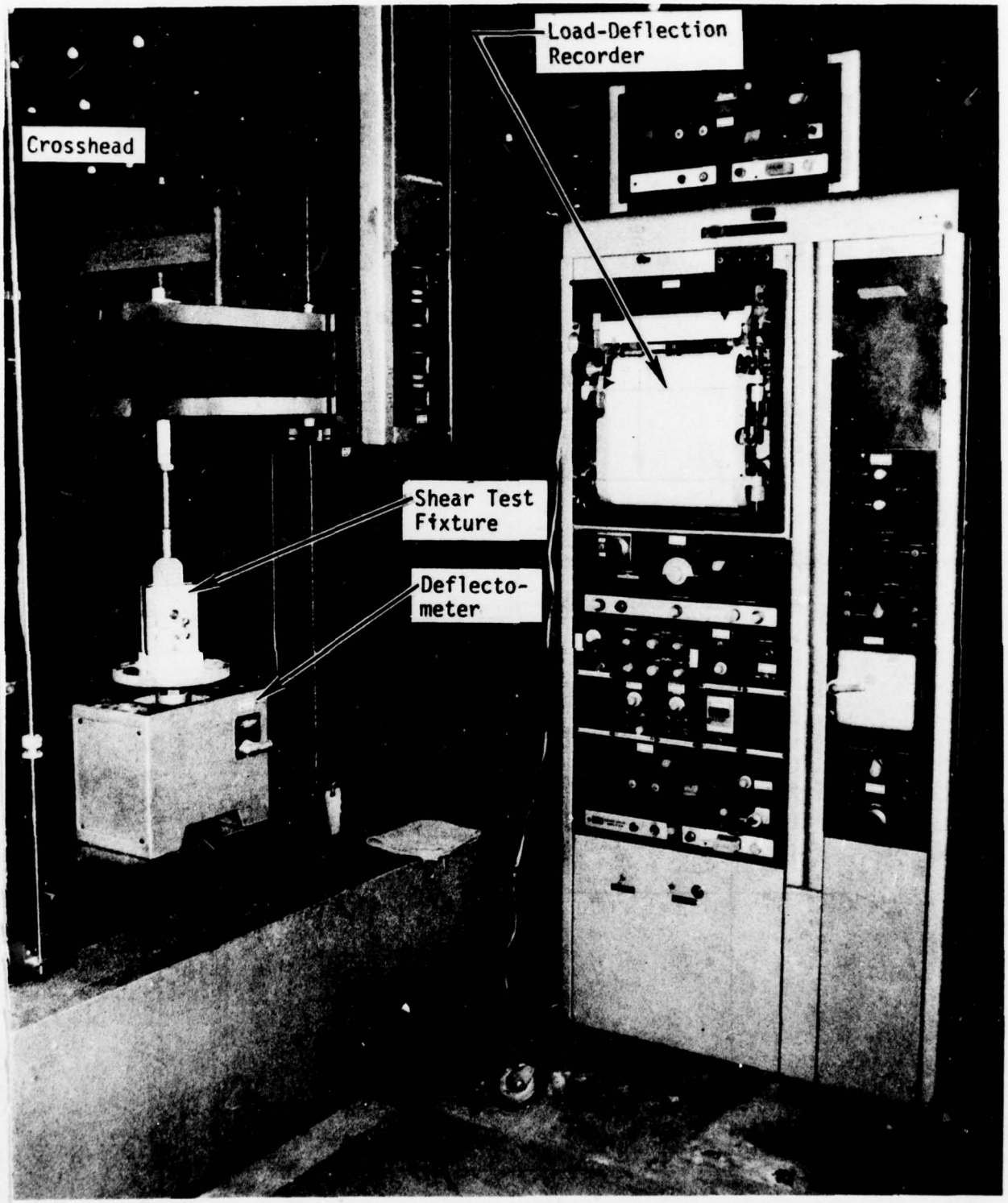

FIGURE 46. Compressive Shear Test Setup

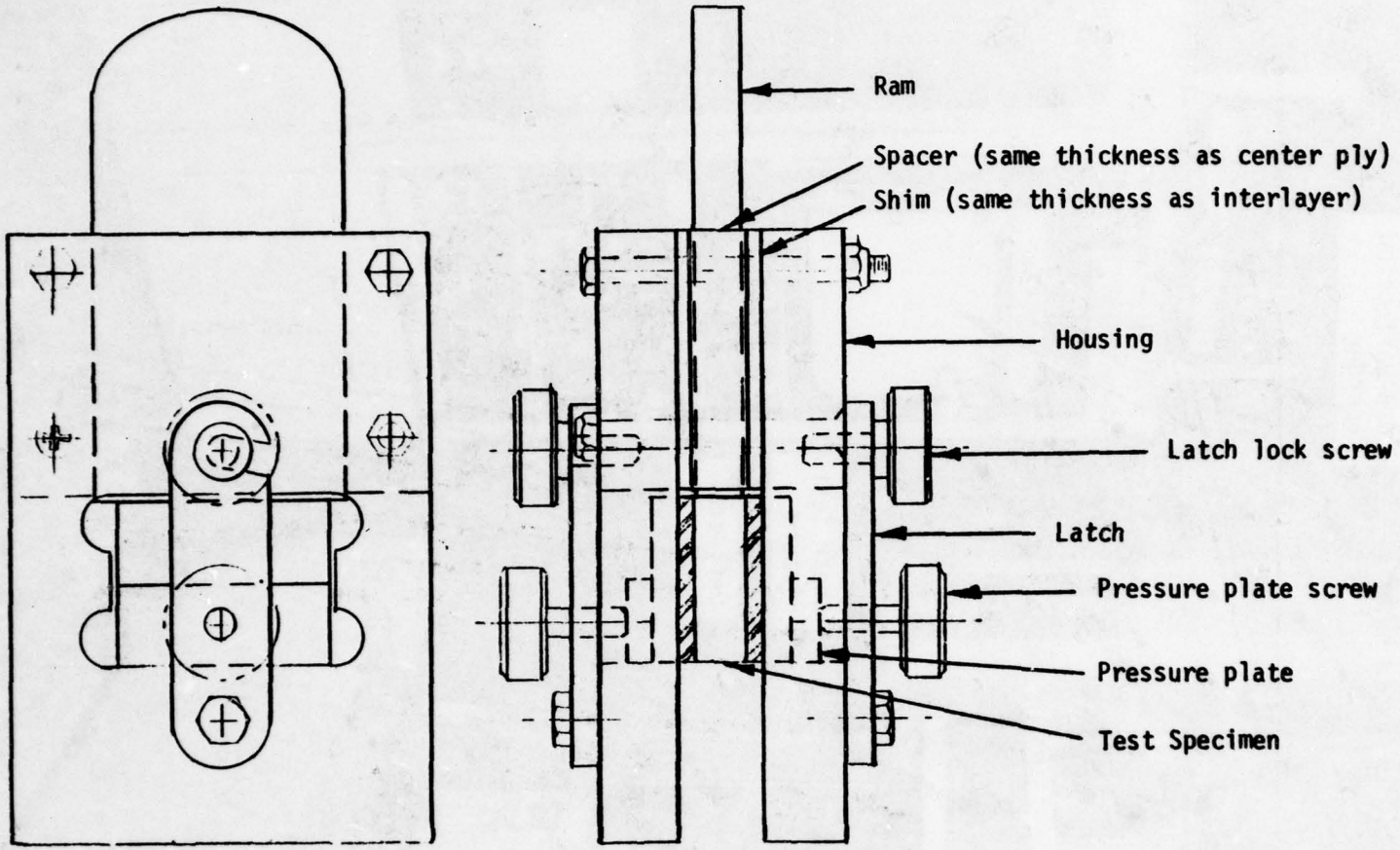

Figure 47. Shear Test Fixture.

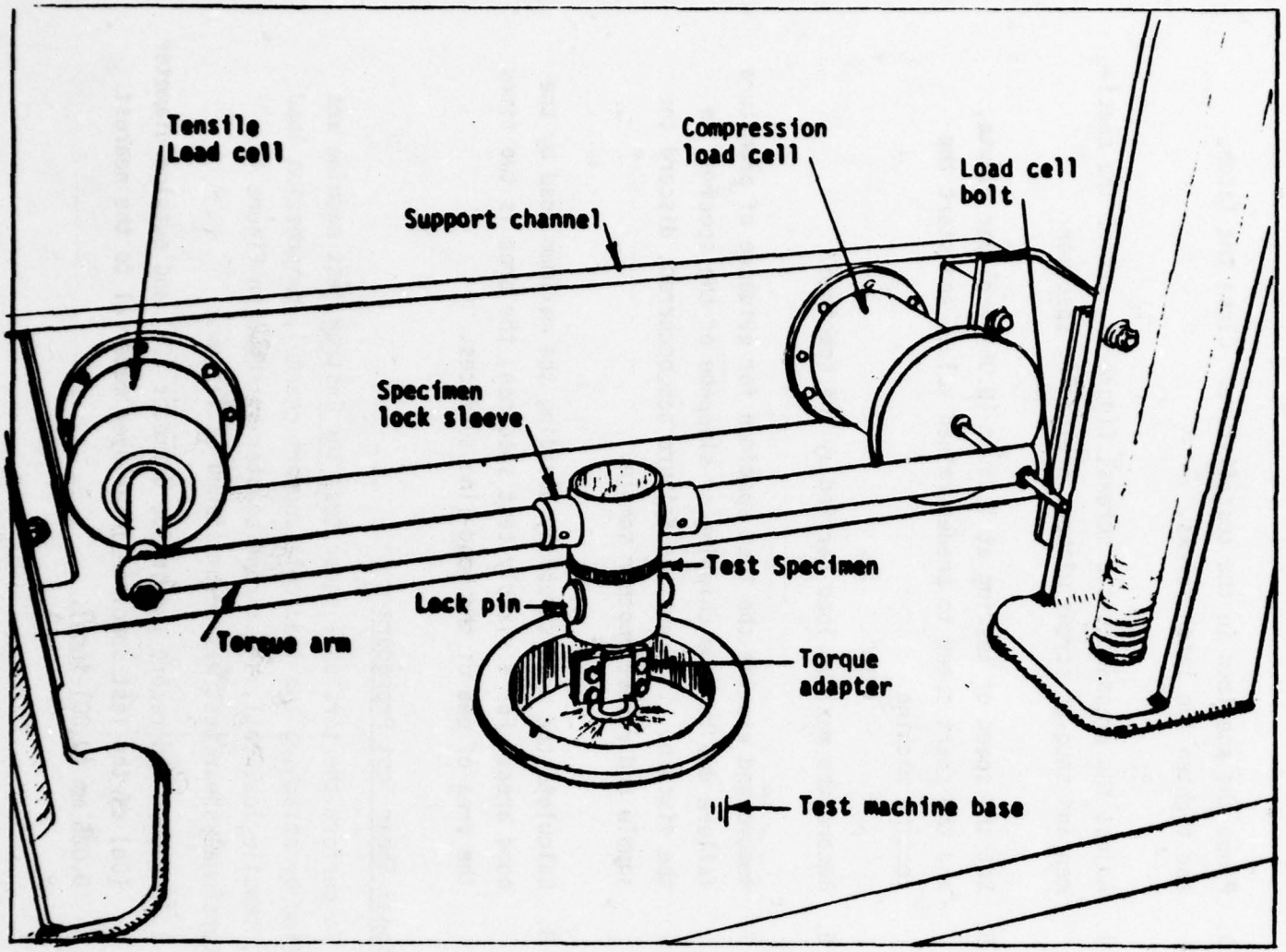

Figure 48. Torsional Shear Test Setup.

2. Loosen the test fixture, latch screws, Figure 47, and position one latch to a horizontal position.

3. Place the specimen in the test fixture. Close the latch, and tighten the latch screws.

4. Adjust the pressure plate screws, Figure 47, center the specimen and snug-up screws without preloading specimen.

5. Set the speed of testing at 1.25 mm (0.05-inch) per minute, and the chart speed to predetermined values and start the testing machine.

6. Record the maximum load carried by the specimen.

7. Remove and examine the test specimen for evidence of premature failure due to edge chipping or slippage of the specimen in the fixture. If premature failure has occurred, discard the sample and retest another sample.

8. Calculate the bond stress by dividing the maximum load by the bond area. For a six-ply test specimen, the area is two times the area of one of the bond-line surfaces.

Torsional Shear Test Procedure

To perform the torsional shear test the Instron test machine was modified by attaching the load cell support channel, compression load cell, tensile load cell, and torque adapter as shown in Figure 48. The torsional shear test was accomplished as follows:

1. Measure and record the inside diameter (Di) and outside diameter (Do) of the test specimen interlayer material to the nearest 0.025 mm (0.001-inch).

2. Install the test specimen on the torque adapter and insert the lock pin per Figure 48.

3. Install the torque arm and specimen lock sleeves per Figure 48.

4. Install the torque arm and balance the load cells by adjusting the compression load cell bolt for a 10- to 20-pound preload.

5. Adjust the recorder chart speed and crosshead rate to predetermined values and mark the specimen for 0 deflection.

6. Record the maximum load carried by the specimen and mark the specimen to indicate deflection.

7. Calculate the rupture shear stress (τ) by the formula

$$\tau = \frac{2T\ r_o}{\pi(r_o^4 - r_i^4)}$$

where: T = maximum load x load arm
r_o = outer radius of interlayer
r_i = inside radius of interlayer

TEST REQUIREMENTS

Douglas provided facilities and services required for testing. The mechanical testing machines were verified for accuracy per ASTM E4-72 procedures within $\pm$0.5 percent traceable to NBS. Instrumentation equipment was verified for a class accuracy of B-1 per ASTM E83-67 procedures. The speed of testing was 0.05-inch/minute for compression shear tests, and 0.002-inch/minute for torsional shear tests. A load deflection curve was recorded for each specimen tested through the peak load portion of the curve. A minimum of 5 test specimens for each test condition was provided. The peak load was recorded for each

specimen. Test temperatures were -30°F, +75°F and +190°F for compressive shear tests, and +75°F for torsion shear testing.

TEST RESULTS AND ANALYSIS

Three tasks were accomplished and documented in this section of the report. Task I provides average (actual) compressive shear properties data for test windshields for development of a bird strike computer program (Reference 7) and in support of the analysis of laminated beams representative of aircraft transparencies (Reference 12). Task II provides average and specific design allowable compressive shear properties of two types of silicone interlayer materials, two types of polyurethane materials, and a co-polymer interlayer material as laminated by three transparency manufacturers. Task III provides average torsional shear properties for two types of silicone interlayer materials, and a polyurethane interlayer material as laminated by three transparency manufacturers.

The mechanical property design allowables presented were computed on a "B" basis by methods outlined in Section III. Where "B" basis data could not be computed, the "C" basis data was computed and is presented. Where no design allowable is presented, the design data could not be computed due to large deviations in test results that gave negative or illogical stress and/or strain values.

Test Data

Task I shear strength data are given in Table 18. The average stress-strain curves from which the tabulated data were derived are presented in Appendix C, Figures C1 through C6 (Pages 241 to 246).

Task II shear strength data are given in Table 19. The average and design stress-strain curves from which the tabulated data were derived are presented in Appendix C, Figures C7 through C33 (Pages 247 to 271).

TABLE 18. SHEAR STRENGTH DATA, TASK I

TEST SPECIMEN IDENT	NO.*	THICK-NESS	TEST TEMP (°F)	STRAIN RATE (IN./IN. MIN)	FAILURE MODE	AVERAGE STRENGTH DATA						MATERIAL IDENTIFICATION - BEAM NUMBER OR TRANSPARENCY IDENTIFICATION
						ULTIMATE				SHEAR MOD (PSI)	STD DEV (PSI)	
						STRESS (PSI)	STD DEV (PSI)	STRAIN (IN./IN.)	STD DEV IN./IN)			
PPG529	5	0.06	75	0.03	BOND	328	57	0.881	0.288	594	164	Z5942626-505 BEAM
PPG531	6	0.12	75	0.07	SHEAR	2800	208	5.927	0.386	497	43	Z5942626-1 BEAM
PPG533	7	0.12	75	0.07	SHEAR	3694	712	5.390	0.291	677	99	Z5942639-505 WINDSHIELD
SK531	3	0.12	75	0.03	SHEAR	167	1	1.555	0.034	63	7	Z5942626-501 BEAM
SWU533/8	5	0.12	75	0.05	BOND	61	16	0.369	0.072	157	76	B-1 WINDSHIELD
SWU533/7	5	0.12	75	0.05	BOND	77	12	0.757	0.147	105	8	B-1 WINDSHIELD

* Number of specimens used in the generation of data presented.

TABLE 19. SHEAR STRENGTH DATA TASK II

TEST SPECIMEN		THICKNESS (IN.)	TEST TEMP (°F)	STRN RATE (IN/IN/MIN)	AVERAGE STRENGTH DATA						DESIGN ALLOWABLE			
						ULTIMATE							ULTIMATE	
IDENT	NO.*				FAILURE MODE	STRESS (PSI)	STD DEV (PSI)	STRAIN (IN/IN)	STD DEV (IN/IN)	SHEAR MOD (PSI)	STD DEV (PSI)	DES BAS	STRESS (PSI)	STRAIN IN/IN)	SHEAR MOD (PSI)
PPG531	5	.12	-30	0.07	BOND	3981	700	4.782	0.177	1116	75	B	1377	3.460	910
PPG531	6	.12	195	0.05	SHEAR	221	19	3.949	0.483	144	14	B	126	2.497	112
PPG533	6	.12	75	0.07	SHEAR	3694	712	5.390	0.291	677	99	B	1732	4.588	428
SK531	3	.12	75	0.03	SHEAR	167	1	1.555	0.034	63	7	B	143	1.344	23
SK531	5	.12	-30	0.03	SHEAR	315	54	3.349	0.193	59	14	C	187	2.935	32
SK531	6	.12	195	0.03	SHEAR	143	4	1.584	0.088	60	2	B	108	1.319	56
SK623	5	.12	75	0.03	BOND	1051	42	2.222	0.096	1244	134	B	924	1.896	856
SK623	6	.12	-30	0.07	BOND	1947	42	1.841	0.101	2564	217	B	1710	1.538	2063
SK623	5	.12	195	0.07	BOND	61	3	3.367	0.410	49	3	B	47	1.968	41
SK627	6	.03	76	0.03	BOND	1291	93	5.657	0.402	754	100	B	876	4.449	1012
SK531U	4	.12	85	0.03	BOND	132	37	0.578	0.174	367	130				
SWU531	6	.12	75	0.03	SHEAR	242	17	3.736	0.153	33	3	B	159	3.276	24
SWU531	7	.12	-30	0.03	SHEAR	320	14	2.891	0.165	57	9	B	275	2.437	33
SWU531	6	.12	195	0.03	SHEAR	170	13	1.439	0.115	70	9	B	61	1.093	58

* Number of specimens used in the generation of data presented.

Task III shear strength data are given in Table 20. The average stress-strain curves from which the tabulated data were derived are presented in Appendix C, Figures C34 through C36 (Pages 272 to 274).

Experimental test data and engineering stress-strain curves for test specimens are contained in Part 2, Appendix K.

ANALYSIS

In this analysis average shear stress-strain curves are plotted to show temperature effects on mechanical properties for four types of interlayer materials: plyurethane, two silicones and a co-polymer. Average shear stress-strain curves are superimposed for comparison between two types of silicones, a co-polymer, and a polyurethane interlayer material at three temperature conditions. Comparisons are made between two types of test methods, compressive shear testing and torsional shear testing.

Temperature Effects

A plot of average shear stress-strain curves for PPG Industries PPG-112 polyurethane interlayer material at three temperature conditions is presented in Figure 49. The plot illustrates the large loss in strength and elongation at 195°F and the small gain in strength with a small loss in elongation at -30°F when compared to the room temperature stress-strain curve.

A plot of average shear stress-strain curves for Sierracin S-130 co-polymer interlayer material at three temperatures is presented in Figure 50. The plot illustrates the loss in strength with gain in elongation at 195°F and a gain in strength with a loss in elongation at -30°F when compared to the room temperature stress-strain curve.

A plot of average shear stress-strain curves for Sierracin S100 silicone interlayer material at three temperatures is presented in

TABLE 20. SHEAR STRENGTH DATA, TASK III

TEST SPECIMEN IDENT.	NO.*	THICKNESS (IN)	TEST TEMP (°F)	STRAIN RATE (IN./IN./MIN)	FAILURE MODE	ULTIMATE STRESS (PSI)	STD DEV (PSI)	ULTIMATE STRAIN (IN/IN)	STD DEV (in./in.)	SHEAR MODULUS (PSI)	STD DEV (PSI)
SWU537	4	.12	75	.002	Shear	496	42	1.55	.06	131	34
PPG539	5	.12	75	.008	Bond	707	54	2.47	.62	443	127
SK535	4	.12	75	.002	Shear	244	16	1.80	.32	62	15

* Number of specimens used in the generation of data presented.

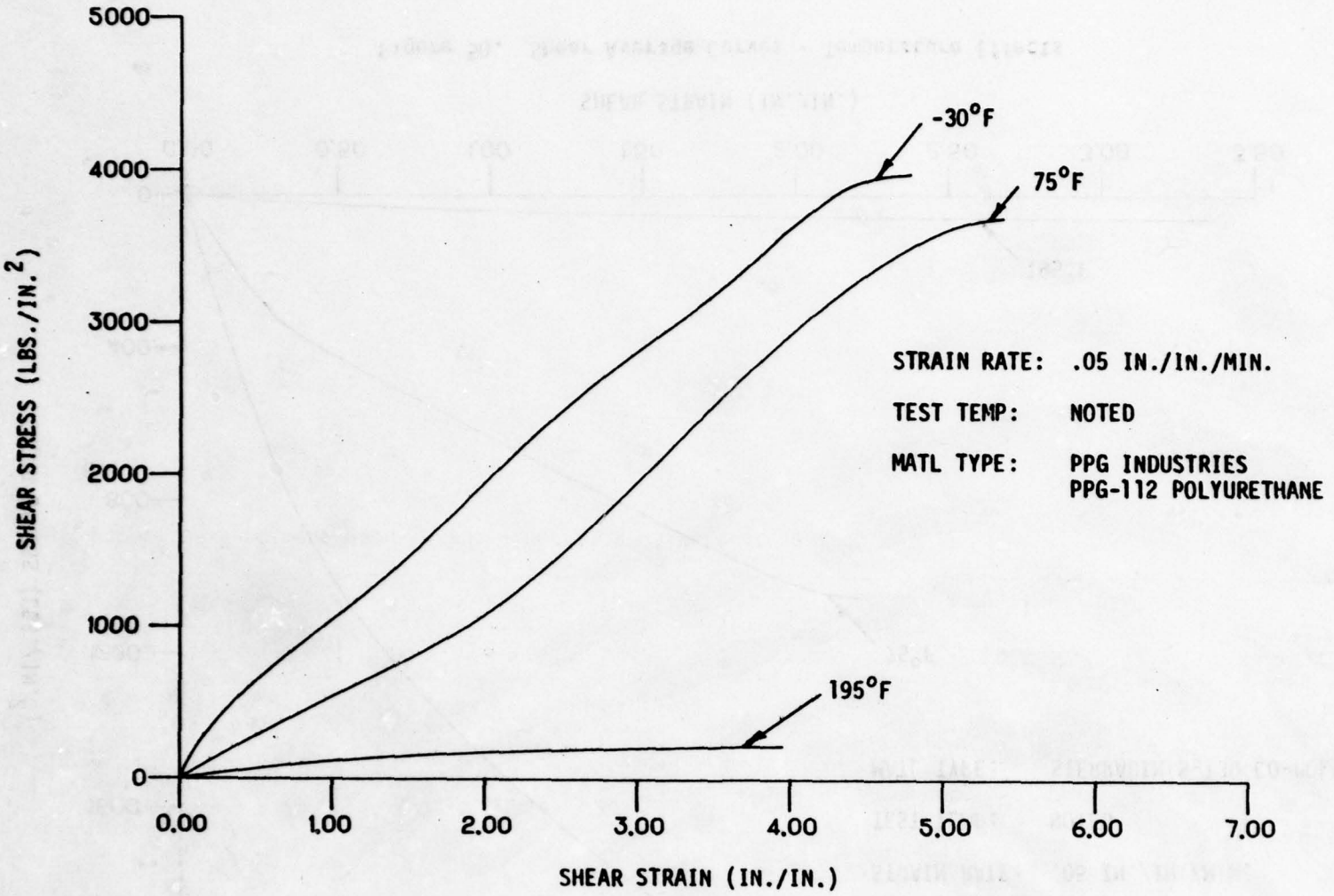

Figure 49. Shear Average Curves - Temperature Effects

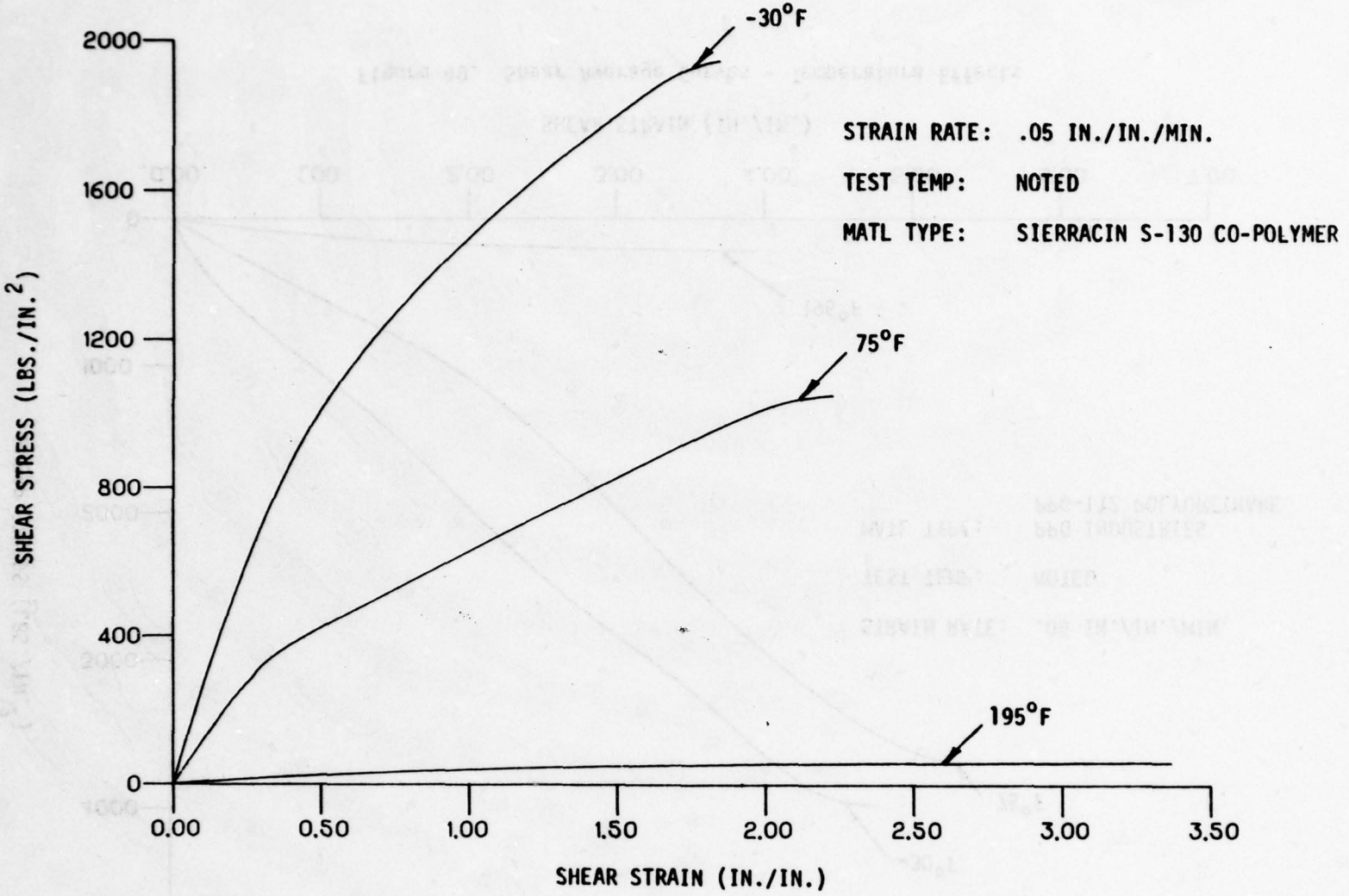

Figure 50. Shear Average Curves - Temperature Effects

Figure 51. The plot illustrates the gain in strength with loss in elongation at -30°F and the loss in strength with loss in elongation at 195°F when compared to the room temperature stress-strain curve.

A plot of average shear stress-strain curves for Swedlow SS 5272Y (HT) silicone interlayer material at three temperatures is presented in Figure 52. The plot illustrates the gain in strength with loss in elongation at -30°F and the loss in strength with loss in elongation at 195°F when compared to the room temperature stress-strain curve.

Material Comparisons

A plot of average shear stress-strain curves at 75°F for four types of interlayer materials is presented in Figure 53. The plot illustrates the increased shear strength and elongation capabilities of polyurethane material and increased strength of the co-polymer over the silicone materials at room temperature conditions. The plot also illustrates the differences in elongation capabilities of two types of silicones at room temperature conditions.

A plot of average shear stress-strain curves at -30°F test condition for four types of interlayer materials is presented in Figure 54. The plot illustrates the increased shear strength and elongation capabilities of polyurethane and increased shear strength of the co-polymer over the silicone materials at -30°F.

A plot of average shear stress-strain curves at 195°F test condition for the four types of interlayer materials is presented in Figure 55. The plot illustrates the increased shear strength and elongation capabilities of polyurethane and the decreased shear strength of the co-polymer material as compared to silicone at 195°F.

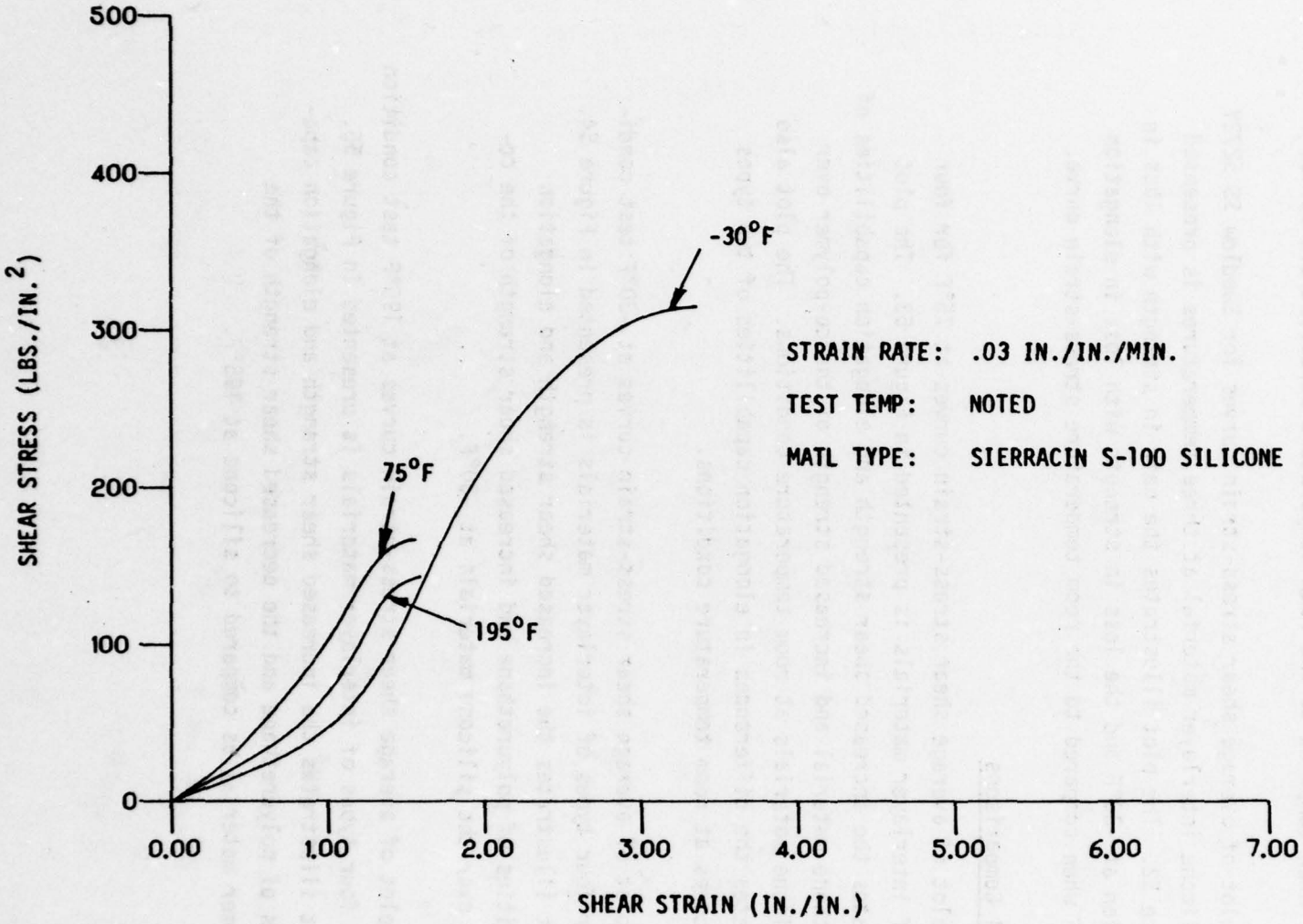

Figure 51. Shear Average Curves - Temperature Effects

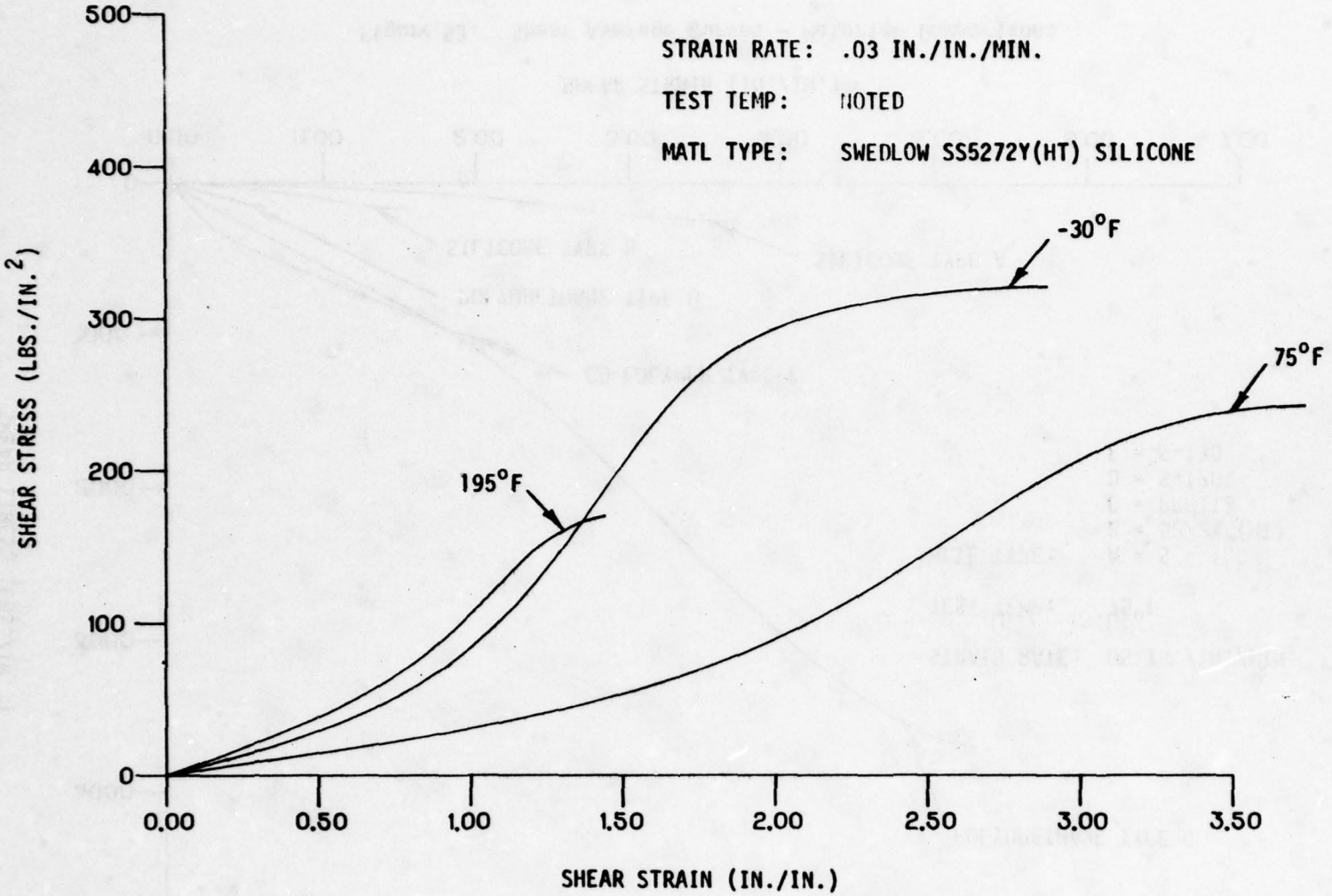

Figure 52. Shear Average Curves - Temperature Effects

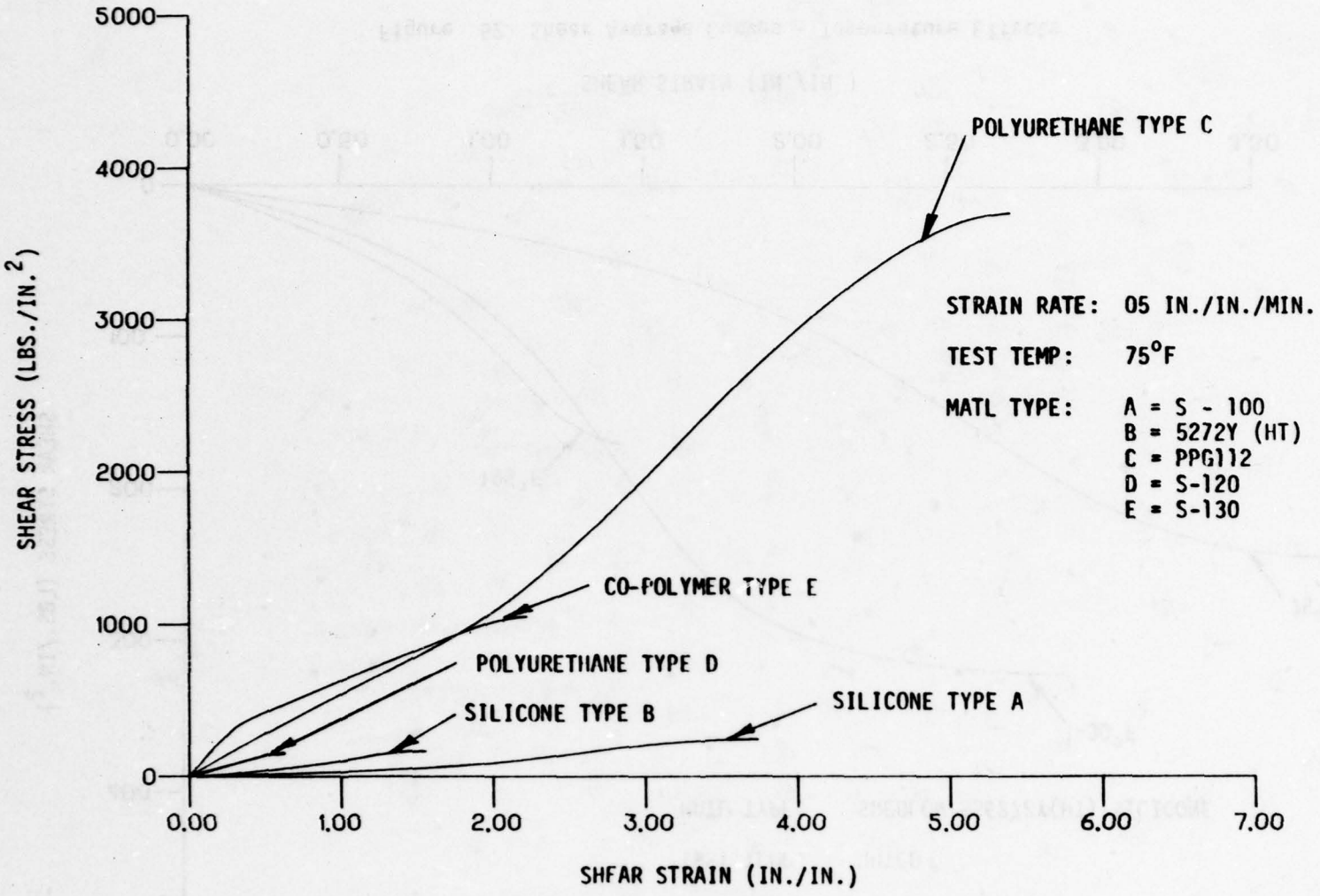

Figure 53. Shear Average Curves - Material Comparisons

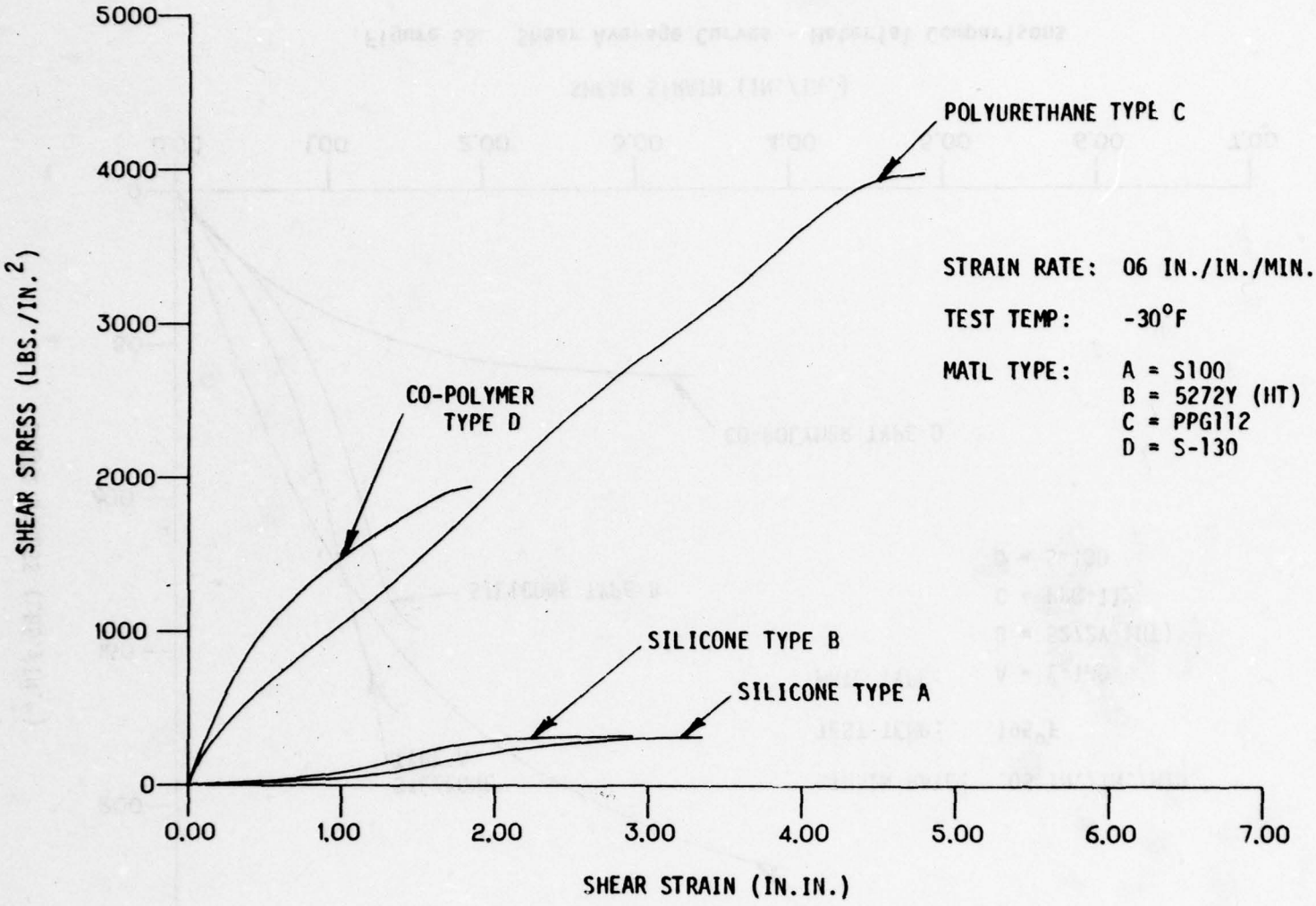

Figure 54. Shear Average Curves - Material Comparisons

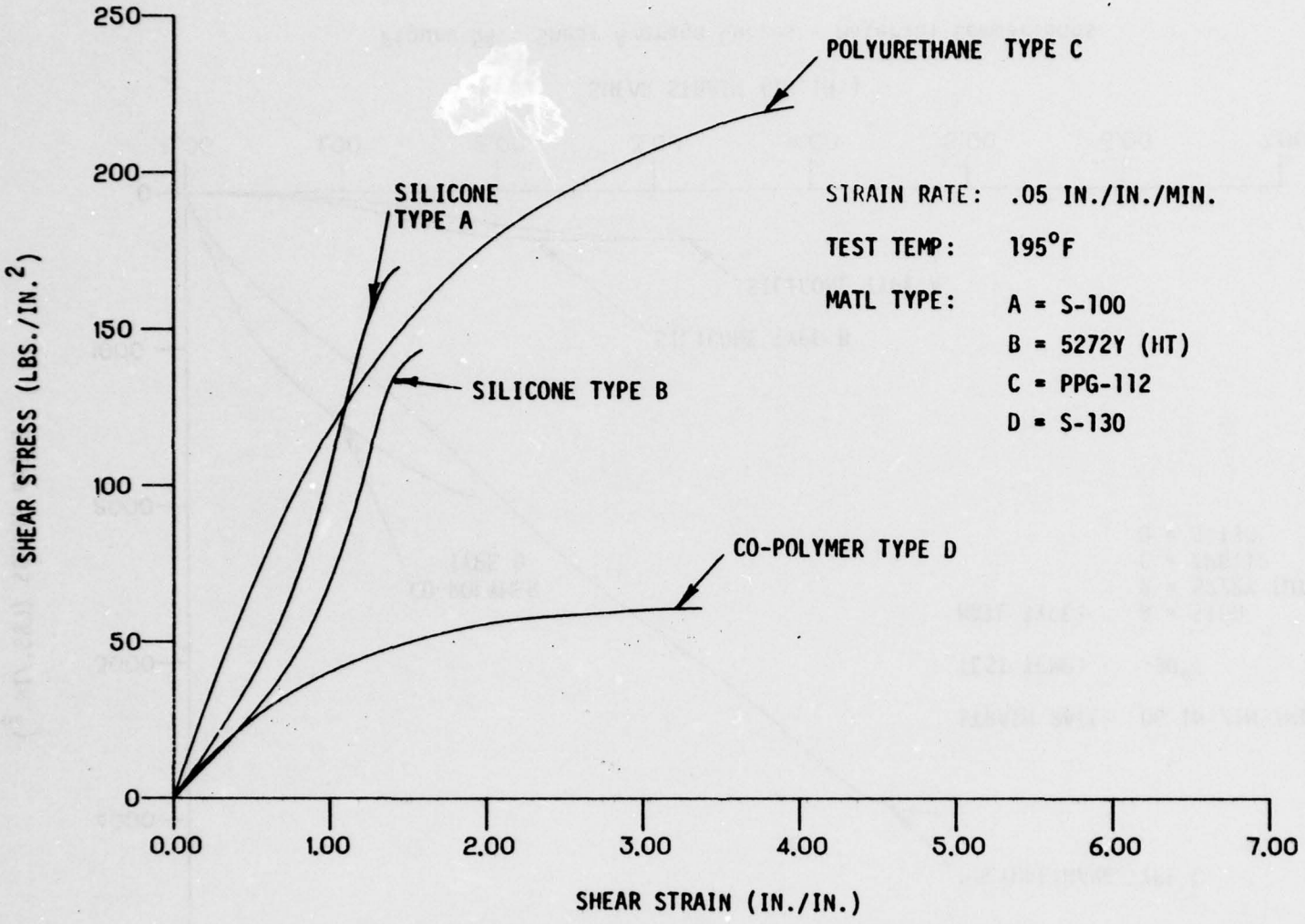

Figure 55. Shear Average Curves - Material Comparisons

Test Method Comparisons

Comparison of test results between two test methods, compressive shear and torsion shear, are presented for two types of silicone interlayer materials in Figure 56. It can be seen that there was close correlation of test results for type B material and a large variation in test results for type A material. The shear modulus for the type B material torsional test is illogically high for silicone material under these test conditions. Torsional test curves were erratic and standard deviation large for these tests resulting in illogical design curves. This was due to a sideways displacement of the upper test adapter tube during test. For these reasons the torsional shear test method was discarded.

CONCLUSIONS

Conclusions based on data contained in this section and other applicable data are contained in Section XI of this report.

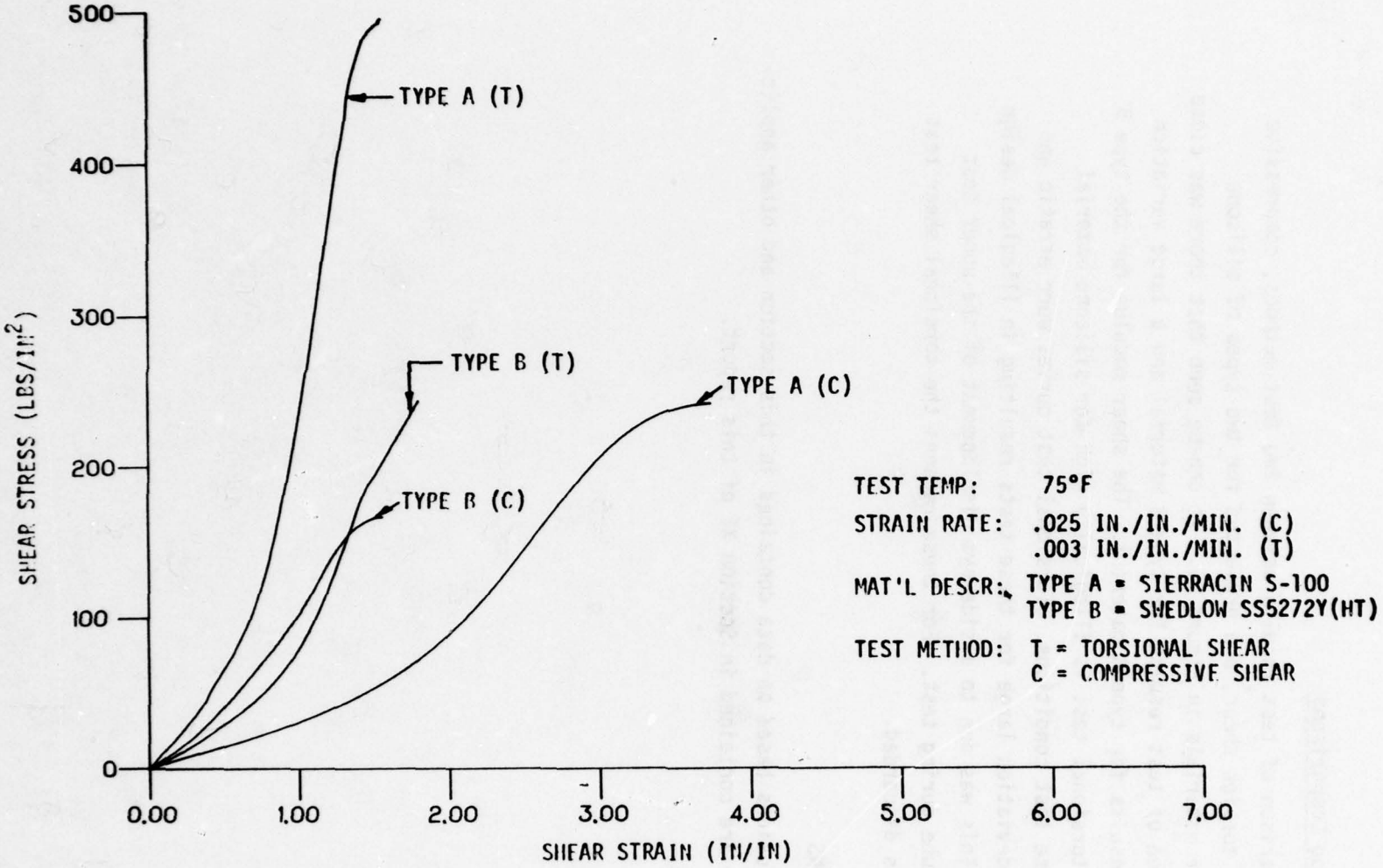

Figure 56. Shear Average Curves - Test Methods Comparison.

APPENDIX C

SHEAR STRESS-STRAIN CURVE DATA

The following stress-strain data are presented for use in conjunction with tabulated strength data presented in the following listed tables of this section.

PAGES

Table 18 (Page 225)

Shear stress-strain curves - Figures C1 through C6 . . . . 241 - 246

Figure 19 (Page 226)

Shear stress-strain curves - Figures C7 through C33 . . . 247 - 271

Figure 20 (Page 228)

Shear stress-strain curves - Figures C34 through C36 . . . 272 - 274

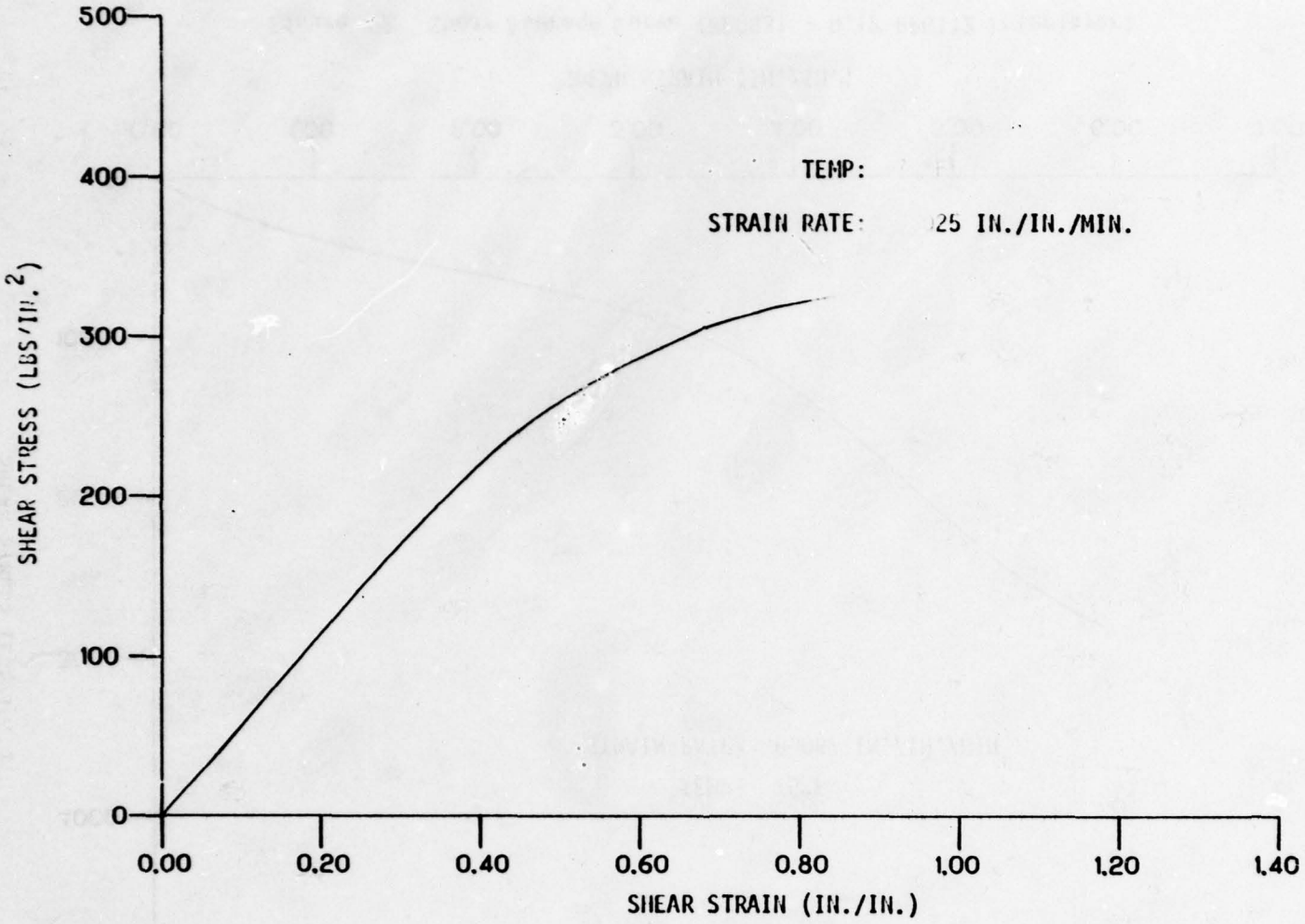

Figure C1. Shear Average Curve (PPG529 - 0.06 PPG112 Interlayer)

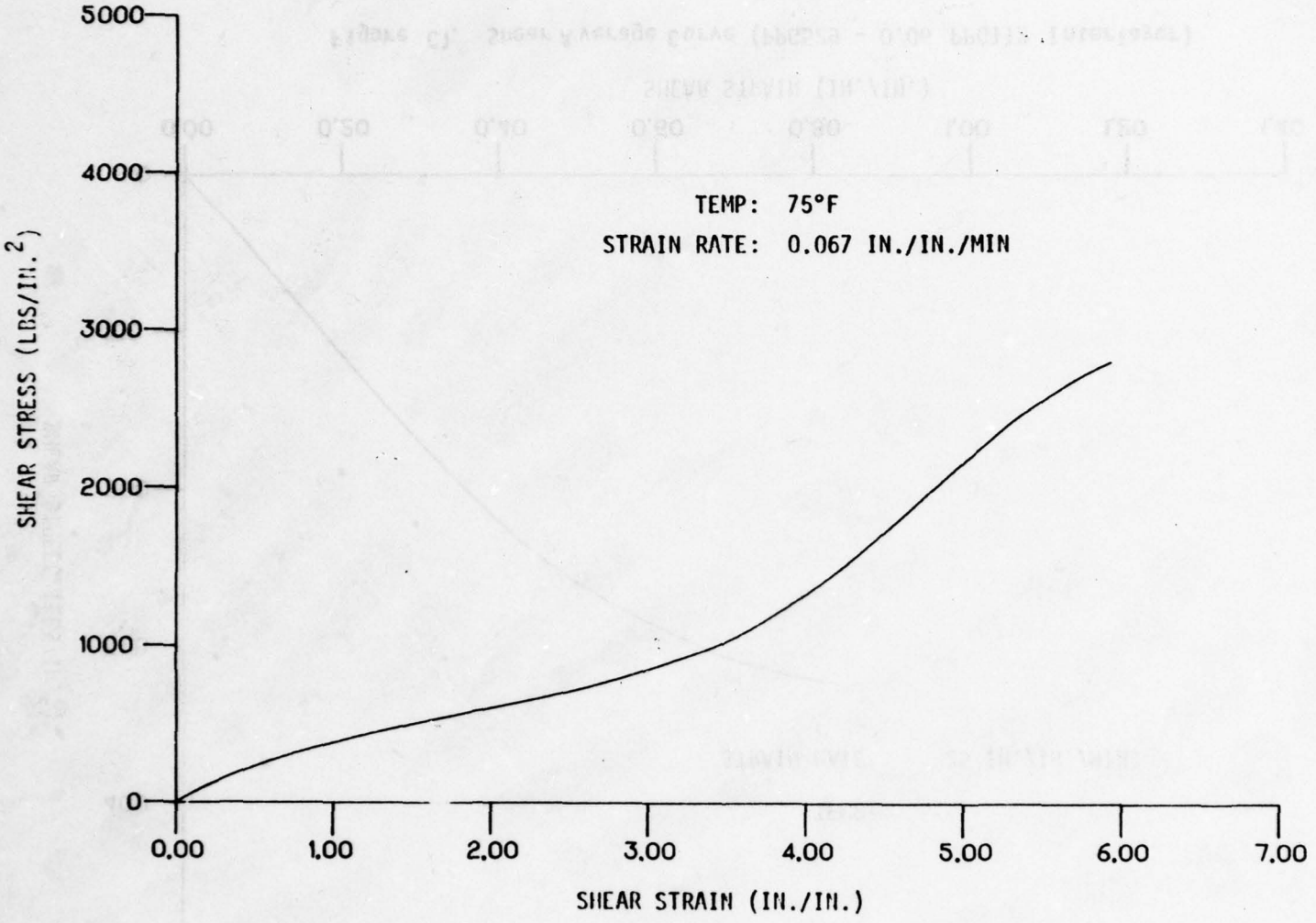

Figure C2. Shear Average Curve (PPG531 - 0.12 PPG112 Interlayer).

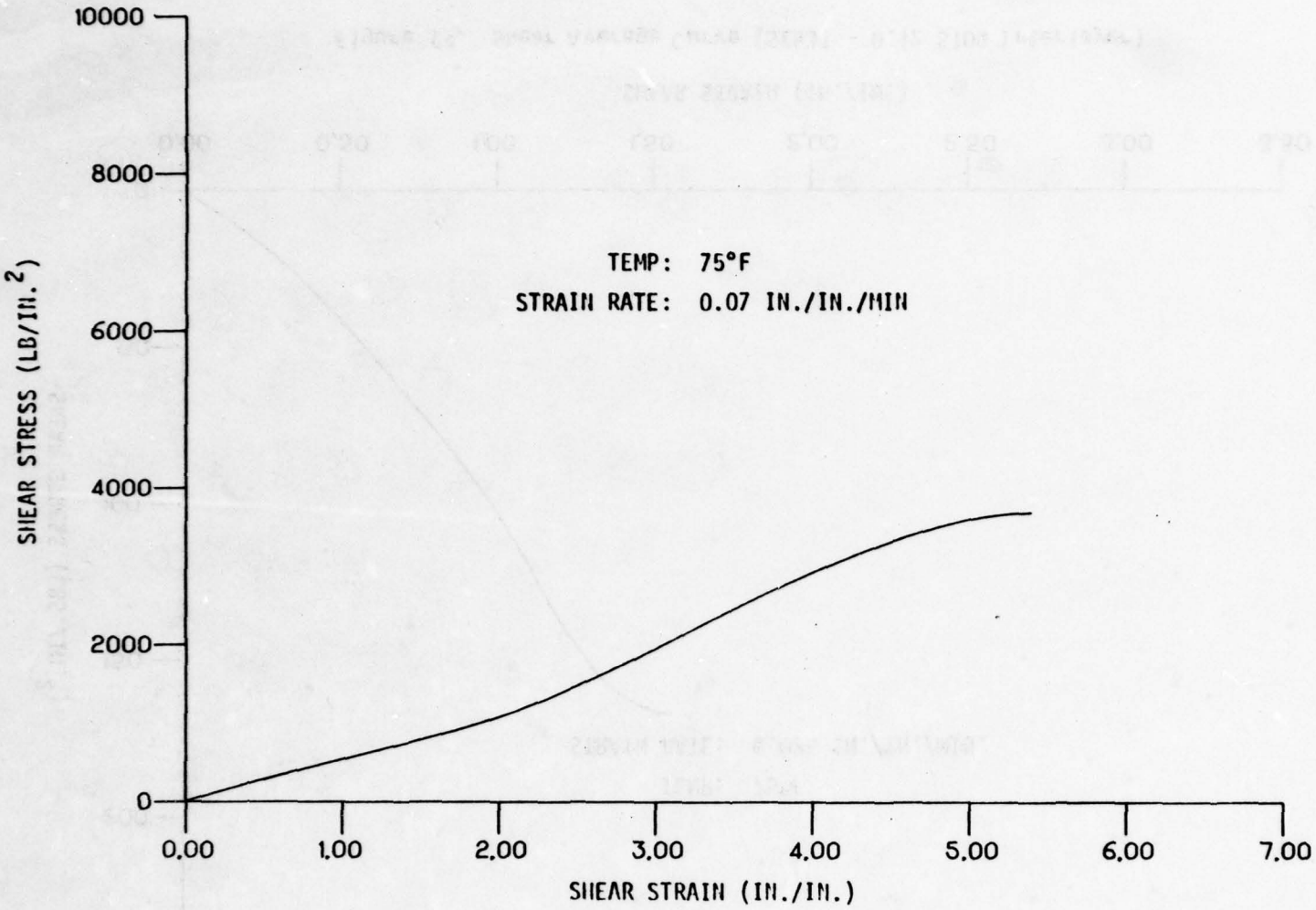

Figure C3. Shear Average Curve (PPG533 - 0.12 PPG112 Interlayer).

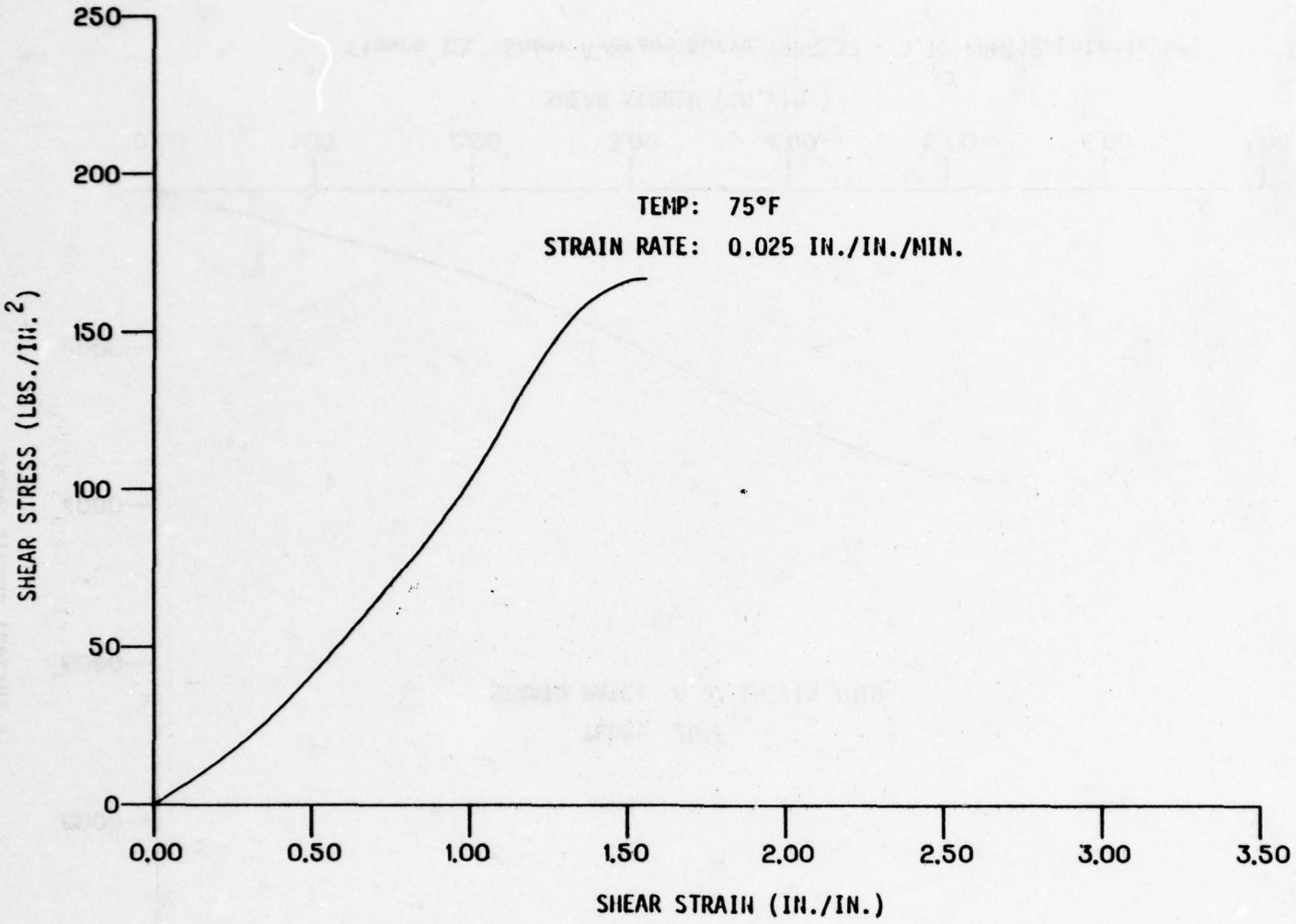

Figure C4. Shear Average Curve (SK531 - 0.12 S100 Interlayer)

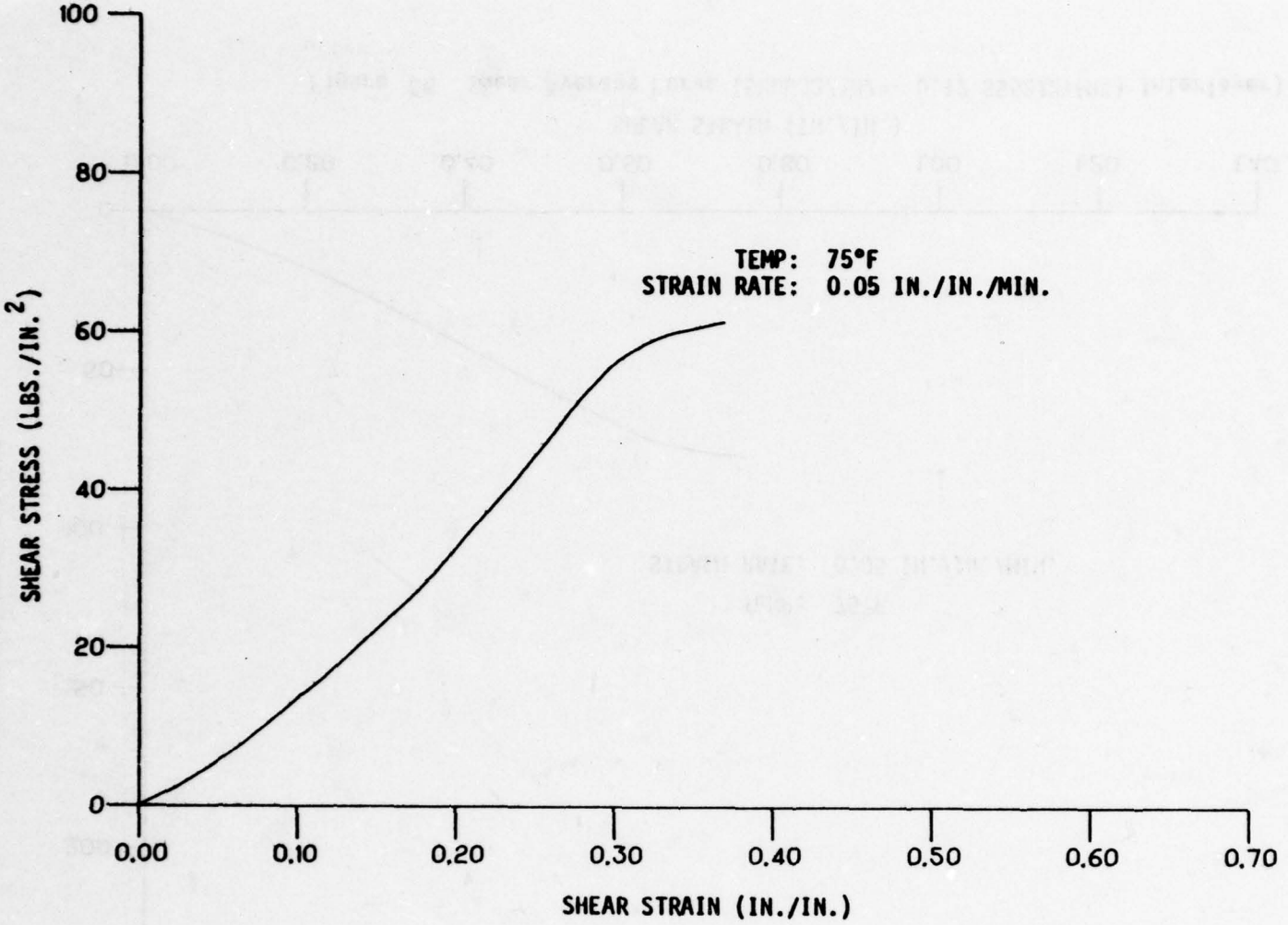

Figure C5. Shear Average Curve (SWU533/108 - 0.12 SS5272Y(HT) - Interlayer).

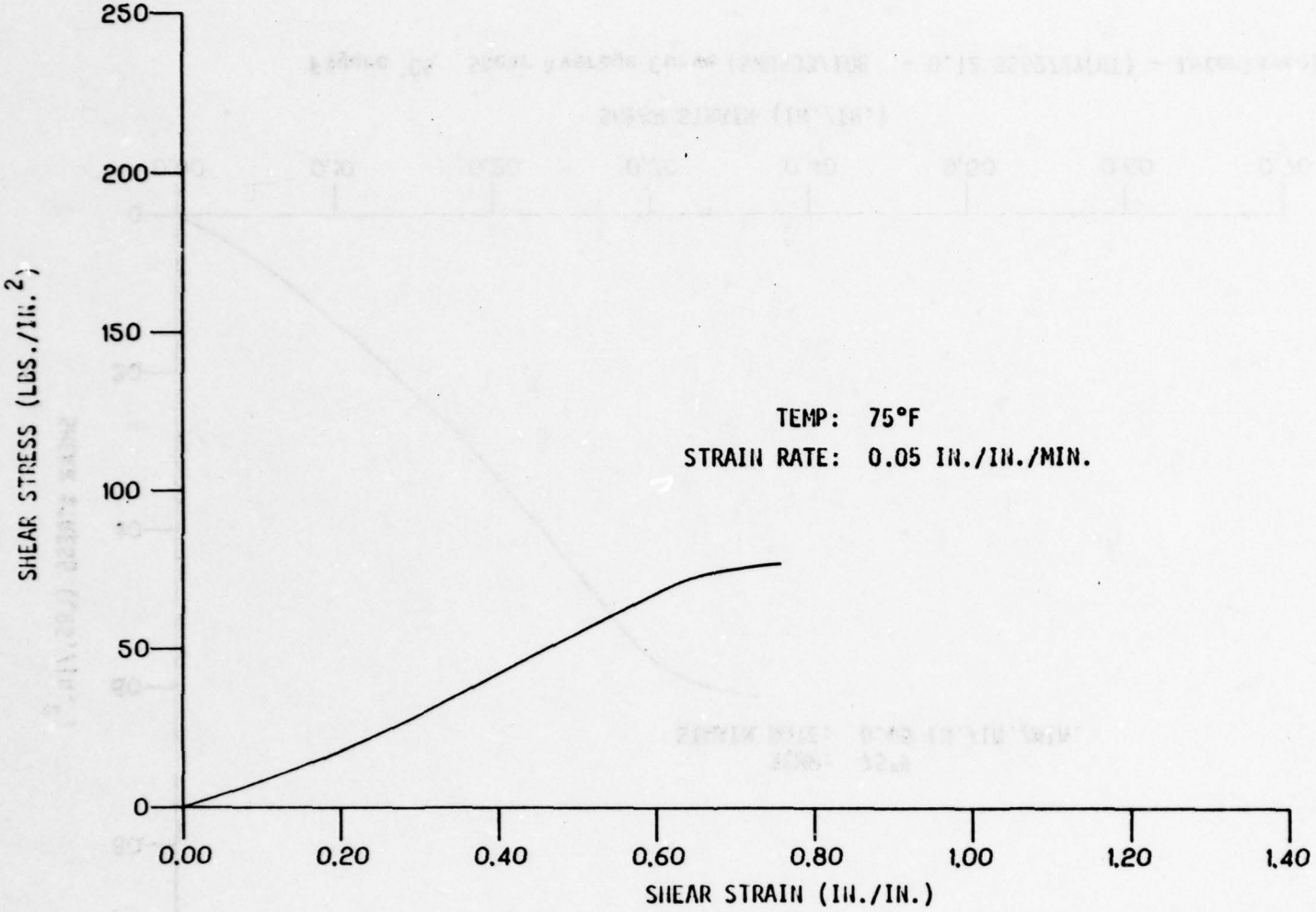

Figure C6 Shear Average Curve (SWU533/107 - 0.12 SS5272Y(HT) Interlayer).

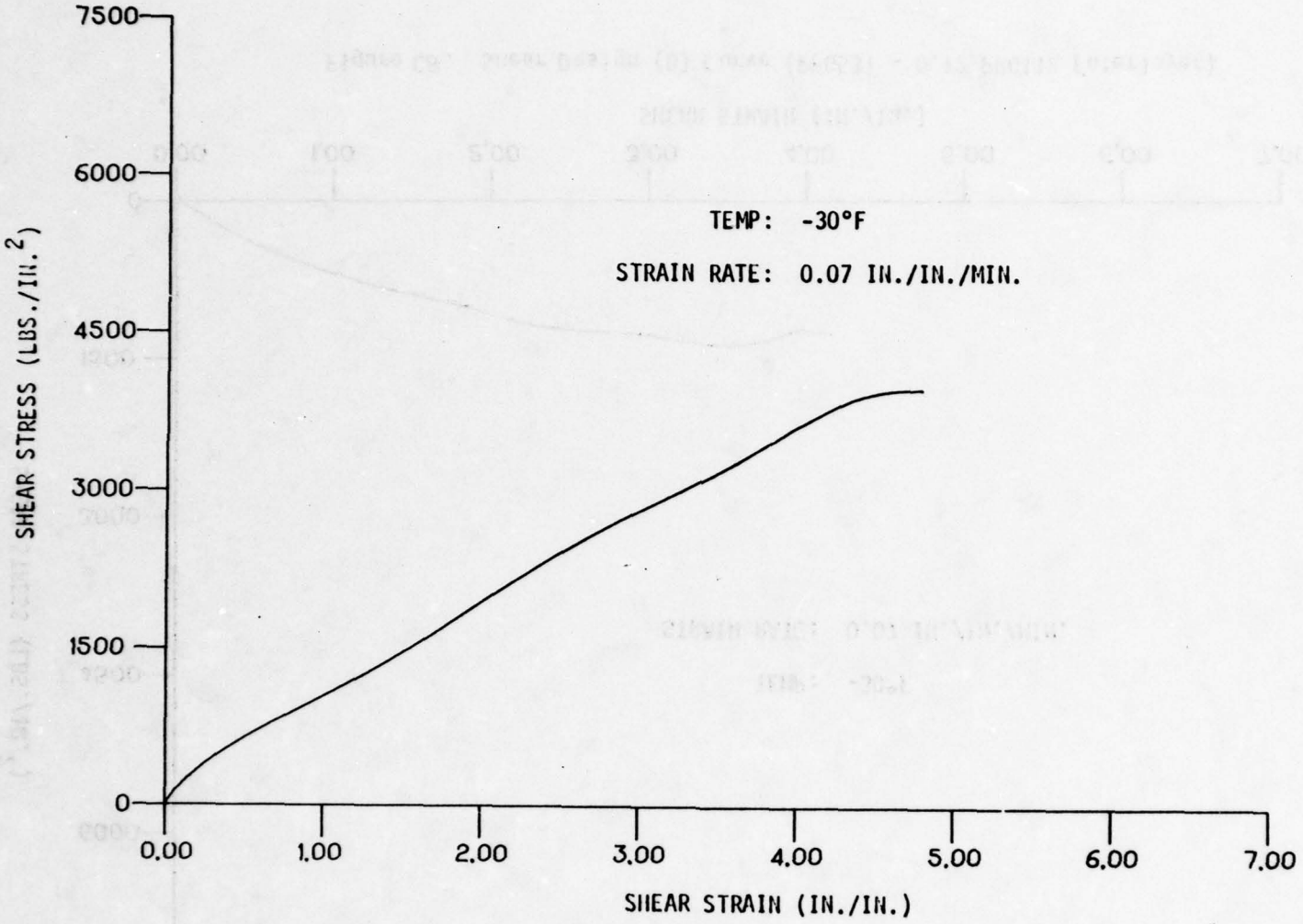

Figure C7. Shear Average Curve (PPG531 - 0.12 PPG112 Interlayer)

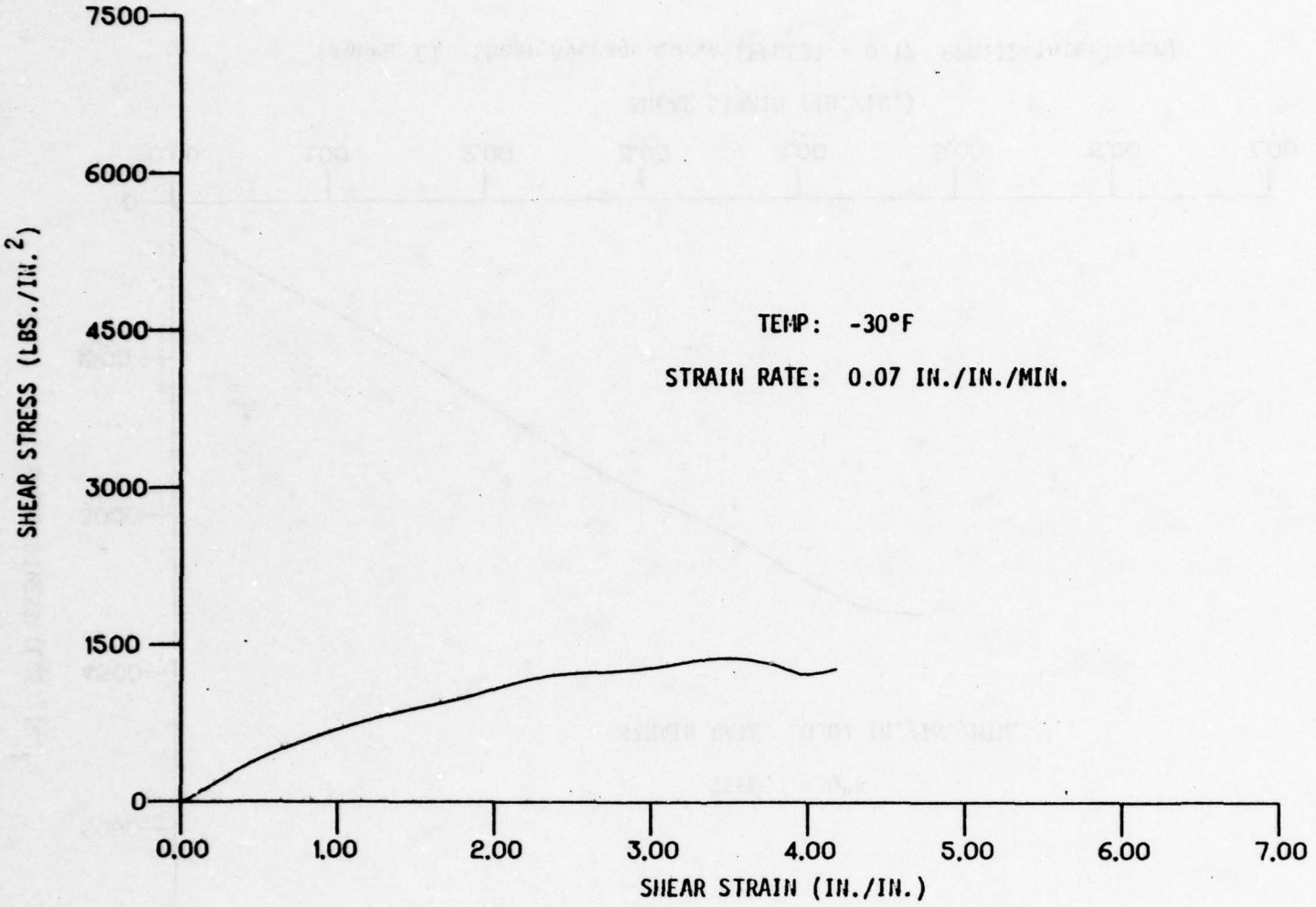

Figure C8. Shear Design (B) Curve (PPG531 - 0.12 PPG112 Interlayer)

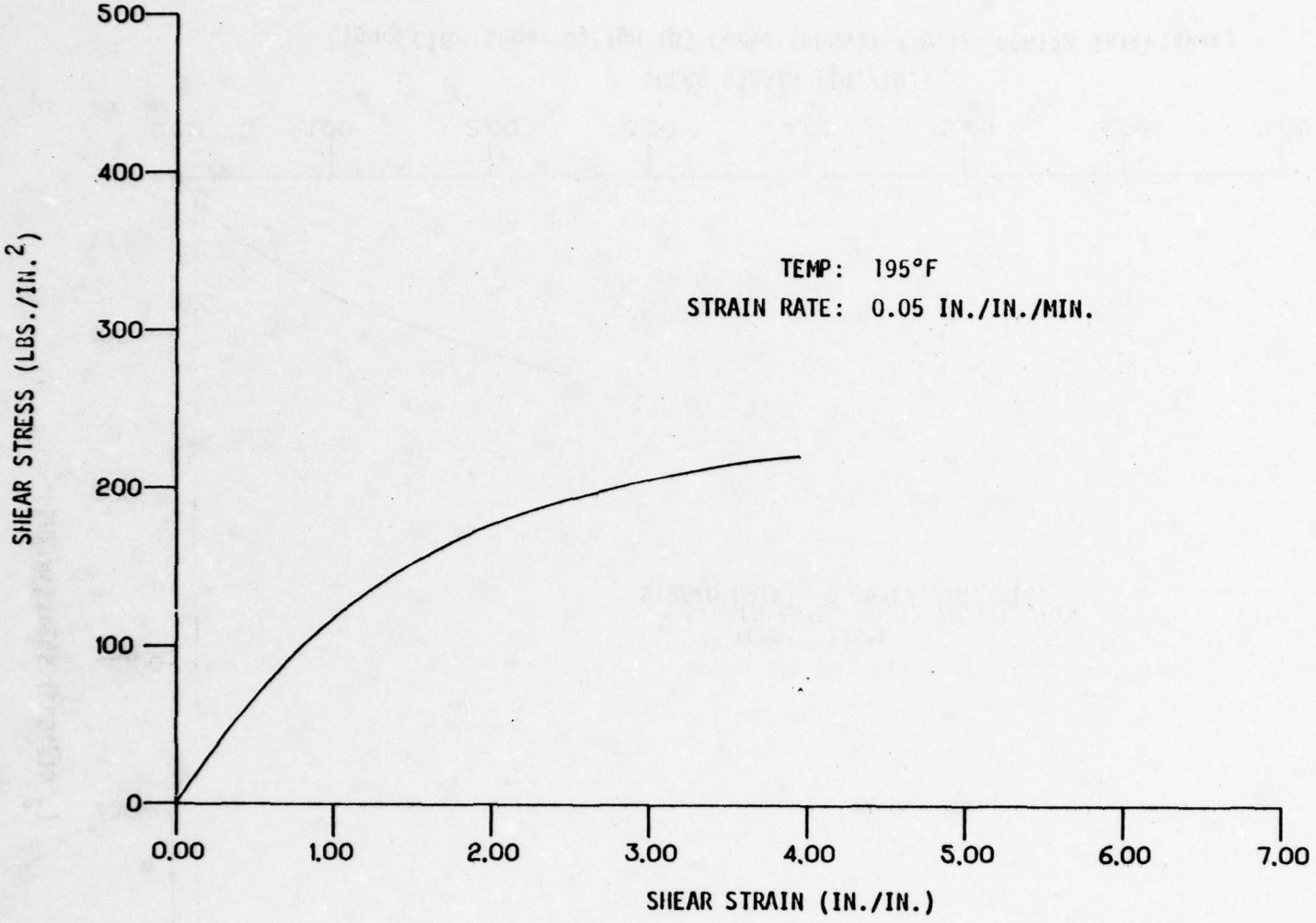

Figure C9. Shear Average Curve (PPG531 - 0.12 PPG112 Interlayer)

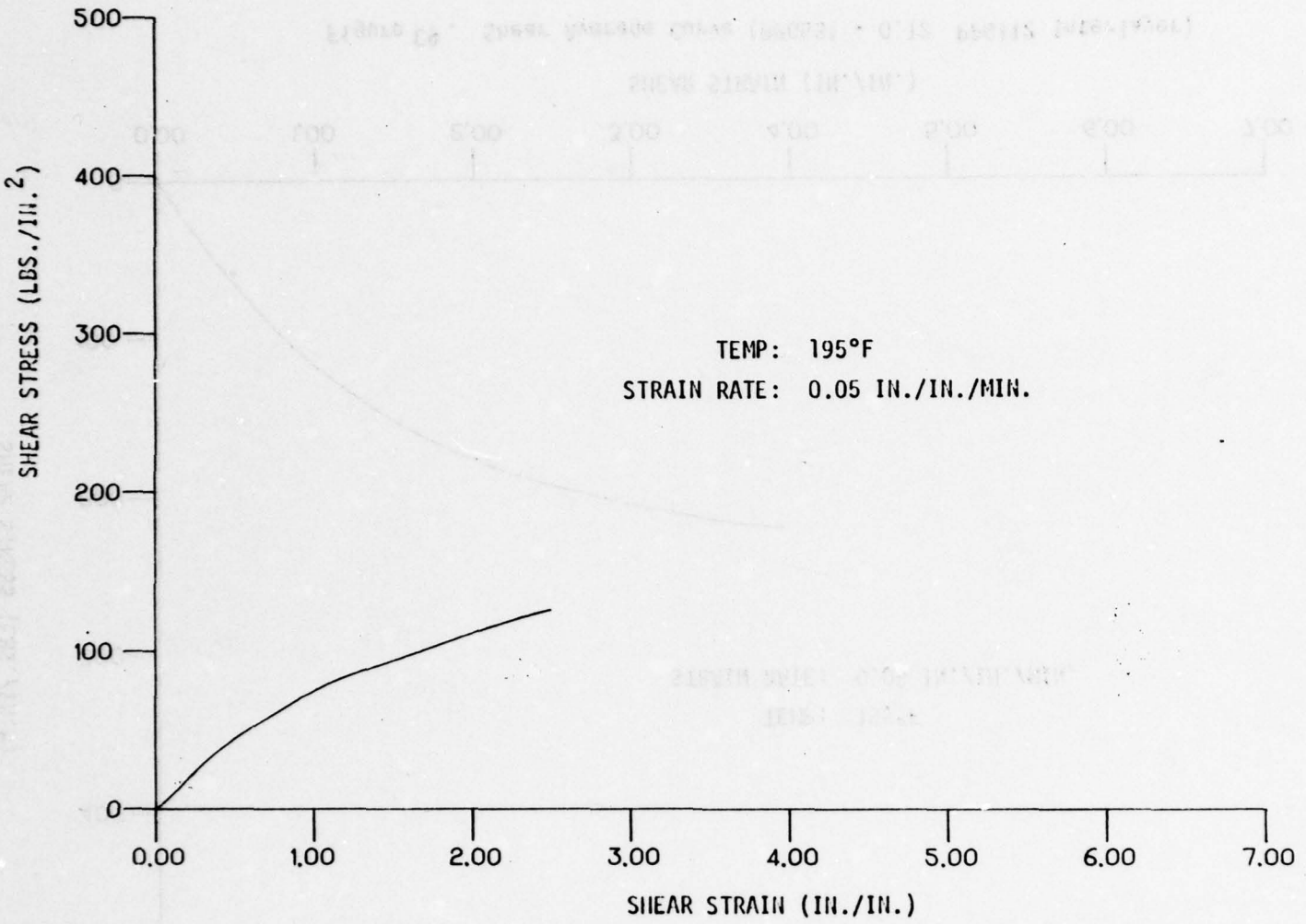

Figure C10 Shear Design (B) Curve (PPG531 - 0.12 PPG112 Interlayer)

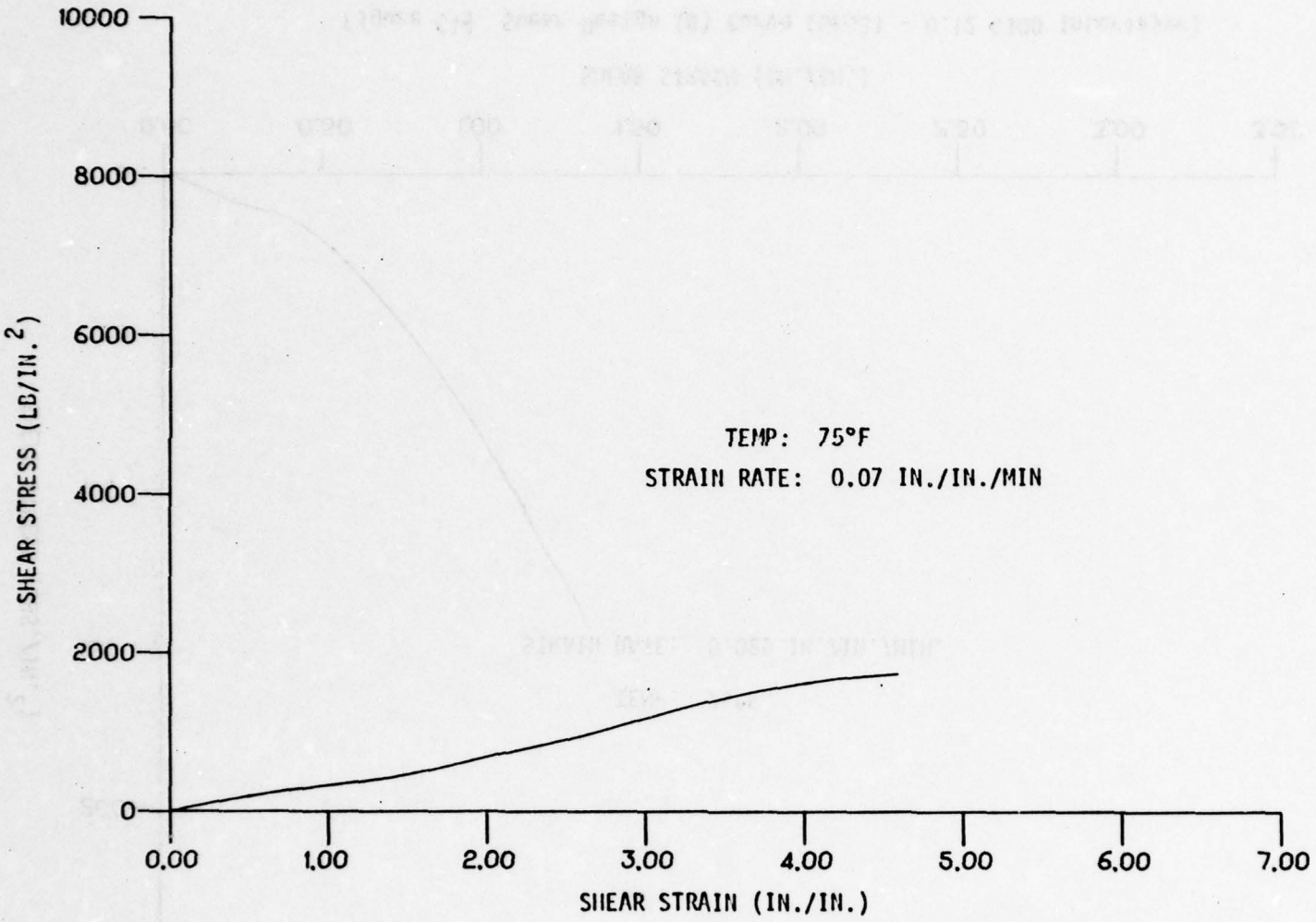

Figure C13 Shear Design (B) Curve (PPG533 - 0.12 PPG112 Interlayer)

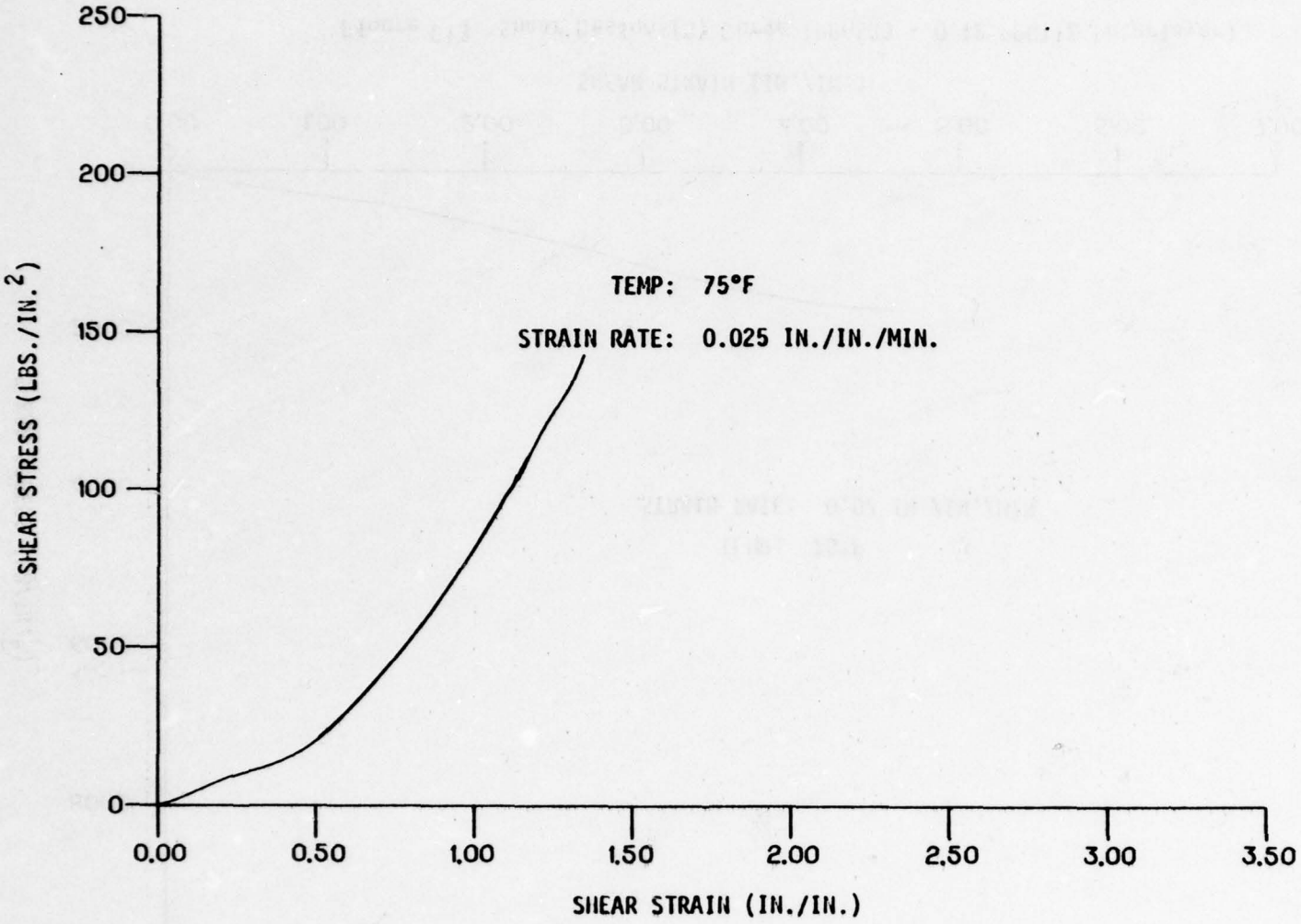

Figure C14 Shear Design (B) Curve (SK531 - 0.12 S100 Interlayer)

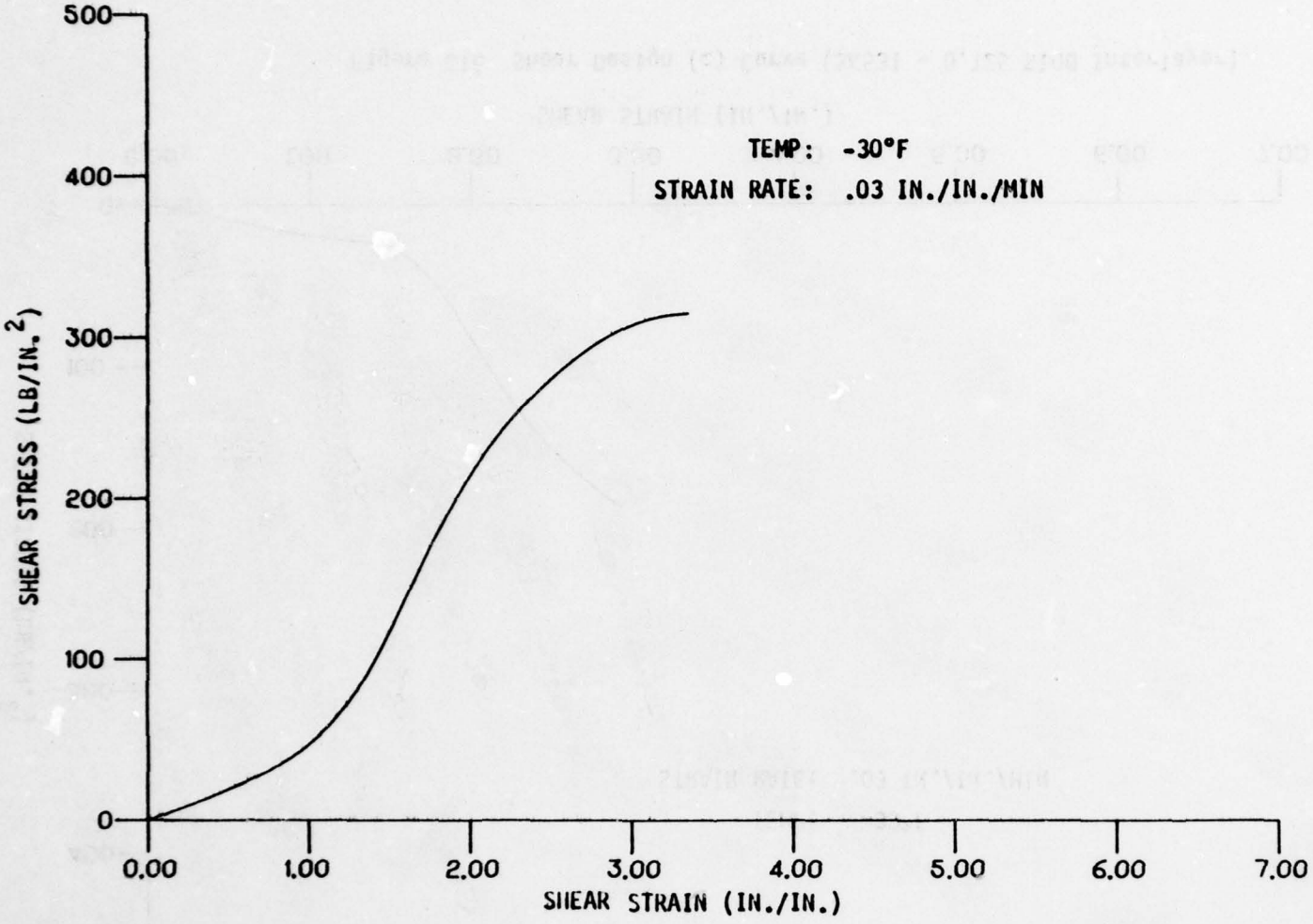

Figure C15. Shear Average Curve (SK531 - 0.125 S100 Interlayer).

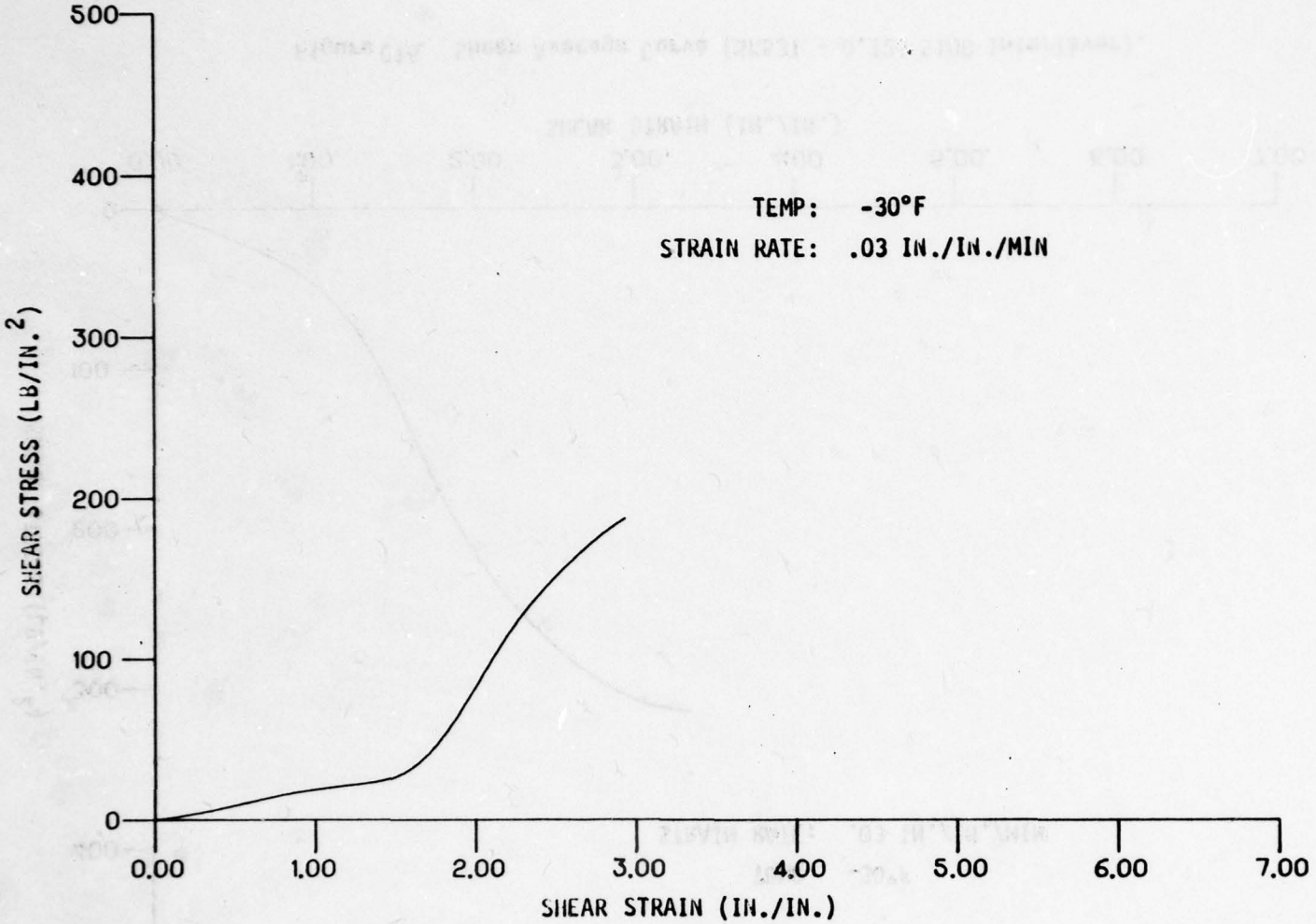

Figure C16 Shear Design (c) Curve (SK531 - 0.125 S100 Interlayer).

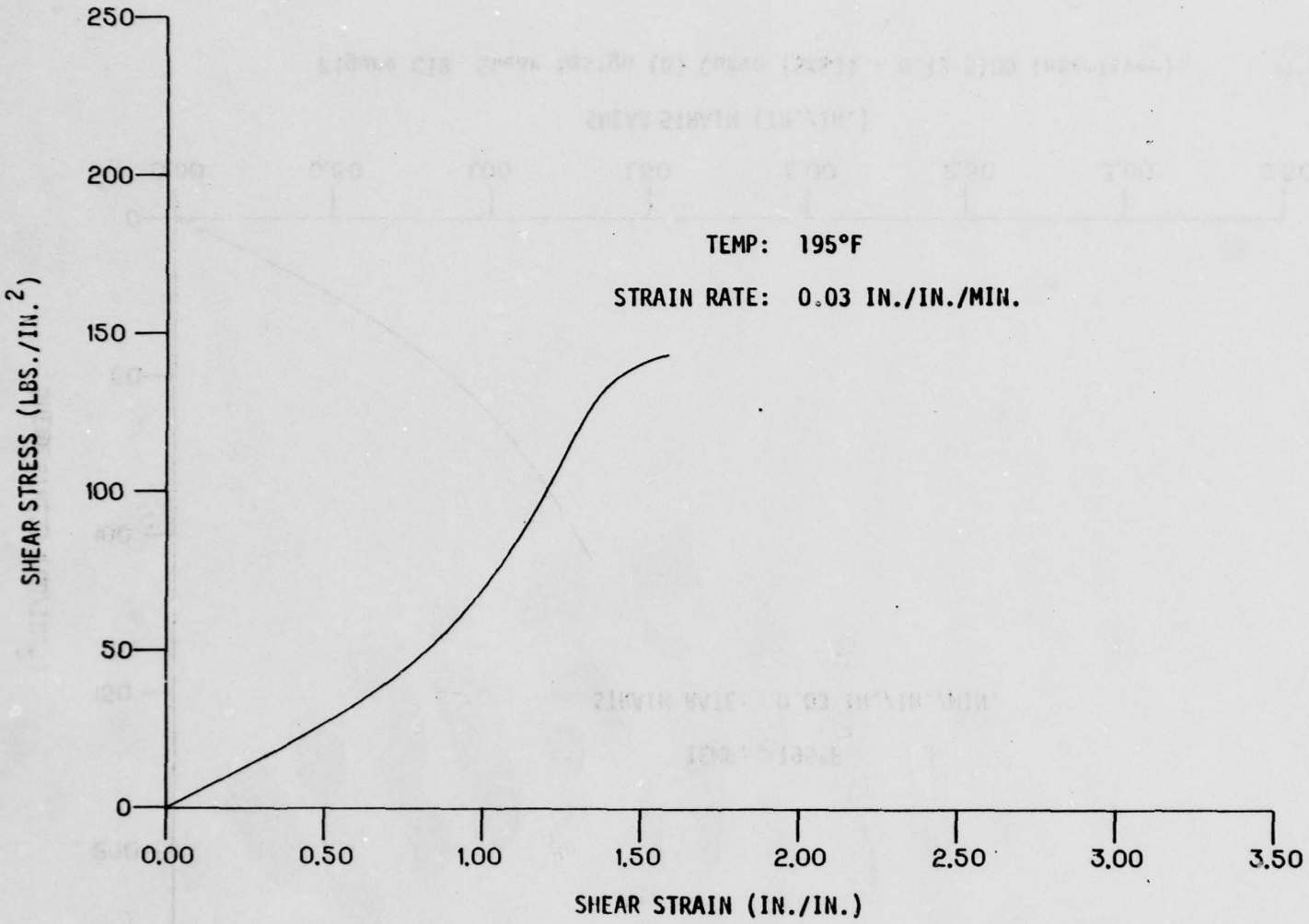

Figure C17 Shear Average Curve (SK531 - 0.12 S100 Interlayer).

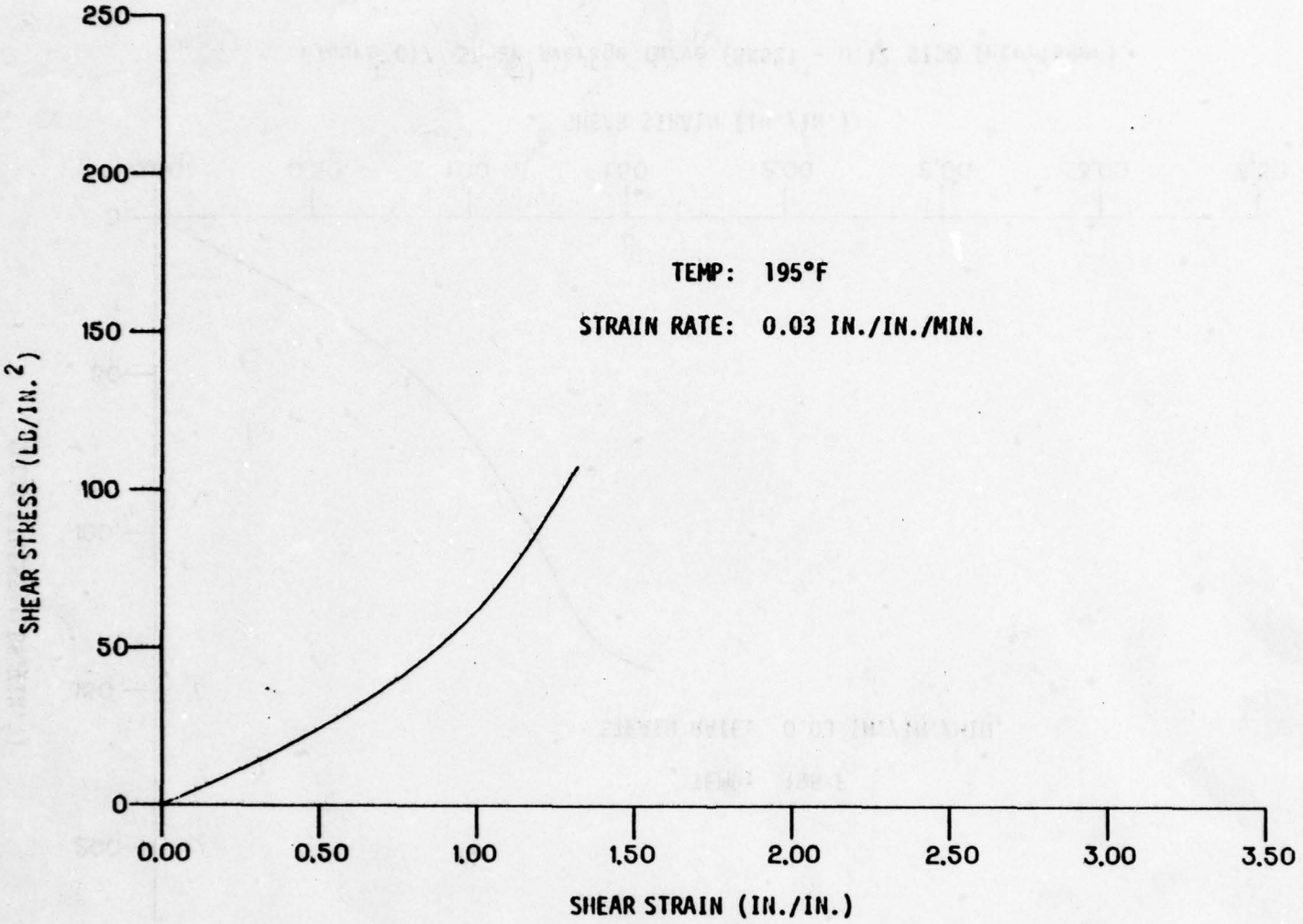

Figure C18 Shear Design (B) Curve (SK531 - 0.12 S100 Interlayer).

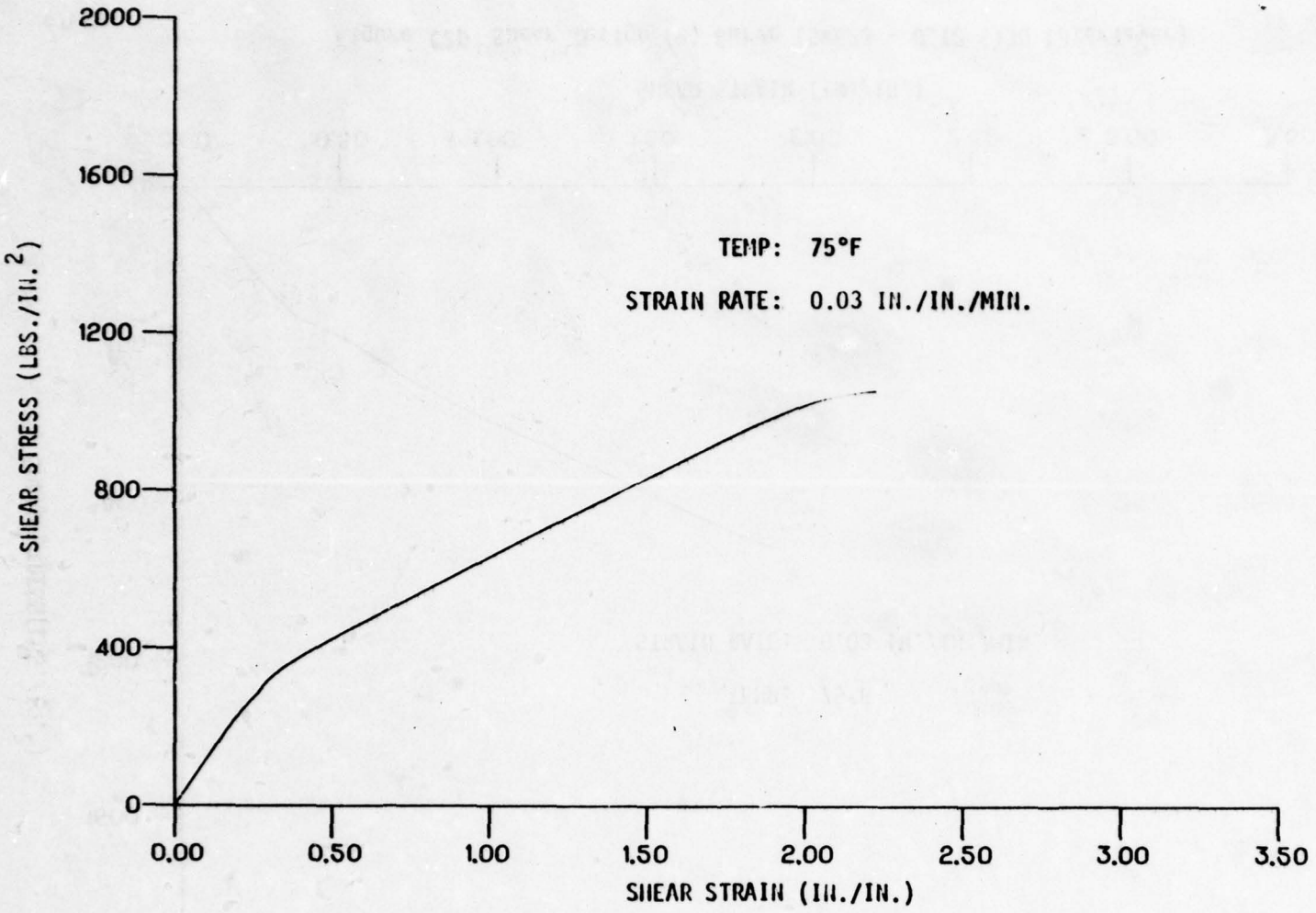

Figure C19 Shear Average Curve (SK623 - 0.12 S130 Interlayer)

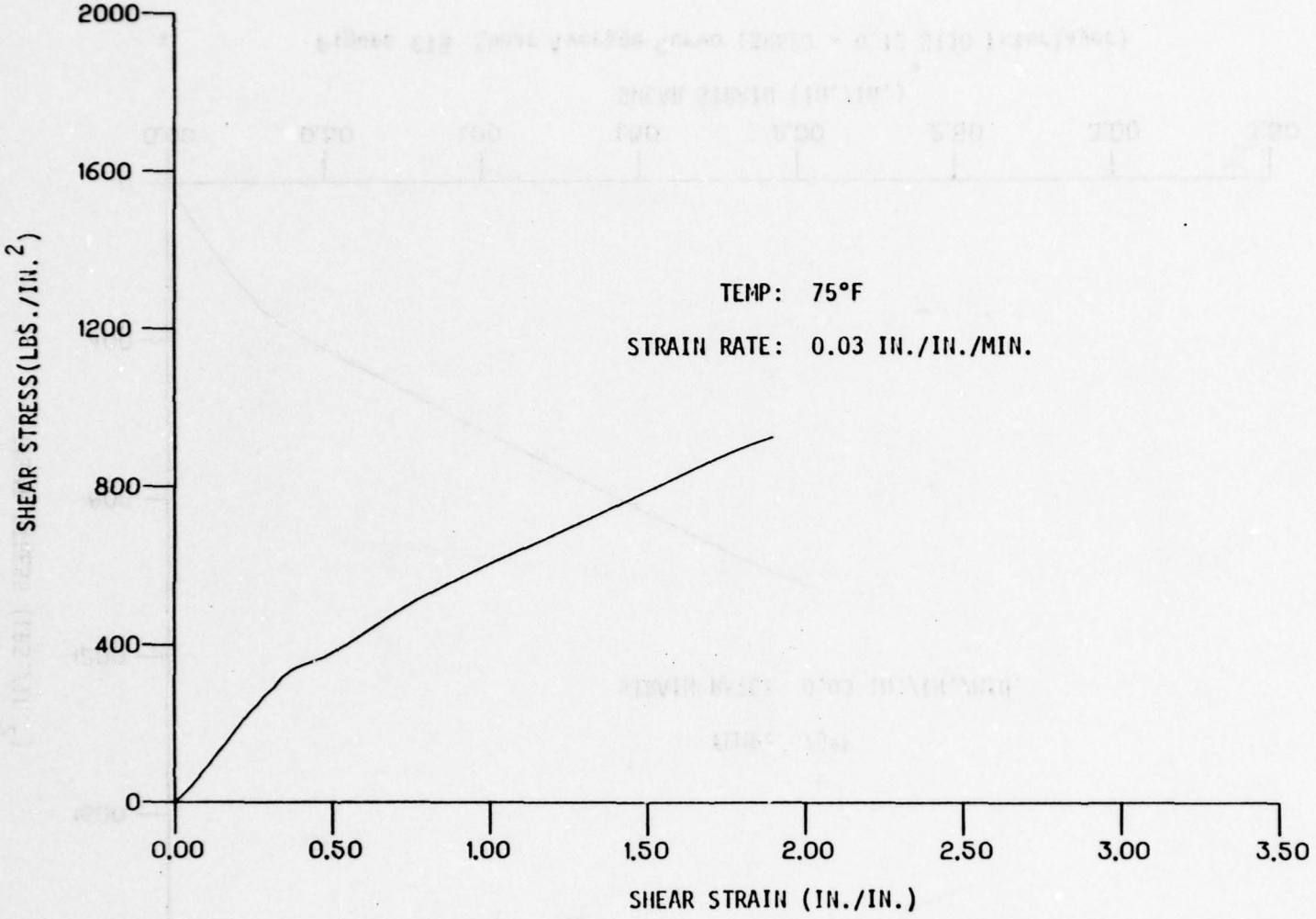

Figure C2D Shear Design (B) Curve (SK623 - 0.12 S130 Interlayer)

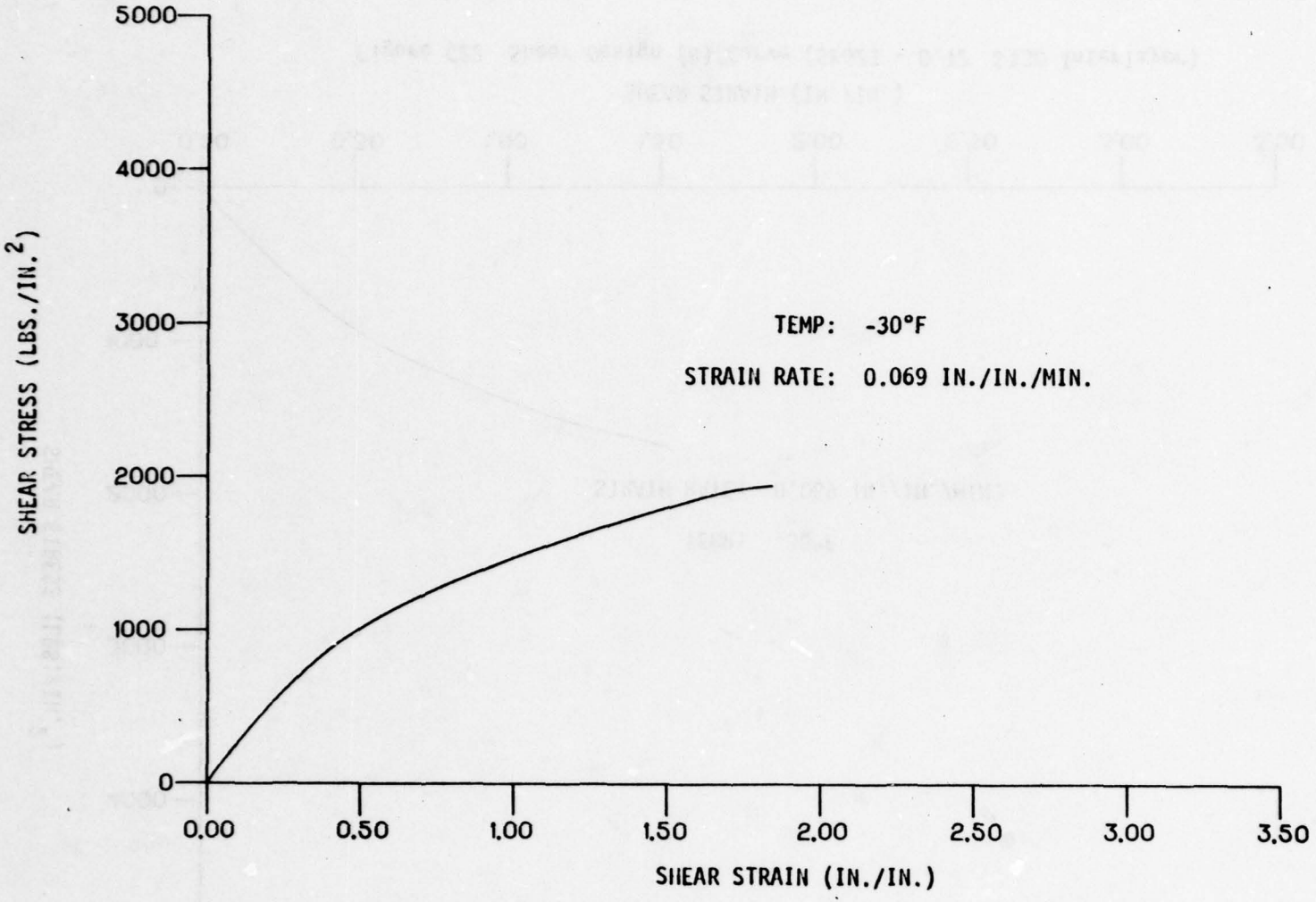

Figure C21 Shear Average Curve (SK623 - 0.12 S130 Interlayer)

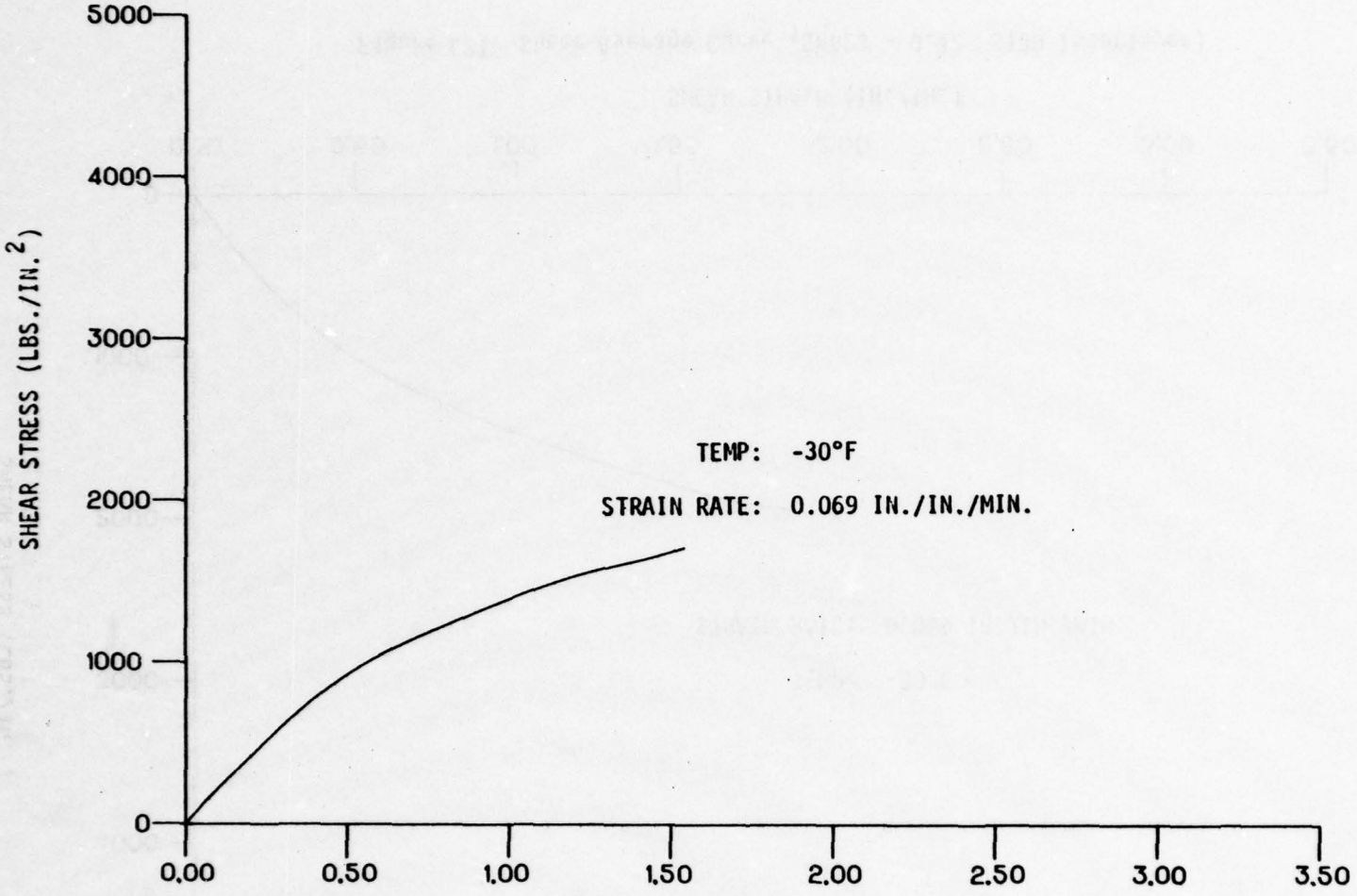

Figure C22 Shear Design (B) Curve (SK623 - 0.12 S130 Interlayer)

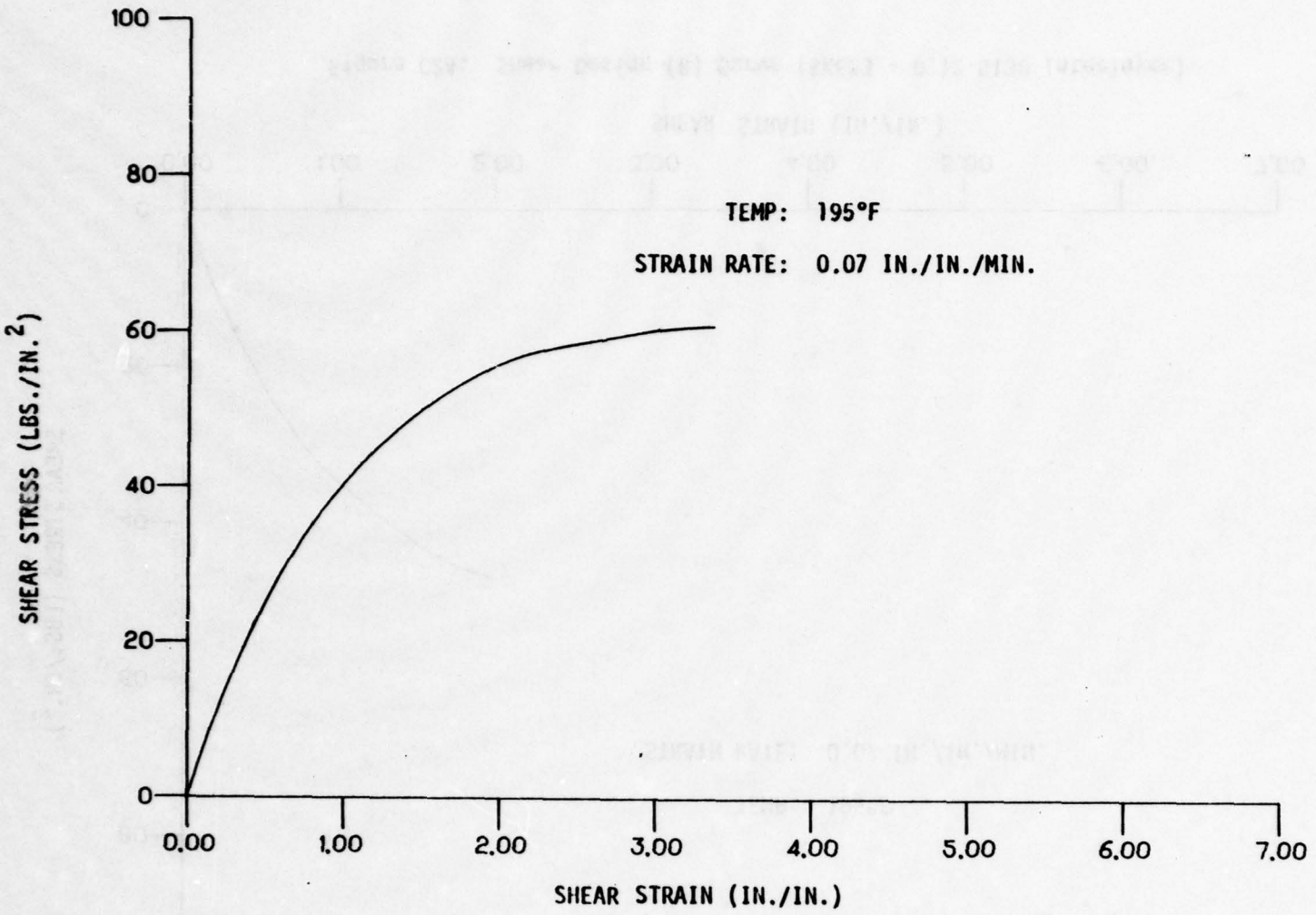

Figure C23 Shear Average Curve (SK623 - 0.12 S130 Interlayer).

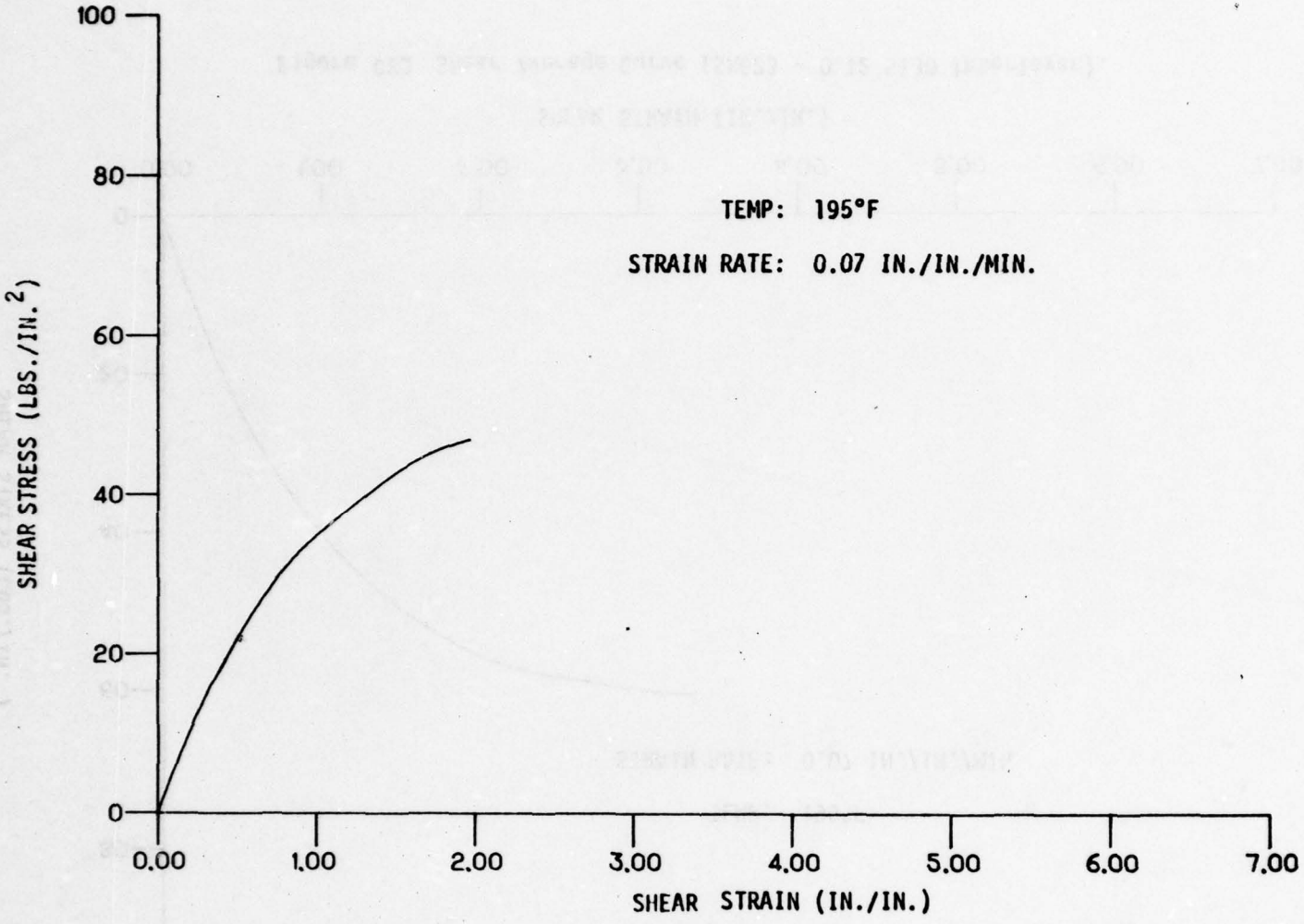

Figure C24. Shear Design (B) Curve (SK623 - 0.12 S130 Interlayer).

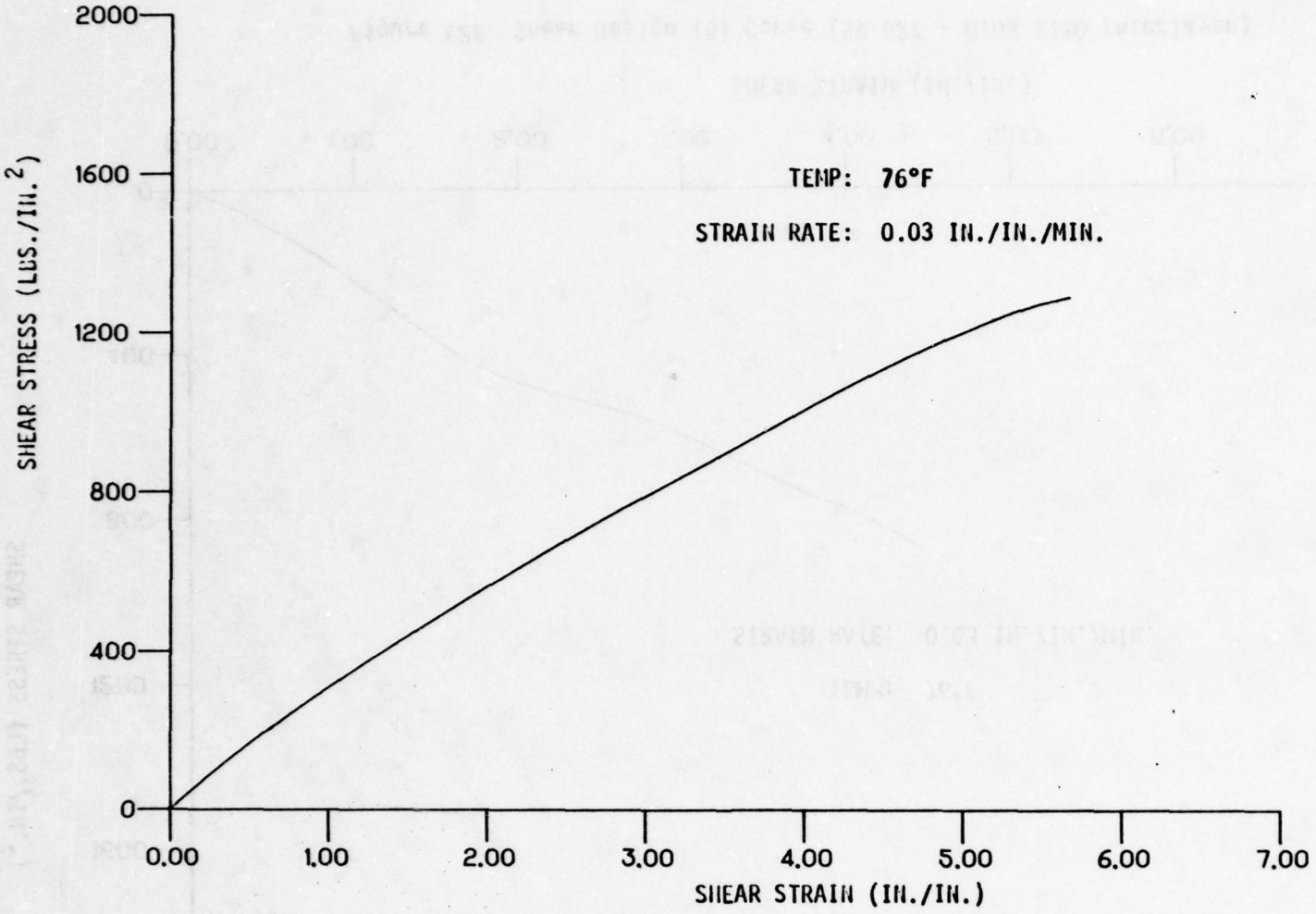

Figure C25. Shear Average Curve (SK627 - 0.03 S130 Interlayer)

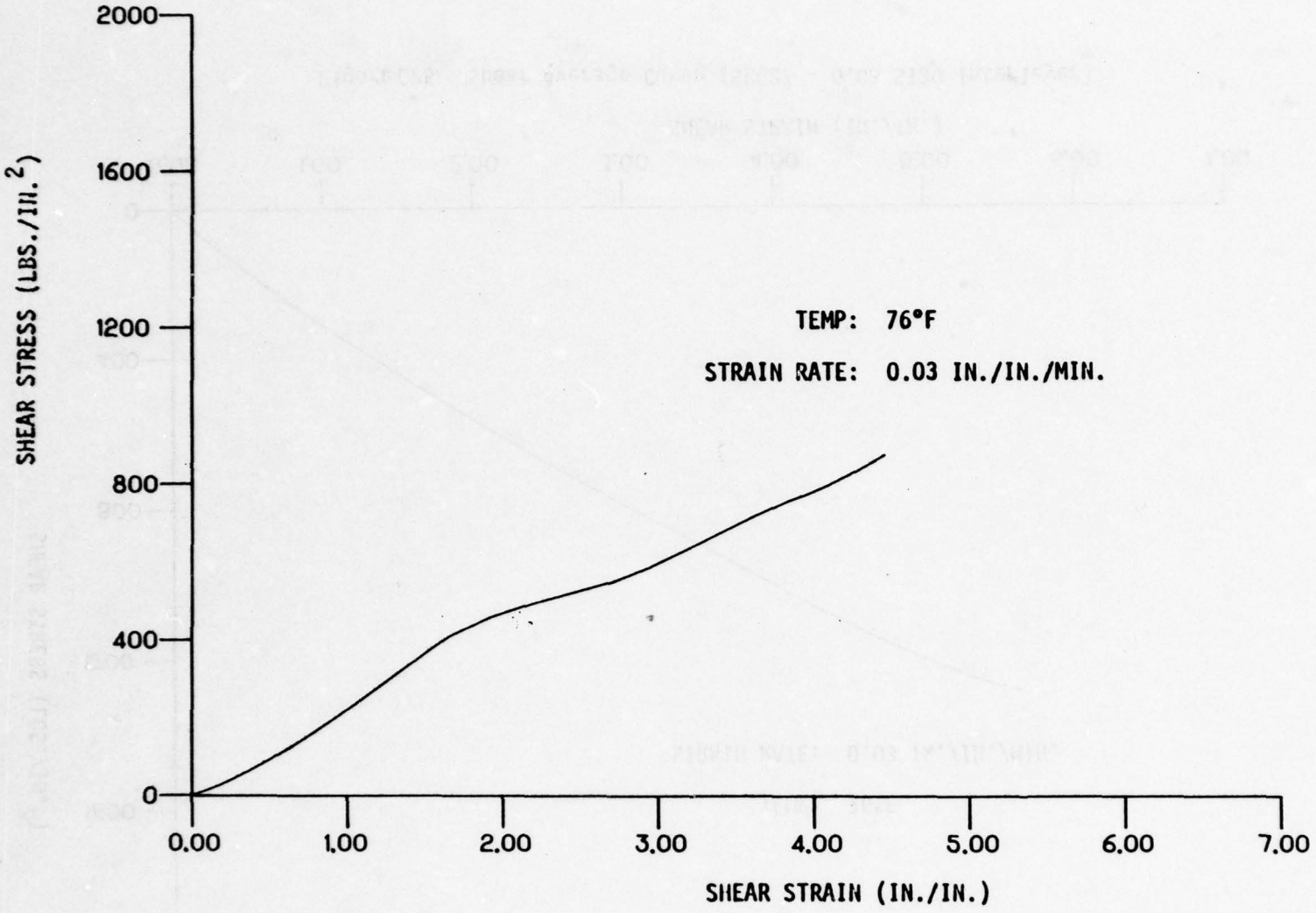

Figure C26 Shear Design (B) Curve (SK 627 - 0.03 S130 Interlayer)

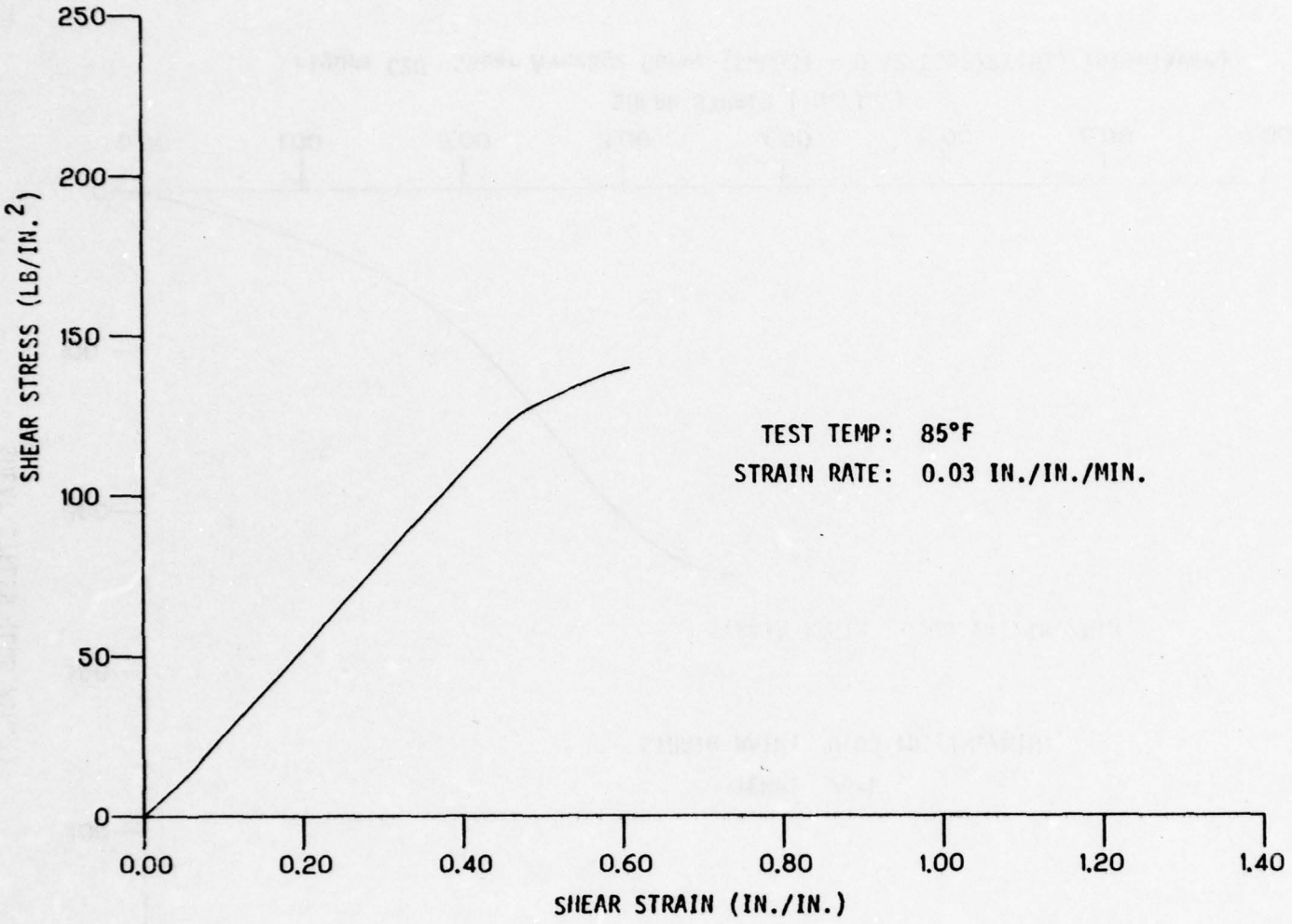

Figure C27. Shear Average Curve (SK531U - S-120 Interlayer).

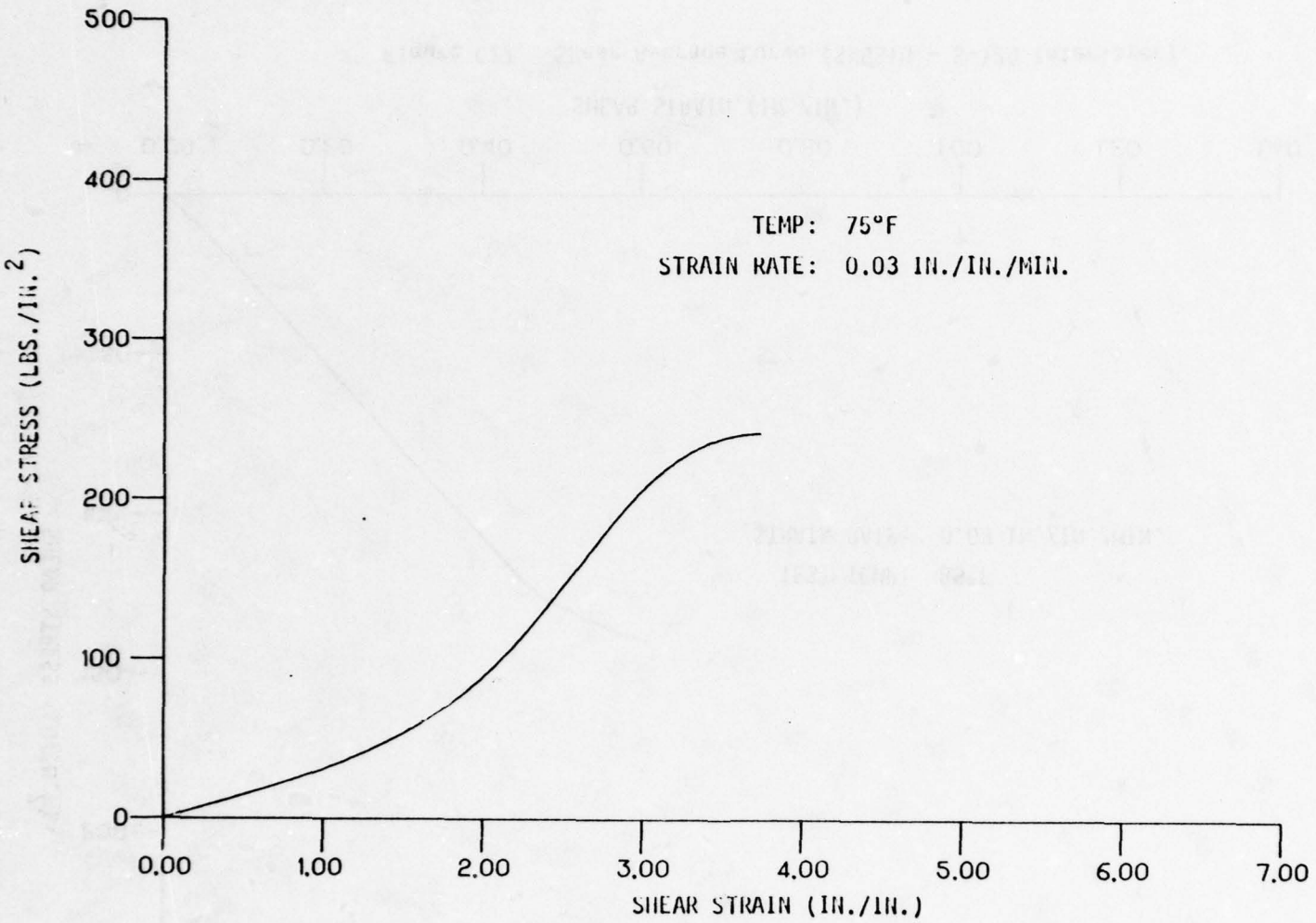

Figure C28 Shear Average Curve (SWU531 - 0.12 SS5272Y(HT) Interlayer).

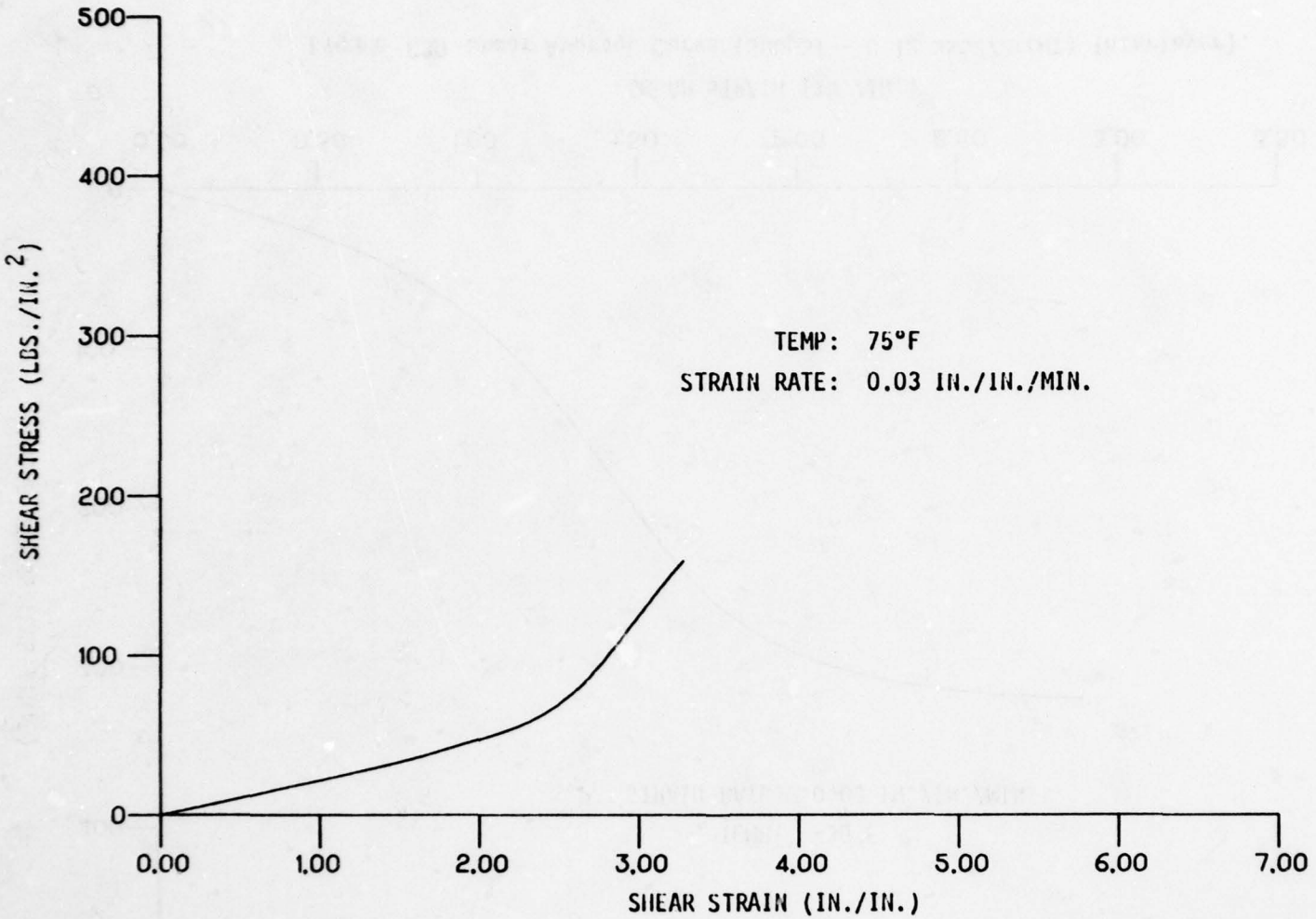

Figure C29. Shear Design (B) Curve (SWU531 - 0.12 SS5272Y(HT) Interlayer).

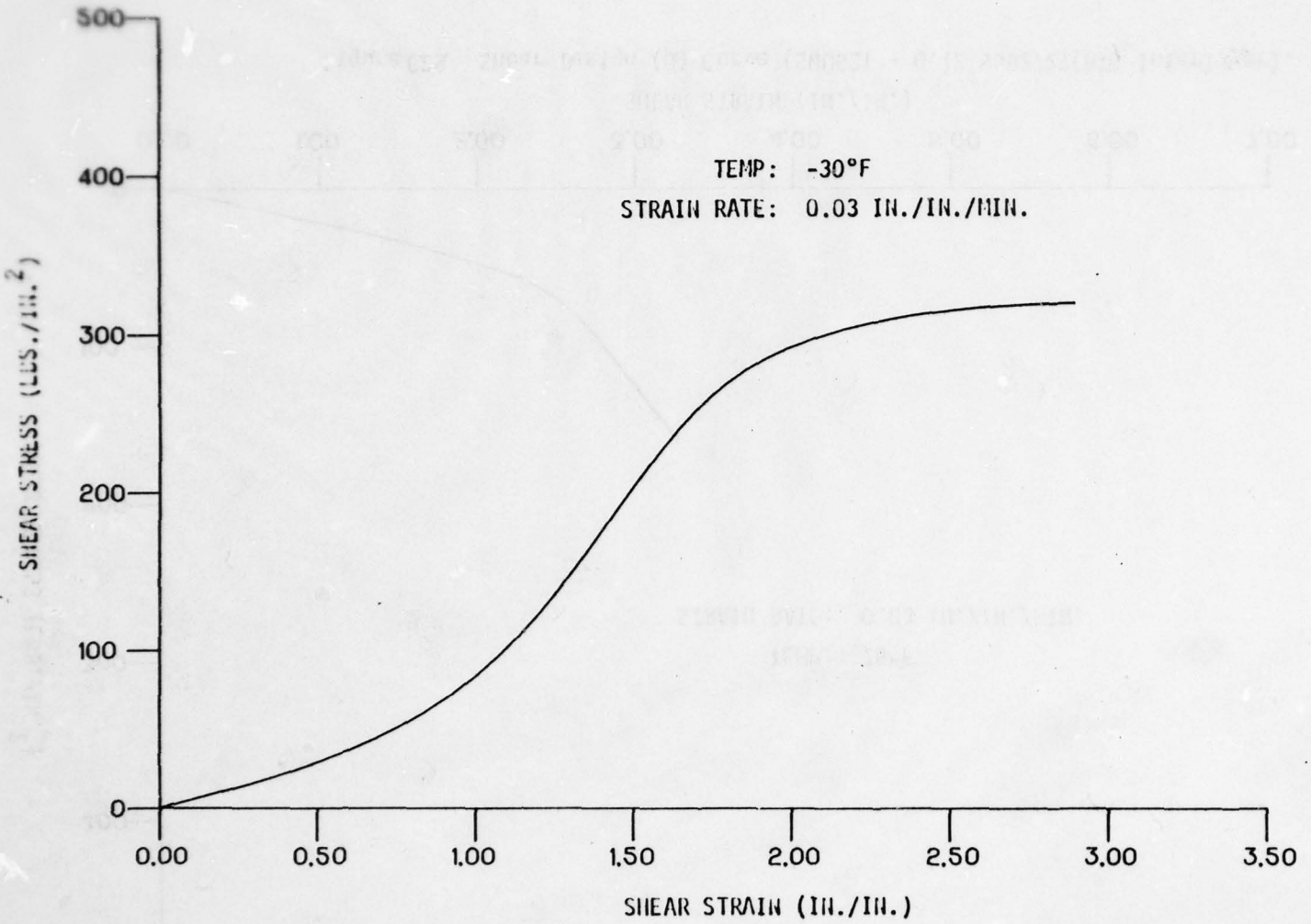

Figure C30 Shear Average Curve (SW0531 - 0.12 SS5272Y(HT) Interlayer).

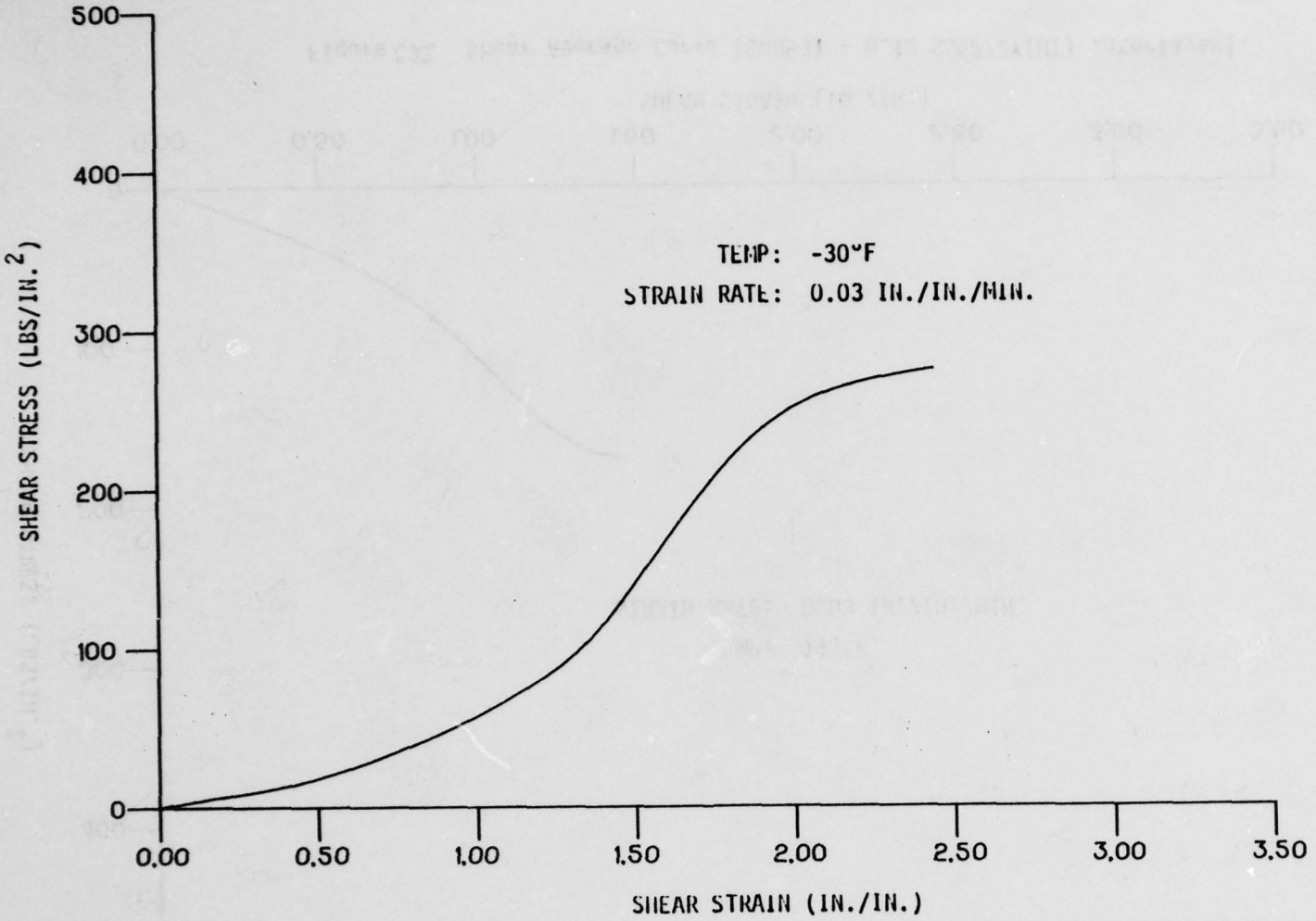

FigureC31. Shear Design (B) Curve (SWU531 - 0.12 SS5272Y(HT) Interlayer).

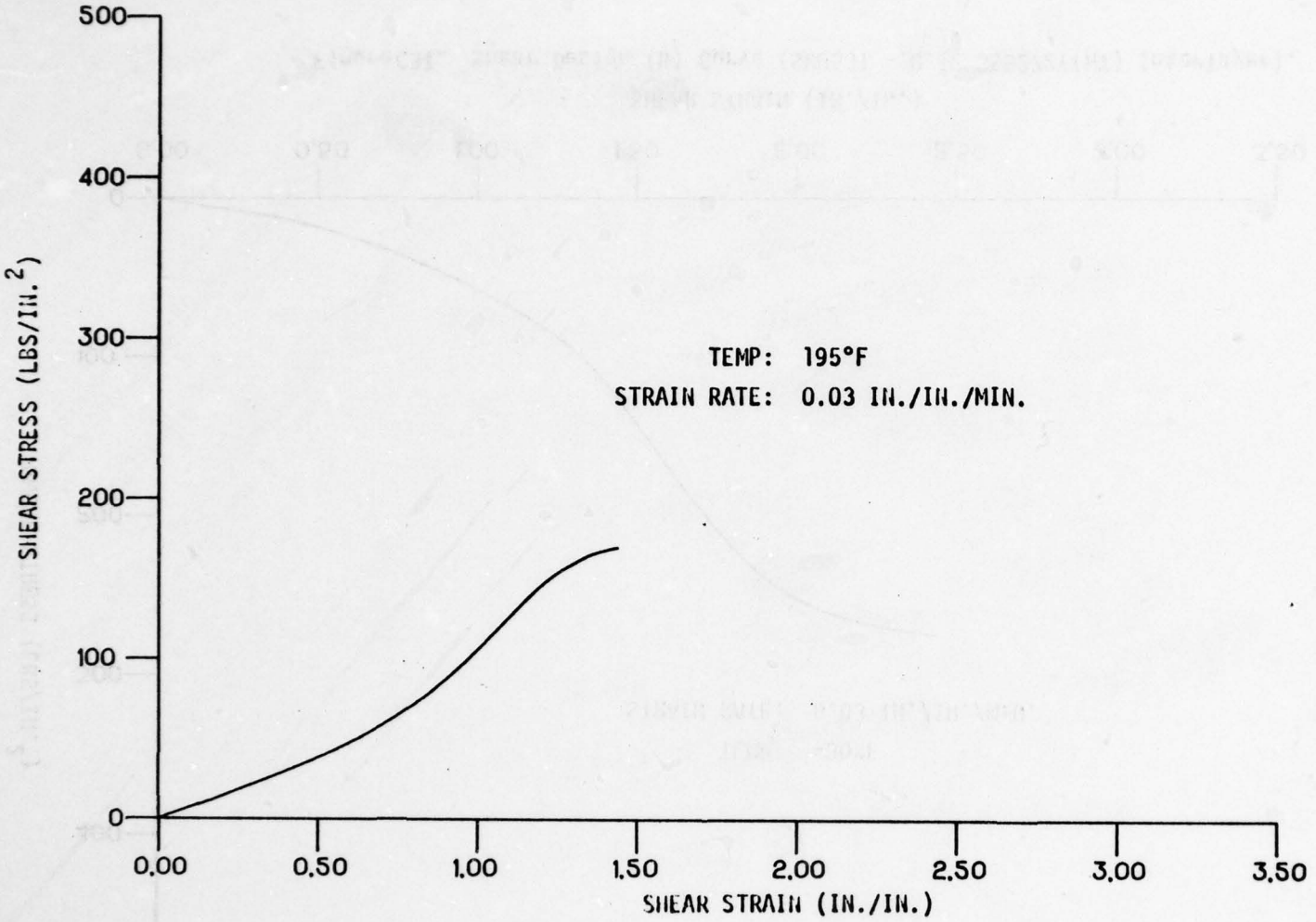

Figure C32. Shear Average Curve (SWU531 - 0.12 SS5272Y(HT) Interlayer).

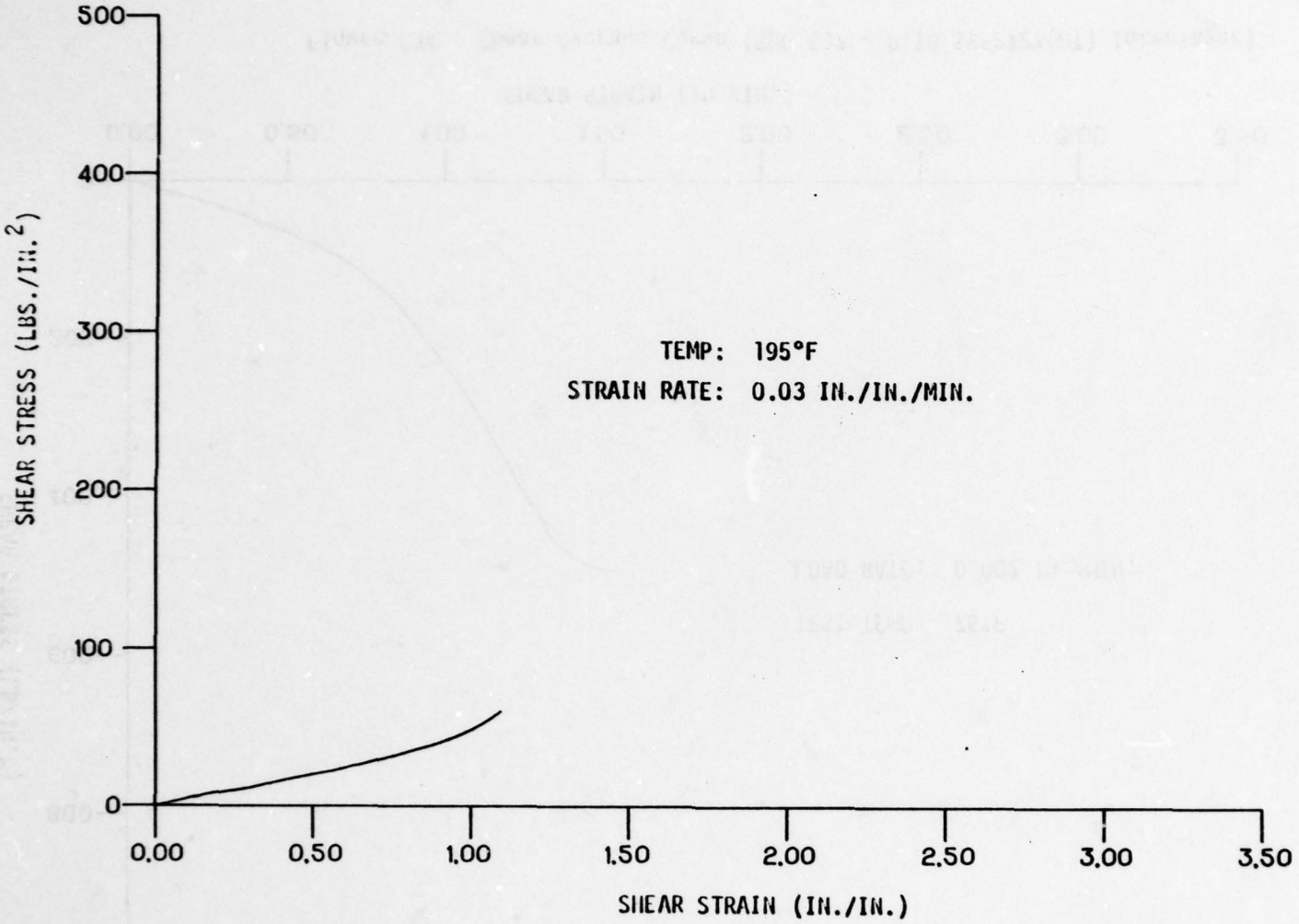

Figure C33 Shear Design (B) Curve (SWU531 - 0.12 SS5272Y(HT) Interlayer).

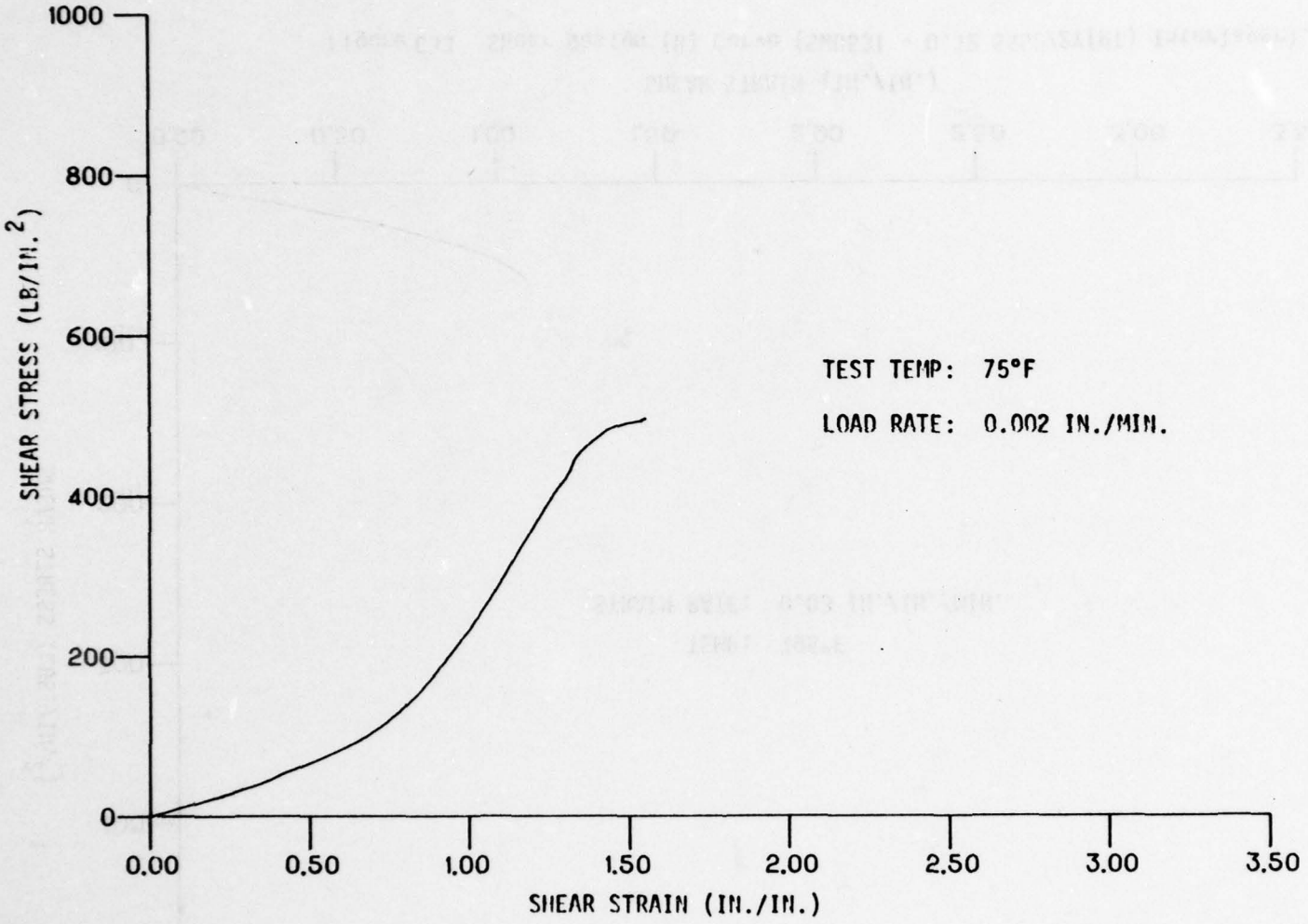

Figure C34. Shear Average Curve (SWU 537 - 0.10 SS5272Y(HT) Interlayer).

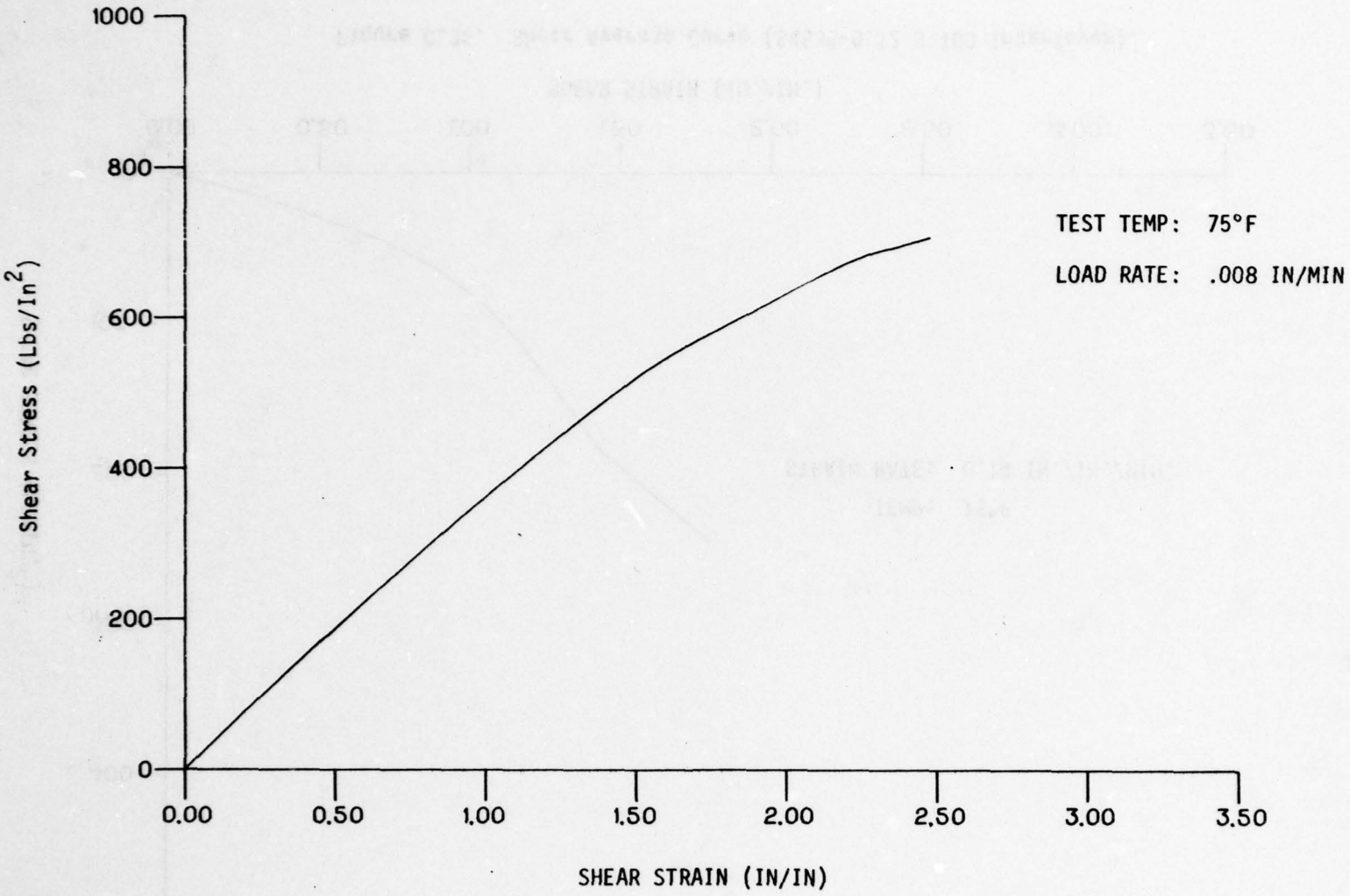

Figure C35. Shear Average Curve (PPG 539 - 0.125 PPG112 Interlayer)

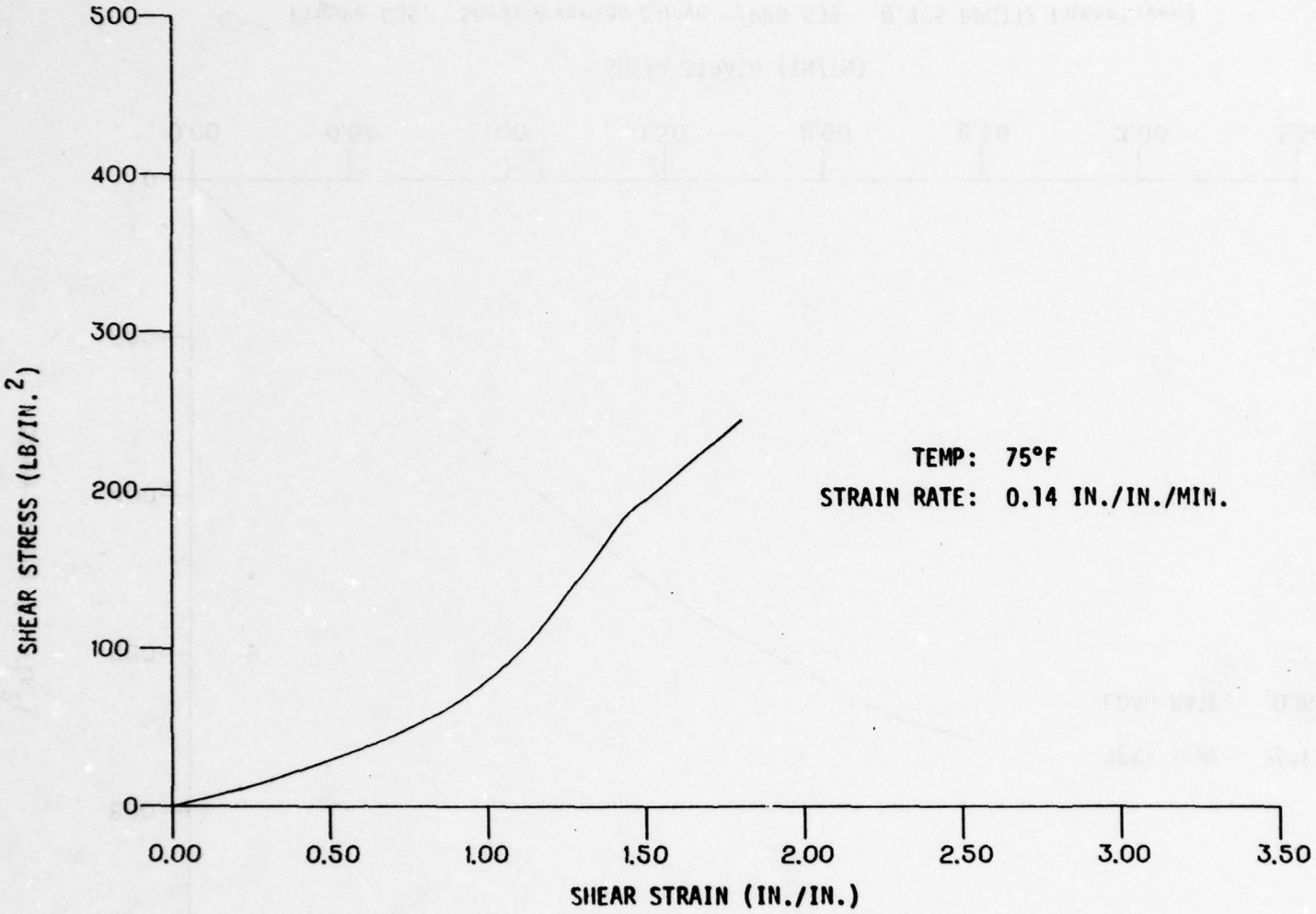

Figure C.36. Shear Average Curve (SK535-0.12 S-100 Interlayer).

SECTION VIII
HIGH STRAIN RATE TENSILE MECHANICAL PROPERTIES TESTING OF MONOLITHIC POLYCARBONATE MATERIALS

This series of tests were conducted to provide average (actual) and design allowable tensile mechanical properties at high strain rates for monolithic polycarbonate materials processed by specific aircraft transparency fabricators. The primary use for these mechanical properties was for development of and future design use in computer analysis of a bird strike. Additional uses were to provide for evaluation of materials and processors, and design trade-off studies. Tests were conducted at the maximum and minimum temperature conditions established by the flight profile of a supersonic aircraft. Maximum strain rates due to a bird strike were determined from bird impact tests of actual full size transparencies. Tests were accomplished at Terra Tek, Salt Lake City, Utah, under contract to Douglas for high strain rate testing. Test specimens were designed by Douglas to specifications furnished by Terra Tek, Inc., and manufactured by specific fabricators. These specimens received the same processing as a laminated aircraft transparency.

TEST SPECIMEN DESCRIPTION

The test specimens required for this series of tests are shown in Figures 57 through 60. All test specimens were examined under polarized light to expose stress risers from machining operations which could have affected test results. Specimens displaying stress were refinished (sanded and polished) to remove such discrepancies. Machine cutting speed and feed rates were controlled to prevent heating parts above 150°F during machining to eliminate adverse thermal conditioning effects. Specimens of a particular test series were orientated in the same length-width relation with respect to the basic stock. Polycarbonate materials tested

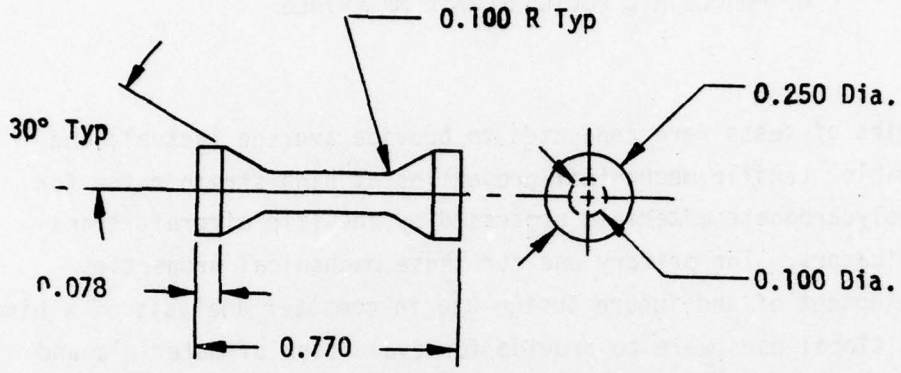

Figure 57. Tensile Specimen (Z7942633-523).

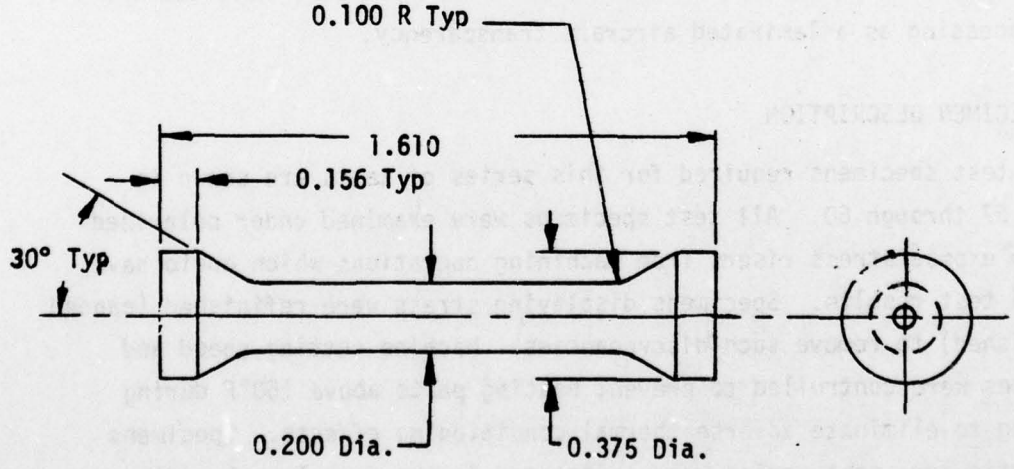

Figure 58. Tensile Specimen (Z7942633-569).

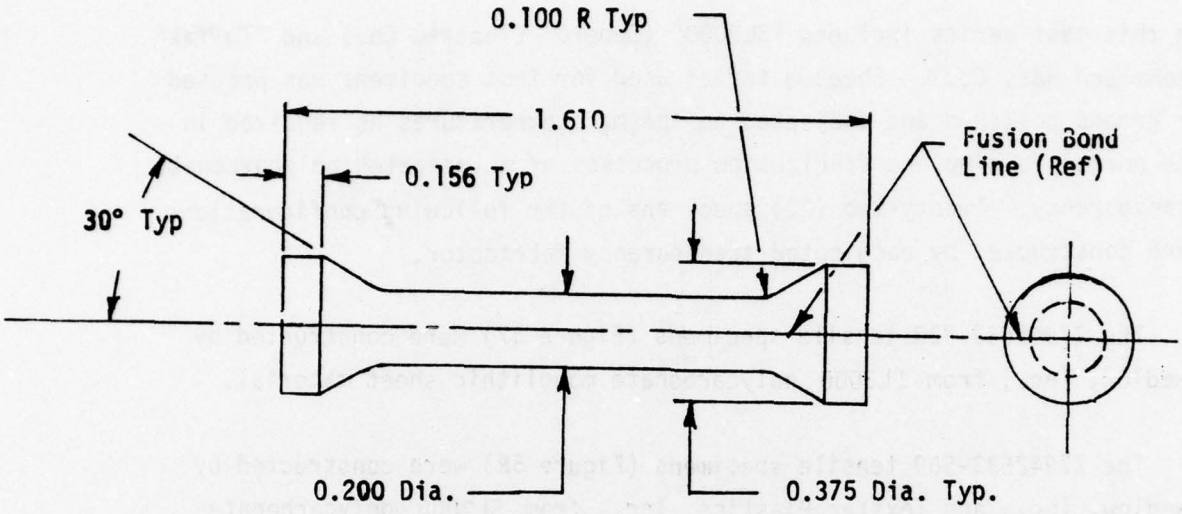

Figure 59. Tensile Specimen (Z7942633-601).

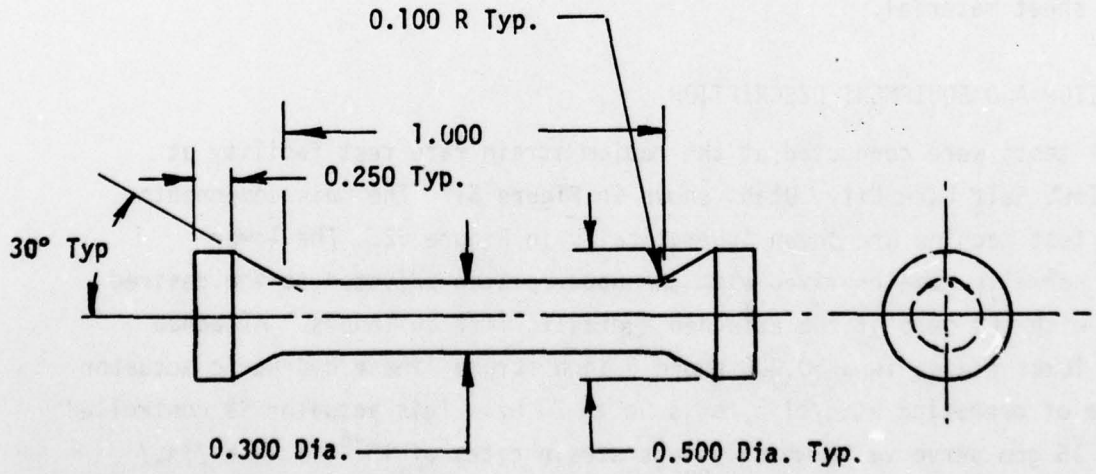

Figure 60. Tensile Specimen (Z7942633-611).

in this test series included "SL3000" (General Electric Co.) and "Tuffak" (Rohm and Haas Co.). Sheet material used for test specimens was pressed or ground polished and subjected to thermal temperatures as required in the normal forming and fabrication processes of a laminated polycarbonate transparency. Twenty-two (22) specimens of the following configurations were constructed by each noted transparency fabricator.

The Z7942633-523 tensile specimens (Figure 57) were constructed by Swedlow, Inc., from SL3000 polycarbonate monolithic sheet material.

The Z7942633-569 tensile specimens (Figure 58) were constructed by Swedlow, Inc., and Texstar Plastics, Inc., from SL3000 polycarbonate monolithic sheet material.

The Z7942633-601 tensile specimens (Figure 59) were constructed by Swedlow, Inc., Sierracin, Inc., and Texstar Plastics, Inc., from SL3000 and "Tuffak" polycarbonate fusion bonded sheet material.

The Z7942633-611 tensile specimens (Figure 60) were constructed by Swedlow, Inc., and Sierracin, Inc., from SL3000 polycarbonate fusion bonded sheet material.

TEST SETUP AND EQUIPMENT DESCRIPTION

All tests were conducted at the medium strain rate test facility at Terra Tek, Salt Lake City, Utah, shown in Figure 61. The main components of the test machine are shown schematically in Figure 62. The lower platen normally remains fixed with the upper platen adjusted to the desired height with the help of the attached hydraulic lift cylinders. Attached to the lower platen is a 50,000 pound 6-inch stroke linear hydraulic actuator capable of operating at cyclic rates up to 20 Hz. This actuator is controlled with a 15 gpm servo valve which allows strain rates of 10^{-6} to 1 in./in./sec. Through the use of a 50 gpm 4-way solenoid operated valve, in conjunction with a flow-control subplate manifold to vary the flow during open-loop operation, the strain rate is extended to 10 in./in./sec.

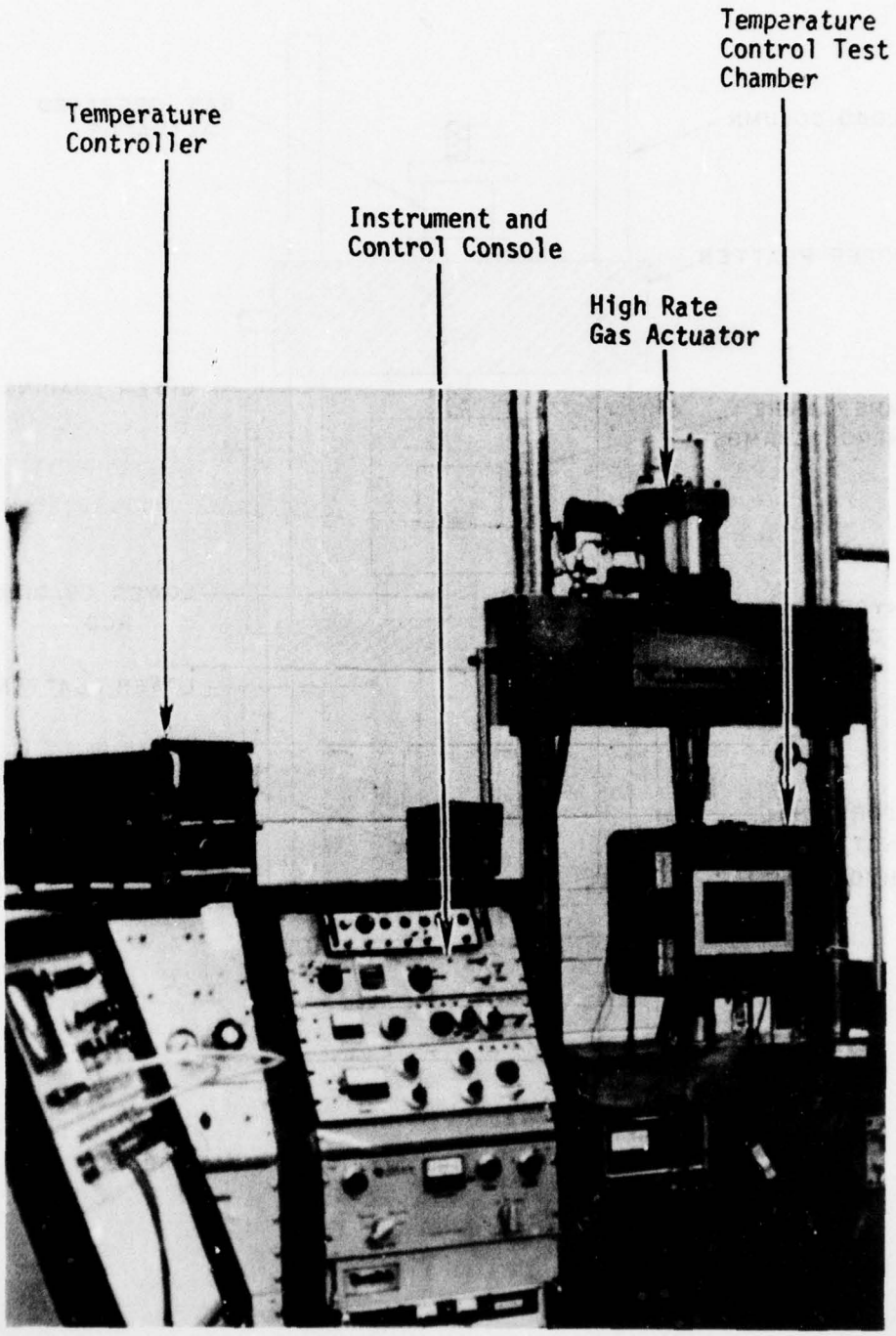

Figure 61. Medium Strain Rate Test Facility.

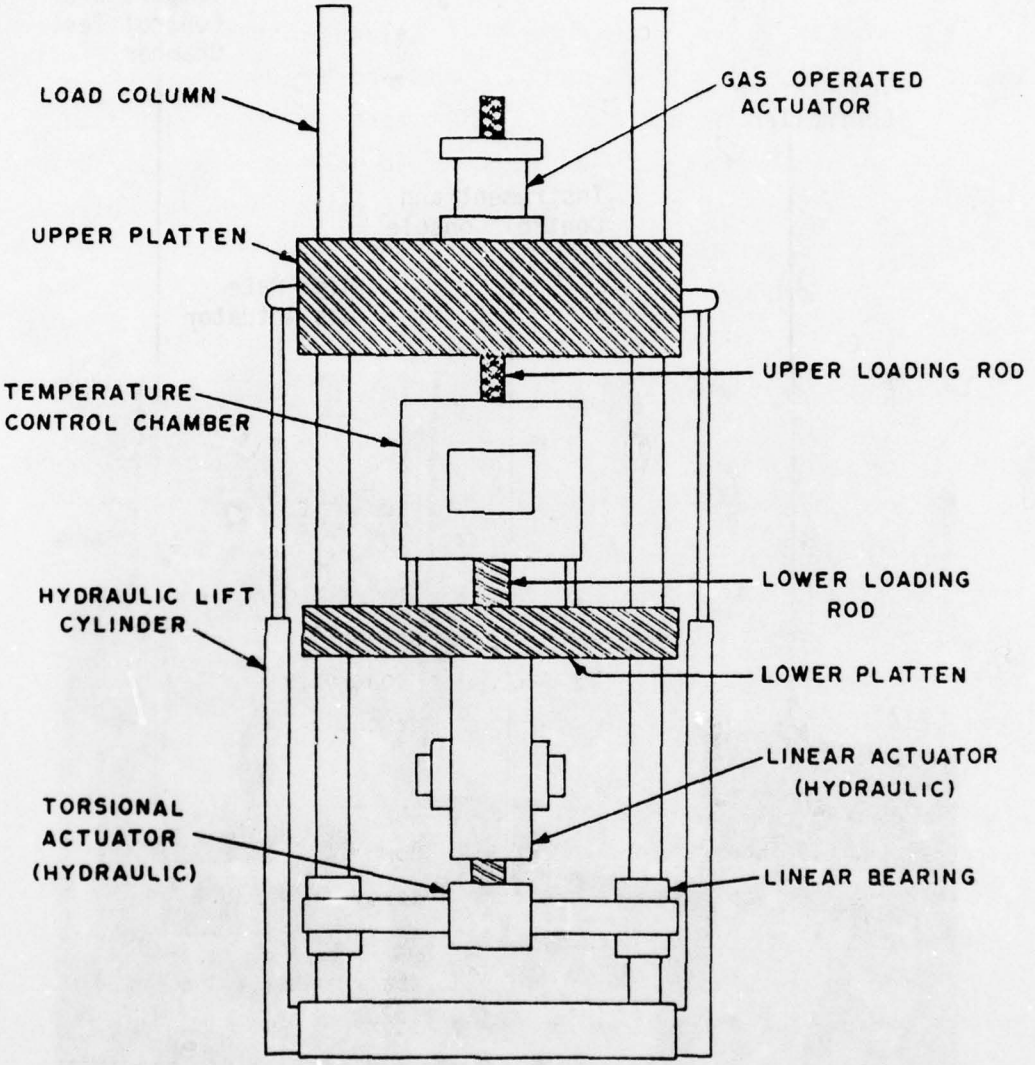

Figure 62. Schematic of Medium Strain Rate Machine.

For all but the very low strain rate tests presented here the high pressure gas actuator mounted above the upper platen was used. This actuator (Figure 63) is operated by charging a reservoir on either side of the piston to equal pressure. The piston is accelerated when the gas is released from one reservoir, the direction is toward the one that is exhausted. The orifice size can be adjusted to control the exhaust rate. Motion is initiated through a fast acting solenoid valve mounted downstream from the orifice. Piston velocity, and hence rate of loading, is controlled by the gas charging pressure, the orifice size, and, to some extent, the specimen. Piston velocities up to 500 in./sec can be achieved. Actuators are supplied by a 100 h.p. 50 gpm hydraulic power supply. Accumulators are provided to supply the peak flow rates.

Controls for the medium strain rate machine are located in the adjacent cabinets shown in Figure 61. These cabinets house servo controllers for the hydraulic actuators, each capable of three feedback modes of operation (displacement, strain, load) thus allowing independent selection of the feedback control. Digital ramp generators and a function generator are also available for test control. The pneumatic controls for the fast acting gas actuator system are also housed in the cabinets.

Specimen temperatures can be maintained in the range of -100°F to 300°F with the use of the temperature chamber shown in Figure 62. The lower temperatures are achieved by injecting a spray from a liquid nitrogen bottle. The system operates in a closed loop mode with a thermocouple, attached to the sample, providing a feedback signal to a Research Incorporated Series 6000 Termac Combined Temperature-Power Controller which in turn controls a solenoid on the nitrogen supply. High temperatures are maintained in a similar fashion except that a nicrome wire heater encased in an Iconel sheath is substituted for the solenoid valve. In this case, the error signal controls the amount of power supplied to the heaters by the power controller.

AD-A064 436 DOUGLAS AIRCRAFT CO LONG BEACH CALIF F/G 11/9
TESTING FOR MECHANICAL PROPERTIES OF MONOLITHIC AND LAMINATED P--ETC(U)
OCT 78 F E GREENE, L P KOEGEBOEHN F33615-75-C-3105
UNCLASSIFIED MDC-J6950 AFFDL-TR-77-96-PT-1 NL

4 OF 5
AD
A064438

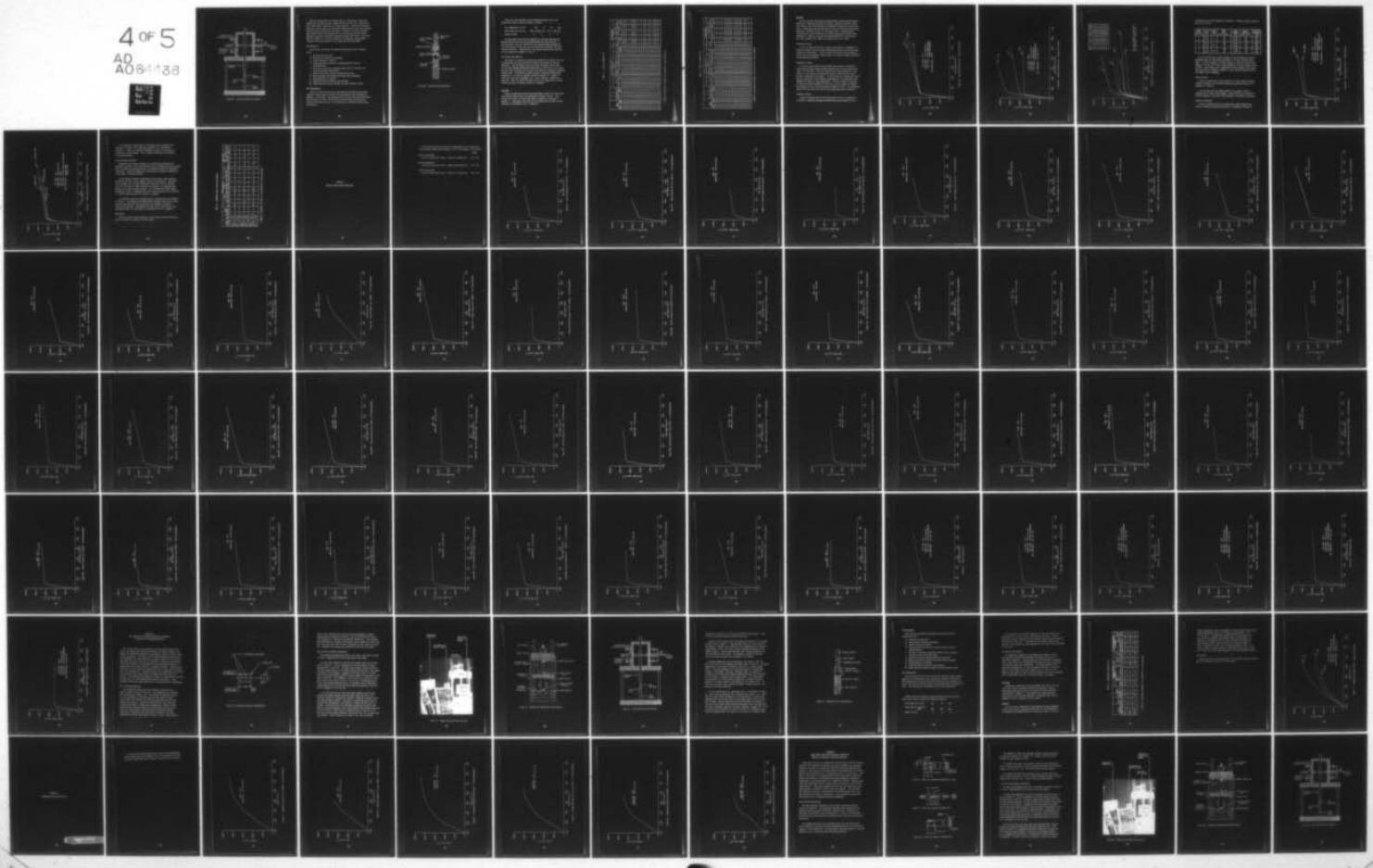

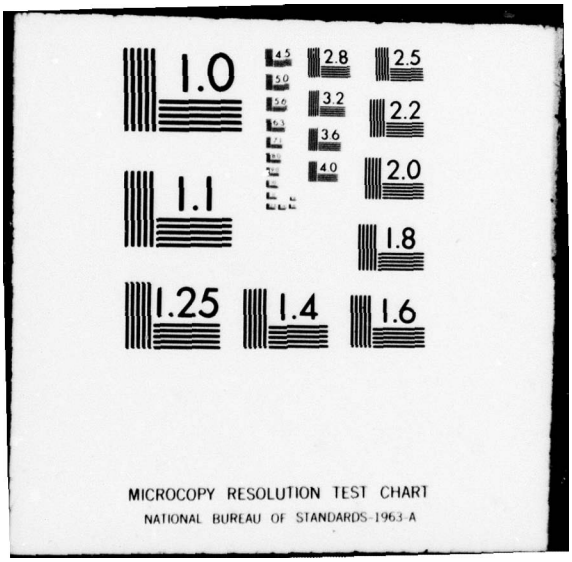
1.0
1.1
1.25
1.4
1.6
2.8
3.2
3.6
4.0
2.5
2.2
2.0
1.8
MICROCOPY RESOLUTION TEST CHART
NATIONAL BUREAU OF STANDARDS-1963-A

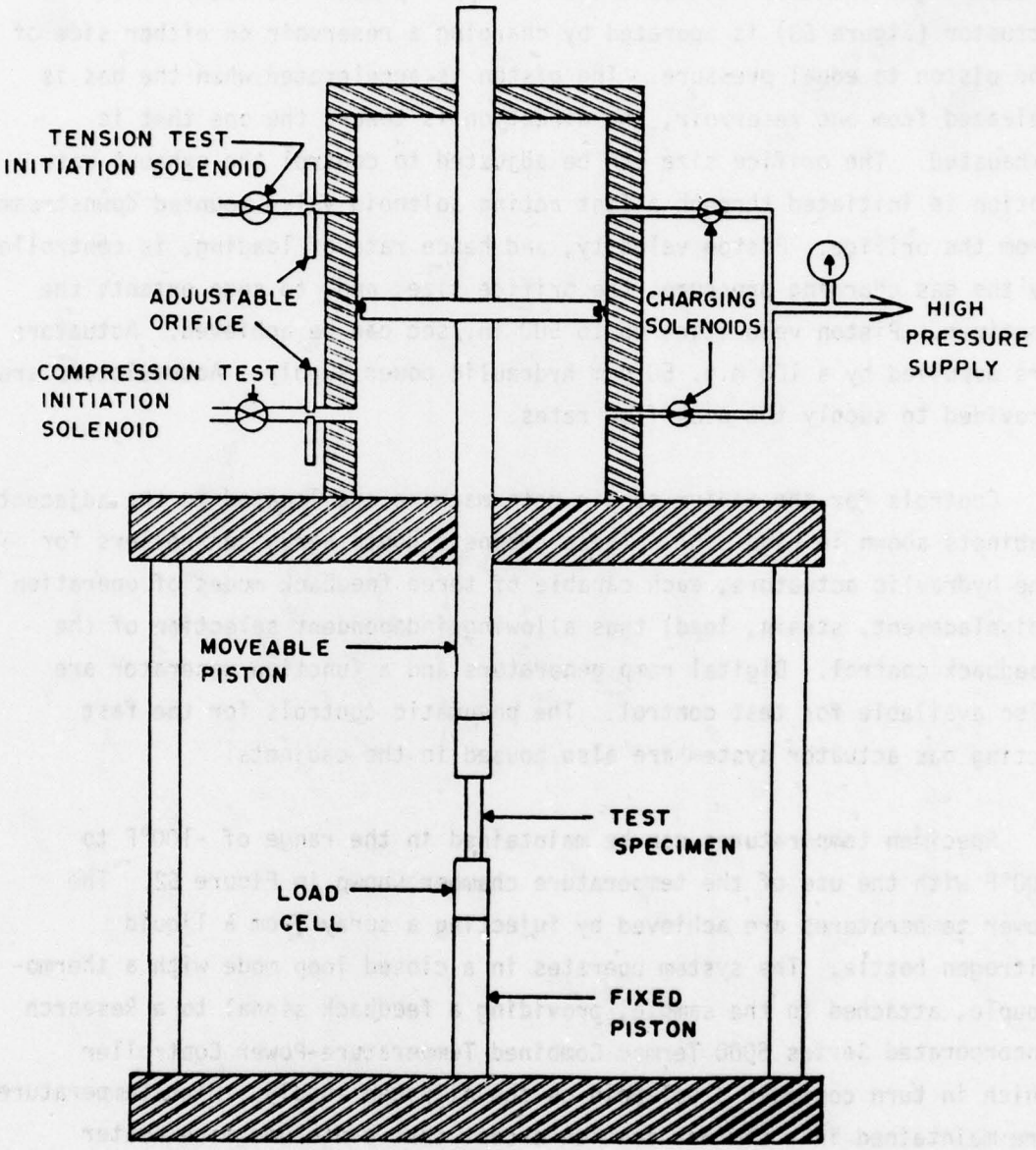

Figure 63. High Strain Rate Gas Actuator.

The test configuration for tension tests is illustrated in Figure 64. Sample load was measured with a Sundstrand Data Control, Inc., Quartz Load Cell, Model 923F2, interfaced to a charge amplifier. Strains were measured during the tension tests by strain gages bonded directly to the test specimen. Both the load and strain were recorded as a function of time on a Nicolet Model 1090AR Digital Oscilloscope, which was interfaced with the Digital Equipment Corporation multiuser timesharer computer (PDP 11/34). The strain data was plotted as a function of stress on a cathode-ray tube terminal (Tektronix 4010) and copied on a hard copy unit (Tektronix 4610).

TEST PROCEDURE

The following procedures are typically used by Terra Tek in tension tests.

1. Calibrate the load cell.
2. Record exact dimensions of specimen.
3. Install specimen in machine.
4. Attach appropriate coolant or heating enclosures and all instrumentation.
5. Run test as specified, recording stress-strain to failure, and load at yield and break points.
6. Record exact piston velocity achieved during test.
7. Remove specimen from machine and record exact dimensions.
8. Take photograph of specimen.
9. Positively mark and identify each specimen.
10. Repeat applicable above procedure for each specimen in turn.

TEST REQUIREMENTS

Terra Tek, Salt Lake City, Utah, provided the facilities and services required to apply dynamic loading on the polycarbonate test specimens to simulate a bird strike. Test temperatures and strain rates were established from supersonic aircraft flight profiles and bird impact test data contained in References 1 and 2. The following test conditions reflect these requirements.

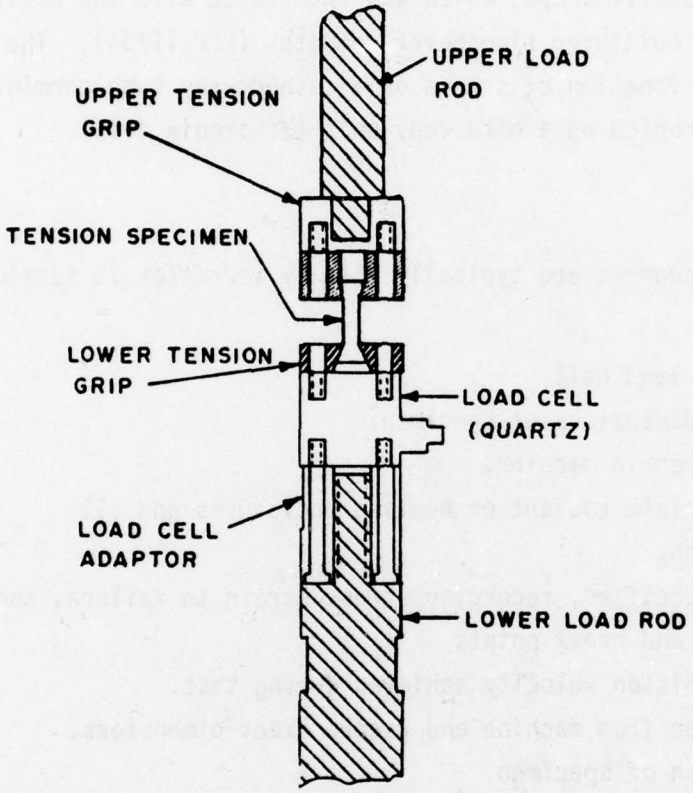

Figure 64. Tensile Test Configuration.

Twenty (20) test specimens of each processed material were to be tested under uniaxial tension loading as follows:

Test Temperature (°F ±5°)	-30	76	76	190
Strain-Rate (in./in./sec.)	200 ± 50	200 ± 50	10 ± 5	200 ± 50
Number of Tests	5	5	5	5

The gage length cross section dimensions of each test specimen was measured within ±0.001-inch and recorded before and after each test. A load-deflection curve was recorded for each specimen tested through the peak load portion of the curve, and the yield load and rupture load were recorded seperately. Photographs of the ruptured specimen were supplied, and are presented in Appendix L (Part 2).

TEST RESULTS AND ANALYSIS

The mechanical properties strength data presented is based on five test specimens made from the same batch of material and tested at identical conditions. Test specimens that broke at some fortuitous flaw or that did not break between predetermined gage marks or that failed in the fusion bond area were discarded and not used in calculation of mechanical properties strength data. The mechanical property design allowables presented were computed on a "B" basis by methods outlined in Section III. Where "B" basis data could not be computed, the "C" basis data was computed and is presented. Where the design allowable could not be computed due to insufficient test data, no design allowable is presented.

Test Data

Tensile strength data derived from experimental results for high strain rate uniaxial tensile tests are summarized in Tables 21 and 22. True stress-strain plots for average and design allowables is contained in Appendix D. Experimental test data and true stress-strain curves for test specimens are contained in Part 2, Appendix L.

TABLE 21. TENSILE STRENGTH DATA

TEST SPECIMEN IDENT	TEST SPECIMEN NO.*	THICKNESS (IN.)	TEST TEMP (° F)	STRAIN RATE (IN/IN/SEC)	AVERAGE STRENGTH DATA: YIELD (PSI)	STD DEV (PSI)	SEC YLD MOD (PSI 10^{-5})	ULTIMATE: TRUE STRESS (PSI)	STD DEV (PSI)	TRUE STRAIN (IN/IN)	STD DEV (IN/IN)	ELAST MOD (PSI 10^{-5})	STD DEV (PSI x 10-5)	DESIGN ALLOWABLE: DES BAS	YIELD (PSI)	SEC YLD MOD (PSI 10^{-5})	ULTIMATE: TRUE STRESS (PSI)	TRUE STRAIN (IN/IN)	ELAST MOD (PSI 10^{-5})
SWU523	4	.10	72	161	11395	569	1.48	13466	211	0.358	0.032	2.81	0.142	B	9025	1.17	12587	0.227	2.26
SWU523	8	.10	78	276	12423	1076	1.20	15320	2753	0.423	0.077	3.08	0.434	C	10683	1.03	10865	0.298	2.30
SWU523	4	.10	-30	200	14974	1604	1.58	19035	2510	0.388	0.137	3.58	0.481						
SWU523	3	.10	190	200	8502	623	1.07	11175	863	0.485	0.180	1.90	0.057						
SWU569	5	.20	72	50	18769	1732	2.98	27601	2149	0.572	0.027	4.69	0.727	B	12868	2.04	20277	0.480	2.23
SWU569	4	.20	72	141	18995	1632	3.34	28422	1962	0.558	0.025	4.88	0.766	B	12203	2.15	20258	0.456	1.69
SWU569	3	.20	-30	145	20550	2434	2.79	24932	3031	0.362	0.179	4.12	1.051						
SWU569	5	.20	190	183	14158	1899	2.42	16032	3862	0.588	0.025	3.55	0.599						
SWU601	4	.20	-30	200	13509	718	2.76	13509	718	0.049	0.004	3.68	0.227						
SWU601	6	.20	73	180	12004	929	1.99	16606	2921	0.599	0.115	4.02	0.315	C	10244	1.70	11071	0.380	3.67
SWU601	4	.20	190	209	9724	212	1.62	10634	593	0.540	0.045	3.22	0.051						
SWU601RH	4	.20	73	200	11972	204	2.03	14283	830	0.468	0.063	3.63	0.102	C	11439	1.94	12109	0.303	3.40
SWU611	5	.30	-30	93	20086	600	2.57	25559	3763	0.420	0.206	4.24	0.302						
SWU611	5	.30	72	119	13831	234	2.13	17162	1709	0.520	0.078	3.43	0.133	C	13327	2.05	13487	0.351	3.36
SWU611	5	.30	72	E	12298	155	1.76	14777	499	0.475	0.027	4.44	0.427	B	11771	1.69	13077	0.361	4.90
SWU611	5	.30	190	154	11270	295	2.04	13764	1676	0.662	0.119	3.48	0.204						

* Number of specimens included in generation of data presented.

TABLE 22. TENSILE STRENGTH DATA

TEST SPECIMEN		THICKNESS (IN.)	TEST TEMP (°F)	STRAIN RATE (IN./IN. SEC)	AVERAGE STRENGTH DATA								DESIGN ALLOWABLE					
								ULTIMATE								ULTIMATE		
IDENT	NO.*				YIELD (PSI)	STD DEV (PSI)	SEC YLD MOD (PSI x 10^{-5})	TRUE STRESS (PSI)	STD DEV (PSI)	TRUE STRAIN (IN/IN)	STD DEV (IN/IN)	ELAST MOD (PSI x 10^{-5})	STD DEV	DES BAS	YIELD (PSI)	SEC YLD MOD (PSI x 10^{-5})	TRUE STRESS (PSI)	TRUE STRAIN (IN/IN)	ELAST MOD (PSI x 10^{-5})
SK601	8	.20	-30	98	15193	307	2.23	21856	2021	0.578	0.035	3.67	0.398						
SK601	3	.20	72	108	12133	114	1.91	17831	1785	0.598	0.069	3.41	0.081						
SK601	8	.20	72	5	11387	122	1.83	15166	1887	0.480	0.117	3.91	0.303						
SK601	5	.20	190	190	10402	322	1.74	11535	1418	0.551	0.073	2.90	0.214						
SK611	8	.30	76	124	13837	69	2.20	17718	1335	0.514	0.063	4.11	0.153	C	13688	2.18	14849	0.378	3.90
SK611	5	.30	72	8	12287	341	1.70	14713	1012	0.465	0.050	4.08	0.326	C	11553	1.60	12533	0.357	3.63
SK611	5	.30	-30	94	20324	1042	2.75	28411	3531	0.542	0.092	4.41	0.295	C	18085	2.44	20820	0.343	3.91
SK611	4	.30	190	145	11958	49	1.95	13753	1798	0.606	0.102	3.59	0.157						
TEX601RH	5	.20	72	211	12643	360	2.08	13675	563	0.394	0.030	4.04	0.122	B	11416	1.88	11958	0.291	3.61
TEX601	5	.20	72	213	12413	297	1.90	13545	374	0.428	0.056	3.71	0.316	B	11401	1.75	12270	0.237	2.84
TEX601	5	.20	72	230	12366	219	1.90	14260	571	0.490	0.029	3.55	0.384	B	11621	1.78	12316	0.393	2.40
TEX601	5	.20	75	206	12915	169	1.59	13597	860	0.419	0.059	3.75	0.290						
TEX601	4	.20	75	217	13144	383	1.63	15535	1071	0.464	0.041	3.54	0.362	C	12141	1.50	12731	0.357	2.60
TEX601	2	.20	-30	94	16363	167	2.01	22271	2419	0.479	0.084	3.81	0.100						
TEX601	4	.20	190	169	10621	212	2.04	10565	312	0.490	0.027	3.42	0.415						

*Number of specimens included in the generation of data presented.

Analysis

In this analysis comparisons are made between processed polycarbonate materials to demonstrate processing effects, temperature effects, thickness effects, and forming effects on mechanical properties at high strain rates. Comparisons were made between two types of processed polycarbonate materials, SL3000 and Tuffak, at high strain rates. Proposed design allowables for tensile properties of SL3000 polycarbonate material were generated by combining test data of processed materials from Sierracin, Inc. (SK), Swedlow, Inc. (SWU), and Texstar Plastics Co. (TEX).

Processing Effects

A plot of average tensile true stress-strain curves is presented in Figure 65 comparing the processed SL3000 polycarbonate from three aircraft transparency fabricators. It can be seen from Figure 65 that processing affects the yield strength, rupture strain, and rupture strength properties of polycarbonate materials.

Temperature Effects

A plot of average tensile true stress-strain curves is presented in Figure 66 comparing processed SL3000 polycarbonate at three temperatures; -30°F, 75°F and 190°F. The true stress-strain curves plotted are a test average of the processed polycarbonate materials from the three noted aircraft transparency fabricators. It can be seen that temperature affects plastic properties of the processed polycarbonate to a large extent when compared to results at room temperatures. The plot reveals a large gain in yield and rupture strength at -30°F with a loss in strain to rupture and a smaller loss in yield and rupture strength at 190°F. This comparison agrees with low strain rate tensile test comparisons made in Section V.

Thickness Effects

A plot of average tensile true stress-strain curves is presented in in Figure 67 comparing processed SL3000 polycarbonate materials of two

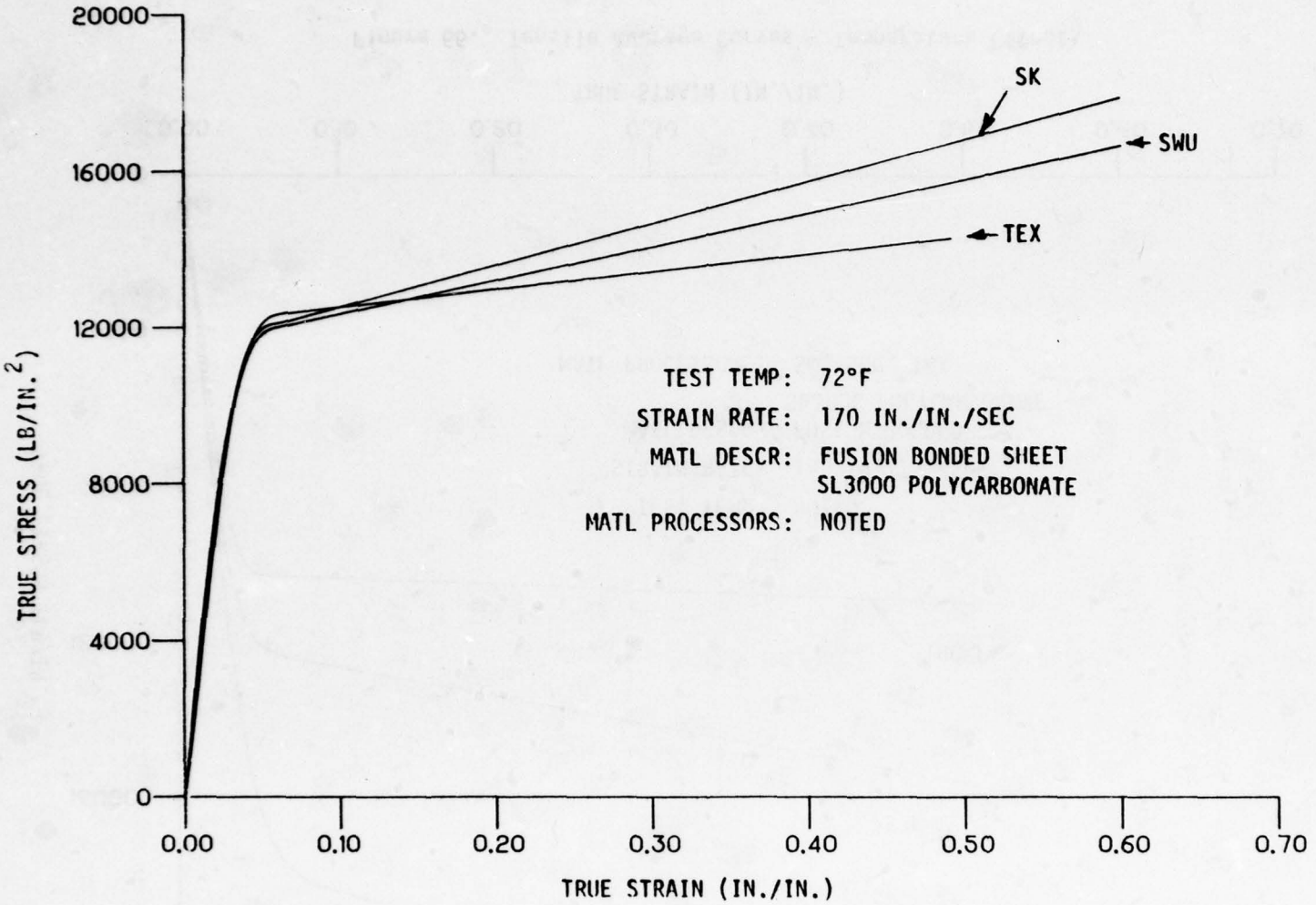

682

Figure 65. Tensile Average Curves - Processing Effects.

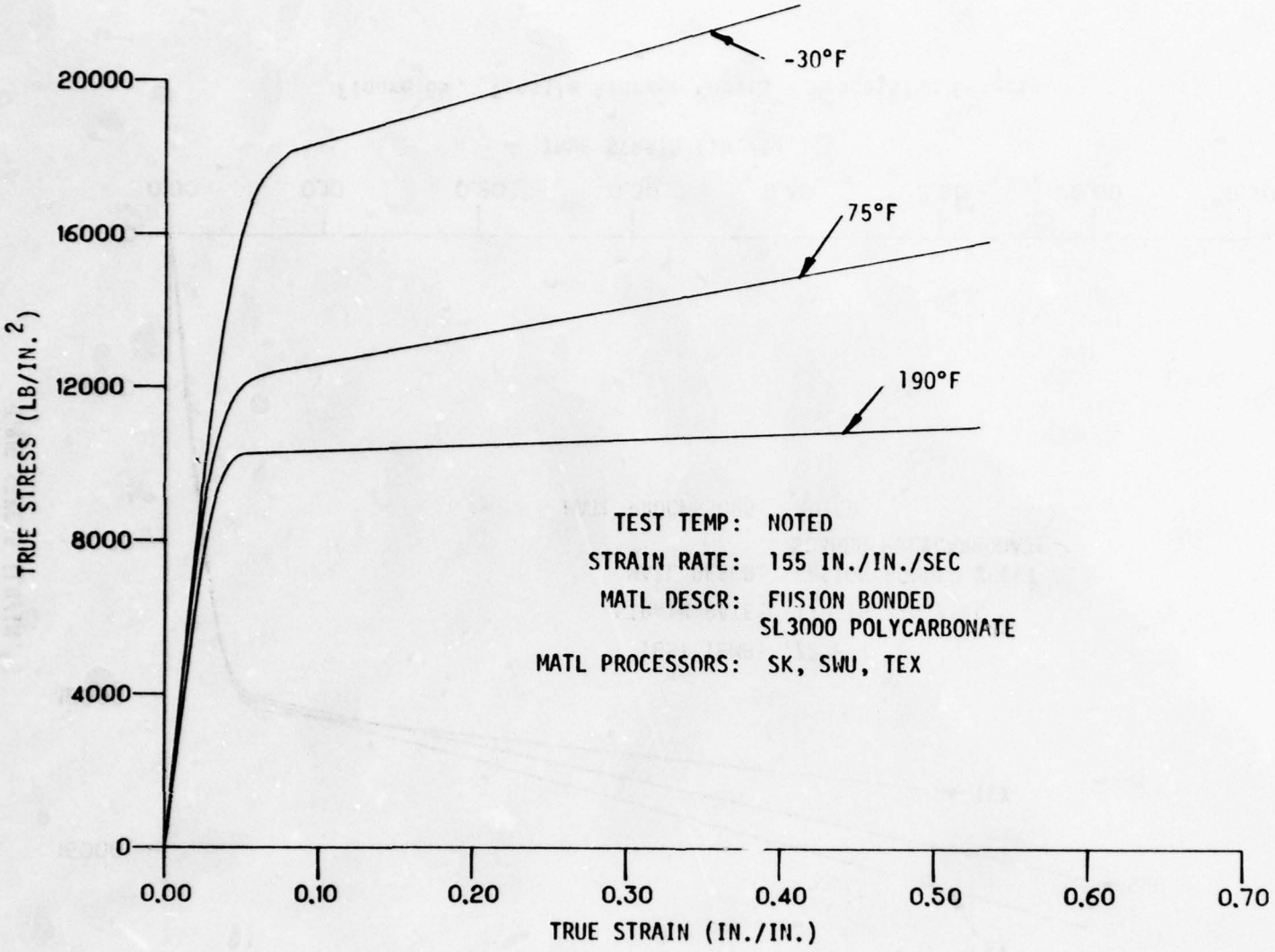

Figure 66. Tensile Average Curves - Temperature Effects.

CURVE NO.	THICK-NESS	TEST TEMP	STRAIN RATE
A	0.10	72°F	161
B	0.30	72°F	119
C	0.10	-30°F	200
D	0.30	-30°F	93
E	0.10	190°F	200
F	0.30	190°F	154

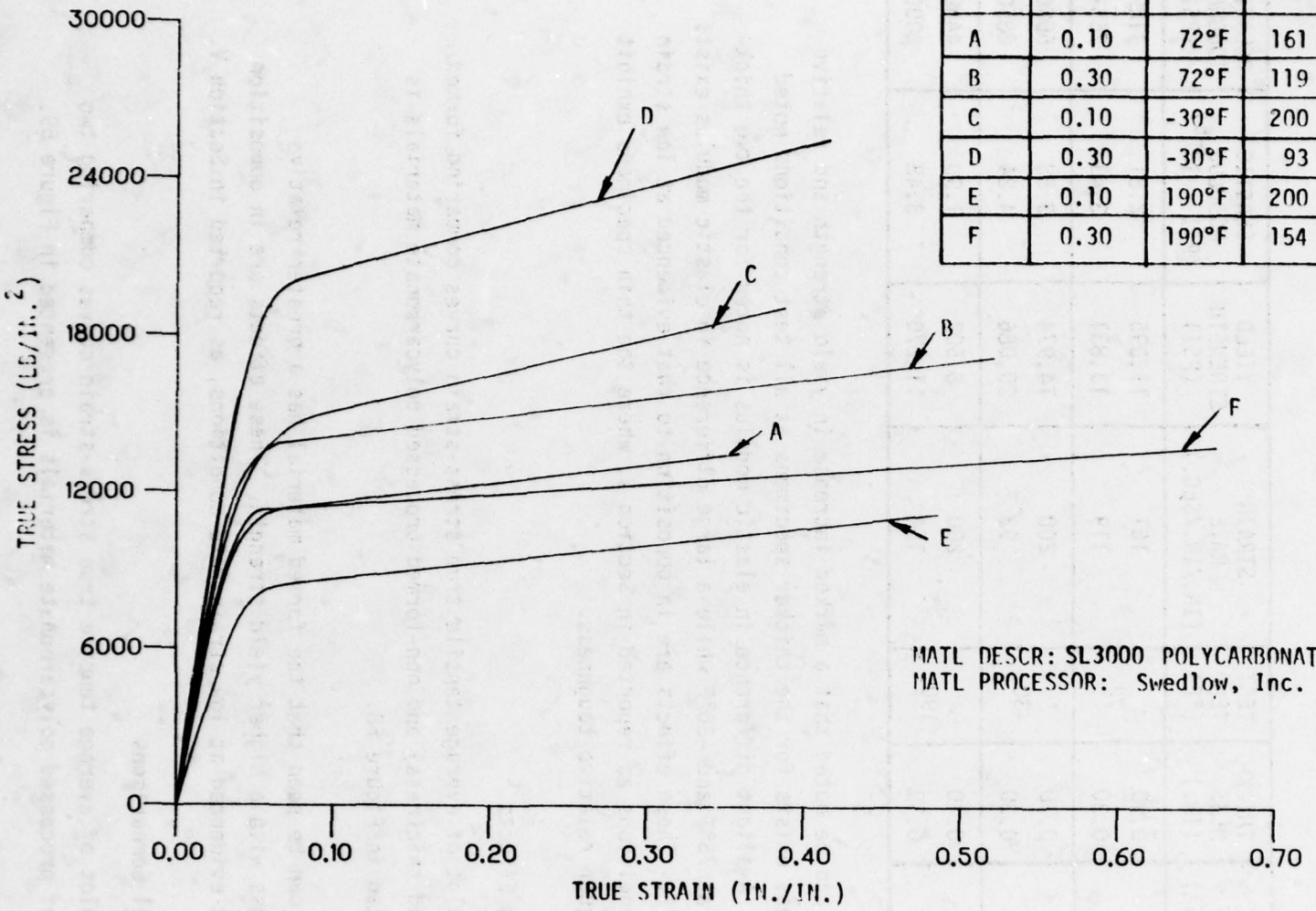

Figure 67. Tensile Average Curves - Thickness Effects.

thicknesses and at three temperature conditions. Affected strength properties data are as follows:

CURVE IDENT (FIG. 67)	THICK-NESS (IN.)	TEST TEMP (°F)	STRAIN RATE (IN./IN./SEC.)	YIELD STRENGTH (PSI)	ELASTIC MODULUS ($PSI \times 10^{-5}$)	RELATIVE TOUGHNESS (PSI)
A	0.10	72	161	11,395	2.81	4129
B	0.30		119	13,831	3.43	7658
C	0.10	-30	200	14,974	3.58	6006
D	0.30		93	20,086	4.24	8850
E	0.10	190	200	8,502	1.90	4462
F	0.30		154	11,270	3.48	8000

It can be noted that a marked increase in yield strength and relative toughness exists for the thicker specimens at all test conditions noted above. A slight difference in elastic modulus is noted for the two thicknesses at 75°F and -30°F while a large difference in elastic modulus exists at 190°F. These effects are in opposition to that evidenced at low strain rate conditions as reported in Section V, where the thin specimens exhibit the higher relative toughness.

Forming Effects

A plot of average tensile true stress-strain curves comparing formed (reduced thickness) and non-formed processed polycarbonate materials is presented in Figure 68.

It can be seen that the formed material has a greater relative toughness with a higher yield strength. These effects are in opposition to that evidenced at low strain rate conditions, as reported in Section V.

Material Comparisons

A plot of average tensile true stress-strain curves comparing two types of processed polycarbonate materials is presented in Figure 69.

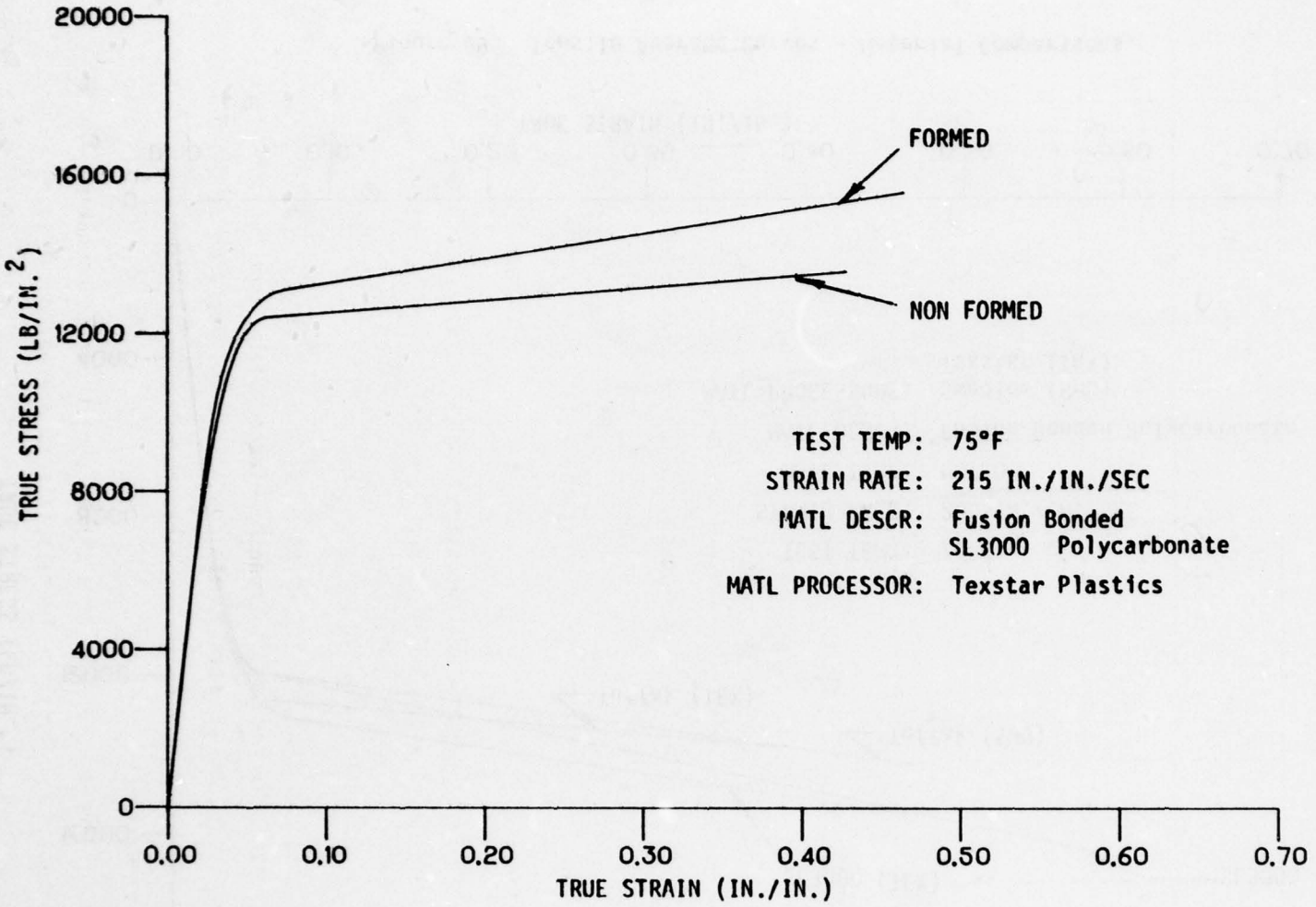

Figure 68. Tensile Average Curves - Forming Effects.

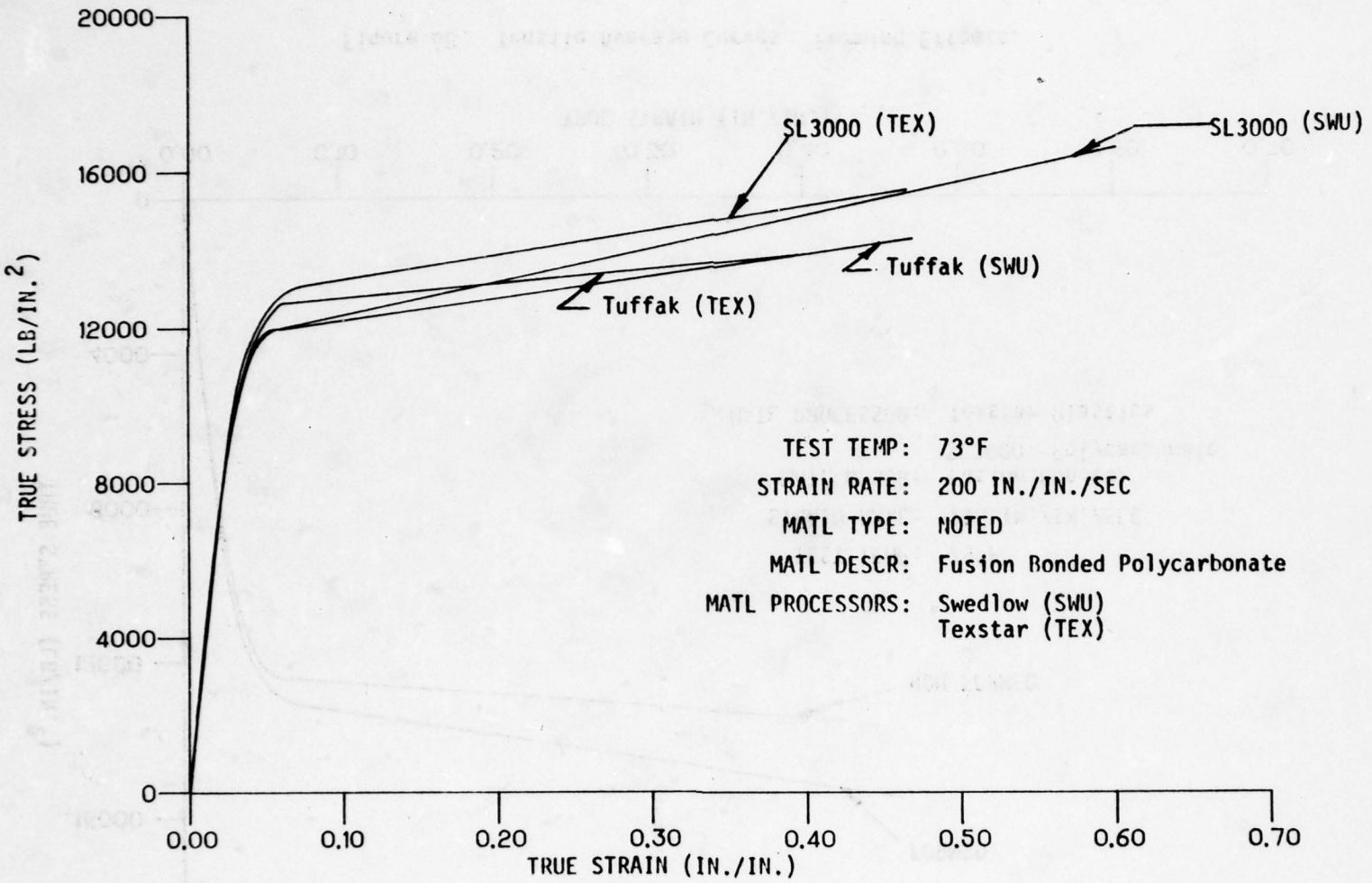

Figure 69. Tensile Average Curves - Material Comparisons.

It is noted that SL3000 shows an increased relative toughness when compared to "Tuffak" at the noted test conditions for both material processors. Little or no material difference is seen in the modulus of elasticity or yield strength. Yield strength differences are attributed to processing effects.

Proposed Design Allowables

Proposed tensile design allowables for processed polycarbonate were developed from tensile test data previously used in determining design strength data for SL3000 polycarbonate material as processed by specific transparency fabricators. These were combined to provide design allowables representing a wide range of processed material.

The fabrication processes represented include drying, press polishing, mechanical polishing, fusion bonding, forming, and laminating. Representative specimens from all known transparency fabricators are not included, but it is felt that all normal fabrication processes of a laminated transparency are included in these averages. It is intended that these design allowables be used by the designer for bird strike analysis and for selection of materials where the specific processor is unknown.

The developed averages and proposed design allowables data are presented in Table 23. The average and proposed design allowable stress-strain curves from which the tabulated data was derived are presented in Appendix D, Figure D47 through D52. Experimental test data, test stress-strain curves, and computer data for this analysis are contained in Part 2, Appendix L.

CONCLUSIONS

Conclusions based on data contained in this section and other applicable data are contained in Section XI of this report.

TABLE 23. PROPOSED TENSILE DESIGN ALLOWABLES

TEST SPECIMEN IDENT.	NO.	THICK-NESS (IN.)	TEST TEMP (°F)	STRAIN RATE (IN/IN SEC)	AVERAGE STRENGTH DATA									DESIGN ALLOWABLE					
					YIELD (PSI)	STD DEV (PSI)	SEC YLD MOD (PSI x 10^{-5})	ULTIMATE				ELAST MOD (PSI x 10^{-5})	STD DEV (PSI x 10^{-5})	DES BAS	YIELD (PSI)	SEC YLD MOD (PSI x 10^{-5})	ULTIMATE		ELAST MOD (PSI x 10^{-5})
								TRUE STRESS (PSI)	STD DEV (PSI)	TRUE STRAIN (IN/IN)	STD DEV (IN/IN)						TRUE STRESS (PSI)	TRUE STRAIN (IN/IN)	
SKE01		0.20																	
SMU601		0.20																	
TEX601	24	0.20	75	144	13,090	925	1.61	16,480	2358	0.527	0.101	3.89	0.38	C	12,059	1.49	13,853	0.414	3.55
SK611		0.30																	
SMU611		0.30																	
SK601		0.20																	
SMU569		0.20																	
TEX601	18	0.20	-30	102	19,353	2295	2.38	24,747	4523	0.450	0.180	4.06	0.58	C	16,597	2.04	19,315	0.234	3.41
SK611		0.30																	
SMU611		0.30																	
SKE01		0.20																	
SMU601		0.20																	
TEX601	22	0.20	190	170	10,805	790	1.76	12,105	1886	0.573	0.097	3.28	0.42	C	9,905	1.61	9,958	0.463	2.85
SK611		0.30																	
SMU611		0.30																	

* Number of specimens included in the generation of data presented.

APPENDIX D

TENSILE STRESS-STRAIN CURVE DATA

The following stress-strain data are presented for use in conjunction with tabulated strength data presented in the listed tables of this section.

PAGES

Table 21 (Page 286)

Tensile stress-strain curves - Figures D1 through D24 . . 229 - 322

Table 22 (Page 287)

Tensile stress-strain curves - Figures D25 through D46 . 323 - 344

Table 23 (Page 296)

Tensile stress-strain curves - Figures D47 through D52 . 345 - 350

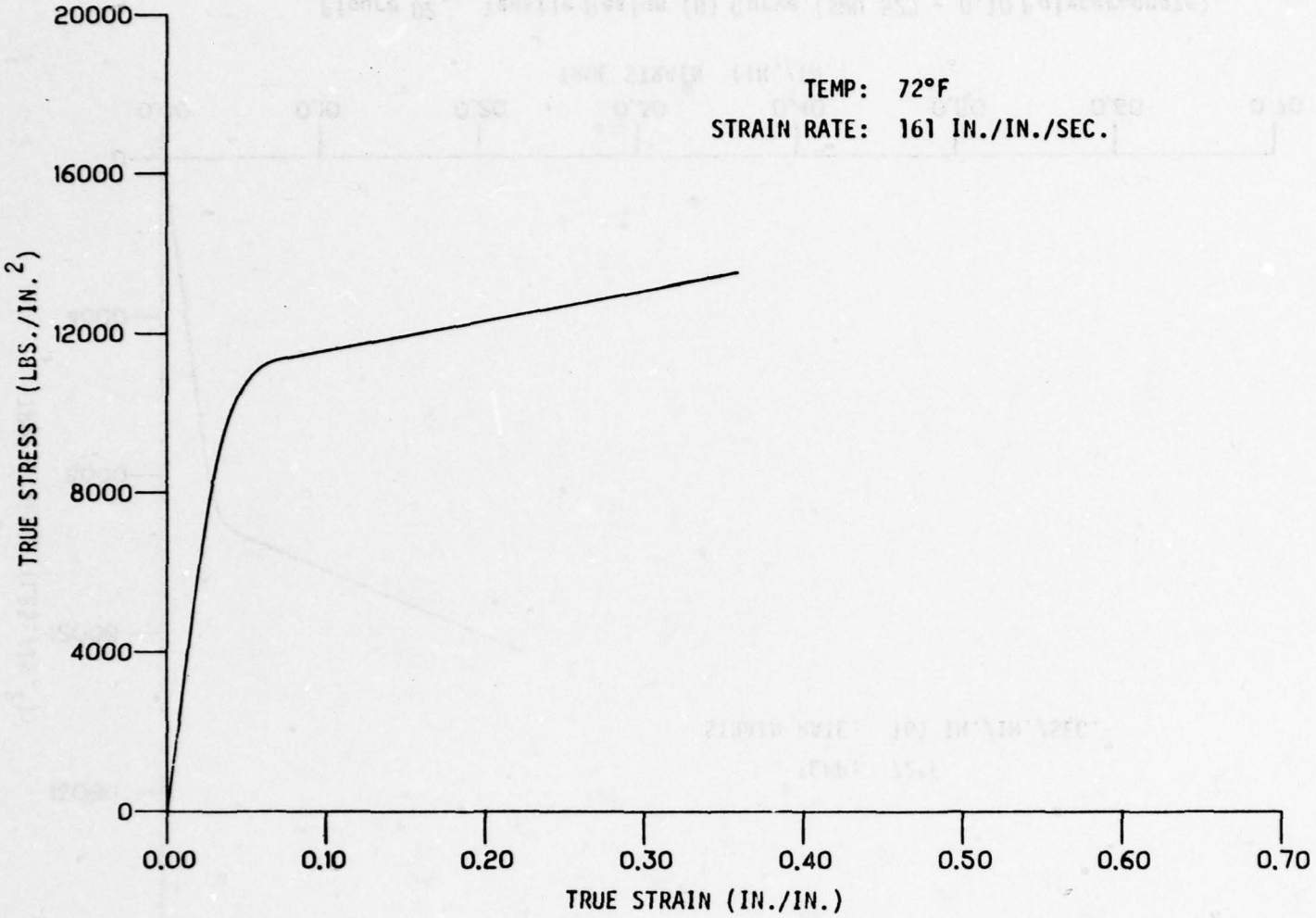

Figure D1. Tensile Average Curve (SWU 523 - 0.10 olycarbonate).

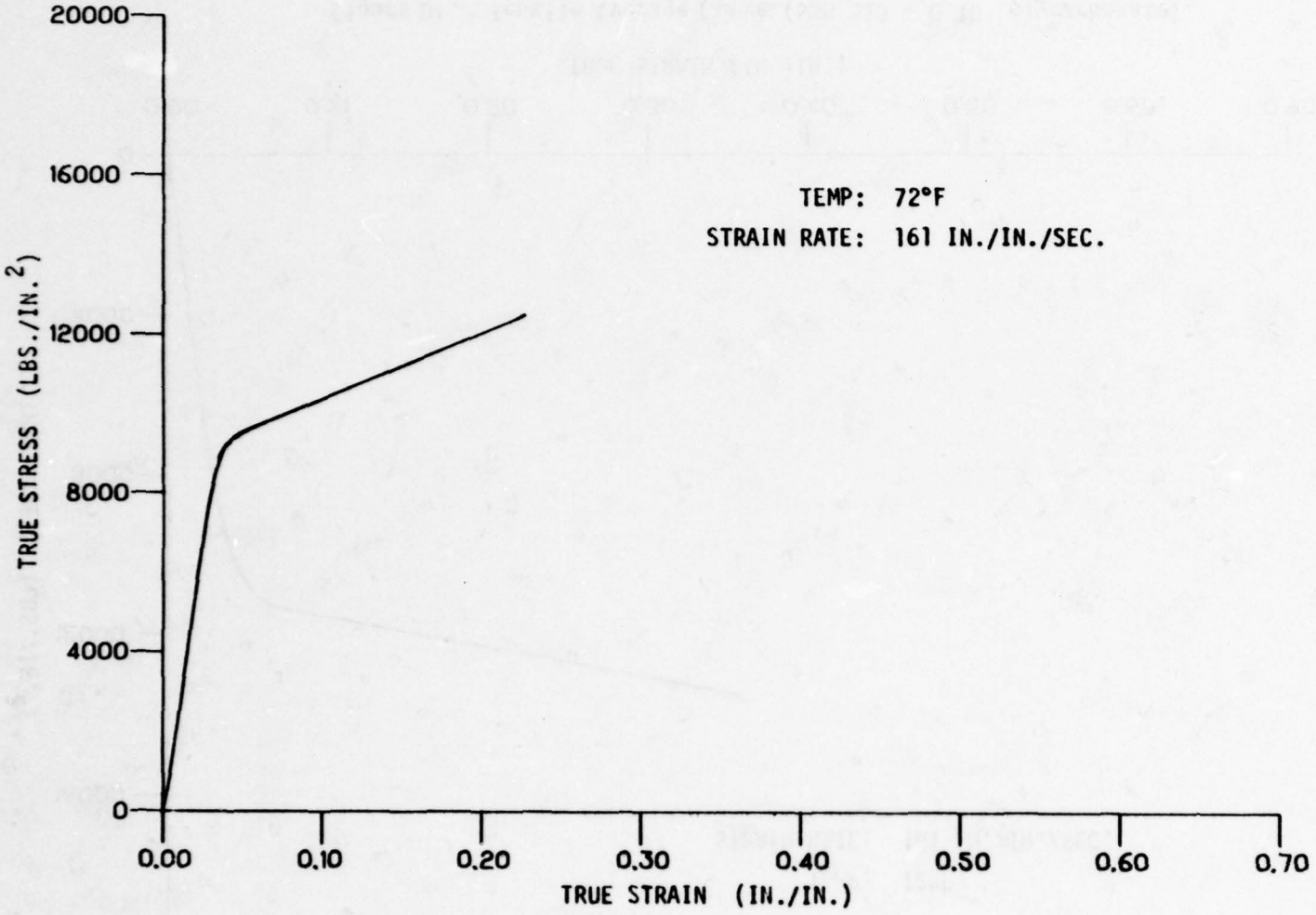

Figure 02. Tensile Design (B) Curve (SWU 523 - 0.10 Polycarbonate).

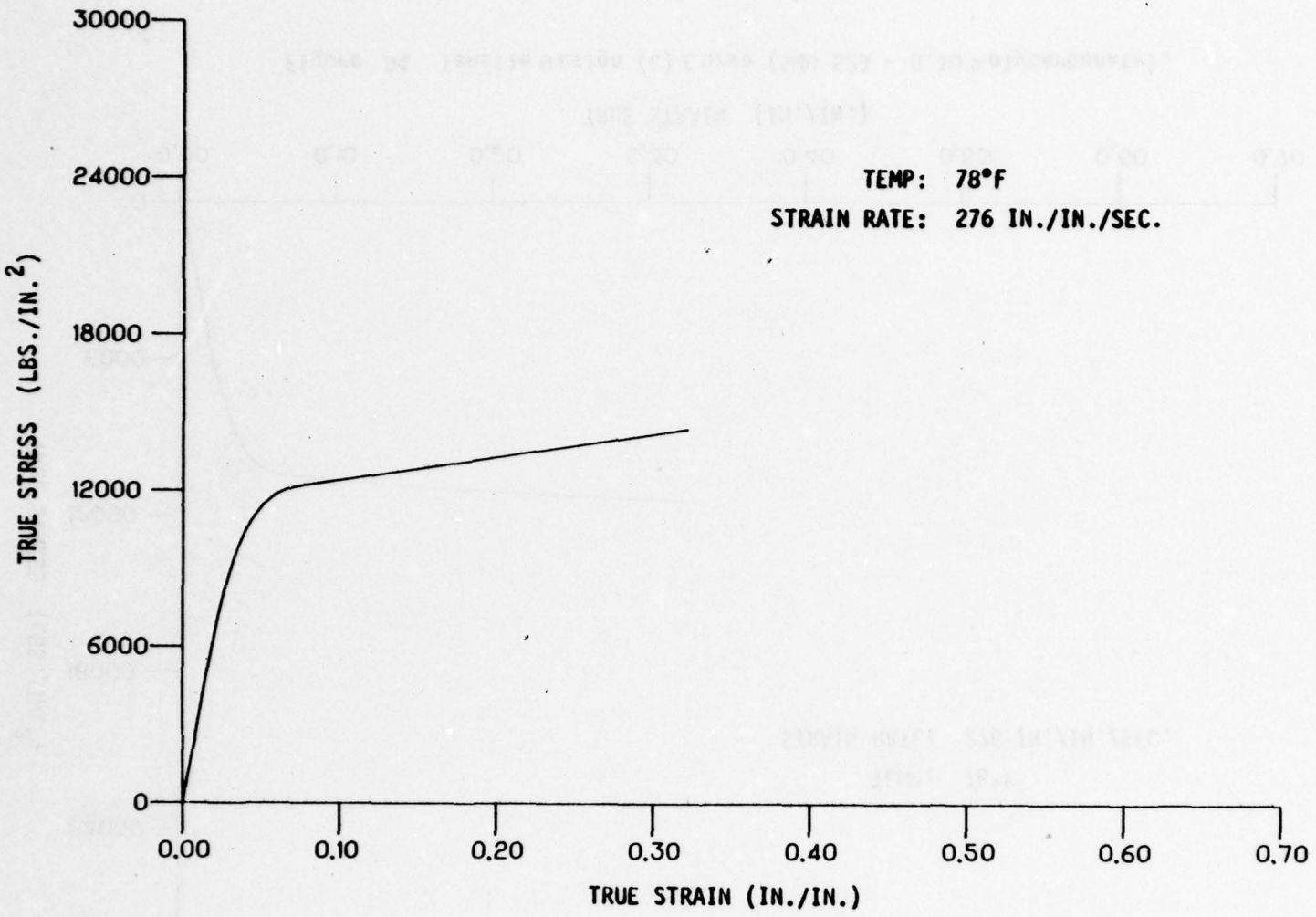

Figure D3. Tensile Average Curve (SWU 523 - 0.10 Polycarbonate).

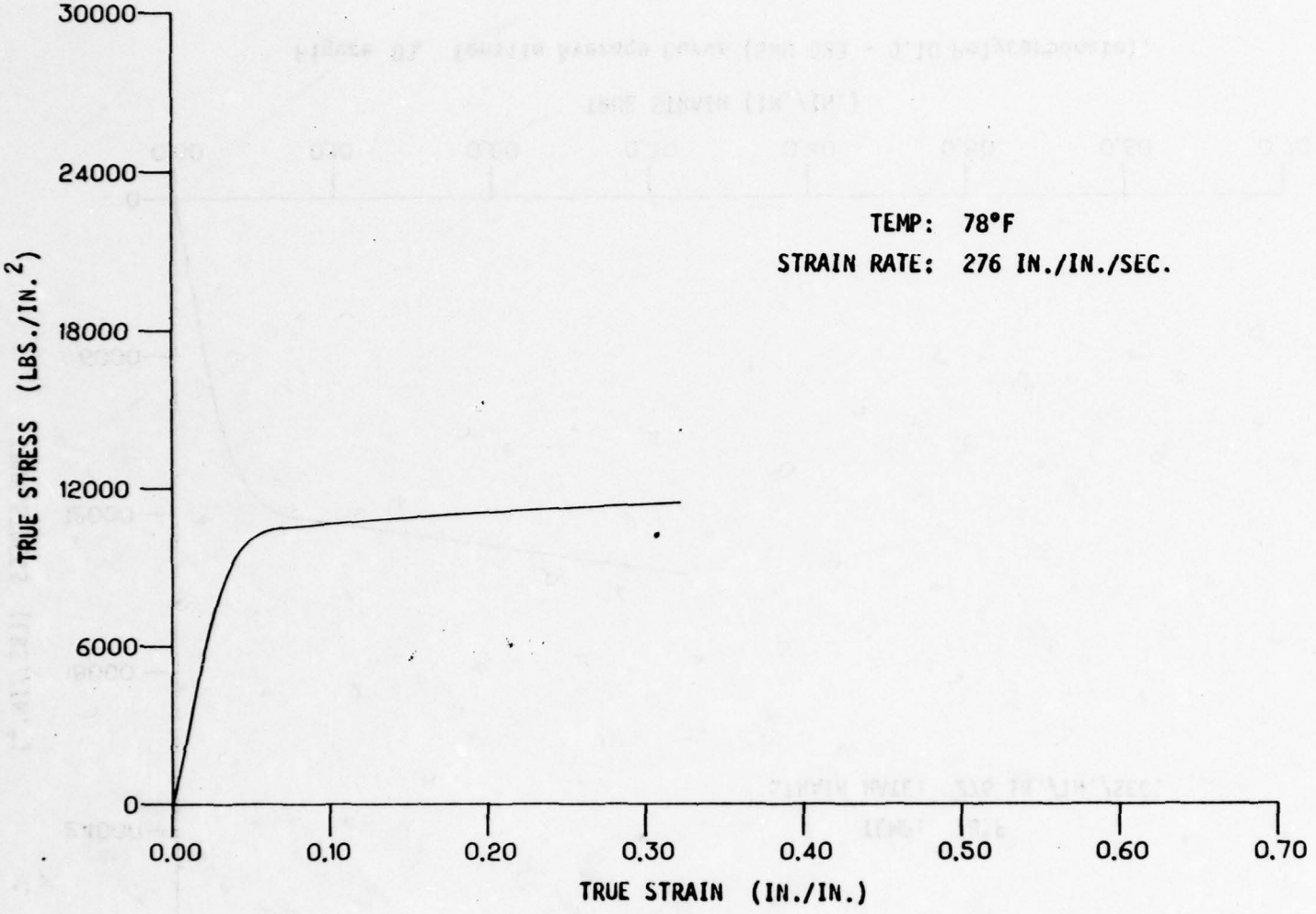

Figure D4 Tensile Design (C) Curve (SWU 523 - 0.10 Polycarbonate).

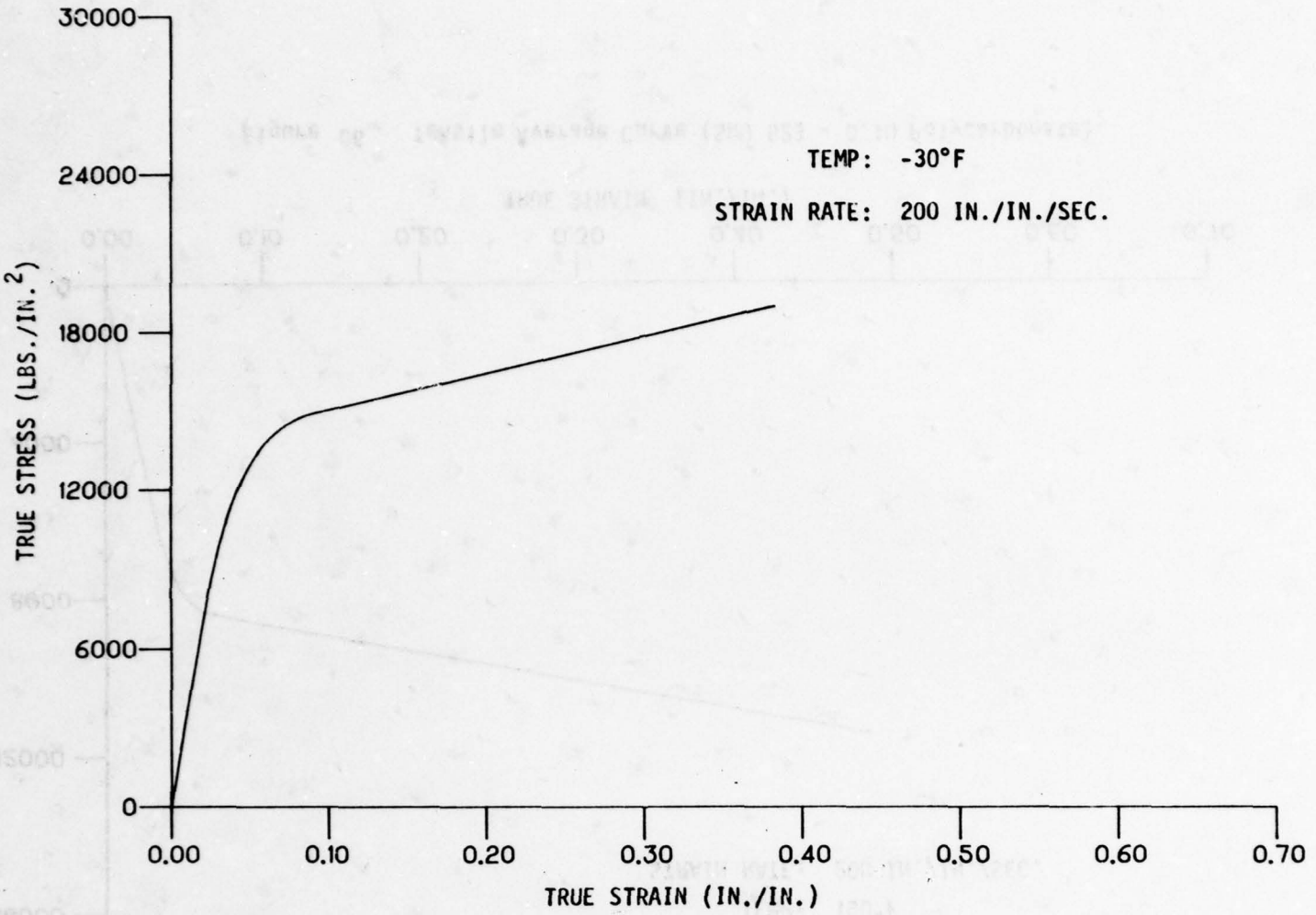

Figure D5. Tensile Average Curve (SWU 523 - 0.10 Polycarbonate).

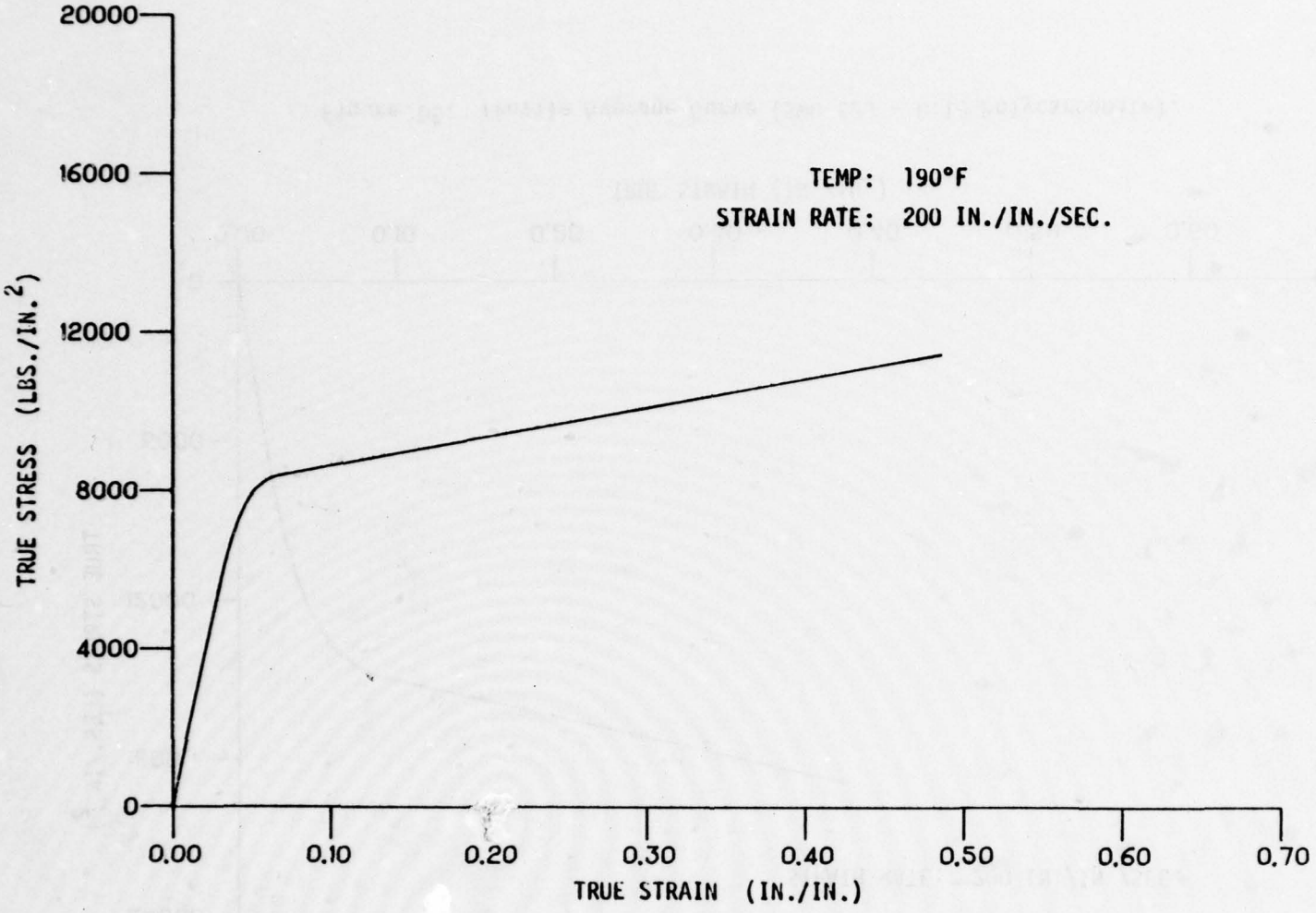

Figure D[illegible]. Tensile Average Curve (SWU 523 - 0.10 Polycarbonate).

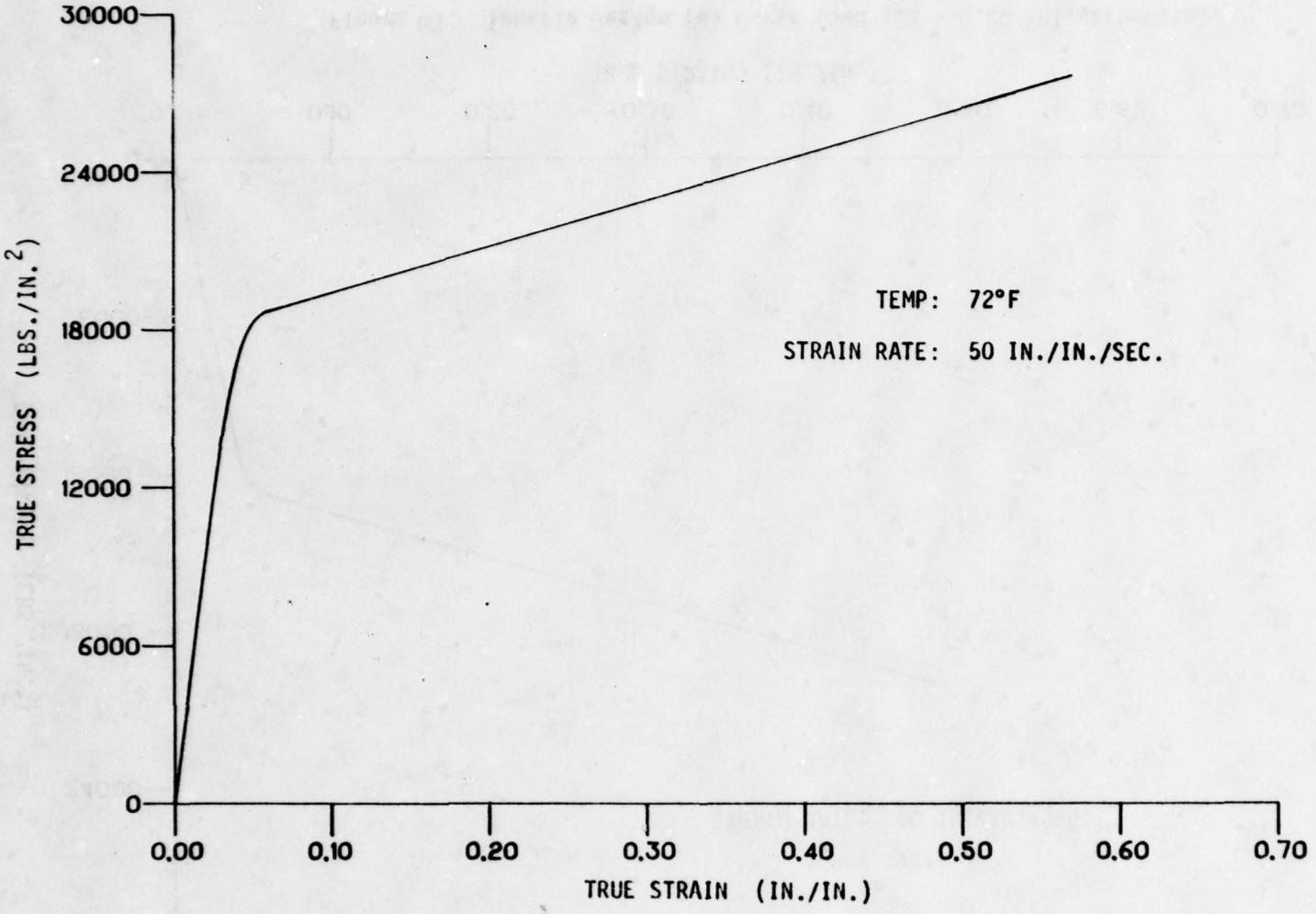

Figure D7. Tensile Average Curve (SWU 569 - 0.20 Polycarbonate).

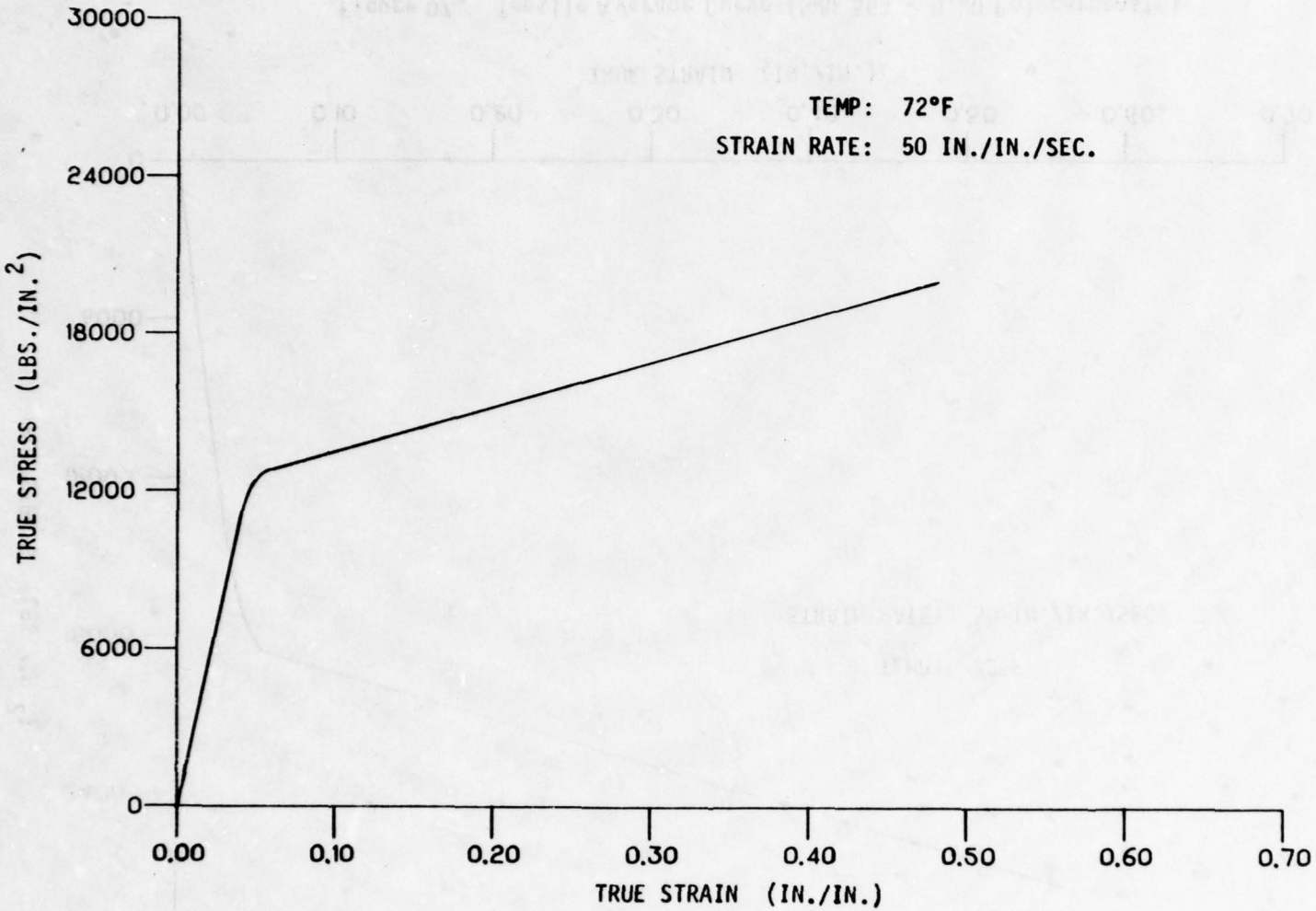

Figure D8. Tensile Design (B) Curve (SWU 569 - 0.20 Polycarbonate).

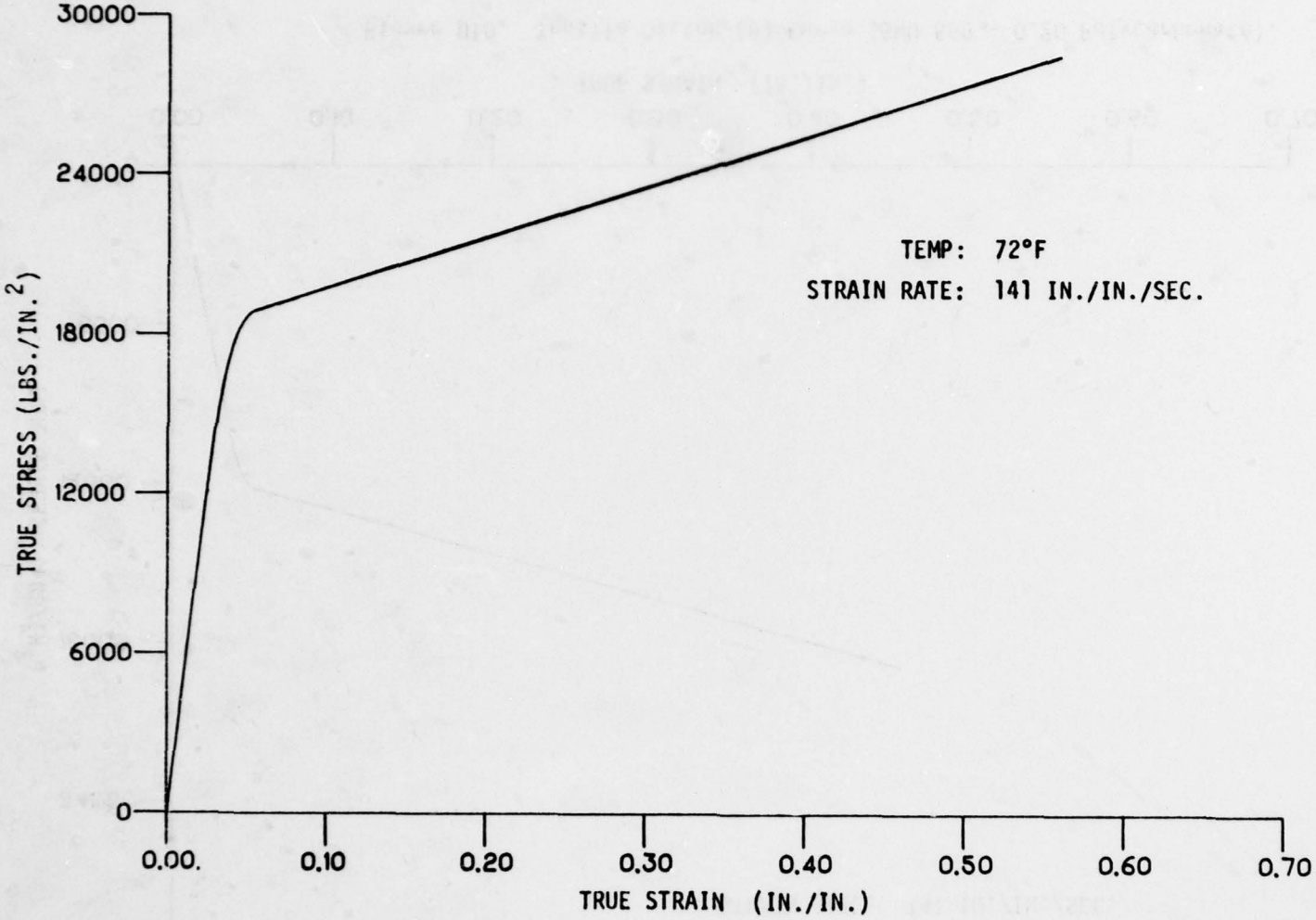

Figure D9. Tensile Average Curve (SWU 569 - 0.20 Polycarbonate).

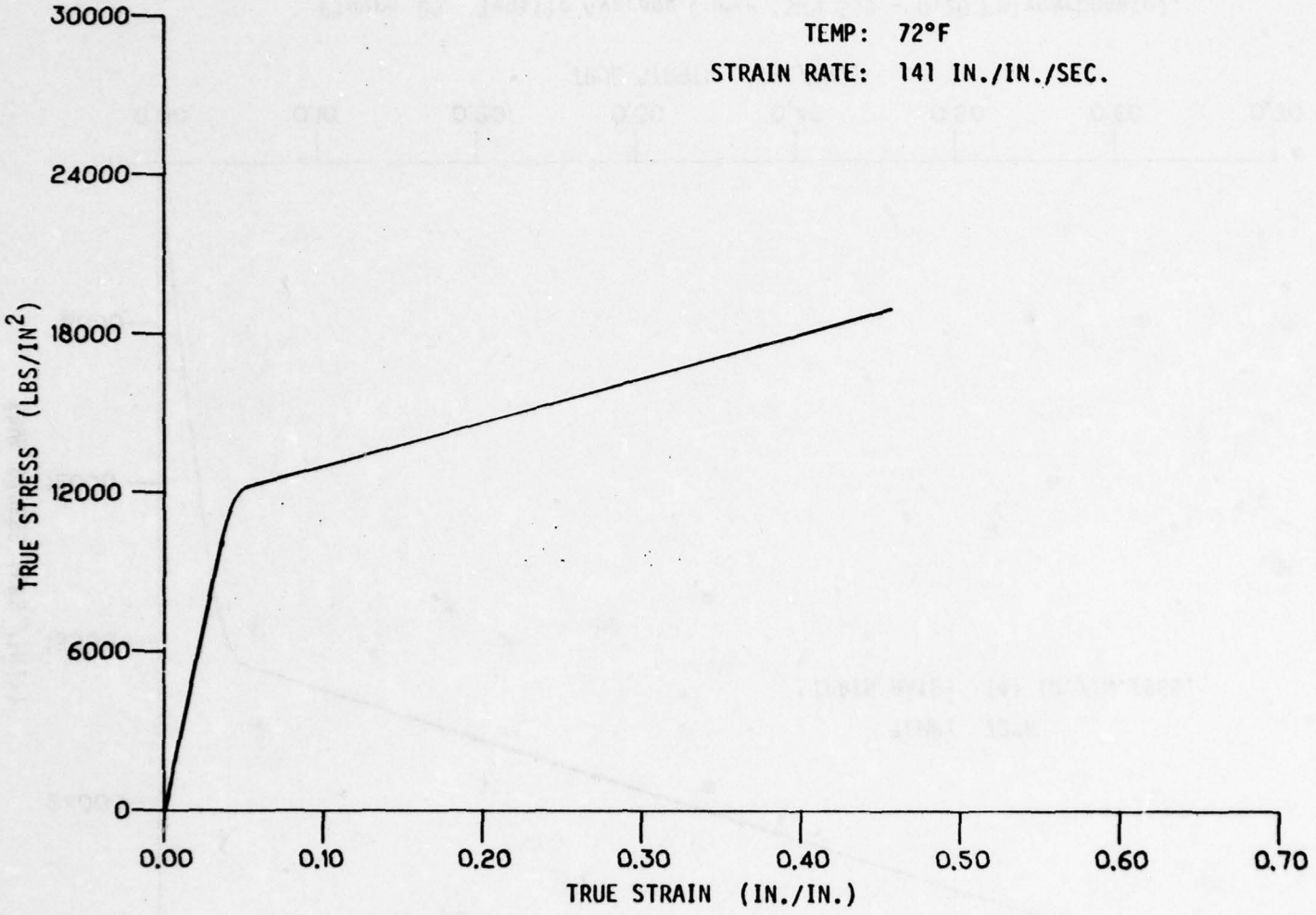

Figure D10. Tensile Design (B) Curve (SWU 569 - 0.20 Polycarbonate).

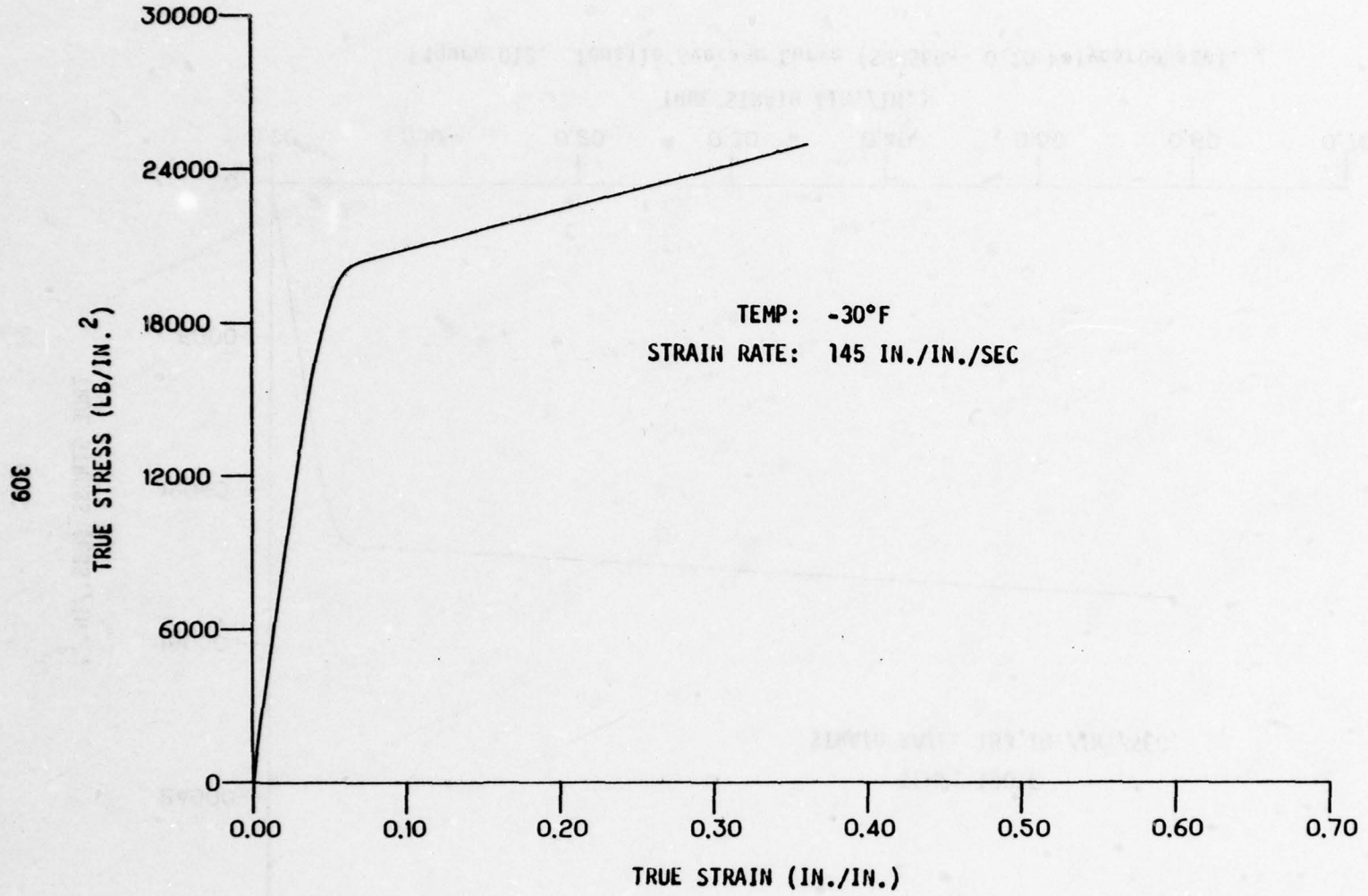

Figure D11. Tensile Average Curve (SWI569 - 0.20 Polycarbonate).

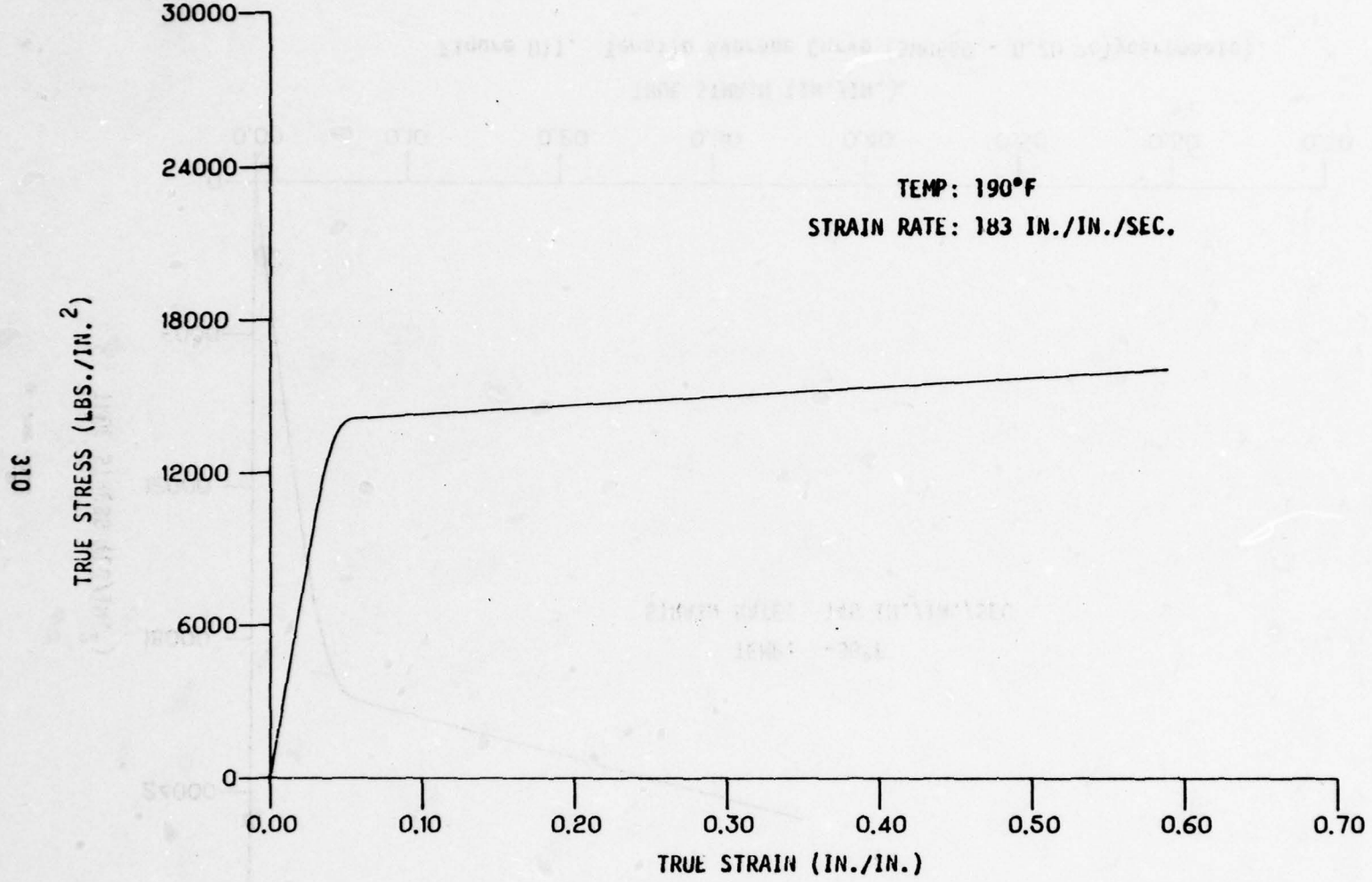

Figure D12. Tensile Average Curve (SHU569 - 0.20 Polycarbonate).

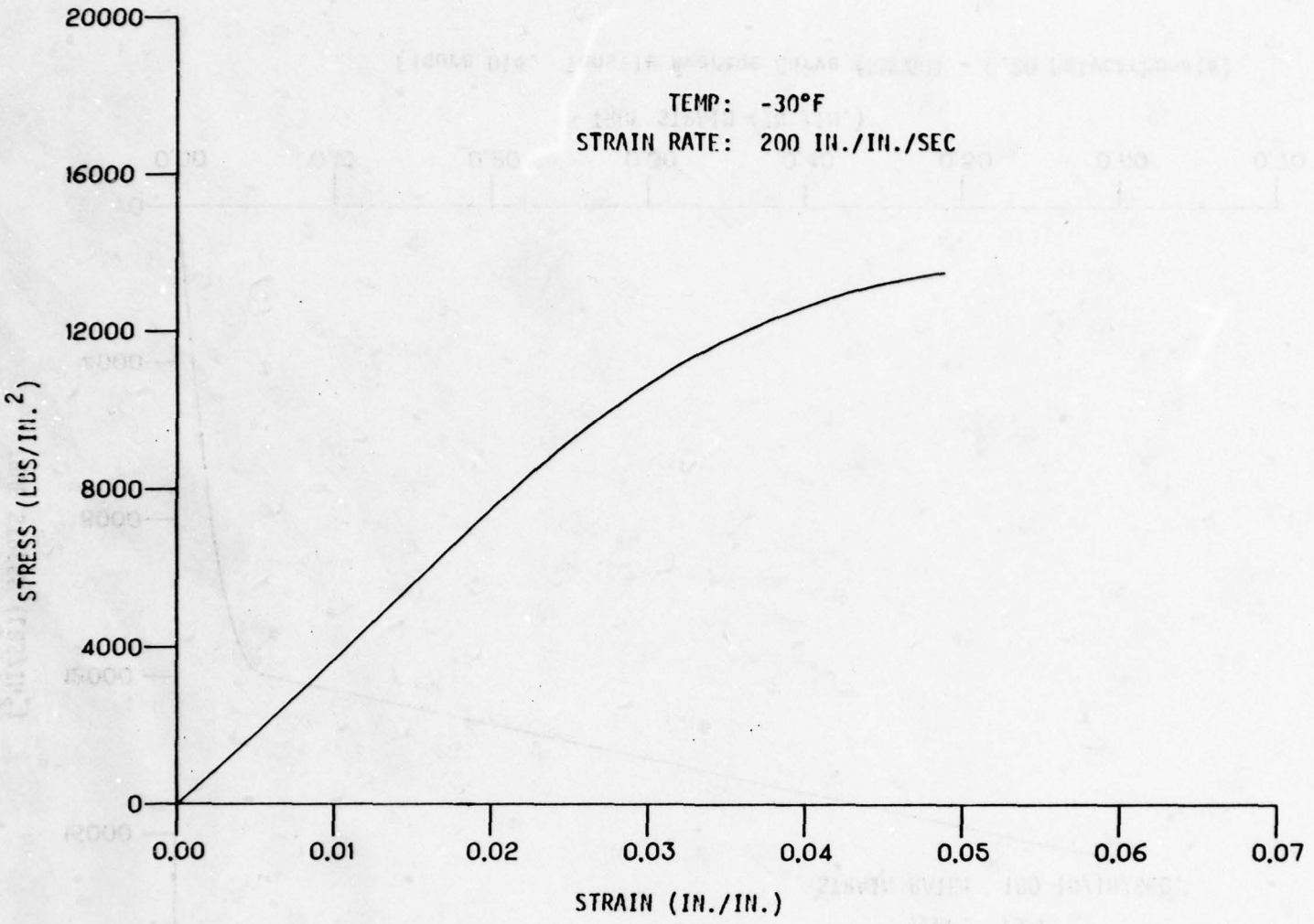

Figure D13. Tensile Average Curve (SWU601 - 0.20 Polycarbonate).

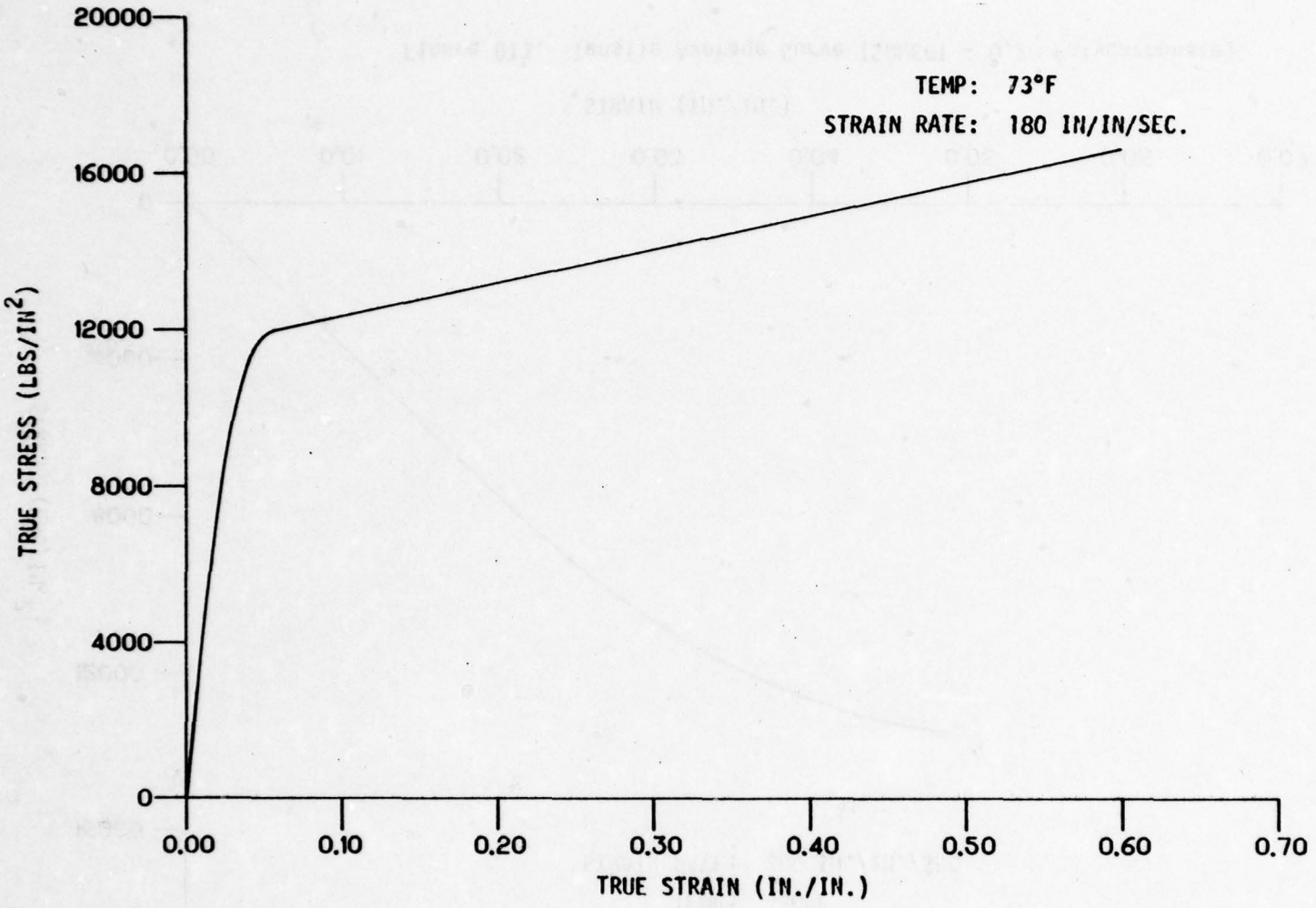

Figure D14. Tensile Average Curve (SWU601 - 0.20 Polycarbonate).

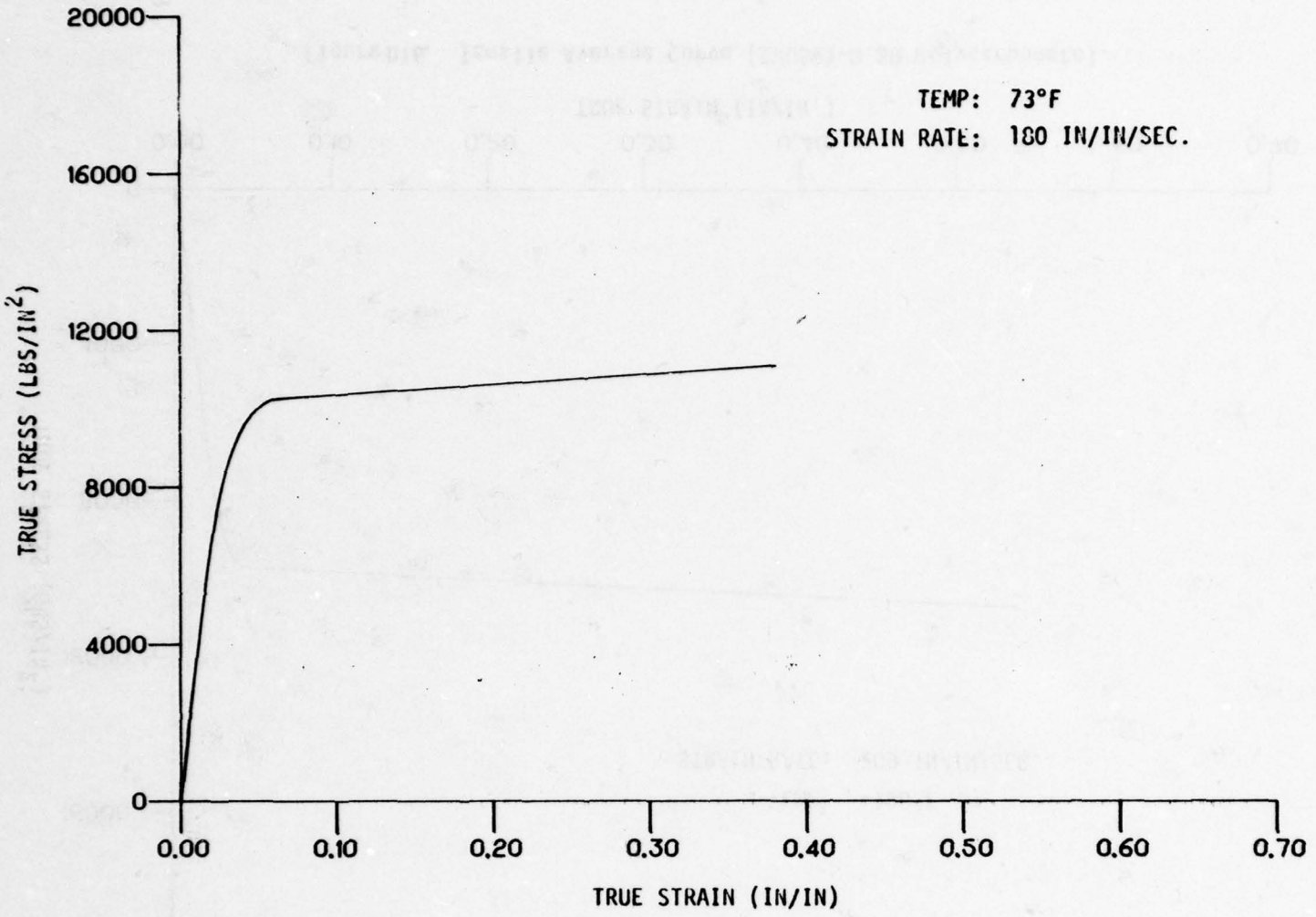

Figure D15.Tensile Design (C) Curve (SWU601 - 0.20 Polycarbonate)

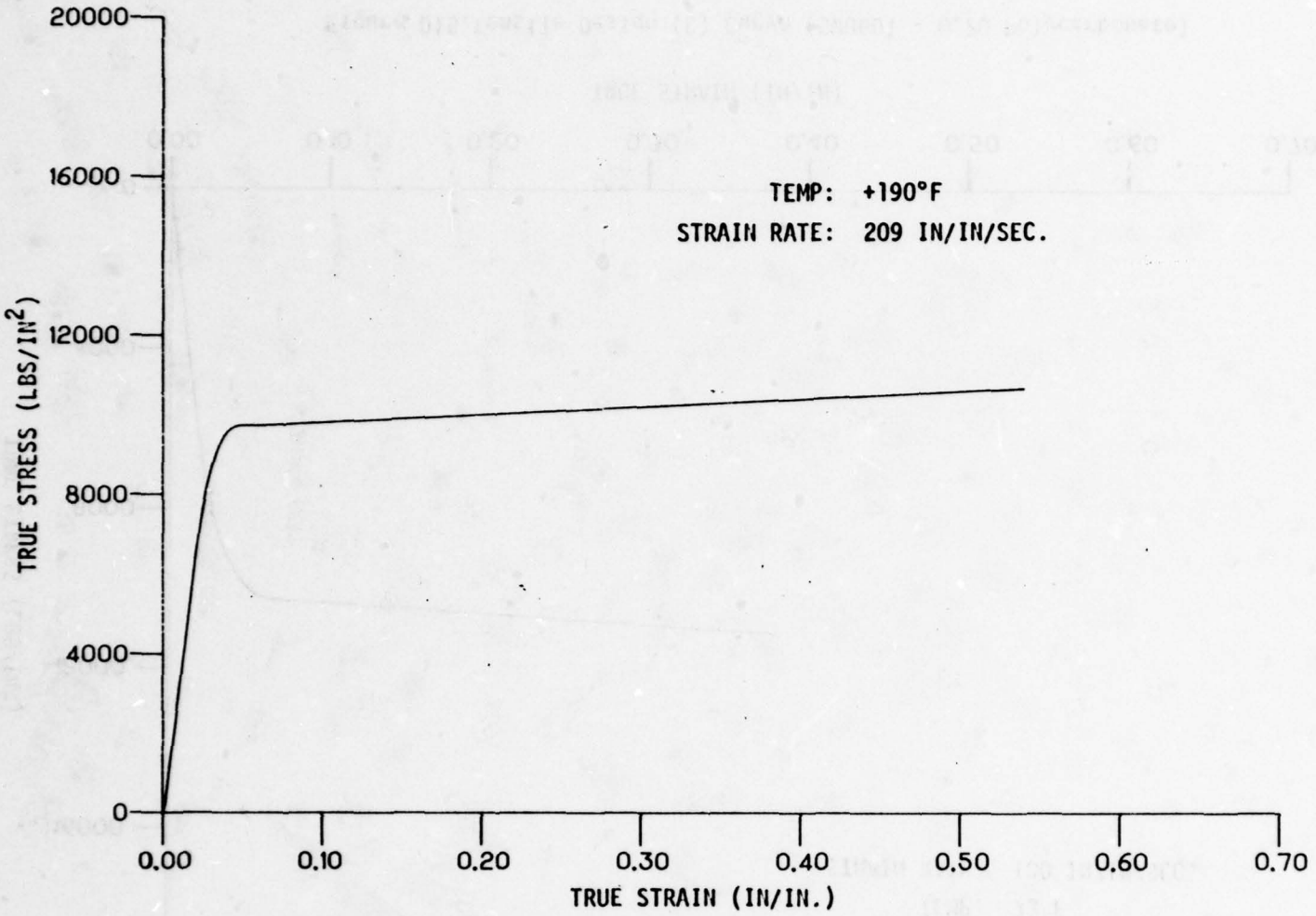

Figure D16. Tensile Average Curve (SWU601-0.20 Polycarbonate).

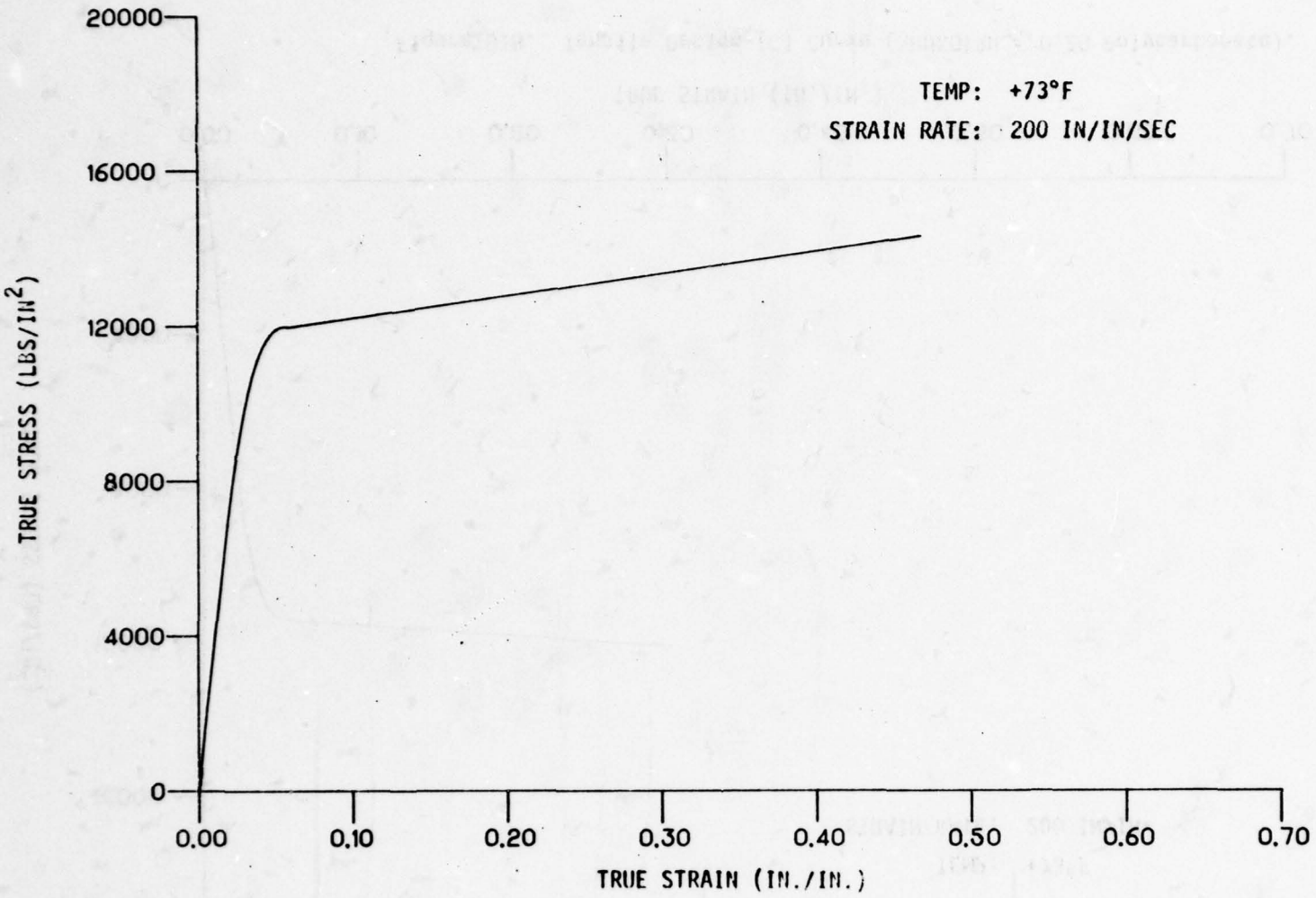

Figure D17. Tensile Average Curve (SWU601RH - 0.20 Polycarbonate).

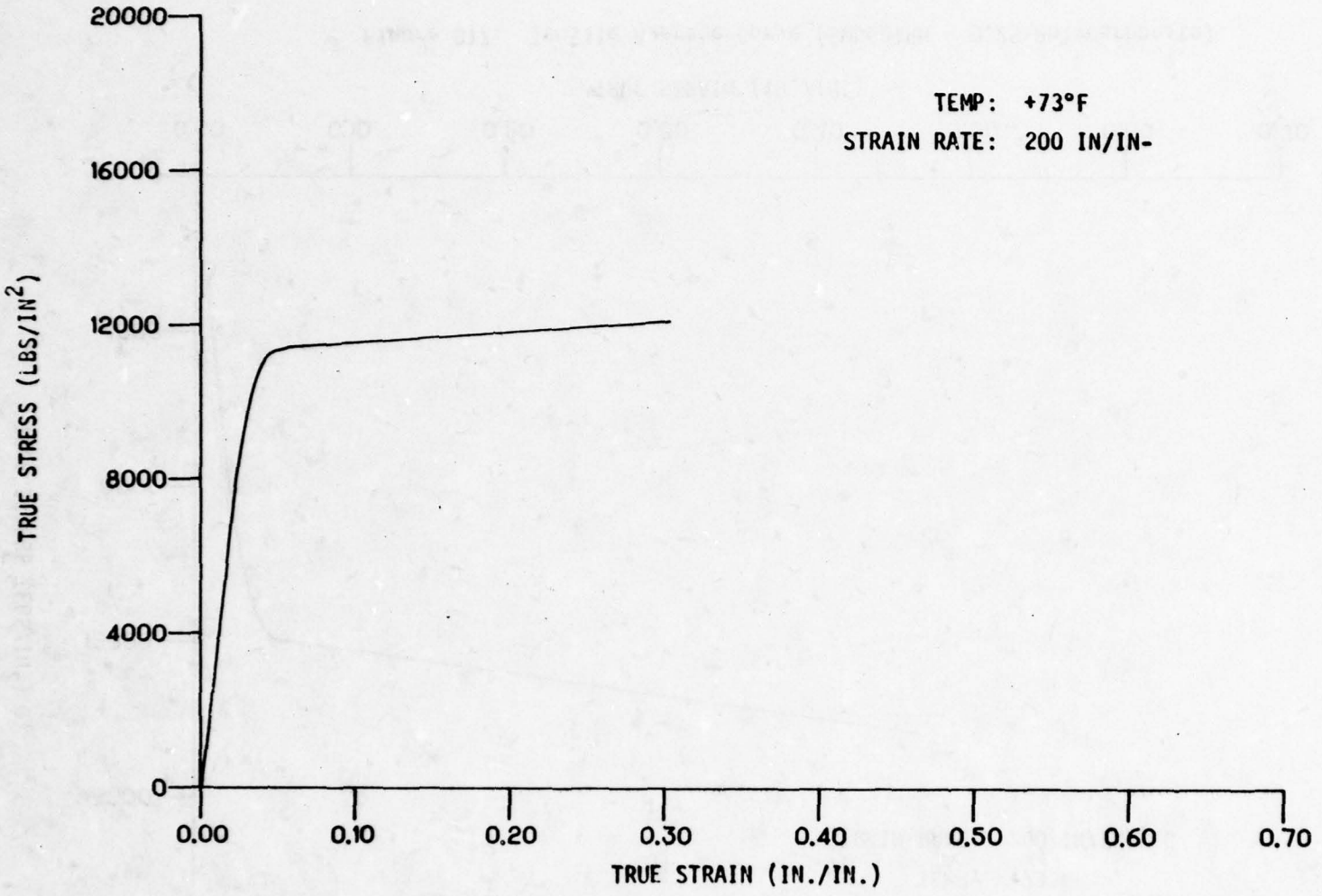

Figure D18. Tensile Design (C) Curve (SWU601RH - 0.20 Polycarbonate).

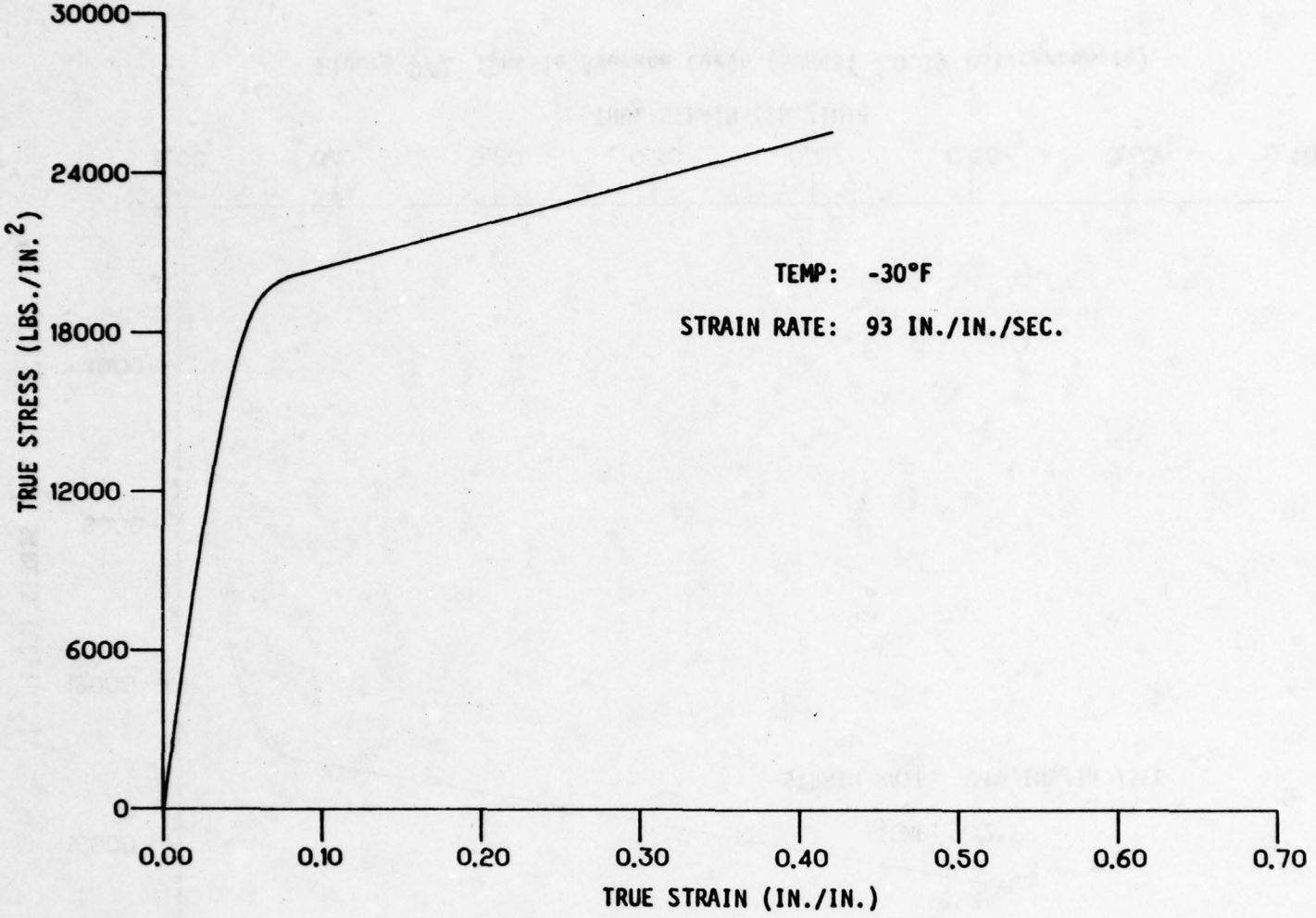

Figure D19 Tensile Average Curve (SWU 611 - 0.30 Polycarbonate)

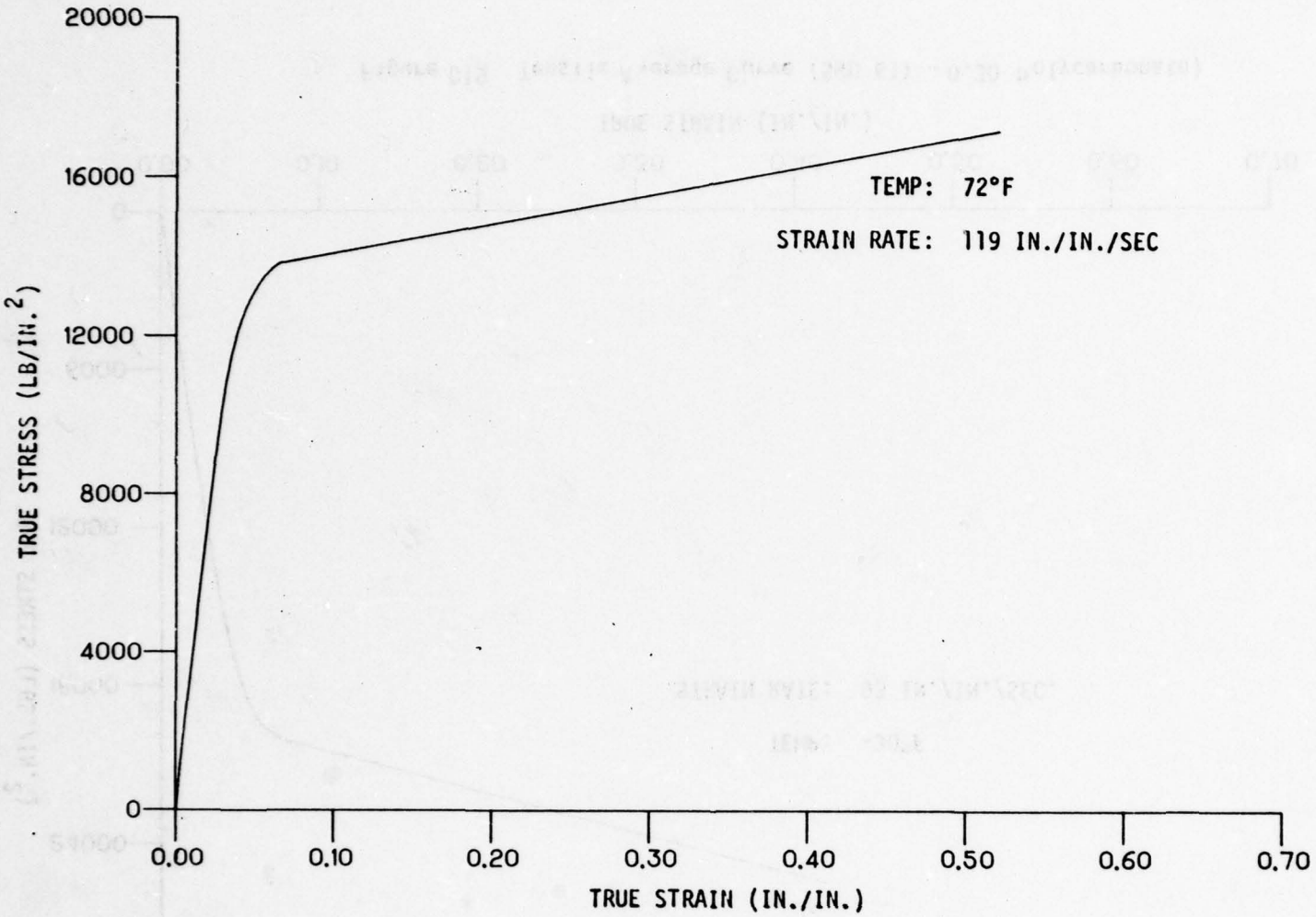

Figure D20 Tensile Average Curve (SWU611 - 0.30 Polycarbonate).

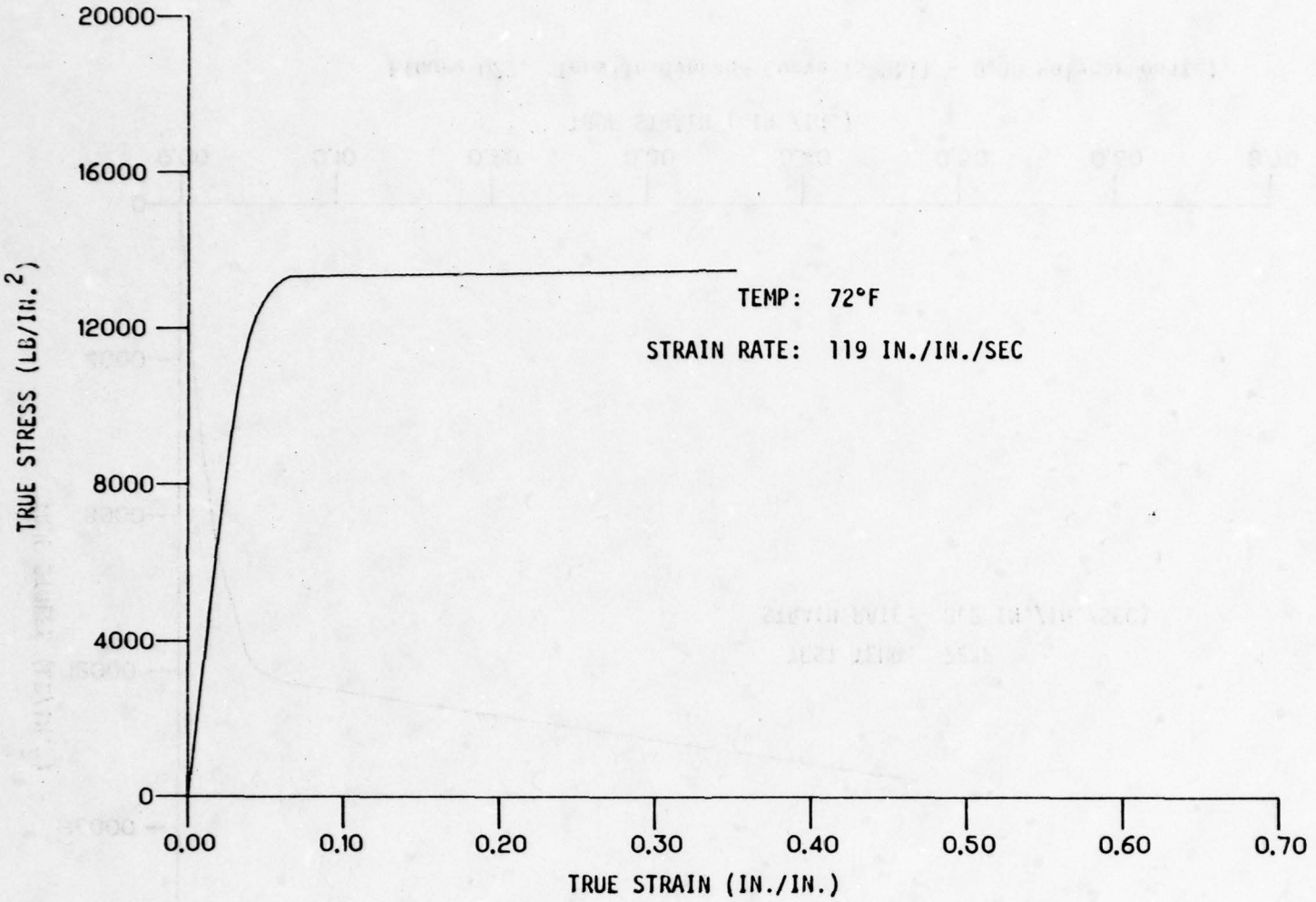

Figure D21 Tensile Design (C) Curve (SWU 611 - 0.30 Polycarbonate).

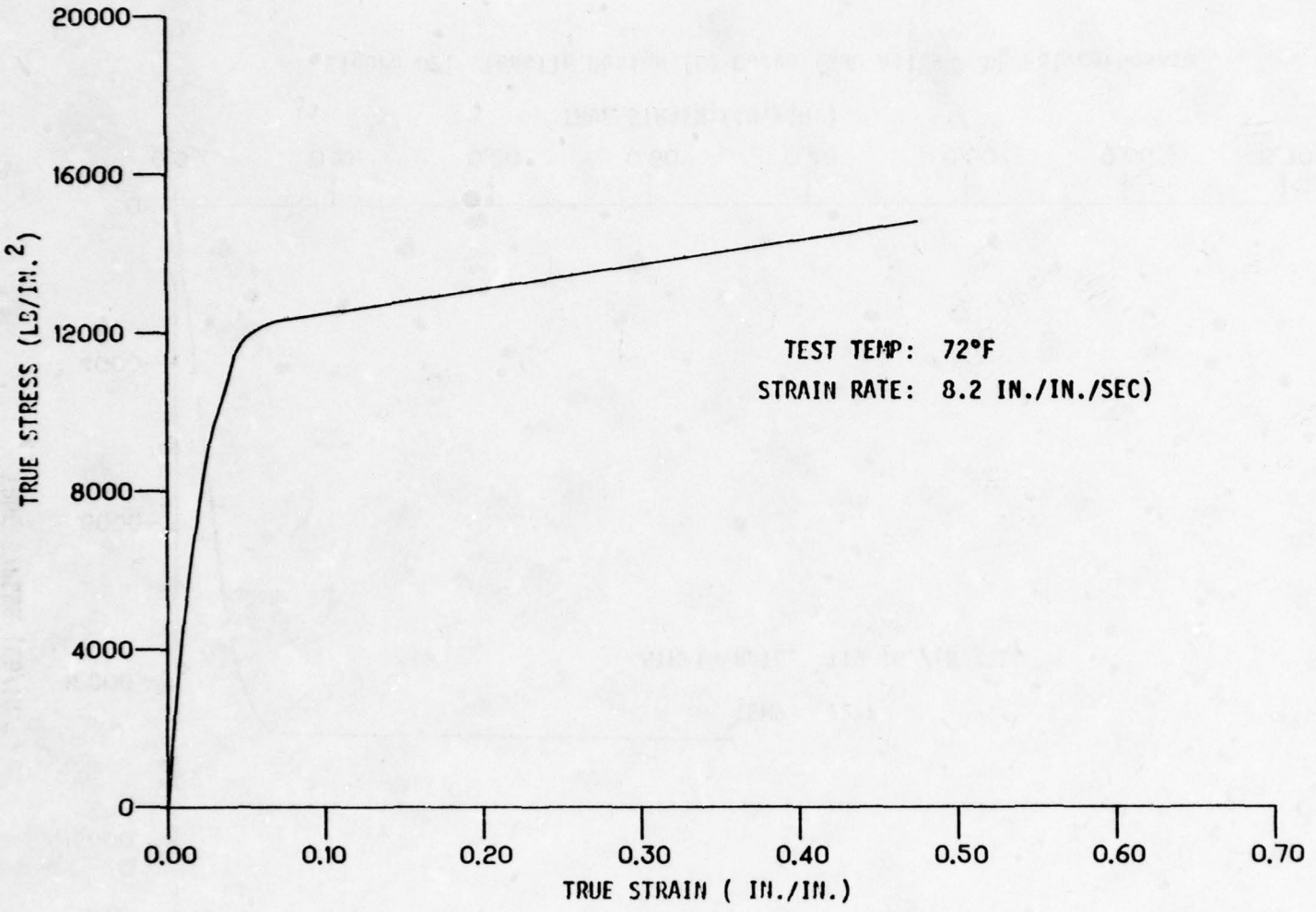

Figure D22. Tensile Average Curve (SHU611 - 0.30 Polycarbonate).

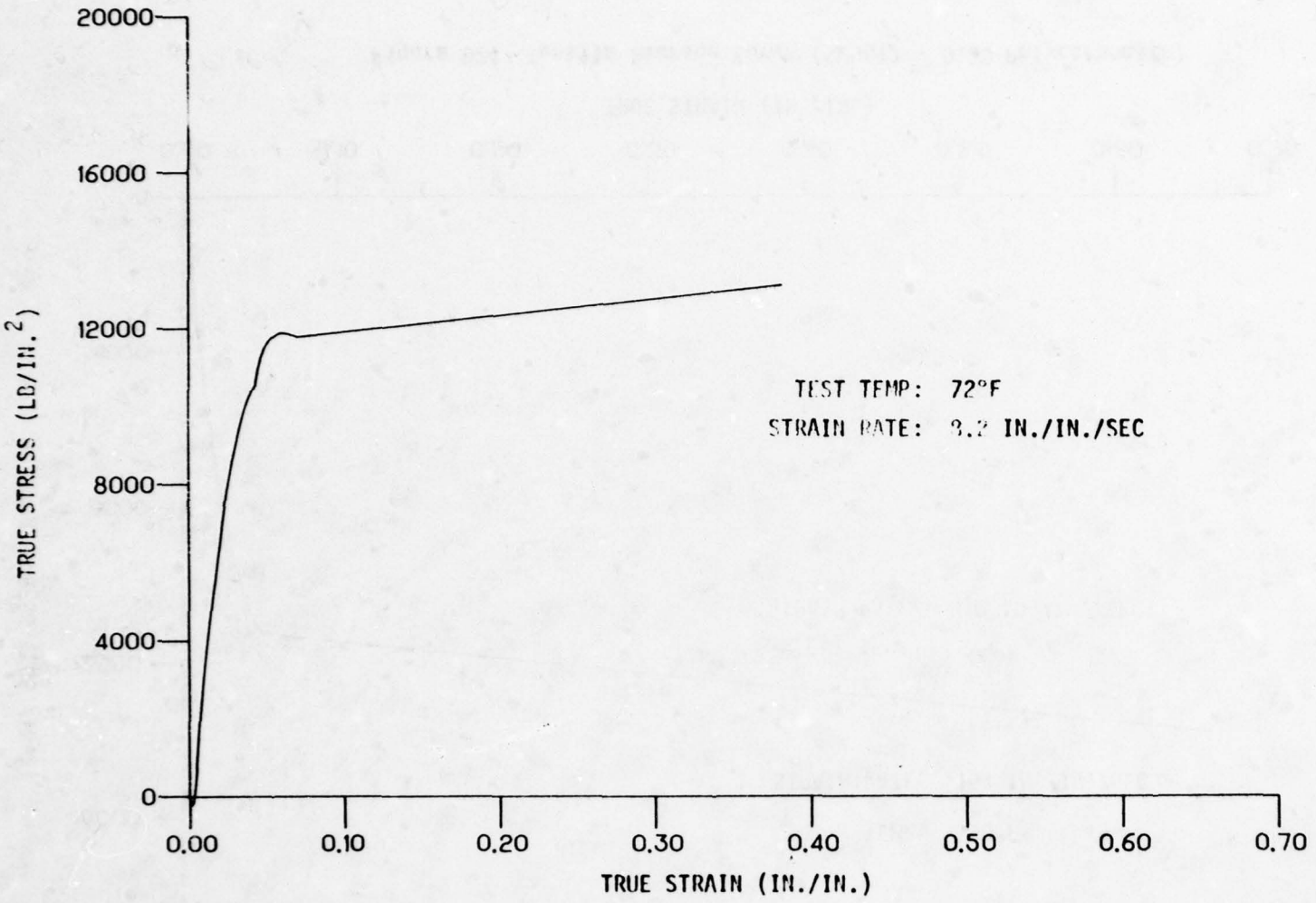

Figure D23. Tensile Design (B) Curve (SWU611 - 0.30 Polycarbonate)

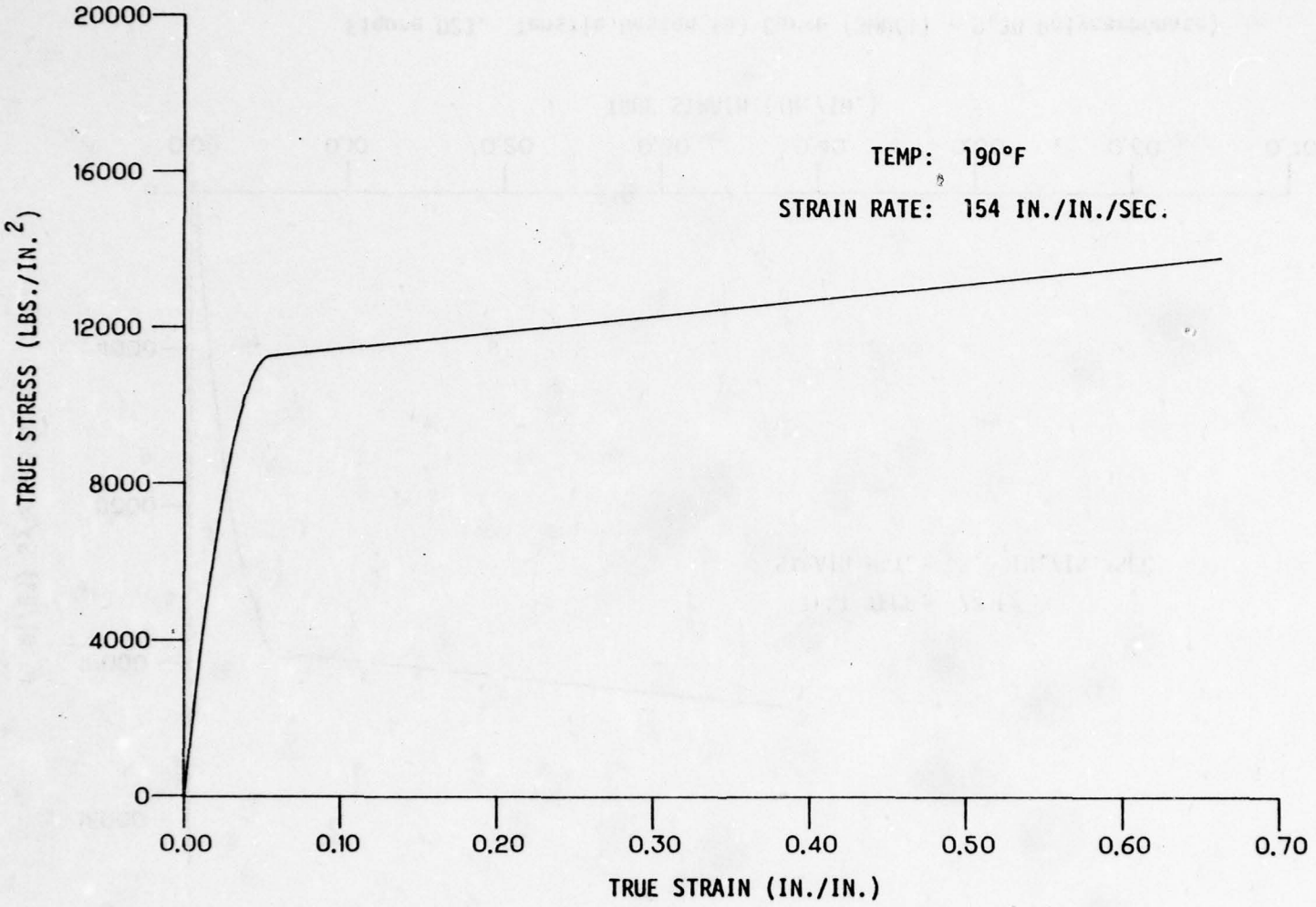

Figure D24 Tensile Average Curve (SWU611 - 0.30 Polycarbonate)

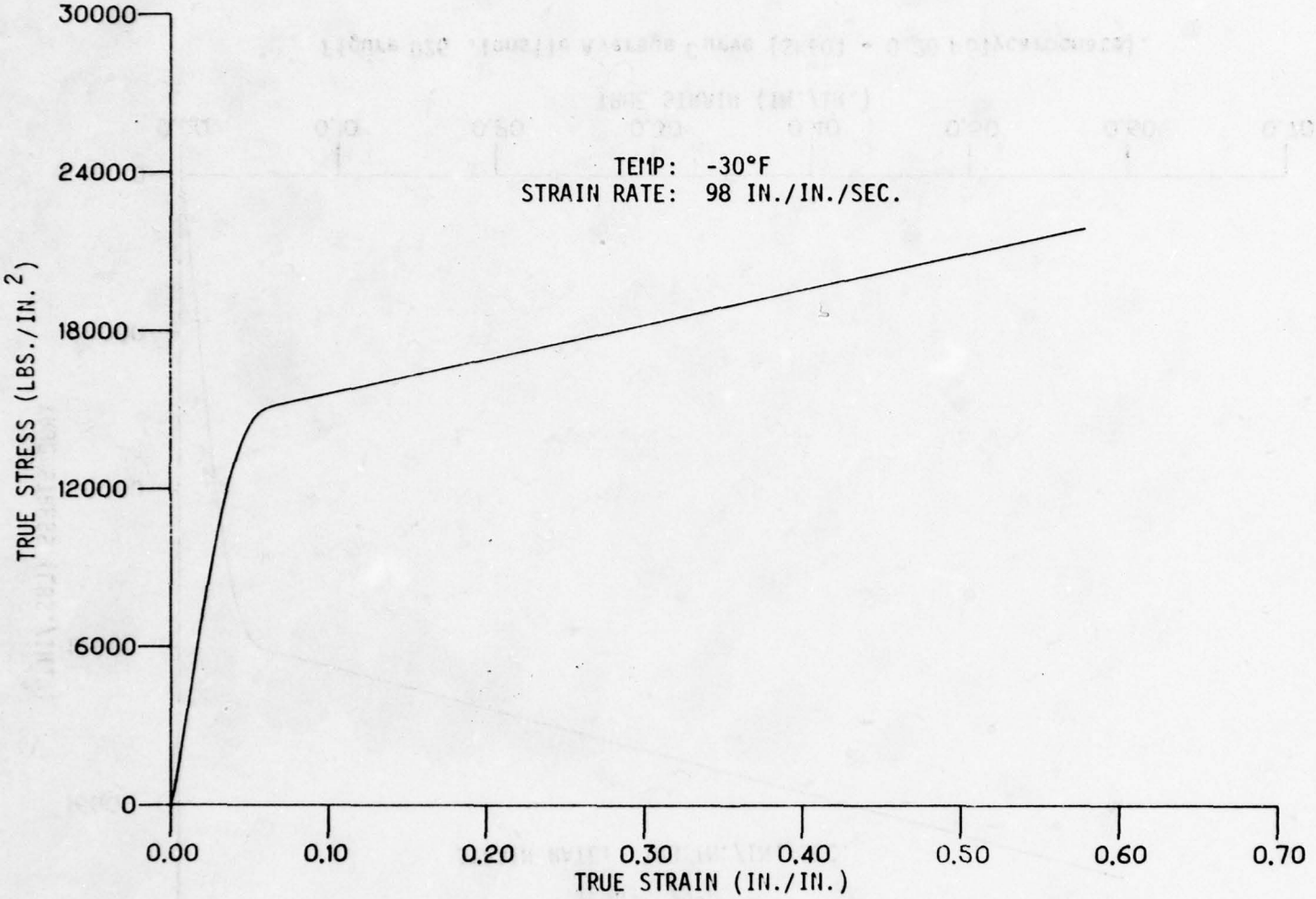

Figure D25. Tensile Average Curve (SK601 - 0.20 Polycarbonate).

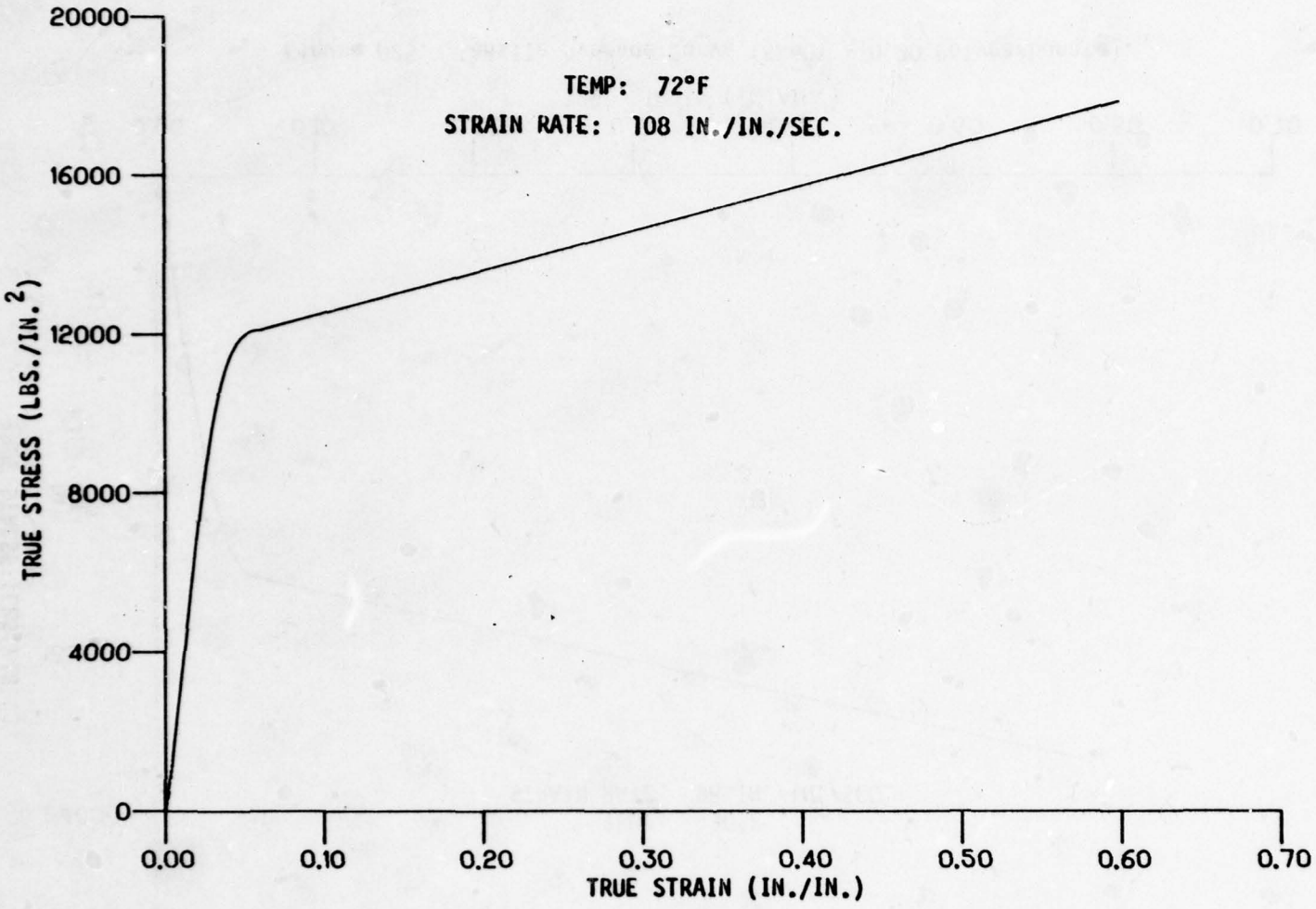

Figure D26 Tensile Average Curve (SK601 - 0.20 Polycarbonate).

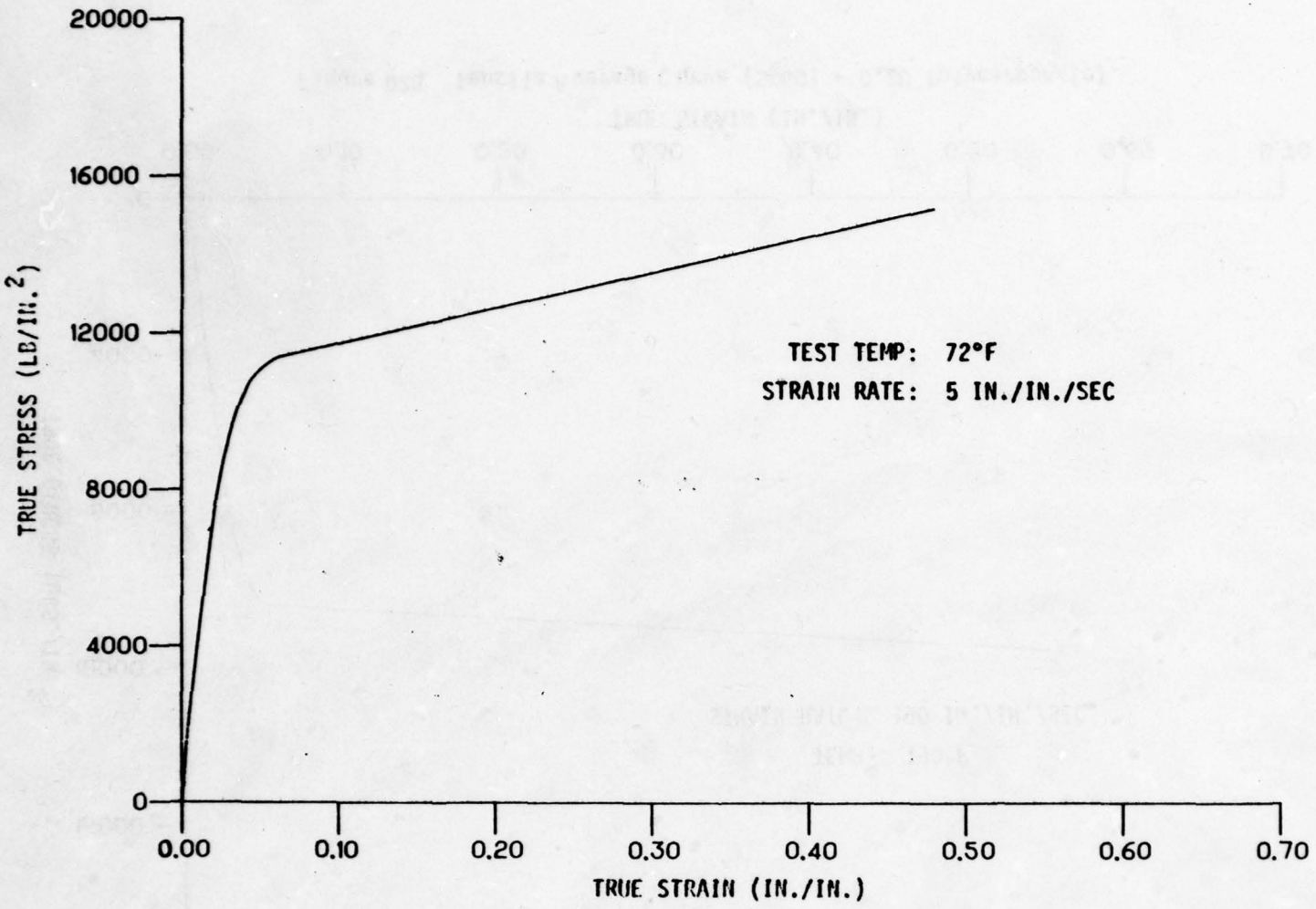

Figure D27. Tensile Average Curve (SK601 - 0.200 Polycarbonate).

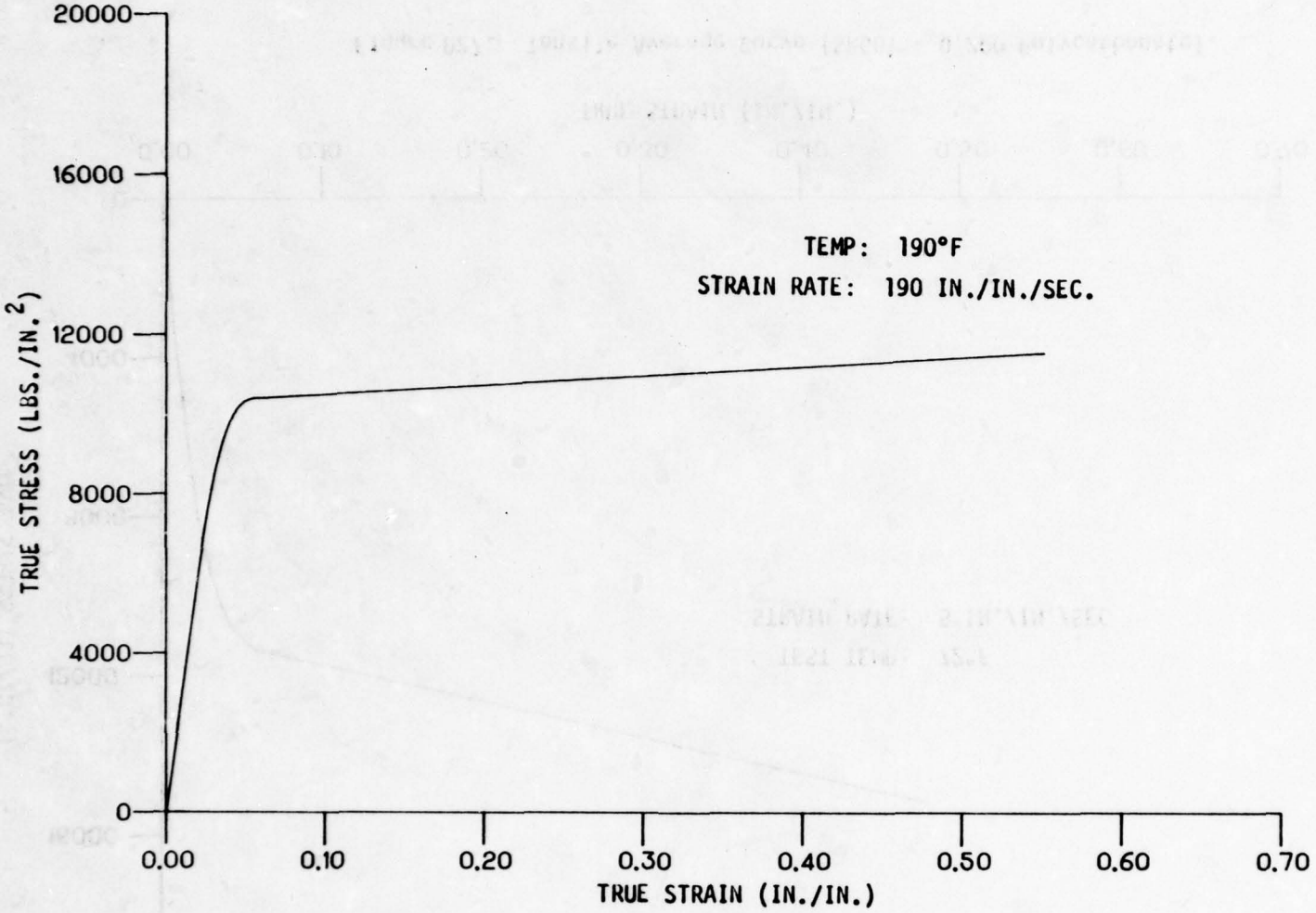

Figure D28 Tensile Average Curve (SK601 - 0.20 Polycarbonate).

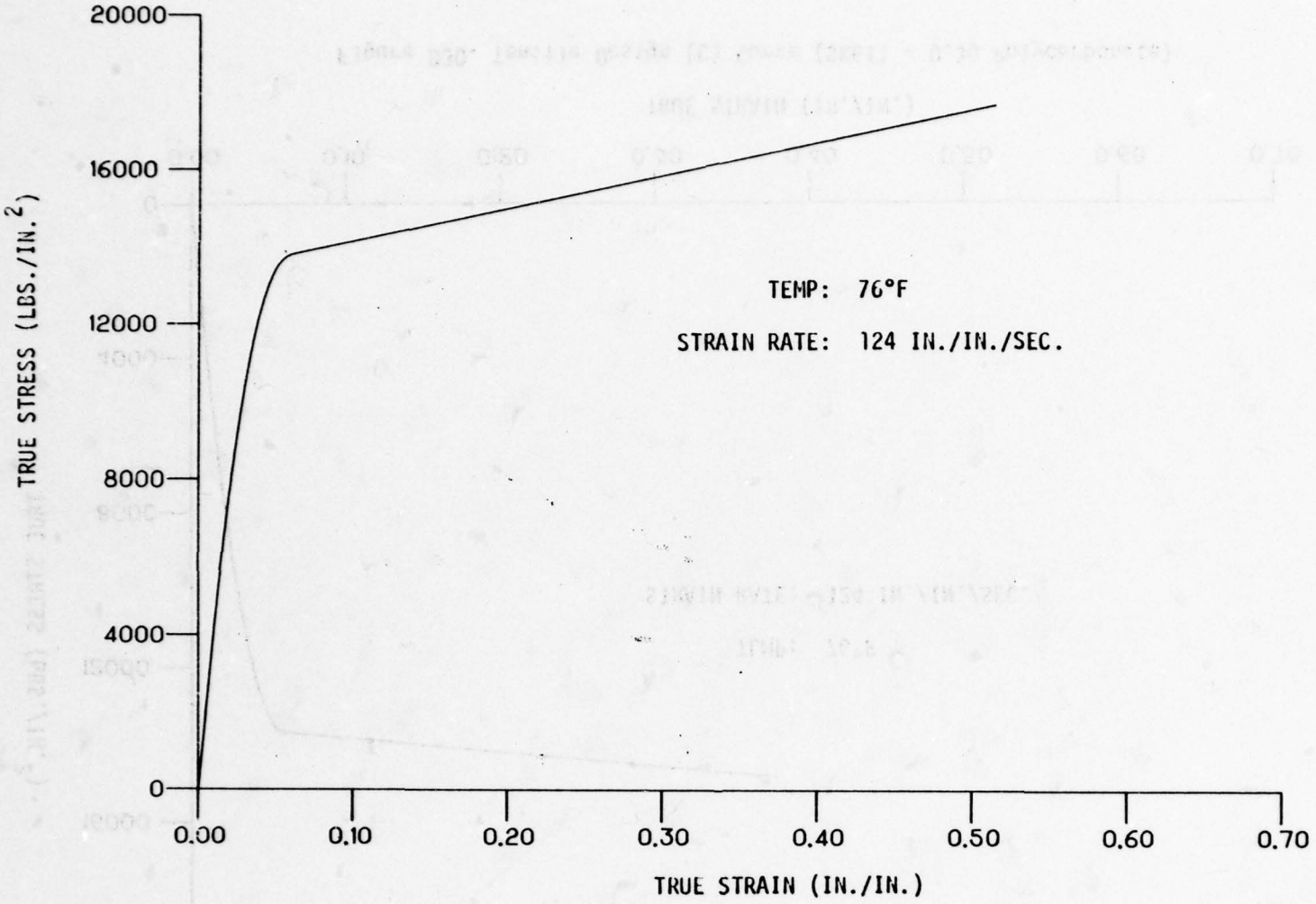

Figure D29. Tensile Average Curve (SK611 - 0.30 Polycarbonate)

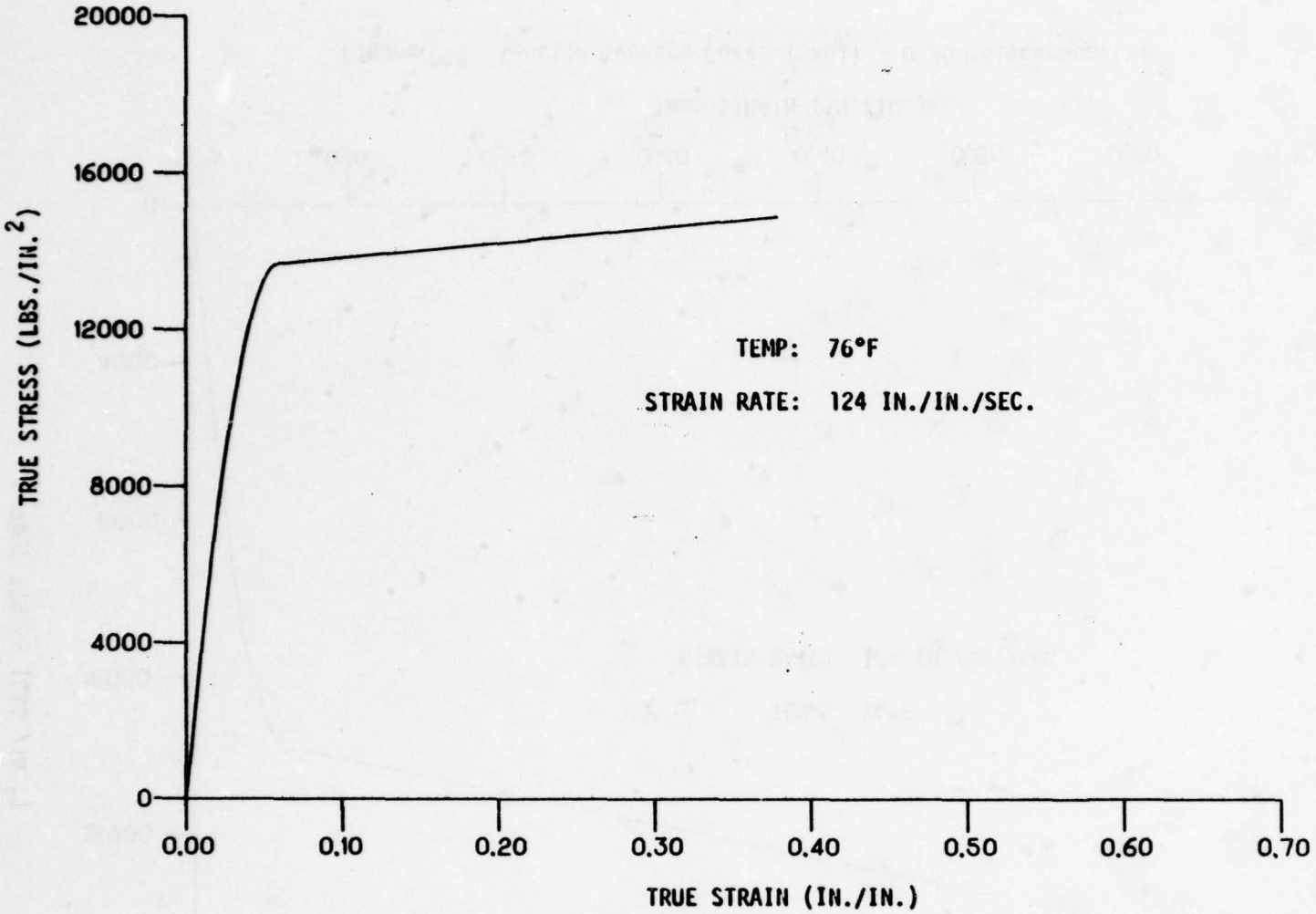

Figure D30. Tensile Design (C) Curve (SK611 - 0.30 Polycarbonate)

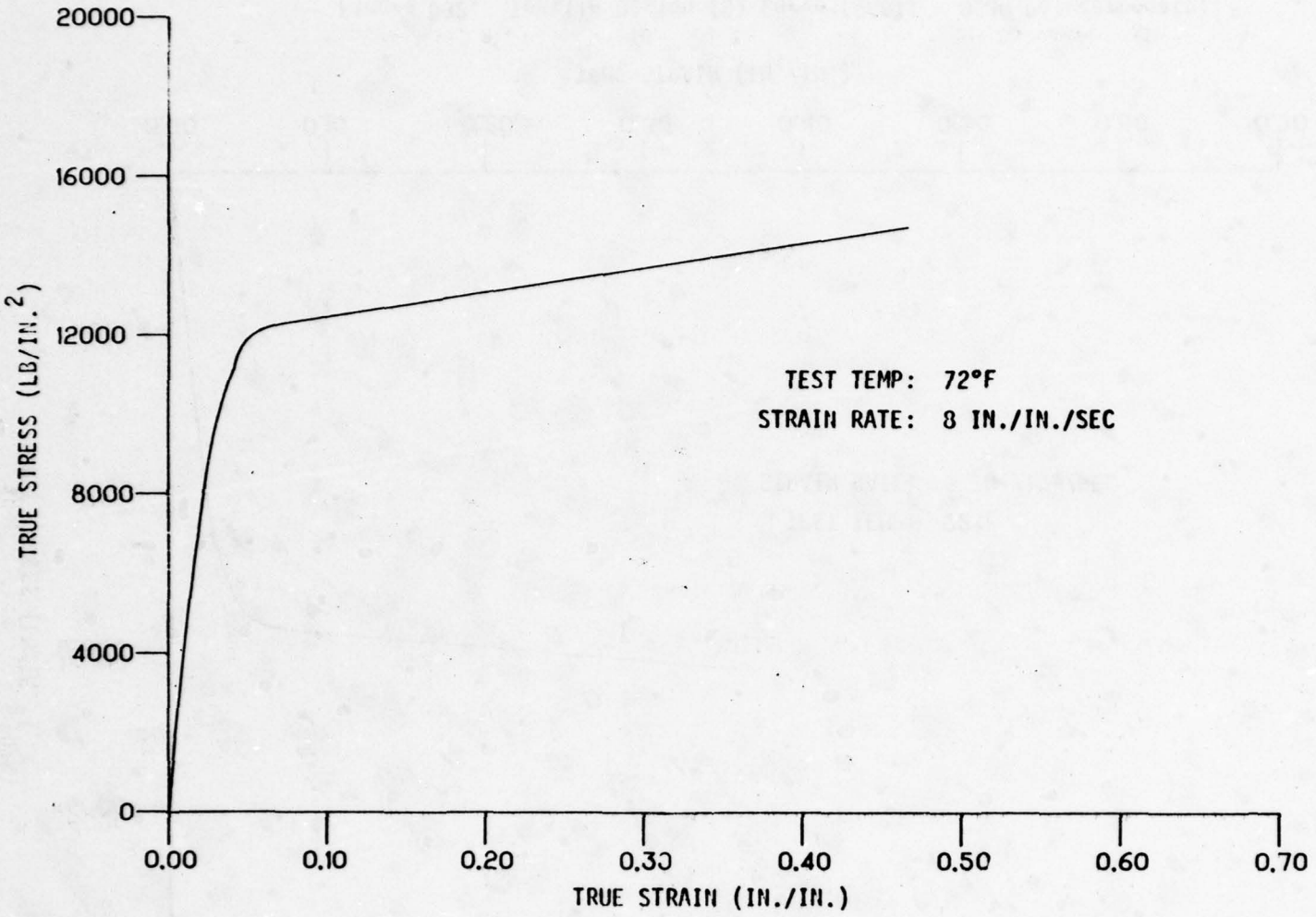

Figure D31. Tensile Average Curve (SK611 - 0.30 Polycarbonate).

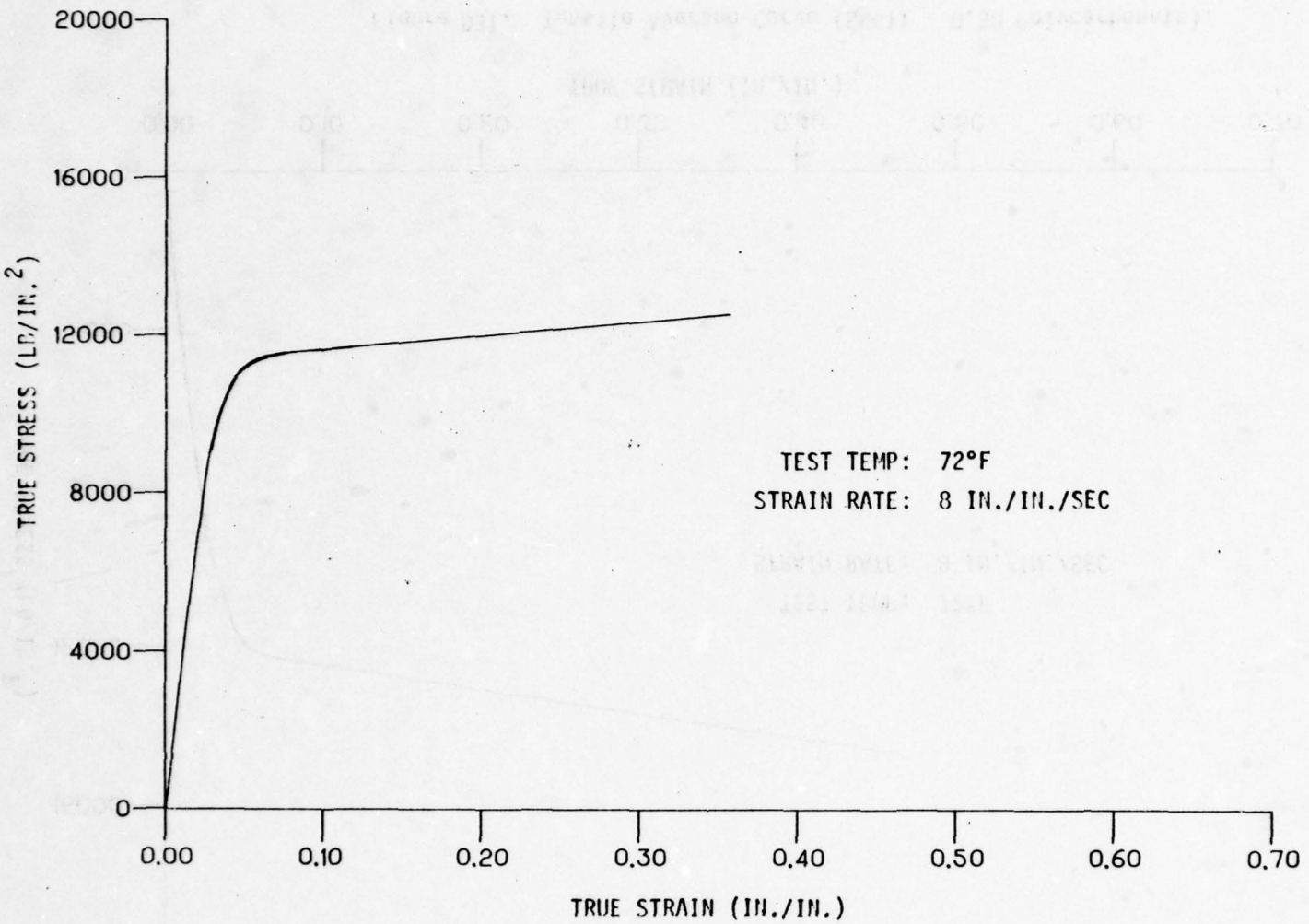

Figure D32. Tensile Design (C) Curve (SK611 - 0.30 Polycarbonate).

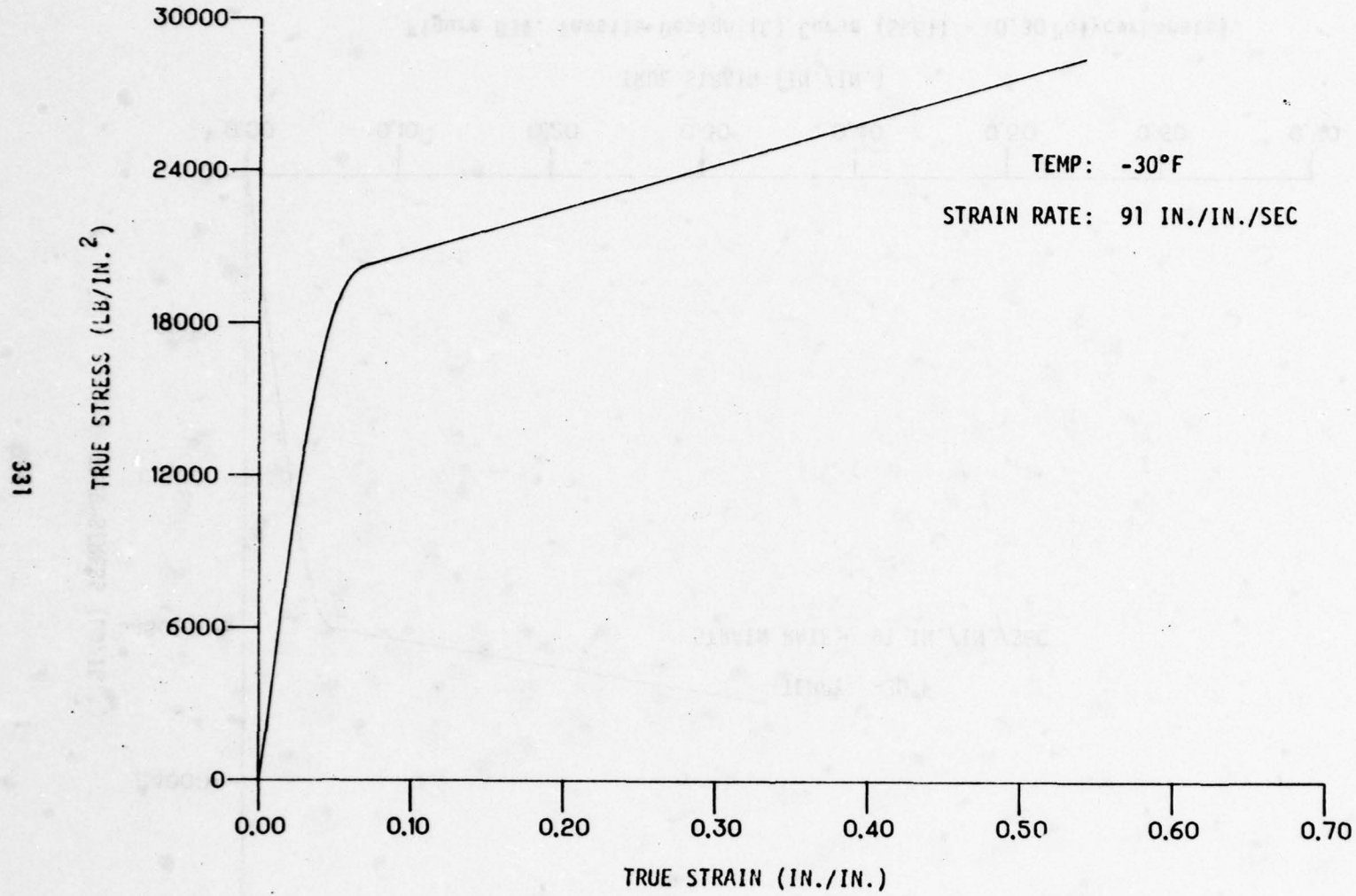

Figure D33. Tensile Average Curve (SK611 - 0.30 Polycarbonate).

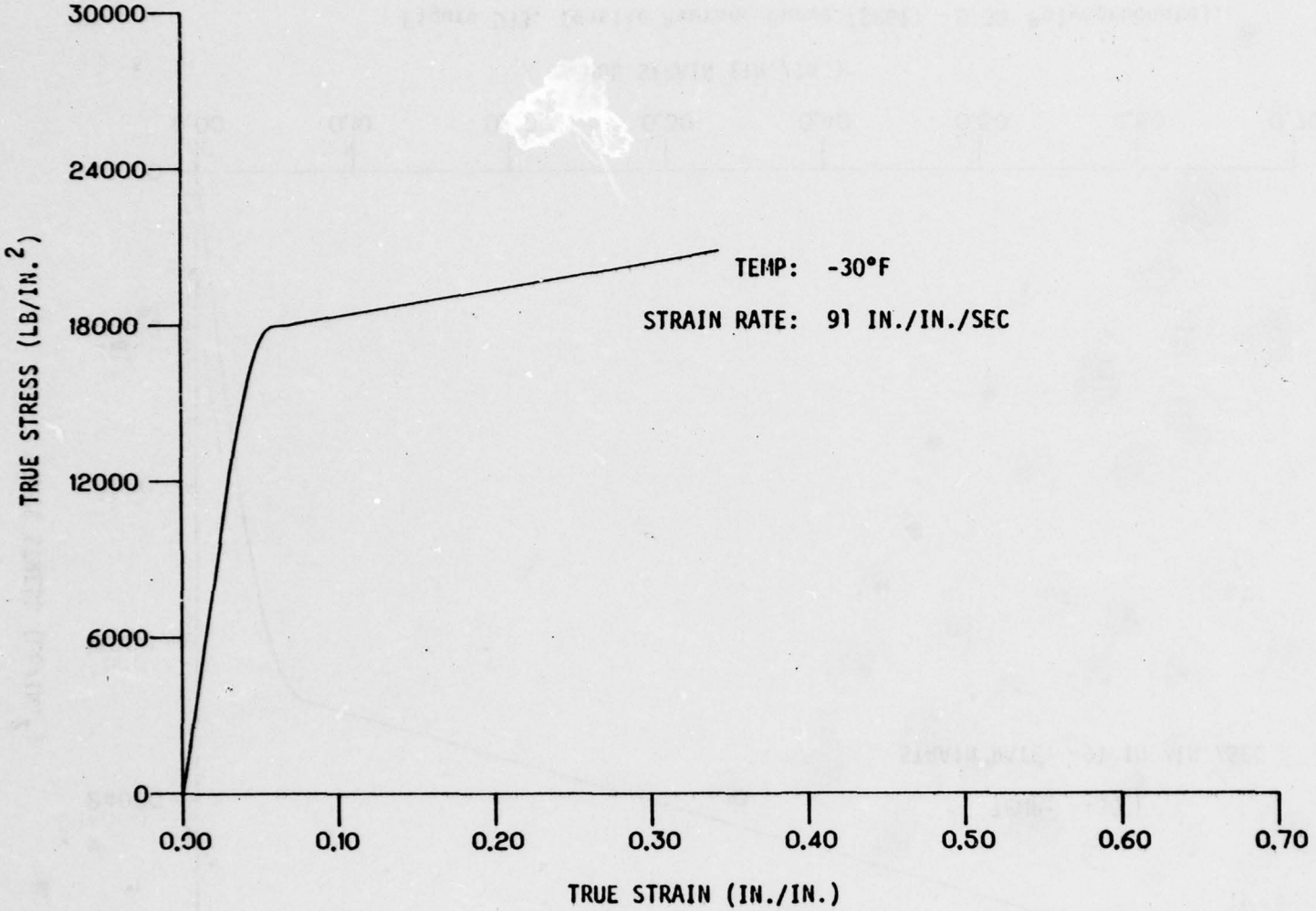

Figure D34. Tensile Design (C) Curve (SK611 - 0.30 Polycarbonate).

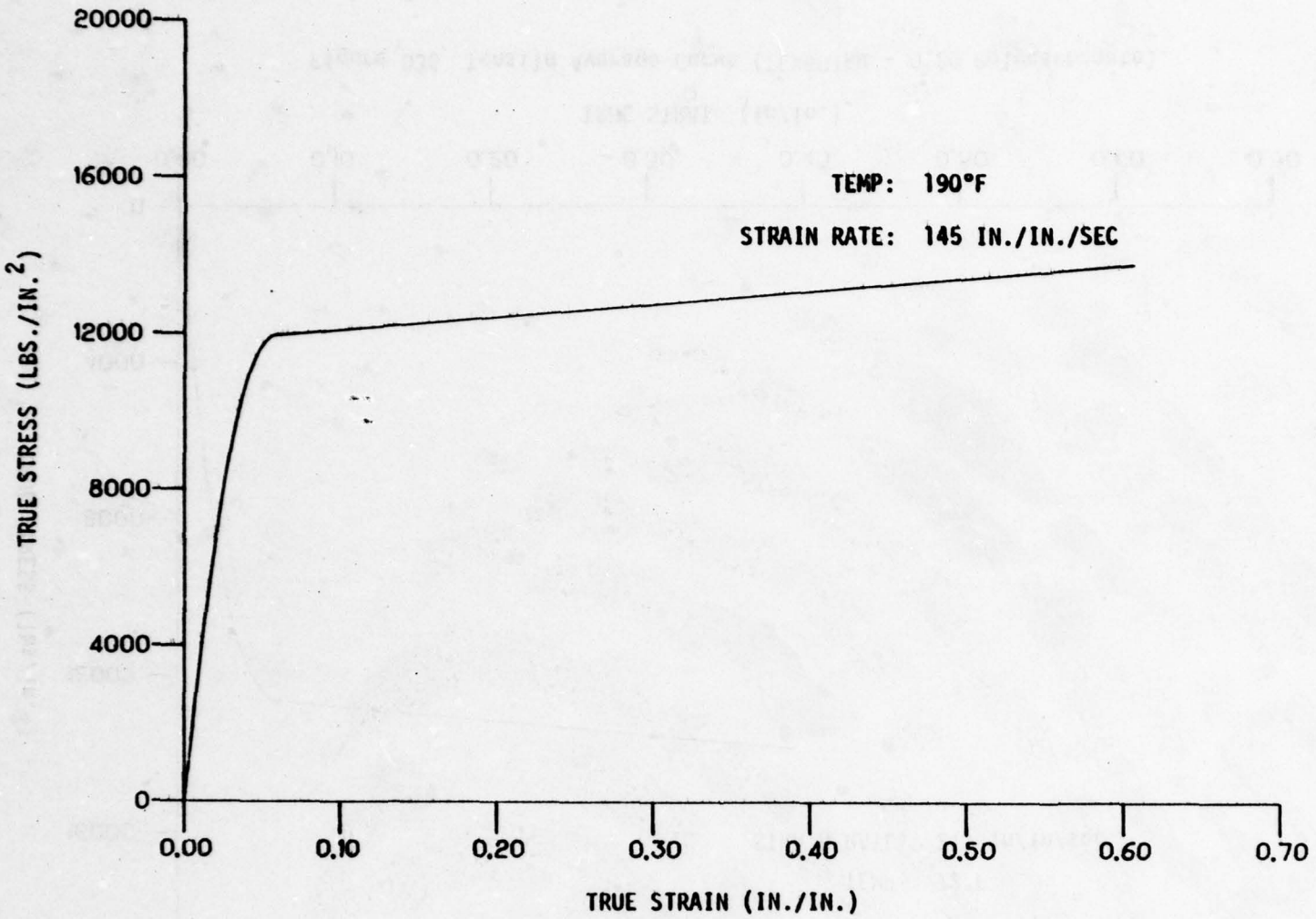

Figure D35 Tensile Average Curve (SK611 - 0.30 Polycarbonate)

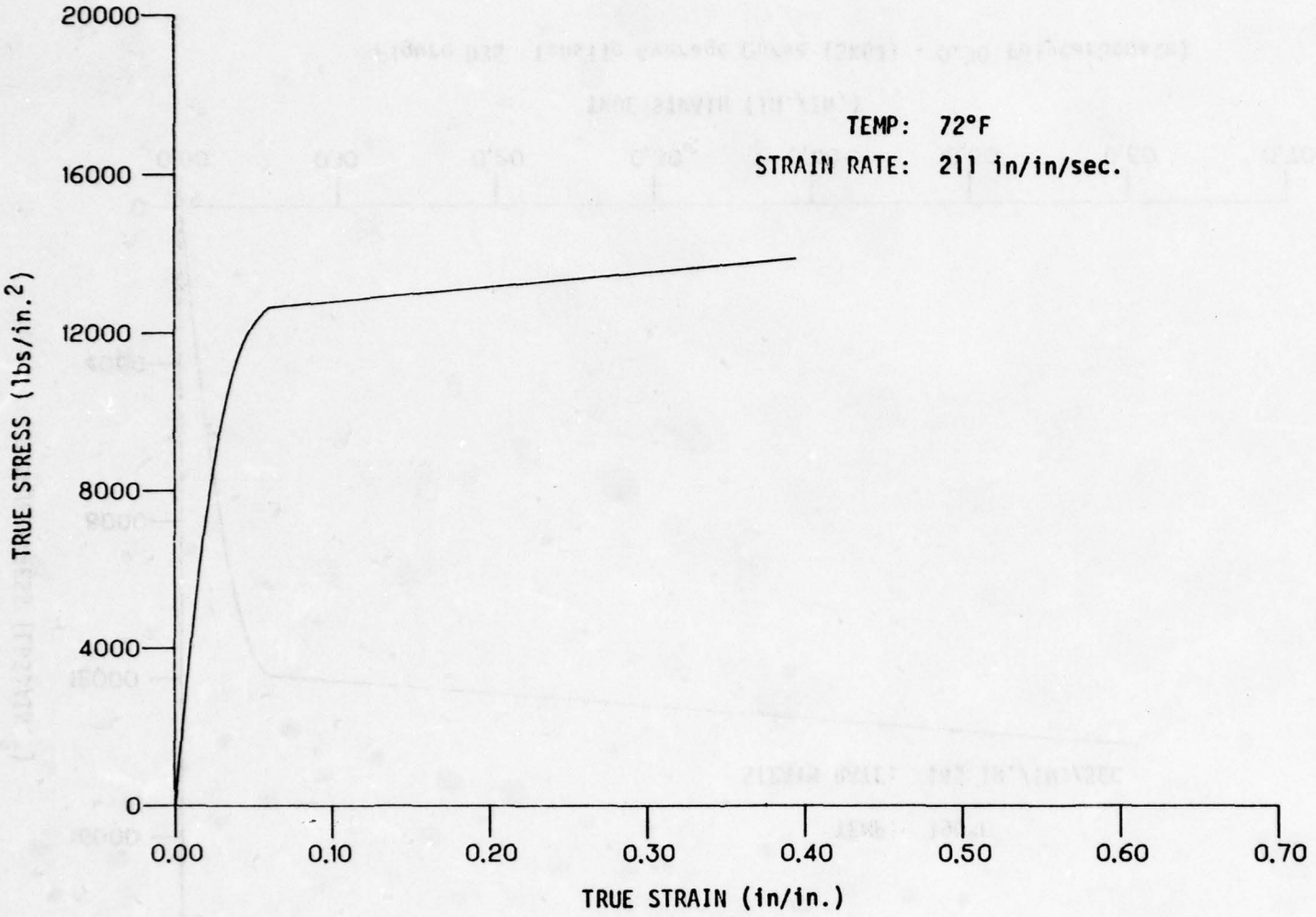

Figure D36 Tensile Average Curve (TEX601RH - 0.20 Polycarbonate).

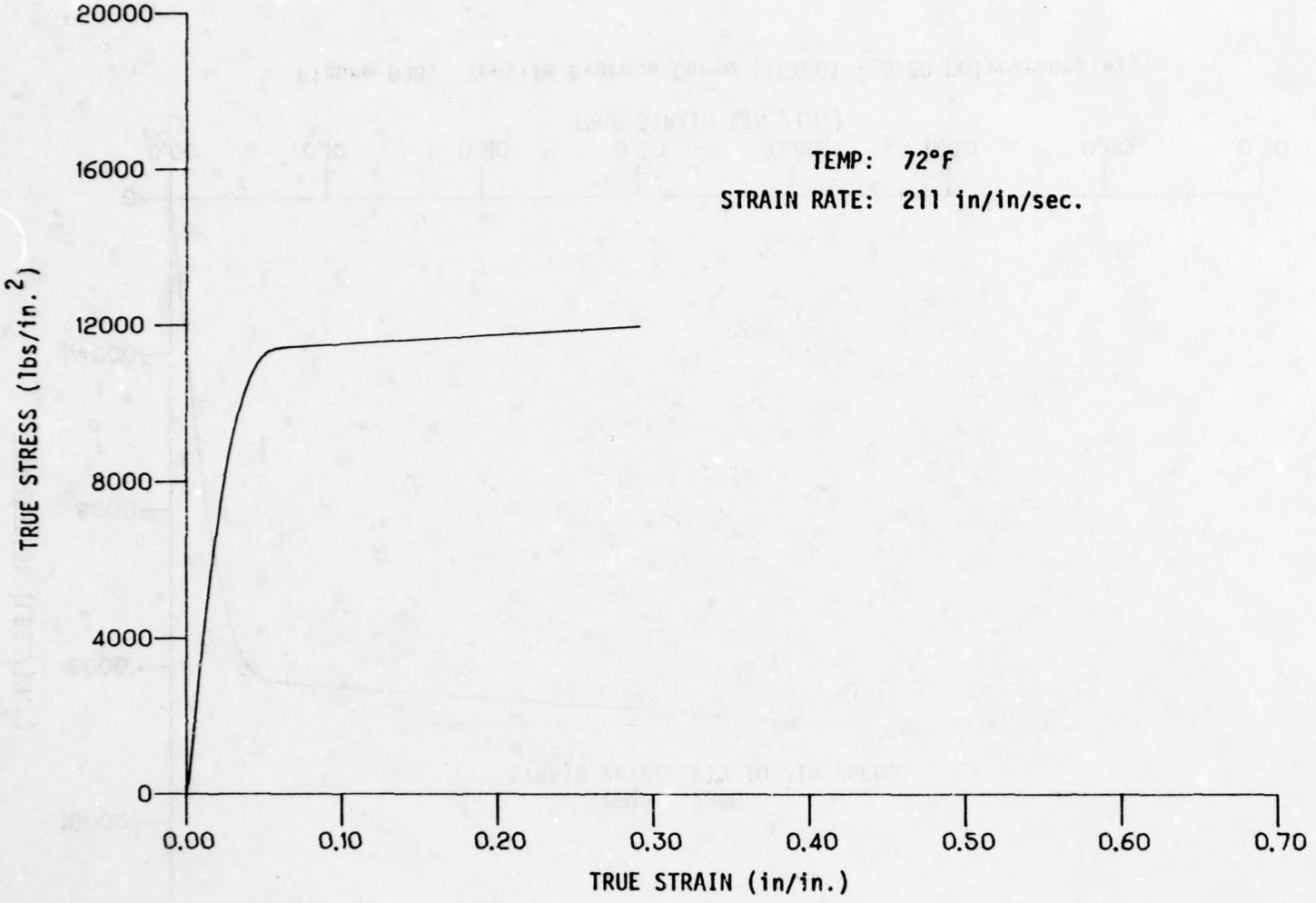

Figure D37 Tensile Design (B) Curve (TEX601RH - 0.20 Polycarbonate).

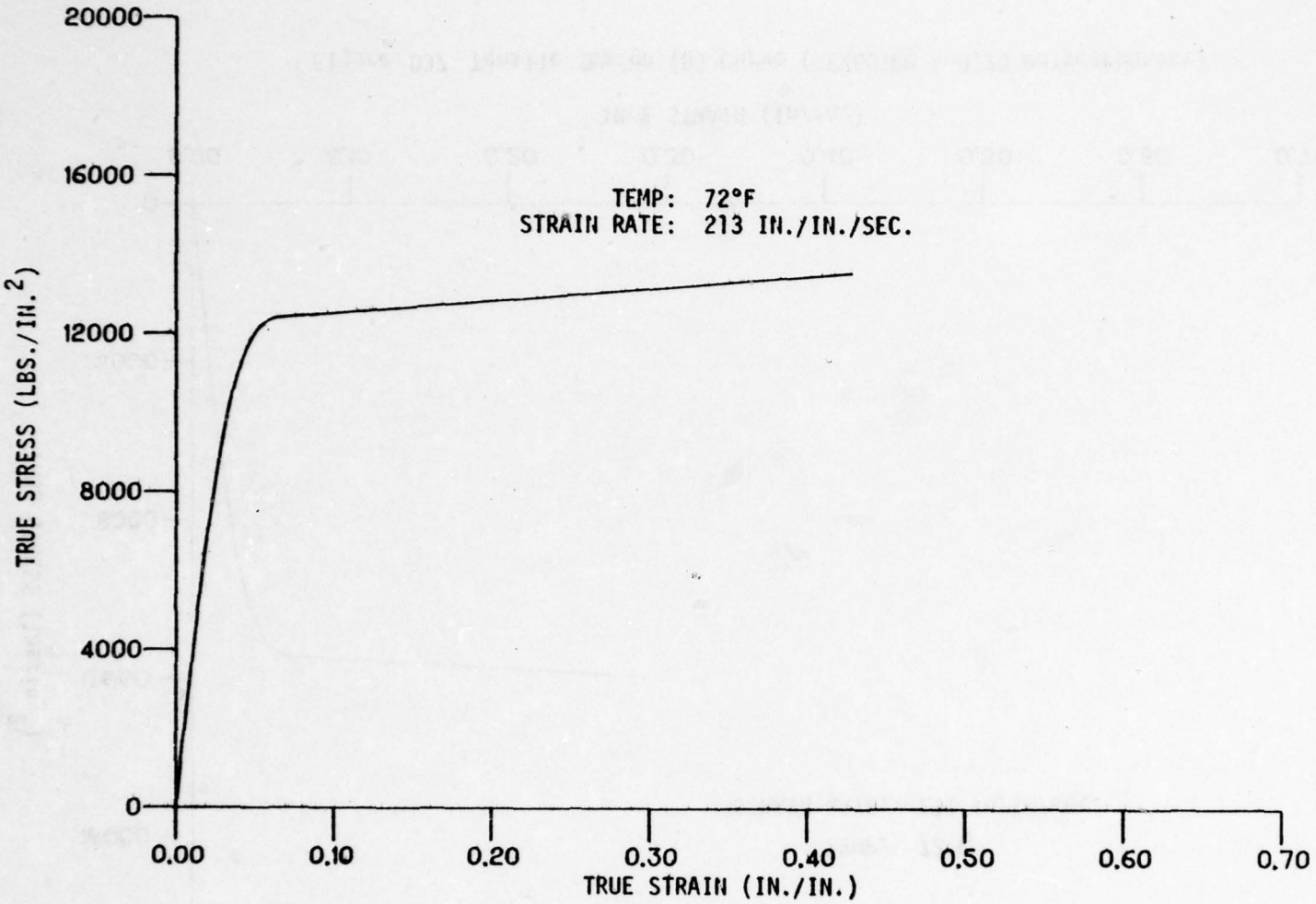

Figure D38. Tensile Average Curve (TEX601 - 0.20 Polycarbonate).

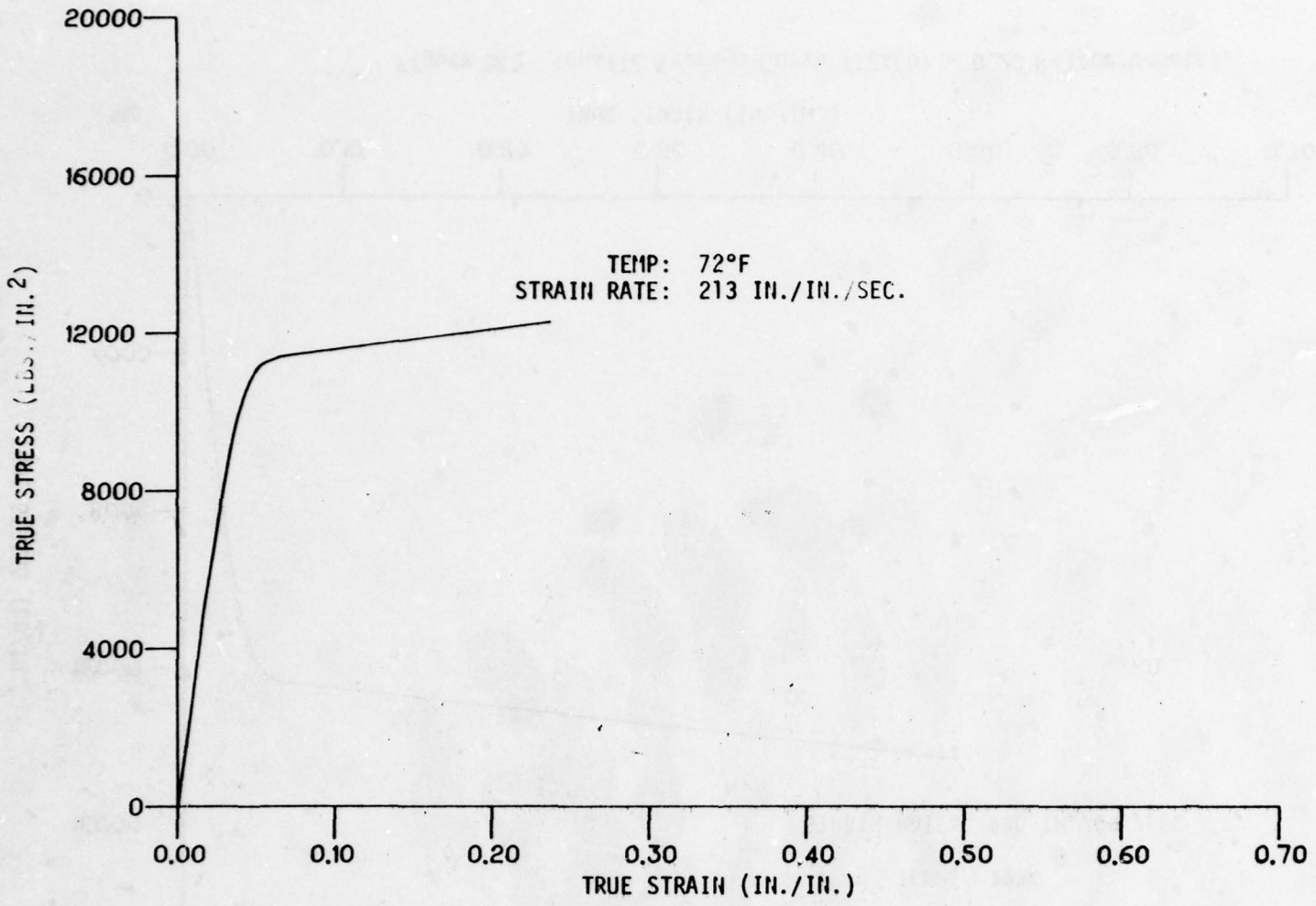

Figure D39. Tensile Design (B) Curve (TEX601 - 0.20 Polycarbonate).

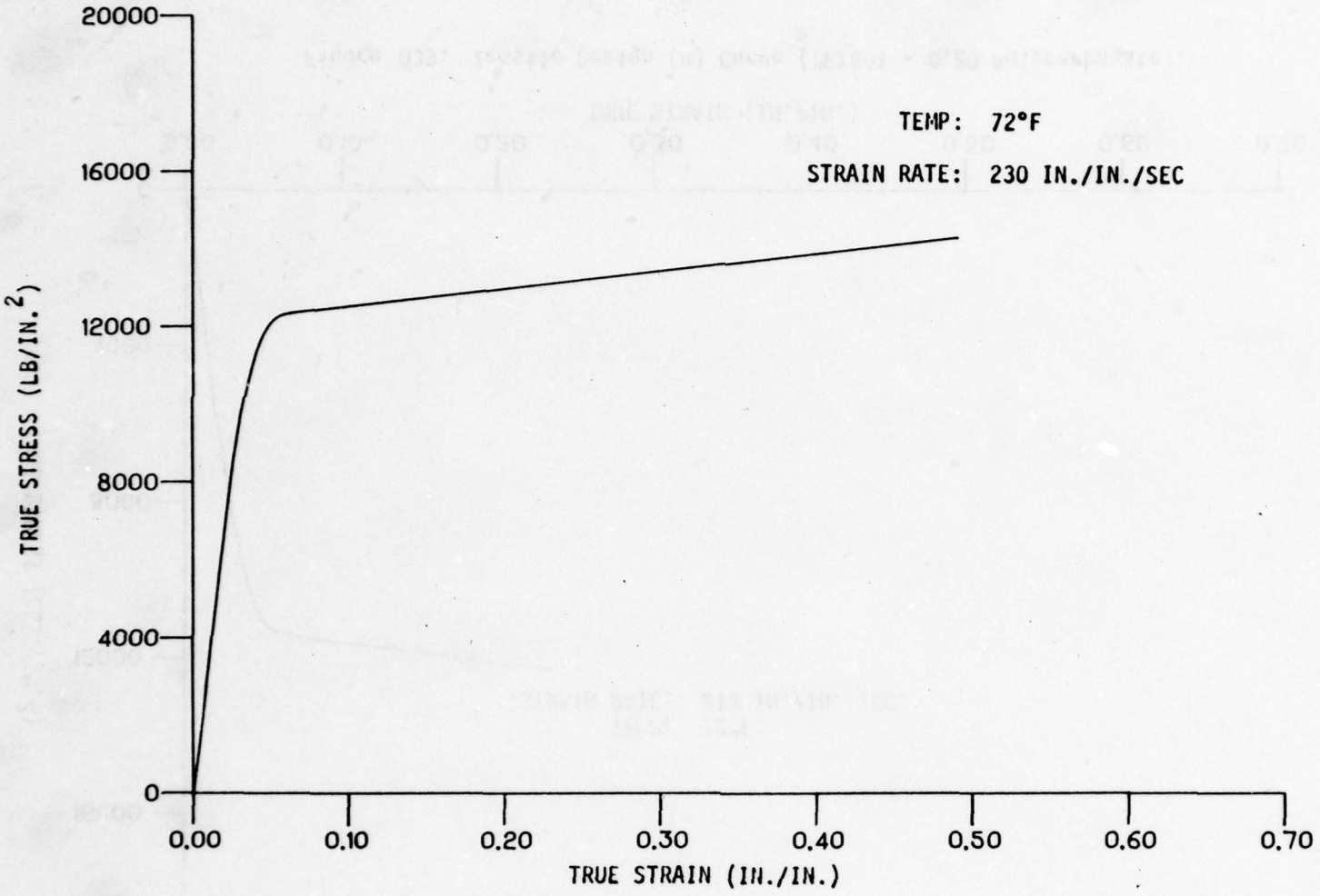

Figure D4Q Tensile Average Curve (TEX601 - 0.20 Polycarbonate).

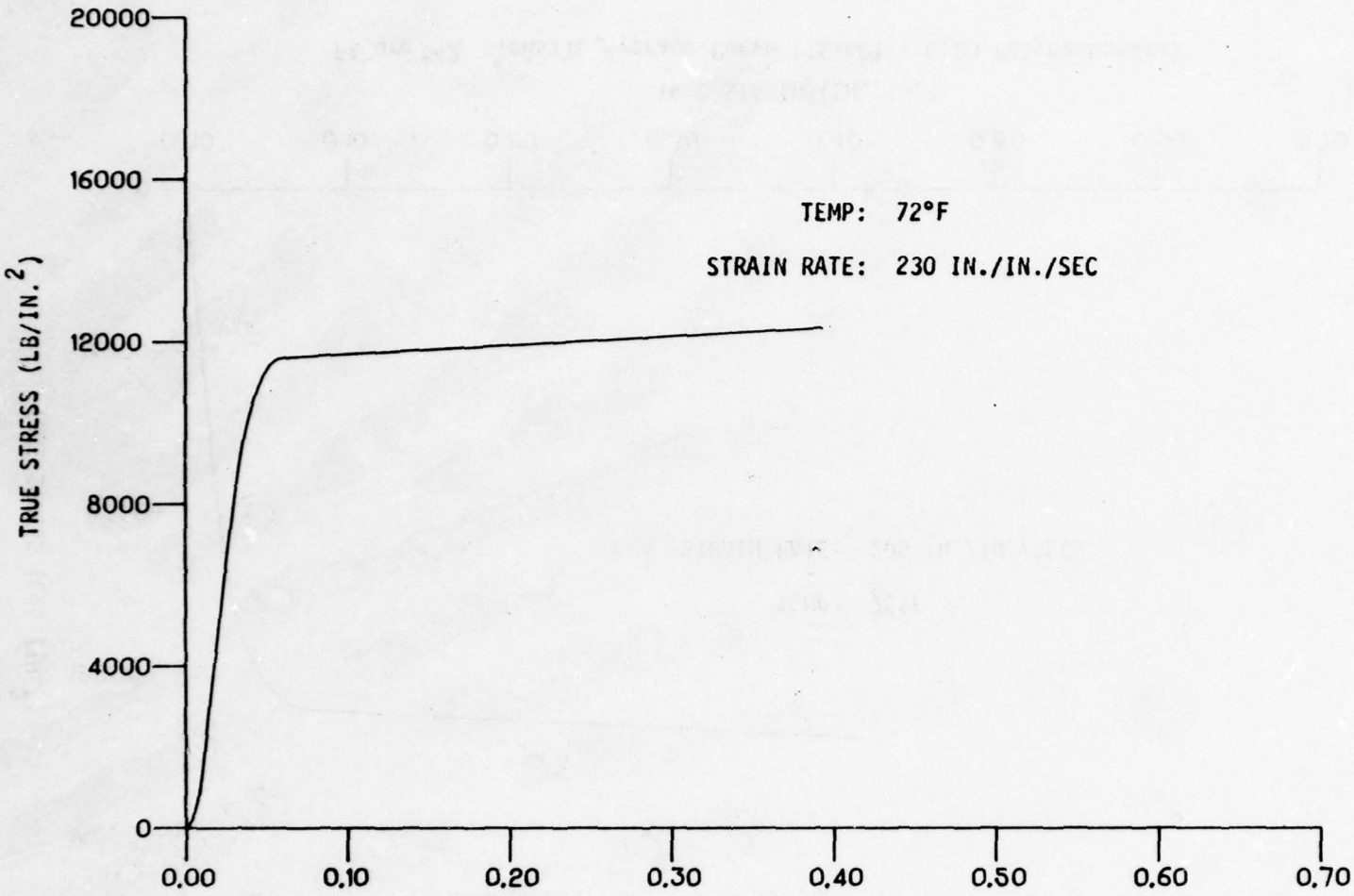

Figure D41 Tensile Design (B) Curve (TEX601 - 0.20 Polycarbonate).

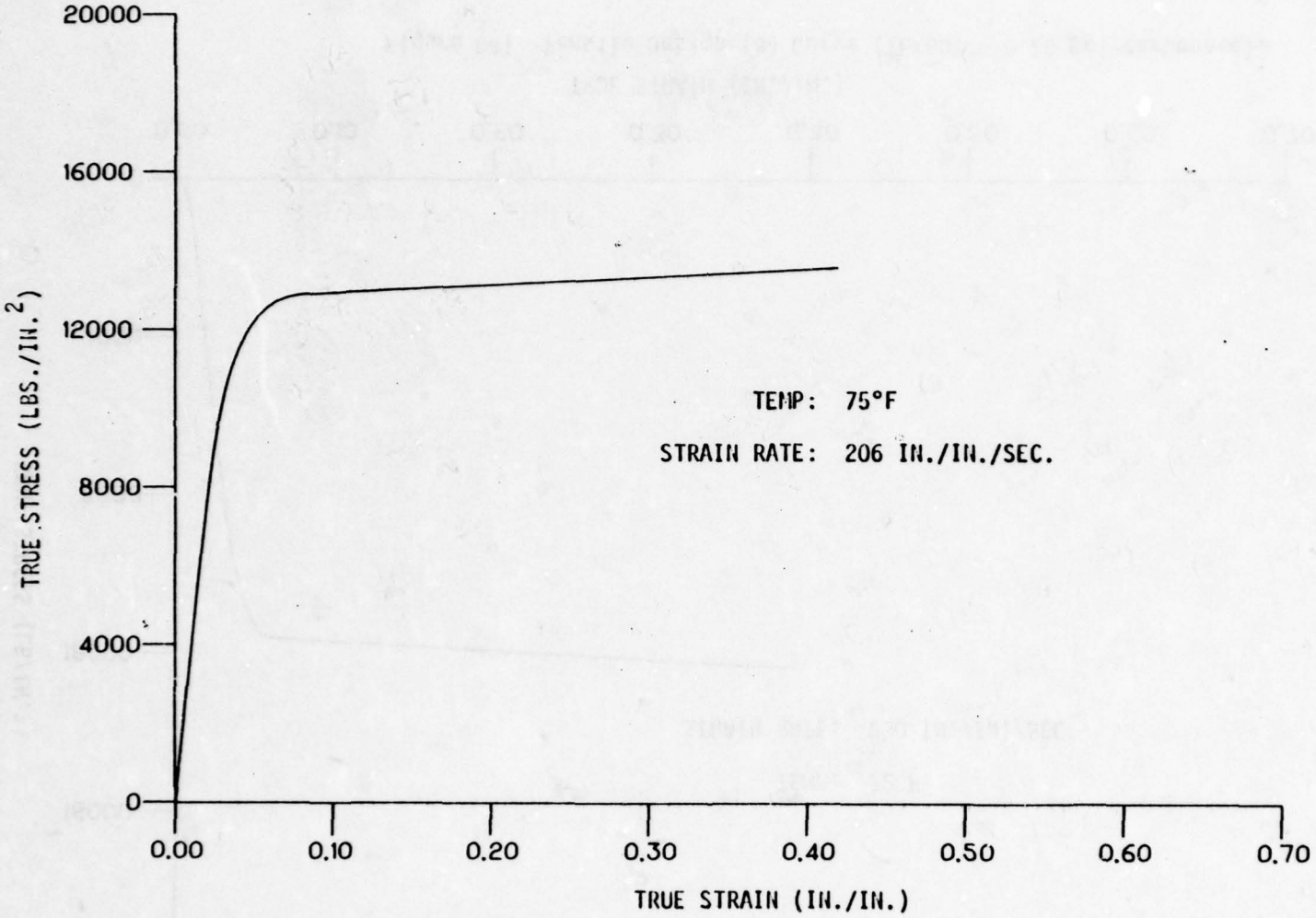

Figure D42. Tensile Average Curve (TEX601 - 0.20 Polycarbonate)

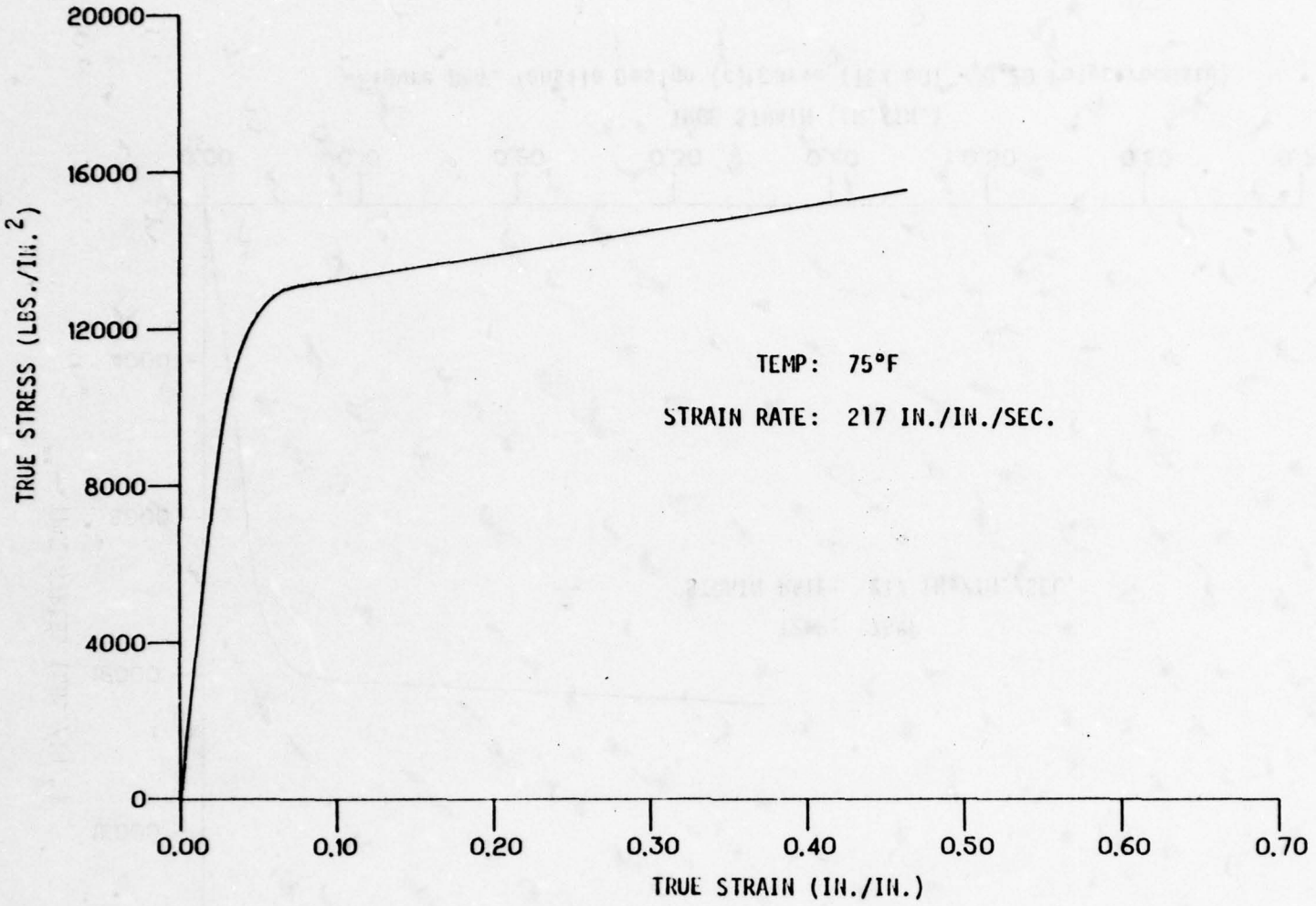

Figure D43 Tensile Average Curve (TEX601 - 0.20 Polycarbonate)

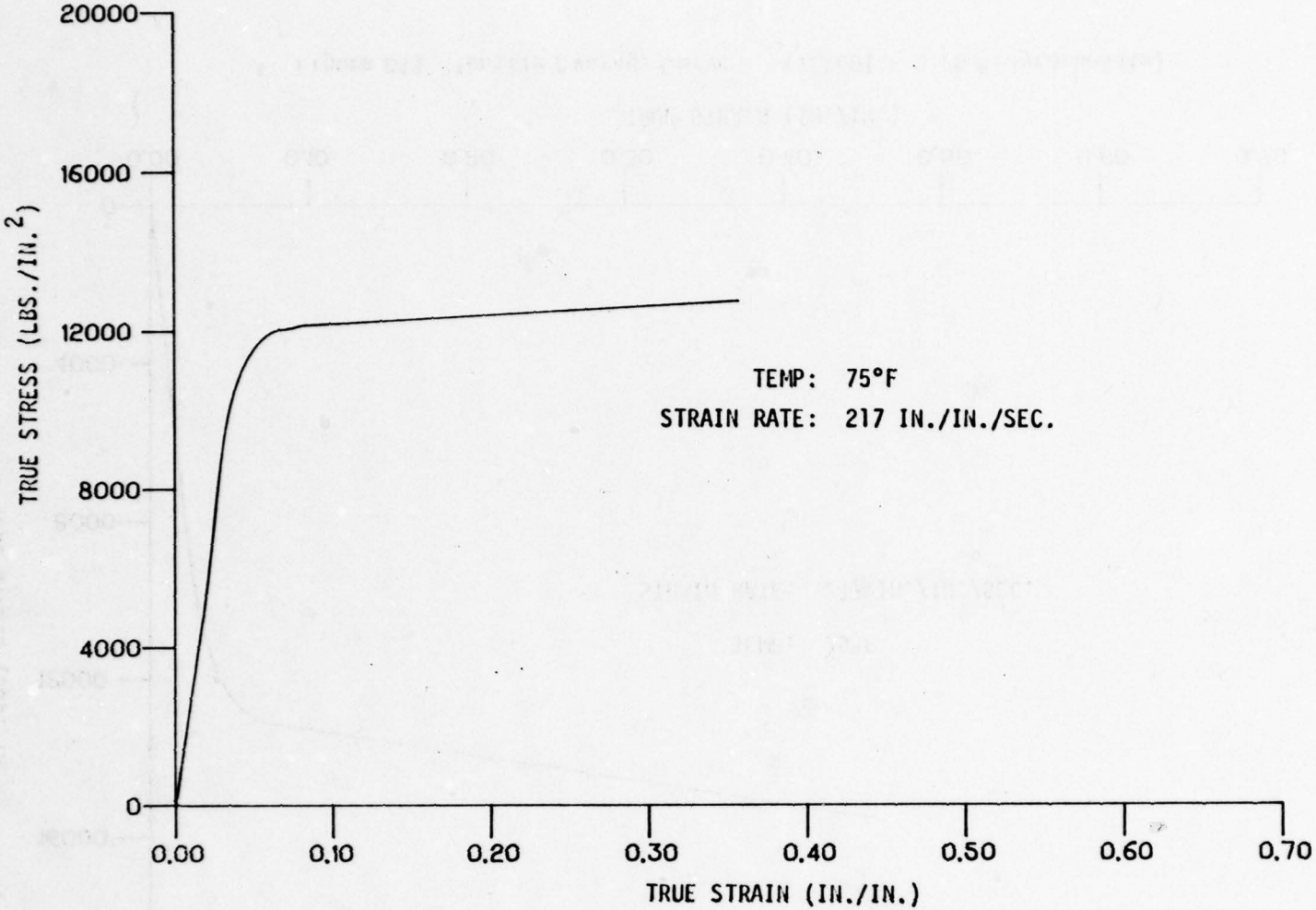

Figure D44. Tensile Design (c) Curve (TEX 601 - 0.20 Polycarbonate)

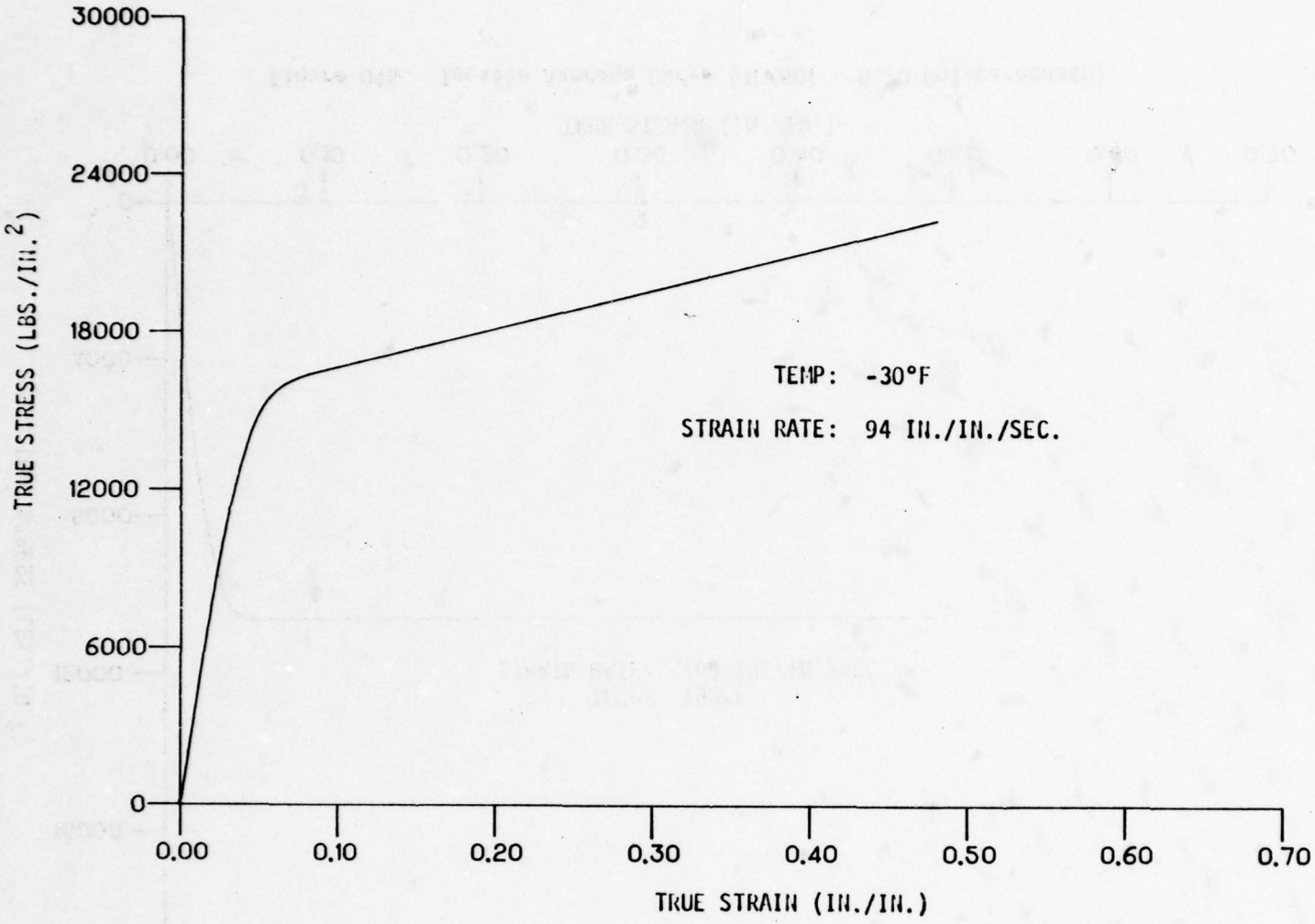

Figure 045. Tensile Average Curve (TEX601 - 0.20 Polycarbonate)

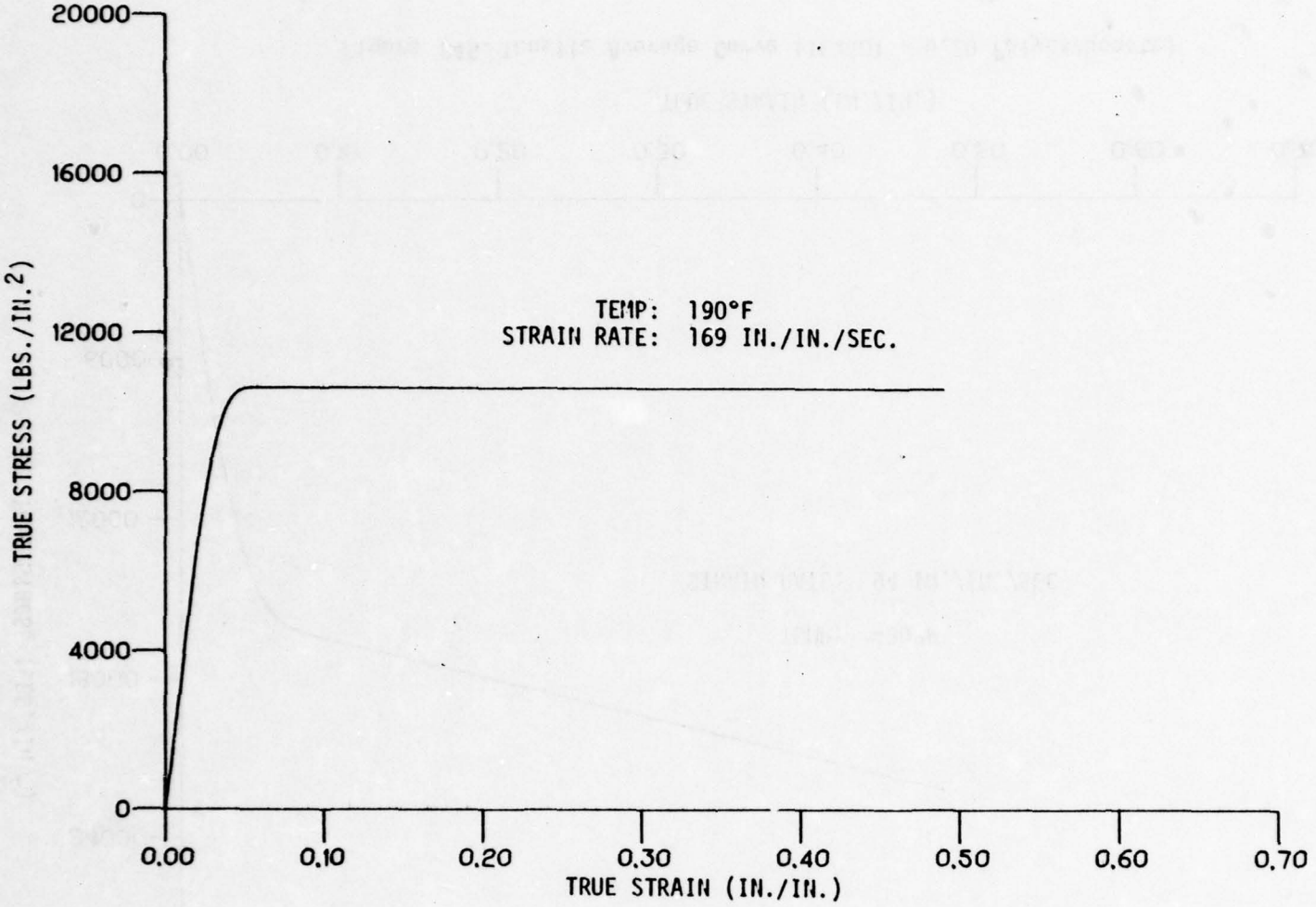

Figure D46. Tensile Average Curve (TEX601 - 0.20 Polycarbonate).

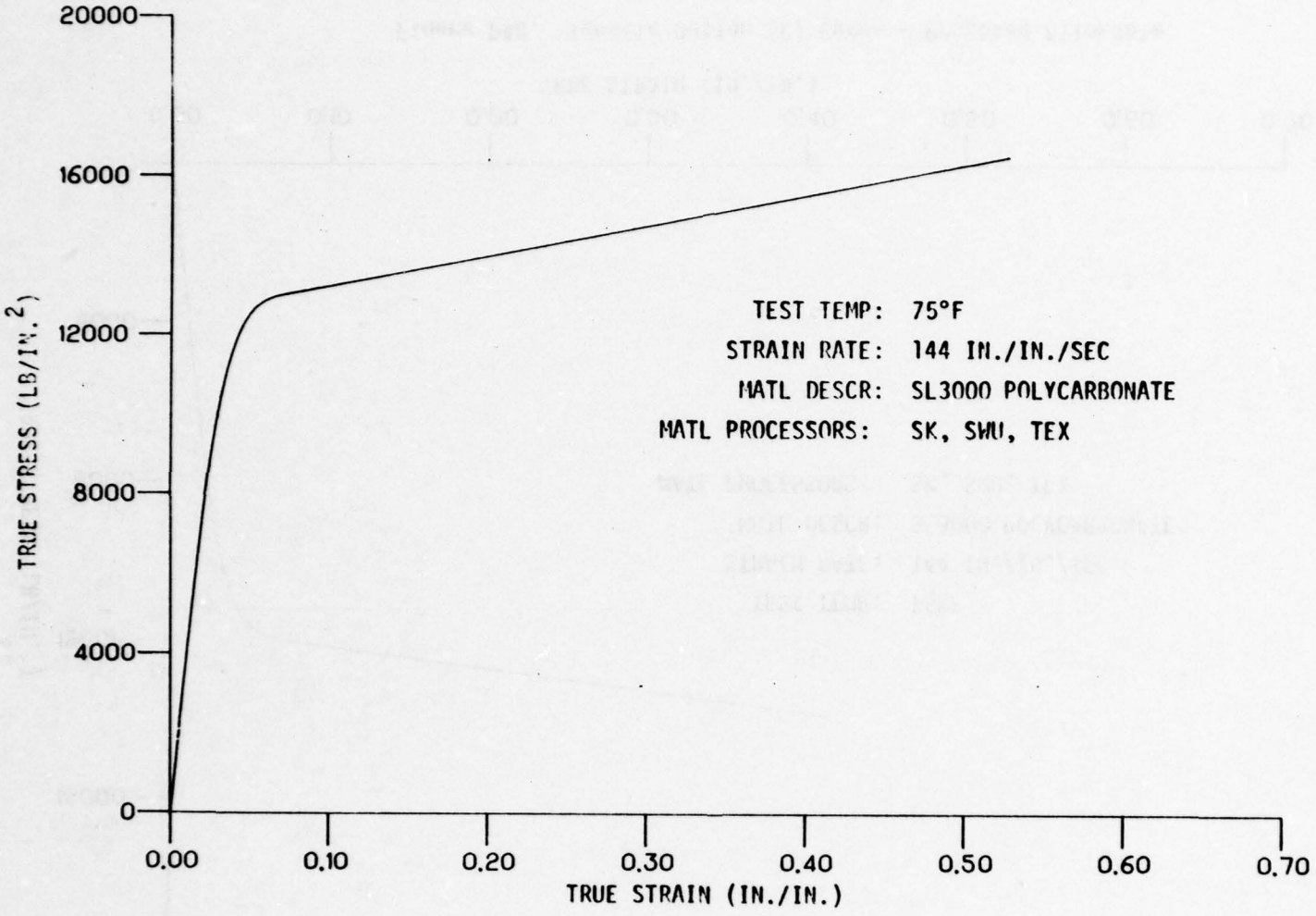

Figure D47. Tensile Average Curve.

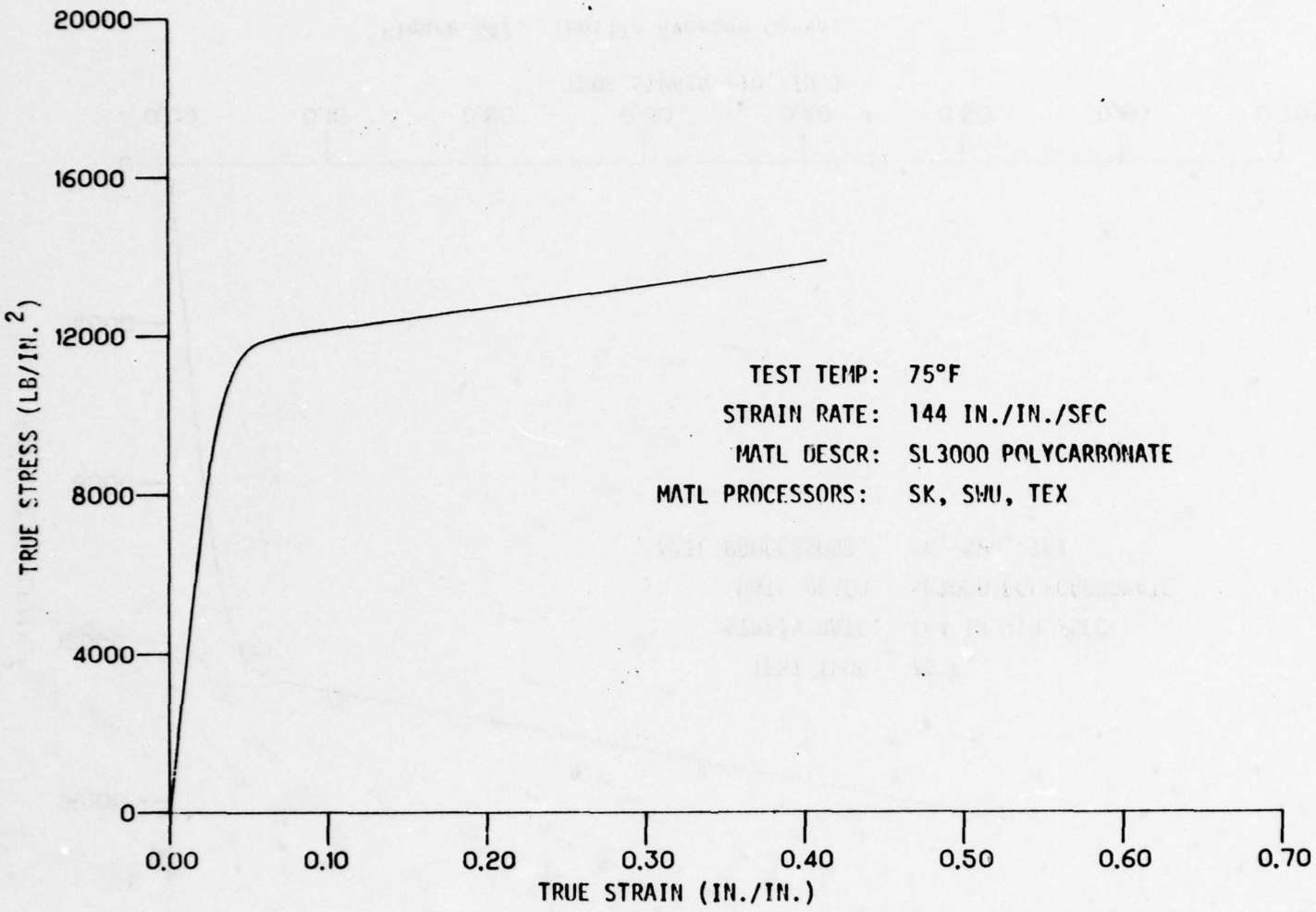

Figure D48. Tensile Design (C) Curve - Proposed Allowable.

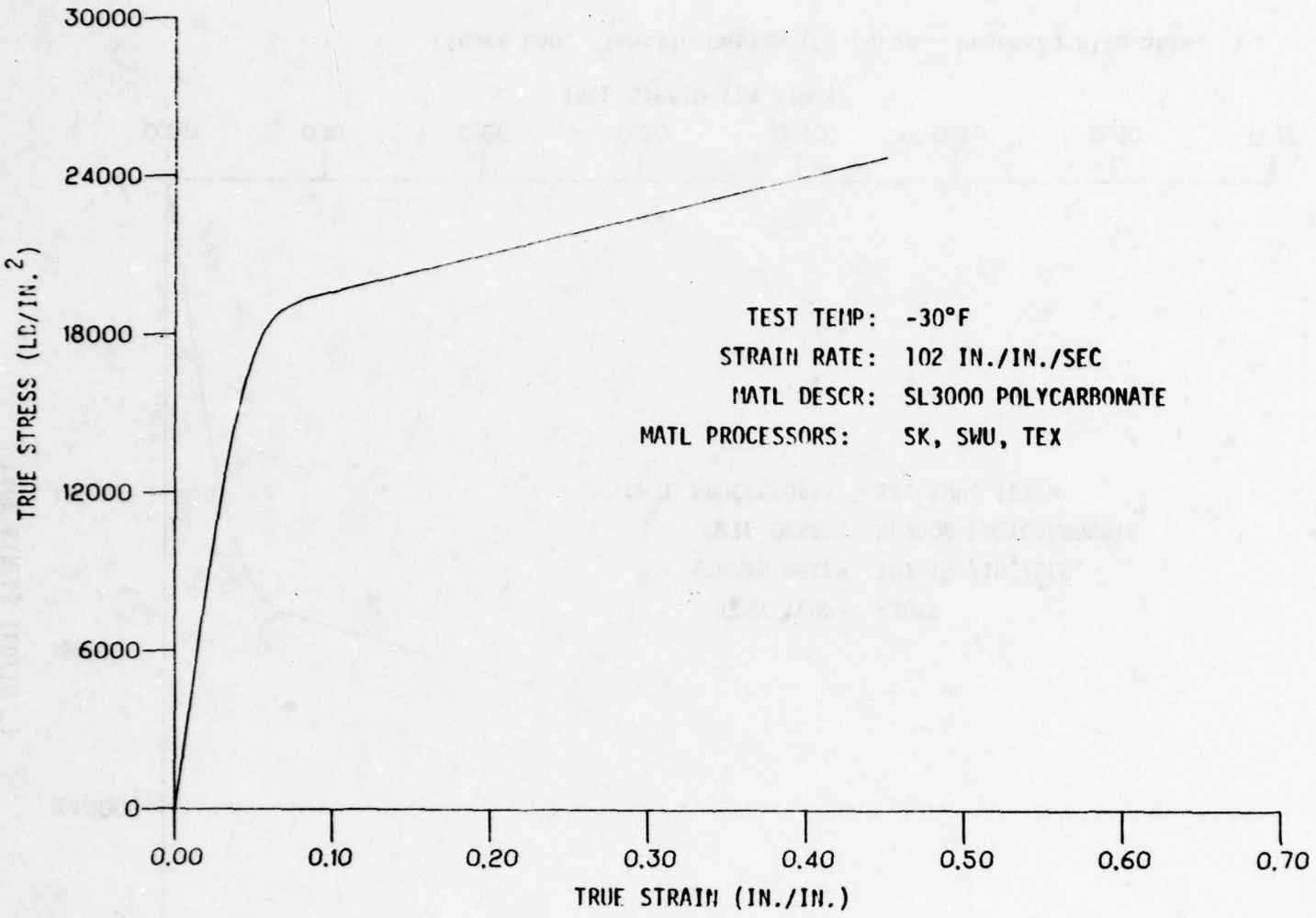

Figure D49. Tensile Average Curve.

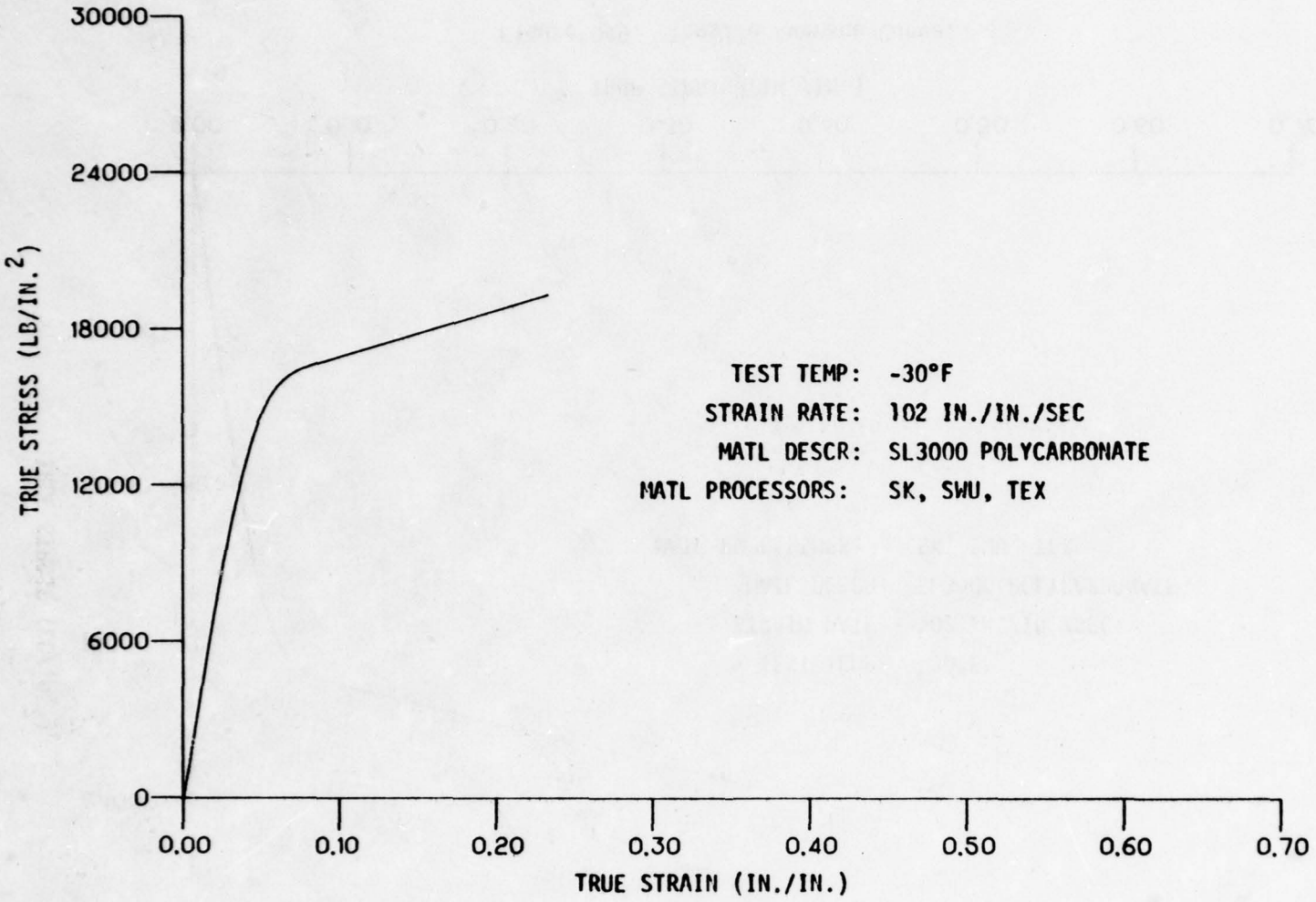

Figure D50. Tensile Design (C) Curve - Proposed Allowable.

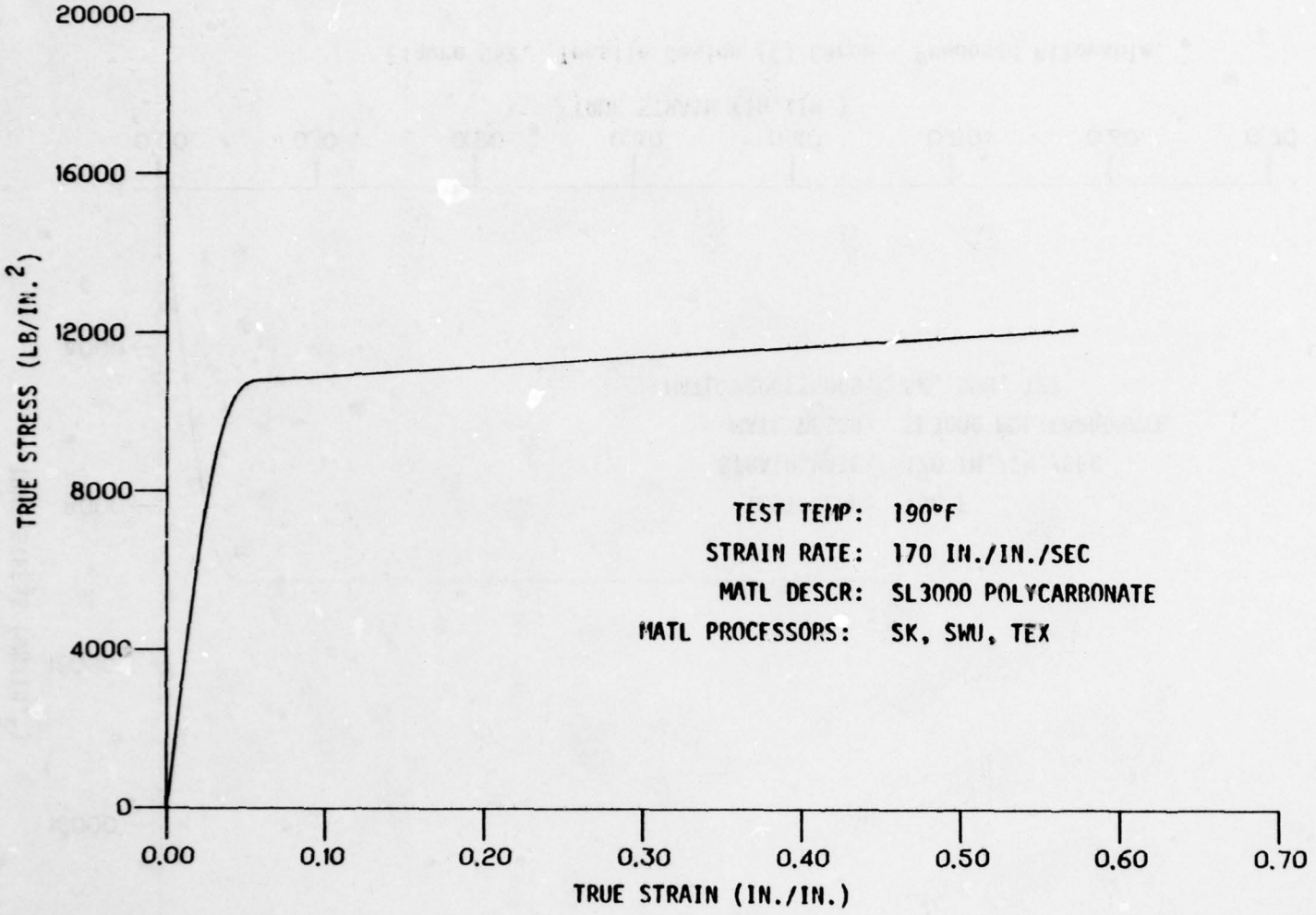

Figure D51. Tensile Average Curve.

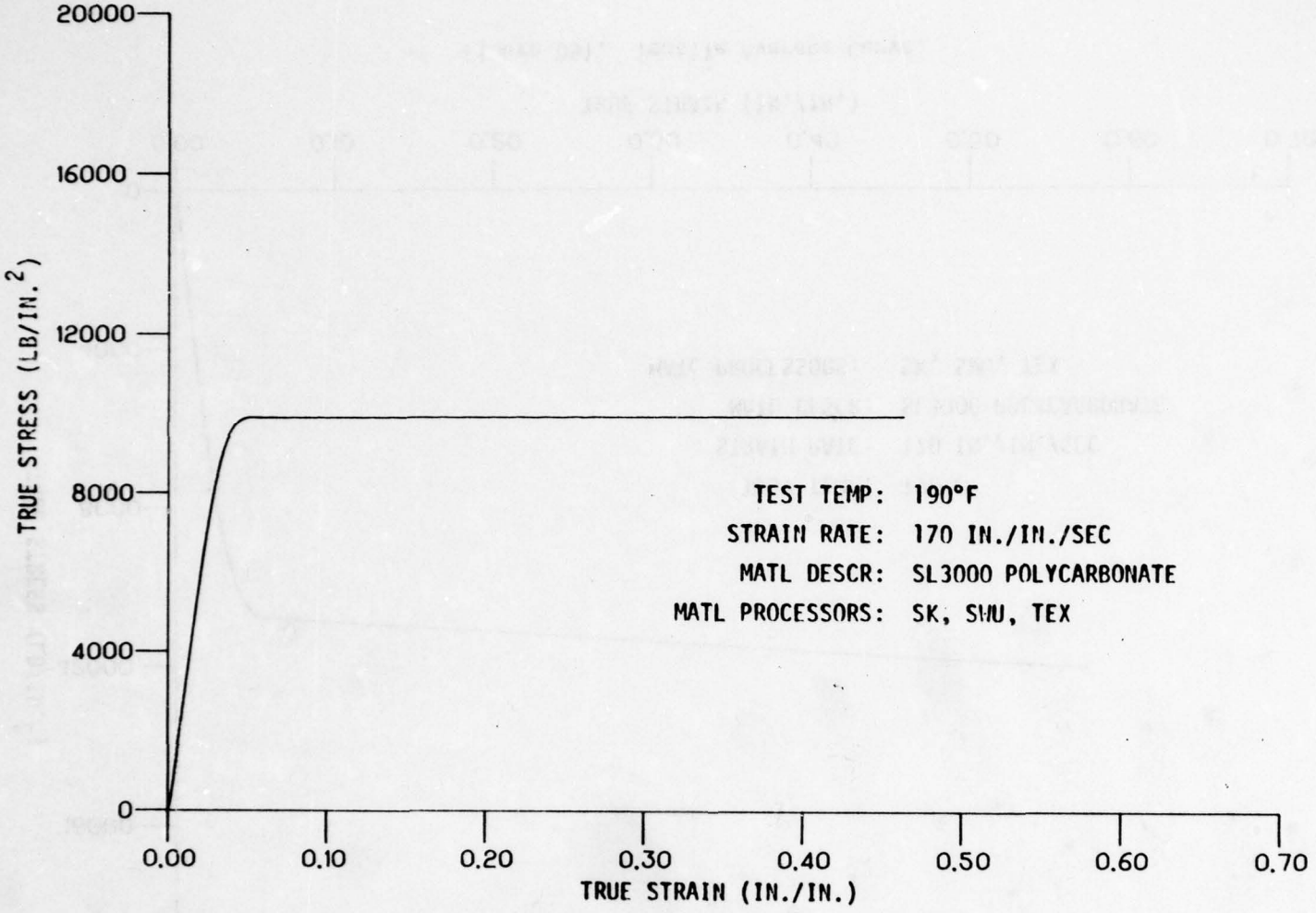

Figure D52. Tensile Design (C) Curve - Proposed Allowable.

SECTION IX
HIGH STRAIN RATE COMPRESSIVE MECHANICAL PROPERTIES OF MONOLITHIC POLYCARBONATE MATERIAL

This series of tests was conducted to provide average (actual) high strain rate compressive mechanical properties, and design allowables for monolithic polycarbonate materials as processed by specific aircraft transparency fabricators. The primary use for these mechanical properties was for development and future design use in computer analysis of bird strike. Additional uses were to provide for evaluation of materials and processors. Tests were conducted at the maximum and minimum temperature conditions established by the flight profile of a supersonic aircraft. Maximum strain rates due to a bird strike were determined from bird impact tests of actual full size transparencies. Compression testing was accomplished at Terra Tek, Salt Lake City, Utah, under contract to Douglas for high strain rate testing. Test specimens were designed by Douglas to specifications furnished by Terra Tek, Inc., and manufactured by specific fabricators. These specimens received the same processing as a laminated aircraft transparency.

TEST SPECIMEN DESCRIPTION

The Z7942633-525 compression test specimens required for this series of tests is shown in Figure 70. The compression test specimens were constructed by Swedlow, Inc., from SL3000 polycarbonate material. All test specimens were examined under polarized light to expose stress risers that resulted from machining operations and could have affected test results. Specimens displaying stress were refinished (sanded and polished) to remove such discrepancies. Machine cutting speed and feed rates were controlled to prevent heating parts above 150°F which could result in adverse thermal conditioning effects. Specimens of a particular test series were orientated in the same length-width relation with respect to the basic stock. Sheet material

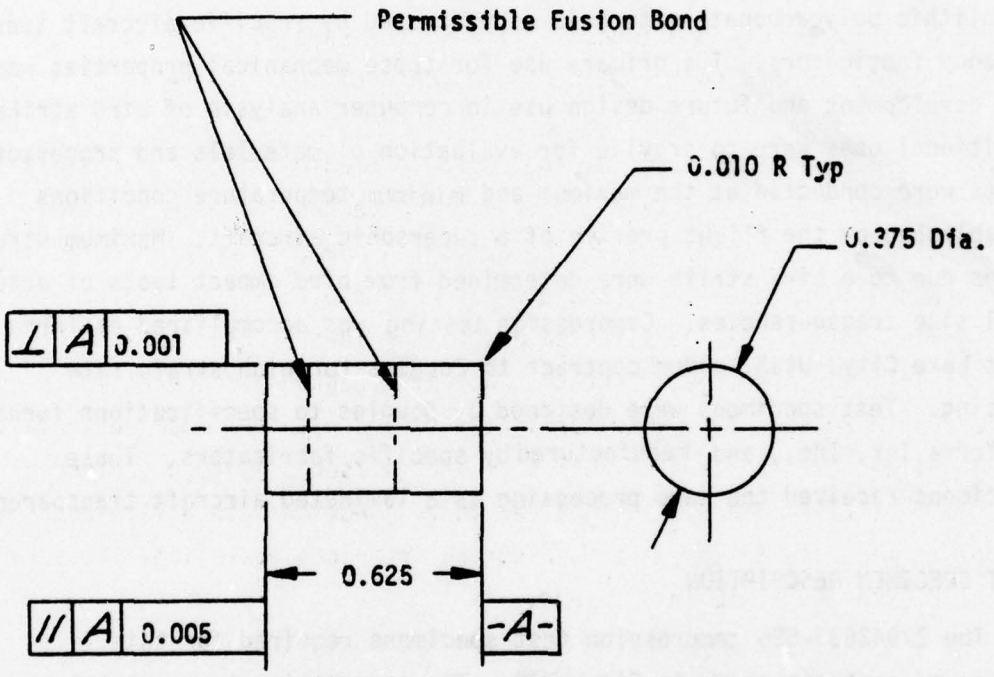

Figure 70. Compression Specimen (Z7942633-525).

used for test specimens was ground polished and subjected to thermal temperatures and frequencies required in the normal forming and fabrication processes of a laminated polycarbonate transparency. Test specimens were constructed in accordance with design criteria specified by Terra Tek, Salt Lake City, Utah, under contract to Douglas for high strain rate testing. Eighteen (18) specimens were supplied to Terra Tek for testing.

TEST SETUP AND EQUIPMENT DESCRIPTION

The following equipment description is the same as outlined in Section VIII and is repeated here for the convenience of the reader.

All tests were conducted at the Terra Tek medium strain rate facility shown in Figure 71. The main components of the test machine are shown schematifally in Figure 72. The lower platen normally remains fixed with the upper platen adjusted to the desired height with the help of the attached hydraulic lift cylinders. Attached to the lower platen is a 50,000 pound 6-inch stroke linear hydraulic actuator capable of operating at cyclic rates up to 20 Hz. This actuator is controlled with a 15 gpm servo valve which allows strain rates of 10^{-6} to 1 in./in./sec. Through the use of a 50 gpm 4-way solenoid operated valve, in conjunction with a flow-control subplate manifold to vary the flow during open-loop operation, the strain rate is extended to 10 in./in./sec.

For all but the very low strain rate tests presented here the high pressure gas actuator mounted above the upper platen was used. This actuator, Figure 73, is operated by charging a reservoir on either side of the piston to equal pressure. The piston is accelerated when the gas is released from one reservoir, the direction is toward the one that is exhausted. The orifice size can be adjusted to control the exhaust rate. Motion is initiated through a fast acting solenoid valve mounted downstream from the orifice. Piston velocity, and hence, rate of loading, is controlled by the gas charging pressure, the orifice size, and, to some extent, the specimen. Piston velocities up to 500 in./sec. can be achieved.

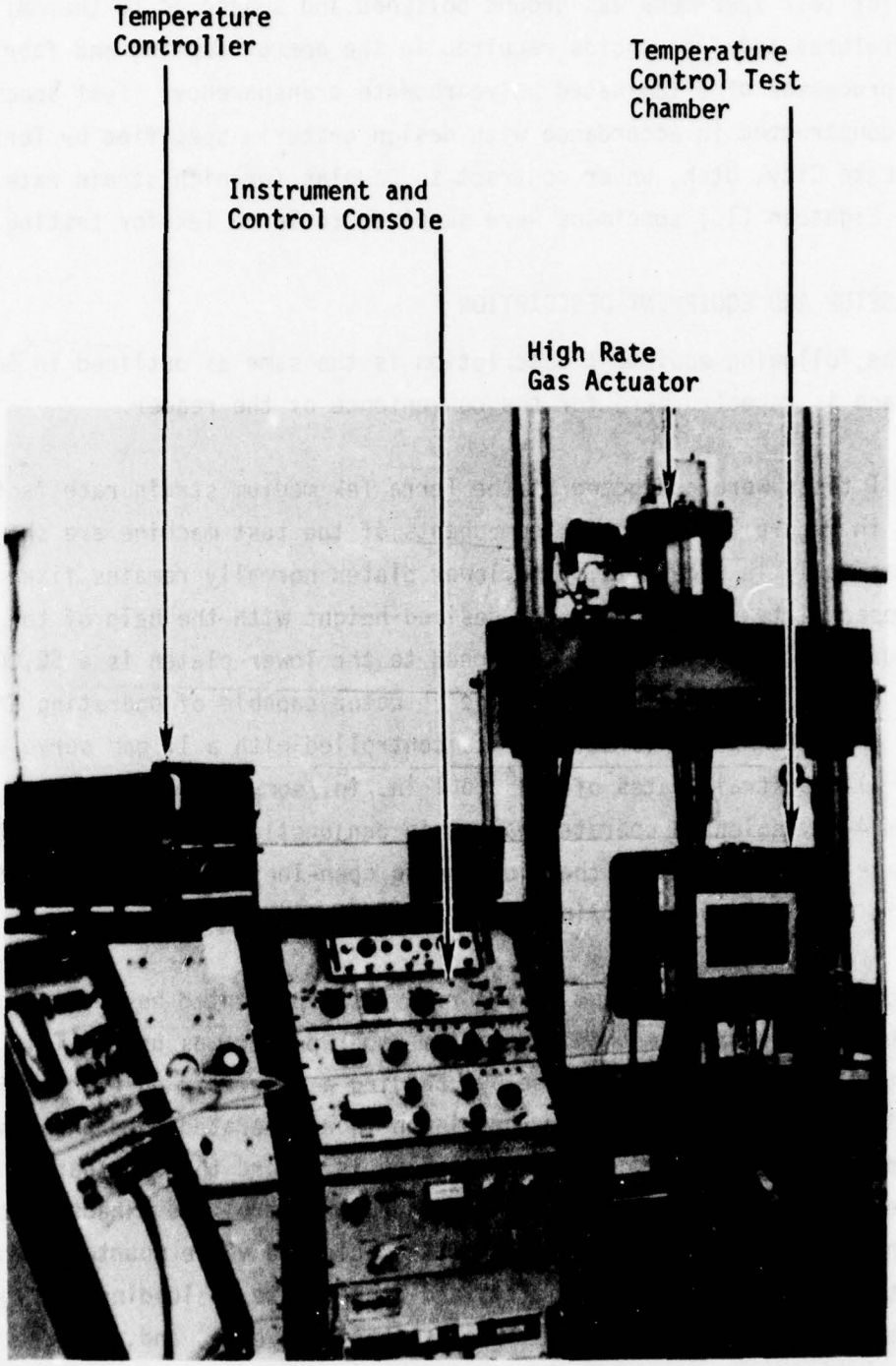

Figure 71. Medium Strain Rate Test Facility.

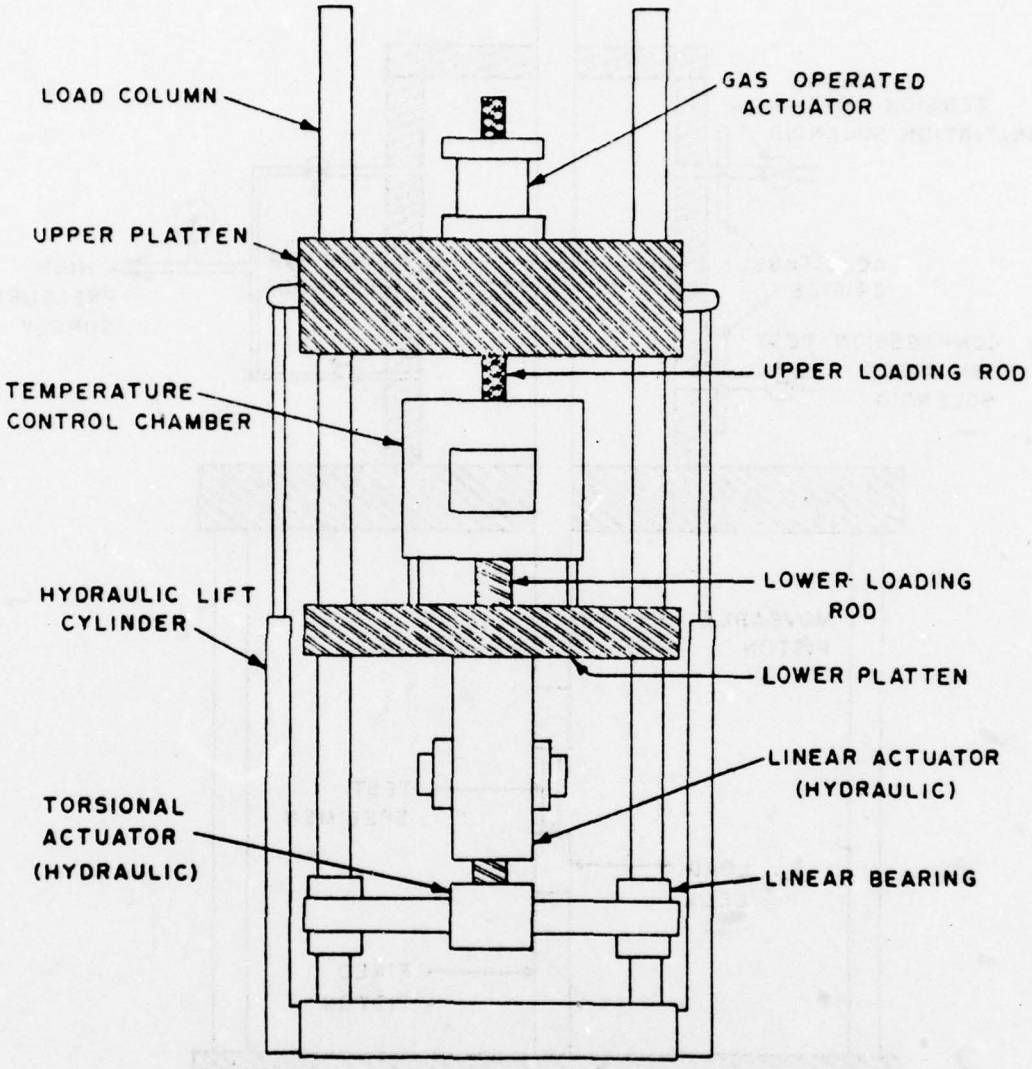

Figure 72. Schematic of Medium Strain Rate Machine.

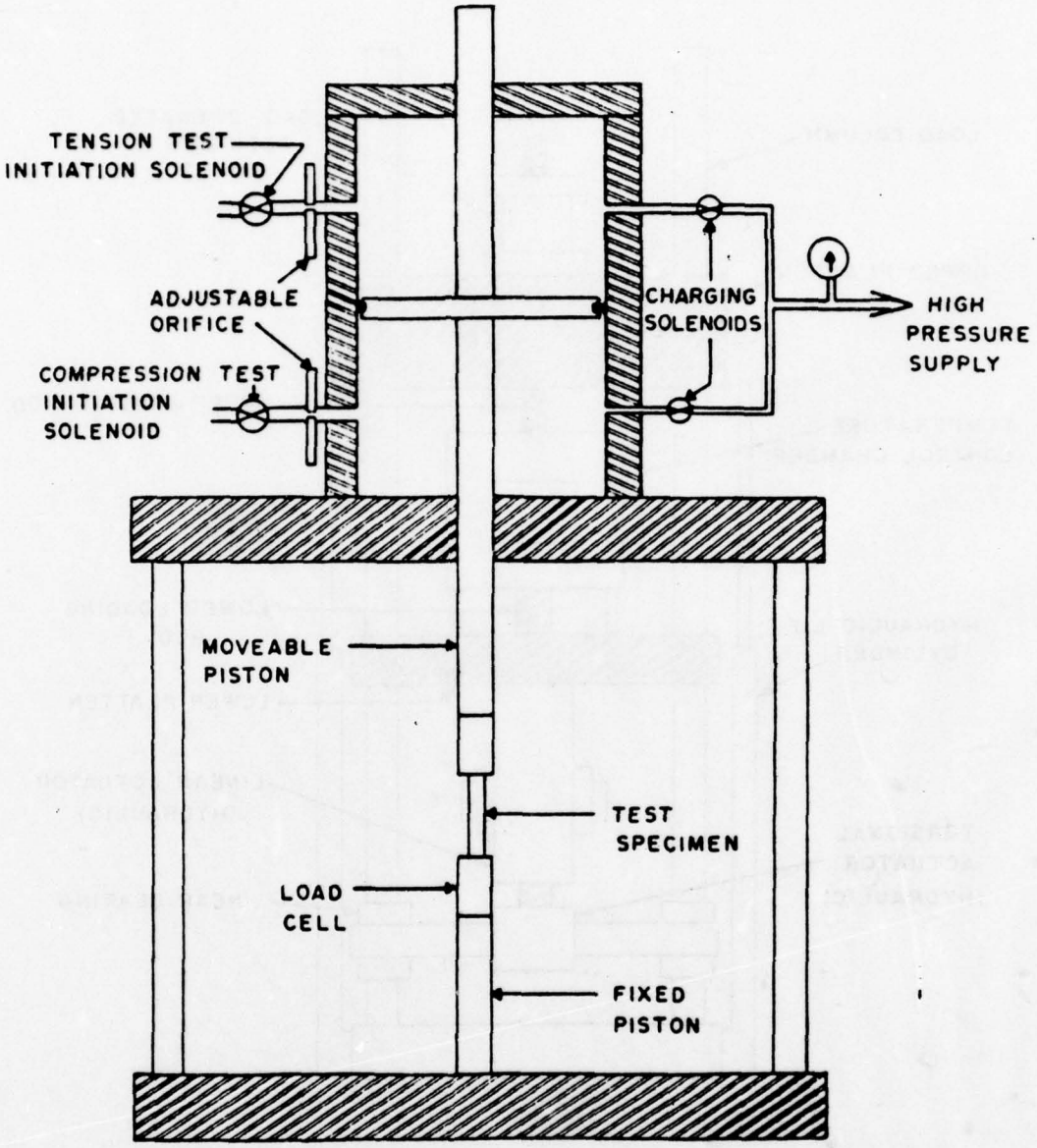

Figure 73. High Strain Rate Gas Actuator.

Actuators are supplied by a 100 hp 50 gpm hydraulic power supply. Accumulators are provided to supply the peak flow rates.

Controls for the medium strain rate machine are located in the adjacent cabinets shown in Figure 71. These cabinets house servo controllers for the hydraulic actuators, each capable of three feedback modes of operation (displacement, strain, load) thus allowing independent selection of the feedback control. Digital ramp generators and a function generator are also available for test control. The pneumatic controls for the fast acting gas actuator system are also housed in the cabinets.

Specimen temperatures can be maintained in the range of -100°F to 300°F with the use of the temperature chamber shown in Figure 71. The lower temperatures are achieved by injecting a spray from a liquid nitrogen bottle. The system operates in a closed loop mode with a thermocouple, attached to the sample, providing a feedback signal to a Research Incorporated Series 6000 Termac Combined Temperature-Power Controller which in turn controls a solenoid on the nitrogen supply. High temperatures are maintained in a similar fashion except that a nicrome wire heater encased in an Inconel sheath is substituted for the solenoid valve. In this case, the error signal controls the amount of power supplied to the heaters by the power controller.

The test configuration for compression tests is illustrated in Figure 74. Sample load was measured with a Sundstrand Data Control, Inc., quartz load cell, model 923F2, interfaced to a charge amplifier. Strains were measured during the tension tests by strain gages bonded directly to the test specimen. Both the load and strain were recorded as a function of time on a Nicolet model 1090AR Digital Oscilloscope, which interfaced with the Digital Equipment Corporation multiuser timesharer computer (PDP 11/34). The strain data is plotted as a function of stress on a cathode-ray tube terminal (Tektronix 4010) and copies on a hard copy unit (Tektronix 4610).

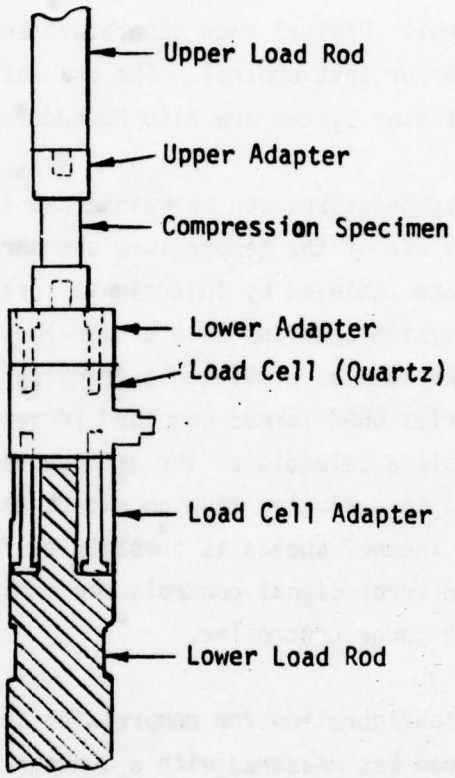

Figure 74. Compression Test Configuration.

TEST PROCEDURE

The following procedures are typically used by Terra Tek in compression tests:

1. Calibrate the load cell.
2. Record exact dimensions of specimen.
3. Install specimen in machine.
4. Attach appropriate coolant or heating enclosures and all instrumentation.
5. Run test as specified, recording stress-strain to failure, and load at yield and break points.
6. Record exact piston velocity achieved during test.
7. Remove specimen from machine and record exact dimensions.
8. Take photograph of specimen.
9. Positively mark and identify each specimen.
10. Repeat applicable above procedure for each specimen in turn.

TEST REQUIREMENTS

Terra Tek provided facilities and services required to apply dynamic loading on the polycarbonate test specimens to simulate a bird strike. Test temperatures and strain rates were established from supersonic aircraft flight profiles and bird impact test data contained in References 1 and 2. The following test conditions reflect these requirements.

Fifteen (15) test specimens of each processed material were to be tested under uniaxial compression loading as follows:

Test Temperature ($\pm$5°F)	-30	76	190
Strain-Rate (in./in./sec. $\pm$50)	200	200	200
Number of Tests	5	5	5

The gage length cross section dimensions of each test specimen was measured within ± 0.001-inch and recorded before each test. A load-deflection curve was recorded for each specimen tested through the maximum load portion of the curve. Photographs of the ruptured specimen were supplied. The maximum load, exact temperature and strain rate was recorded for each test.

TEST RESULTS AND ANALYSIS

The compression properties data presented are based on five (5) test specimens made from the same batch of material and tested at identifical conditions. Test specimens that failed at some fortuitous flaw or that failed in the fusion bond area were not used in calculation of mechanical properties strength data. The design allowables presented were computed on a "B" basis by methods outlined in Section III. Where "B" basis data could not be computed, the "C" basis data was computed and presented. Where the design allowable could not be computed due to insufficient test data, no design allowable is presented.

Test Data

Compression strength data from experimental test results for high strain rate uniaxial compression tests are presented in Table 24. Compression stress-strain curves for average and design allowables are contained in Appendix E. Experimental test data, compression stress-strain curves for test specimens, and computer data runs are contained in Part 2, Appendix M of this report.

Analysis

In this analysis comparisons are made between average compression stress-strain curves to demonstrate the effect of test temperatures on processed polycarbonate material at high strain rates. A plot of

TABLE 24. COMPRESSION STRENGTH DATA

TEST SPECIMEN IDENT	TEST SPECIMEN NO.*	THICK-NESS (IN.)	TEST TEMP (°F)	STRAIN RATE (IN./IN. SEC.)	AVERAGE STRENGTH DATA MAXIMUM STRESS (PSI)	STD DEV (IN./IN.)	MAXIMUM STRAIN (IN./IN.)	STD DEV (IN./IN.)	ELAST MOD (PSI 10-5)	STD DEV (PSI x 10-5)	DESIGN ALLOWABLE DES BAS	MAXIMUM STRESS (PSI)	MAXIMUM STRAIN (IN./IN.)	ELAST MOD (PSI* 10-5)
SWU525	4	.38	-30	197	25,594	407	0.106	0.011	4.54	0.091	B	20,408	0.059	4.28
SWU525	6	.38	72	227	17,427	270	0.114	0.008	4.39	0.518	B	16,311	0.089	2.79
SWU525	4	.38	190	263	13,791	325	0.078	0.002	2.88	0.249	B	12,152	0.072	1.95

* Number of specimens included in the generation of data presented.

average compression curves is presented in Figure 75 comparing processed SL3000 polycarbonate materials at three test temperatures: -30°F, 75°F and 190°F. The compression stress-strain curves plotted are a test average of processed polycarbonate material from Swedlow, Inc. Comparison of compression tests at -30°F and 190°F with respect to room temperature tests reveal a large gain in maximum strength at -30°F as compared to a small loss in maximum strength at 190°F. The opposite effect on elastic modulus is noted with a small gain at -30°F and a large loss at 190°F when compared to the room temperature modulus.

CONCLUSIONS

Conclusions based on data contained in this section and other applicable data are contained in Section XI of this report.

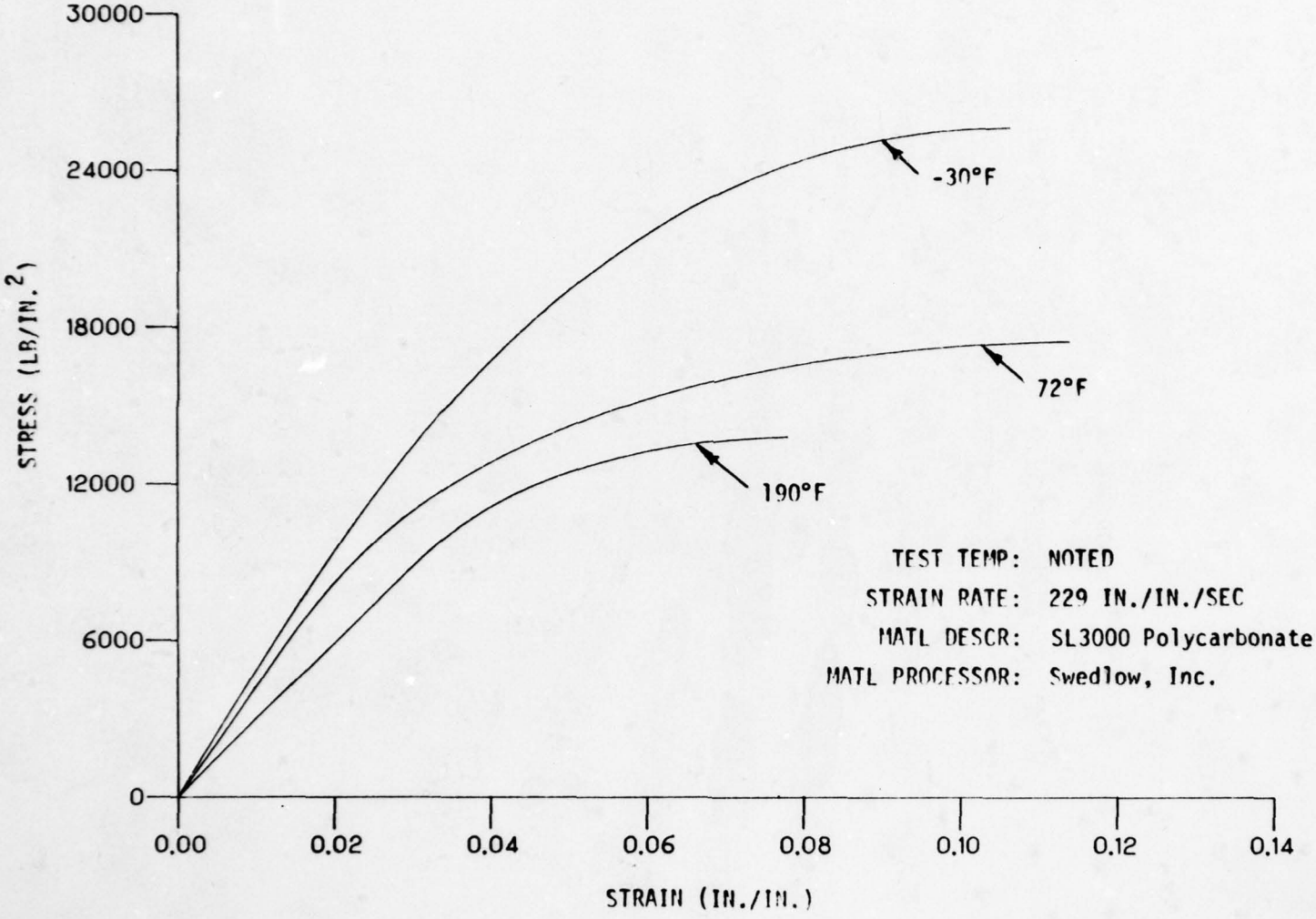

Figure 75. Compression Average Curves - Temperature Effects.

APPENDIX E

COMPRESSION STRESS-STRAIN DATA

PRECEDING PAGE NOT FILMED
BLANK

The following average stress-strain curves and developed design stress-strain curves are presented for use in conjunction with compression strength data given in Table 24, Page 361 of this section.

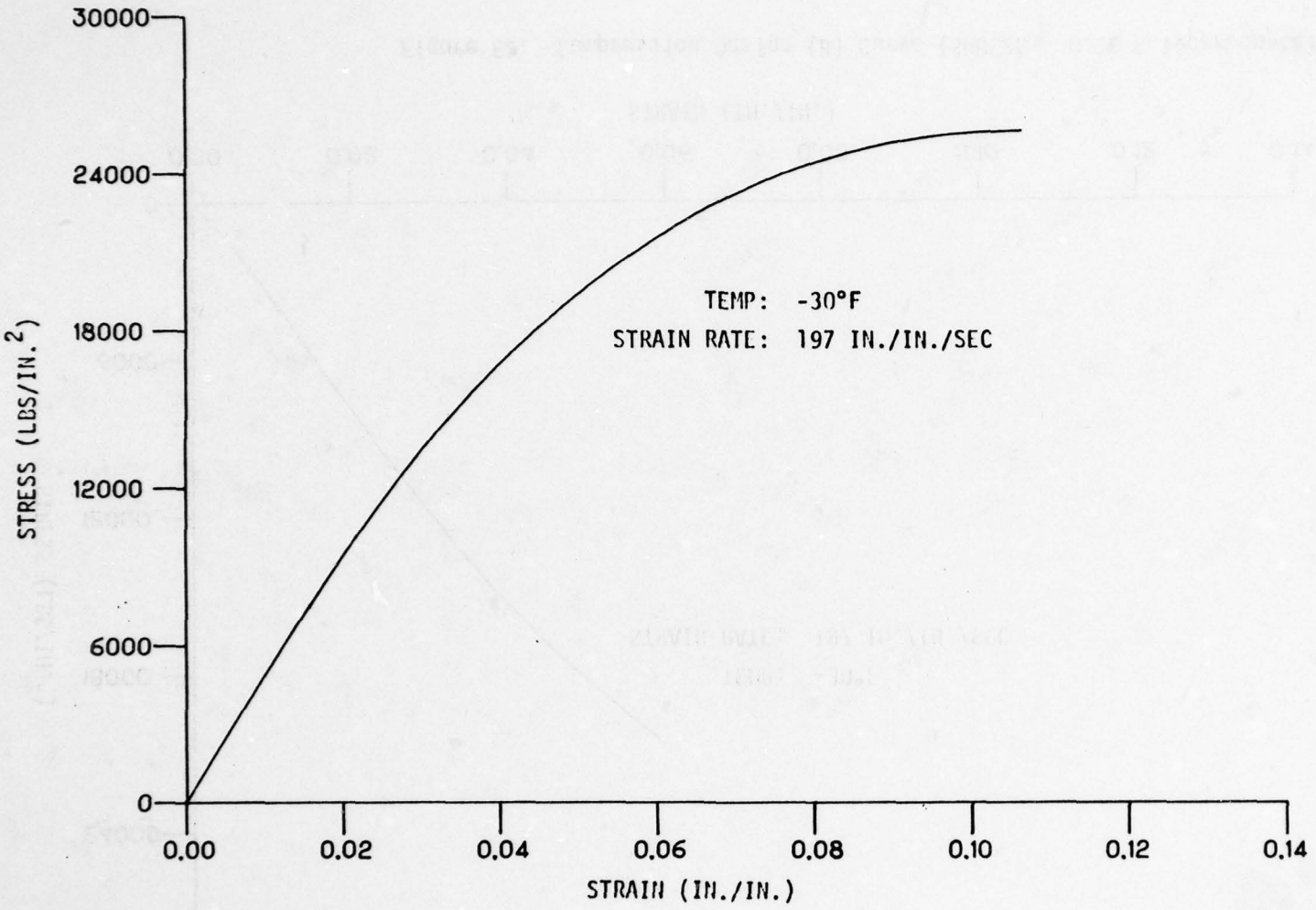

Figure E1. Compression Average Curve (SWU525 - 0.38 Polycarbonate).

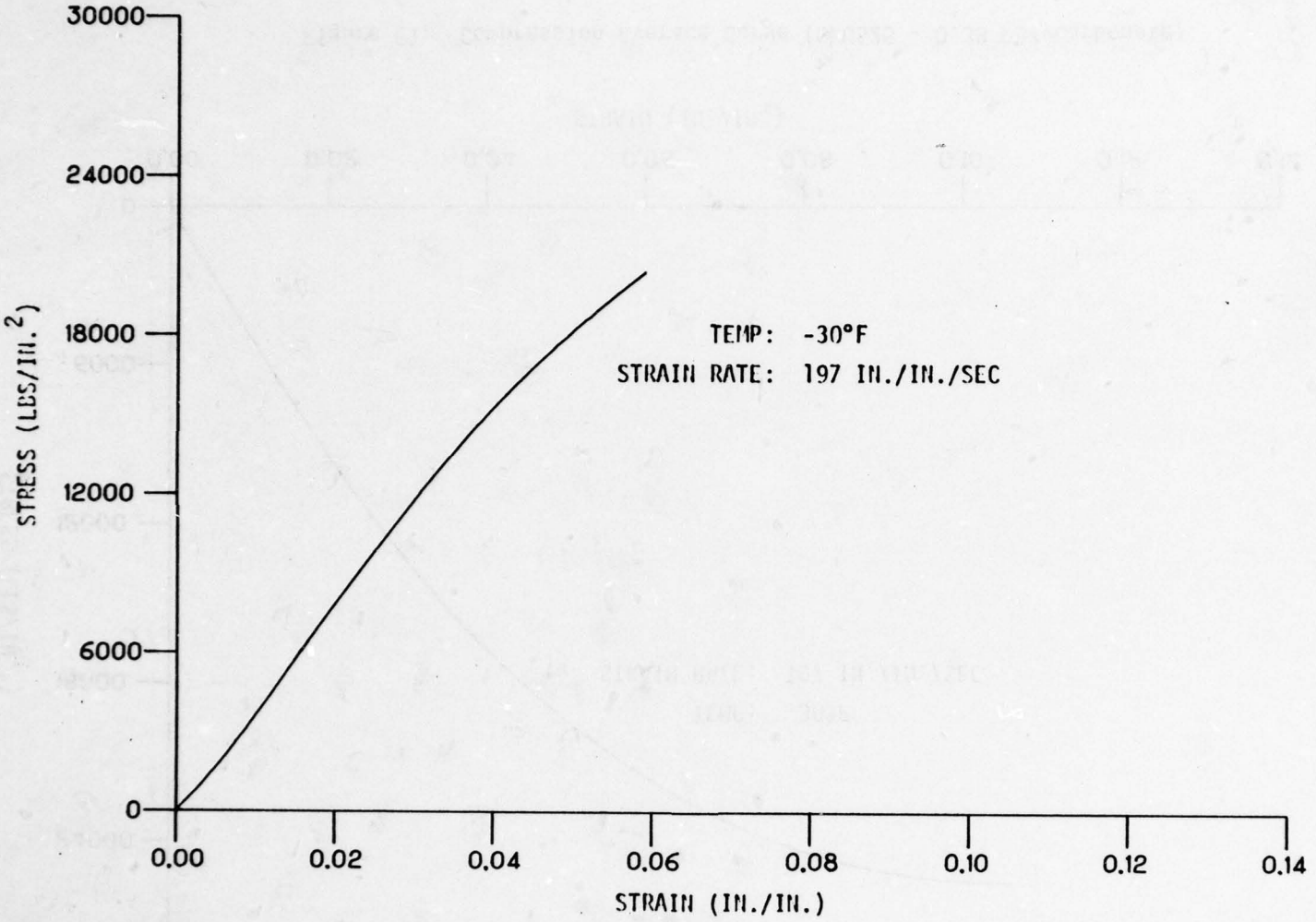

Figure E2. Compression Design (B) Curve (SWU525 - 0.38 Polycarbonate).

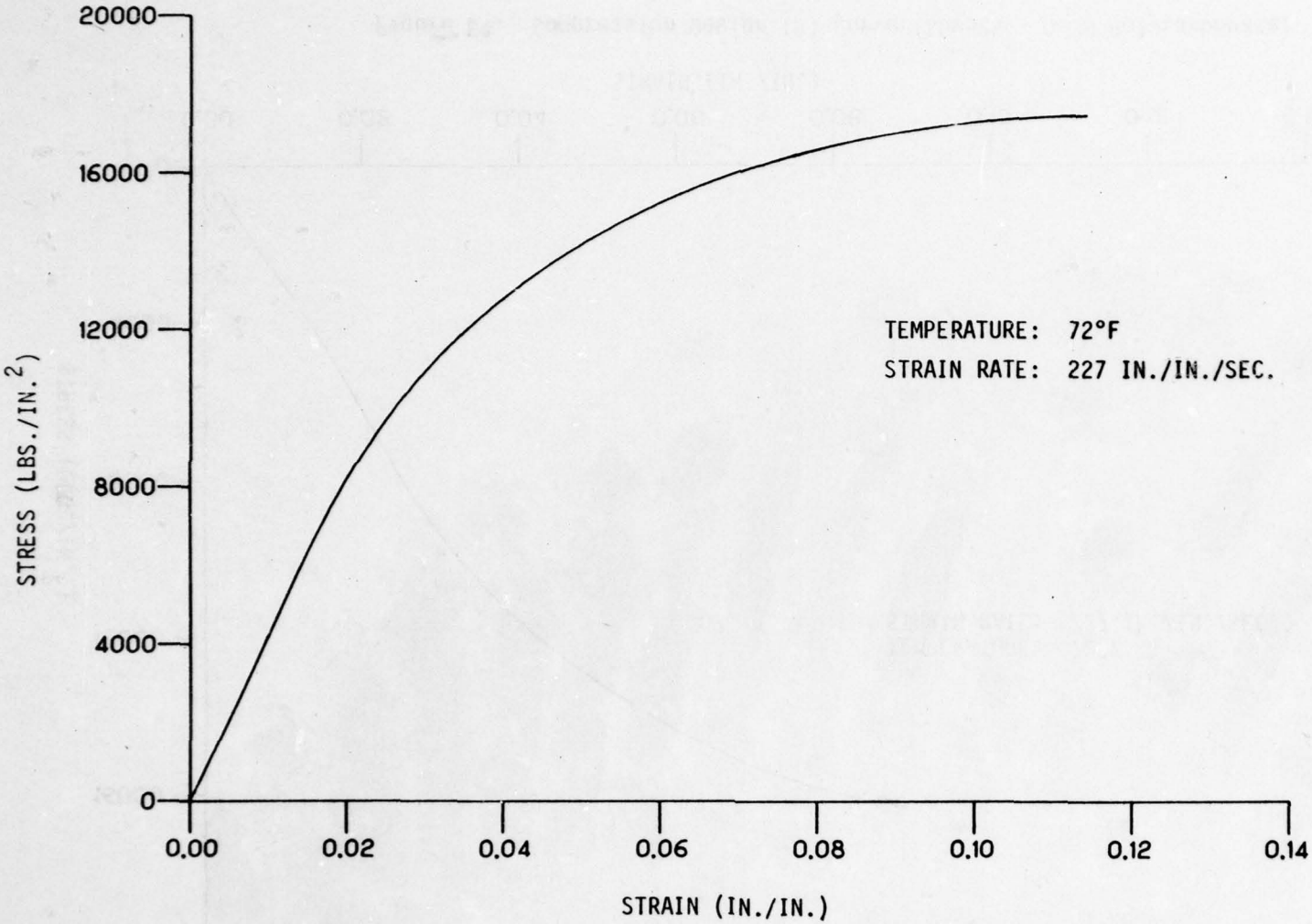

Figure E3. Compression Average Curve (SWU525 - 0.38 Polycarbonate).

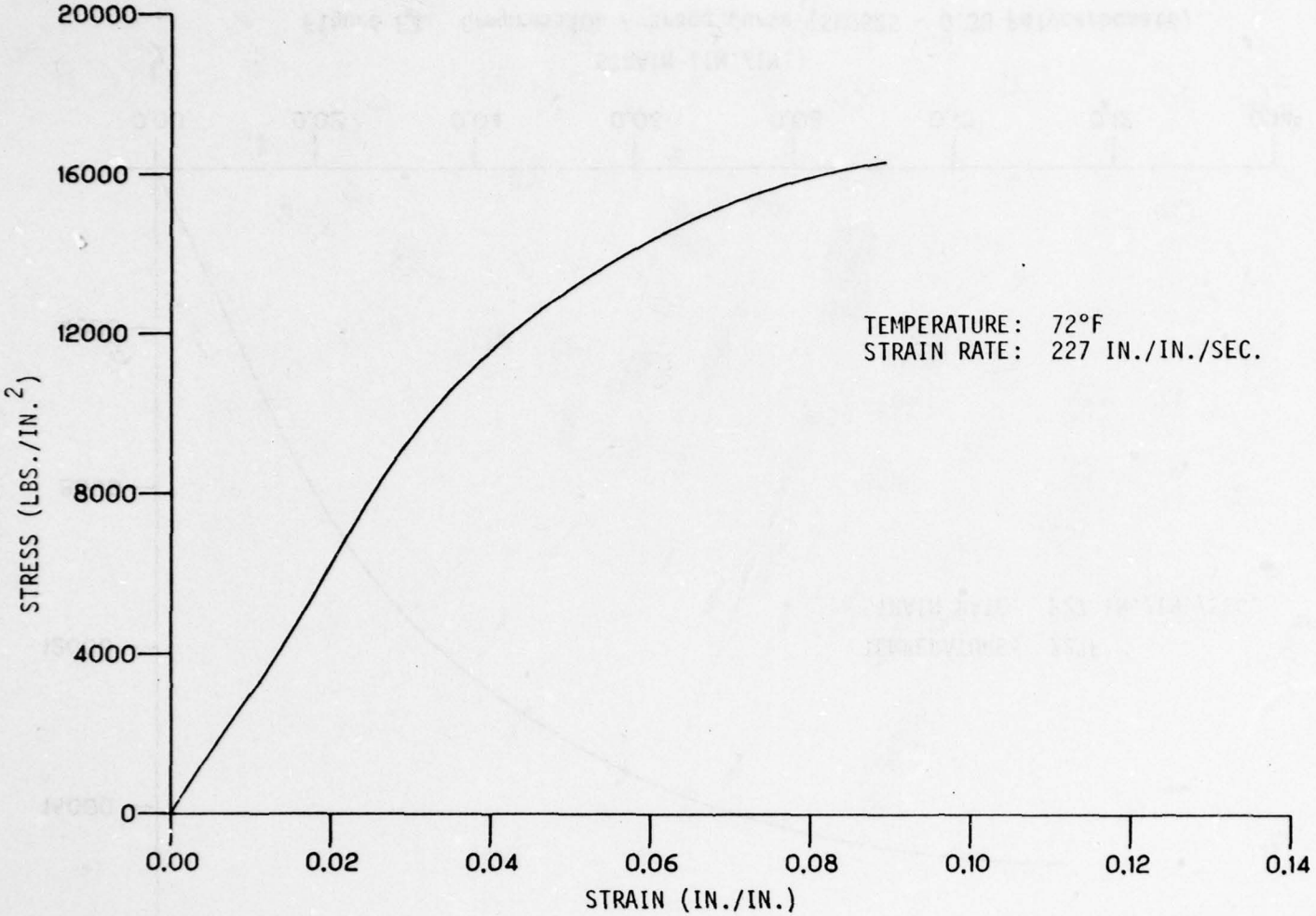

Figure E4. Compression Design (B) Curve (SWU525 - 0.38 Polycarbonate).

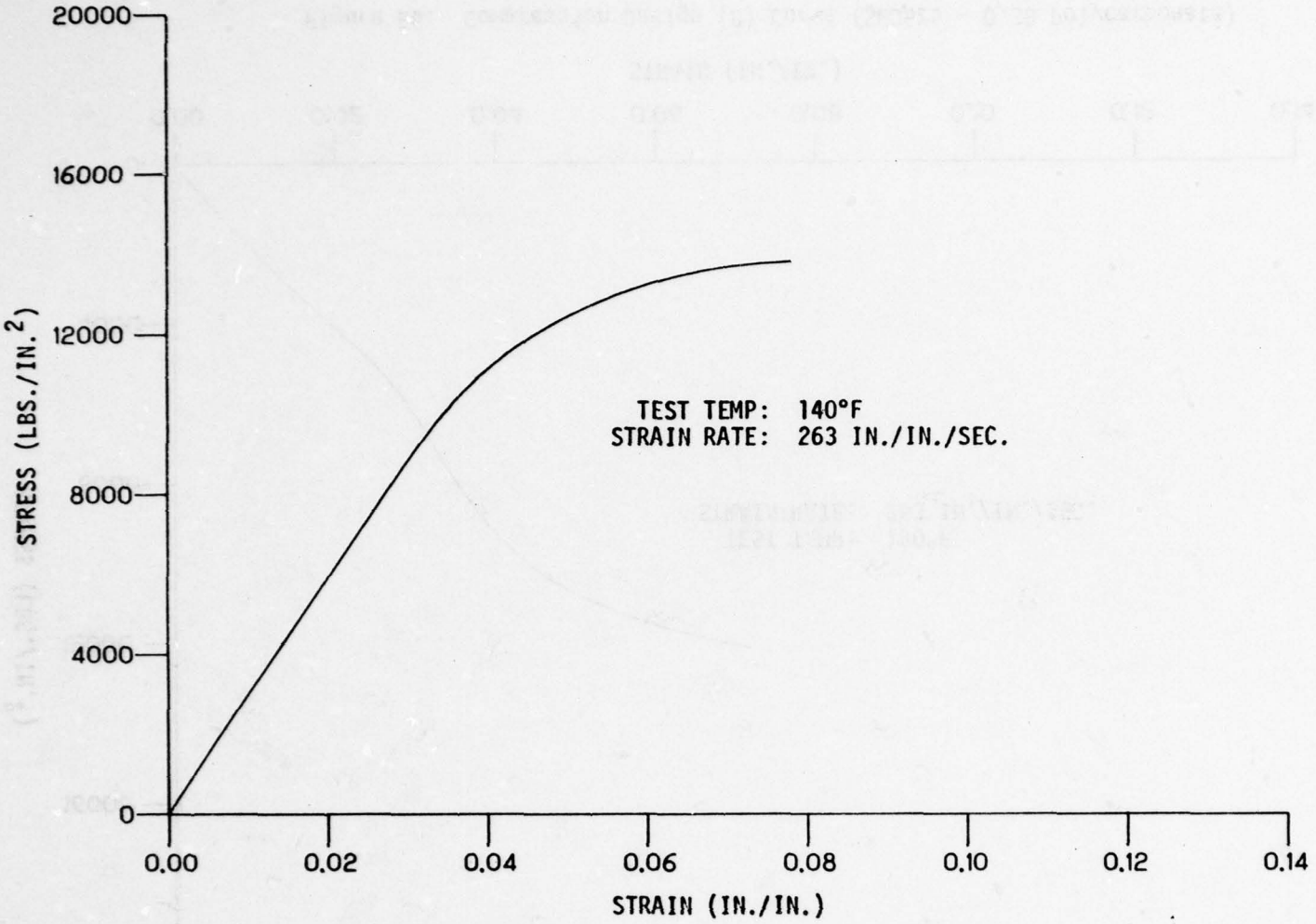

Figure E5. Compression Average Curve (SWU525 - 0.38 Polycarbonate).

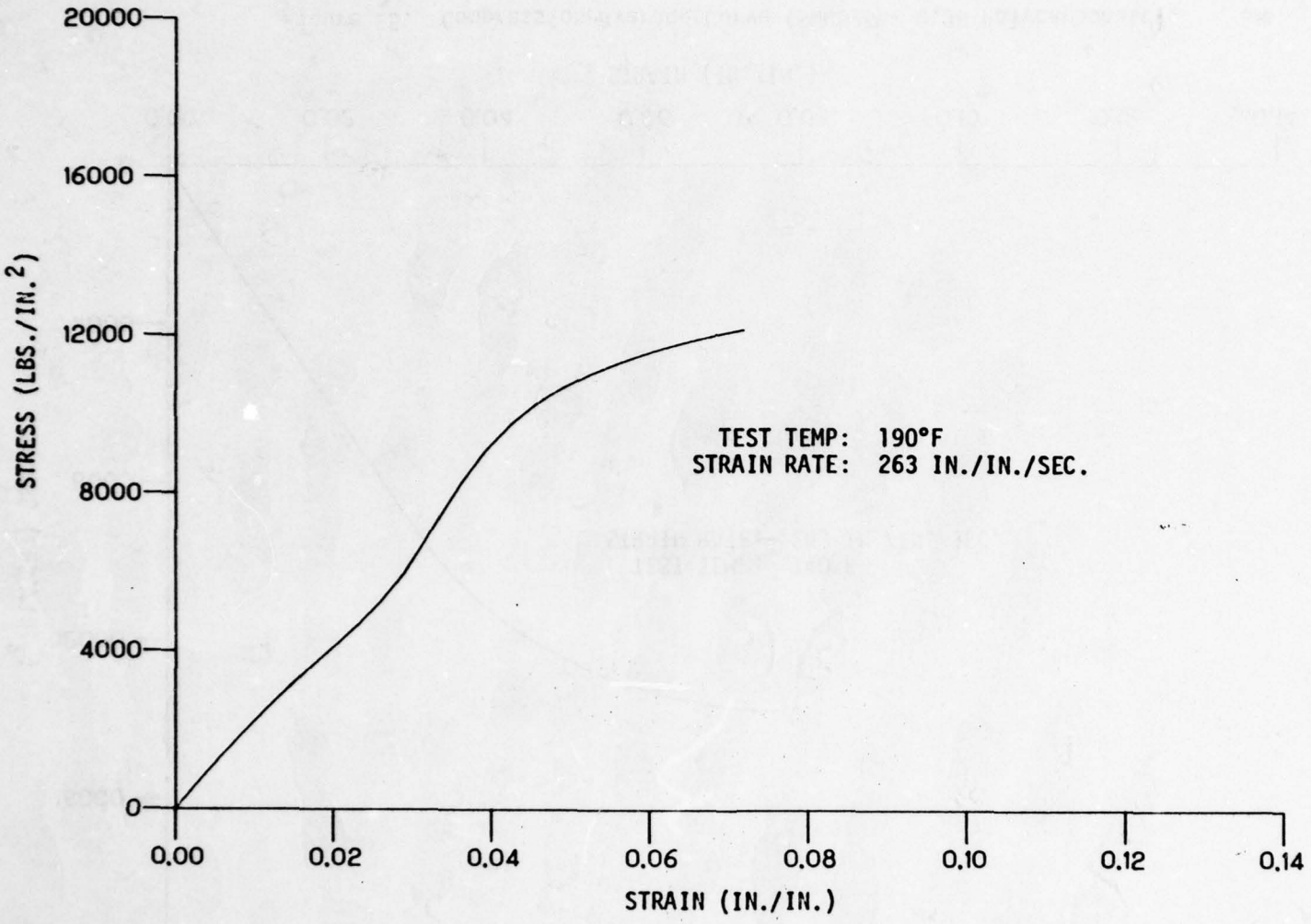

Figure E6. Compression Design (B) Curve (SWU525 - 0.38 Polycarbonate).

SECTION X
HIGH STRAIN RATE SHEAR MECHANICAL PROPERTIES TESTING OF LAMINATED INTERLAYER MATERIALS

This series of tests was conducted to provide high strain rate average (actual) shear mechanical properties and design allowables for laminated interlayer materials as processed by specific aircraft transparency fabricators. The primary use for these mechanical properties was for development of and future design use in computer analysis of a bird strike. This data is also useful in evaluating materials and transparency fabricators. Tests were conducted at the maximum and minimum temperature conditions established by the flight profile of a supersonic aircraft. Maximum strain rates were determined from bird impact tests of actual full size aircraft transparencies. Tests were conducted at Terra Tek, Salt Lake City, Utah, under contract to Douglas for high strain rate testing. Test specimens were designed by Douglas to specifications furnished by Terra Tek, Inc., and manufactured by specific fabricators. These specimens received the same processing as a laminated aircraft transparency.

TEST SPECIMEN DESCRIPTION

The test specimens required for this series of tests are shown in Figures 76 through 78. The shear test specimens were subjected to the same fabrication processes and thermal treatment that is received by a laminated polycarbonate aircraft transparency. A total of 110 specimens of the following configurations were constructed by the noted transparency fabricators.

The Z7942633-519 shear test specimens (Figure 76) were constructed from a laminate containing 2 plies of SL3000 polycarbonate sheet laminated together with PPG Industries 112 polyurethane interlayer material, and with Sierracin, Inc., S-120 polyurethane interlayer materials.

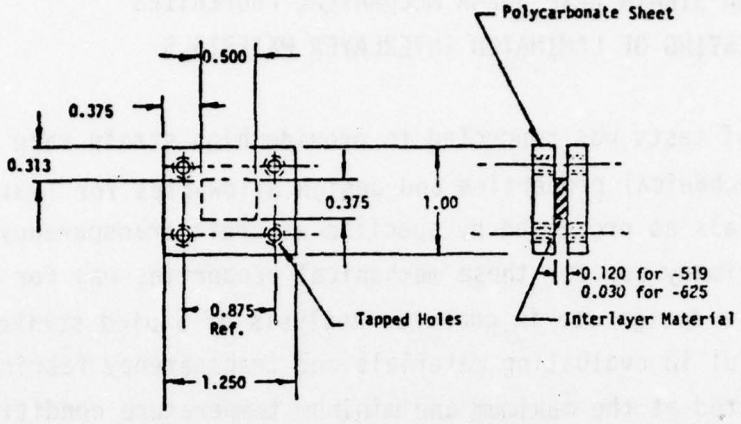

Figure 76. Shear Test Specimen (Z7942633-519, -625).

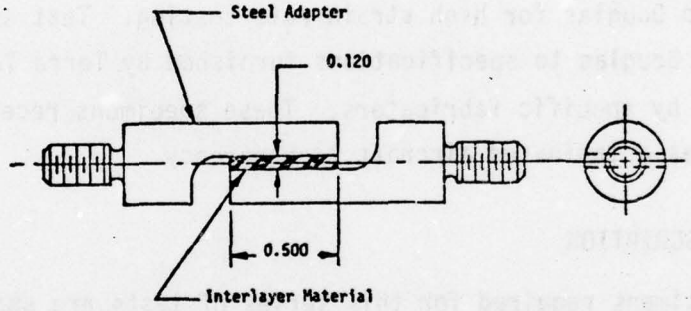

Figure 77. Shear Test Specimen (Z7942633-521).

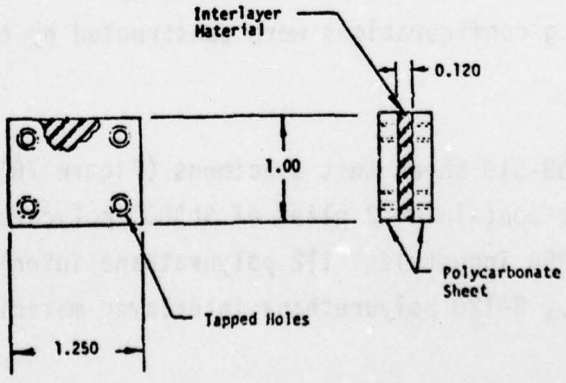

Figure 78. Shear Test Specimen (Z7942633-603).

The Z7942633-521 shear test specimens (Figure 77) were constructed by laminating Swedlow, Inc. SS5272Y (HT) silicone interlayer material between two steel adapter fittings.

The Z7942633-625 shear test specimens (Figure 76) were constructed from a laminate containing 2 plies of SL3000 polycarbonate sheet laminated together with Sierracin, Inc., S-130 co-polymer interlayer material.

The Z7942633-603 shear test specimens (Figure 78) were constructed from a laminate containing 2 plies of SL3000 polycarbonate sheet laminated together with Sierracin, Inc., S-100 silicone interlayer material.

TEST SETUP AND EQUIPMENT DESCRIPTION

The following equipment description is the same as outlined in Section VIII and is repeated here for the convenience of the reader.

All tests were conducted at the Terra Tek medium strain rate facility shown in Figure 79. The main components of the test machine are shown schematically in Figure 80. The lower platen normally remains fixed with the upper platen adjusted to the desired height with the help of the attached hydraulic lift cylinders. Attached to the lower platen is a 50,000 pound 6-inch stroke linear hydraulic actuator capable of operating at cyclic rates up to 20 Hz. This actuator is controlled with a 15 gpm servo valve which allows strain rates of 10^{-6} to 1 in./in./sec. Through the use of a 50 gpm 4-way solenoid operated valve, in conjunction with a flow-control subplate manifold to vary the flow during open-loop operation, the strain rate is extended to 10 in./in./sec.

For all but the very low strain rate tests presented here, the high pressure gas actuator mounted above the upper platen was used. This actuator, Figure 81, is operated by charging a reservoir on either side of the piston to equal pressure. The piston is accelerated when the gas is released from one reservoir, the direction is toward the one that is exhausted. The orifice size can be adjusted to control the exhaust

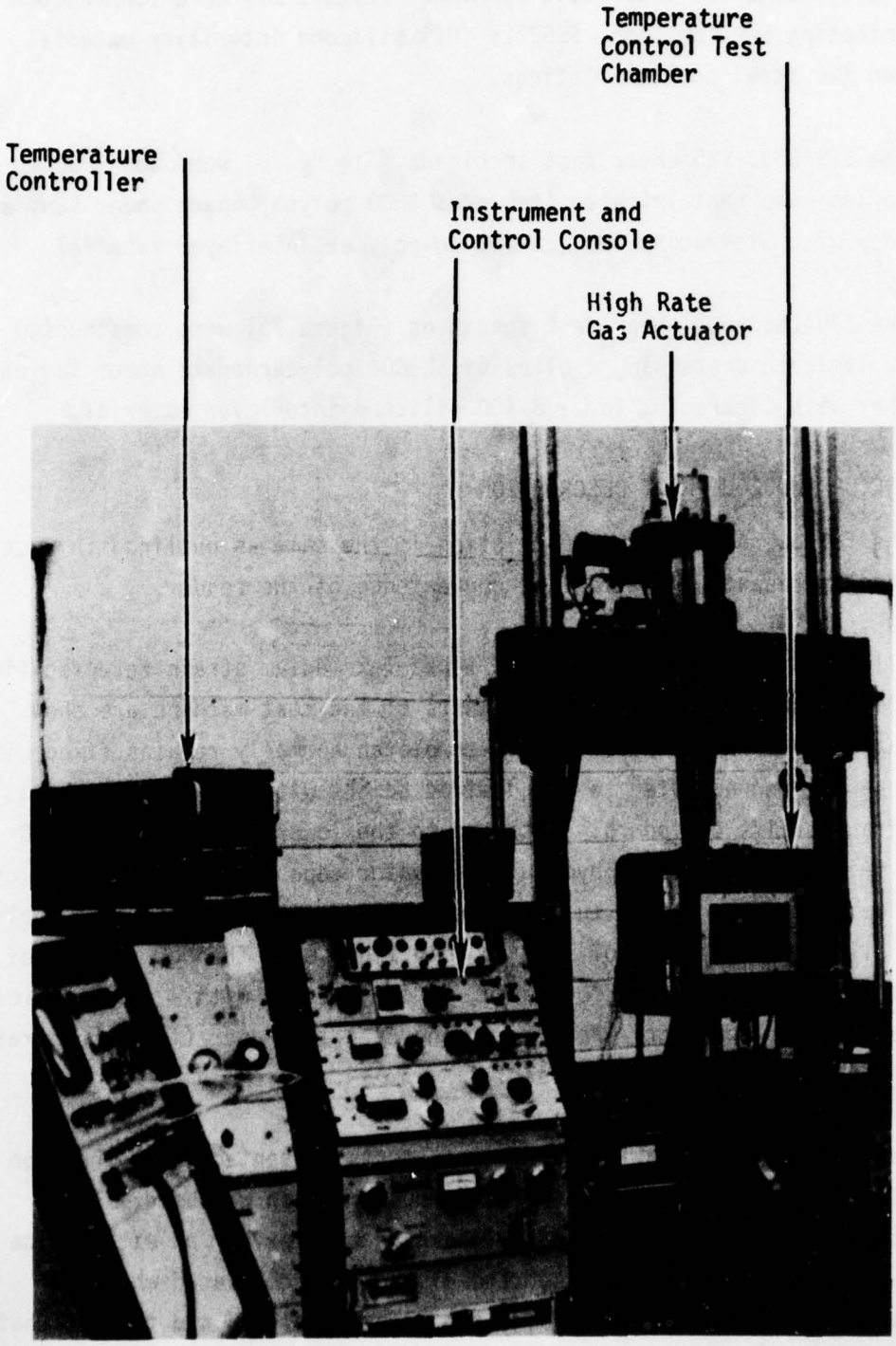

Figure 79. Medium Strain Rate Test Facility.

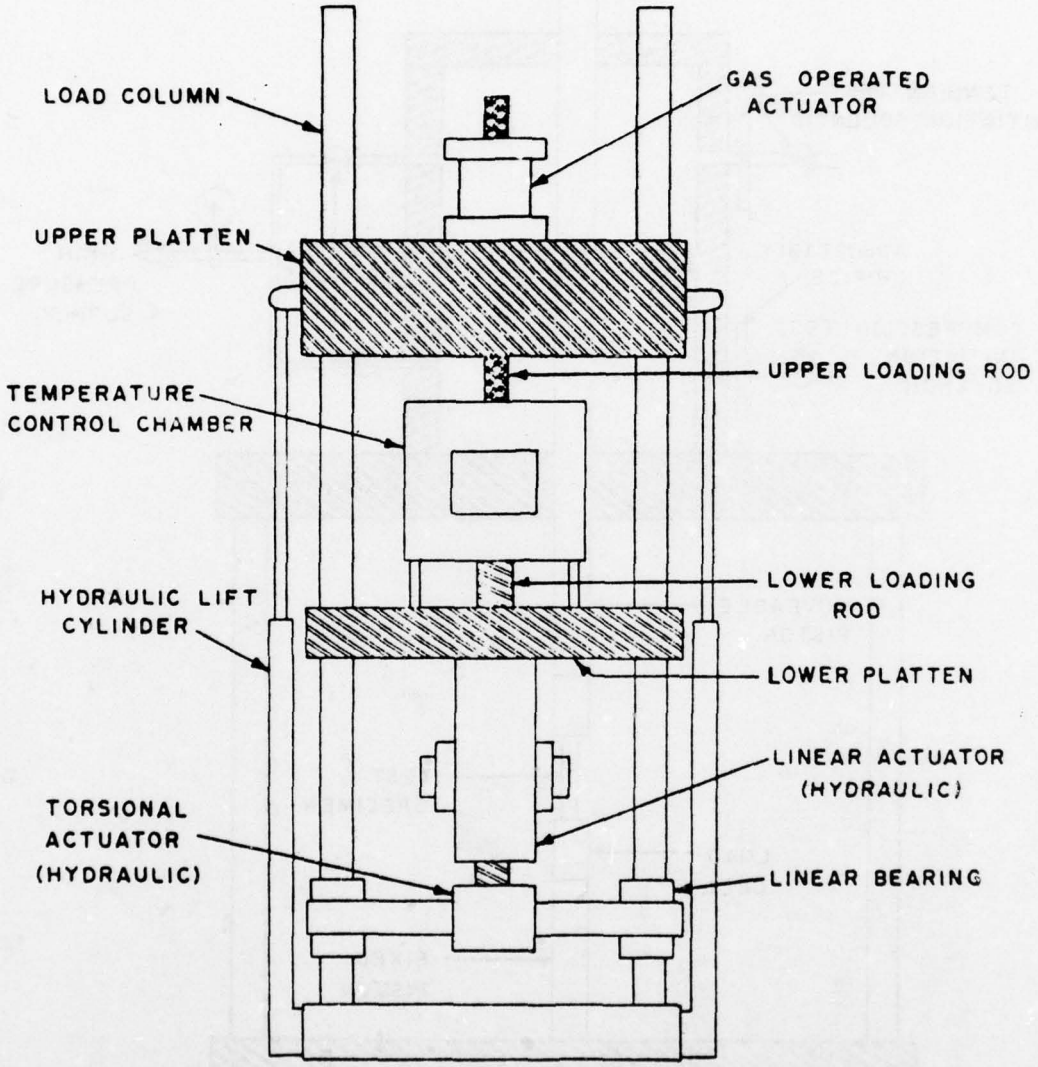

Figure 80. Schematic of Medium Strain Rate Machine.

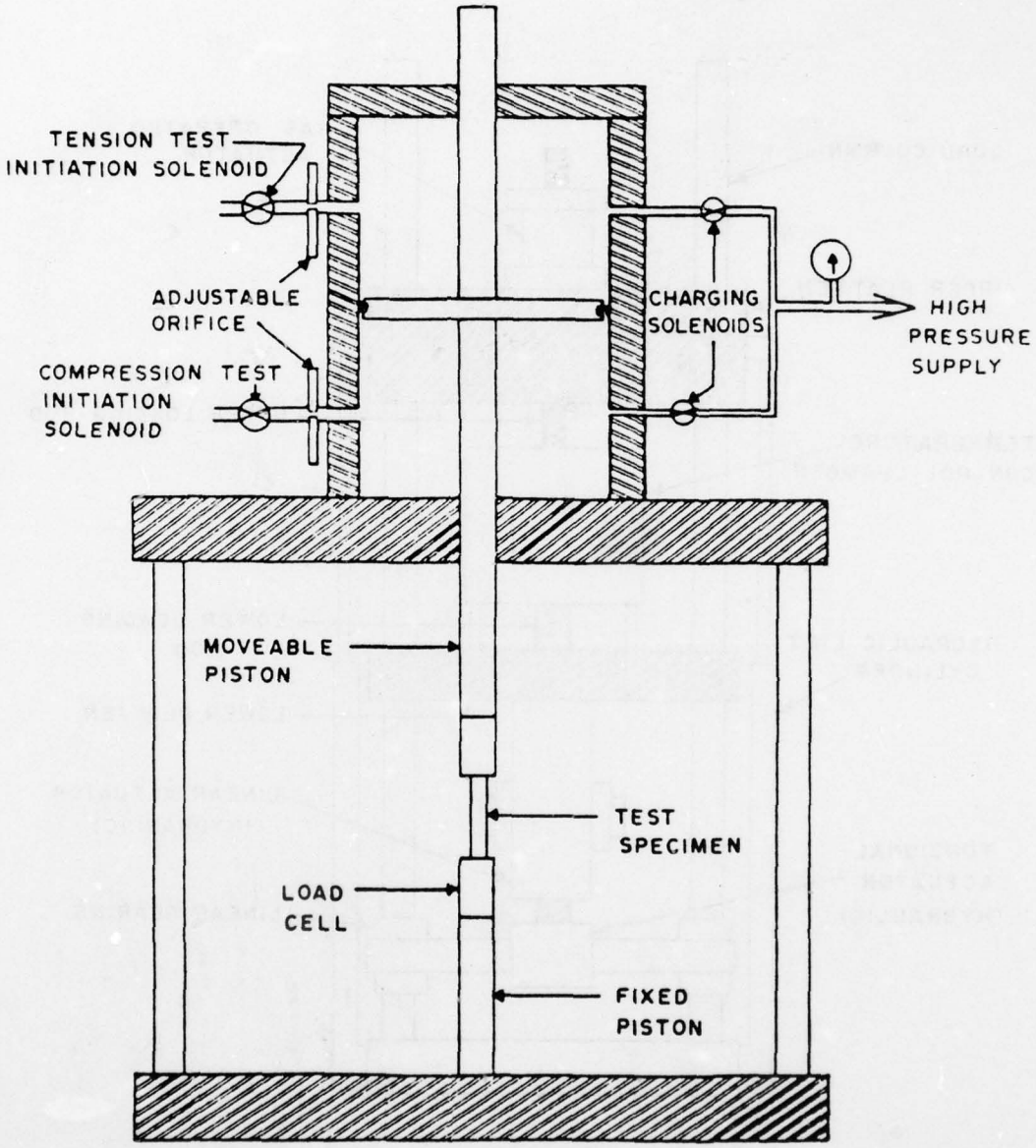

Figure 81. High Strain Rate Gas Actuator.

AD-A064 436 DOUGLAS AIRCRAFT CO LONG BEACH CALIF F/G 11/9
TESTING FOR MECHANICAL PROPERTIES OF MONOLITHIC AND LAMINATED P--ETC(U)
OCT 78 F E GREENE, L P KOEGEBOEHN F33615-75-C-3105
UNCLASSIFIED MDC-J6950 AFFDL-TR-77-96-PT-1 NL

5 OF 5
AD
A064436

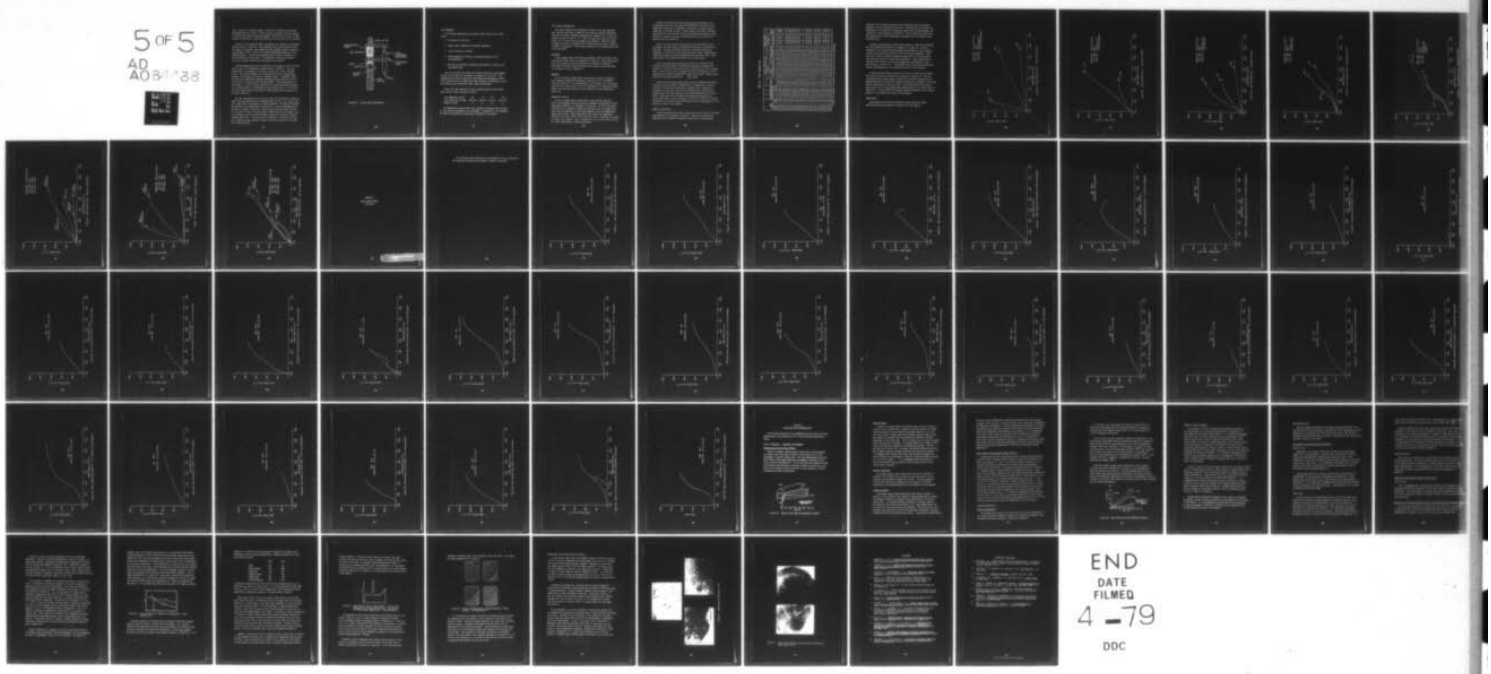

END
DATE
FILMED
4-79
DDC

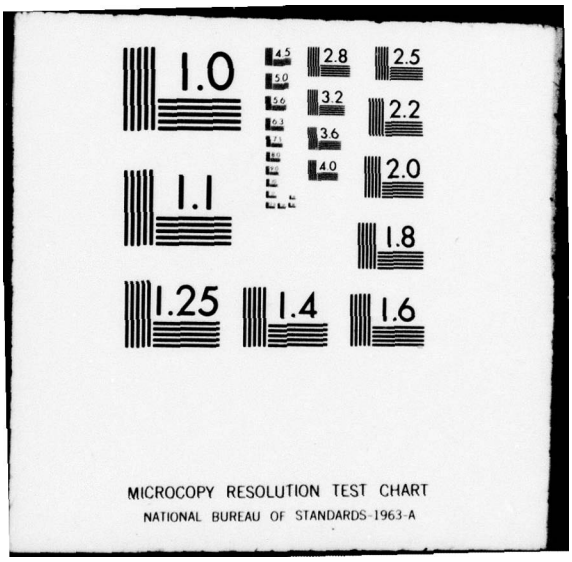
1.0
1.1
1.25
1.4
1.6
1.8
2.0
2.2
2.5
2.8
3.2
3.6
4.0
4.5
5.0
5.6
MICROCOPY RESOLUTION TEST CHART
NATIONAL BUREAU OF STANDARDS-1963-A

rate. Motion is initiated through a fast acting solenoid valve mounted downstream from the orifice. Piston velocity, and hence, rate of loading, is controlled by the gas charging pressure, the orifice size, and, to some extent, the specimen. Piston velocities up to 500 in./sec. can be achieved.

Controls for the medium strain rate machine are located in the adjacent cabinets shown in Figure 79. These cabinets house servo controllers for the hydraulic actuators, each capable of three feedback modes of operation (displacement, strain, load) thus allowing independent selection of the feedback control. Digital ramp generators and a function generator are also available for test control. The pneumatic controls for the fast acting gas actuator system are also housed in the cabinets.

Specimen temperatures can be maintained in the range of -100°F to 300°F with the use of the temperature chamber shown in Figure 79. The lower temperatures are achieved by injecting a spray from a liquid nitrogen bottle. The system operates in a closed loop mode with a thermocouple, attached to the sample, providing a feedback signal to a Research Incorporated Series 6000 Termac Combined Temperature-Power Controller which in turn controls a solenoid on the nigrogen supply. High temperatures are maintained in a similar fashion except that a nicrome wire heater encased in an Inconel sheath is substituted for the solenoid valve. In this case, the error signal controls the amount of power supplied to the heaters by the power controller.

The test configuration for the shear tests are illustrated in Figure 82. Sample load was measured with a Sundstrand Data Control, Inc., quartz load cell, Model 923F2, interfaced to a change amplifier. The shear displacement was obtained on the shear tests by the use of a linear displacement potentiometer, as shown in Figure 82. Both the load and strain were recorded as a function of time on a Nicolet model 1090AR digital oscilloscope, which was interfaced with the Digital Equipment Corporation multiuser timeshare computer (PDP 11/34). The strain data is plotted as a function of stress on a cathode-ray tube terminal (Tektronix 4010) and copied on a hard copy unit (Tektronix 4610).

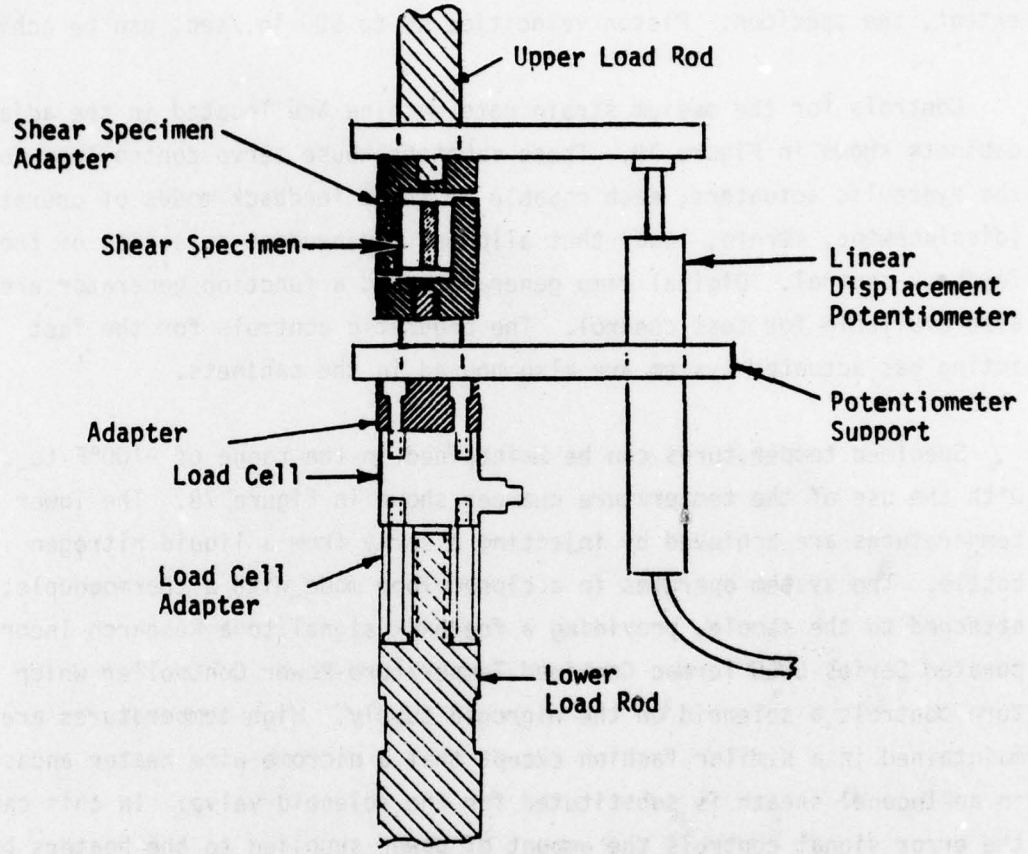

Figure 82. Tensile Test Configuration.

TEST PROCEDURE

The following procedures are typically used by Terra Tek in shear tests;

1. Calibrate the load cell.

2. Record exact dimensions of specimen interlayer.

3. Install specimen in machine.

4. Attach appropriate coolant or heating enclosures and all instrumentation.

5. Run test as specified, recording stress-strain to failure, and the maximum load.

Terra Tek provided facilities and services required to apply dynamic loading on the shear test specimens to simulate a bird strike. Test temperatures and strain rates were established from supersonic aircraft flight profiles and bird impact test data contained in References 1 and 2. The following test conditions reflect these requirements.

Twenty (20) test specimens of each processed material were tested under uniaxial shear loading as follows:

Test Temperature (±5°F)	-30	76	76	190
Strain Rate (in./in./sec)	200 ± 50	200 ± 50	10 ± 2.5	200 ± 50
Number of Tests	5	5	5	5

The engineering stress-strain curve through the maximum stress portion of the curve was recorded for each specimen. A minimum of 5 test specimens for each test condition and each type of material was provided.

TEST RESULTS AND ANALYSIS

The shear strength data presented are based on five test specimens made from the same batch of material and tested at identical conditions. The specific design allowables presented were computed on a "B" basis by methods outlined in Section III. Where "B" basis data could not be computed, the "C" basis data was computed and presented. Where the design allowable could not be computed due to insufficient test data, no design allowable is presented. Strain rates indicated are an average strain rate of the test data.

Test Data

Shear strength data derived from experimental results for high strain rate uniaxial shear tests are summarized in Table 25. Shear stress-strain plots for average and design allowables are contained in Appendix F. Experimental test data and true stress-strain curves for test specimens are contained in Part 2, Appendix N.

Analysis

In this analysis average shear stress-strain curves are plotted to show temperature effects on mechanical properties for five different interlayer materials: two polyurethanes, two silicones, and a co-polymer. Average shear stress-strain curves are superimposed for comparison between these five interlayer materials at cold, ambient, and hot temperature conditions.

Temperature Effects

A plot of average shear stress-strain curves for PPG Industries PPG-112 polyurethane interlayer material (Z7942633-519 specimen) at three temperature conditions is presented in Figure 83. The plot illustrates the large loss in strength at 190°F and the small gain in strength with a large loss in elongation at -30°F when compared to the room temperature stress-strain curve. These conditions do not agree with temperature effects at low strain rates in that the large loss in elongation to rupture at -30°F is not evident. This is assumed to be due to bond failure (Table 25) rather than material cohesive properties.

A plot of average shear stress-strain curves for Sierracin, Inc., S-120 polyurethane interlayer material (Z7942633-625 specimen) at two temperature conditions is presented in Figure 84. The plot denotes a large loss in strength at 190°F. Since a bond failure mode is evident per Table 25 for this material at all test temperature conditions these results are assumed to be due to bond failure and do not reflect the material cohesive properties.

A plot of average shear stress-strain curves for Sierracin S-130 co-polymer interlayer material (Z7942633-625 specimen) is presented in Figure 85. The plot illustrates the loss in strength with gain in elongation at 190°F and a gain in strength with a loss in elongation at -30°F when compared to the room temperature stress-strain curve. These results agree with temperature effects at low strain rates.

A plot of average shear stress-strain curves for Sierracin S-100 silicone interlayer material (Z7942633-603 specimen) is presented in Figure 86. The plot illustrates the gain in strength with loss in elongation at -30°F and the loss in strength with loss in elongation at 195°F when compared to the room temperature stress-strain curve. These results agree with temperature effects at low strain rates.

A plot of average shear stress-strain curves for Swedlow SS5272Y(HT) silicone interlayer material (Z7942633-521) is presented in Figure 87. The plot illustrates the large gain in strength with a large gain in elongation at -30°F and a small loss in strength with a small loss in elongation at 190°F when compared to the room temperature stress-strain curve. These results do not agree with temperature effects at low strain rates where a loss in elongation to failure at -30°F was indicated. The mechanism that caused these differences was not investigated as it was beyond the scope of this program.

Material Comparisons

A plot of average shear stress-strain curves at 75°F for the five interlayer materials is presented in Figure 88. The plot illustrates the increased shear strength and elongation capabilities of polyurethane

TABLE 25. SHEAR STRENGTH DATA

TEST SPECIMEN IDENT	NO*	THICKNESS (IN.)	TEST TEMP (° F)	STRN RATE (IN/IN/SEC	AVERAGE STRENGTH DATA: FAILURE TYPE	ULTIMATE: STRESS (PSI)	ULTIMATE: STD DEV (PSI)	ULTIMATE: STRAIN (IN/IN)	ULTIMATE: STD DEV IN/IN)	SHEAR MOD (PSI	STD DEV (PSI)	DESIGN ALLOWABLE: DES BAS	ULTIMATE: STRESS (PSI)	ULTIMATE: STRAIN (IN/IN)	SHEAR MOD (PSI
PPG519	5	.12	72	50	SHEAR	2803	96	4.207	0.109	1037	87	C	2583	3.972	898
PPG519	5	.12	72	160	SHEAR	2644	97	4.914	0.338	779	24	B	2145	3.761	700
PPG519	4	.12	-30	98	BOND	3593	294	0.910	0.280	7061	2453				
PPG519	4	.12	190	180	SHEAR	626	114	4.962	0.332	340	65	C	296	4.093	174
SK519	5	.12	73	150	BOND	1393	735	3.734	0.967	355	154	C	288	1.655	102
SK519	4	.12	73	8	BOND	451	38	1.547	0.117	437	38	C	328	1.242	339
SK519	3	.12	190	222	SHEAR	381	24	3.051	0.203	337	79	C	258	2.279	319
SK603	5	.12	73	10	SHEAR	374	6	2.544	0.115	88	20	C	328	2.296	51
SK603	6	.12	73	209	SHEAR	446	17	4.810	0.914	64	13				
SK603	2	.12	-30	159	SHEAR	575	24	3.709	0.260	232	103				
SK603	5	.12	190	236	SHEAR	366	20	2.390	0.257	125	11	C	148	1.837	119
SK625	5	.03	73	8	BOND	1393	137	3.235	0.386	664	158	C	926	2.405	371
SK625	4	.03	73	450	BOND	1961	286	3.148	1.161	1262	294				
SK625	5	.03	-30	184	BOND	3440	343	2.935	0.225	1967	809	C	2758	2.452	317
SK625	5	.03	190	327	BOND	736	126	4.880	0.885	217	53	C	394	2.978	101
SWU521	5	.120	72	55	SHEAR	322	50	4.185	0.962	52	10				
SWU521	4	.12	72	195	SHEAR	322	29	3.421	0.814	66	18	C	26	1.183	20
SWU521	4	.12	-30	200	SHEAR	563	73	5.509	0.483	64	7	C	314	4.244	46
SWU521	3	.12	190	195	SHEAR	310	71	3.032	0.716	51	13				

* Number of specimens included in the generation of data presented.

materials and increased strength of the co-polymer over the silicone materials at room temperature conditions. The plot also illustrates the differences in strength and elongation capabilities of polyurethanes and silicones at room temperature conditions. These comparisons agree with the results for the same temperature and materials at low strain rates in Section VII.

A plot of average shear stress-strain curves at -30°F test condition for four interlayer materials is presented in Figure 89. The plot illustrates the increased shear strength capabilities of the co-polymer (S-130) and polyurethane (PPG-112) over the silicone materials. This plot also reveals increased elongation capabilities of the co-polymer over the polyurethanes at these test conditions. These comparisons do not agree with results for the same temperature and material at low strain rates in Section VII. The mechanism that caused these differences was not investigated as it was beyond the scope of this program.

A plot of average shear stress-strain curves at 195°F test condition for the five interlayer materials is presented in Figure 90. The plot illustrates the increased shear strength and elongation capabilities of polyurethane (PPF-112) and the co-polymer material as compared to silicones, and the polyurethane (S-120) at 190°F. These comparisons do not agree with results for the same temperature and materials at low strain rates in Section VII. The mechanism that caused these differences was not investigated as it was beyond the scope of this program.

CONCLUSIONS

Conclusions based on data contained in this section and other applicable data are contained in Section XI of this report.

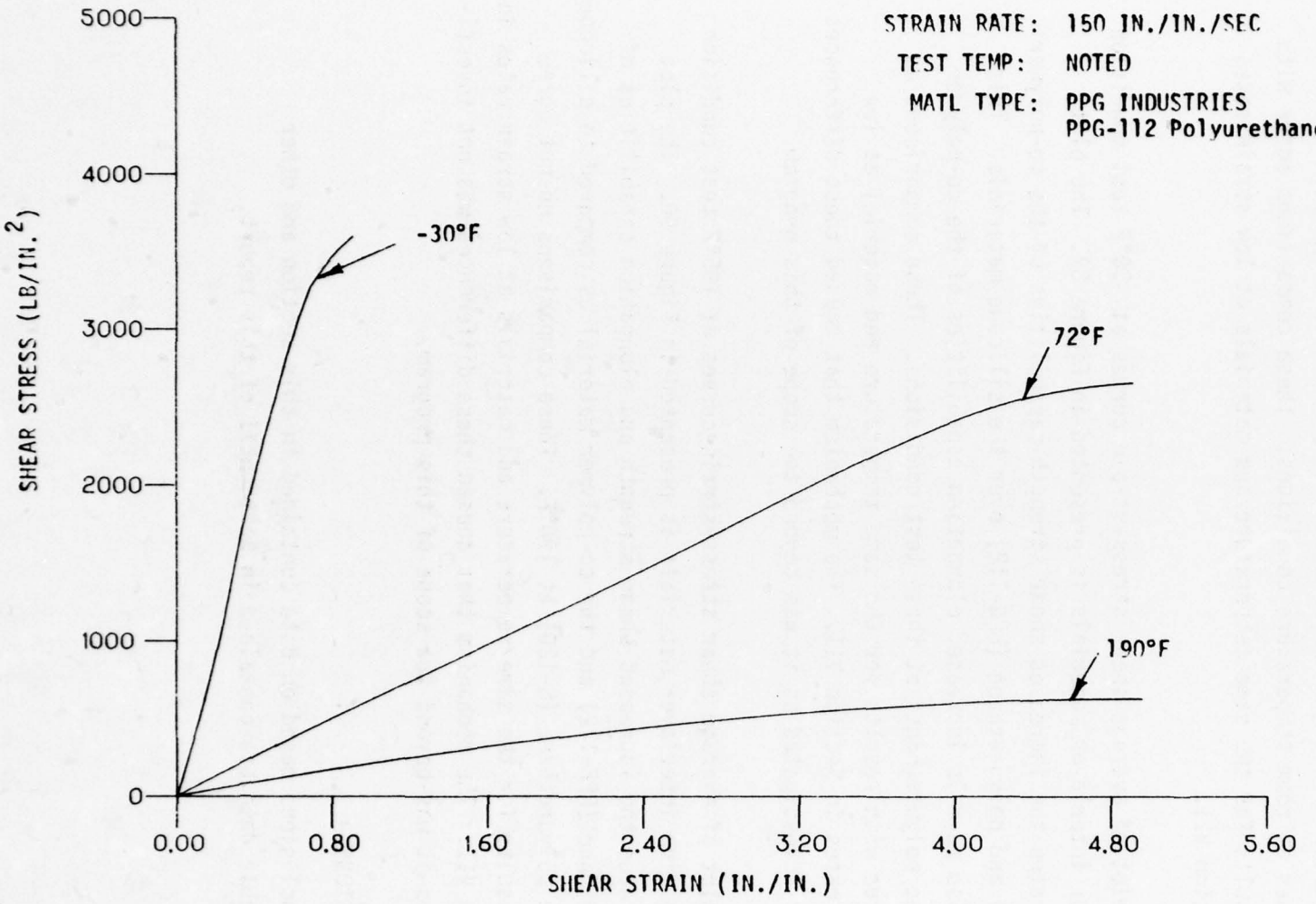

Figure 83. Shear Average Curves - Temperature Effects.

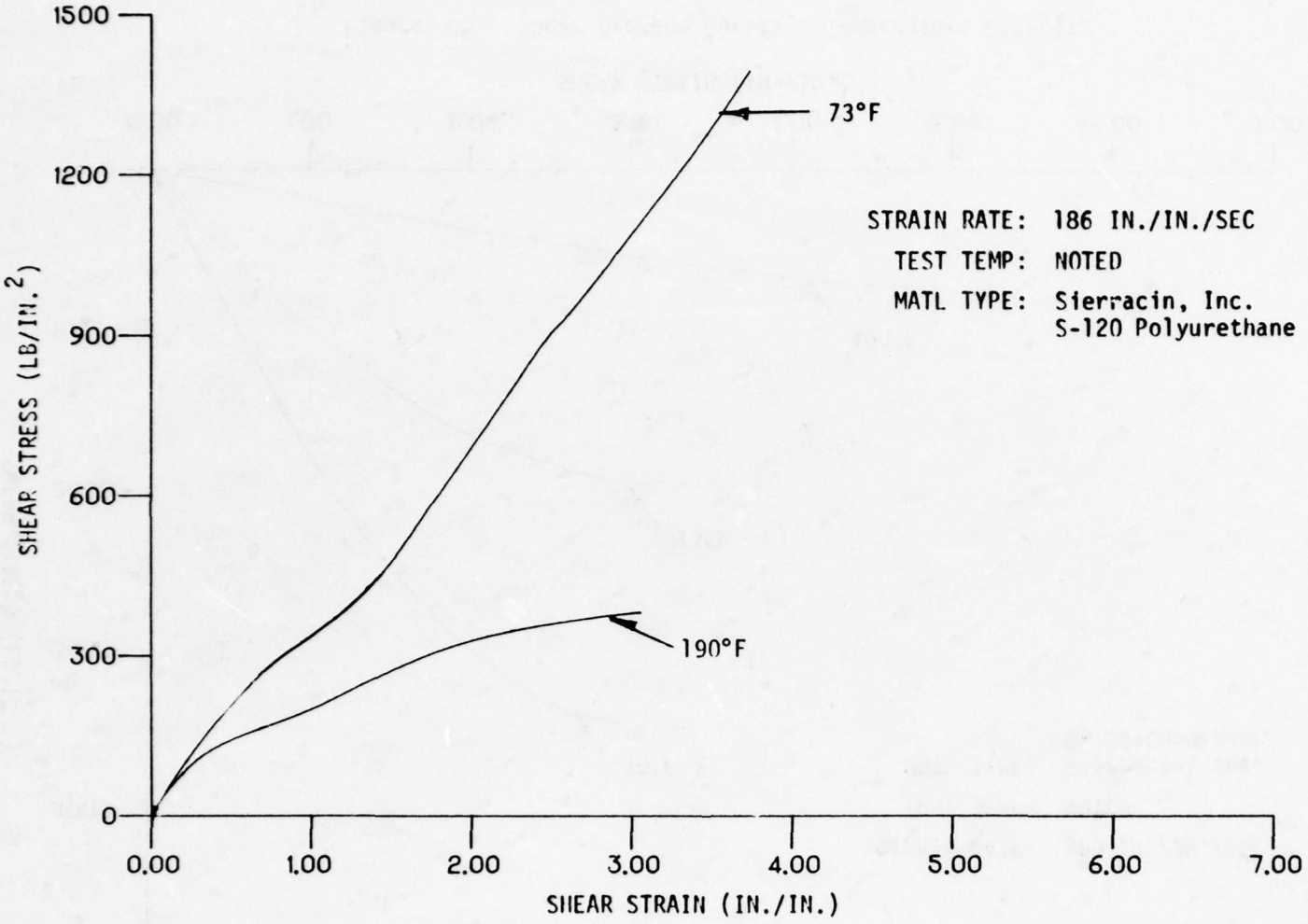

Figure 84. Shear Average Curves - Temperature Effects.

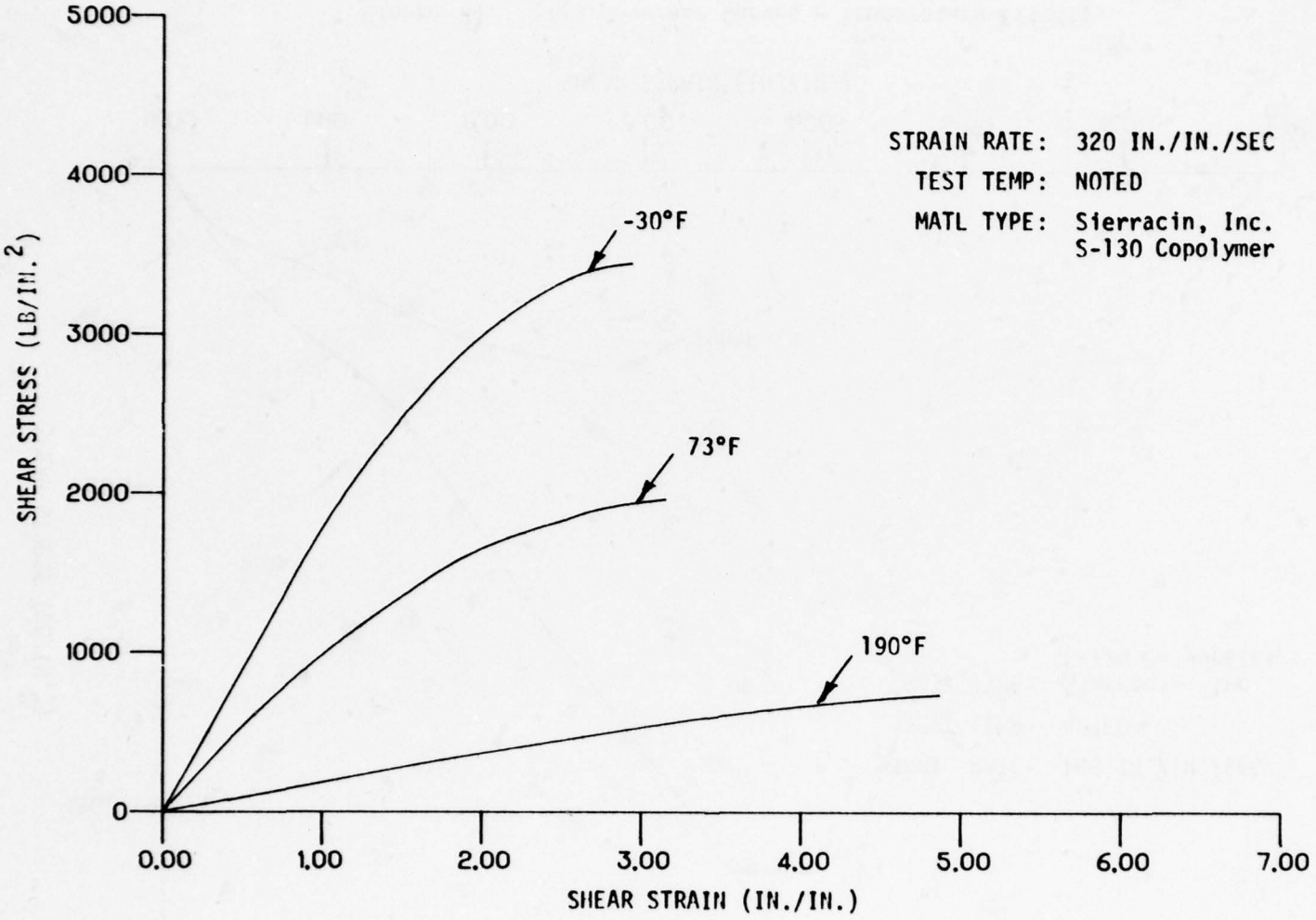

Figure 85. Shear Average Curves - Temperature Effects.

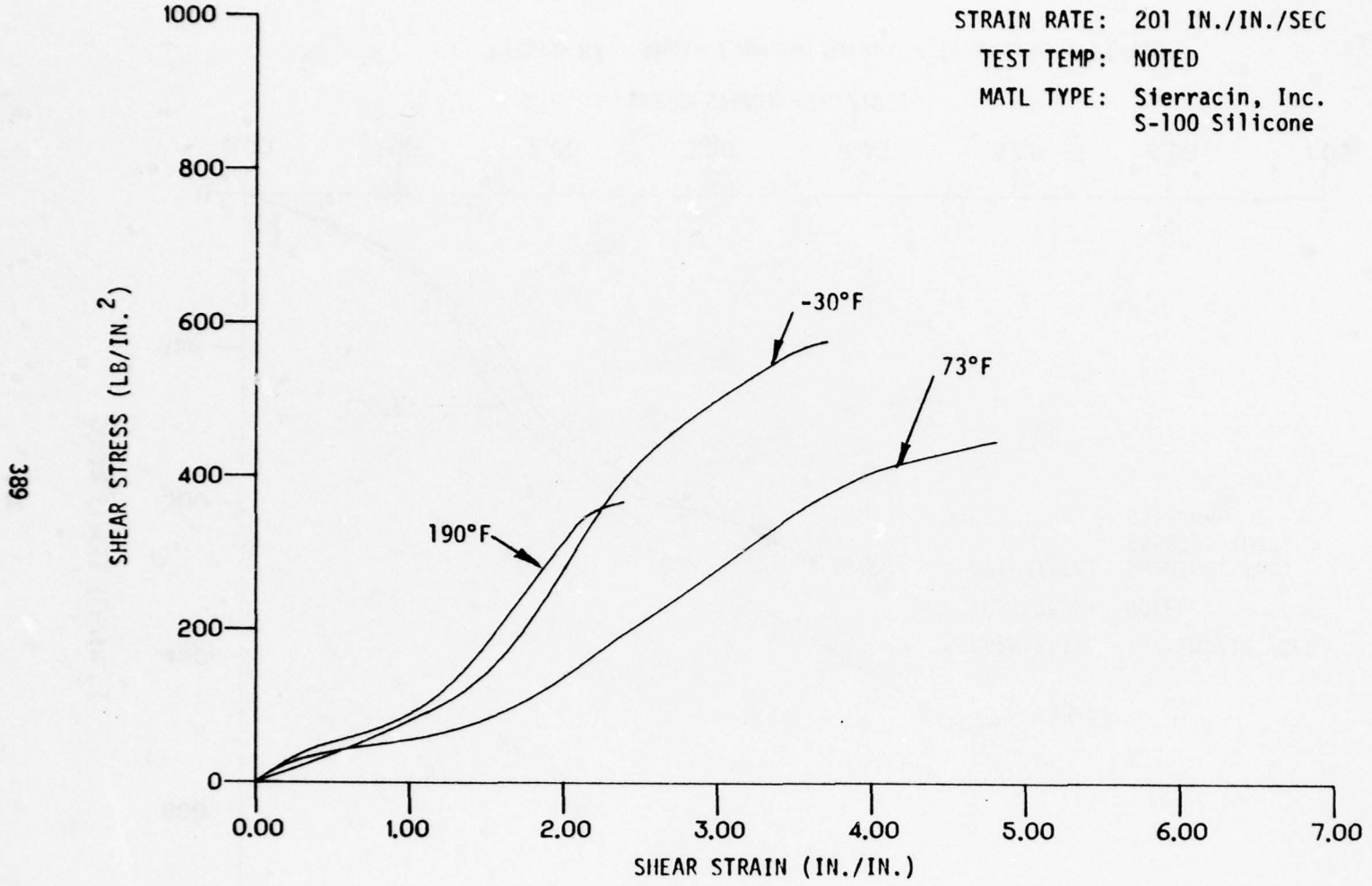

Figure 86. Shear Average Curves - Temperature Effects.

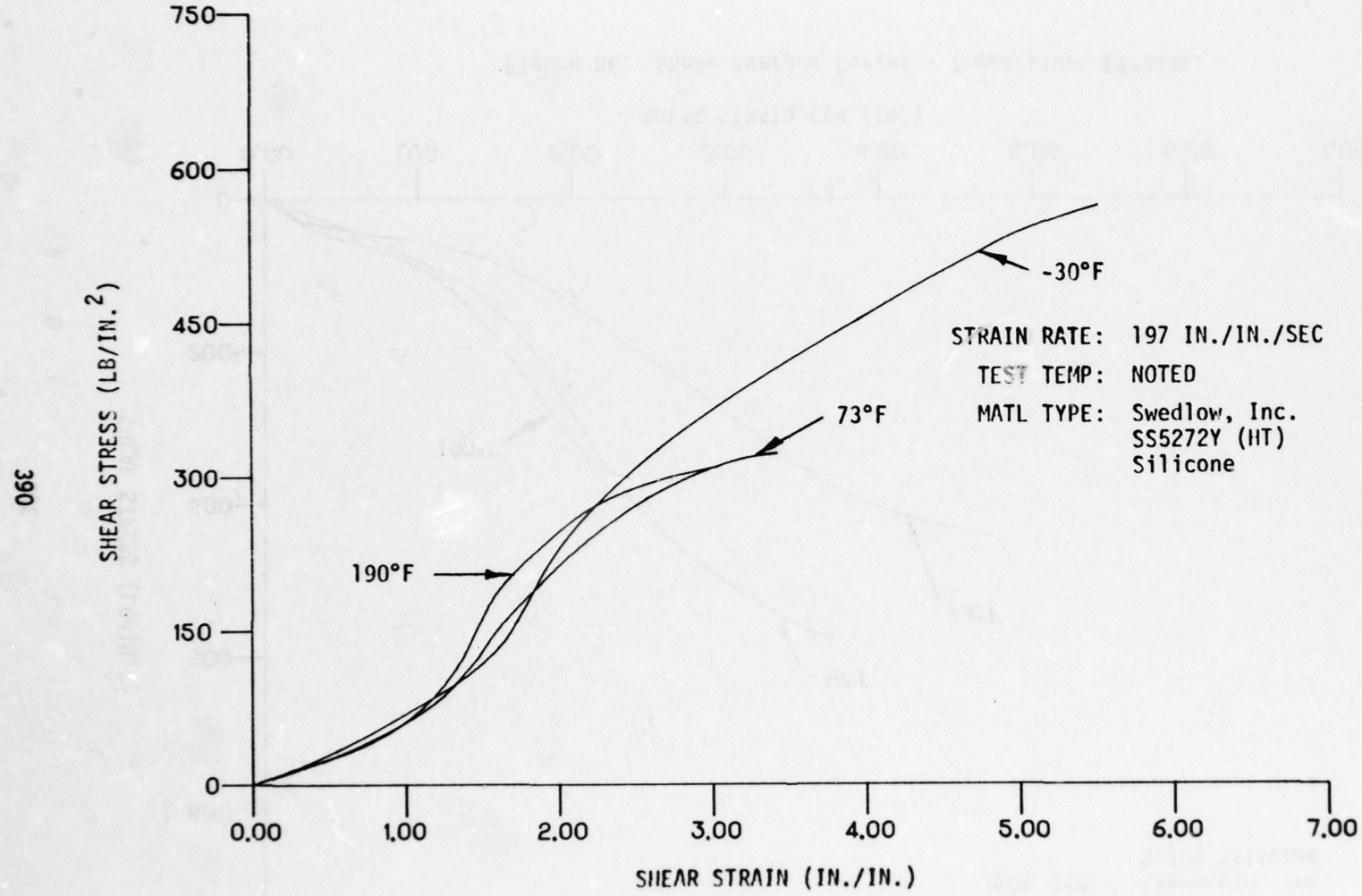

Figure 87. Shear Average Curves - Temperature Effects.

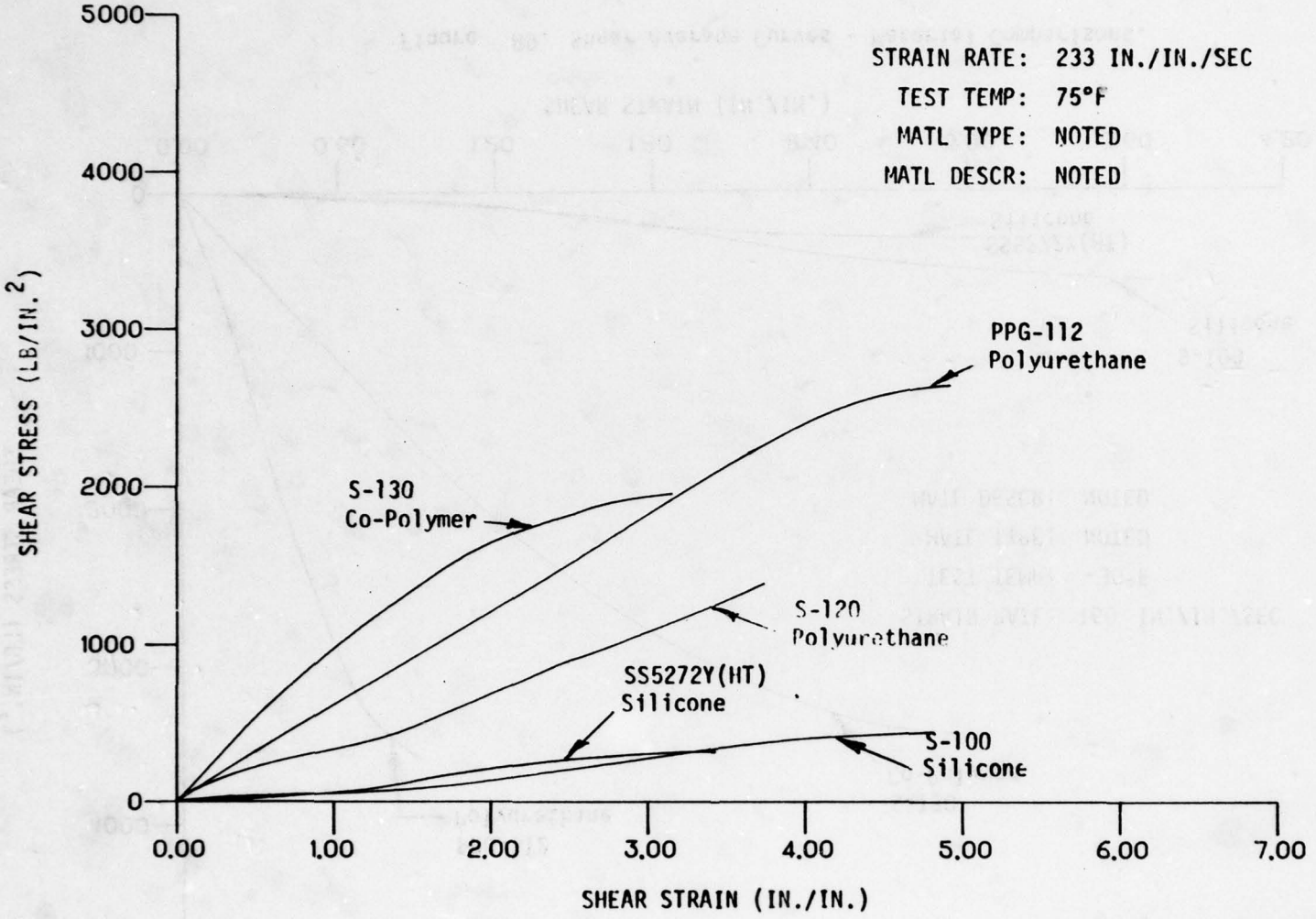

Figure 88. Shear Average Curves - Material Comparisons.

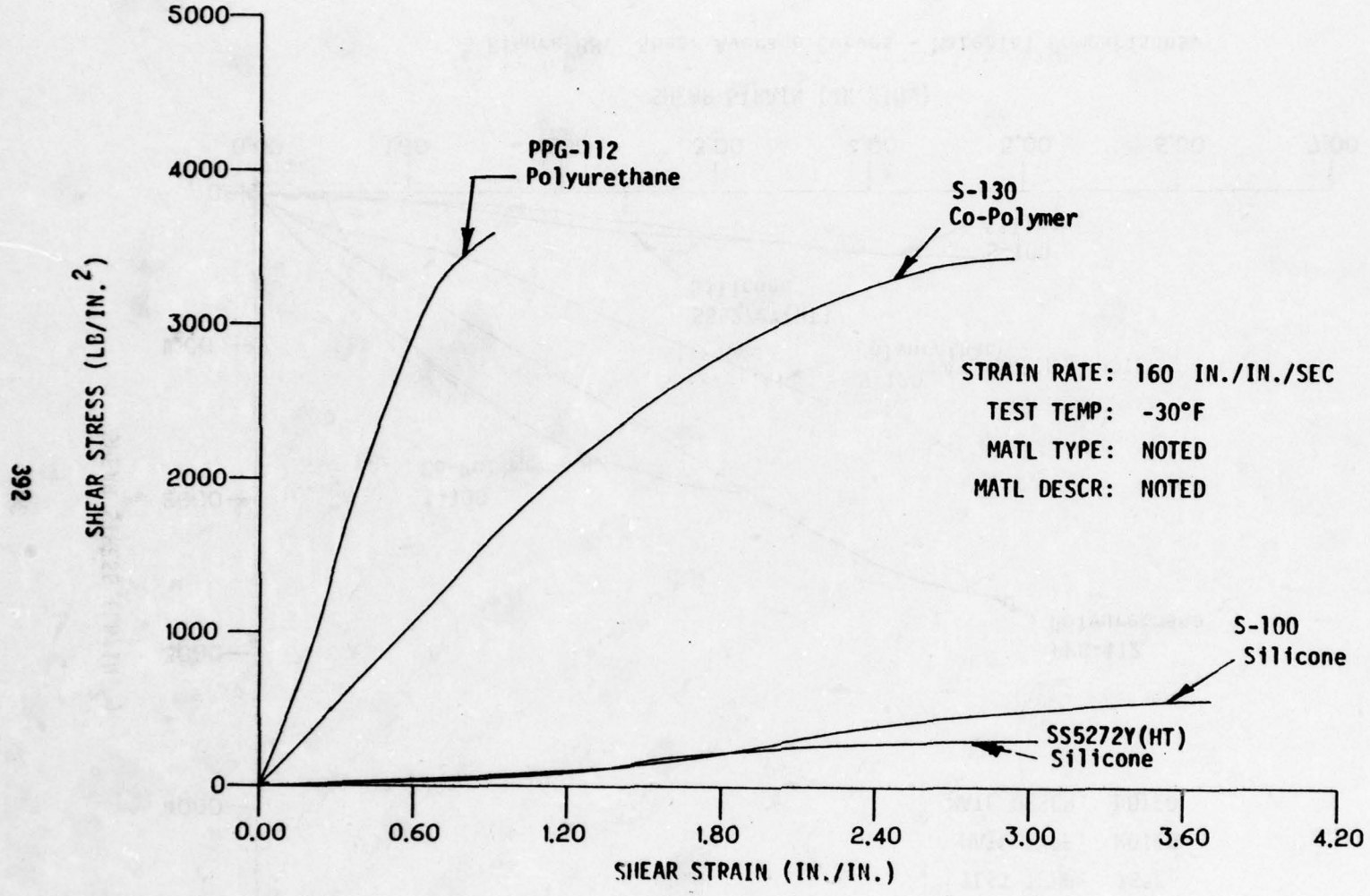

Figure 89. Shear Average Curves - Material Comparisons.

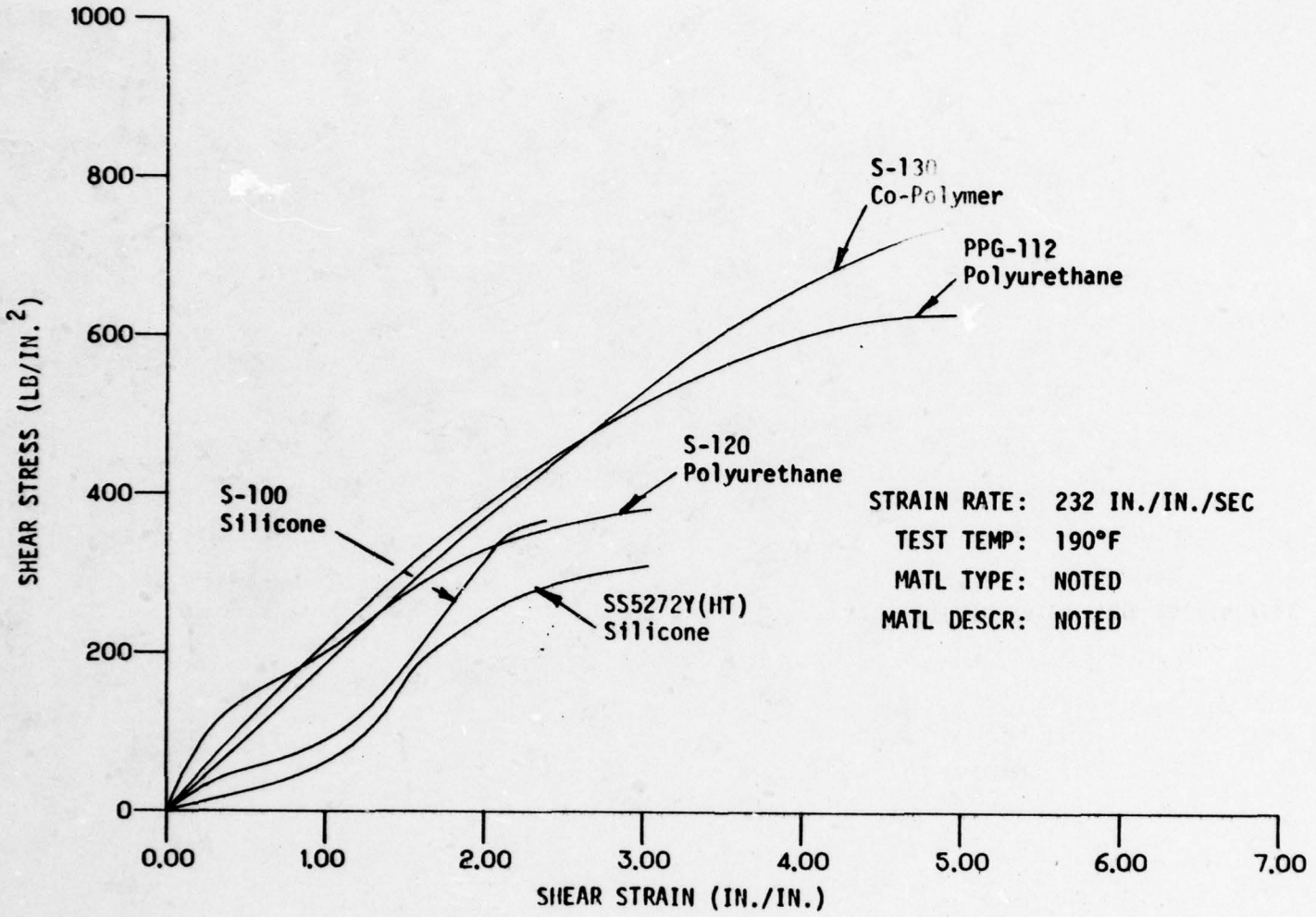

Figure 90. Shear Average Curves - Material Comparisons.

APPENDIX F

SHEAR STRESS-STRAIN CURVE DATA

The following stress-strain data are presented for use in conjunction with tabulated strength data presented in Table 25, Page 383.

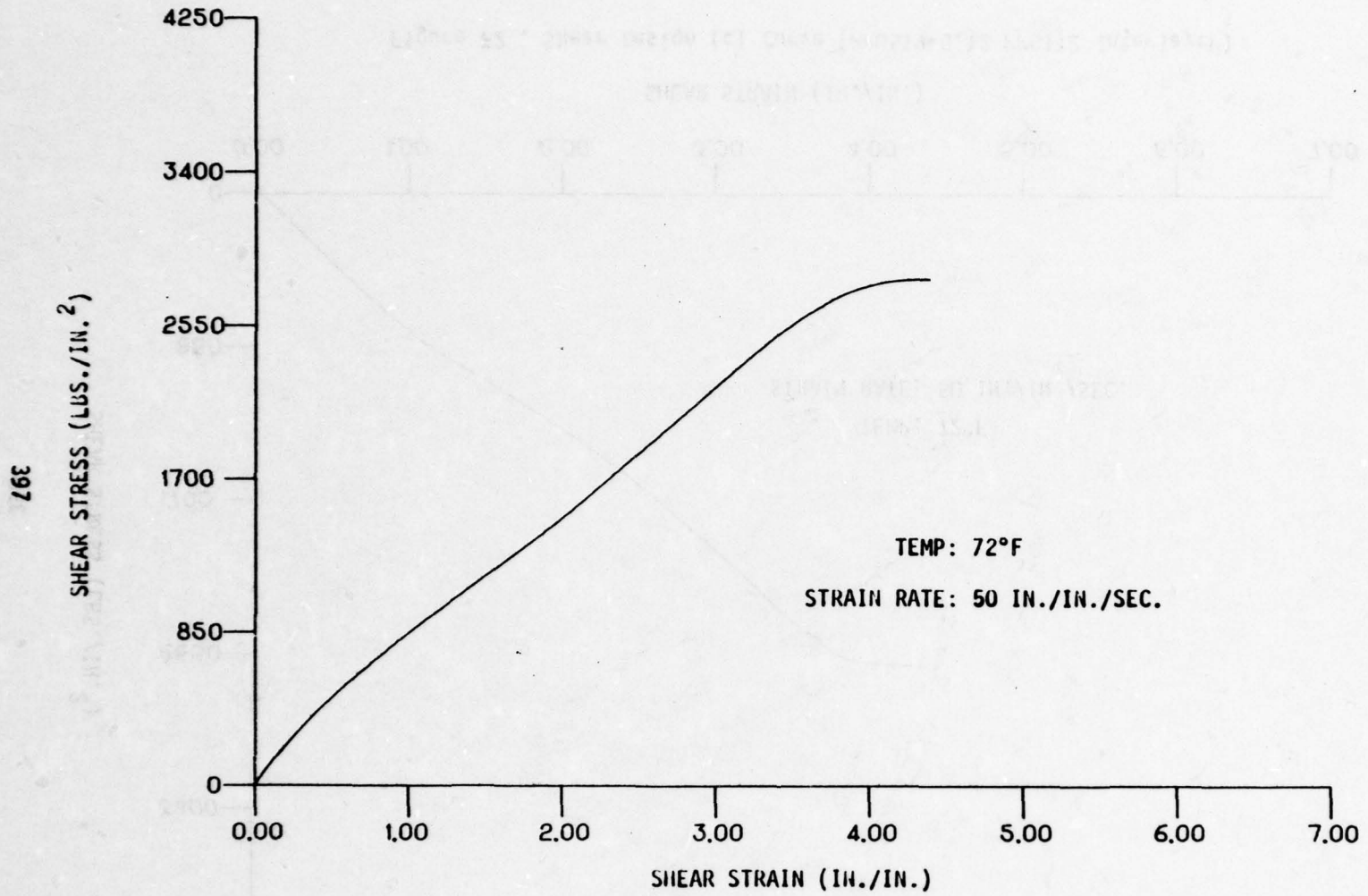

Figure F1 . Shear Average Curve (PPG 519-0.12 PPG112 Interlayer).

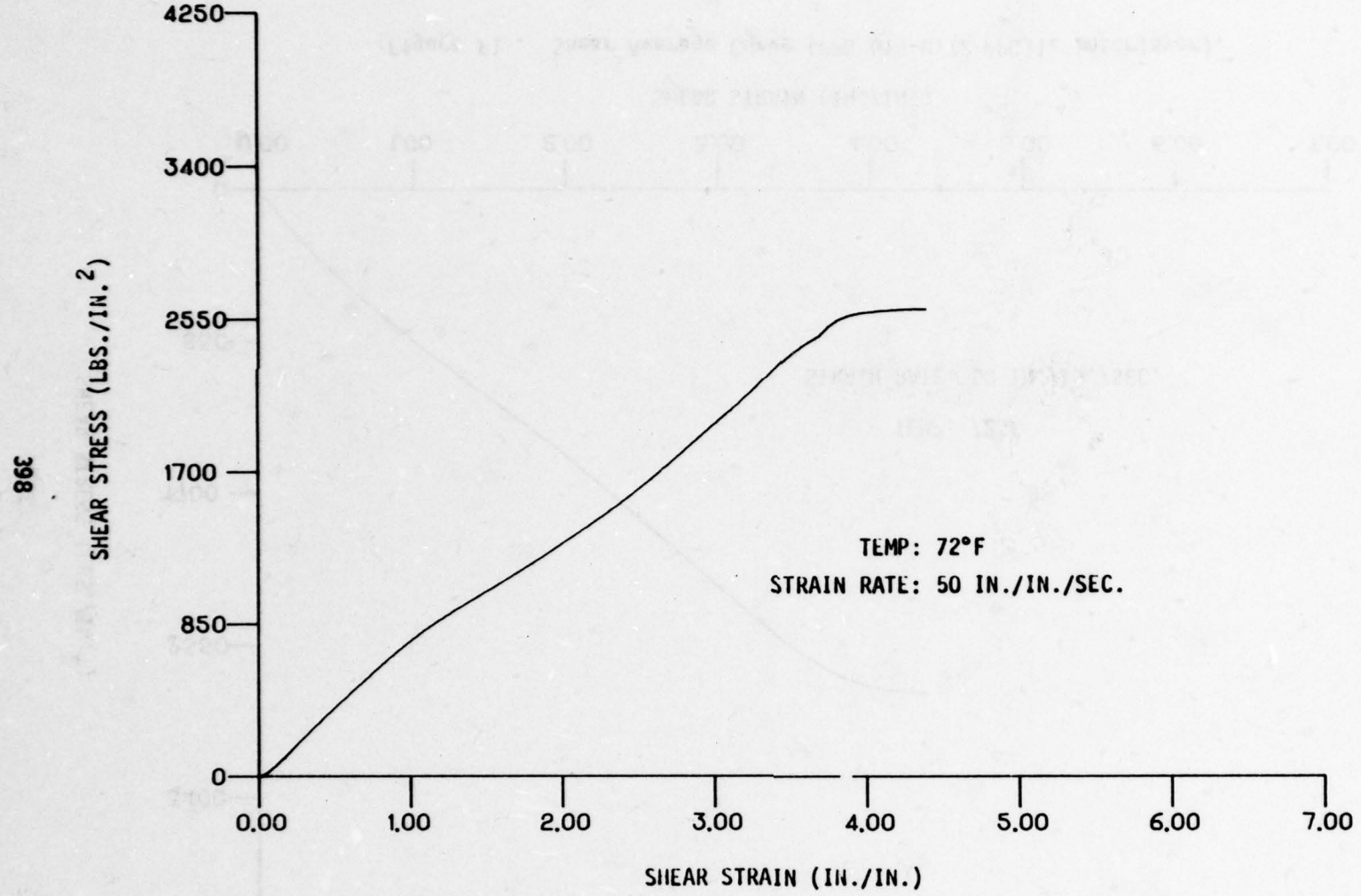

Figure F2 . Shear Design (c) Curve (PPG519-0.12 PPG112 Interlayer)

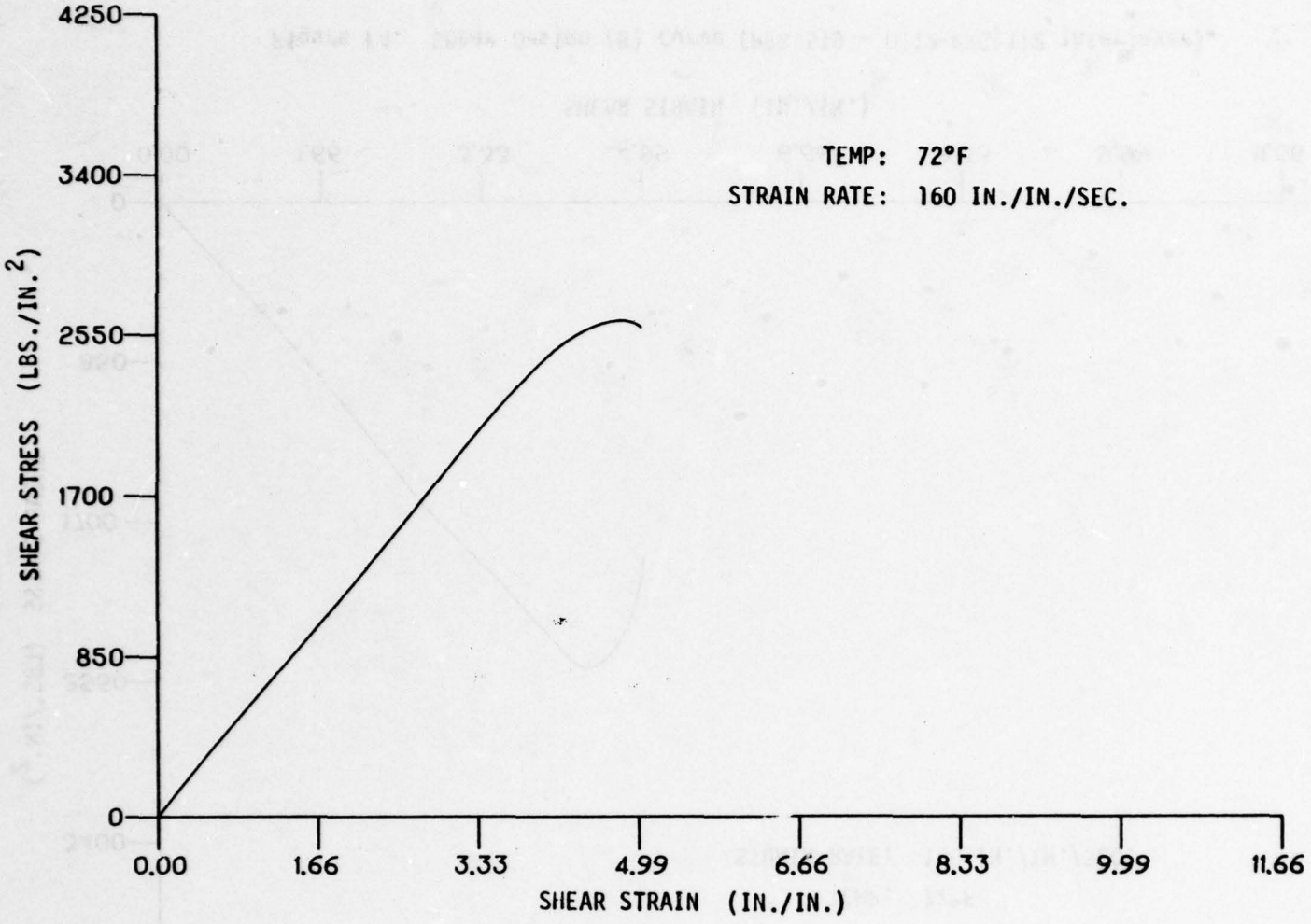

Figure F3. Shear Average Curve (PPG 519 - 0.12 PPG 112 Interlayer).

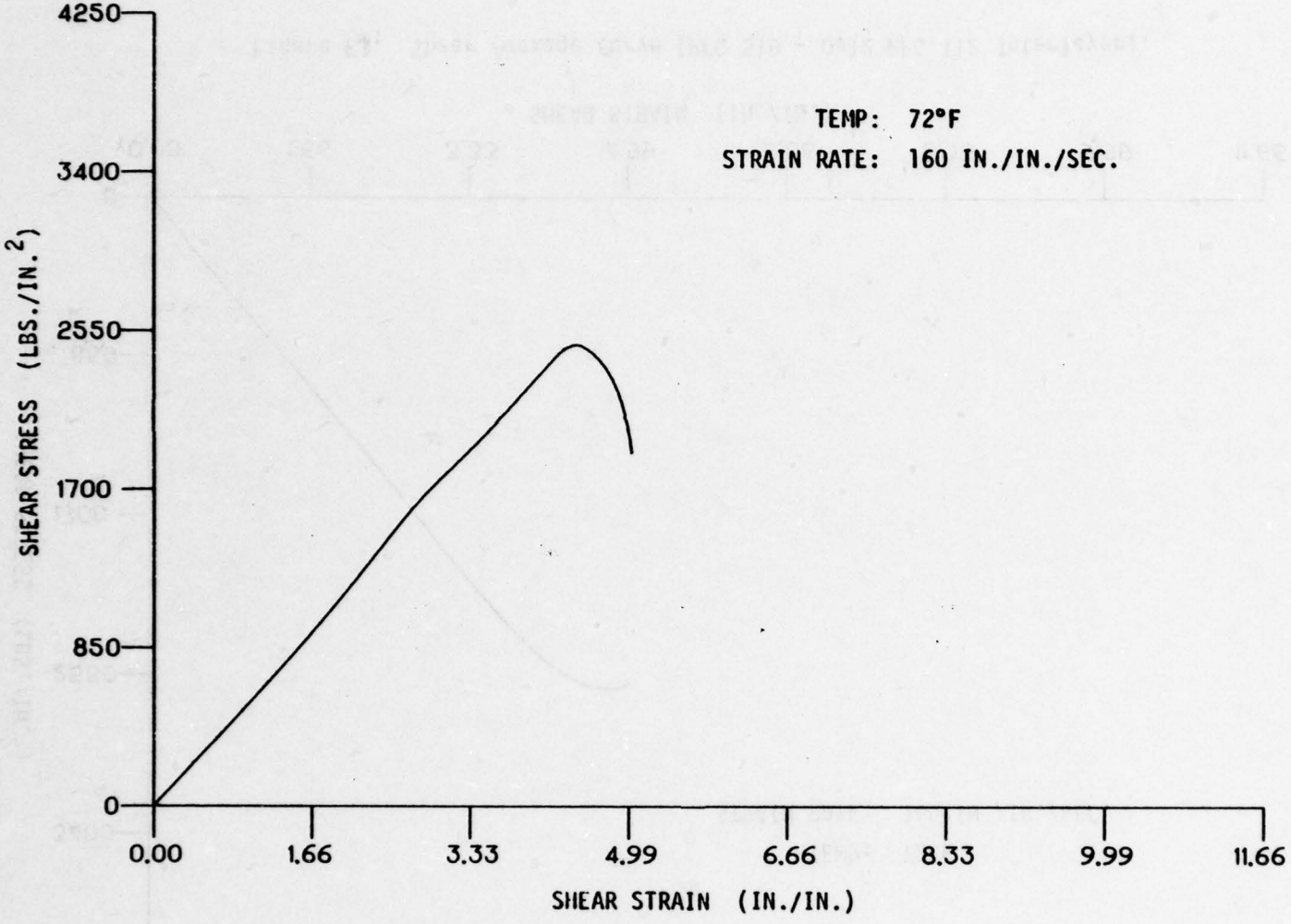

Figure F4. Shear Design (B) Curve (PPG 519 - 0.12 PPG 112 Interlayer).

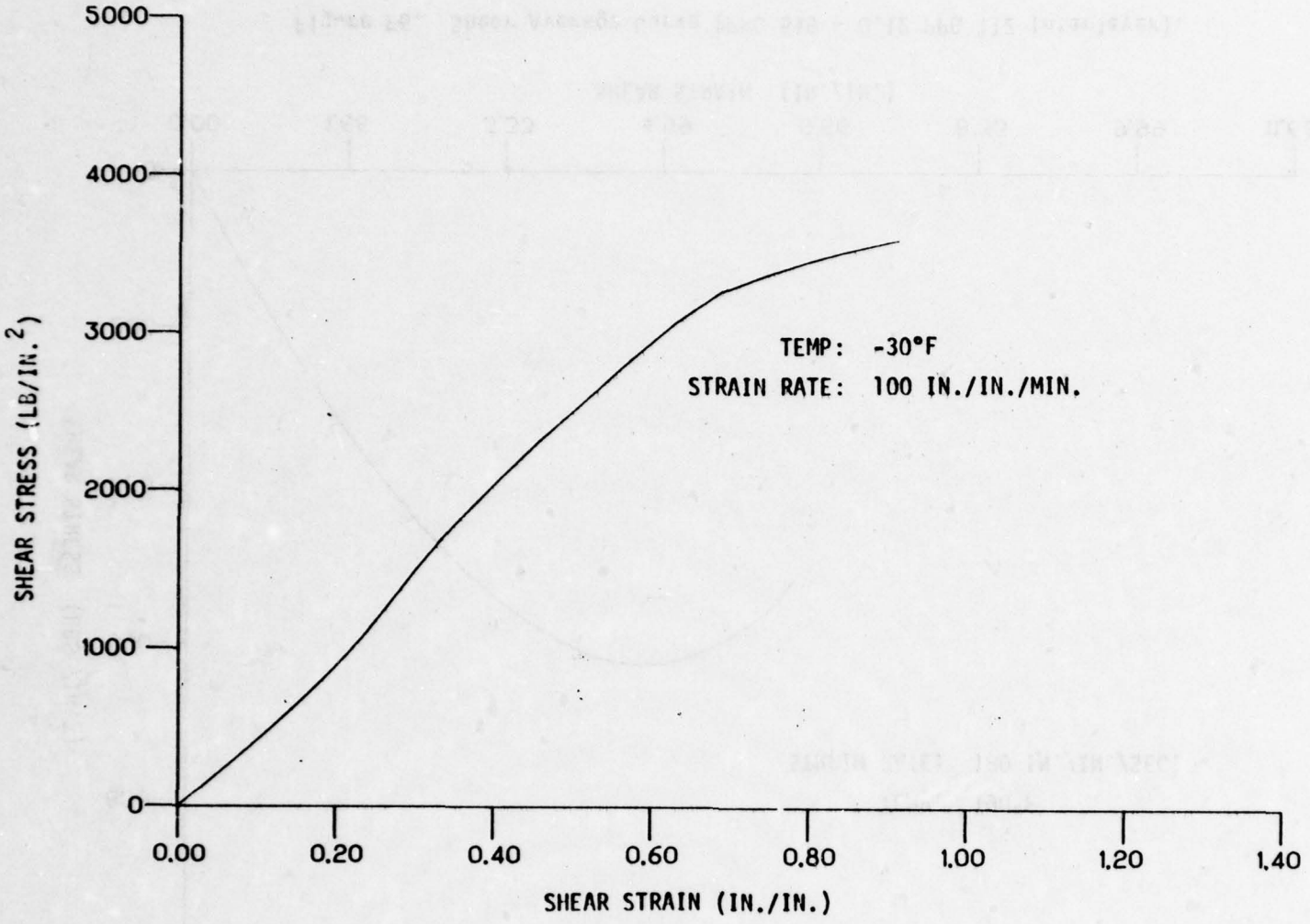

Figure F5 . Shear Average Curve (PPG519-0.12 PPG112 Interlayer).

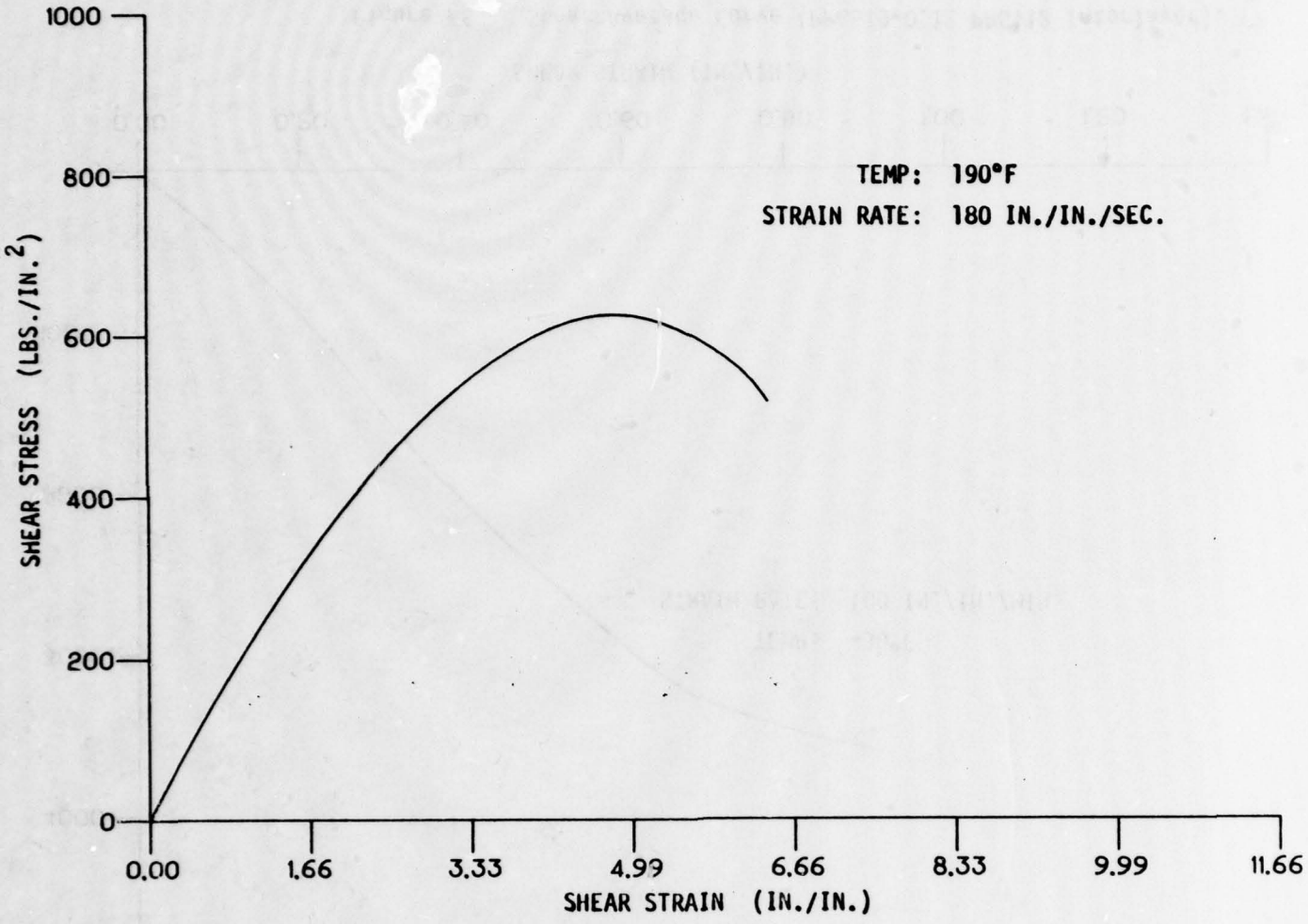

Figure F6. Shear Average Curve (PPG 519 - 0.12 PPG 112 Interlayer).

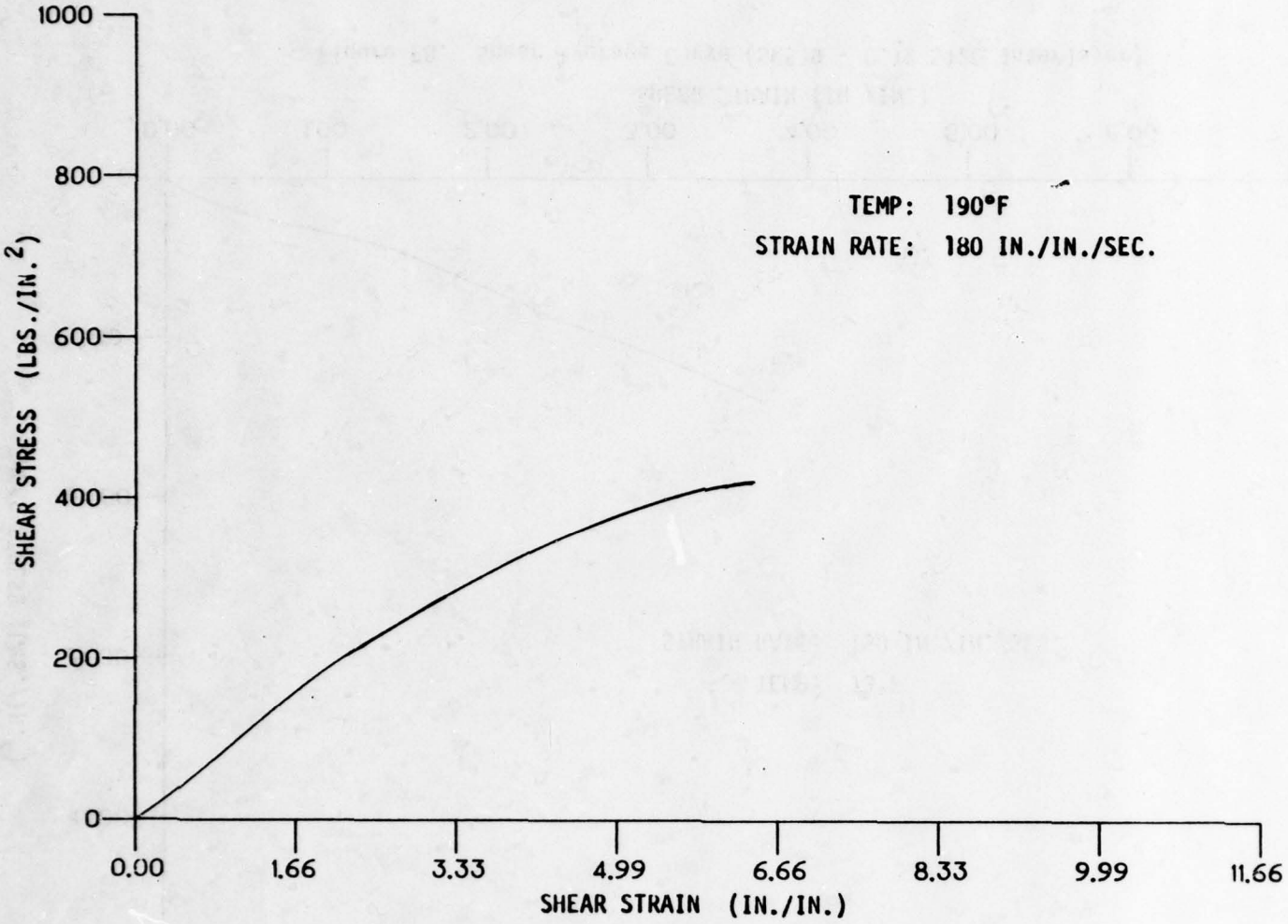

Figure F7. Shear Design (C) Curve (PPG 519 - 0.12 PPG 112 Interlayer).

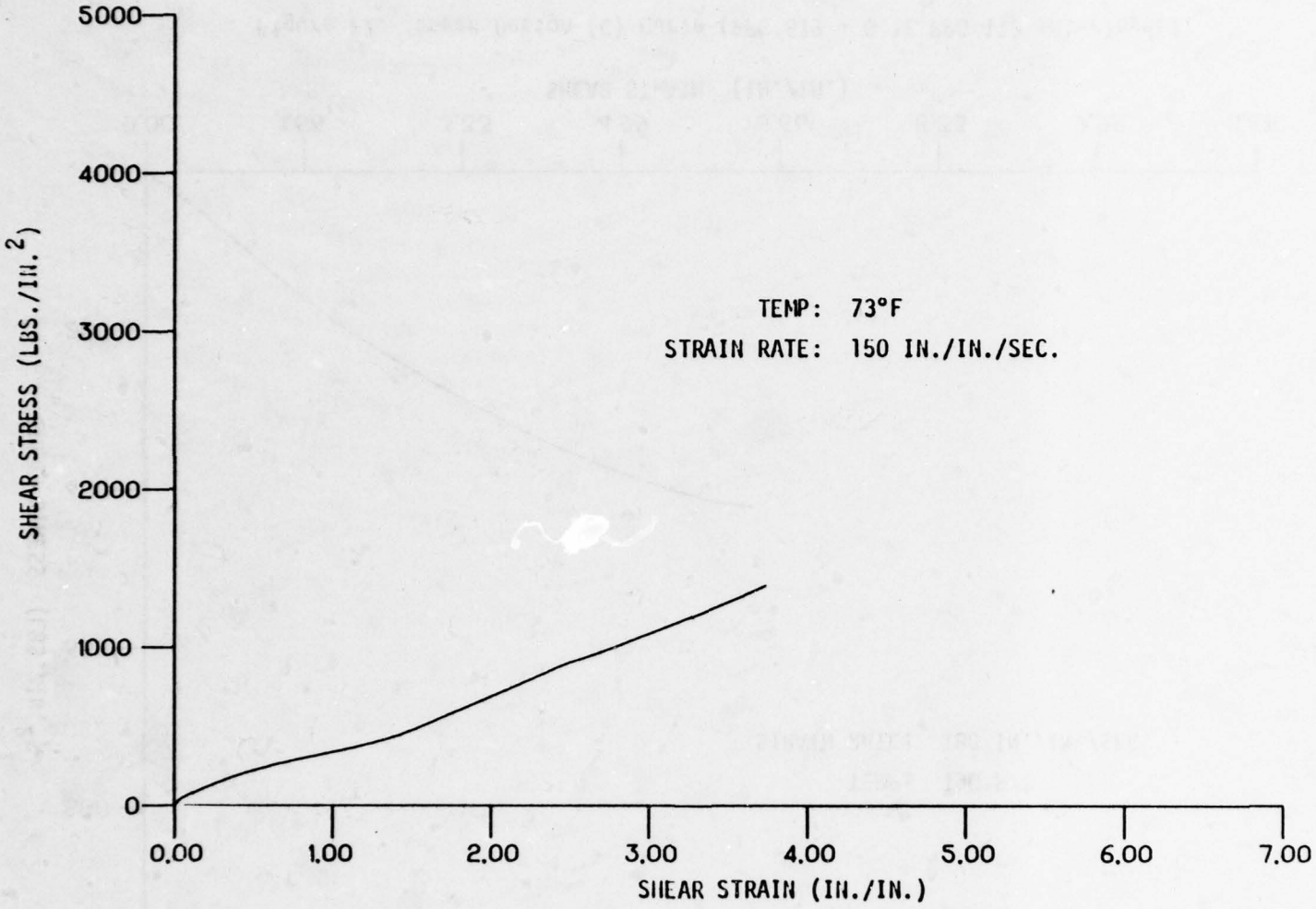

Figure F8. Shear Average Curve (SK519 - 0.12 S120 Interlayer)

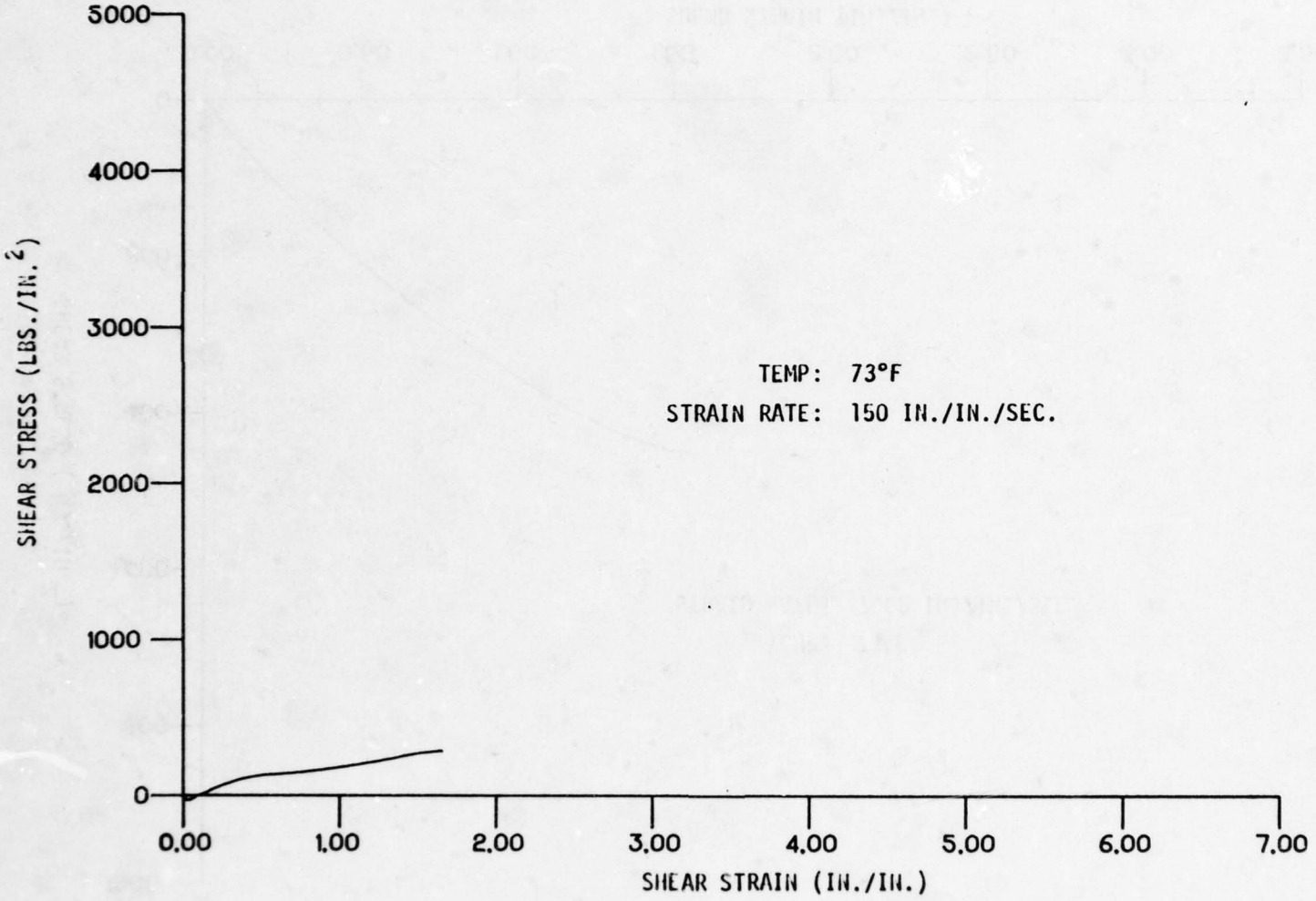

Figure F9. Shear Design (c) Curve (SK519 - 0.12 S120 Interlayer)

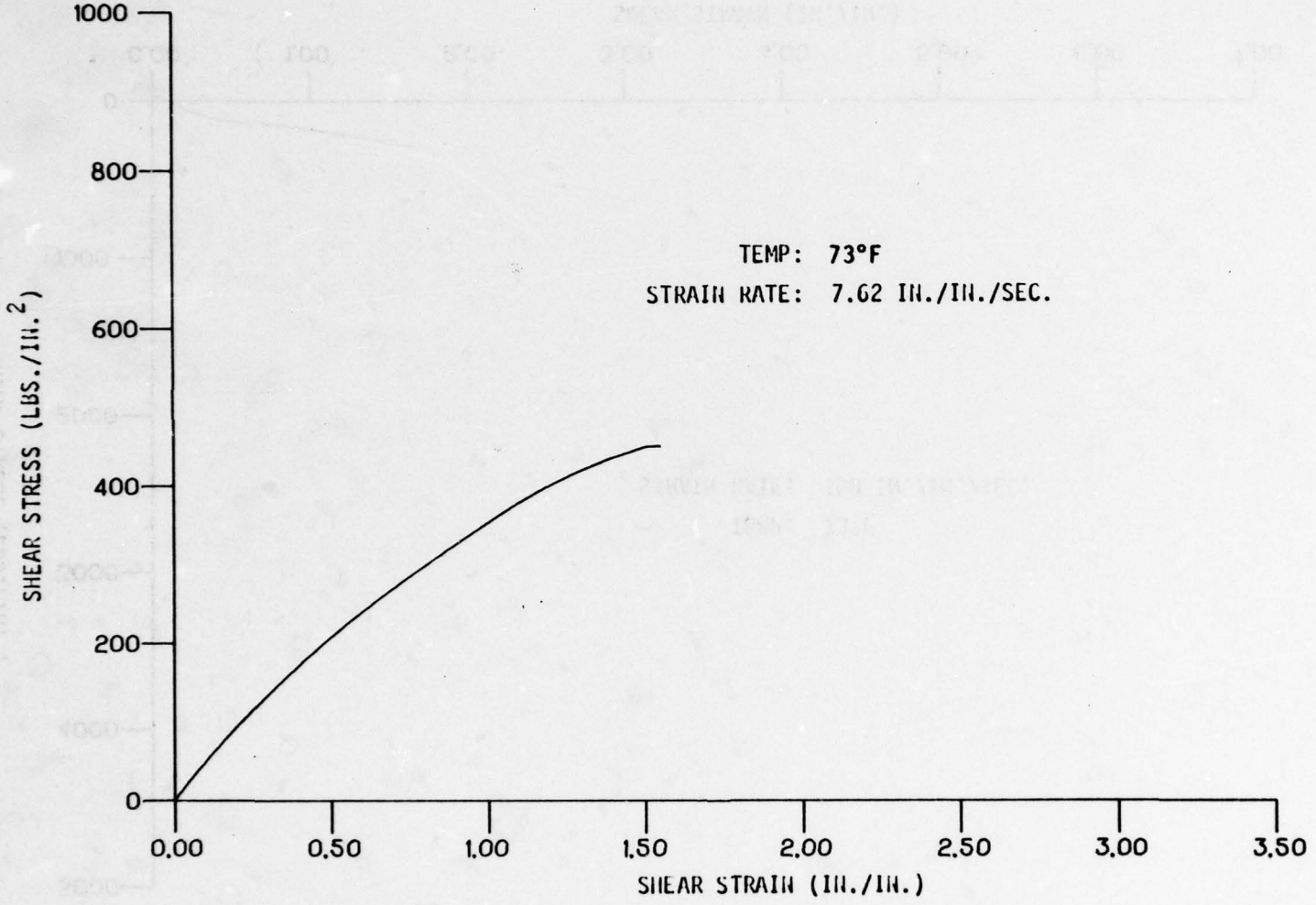

Figure F10. Shear Average Curve (SK519 - 0.12 S120 Interlayer)

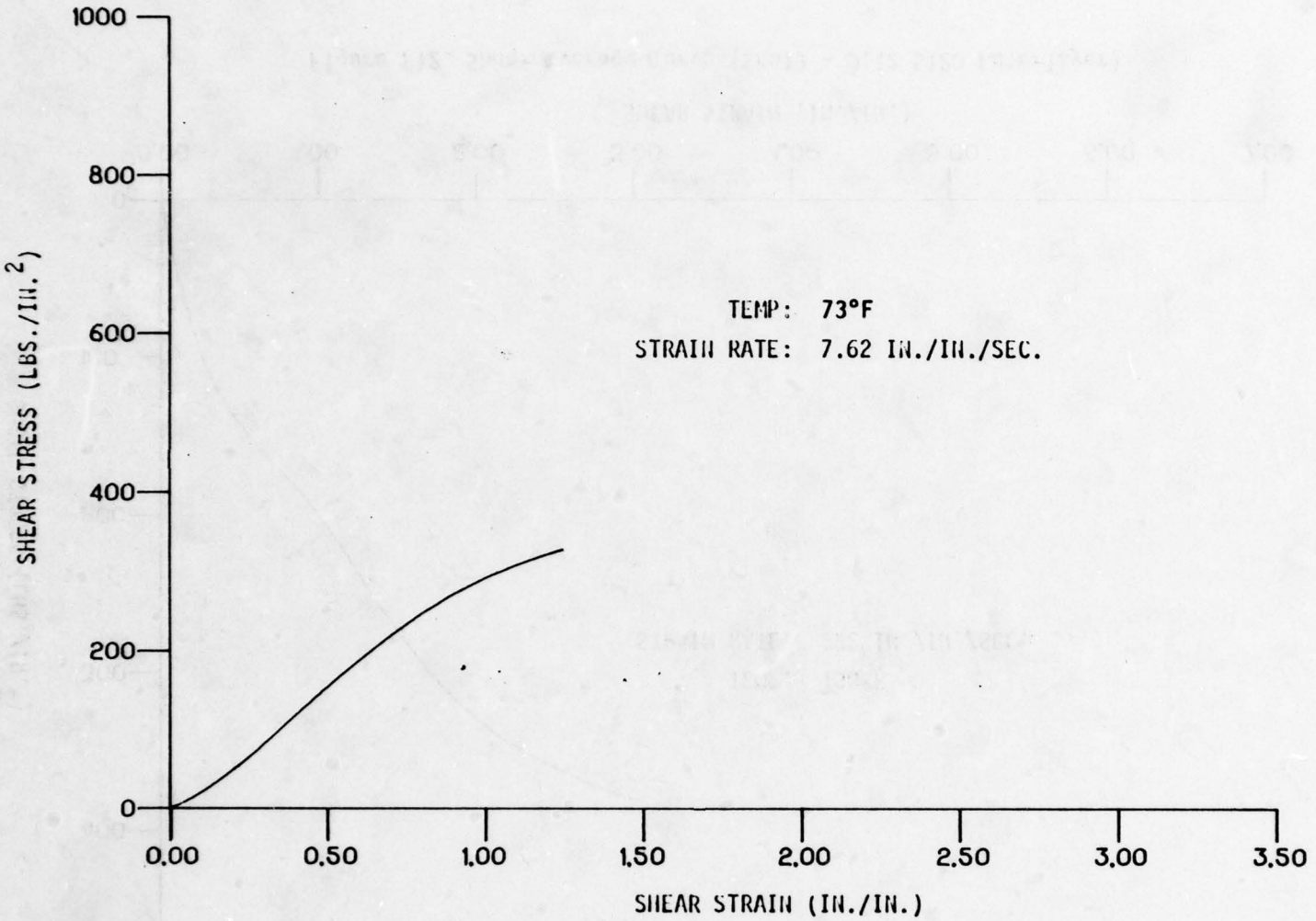

Figure F11. Shear Design (c) Curve (SK519 - 0.12 S120 Interlayer)

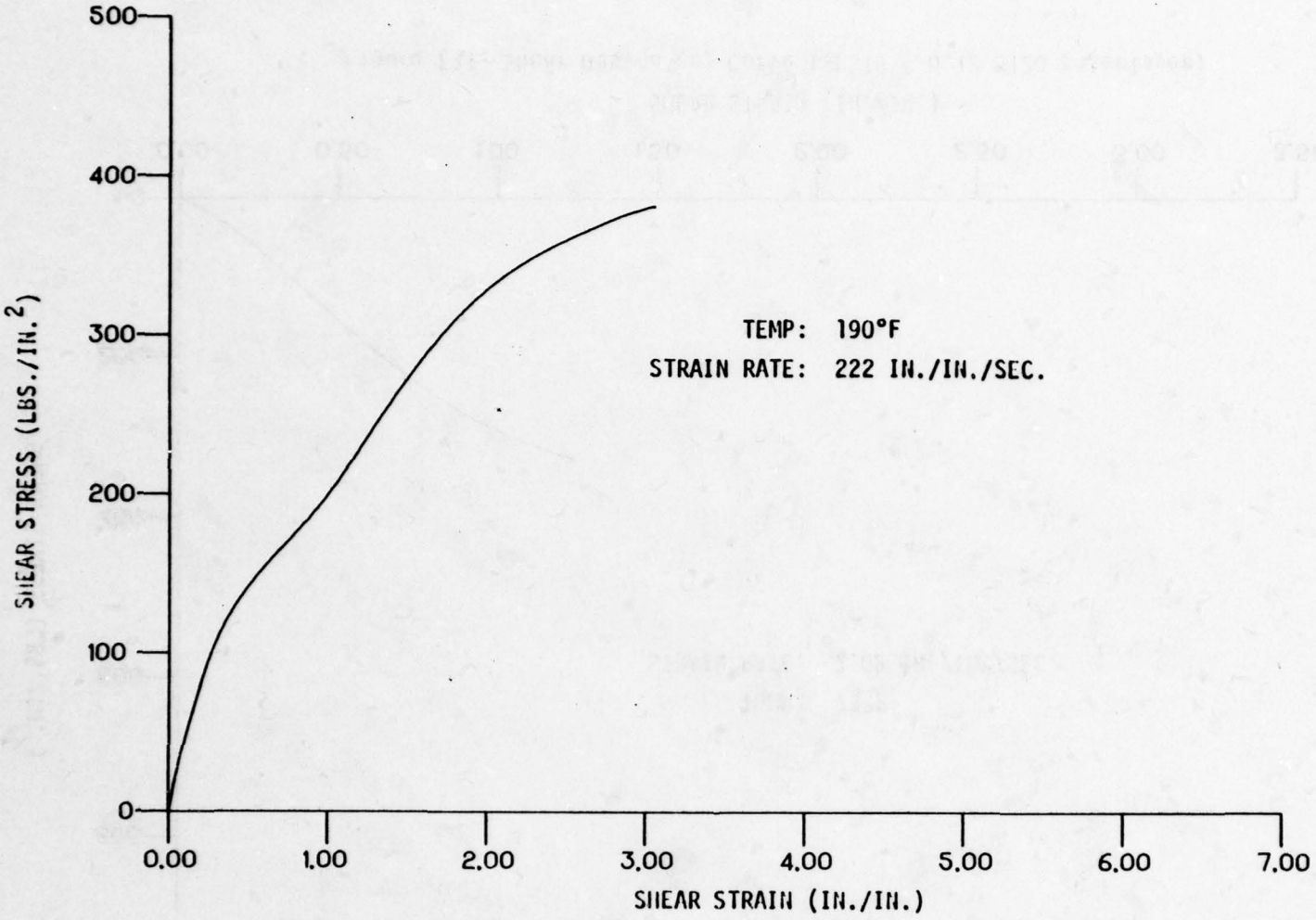

Figure F12. Shear Average Curve (SK519 - 0.12 S120 Interlayer)

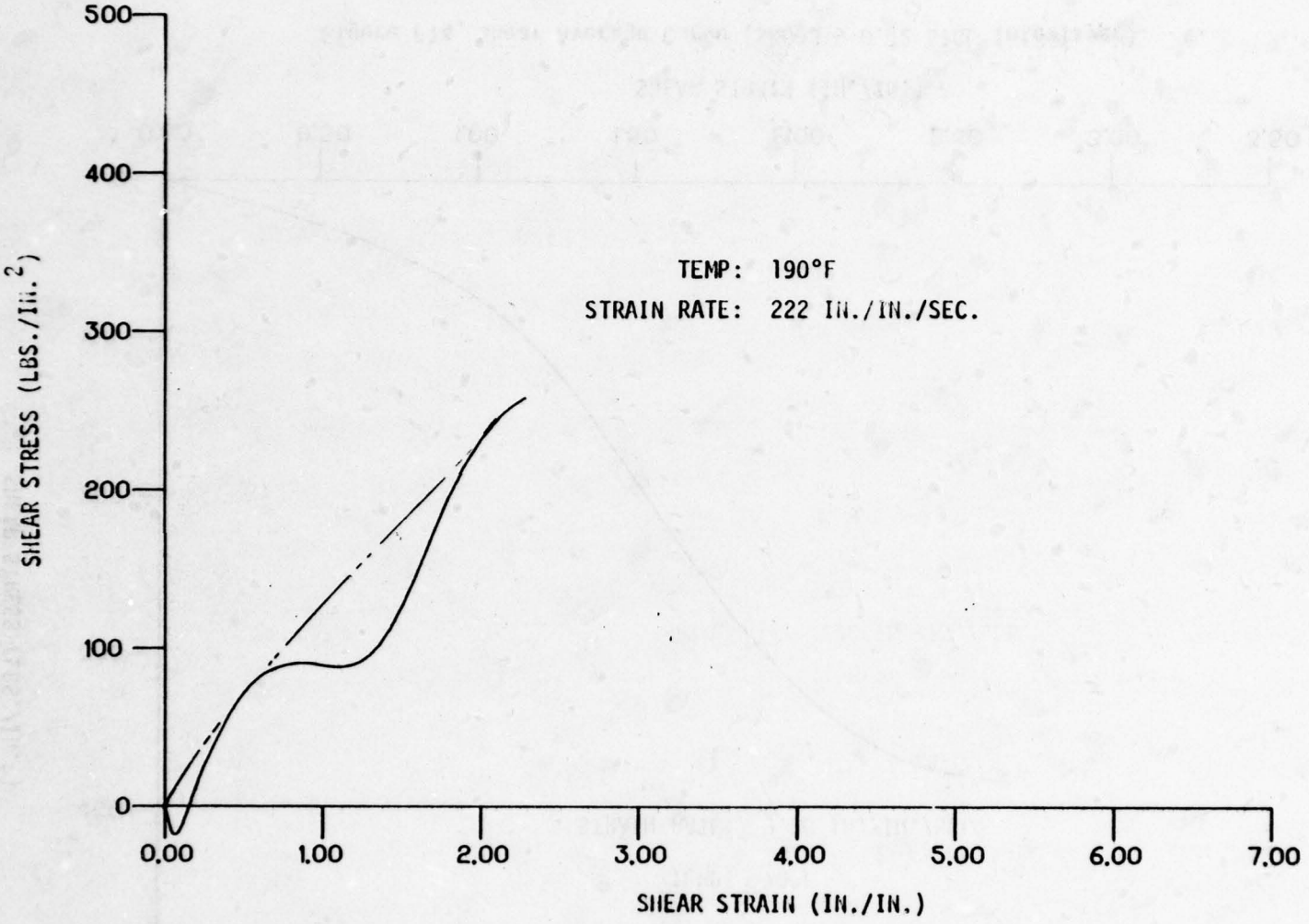

Figure F13. Shear Design (c) Curve (SK519 - 0.12 S120 Interlayer)

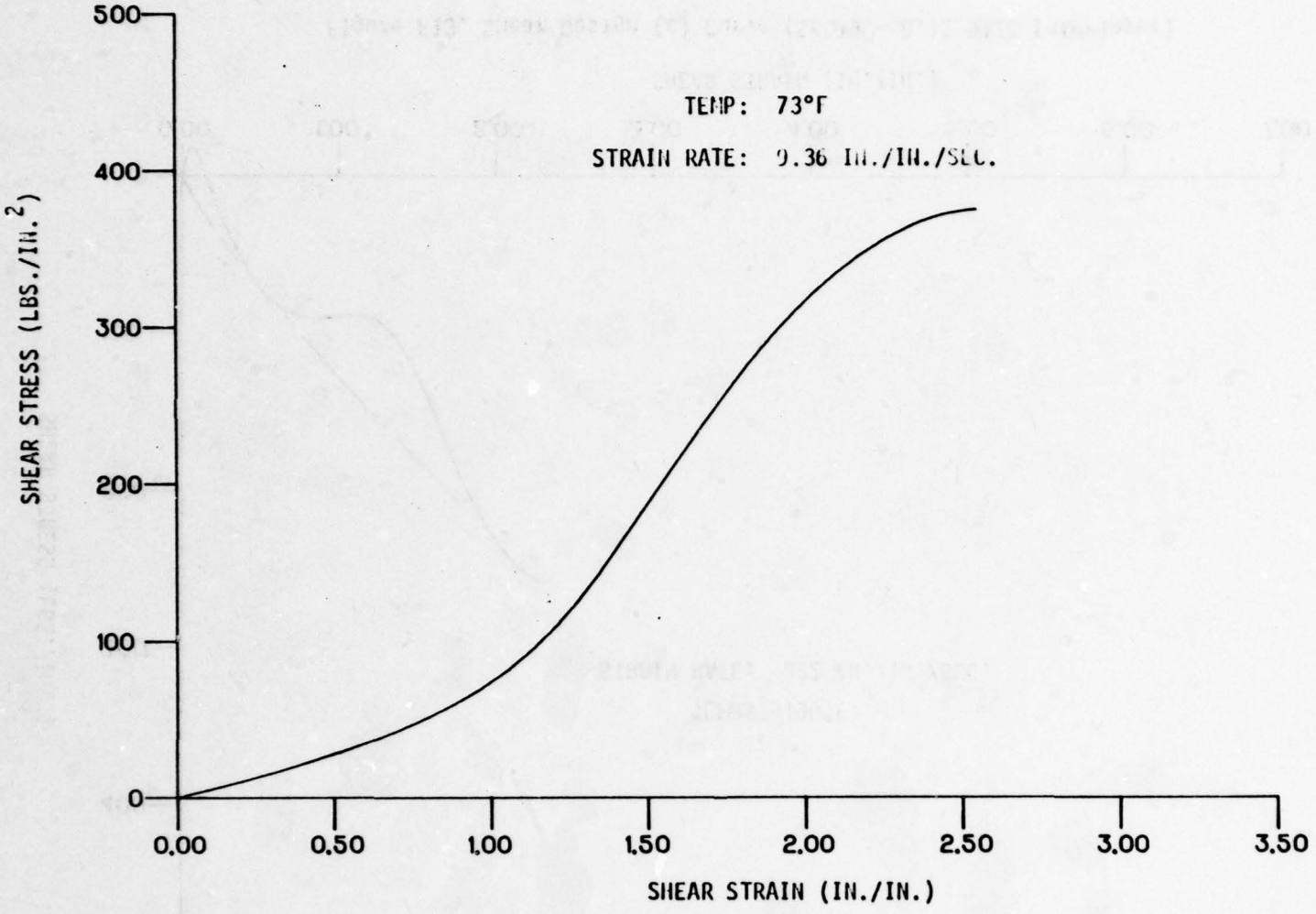

Figure F14. Shear Average Curve (SK603 - 0.12 S10C Interlayer).

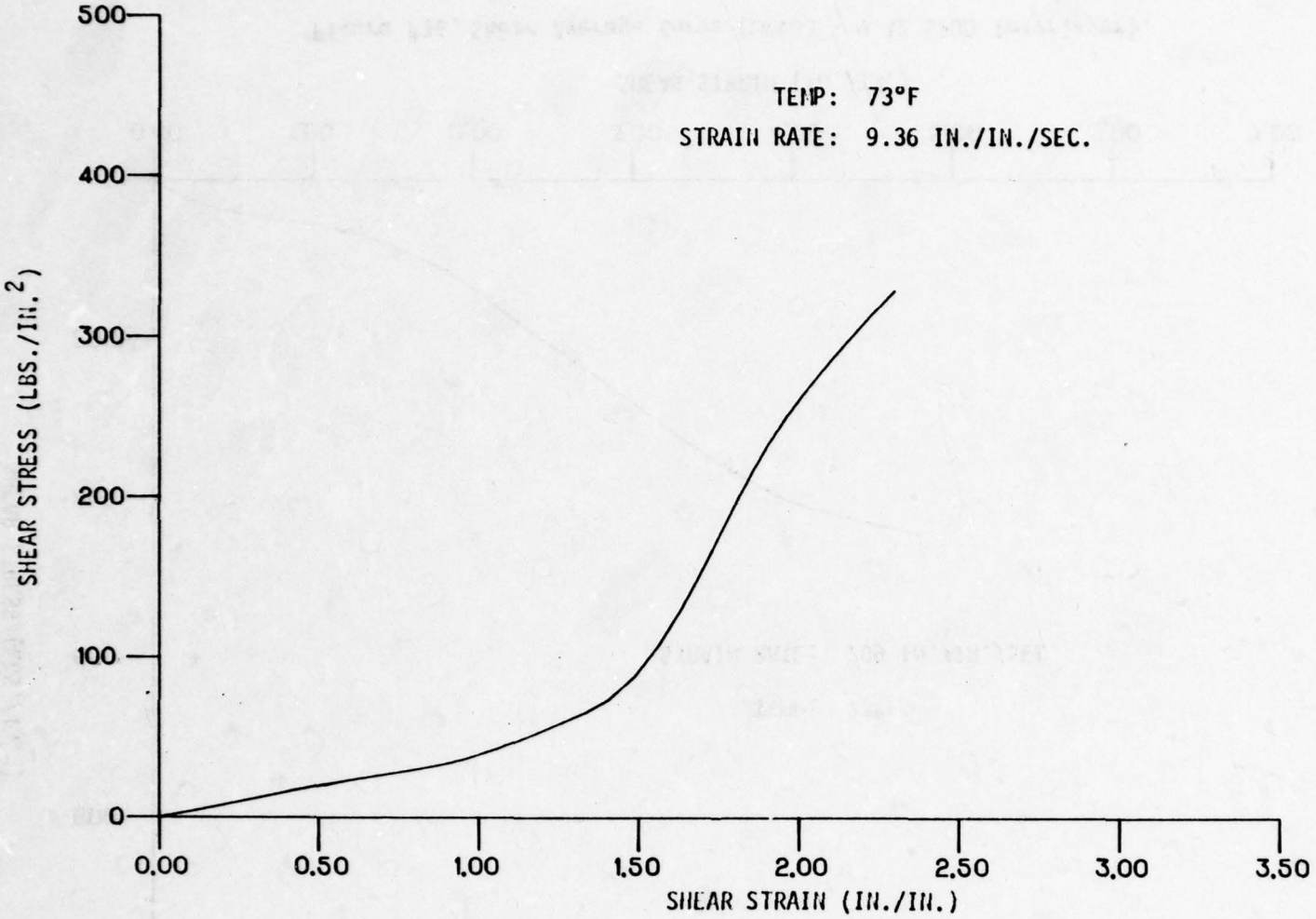

Figure F15. Shear Design (c) Curve (SK603 - 0.12 S10[illegible] Interlayer).

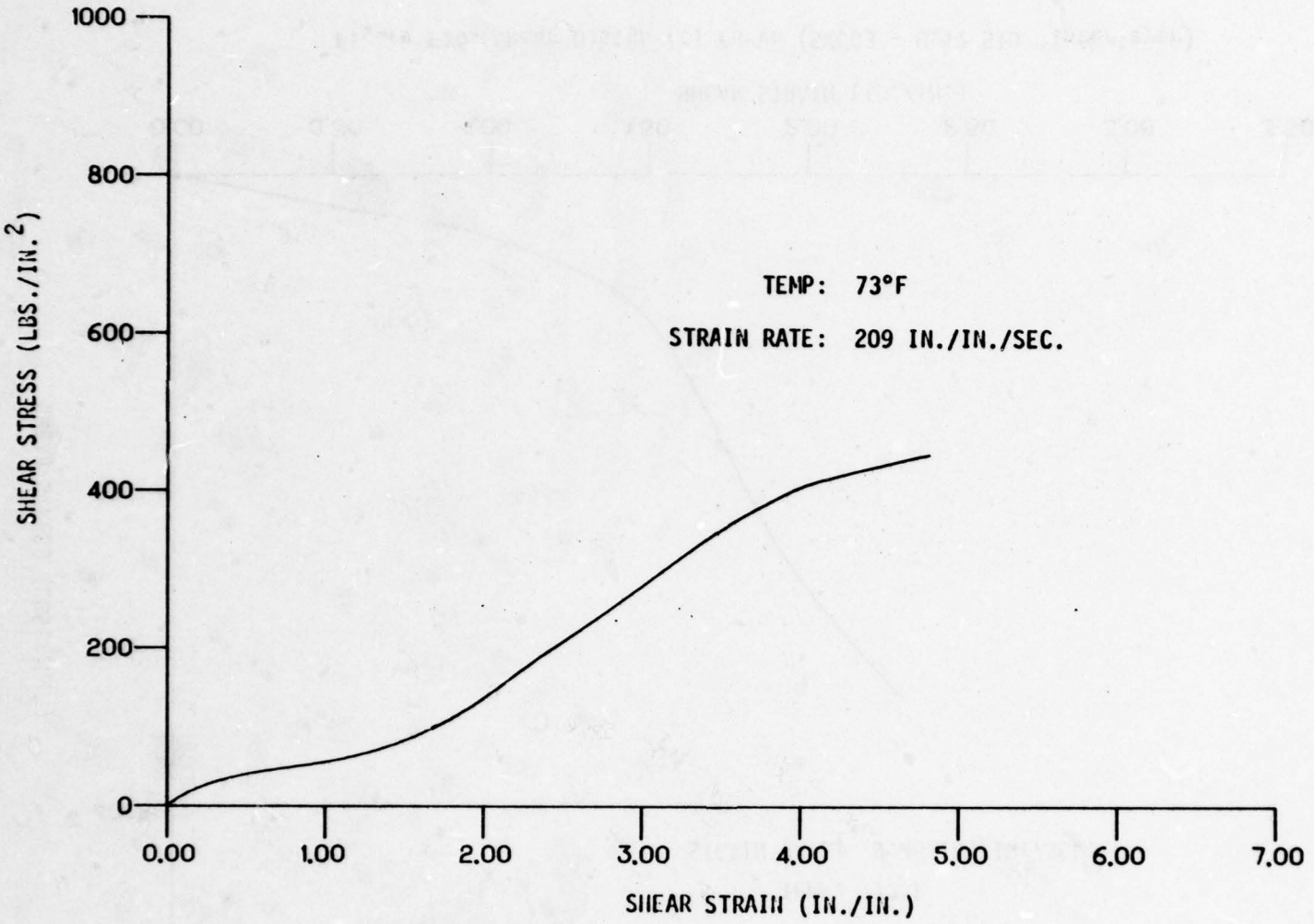

Figure F16. Shear Average Curve (SK603 - 0.12 S100 Interlayer).

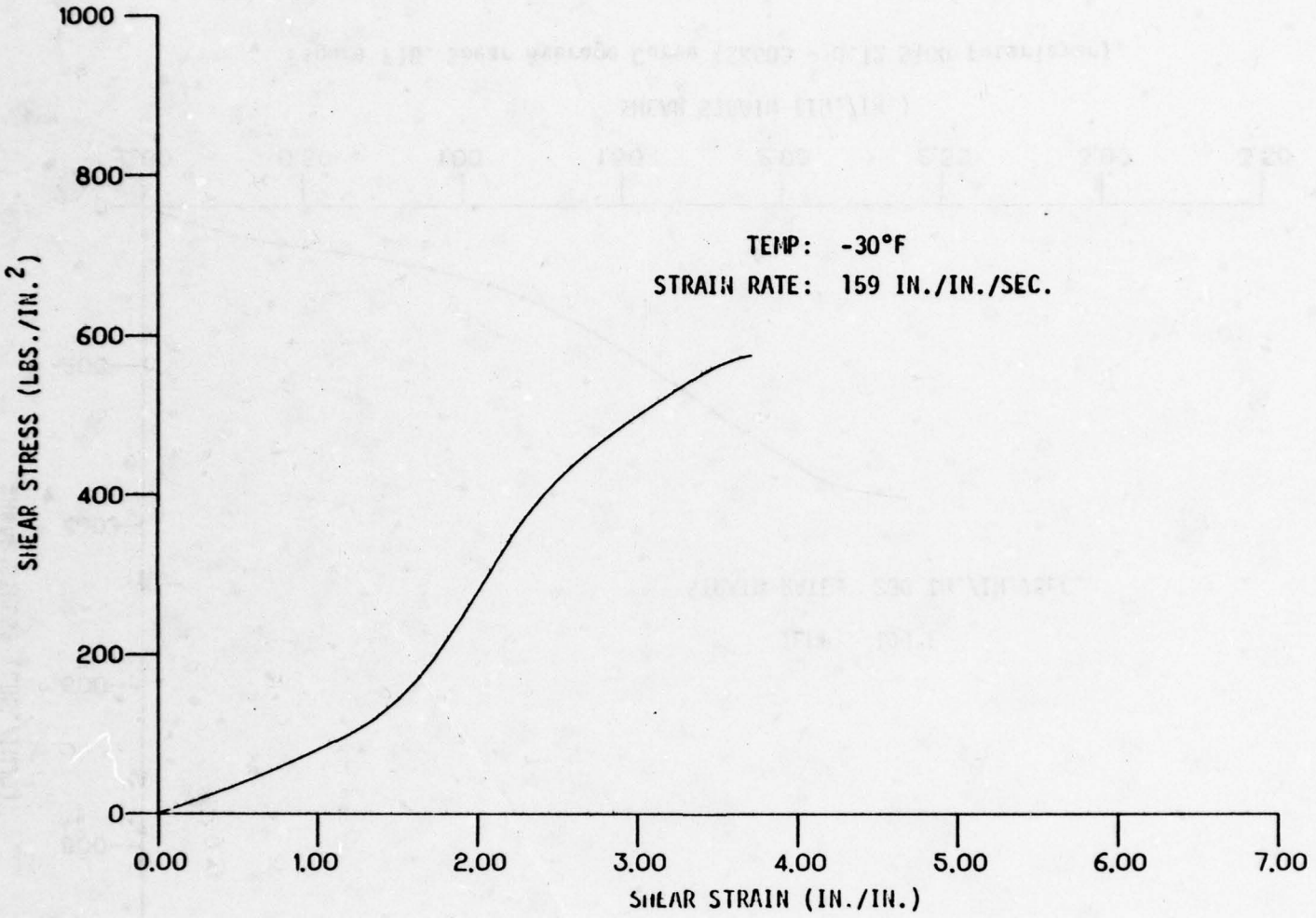

Figure F17. Shear Average Curve (SK603 - 0.12 S100 Interlayer).

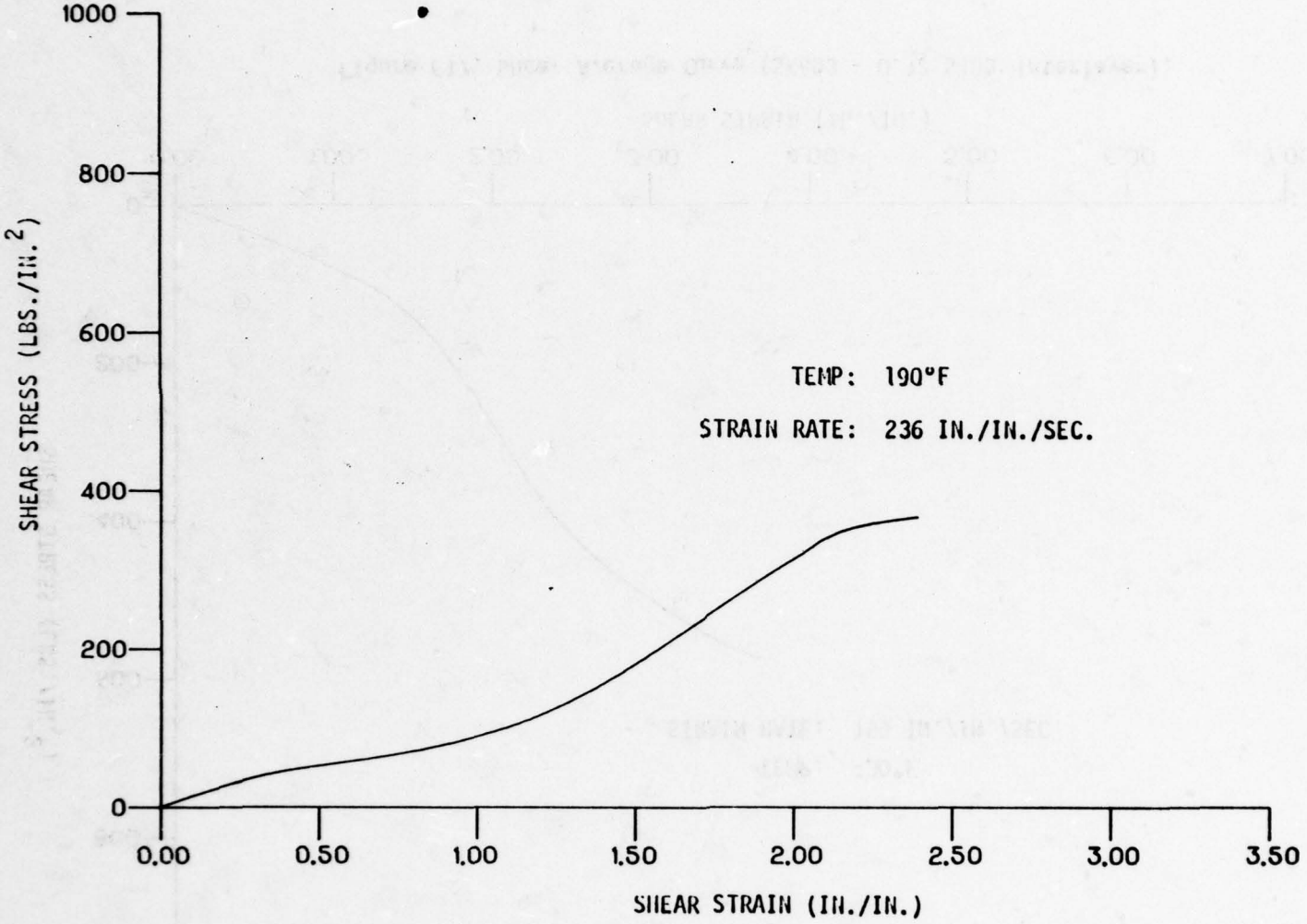

Figure F18. Shear Average Curve (SK603 - 0.12 S100 Interlayer)

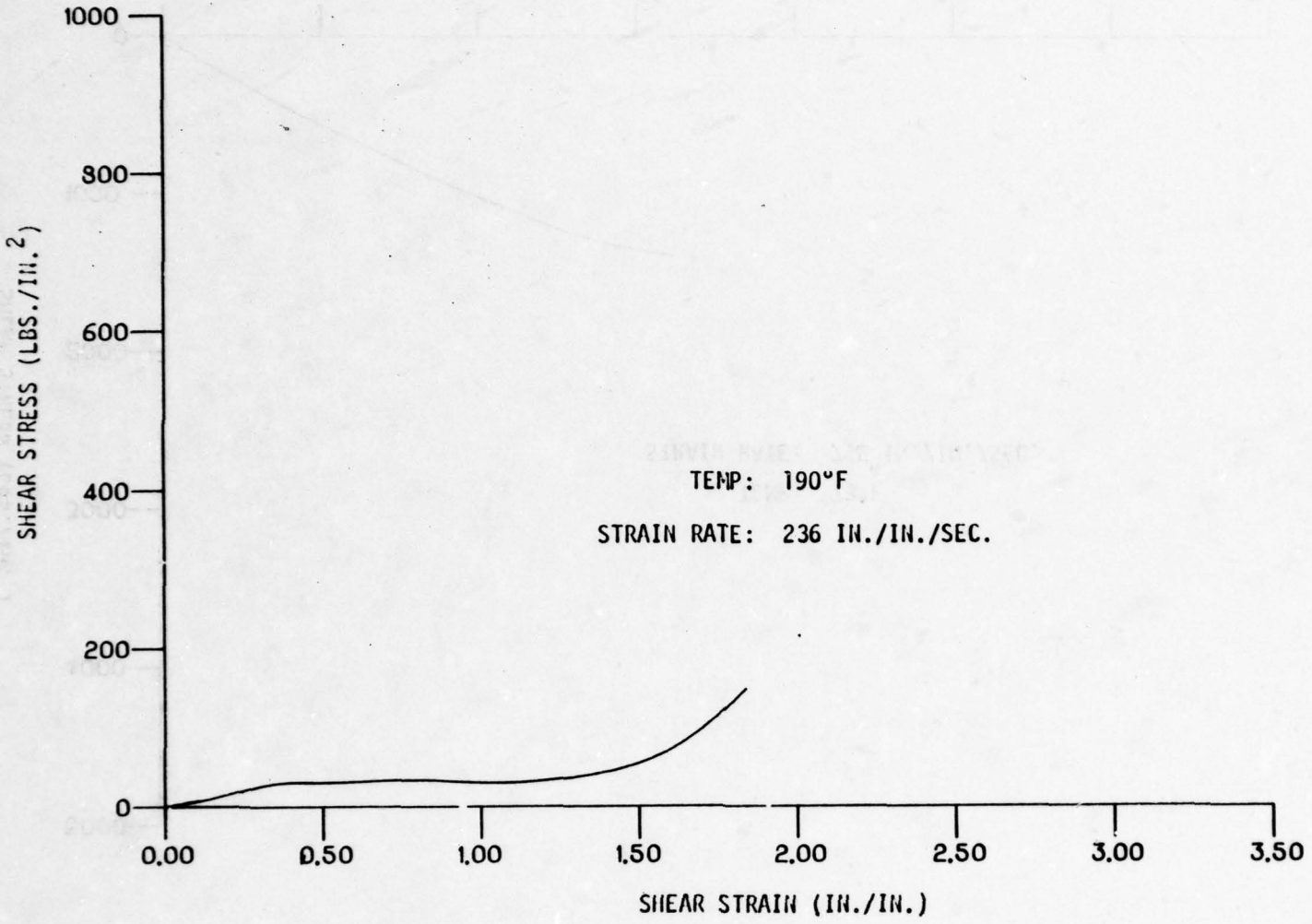

Figure F19. Shear Design (c) Curve (SK603 - 0.12 S100 Interlayer)

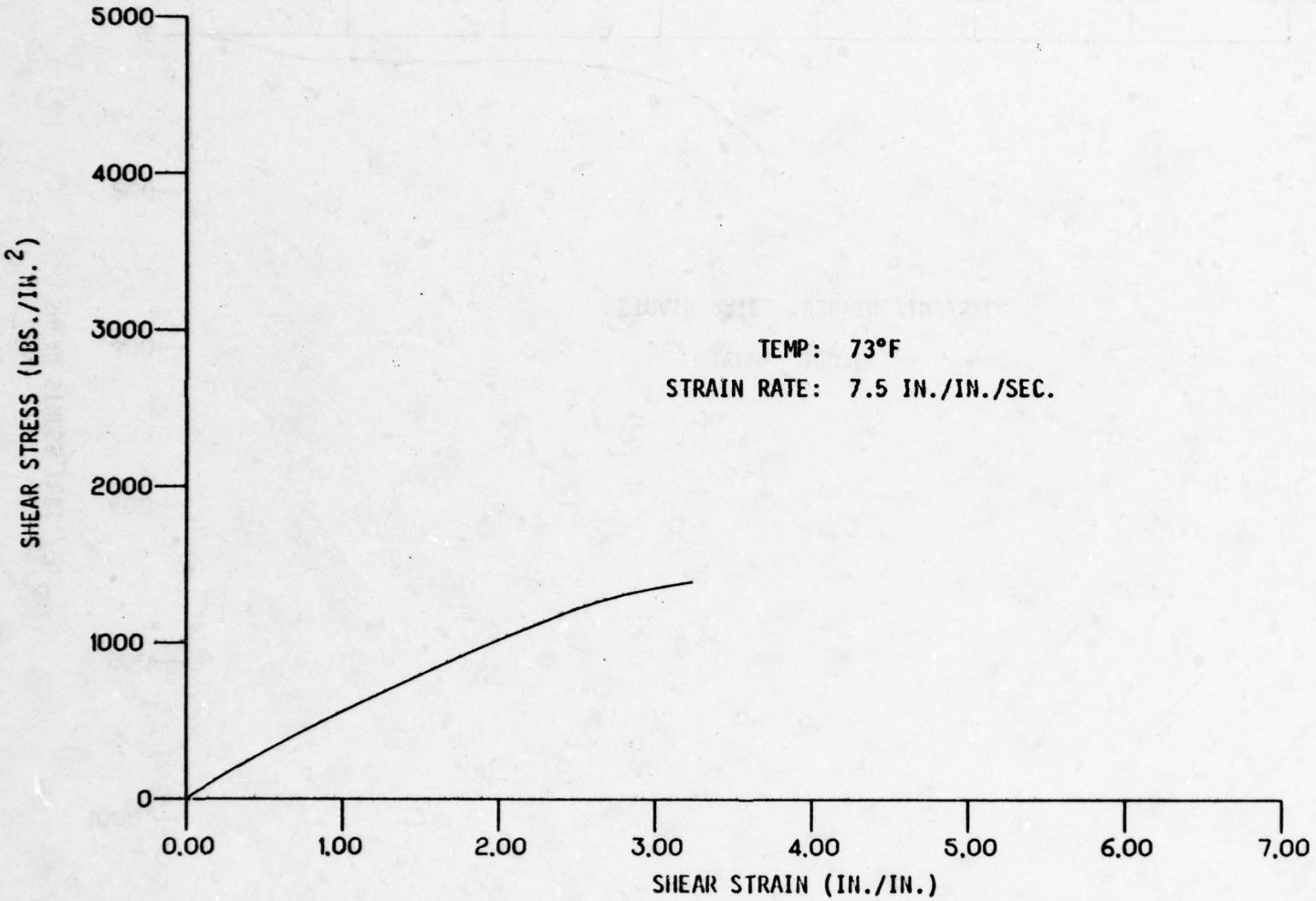

Figure F20. Shear Average Curve (SK625 - 0.03 S130 Interlayer)

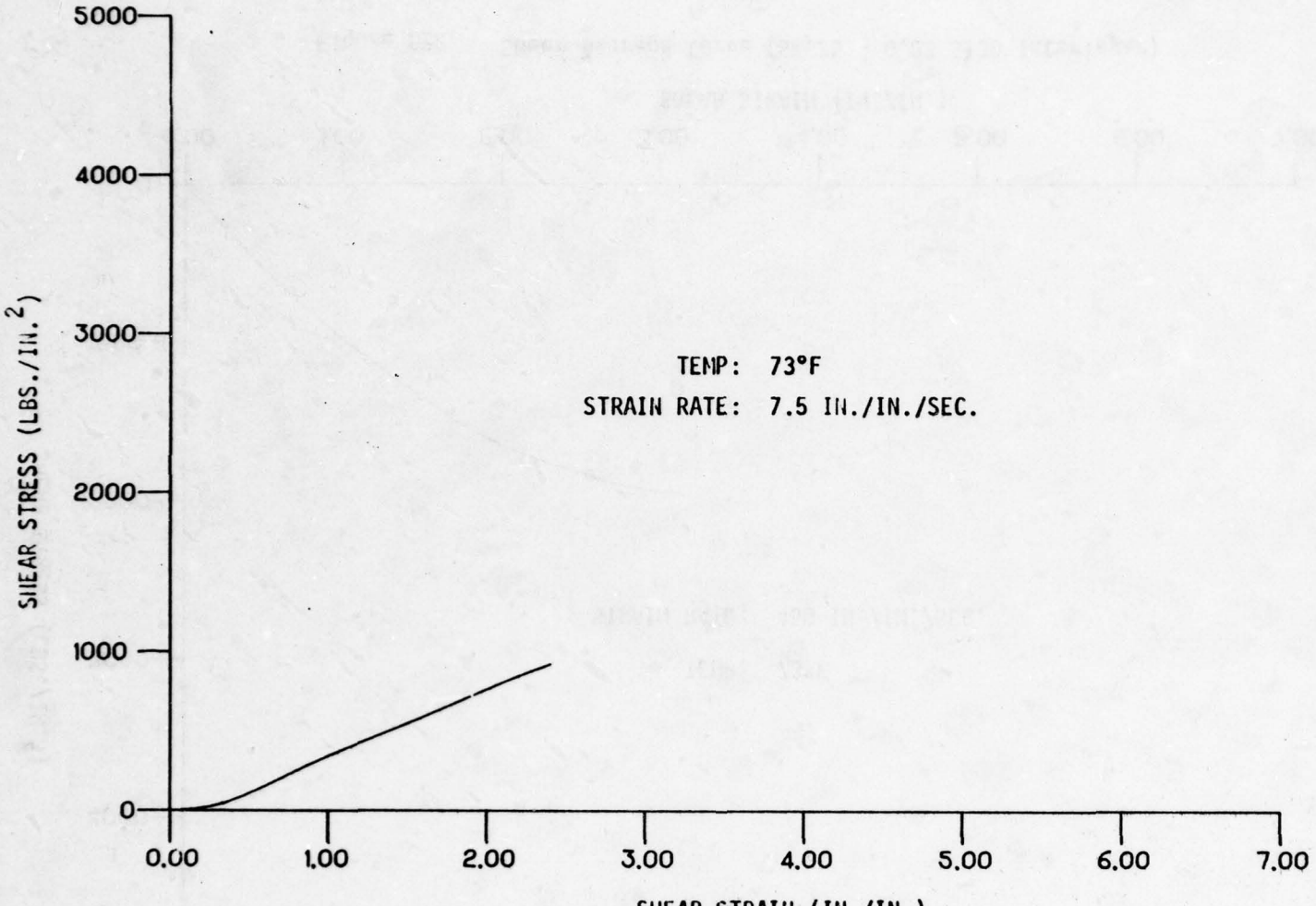

Figure F21. Shear Design (c) Curve (SK625 - 0.03 S130 Interlayer)

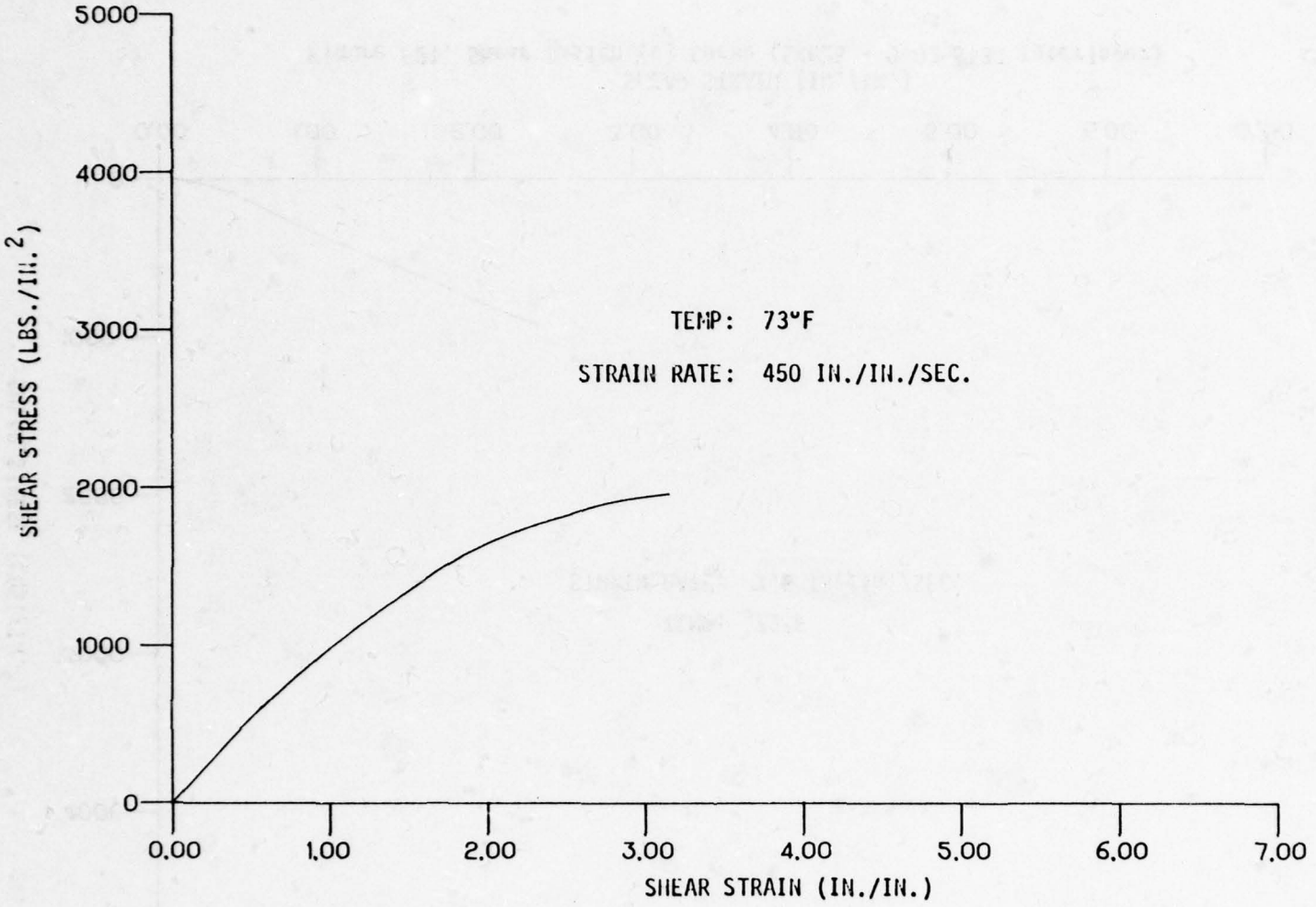

Figure F22. Shear Average Curve (SK625 - 0.03 S130 Interlayer)

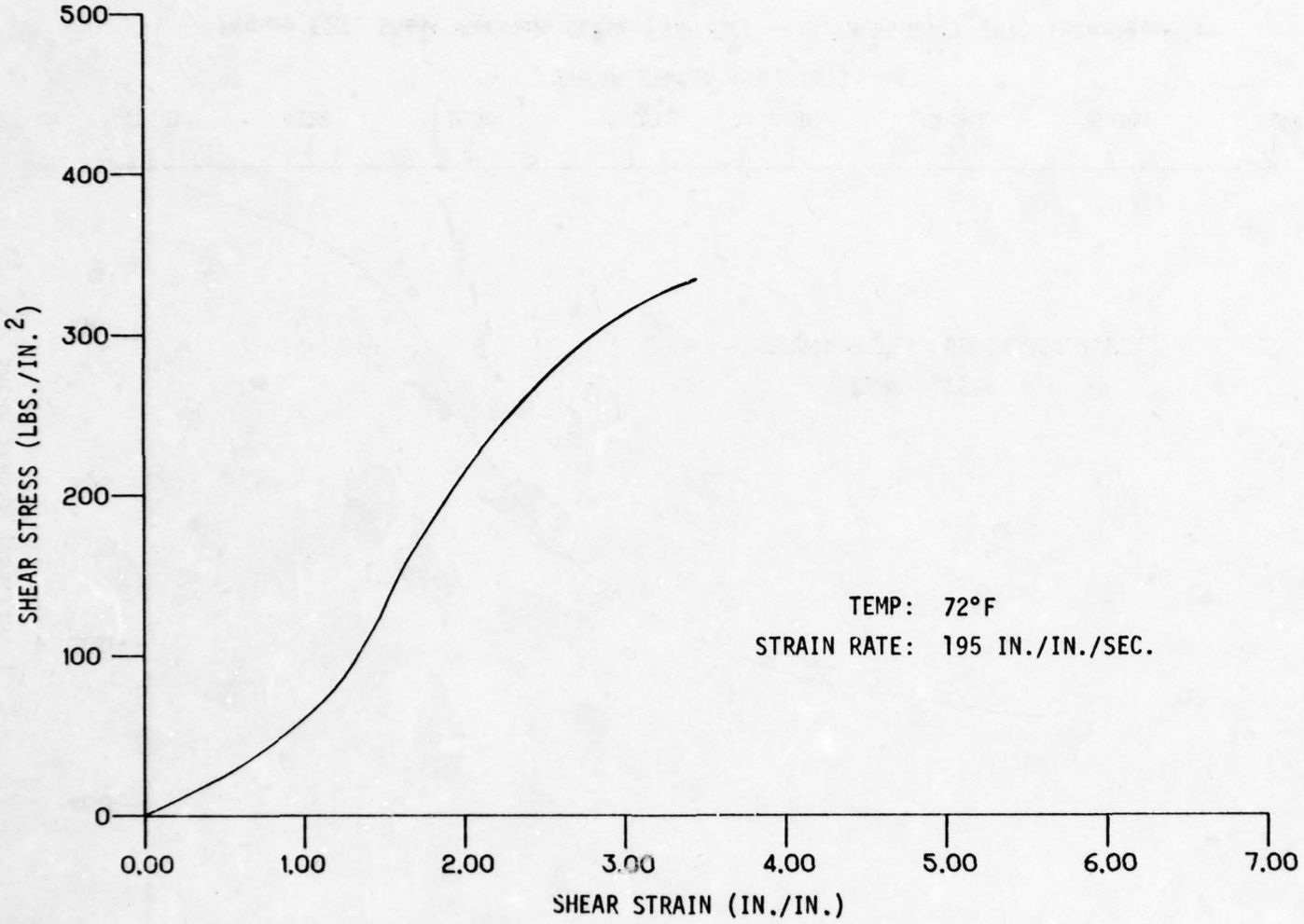

Figure F28. Shear Average Curve [SWU 521 -- 0.12 SS5272 (HT) Interlayer].

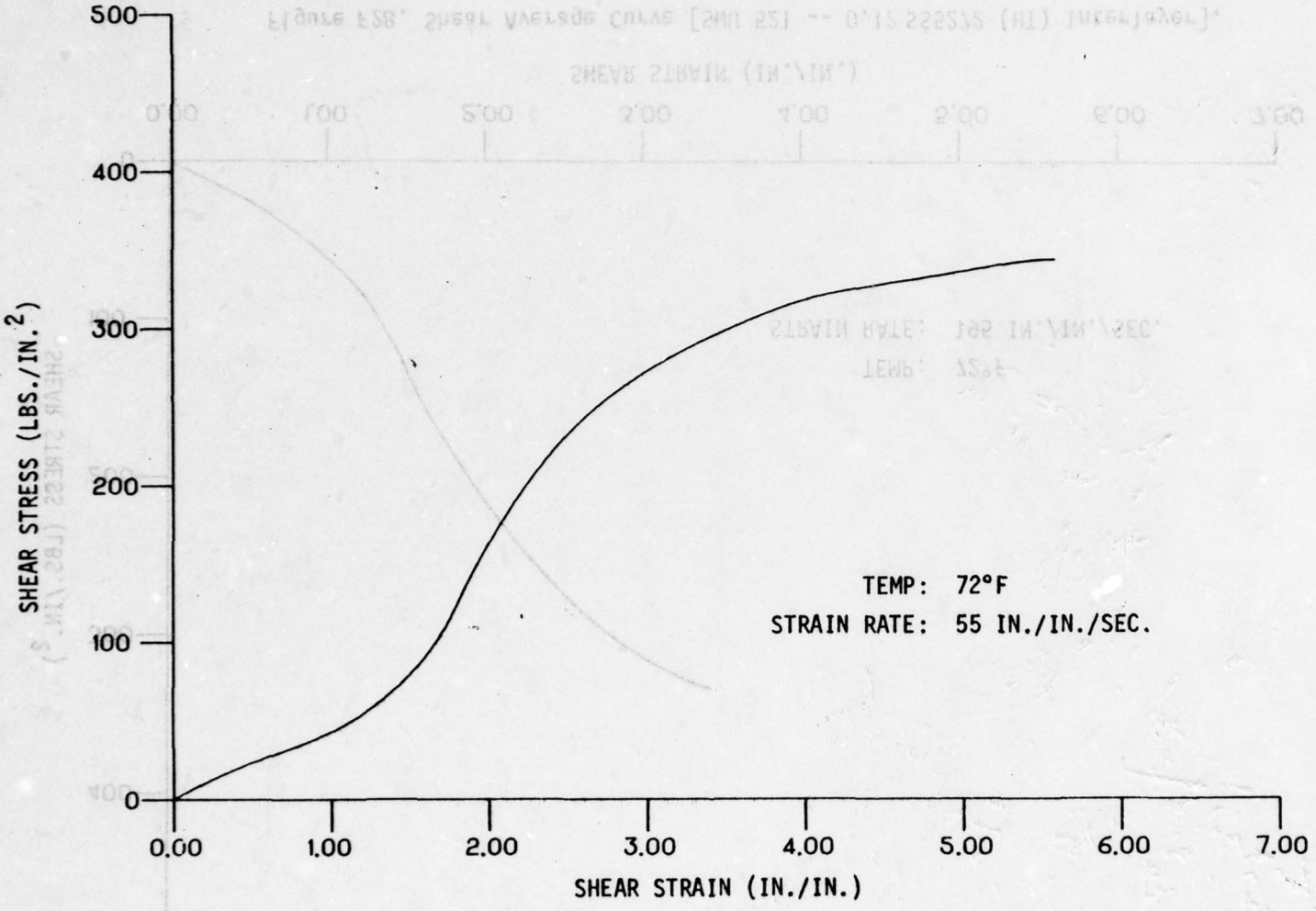

Figure F27. Shear Average Curve [SWU 521 -- 0.12 SS5272Y (HT) Interlayer].

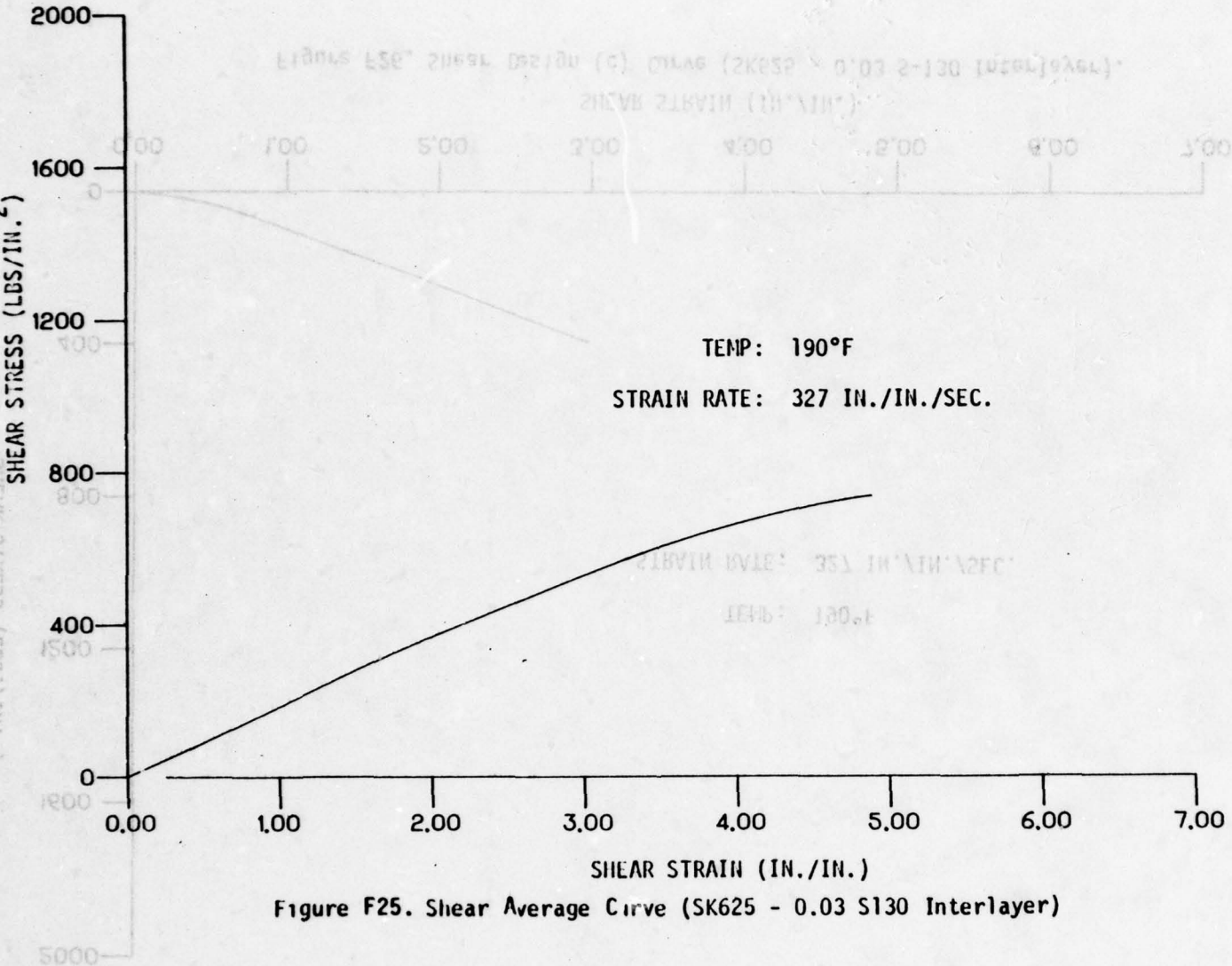

Figure F25. Shear Average Curve (SK625 - 0.03 S130 Interlayer)

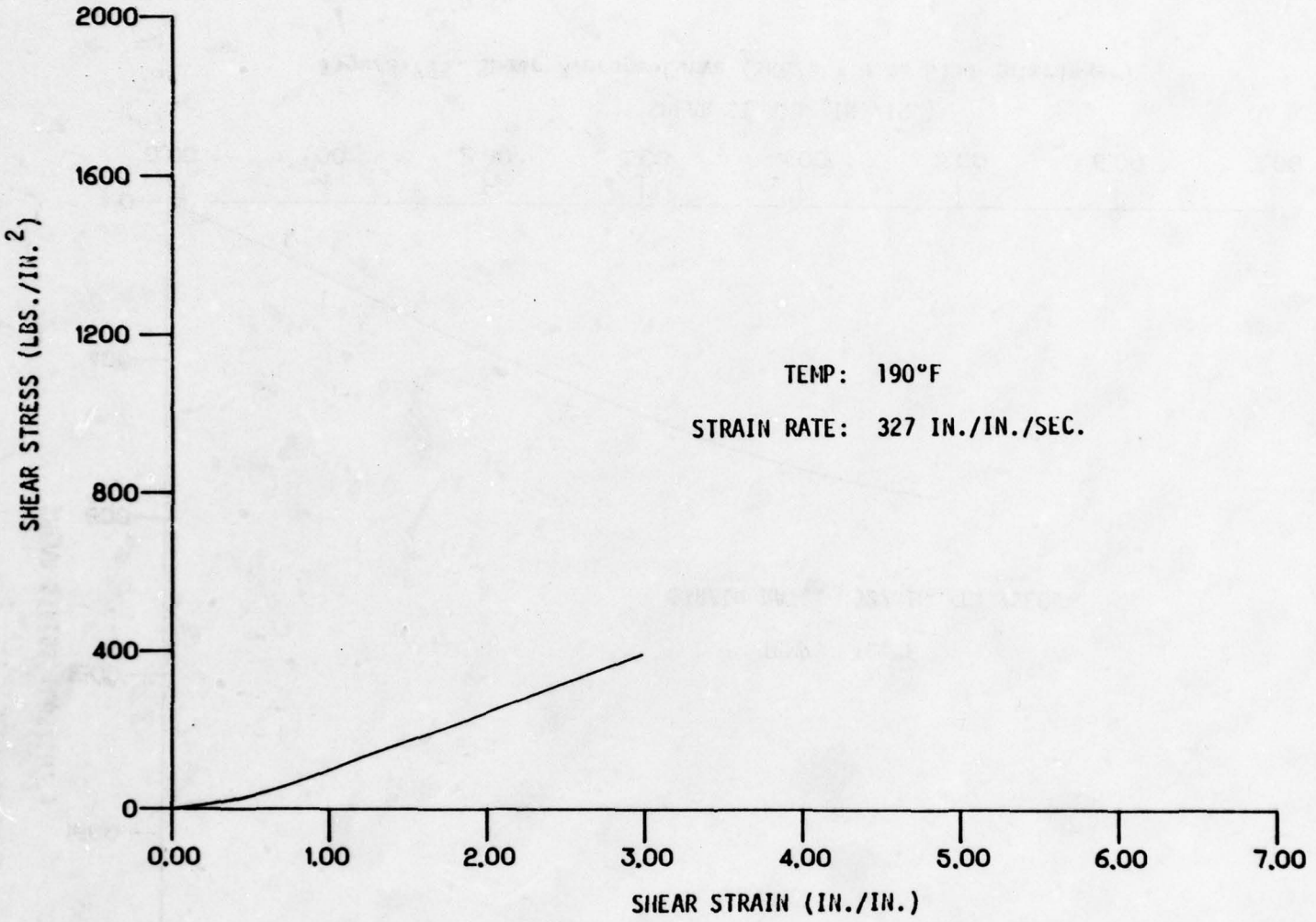

Figure F26. Shear Design (c) Curve (SK625 - 0.03 S-130 Interlayer).

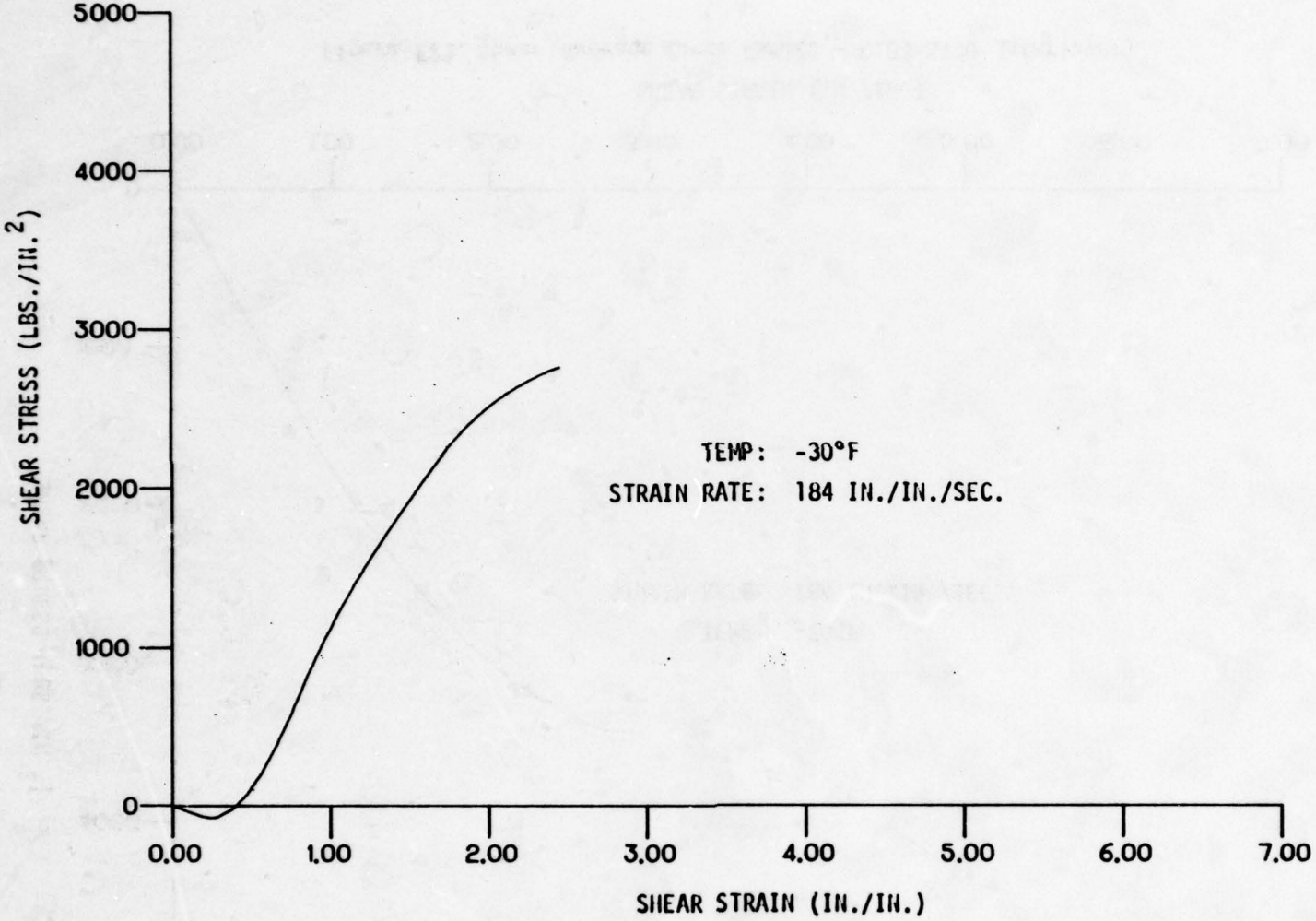

Figure F24. Shear Design (c) Curve (SK625 - 0.03 S130 Interlayer)

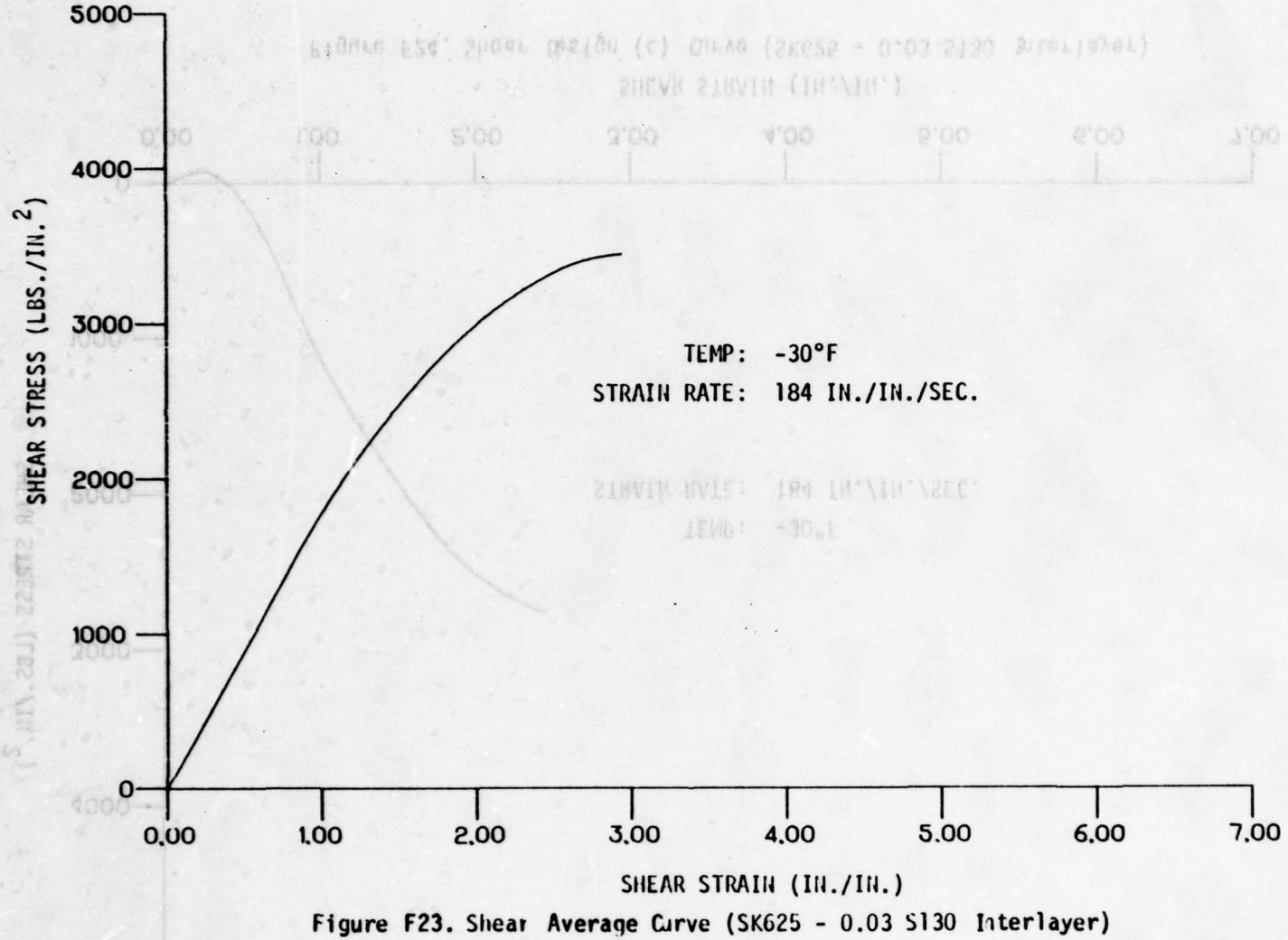

Figure F23. Shear Average Curve (SK625 - 0.03 S130 Interlayer)

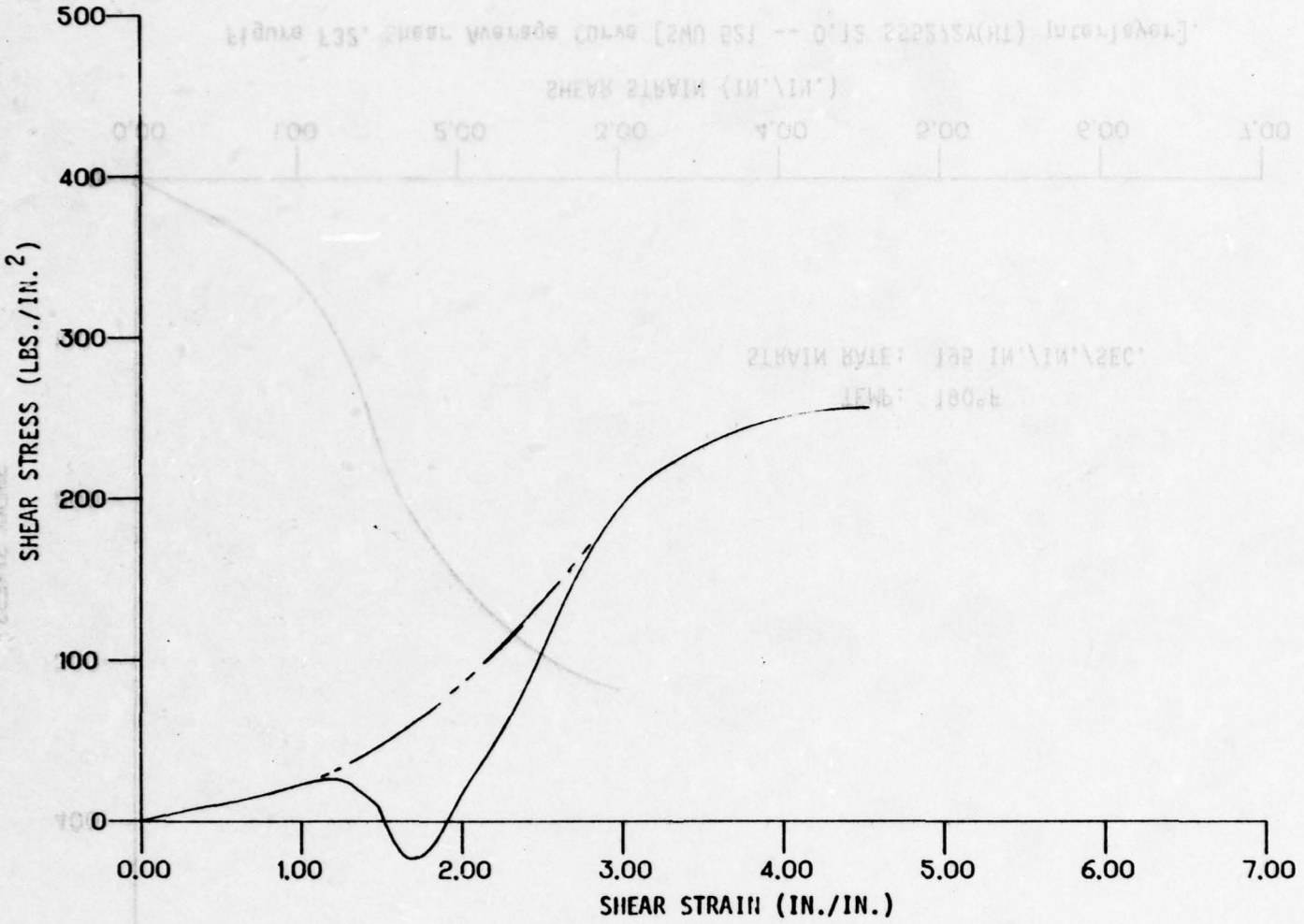

Figure F29. Shear Design (C) Curve (SWU 521-0.12 SS5272Y(HT) Interlayer)

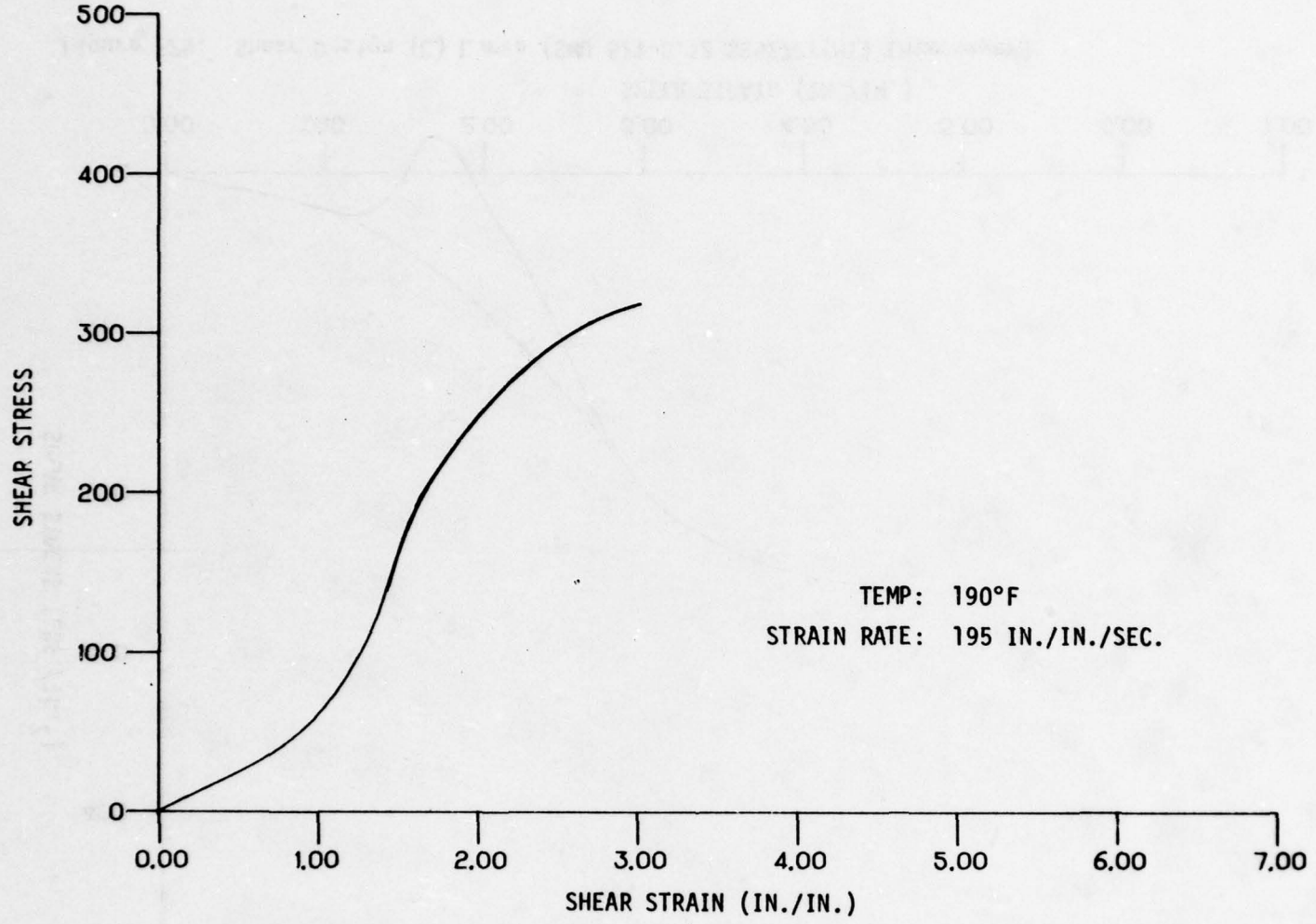

Figure F32. Shear Average Curve [SWU 521 -- 0.12 SS5272Y(HT) Interlayer].

SECTION XI
CONCLUSIONS AND RECOMMENDATIONS

The following conclusions and recommendations are based on data and observations on this program as well as data previously generated by others.

CORE PLY MATERIALS - PROCESSED POLYCARBONATE

Temperature and Strain Rate Effects

Figure 91 presents average tensile stress-strain curves prepared from tensile test data used in Section V and Section VIII for the development of specific design data. The test temperatures and strain rates reflect the extreme operating environmental conditions of the design aircraft transparencies. It was concluded that processed SL3000 polycarbonate sheet maintains sufficient strength and ductility to be used as the structural core ply material for the supersonic aircraft transparencies under consideration.

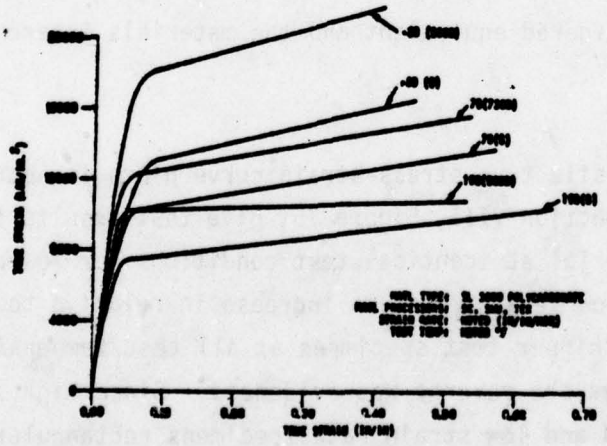

Figure 91. Tensile Strain Rate and Temperature Effects.

Forming Effects

The plots of average tensile true stress-strain curves in Section V, Figure 29, and in Section VIII, Figure 76, show test results for formed (reduced thickness) and non-formed polycarbonate materials at low and high strain rates. Formed parts with thickness reduction above 10 percent appears to decrease relative toughness and mechanical strength properties at low strain rates. This is possibly due to residual stresses within the part due to forming. The reverse seems to be evident at high strain rates where the reduction in thickness was unknown. This was possibly due to strain rate or specimen configuration effects (see thickness effects) where the thickness reduction was less than 10 percent. It is recommended that further high strain rate testing be conducted to verify effects on polycarbonate to establish a maximum allowable thinning of a bird proof canopy. It is recommended that thinning due to forming not exceed 18 percent based on this analysis and prior bird impact tests on canopies.

Material Comparison

The average tensile true stress-strain curve plots in Section V, Figure 26, and in Section VIII, Figure 77, show test results for two processed polycarbonates, "SL3000" and "Tuffak". From the standpoint of these tests and for the purposes of this program, the strength properties are considered equivalent and the materials interchangeable.

Thickness Effects

The average tensile true stress-strain curve plots in Section V, Figure 34, and in Section VIII, Figure 75, give test results for several thicknesses of material at identical test conditions for low and high strain rates. At low strain rates an increase in relative toughness was noted for the thinner test specimens at all test temperatures, and at high strain rates the reverse was evidenced. Since high strain rate specimens are round and low strain rate specimens rectangular, specimen configuration may have effected test results. From previous investigations

into this subject (References 10 and 15) and based on these test results, it appears that thickness is not the variable, but strain rate in combination with specimen configuration. Previous investigation (Reference 10) suggests an optimum testing speed for identical test results within these thickness ranges with temperature being entered as the variable. It is recommended that biaxial stress tests at high strain rate be conducted to establish the optimum laminate core ply thickness for bird strike resistance at a given strain rate and temperature condition. Tension-tension biaxial stress tests would provide a test more representative of actual stress conditions. These tests have been accomplished at Terra Tek for aluminum alloy per Reference 21.

Service Aging and Aerodynamic Heating Effects

A comparison of impact test data and tensile stress-strain data before and after thermal treatment and/or storage as contained in Section IV and other data (References 9 and 11) show that mechanical properties of polycarbonate materials are affected by in-service aging and aerodynamic heating above 176°F (80°C). The thermal processing results in a decrease in: impact strength, fracture energy, and elongation to break. Therefore, the high-impact properties of a newly made polycarbonate transparency cannot be fully utilized for aircraft applications. Other materials used in the construction of a laminated transparency may also be affected by in-service environmental conditions. Present practice for qualification testing of a transparency design and/or materials testing does not require in-service aging and simulated aerodynamic heating effects to be imparted to the test material and/or transparency prior to burst pressure, bird strike and/or material tests. It is therefore recommended that consideration be given to these areas in future design qualification tests and/or material testing to take into account these degrading effects of in-service heating and aging based on the life expectancy of the transparency.

INTERLAYER MATERIALS

Material Comparisons

The average shear stress-strain curve plots for material comparisons at low strain rates are presented in Section VII, Figures 53 through 55, and at high strain rates in Section X, Figures 88 through 90.

At low strain rate test conditions (Figure 61 through 63) it is noted that polyurethane (PPG-112) interlayer material is superior in load carrying and elongation capabilities to all other materials at all test temperature conditions.

At high strain rate test conditions (Figures 88 through 90) it can be noted that polyurethane (PPG-112) interlayer material is superior in load carrying ability at room temperature and at the low temperature extreme (-30°F) test conditions. The co-polymer is superior in load carrying ability at the high temperature extreme (+190°F) test condition and silicones are superior to all other materials in elongation to failure at room temperature and low temperature extremes (-30°F). Polyurethane (PPG-112) is superior in elongation to failure at the high temperature extremes (+190°F).

Figure 92 presents average shear stress-strain curves prepared from test data used in Section VII and Section X for development of specific design data for PPG-112. The test temperatures and strain rates reflect the extreme operating conditions of the design aircraft. Based on the preceding comparisons and the overall performance of PPG-112 as shown in Figure 92, this material was selected for use in the laminated core ply design transparency.

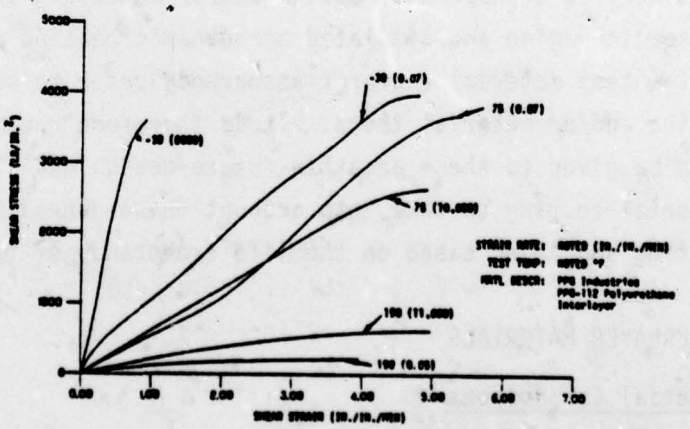

Figure 92. Shear Strain Rate and Temperature Effects.

MATERIAL DESIGN ALLOWABLES

The processes involved in manufacturing transparency materials and the processes used during the manufacture of a transparency is proprietary and may change without notice. It is therefore recommended that sufficient testing be initiated by design specification and/or material specification control documents to provide quality control and assurance of acceptable strength properties in the finished product. The design allowables published in this report can be used as the minimum acceptable material strength property for design and/or material specification control testing where the material is within the statistical population of the design allowable. It is therefore recommended that a sample of the selected processor material be compared to test material used to determine design allowables by methods specified in Section III, tests of significants.

Intrinsic viscosity tests are used by industries as the quality control tool for determining the molecular weight spectrum of polycarbonate resins. Mechanical properties can be correlated to specific molecular weight or ranges (Reference 4). These records are said to be available at General Electric Co., for each heat-lot of extruded sheet material. It is recommended that further investigations be made to establish intrinsic viscosity limits to maintain extruded sheet strength properties within design allowable limits after processing. Extruded sheet records can then be compared to established viscosity limits to determine acceptability of a heat-lot of material.

Proposed design allowables documented in this report are presented for general industry use and are submitted for consideration of inclusion in MIL-HDBK-17. It is recommended that guidelines for the preparation of design allowables of plastics be included in this document similar to that outlined for metals in MIL-HDBK-5C.

TEST OBSERVATIONS

The test methods described in this report proved satisfactory in the establishment of design mechanical properties for the transparency materials tested with the exception of the torsional shear tests. The following recommendations and conclusions are based on observations made during tests, and from a review of test data.

Low Strain-Rate Testing (Douglas Facility)

Tensile Tests

Comparison of calculated strain data of known strain gage length (tests using an extensometer), revealed that a large error existed in strain calculations where a measured gage length was used. It was determined by tests that the specimen measured gage length must be doubled to account for this error. It is therefore recommended that an extensometer or other means to determine an accurate gage length be used for all tensile tests of polymer materials.

Low strength values in a series of tensile tests were found to be attributable to edge chipping of specimens during machining. These defects show up as stress risers on the specimen when viewed through a polarascope. It is therefore recommended that all polycarbonate machined parts be inspected using polarized light. These defects can be removed by sanding and polishing edges.

Shear Tests

In shear testing of polyurethane materials at 75°F and -30°F it was found that ultimate shear loads exceeded the bearing strength of polycarbonate face plies of the Z7942633-531, and -533 test specimens. It was found that the polyurethane material shear area had to be reduced 70 percent to eliminate this condition. It is therefore recommended that in construction of shear test specimens, the polyurethane material be undercut similar to the high strain rate specimens Z7942633-519, and

-625 so that the ratio of bearing area of polycarbonate (A_b) to the total shear area of polyurethane (A_s) be equal to or greater than $.7\left(\frac{A_b}{A_s} \geq .7\right)$.

Design allowables given for shear tests where a bond failure mode is tabulated do not reflect the true strength of a material, but is only indicative of the adhesive strength of a laminate. These materials are not recommended for structural laminates due to inconsistency of bonding processes and the possibility of bond deterioration during service. It is recommended that these material bonding techniques be improved, or the interlayer material be restructured to provide a cohesive failure mode and re-test made to establish design allowables.

Izod Notch Tests

Test results were found to be inconsistent due to methods used in machine operations. To provide consistent test results all materials to be compared should be machined in a single setup to provide the same notch configuration. It is recommended to use tensile tests for a more consistent method in determining fracture energy for comparison of materials.

High Strain-Rate Testing (Terra Tek Facility)

Tensile Tests

It is recommended that a minimum of ten (10) tests be conducted for each material and test condition at high strain rates to establish design allowables. This requirement is based on the many recorded test failures due to instrumentation failures, specimen failures, and the large deviations in strain rates.

Discussion of Tension Specimen Failures and Related Polymer Fracture Theory

The following discussion is submitted by Terra Tek, Inc., to provide an explanation for the brittle fracture mode seen in tensile tests of polycarbonate specimens at high strain rates and low temperatures.

Fracture is at best a complex phenomenon that is not completely understood. Fracture involving macromolecules, such as in plastics, is particularly complex. Depending on polymer type, temperature of testing, rate of loading, environmental conditions, etc., deformation loading to failure may involve: (1) on a macroscopic scale, brittle fracture, shear slippage and/or crazing; (2) on a molecular scale, chain slippage resulting from breakage of secondary bonds and/or primary bond scission resulting in rupture of the long polymer chains or cross links.

The properties of polymers are extremely sensitive to loading conditions. The amount of variance of properties is usually surprising to those who have not made such measurements. There are many examples in the literature to which the reader interested in more detail is referred in References 15 through 18. It is not uncommon in polymers that by varying the temperature from -50°F to 100°C and the frequency over four orders of magnitude, the shear compliance, or modulus varies over more than three orders of magnitude. As described in References 15, 16 and 17, a shift in time will produce the same change in mechanical properties (at least in those dependent upon the rotational movement of molecular segments) as will a corresponding change in temperature. That is, in general, a decrease in temperature is equivalent to an increase in loading rate. Formal theories and models of this phenomenon have been developed and are sometimes known as the Williams-Landel-Ferry (WLF) theory. Yield stress, strain at fracture, ultimate strength and indeed the general stress-strain curve are drastically altered by temperature and/or loading rate.

Andrews (Reference 16) suggests that much of the fracture behavior of polymers can be explained by using the hypothesis that the phenomenon of yield is independent of that of brittle fracture. He states, for

example, that a satisfactory explanation of the transition from ductile to brittle behavior (often called the ductile-brittle transition) can be deduced from the fact that phenomena of brittle fracture and yield appear to be quite independent, and that which of these occur first is determined by the testing conditions. This explanation is simply that at any temperature the material has both a yield strength and a brittle fracture strength which both vary with temperature. The yield strength, however, is often much more dependent upon temperature than the brittle strength. This is shown schematically in Figure 93. The point of intersection between the yield strength σ_y and the brittle fracture strength of σ_f might be termed the ductile-brittle transition temperature T_b. Below this temperature, the material will embrittle while above T_b fracture will always be ductile.

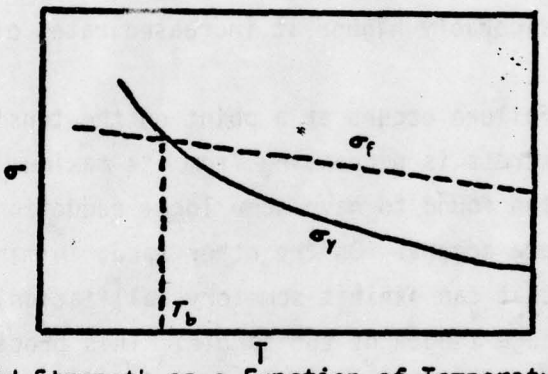

Figure 93. Yield Strength as a Function of Temperature. From Reference 16.

For some polymers T_b is quite close to the glass transition temperature (T_g) but for others it may be very far removed. T_g, it may be noted, is the temperature at which the elastic modulus of a polymer shows an abrupt increase with decreasing temperature. It has been supposed by some that this high modulus alone causes a material to embrittle. This,

however, is a fallacy since many polymeric materials are ductile well below their glass transition temperature. Andrews (Reference 16) lists the following values:

	T_g°C	T_b°C
PMMA	105	45
Polycarbonate	150	-200
Rigid PVC	74	-20
Natural Rubber	-70	-65
Polystyrene	100	90
Polyisobutylene	-70	-60

It should be noted that the first three of these materials have $T_b < T_g$ while the last three are very near T_g. It is also important to note that these T_g's and T_b's are for slow loading rates; both temperatures would generally be considerably higher at increased rates of loading.

When sample failure occurs at a point on the tensile stress-strain curve where the stress is decreasing from its maximum value, the specimen under test is often found to have some local reduction in cross-sectional area until fracture occurs. On the other hand, in many polymers (particularly those that can exhibit some crystallization) the neck may run over the whole gauge length of the sample. This process, shown schematically in Figure 94 is often called drawing and generally involves some form of cold "strain hardening" since the reduced cross-section could not otherwise bear the full load on the specimen while the larger unoriented part continued to be drawn out into the smaller sections. Processes similar to this area are used to produce orientated fibers that may have strengths nearly on order of magnitude higher than unorientated bulk material.

Whether a specimen will fail to embrittle, have a sharp neck to failure or draw depends on factors such as loading rate, temperature and presence of flaws. Flaws, whether they be internal flaw, notches on the surface, or even almost microscopic machine marks, can have a pronounced effect on

fracture behavior. Not only do such flaws act as stress rises that increase the value of the static elastic stresses but they can also affect the local strain rate. For example, unnotched specimens tested in a Charpy test may fracture ductilely with the absorption of a large amount of energy from the striking arm while a notched sample of the same material tested the same way will fracture in a brittle manner while absorbing very little energy.

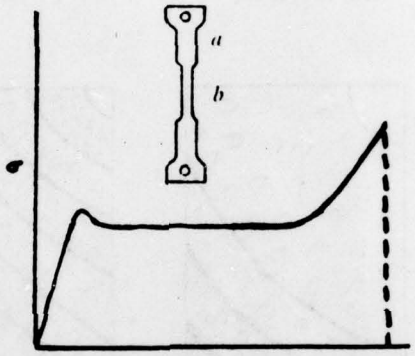

Figure 94. Stress-Strain Curve in Cold Drawing. Inset is the Appearance of the Test-Piece Itself. (a) Undrawn (b) Drawn Regions Respectively. From Reference 16.

The topography of the fracture surfaces for the samples tested in the present study are typical of these reported by others for polymers. Wolock and Newman review fractography studies in Reference 19. They cite the work of Sandman (Reference 20) who examined a large number of fracture surfaces produced in tensile specimens in various plastics by tension. These surfaces (and the ones in the current study) where characterized by the usual mirror-like area surrounded by concentric ribs covered with closely packed hyperbolic "figures".

Sandman's analysis (Reference 20) revealed that the portion of the surface of the broken section containing these circular ribs can be reduced considerably by loading at a slow rate. It is even possible to

completely eliminate these ribs by loading at very slow rates. His results are shown schematically in Figure 95.

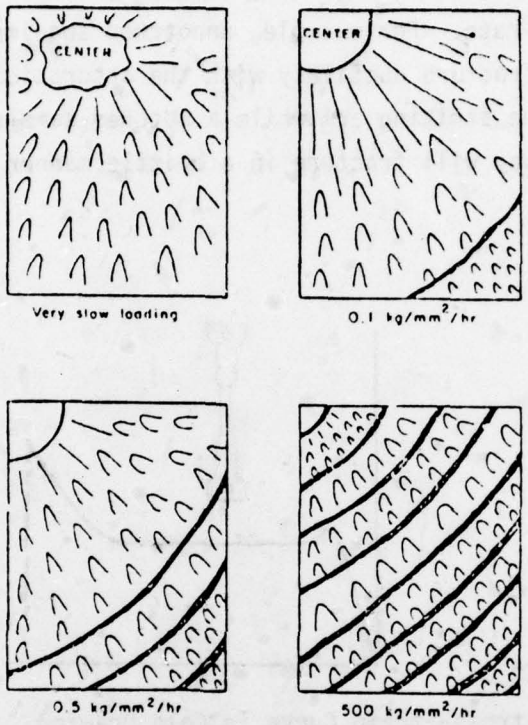

Figure 95. Effect of Loading Rate on Fracture Surface of Glassy Polymers. From Reference 20.

It is interesting to compare the effects of changing molecular weight and temperature with the effect of rate of loading on the nature of the fracture surface. Wolock and Newman (Reference 19) report that increasing molecular weight is analogous to decreasing loading rate as far as appearance of the fracture surface goes. When the molecular weight drops, the surface has less hyperbolic-figure area analogous to increasing the loading rate. The explanation is analogous to that for rate effects. Quoting from these authors, "An increased temperature, consistent with its effect on the properties, has an effect on the fracture surface analogous to decreasing the loading rate and vice versa".

Description of Observed Fracture Surfaces

In the current study some of the samples tested at -30°F were observed to fail in either a comparatively brittle manner with little or no necking while others exhibited considerable drawing. Temperature, loading rate and sample material were as near the same as possible. The exact reason for the difference in behavior is not known with certainty. Photographs of samples of both types are shown in Figures 96 and 97. In either case, the final fracture surface was perpendicular to the axis of the tensile specimen; that is, the failure occurred across the plane of maximum tensile stress.

Micrographs (obtained with a Unitron series N optical metagraph) revealed that the fracture surfaces were very different for these two types of observed behavior. Figure 95 shows a fracture surface typical of the samples which failed with almost no drawing. Figure 96 is typical of the -30°F samples that exhibited extensive drawing before final fracture. Obviously the first of these is typical of high loading rate fracture described previously while the latter is characteristic of a low-loaded rate failure.

The big question is why this difference in behavior for samples that are supposedly the same and are fractured under as near identical conditions as possible. The most likely explanation, in our opinion, is that the testing conditions (high strain rate and low temperatures) is approaching the T_b for these samples. If this is the case, slight differences in specimens and/or testing conditions could result in the sample falling to either side of the transition point. Specimen differences that might result in these differences in behavior include slight variations in composition, orientation (i.e., exactly how the sample was cut from the material), internal flaws, machine marks or scratches on the surface, etc.

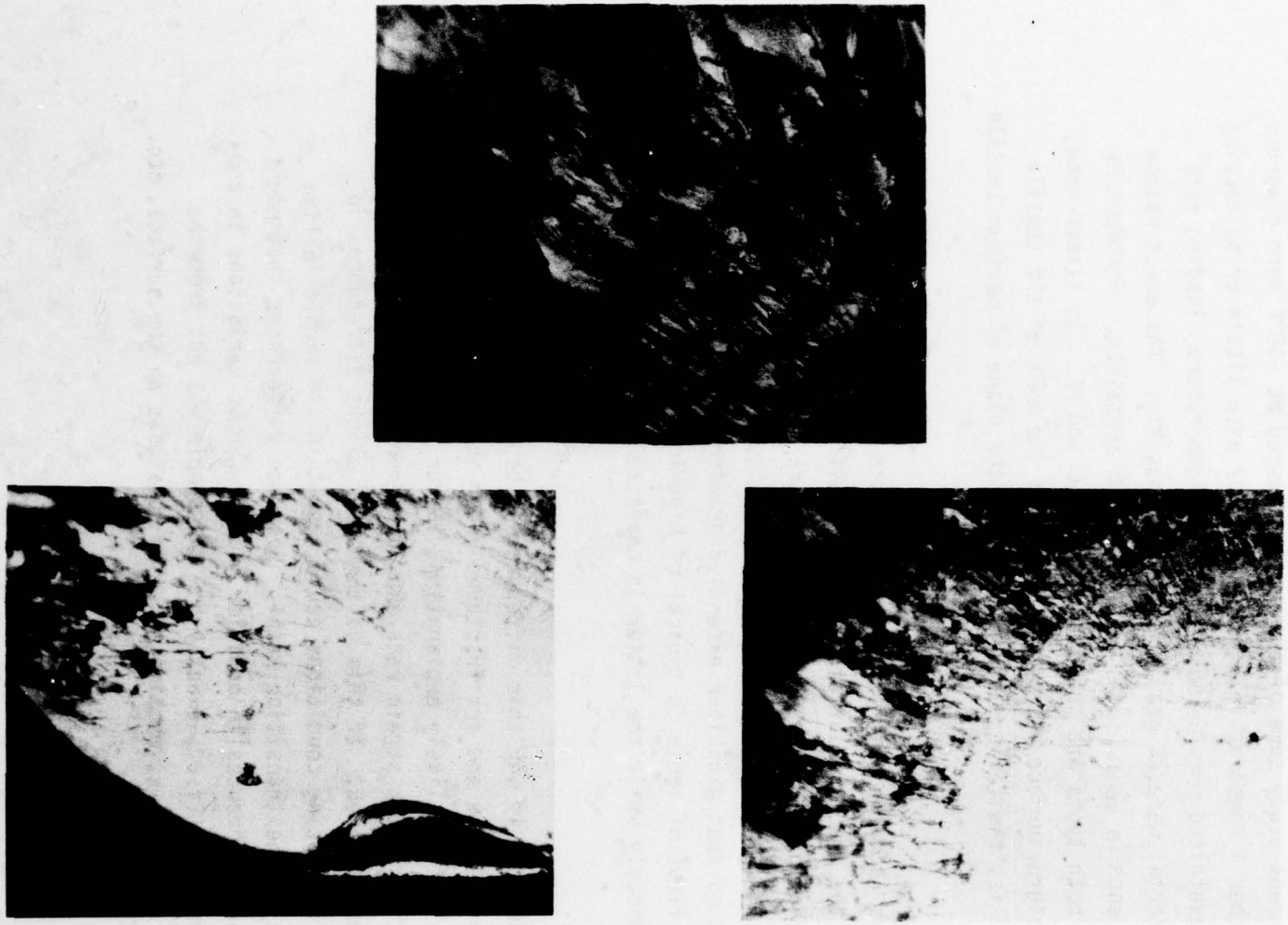

Figure 96. Sample That Did Not Draw (x 40).

Figure 97. Sample That Necked and was Drawn Over Large Part of Gauge Length (x 40).

REFERENCES

1. Lawrence, J. H., Jr., Windshield Technology Demonstrator Program - Detail Design Options Study (Douglas Aircraft Co.) AFFDL-TR-77-1.

2. Lawrence, J. H., Jr., Windshield Technology Demonstrator Program - Canopy Detail Design Options Study (Douglas Aircraft Co.), AFFDL-TR-78-114.

3. Sorenson, W. R. and Campbell, T. W., Preparative Methods of Polymer Chemistry by Inter Sciences Publisher, New York, 1961

4. Ryan, J. T., Impact and Yield Properties of Polycarbonate as a Function of Strain Rate, Molecular Weight, Thermal History, and Temperature", Polymer Engineering and Science, March 1978.

5. Ramberg, W., and Osgood, W., T.N. 902, National Advisory Committee for Aeronautics.

6. Lilliefors, H. W., "On the Kolomgorov-Smirnov Test for Normality with Mean and Variance Unknown", American Statistical Association Journal, June 1967, Pages 399-402.

7. Denke, P. H., Aircraft Windshield Bird Impact Math Model (Douglas Aircraft Co.) AFFDL-TR-77-99.

8. Eshleman, A. L., and Meriwether, H. D., Graphics Applications to Aerospace Structural Design Problems, (Douglas Paper 4650), dated June 1967.

9. Morgan, R. J. and O'Neal, J. E., "The Effect of Thermal History on the Mechanical Properties and Crystallinity of Polycarbonate", Conference on Aerospace Transparent Materials and Enclosures, AFML-TR-76-54, April 1976.

10. Hassard, R. S., Design Criteria Transparent Polycarbonate Plastic Sheet (Goodyear Aerospace Corp.), ARML-TR-72-117, August 1972.

11. Schramm, R. E., Clark, A. F., and Feed, R. P., A Compilation and Evaluation of Mechanical, Thermal and Electrical Properties of Selected Polymers, U. S. Department of Commerce, NBS Monograph 132, September 1973.

12. Rhodes, G. F., Damping, Static/Dynamic, and Impact Characteristics of Laminated Beams Typical of Windshield Construction (Douglas Aircraft Co.) AFFDL-TR-76-156.

13. Magnusson, R. H., and Coker M. H., High Speed Bird Impact Testing of Aircraft Transparencies (Douglas Aircraft Co.), AFFDL-TR-77-98.

REFERENCES (Continued)

14. Goldblum, K. B., "Detective Work with High-Speed Testing - The Location of a Phase Change Area", Journal of Applied Polymer Science, Volume 8, January 1964, pp. 111-117.

15. Williams, M. L., Landel, R. F., and Ferry J.D.H., Am. Chem. Soc., 77, 3701, 1955.

16. Andrews, E. H., Fracture in Polymers, Elsevier, New York, 1968.

17. Fitzgerald, E. R., Grandine, L. D., and Ferry J.D.H., J. Appl. Phys., 24, 650, 1953.

18. Rosen, B., "Chapter IC - Mechanical Aspects", in Fracture Processes in Polymer Solids, ed. by Rosen, J., Wiley & Sons, New York, 1966.

19. Wolock, I., and Newman, S., "Chapter IIC - Fracture Topography", in Fracture Processes in Polymer Solids, ed. by B. Rosen, John Wiley & Sons, New York, 1966.

20. Zandman, F., "Etude de la Deformation et de la Rupture des Matieres Plastiques," Publications Scientifique et Technique de Ministere de l'Air, No. 291, Paris, 1954.

21. Reid, R. J., Jones, A. H., Green, S. J., Characterization of 2014-T651 Aluminum Alloy (Terra Tek), AMMRC CTR 74-68.

☆U.S.Government Printing Office: 1979 — 657-002/338